THE ROLE OF SALIVA IN ARTHROPOD-HOST-PATHOGEN RELATIONSHIPS

EDITED BY: Lucas Tirloni, Eric Calvo, Satoru Konnai and Itabajara Silva Vaz Jr
PUBLISHED IN: Frontiers in Cellular and Infection Microbiology

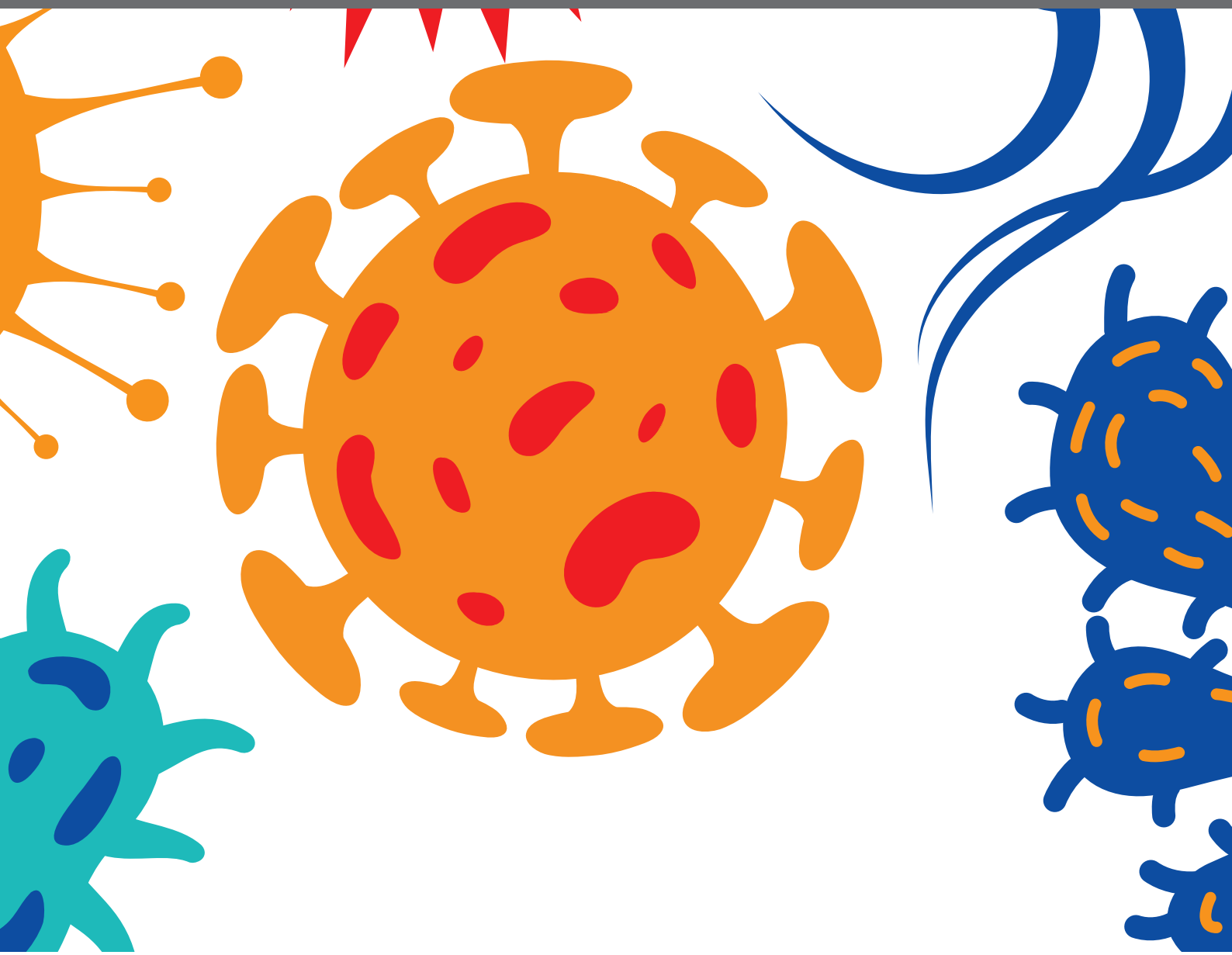

frontiers Research Topics

frontiers

ISSN 1664-8714
ISBN 978-2-88966-552-5
DOI 10.3389/978-2-88966-552-5

About Frontiers

Frontiers is more than just an open-access publisher of scholarly articles: it is a pioneering approach to the world of academia, radically improving the way scholarly research is managed. The grand vision of Frontiers is a world where all people have an equal opportunity to seek, share and generate knowledge. Frontiers provides immediate and permanent online open access to all its publications, but this alone is not enough to realize our grand goals.

Frontiers Journal Series

The Frontiers Journal Series is a multi-tier and interdisciplinary set of open-access, online journals, promising a paradigm shift from the current review, selection and dissemination processes in academic publishing. All Frontiers journals are driven by researchers for researchers; therefore, they constitute a service to the scholarly community. At the same time, the Frontiers Journal Series operates on a revolutionary invention, the tiered publishing system, initially addressing specific communities of scholars, and gradually climbing up to broader public understanding, thus serving the interests of the lay society, too.

Dedication to Quality

Each Frontiers article is a landmark of the highest quality, thanks to genuinely collaborative interactions between authors and review editors, who include some of the world's best academicians. Research must be certified by peers before entering a stream of knowledge that may eventually reach the public - and shape society; therefore, Frontiers only applies the most rigorous and unbiased reviews.
Frontiers revolutionizes research publishing by freely delivering the most outstanding research, evaluated with no bias from both the academic and social point of view. By applying the most advanced information technologies, Frontiers is catapulting scholarly publishing into a new generation.

What are Frontiers Research Topics?

Frontiers Research Topics are very popular trademarks of the Frontiers Journals Series: they are collections of at least ten articles, all centered on a particular subject. With their unique mix of varied contributions from Original Research to Review Articles, Frontiers Research Topics unify the most influential researchers, the latest key findings and historical advances in a hot research area! Find out more on how to host your own Frontiers Research Topic or contribute to one as an author by contacting the Frontiers Editorial Office: frontiersin.org/about/contact

THE ROLE OF SALIVA IN ARTHROPOD-HOST-PATHOGEN RELATIONSHIPS

Topic Editors:
Lucas Tirloni, National Institutes of Health (NIH), United States
Eric Calvo, National Institutes of Health (NIH), United States
Satoru Konnai, Hokkaido University, Japan
Itabajara Silva Vaz Jr, Federal University of Rio Grande do Sul, Brazil

Citation: Tirloni, L., Calvo, E., Konnai, S., Silva Vaz, I., Jr. eds. (2021). The Role of Saliva in Arthropod-Host-Pathogen Relationships. Lausanne: Frontiers Media SA. doi: 10.3389/978-2-88966-552-5

Table of Contents

frontiers in Cellular and Infection Microbiology

EDITORIAL
published: 28 January 2021
doi: 10.3389/fcimb.2020.630626

Editorial: The Role of Saliva in Arthropod-Host-Pathogen Relationships

Lucas Tirloni[1]*, *Eric Calvo*[2], *Satoru Konnai*[3] and *Itabajara da Silva Vaz Jr*[4,5]

[1] Laboratory of Bacteriology, Tick-Pathogen Transmission Unit, Division of Intramural Research, National Institute of Allergy and Infectious Diseases, Hamilton, MT, United States, [2] Laboratory of Malaria and Vector Research, Molecular Entomology Unit, Division of Intramural Research, National Institute of Allergy and Infectious Diseases, Rockville, MD, United States, [3] Department of Disease Control, Faculty of Veterinary Medicine, Hokkaido University, Sapporo, Japan, [4] Centro de Biotecnologia, Universidade Federal do Rio Grande do Sul, Porto Alegre, Brazil, [5] Faculdade de Veterinária, Universidade Federal do Rio Grande do Sul, Porto Alegre, Brazil

Keywords: arthropod, saliva, host, pathogen, relationship

Editorial on the Research Topic

The Role of Saliva in Arthropod-Host-Pathogen Relationships

INTRODUCTION

Hematophagous arthropods can transmit various pathogens causing diseases to humans, including malaria, Chagas disease, filariasis, leishmaniosis, dengue, Lyme disease, anaplasmosis, babesiosis, among other (WHO, 2020). In addition, these arthropods are vector of disease-causing pathogens to animals generating huge economic losses in livestock.

Saliva was a central component for the adaptation of the hematophagy in blood feeding arthropods and this habit evolved independently in many arthropod orders or even within insect families (Ribeiro, 1995). Saliva has a potent pharmacologically activity that interfere in the hemostatic and immune responses of vertebrate host (Ribeiro, 1995; Francischetti, 2009; Šimo et al., 2017) and pathogen transmission. Additionally, active compounds in arthropod saliva are potential useful as therapeutic tools (Chmelar et al., 2019). The study described by Li et al. shed light on comparative proteomic of a different species of blood feeding parasite, the parasitic isopod *Tachaea chinensis*, a parasite of shrimps. Similar to blood feeding arthropods feeding on mammals, there is evidence that isopod parasites may also inject anticoagulants or other compounds directly into the host to modulate host's hemostasis and immune response. In this study, authors used a tandem mass tag-based quantitative proteomic approach to perform a comparative analysis between unfed and fed individuals, identifying 37 upregulated and 92 downregulated proteins in unfed *T. chinensis*, suggesting that organism's energetic demand is increased during the search for a host. Similar to other hematophagous parasites, isopods may also employ biomolecules that affect host blood coagulation and defense systems. Differentially expressed proteins related to blood feeding identified in this study also were described in the saliva of other hematophagous arthropods (Mans, 2011; Tirloni et al., 2014; Chmelař et al., 2016).

The protein composition of the saliva of hematophagous arthropods and the correlation with expression in salivary glands are essential to understand the feeding process and immunomodulation of host defenses (Tirloni et al., 2017; Antunes et al., 2019). Technological advances, including large-scale DNA sequencing and proteomic analysis, have increased the

OPEN ACCESS

Edited and reviewed by:
Jeroen P. J. Saeij,
University of California, Davis, United States

***Correspondence:**
Lucas Tirloni
lucas.tirloni@nih.gov

Specialty section:
This article was submitted to Parasite and Host, a section of the journal Frontiers in Cellular and Infection Microbiology

Received: *18 November 2020*
Accepted: *30 December 2020*
Published: *28 January 2021*

Citation:
Tirloni L, Calvo E, Konnai S and da Silva Vaz I Jr (2021) Editorial: The Role of Saliva in Arthropod-Host-Pathogen Relationships. Front. Cell. Infect. Microbiol. 10:630626. doi: 10.3389/fcimb.2020.630626

identification of genes and proteins, supporting our comprehension governing vector-host-pathogen interactions. In a fascinating review, Mans performs a historical analysis and reflection of the development of methods used to study and identify the protein composition related to the tick-host interface. This work summarizes the advances made over the years to understand and describe the complexity present within this interface. The high-throughput *in silico* analyses are widening rapidly and the development of new algorithms are increasing the accuracy of analyses and the importance for biological sciences (Hernández-Vargas et al., 2017; Bensaoud et al., 2019; Jia et al., 2020; Polanska et al., 2020; Tirloni et al., 2020). Recent advances in tick transcriptomic and proteomic studies have revealed over thousands of different transcripts coding for proteins in different tick species (Karim et al., 2011; Schwarz et al., 2013; Chmelař et al., 2016; Tirloni et al., 2020). As more and more studies contribute to our knowledge of tick genes and proteins, it becomes increasingly important to develop new approaches to help the annotation and classification of identified sequences. A tick-specific protein database is import since previous studies showed the presence of protein families that are found exclusively in ticks. TickSialoFam (TSFam) is a database aimed to assemble a curated collection of salivary genes and proteins in addition to improve the annotation of their putative functions. The initial version of the database identified 136 tick salivary secreted protein families. Moreover, with the increasing availability of whole-genome sequencing data, the TSFam database can be updated to include these new identified sequences (Ribeiro et al.).

Quantification of the cellular activity in different conditions or times, such as the parasite relationship, is instrumental to understand the cell or organ functions and susceptibility to diseases and several strategies have been developed for the quantification of proteins using mass spectrometry (Van De Merbel, 2019). This approach was used to compare proteins in the saliva of five vector species of the Chaga`s disease pathogen, *Trypanosoma cruzi*, including *Triatoma infestans*, *Triatoma dimidiata*, *Dipetalogaster maxima*, *Rhodnius prolixus*, and *Rhodnius neglectus* (Santiago et al.). Data showed similarities and differences in protein profile in saliva of these species. A notable observation was the presence of unique proteins for each triatomine species that could be useful as marker for species identification.

Another interesting study published in this issue provided evidence that a salivary protein affect vitellogenin uptake in the ovary and thereby play a role in the modulation of tick reproduction. The RH36 is an immunosuppressant protein that regulate the host immune system during tick feeding. Homologous proteins to RH36 were identified in other ticks (Aljamali et al., 2009; Anatriello et al., 2010) and characterized as immunosuppressant molecule, including in *Dermacentor andersoni* (Bergman et al., 1998) and *Haemaphysalis longicornis* (Konnai et al., 2009). Surprisingly, RNAi-mediated gene silencing of RH36 induces a reduction in tick oviposition and also affects HSP70 expression in the immature ovary of engorged ticks. This raises the possibility that RH36 interferes in tick vitellogenin uptake and then control ovary cell maturation by modulating HSP70 expression, and controlling tick oviposition (Wang et al.).

As mentioned, saliva facilitates establishment of infection and increases transmission in the vertebrate host. However, host susceptibility to parasite infection also is markedly affected by genetic differences. Many studies have shown that susceptibility to parasites is influenced by genetic characteristics of both host and pathogen. In addition, there are solid evidences for the existence of host genetic component controlling expression of parasite proteins (Popara et al., 2013; Tirloni et al., 2017). A perfect example is that *Bos taurus* are more susceptible to *Rhipicephalus microplus* infestations than *Bos indicus* (Garcia et al., 2020). The characterization of tick salivary gland gene expression in tick-susceptible and tick-resistant hosts can be important for the identification of potential targets for the development of new control methods. Giachetto et al. study identified 137 sequences as differentially expressed genes between ticks feeding on tick-susceptible or tick-resistant cattle.

Bioinformatics analysis associated to serological data are useful strategies for antigen selection in vaccine development. Sera from rabbits repeatedly infested with *Ixodes ricinus* were used to identify salivary immunogenic antigens. Using this approach, Perner et al. identified metalloproteases essential to tick initial feeding and engorgement, suggesting immunomodulatory or anti-hemostatic properties of these enzymes. To corroborate the role of metalloproteases at the tick/host interface, authors fed ticks micro-injected with a zinc metalloprotease inhibitor, which impacted tick feeding. A proteomic approach was also used to identify potential vector exposure markers (Zeyrek et al., 2011) in mosquitoes. The global spread of the mosquito *Aedes albopictus* increases the risk and burden of *Aedes*-transmitted viruses to temperate areas, highlighting the need to improve vector surveillance methods. With a proteomic approach, Montero et al. identified a correlation between antibodies against an *A. albopictus* salivary gland protein and exposure to mosquito bites. A similar strategy was used by Londono-Renteria et al. to identify a positive correlation among the antibodies against an *Anopheles darlingi* salivary gland antigen (apyrase) and antibodies against the *Plasmodium vivax* and *P. falciparum* antigens in patients infected with malaria. Individuals with high IgG levels are five times more likely to have malaria infection than uninfected persons. Both studies provide strong evidences to use salivary proteins in tools for monitoring the human-mosquito exposure.

Similarly, with the objective to develop diagnostic and research tools Contreras et al. characterized the use the zebrafish as a new animal model to study of allergic reactions and relation among the immune mechanisms in response against the α-gal epitope (Galα1-3Galβ1-(3)4GlcNAc-R) presents in tick saliva and red meat consumption. With the development of new techniques, Hermance et al. used RNA *in situ* hybridization to analyze the cellular localization of Powassan virus at the *Ixodes scapularis* feeding site. Furthermore, this methodology can be used in to identify virus replication in tissues of different mammalian hosts and tick vectors.

Scientific and clinical interest in parasite-derived molecules and their immunomodulatory properties is partially focused in the development of novel drugs for treating diseases. The immunomodulatory effect of the mosquito saliva is reviewed by

Guerrero et al. showing the strongly effect in the transmission and the establishment of pathogens in the host. The focus is on the role of saliva in arboviruses transmission and the potential use of salivary proteins for the control of pathogen transmission through the development of effective vaccines. Sumova et al. showed the immunomodulatory properties of three *Phlebotomus perniciosus* salivary proteins. These proteins inhibited macrophages nitric oxide production and rSP03 proteins increased IL-10 and decreased TNF-α secretions. This data helps understanding the immunomodulatory role of saliva and its participation in *Leishmania* transmission. Similarly, the immunomodulatory effect of parasite saliva also has an effect on pathogen transmission to the vertebrate host (Titus and Ribeiro, 1988; Šimo et al., 2017; Aounallah et al., 2020). Based on *in vitro* experiments with BHK cells expressing a salivary peroxiredoxin from *Haemaphysalis longicornis*, Kusakisako and colleagues demonstrate that this protein facilitates the replication of the tick-borne encephalitis virus by some yet unknown mechanism (Kusakisako et al.).

In conclusion, this Research Topic shed light on the roles of arthropod saliva facilitating blood meal acquisition and pathogen transmission. Moreover, different rationale strategies to develop and improve vaccine efficacy and diagnostic tools were pursued. A better understanding in this field is fundamental to the discovery and implementation of control and prevention strategies, including vaccines, not only against specific pathogens but also the arthropod itself.

AUTHOR CONTRIBUTIONS

All authors listed have made a substantial, direct, and intellectual contribution to the work and approved it for publication.

FUNDING

LT and EC are supported by the Intramural Research Program of the National Institute of Allergy and Infectious Diseases, National Institutes of Health, USA. SK is supported by grants from JSPS KAKENHI, AMED, and JSPS (Japan), and IV is supported by grants from CAPES and CNPq (Brazil).

REFERENCES

Aljamali, M. N., Hern, L., Kupfer, D., Downard, S., So, S., Roe, B. A., et al. (2009). Transcriptome analysis of the salivary glands of the female tick *Amblyomma americanum* (Acari: Ixodidae). *Insect Mol. Biol.* 18, 129–154 doi: 10.1111/j.1365-2583.2009.00863.x

Anatriello, E., Ribeiro, J. M. C., de Miranda-Santos, I. K. F., Brandão, L. G., Anderson, J. M., Valenzuela, J. G., et al. (2010). An insight into the sialotranscriptome of the brown dog tick, *Rhipicephalus sanguineus*. *BMC Genomics*. 11, 450. doi: 10.1186/1471-2164-11-450

Antunes, S., Couto, J., Ferrolho, J., Sanches, G. S., Charrez, J. O. M., De La Cruz Hernández, N., et al. (2019). Transcriptome and Proteome Response of *Rhipicephalus annulatus* Tick Vector to *Babesia bigemina* Infection. *Front. Physiol.* 10, 318. doi: 10.3389/fphys.2019.00318

Aounallah, H., Bensaoud, C., M'ghirbi, Y., Faria, F., Chmelař, J., and Kotsyfakis, M. (2020). Tick Salivary Compounds for Targeted Immunomodulatory Therapy. *Front. Immunol.* 11, 583845. doi: 10.3389/fimmu.2020.583845

Bensaoud, C., Aounallah, H., Sciani, J. M., Faria, F., Chudzinski-Tavassi, A. M., Bouattour, A., et al. (2019). Proteomic informed by transcriptomic for salivary glands components of the camel tick *Hyalomma dromedarii*. *BMC Genomics* 20, 675. doi: 10.1186/s12864-019-6042-1

Bergman, D. K., Ramachandra, R. N., and Wikel, S. K. (1998). Characterization of an Immunosuppressant Protein from *Dermacentor andersoni* (Acari: Ixodidae) Salivary Glands. 35, 505–509. *J. Med. Entomol*. doi: 10.1093/jmedent/35.4.505

Chmelař, J., Kotál, J., Karim, S., Kopacek, P., Francischetti, I. M. B., Pedra, J. H. F., et al. (2016). Sialomes and Mialomes: A Systems-Biology View of Tick Tissues and Tick-Host Interactions. *Trends Parasitol.* 32, 242–254. doi: 10.1016/j.pt.2015.10.002

Chmelar, J., Kotál, J., Kovaríková, A., and Kotsyfakis, M. (2019). The use of tick salivary proteins as novel therapeutics. *Front. Physiol.* 10, 812. doi: 10.3389/fphys.2019.00812

Francischetti, I. M. B. (2009). The role of saliva in tick feeding. *Front. Biosci.* 14, 2051–2088. doi: 10.2741/3363

Garcia, G. R., Chaves Ribeiro, J. M., Maruyama, S. R., Gardinassi, L. G., Nelson, K., Ferreira, B. R., et al. (2020). A transcriptome and proteome of the tick *Rhipicephalus microplus* shaped by the genetic composition of its hosts and developmental stage. *Sci. Rep.* 10, 12857. doi: 10.1038/s41598-020-69793-3

Hernández-Vargas, M. J., Gil, J., Lozano, L., Pedraza-Escalona, M., Ortiz, E., Encarnación-Guevara, S., et al. (2017). Proteomic and transcriptomic analysis of saliva components from the hematophagous reduviid *Triatoma pallidipennis*. *J. Proteomics*. 162, 30–39. doi: 10.1016/j.jprot.2017.04.022

Jia, N., Wang, J., Shi, W., Du, L., Sun, Y., Zhan, W., et al. (2020). Large-Scale Comparative Analyses of Tick Genomes Elucidate Their Genetic Diversity and Vector Capacities. *Cell* 182, 1328–1340.e13. doi: 10.1016/j.cell.2020.07.023

Karim, S., Singh, P., and Ribeiro, J. M. C. (2011). A Deep Insight into the Sialotranscriptome of the Gulf Coast Tick, *Amblyomma maculatum*. *PLoS One* 6, e28525. doi: 10.1371/journal.pone.0028525

Konnai, S., Nakajima, C., Imamura, S., Yamada, S., Nishikado, H., Kodama, M., et al. (2009). Suppression of cell proliferation and cytokine expression by HL-p36, a tick salivary gland-derived protein of *Haemaphysalis longicornis*. *Immunology*. 126, 209–219. doi: 10.1111/j.1365-2567.2008.02890.x

Mans, B. J. (2011). Evolution of Vertebrate Hemostatic and Inflammatory Control Mechanisms in Blood-Feeding Arthropods. *J. Innate Immun.* 3, 41–51. doi: 10.1159/000321599

Polanska, N., Ishemgulova, A., Volfova, V., Flegontov, P., Votypka, J., Yurchenko, V., et al. (2020). *Sergentomyia schwetzi*: Salivary gland transcriptome, proteome and enzymatic activities in two lineages adapted to different blood sources. *PLoS One*. 15, e0230537. doi: 10.1371/journal.pone.0230537

Popara, M., Villar, M., Mateos-Hernández, L., Fernández De Mera, I. G., and De La Fuente, J. (2013). Proteomics approach to the study of cattle tick adaptation to white tailed deer. *BioMed. Res. Int.* 2013, 319812. doi: 10.1155/2013/319812

Ribeiro, J. M. C. (1995). Blood-feeding arthropods: Live syringes or invertebrate pharmacologists? *Infect. Agents Dis.* 4, 143–152.

Schwarz, A., Von Reumont, B. M., Erhart, J., Chagas, A. C., Ribeiro, J. M. C., and Kotsyfakis, M. (2013). De novo *Ixodes ricinus* salivary gland transcriptome analysis using two next-generation sequencing methodologies. *FASEB J.* 27, 4745–4756. doi: 10.1096/fj.13-232140

Šimo, L., Kazimirova, M., Richardson, J., and Bonnet, S.II (2017). The essential role of tick salivary glands and saliva in tick feeding and pathogen transmission. *Front. Cell. Infect. Microbiol.* 7, 281. doi: 10.3389/fcimb.2017.00281

Tirloni, L., Reck, J., Terra, R. M. S., Martins, J. R., Mulenga, A., Sherman, N. E., et al. (2014). Proteomic Analysis of Cattle Tick *Rhipicephalus* (*Boophilus*) *microplus* Saliva: A Comparison between Partially and Fully Engorged Females. *PLoS One* 9, e94831. doi: 10.1371/journal.pone.0094831

Tirloni, L., Kim, T. K., Pinto, A. F. M., Yates, J. R., da Silva Vaz, I., and Mulenga, A. (2017). Tick-Host Range Adaptation: Changes in Protein Profiles in Unfed Adult *Ixodes scapularis* and *Amblyomma americanum* Saliva Stimulated to Feed on Different Hosts. *Front. Cell. Infect. Microbiol.* 7, 517. doi: 10.3389/fcimb.2017.00517

Tirloni, L., Lu, S., Calvo, E., Sabadin, G., Di Maggio, L. S., Suzuki, M., et al. (2020). Integrated analysis of sialotranscriptome and sialoproteome of the brown dog tick *Rhipicephalus sanguineus* (s.l.): Insights into gene expression during blood feeding. *J. Proteomics*. 229, 103899. doi: 10.1016/j.jprot.2020.103899

Titus, R. G., and Ribeiro, J. M. C. (1988). Salivary gland lysates from the sand fly *Lutzomyia longipalpis* enhance leishmania infectivity. *Science (80-)*. 239, 1306–1308. doi: 10.1126/science.3344436

Van De Merbel, N. C. (2019). Protein quantification by LC-MS: A decade of progress through the pages of Bioanalysis. *Bioanalysis*. 11, 629–644. doi: 10.4155/bio-2019-0032

WHO (2020). https://www.who.int/news-room/fact-sheets/detail/vector-borne-diseases.

Zeyrek, F. Y., Palacpac, N., Yuksel, F., Yagi, M., Honjo, K., Fujita, Y., et al. (2011). Serologic markers in relation to parasite exposure history help to estimate transmission dynamics of *Plasmodium vivax*. *PLoS One*. 6, e28126. doi: 10.1371/journal.pone.0028126

Conflict of Interest: The authors declare that the research was conducted in the absence of any commercial or financial relationships that could be construed as a potential conflict of interest.

frontiers in Cellular and Infection Microbiology

ORIGINAL RESEARCH
published: 11 October 2019
doi: 10.3389/fcimb.2019.00350

Comparative Tandem Mass Tag-Based Quantitative Proteomic Analysis of *Tachaea chinensis* Isopod During Parasitism

*Yingdong Li, Xin Li, Zhibin Han, Weibin Xu, Xiaodong Li and Qijun Chen**

College of Animal Science and Veterinary Medicine, Shenyang Agricultural University, Shenyang, China

Parasitic isopods perforate and attach to the host integument via the mandibles and then feed on hemolymph and exudate from the wounds. Such isopods attack a variety of commercially important fish and crustacean hosts. Similar to other hematophagous parasites, isopods may also employ biomolecules that affect host blood conglutination and defense systems. In the present study, a tandem mass tag-based quantitative proteomic approach was used to identify differentially expressed proteins in *Tachaea chinensis* parasites of shrimp, by comparing parasitic (fed) and pre-parasitic (unfed) individuals. We identified 888 proteins from a total of 1,510 peptides, with a significant difference in 129 between the fed and unfed groups. Among these, 37 were upregulated and 92 were downregulated in unfed *T. chinensis*. This indicates that *T. chinensis* may require more energy before parasitism during its search for a host. In addition, as is the case for other blood-sucking parasites, it might secrete antihemostatic, anti-inflammatory, and immunomodulatory molecules to facilitate blood meal acquisition. To our knowledge, this study is the first to use a TMT-based proteomic approach to analyze the proteome of isopod parasites, and the results will facilitate our understanding of the molecular mechanisms of isopod parasitism on crustaceans.

Keywords: comparative proteomic, isopod parasite, *Tachaea chinensis*, blood-sucking, during parasitism

OPEN ACCESS

Edited by:
Itabajara Silva Vaz Jr., Federal University of Rio Grande do Sul, Brazil

Reviewed by:
Marina Amaral Xavier, Federal University of Rio Grande do Sul, Brazil
Ben J. Mans, Agricultural Research Council, South Africa

****Correspondence:***
Qijun Chen
qijunchen759@syau.edu.cn

Specialty section:
This article was submitted to Parasite and Host, a section of the journal Frontiers in Cellular and Infection Microbiology

Received: *23 July 2019*
Accepted: *30 September 2019*
Published: *11 October 2019*

Citation:
Li Y, Li X, Han Z, Xu W, Li X and Chen Q (2019) Comparative Tandem Mass Tag-Based Quantitative Proteomic Analysis of Tachaea chinensis Isopod During Parasitism. Front. Cell. Infect. Microbiol. 9:350. doi: 10.3389/fcimb.2019.00350

INTRODUCTION

Hematophagous parasites such as ticks, mosquitoes, fleas, and leeches can bypass the clotting system of their vertebrate hosts by secreting anticoagulant compounds (Shu et al., 2010; Santiago et al., 2017). Isopod parasites mainly feed on blood (hemolymph) from hosts after perforating the integument with their mandibles, which can cause stress, tissue damage, secondary infection, and mortality (Wilson, 2008; Poore and Bruce, 2012; Williams and Boyko, 2012; Smit et al., 2014). There is evidence that isopod parasites may also inject anticoagulants or other compounds directly into the host so as to evade defensive responses (Nair and Nair, 1983; Manship et al., 2012). At present, only a few proteins for this purpose have been identified, including trypsin inhibitors and anticoagulants in *Paragnathia formica*. Identification of isopod anticoagulant agents may be useful in fully understanding parasite modulation of the host physiological system. This information may be valuable for the identification of novel target antigens and antithrombotic drug development.

Tachaea chinensis, one of the most common ectoparasites of farm-raised shrimps, is widely distributed in China and neighboring countries (Lu et al., 2007; Hua et al., 2018; Li et al., 2018). It is normally approximately 0.7 cm in size and can easily be observed with the naked eye following parasitization. After attacking its host, this isopod invariably remains attached until either the shrimp dies or another shrimp comes within close proximity. Over the past 2 years, *T. chinensis* has been shown to parasitize over 80% of aquacultured *Palaemonetes sinensis* (Li et al., 2018) and 90% of *Exopalaemon carinicauda* (Li et al., 2019). Additional research on isopod parasitization mechanisms is necessary to develop effective methods of control for use in shrimp aquaculture.

We performed tandem mass tag (TMT)-based quantitative proteomic profiling of *T. chinensis* to compare protein expression in fed and unfed parasites and gain insight into their integrated molecular mechanisms and host responses. This will provide an empirical basis for disease prevention and control efforts and support further research on the molecular biology of isopods.

MATERIALS AND METHODS

Ethics Statement

Our study did not involve endangered or protected species. In China, the capture of isopod parasites and their host shrimp from rice fields does not require specific permits. All efforts were made to minimize animal suffering and discomfort. The experimental protocol was approved by the Animal Ethics Committee of Shenyang Agriculture University.

Animals

Tachaea chinensis isopod parasites (0.82 ± 0.17 cm) and their host shrimp *P. sinensis* (3.48 ± 0.35 g) used in this study were collected from a rice field in Panjin City, Liaoning Province, China, in November 2018, and transported to the aquaculture laboratory at Shenyang Agricultural University. They were acclimated in two 300 L^2, fiberglass recirculation tanks with a circular flow system. Water temperature was maintained at 24 ± 0.5°C, and the photoperiod was set at a 12:12 h light:dark cycle. After 2 weeks of acclimatization, 20 healthy *T. chinensis* were transferred to individual plastic tanks (15.8 cm diameter and 32.1 cm height), each containing 5 L water, with the same environmental conditions as during the acclimatization period.

Following this, one *P. sinensis* each was placed in 10 of the prepared tanks, forming the fed group, with the other tanks kept as unfed pre-parasitism controls. After 7 d, fed and unfed *T. chinensis* were removed to individual 2 mL RNAse-free tubes and immediately frozen in liquid nitrogen for storage until protein extraction.

Protein Extraction and SDS-PAGE Analysis

Three fed and three unfed isopods were ground into powder and vortexed in 600 μL SDT buffer (pH 8.0, 4% SDS, 150 mM Tris-HCl, 1 mM DTT), respectively. The mixtures were heated at 100°C for 10 min, then sonicated at 35 W for 4 s, with 7 s intervals, for 10 min. These were centrifuged at 14,000 × *g* for 30 min, and supernatants were collected into 0.22 μm filter tubes. One microliter of the underlayer liquid of each sample was used for BCA quantitative analysis, and 1 μg of the protein sample from each group was subjected to SDS-PAGE (12.5% resolving gels) analysis (**Figure S1**).

Protein Digestion and TMT Labeling

Briefly, six protein concentrates (300 μg each) were mixed in ultrafiltration filtrate tubes (30 kDa cut-off, Sartorius, Gottingen, Germany) with 200 μL urea buffer (8 M urea, 150 mM Tris-HCl, pH 8.0), and the sample was centrifuged at 14,000 × *g* at 20°C for 30 min. The sample was washed twice by adding 200 μL UA and centrifuged at 14,000 × *g* at 20°C for 30 min. The flow-through from the collection tube was discarded. Next, 100 μL of indole-3-acetic acid (IAA) solution (50 mM IAA in UA buffer) was added to the filter tube and vortexed at 600 rpm in a Thermomixer comfort incubator (Eppendorf, Germany) for 1 min. Subsequently, the sample was incubated at room temperature for 30 min in the dark and centrifuged at 14,000 × *g* for 30 min at 20°C. Next, 100 μL UA was added to the filter unit, which was centrifuged at 14,000 × *g* for 20 min; this was carried out three times. The protein suspension in the filtrate tube was subjected to enzyme digestion with 52 μL of trypsin (Promega, Madison, WI, USA) buffer [6 μg trypsin (0.5 μg/μL) in 40 μL of dissolution buffer] for 16–18 h at 37°C. Finally, the filter unit was transferred to a new tube and centrifuged at 14,000 × *g* for 30 min. Peptides were collected in the filtrate and the peptide concentration was measured based on the optical density at 280 nm (OD280).

TMT labeling was performed using the TMT6plex™ Isobaric Label Reagent Set (Thermo Scientific) according to the manufacturer's instructions. The proteins in the unfed group were labeled with reagents 119, 127, and 128, and those in the infected group were labeled with reagents 129, 130, and 131. The labeling solution reaction was then incubated at room temperature for 1.5 h prior to further analysis.

SCX Fractionation and LC-MS/MS Analysis

SCX fractionation and LC-MS/MS analysis were conducted according to a published protocol (Xiao et al., 2019). The TMT-labeled samples were analyzed using an Easy-nLC nanoflow HPLC system connected to Orbitrap-Elite (Thermo Fisher Scientific, San Jose, CA, USA). One microgram of each sample was loaded onto each of two Thermo Scientific EASY columns using an autosampler at a flow rate of 200 nL/min. The sequential separation of peptides on Thermo Scientific EASY trap column (100 μm × 2 cm, 5 μm, 100 Å, C18) and analytical column (75 μm × 25 cm, 5 μm, 100 Å, C18) was achieved using a segmented 1 h gradient from 5 to 28% Solvent B (0.1% formic acid in 100% ACN) for 40 min, followed by 28–90% Solvent B for 2 min, and 90% Solvent B for 18 min. The column was re-equilibrated to its initial highly aqueous solvent composition before each analysis. The mass spectrometer was operated in positive ion mode, and MS spectra were acquired over a range of 350–2,000 m/z. The resolving powers of the MS scan and MS/MS scan at 100 m/z for the Orbitrap Elite were set as 60,000 and 15,000, respectively. The top 16 most intense signals in the acquired MS spectra were selected for further MS/MS analysis.

The isolation window was 2 m/z, and ions were fragmented through high energy collisional dissociation with normalized collision energies of 35 eV. The maximum ion injection times were set at 10 ms for the survey scan and 100 ms for the MS/MS scans, and the automatic gain control target values for full scan modes was set to 1 e 6 and for MS/MS was 5 e 4. The dynamic exclusion duration was 30 s.

Data Analysis

Raw files were analyzed using the Proteome Discoverer 2.1 software (Thermo Fisher Scientific). A search for the fragmentation spectra was performed using the MASCOT search engine embedded in Proteome Discoverer against the NCBI_Peracarida_91190_20190313.fasta database. The following search parameters were used: monoisotopic mass, trypsin as the cleavage enzyme, two missed cleavages, TMT labeling, and carbamidomethylating of cysteine as fixed modifications. Peptide charges of 2^+, 3^+, and 4^+ and the oxidation of methionine were specified as variable modifications. The mass tolerance was set to 20 ppm for precursor ions and to 0.1 Da for fragment ions. The results were filtered based on a false discovery rate of no more than 1%. The relative quantitative analysis of the proteins in the samples based on the ratios of TMT reporter ions from all unique peptides representing each protein was performed using Proteome Discoverer (version 2.1). The relative peak intensities of the TMT reporter ions released in each of the MS/MS spectra were used. Then, the final ratios obtained from the relative protein quantifications were normalized based on the median average protein quantification ratio. The fold change was set to >1.2 for protein upregulation and <0.85 for protein downregulation ($P < 0.05$). Protein functional annotation was conducted using the Universal Protein (UniProt) database. Gene Ontology (GO) and Kyoto Encyclopedia of Genes and Genomes (KEGG) databases were also used.

The mass spectrometry proteomics data have been deposited in the ProteomeXchange Consortium via the PRIDE partner repository (identifier PXD015247). All analyzed data are available from the corresponding author upon reasonable request.

Verification of Protein Quantifications Using PRM Analysis

Parallel reaction monitoring (PRM) was used to verify the TMT-based quantitative proteomics results. Briefly, 2 μg of peptide from each sample was taken for LC-PRM/MS analysis. After sample loading, chromatographic separation was performed using a Thermo Scientific EASY-nLC nano-HPLC system, with two buffers. Solution A was 0.1% formic acid aqueous solution and solution B was a mixed solution of 0.1% formic acid, 95% acetonitrile, and water. The column was first equilibrated with 95% solution A. The sample was injected into a Trap column (100 μm × 20 mm, 5 μm C18, Dr. Maisch GmbH) and subjected to gradient separation through a chromatography column (75 μm × 150 mm, 3 μm C18, Dr. Maisch GmbH) at a flow rate of 250 nL/min. The liquid phase separation gradient was as follows: 0–25 min, linear gradient of B liquid from 5 to 18%; 25–45 min, linear gradient of B liquid from 18 to 50%; 45–48 min, linear gradient of B liquid from 50 to 95%; and 48–60 min, B liquid maintained at 95%. The peptides were separated and subjected to targeted PRM/MS using a Q-Exactive mass spectrometer (Thermo Scientific) for 60 min. The parameters were set as follows: detection mode, positive mode; parent ion scanning range, 350–1,500 m/z; capillary voltage, 1.8 kV; isolation width, 1.6 Th; first-order MS resolution, 70,000 at m/z 200; AGC target, 3 e 6; first-level maximum IT, 250 ms. Peptide secondary MS were obtained as follows: for each full scan, target peptides of precursor m/z were sequentially selected based on the inclusion list for second-order MS (MS2) scan. The parameters used were as follows: resolution, 35,000 at m/z 200; AGC target, 3 e 6; Level 2 maximum IT, 120 ms; MS2 activation type, HCD; peptide fragmentation, nitrogen; isolation window, 2.0 Th; normalized collision energy, 28 eV. Four proteins were randomly selected from the global proteomics analysis (re-labeled peptide GISNEGQNASIK* as the reference standard mixture), including phosphoglucomutase (TFTTQETITNAATSAK), glucose-6-phosphate isomerase (LGAENFVFFHPR), xylose isomerase (YFGNLMDAGR, LSICGEESFGTGSDHIR), and malate dehydrogenase (IFGVTTLDIVR, IQDAGTEVVK). Skyline 3.5 was used to generate an initial PRM transition pair list for the four candidate DEPs.

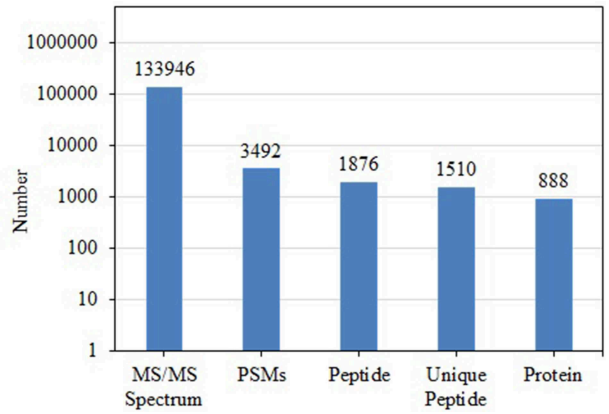

FIGURE 1 | Total numbers of tandem mass spectrometry spectra (MS/MS spectrum), peptide-spectrum matches (PSMs), peptides, unique peptides, and proteins in *Tachaea chinensis*.

RESULTS

SDS-PAGE Analysis and Protein Profiling

BCA results indicated protein concentrations of 15.60, 20.94, and 21.55 μg/μL in fed isopods and 19.06, 25.07, and 22.03 μg/μL in unfed isopods. TMT analysis indicated 3,492 queries in the 133,946 spectra. Among them, a total of 888 unique proteins were identified across 1,510 peptides (**Figure 1**). There were 139 proteins between 0 and 20 kDa, and 282, 241, 92, 45, and 89 proteins of 20–40, 40–60, 60–80, and 80–100 kDa, respectively. Eighty-nine proteins had a mass of over 100 kDa (**Figure 2**).

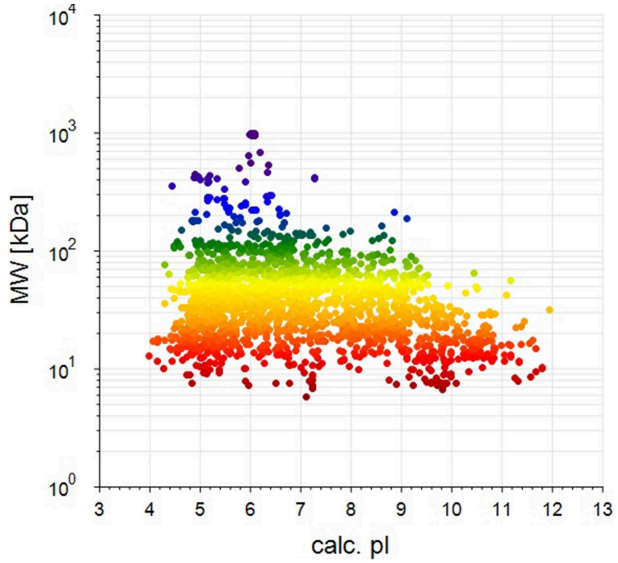

FIGURE 2 | Distribution of identified proteins with different molecular weights (the weight and pI values are for the target proteins from the NCBI_Peracarida_91190_20190313.fasta database).

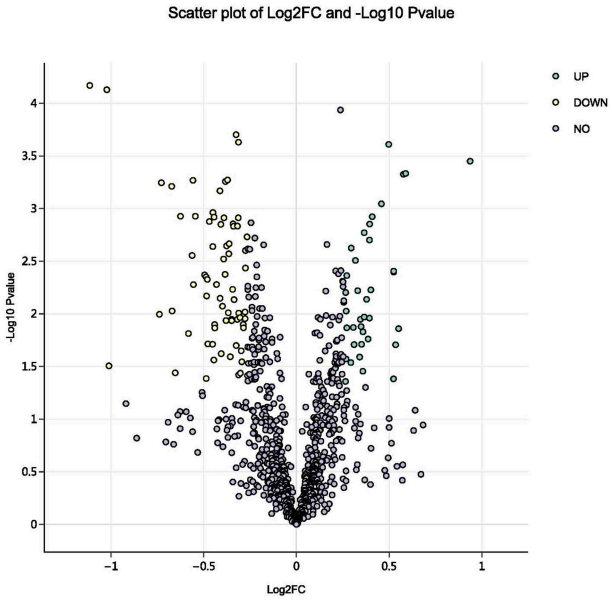

FIGURE 3 | Volcano plot of all proteins identified in the proteome database, for the fed and unfed parasite groups. Yellow points: differentially expressed proteins that were significantly downregulated after parasitism (fold change > 1.2; $p < 0.05$). Green points: differentially expressed proteins that were significantly upregulated after parasitism (fold change < 0.8; $p < 0.05$).

Differentially Expressed Protein Analysis

Using a 1.2-fold increase or decrease in protein expression as a benchmark for a physiologically significant change, 129 differentially expressed proteins (DEPs, $p < 0.05$) were identified between the control and parasitism groups (**Figure 3**). Within these DEPs, 37 were upregulated and 92 were downregulated (**Table S1**, **Figure S2**) before parasitism.

According to GO enrichment analysis, 1,256, 206, and 274 proteins were enriched for the categories biological process, cell component, and molecular function, respectively, and 178, 71, and 83 of these were statistically significant (**Figure S2**). The top 10 significant pathways are shown in **Figure 4**. Fifty-seven KEGG proteins were enriched, and five were statistically significant. Their functions included ECM-receptor interaction, pentose phosphate pathways, protein processing in the endoplasmic reticulum, glutathione metabolism, and phototransduction-fly, with 3, 3, 7, 4, and 3 proteins mapped to them, respectively (**Figure 5**). According to the protein–protein interaction network analysis, the three major clusters of interaction were protein processing in endoplasmic reticulum, ribosomes, and glutathione metabolism (**Figure 6**).

Candidate Proteins Related to Energy and Digestive Metabolism

Some differentially expressed proteins related to energy metabolism were significantly upregulated in unfed *T. chinensis*, including calcium-transporting ATPase sarcoplasmic/endoplasmic reticulum type-like proteins, NADH dehydrogenase [ubiquinone] flavoprotein 1, mitochondrial-like Na^+/K^+-ATPase, partial sodium potassium ATPase alpha subunit, partial smooth endoplasmic reticulum calcium ATPase, NADH dehydrogenase subunit 1 (mitochondrion), and cyclic AMP-responsive element-binding protein 1 (**Table 1**). Among the 92 significantly upregulated differentially expressed proteins, 20 were related to digestive metabolism, including 7, 11, and 2 in carbohydrate, protein, and lipid metabolism, respectively (**Table 1**).

Candidate Proteins Related to Blood Sucking

Three hemocyanin proteins showed the greatest difference in expression between fed and unfed isopods (**Table S1**). Differentially expressed proteins related to blood sucking, including inorganic pyrophosphatase-like isoform X1, alpha-2-macroglobulin, bestrophin homolog, calreticulin, barrier-to-autointegration factor putative salivary alkaline phosphatase, inorganic pyrophosphatase-like isoform X1, neurocalcin homolog isoform X3, and insulin receptor substrate 2-B were significantly upregulated after parasitism (**Table 2**). Four heat shock proteins and two stress-activated proteins were also upregulated.

PRM Results

To validate the proteomic data, three proteins that were upregulated after parasitism (phosphoglucomutase, glucose-6-phosphate isomerase, and xylose isomerase) and one that was downregulated after parasitism (malate dehydrogenase) were selected for PRM analysis. In both the fed and unfed groups, the validated proteins showed expression trends similar to the proteomic expression trends, suggesting that the proteomic data were reliable (**Figure 7**).

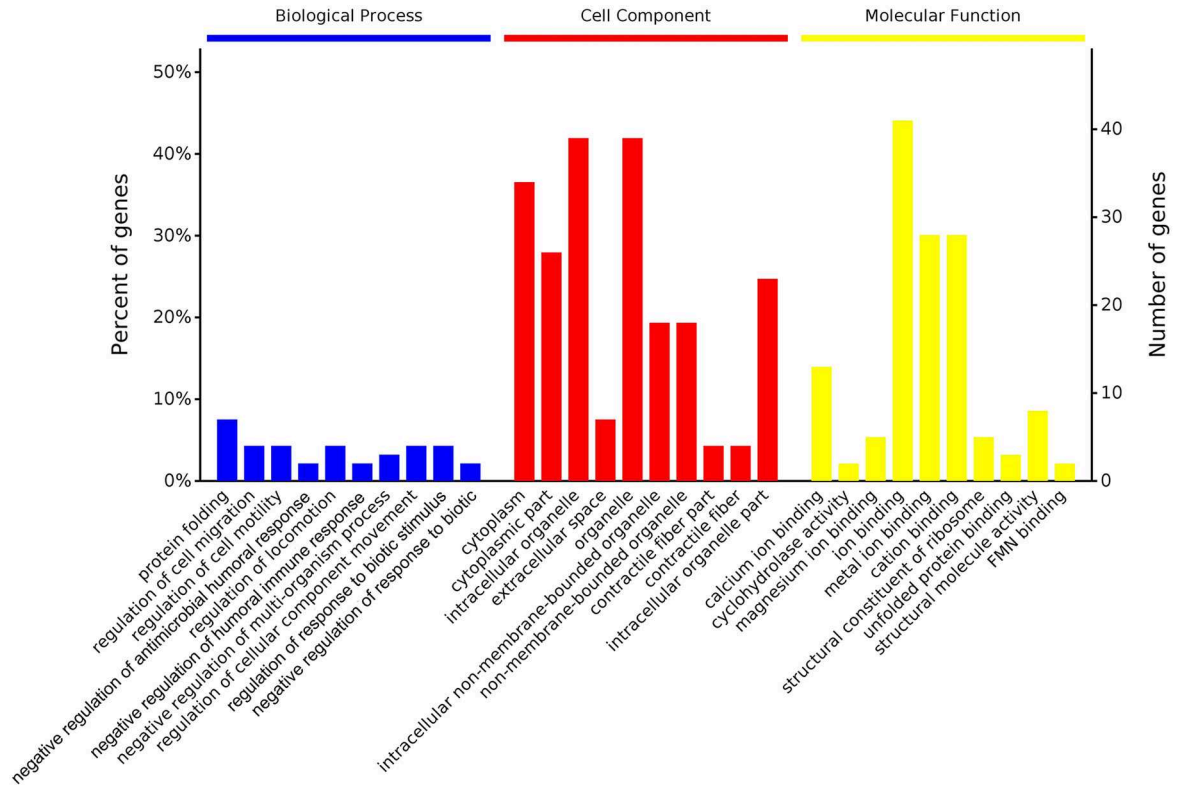

FIGURE 4 | GO functional classification of the identified proteins of the top 10 pathways identified in the proteome database, for the fed and unfed parasite groups, in the biological process, cell component, and molecular function categories.

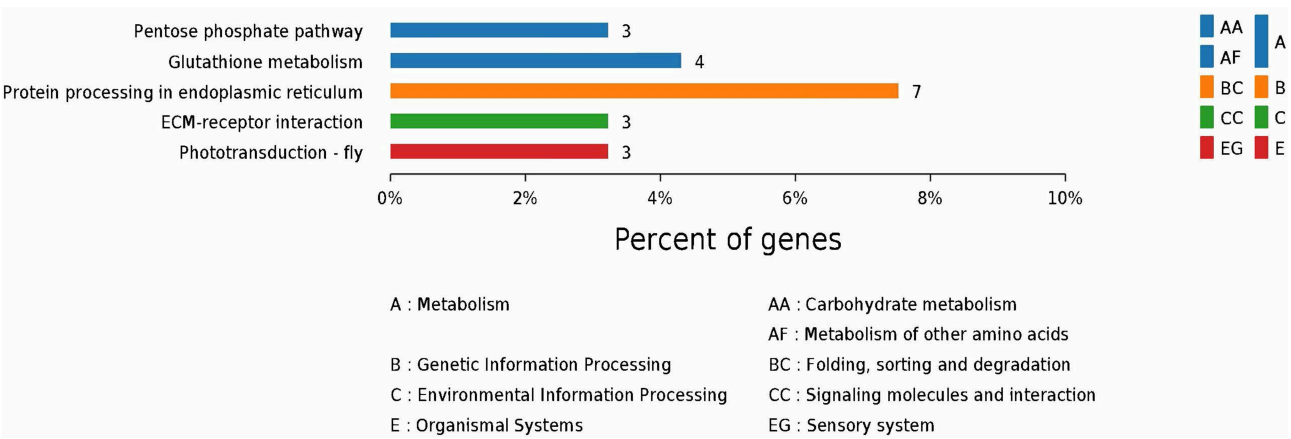

FIGURE 5 | KEGG annotation of the top five pathways from the proteome database of the fed and unfed parasite groups.

DISCUSSION

Hematophagous parasites use antihemostatic, anti-inflammatory, and immunomodulatory compounds to facilitate blood meal acquisition during feeding (Shu et al., 2010; Hajdusek et al., 2013; Eliane et al., 2017; Santiago et al., 2017; Jalovecka et al., 2018). These promote the survival and establishment of pathogens in the host (Boonsriroj et al., 2015; Eliane et al., 2017). Identification and characterization of such compounds can elucidate molecular mechanisms of interaction among parasites, pathogens, and hosts, revealing new vaccine targets (Mcgowan et al., 1982; Slovák et al., 2013; Oleaga et al., 2015; Yu et al., 2015; Eliane et al., 2017; Tirloni et al., 2017). Although many researchers have assumed that isopod parasites are

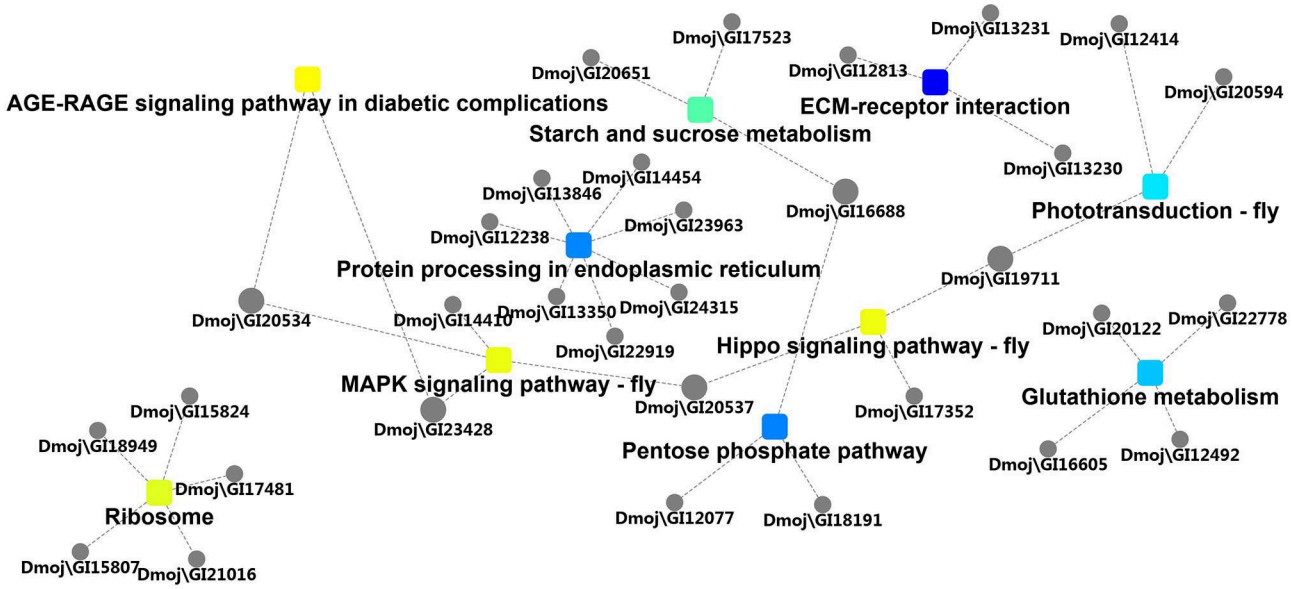

FIGURE 6 | Protein-protein interaction network analysis of the three major network groups.

hematophagous parasites and feed mainly on fish blood or crustacean hemolymph, no prior studies have demonstrated this directly. Moreover, in contrast to ticks and mosquitoes, there is a lack of comprehensive genomic resources for isopod parasites to investigate infection and response mechanisms. We performed, to our knowledge, the first comparative proteomic analysis between fed and unfed *T. chinensis* to gain a better understanding of its feeding and antigen-related proteins. However, because very few protein sequences for isopods are available in the NCBI protein database and all proteins identified were based on homologous proteins, we were able to identify only 888 proteins. Moreover, to avoid potential contamination of the host protein samples and to screen out proteins associated with parasitic processing, we also searched the NCBI protein database for proteins of Peracarida and blood-sucking insects (ticks and mosquitos); we found that proteins from *Armadillidium vulgare* (442, 51.76%), *Hyalella azteca* (227, 26.58%), and *Hirondellea gigas* (143, 16.74%) were similar to those present in our samples (**Table S1**).

Comparative proteomic analysis of unfed and fed *T. chinensis* indicated 129 proteins expressed significantly, with 37 upregulated and 92 downregulated before parasitism. Among the 37 upregulated proteins, seven were identified as contributing to ATP synthesis (**Table 1**). These results suggest that high energy metabolic proteins are expressed in pre-parasitism isopods while searching for hosts. Meanwhile, previous research has shown that genes related to ATP generation in host shrimp *P. sinensis* are upregulated under parasitism, which might be induced by a rapid depletion of ATP content in the parasite itself after parasitism, during its development and reproduction (Li et al., 2018). A similar profile has been demonstrated in fleas, where energy costs for feeding are lower than those in unfed individuals (Sarfati, 2005). Moreover, in crustaceans, because proteins are major contributors to hemolymph density (Simonetta et al., 2011), in their parasites, the major digestive enzymes are thought to be proteases. Eleven proteolytic enzymes were identified among the 129 DEPs, and all were upregulated after parasitism (**Table 1**). Seven carbohydrate metabolism-related proteins were also upregulated, suggesting that hemolymph glucose may also be an important nutrient for *T. chinensis*. Trehalose, which regulates energy metabolism and glucose generation via trehalose catabolism, was also upregulated after parasitism, suggesting that access to host trehalose is an important feature of isopod parasites.

Many researchers have assumed that isopod parasites can feed on fish blood or crustacean hemolymph, comparable to an "aquatic mosquito" (Wilson, 2008; Manship et al., 2012; Smit et al., 2014; Nagler et al., 2017). We previously found that hemocyanin in *P. sinensis* is significantly downregulated following parasitism by *T. chinensis* (Li et al., 2019). The present results indicate that hemocyanin in *T. chinensis* was significantly upregulated after parasitism, suggesting a role in obtaining hemolymph from *P. sinensis*. In hematophagous arthropods such as ticks, mosquitos, fleas, and flies, hematophagy evolved independently over millions of years, leading to various morphological adaptations and diverse strategies to overcome the barriers imposed by hosts (Ribeiro, 1995; Garcia et al., 2015). However, one example of convergent evolution and adaptation for hematophagy is the development of highly functional salivary glands, which produce a large diversity of anticlotting, antiplatelet, vasodilatory, and pathogen-transporting substances (Kim et al., 2016; Tirloni et al., 2016). Although it is known that isopod parasite morphology has been strongly modified for parasitism over 168 million years (Nagler et al., 2017), the type and composition of blood-sucking-related substances remain to be understood.

TABLE 1 | Differentially expressed proteins involved in energy and digestive metabolism, comparing the fed and unfed *Tachaea chinensis*.

Accession	Description	Coverage	Peptides	PSMs	AAs	MW (kDa)	Calc. pI	FC Unfed/Fed	*P*-value
ENERGY METABOLISM									
1371969814	Calcium-transporting ATPase sarcoplasmic/endoplasmic reticulum type-like	13.89	13	36	1,001	109.50	5.52	1.20	0.04
1067084430	NADH dehydrogenase flavoprotein 1, mitochondrial-like	8.55	3	3	468	50.90	8.21	1.20	0.01
1547583175	Na^+/K^+-ATPase, partial	29.70	5	9	202	22.40	6.77	1.28	0.02
1246309936	Sodium potassium ATPase alpha subunit, partial	25.99	5	9	227	25.20	5.39	1.28	0.01
26324131	Smooth endoplasmic reticulum calcium ATPase	18.96	17	46	1,002	109.70	5.36	1.32	0.01
1220106012	NADH dehydrogenase subunit 1 (mitochondrion)	3.56	1	1	309	34.70	8.88	1.41	0.00
1561970059	Cyclic AMP-responsive element-binding protein 1	1.98	1	1	353	37.50	7.56	1.44	0.00
DIGESTIVE METABOLISM									
Carbohydrate Metabolism									
1371969117	Phosphoglucomutase	3.02	1	1	563	61.40	5.26	0.68	0.00
1562001515	Trehalase	1.46	1	1	548	62.80	5.26	0.73	0.03
262305275	Glycogen synthase, partial	6.31	2	3	317	36.20	7.64	0.85	0.01
1067085998	UDP-glucuronosyltransferase 2B14-like	3.85	1	5	156	17.80	9.57	0.76	0.00
1371968467	Fructose 1,6-bisphosphatase	8.33	2	3	276	30.00	5.35	0.78	0.01
1371966397	Kynurenine–oxoglutarate transaminase 3-like, partial	2.69	1	2	484	53.90	7.71	0.83	0.00
1562032021	Ubiquitin carboxyl-terminal hydrolase 7	1.18	1	1	1,267	145.50	5.77	0.83	0.04
Protein Metabolism									
1067064770	Aminopeptidase N-like	0.59	1	2	1,851	208.50	4.91	0.63	0.00
1371969475	26S protease regulatory subunit 6B	5.56	3	3	414	46.70	5.58	0.65	0.00
1562025605	Protein disulfide-isomerase A6	2.27	1	1	441	48.30	5.57	0.68	0.01
1371970147	Nucleoside diphosphate kinase	7.73	1	2	181	20.20	8.40	0.74	0.01
1562030658	Protein disulfide-isomerase	5.17	3	4	522	58.70	4.77	0.75	0.00
1371969013	Dolichyl-diphosphooligosaccharide–protein glycosyltransferase subunit STT3A-like	1.66	1	1	722	82.10	7.87	0.78	0.01
1562029772	Ubiquitin-protein ligase E3C	0.87	1	2	1,032	117.50	6.76	0.78	0.01
1371965865	Serine/threonine-protein phosphatase 4 regulatory subunit 1-like	0.52	1	1	1,340	149.30	4.65	0.80	0.00
1562011562	Peptidyl-prolyl cis-trans isomerase FKBP7	13.81	4	7	210	23.50	4.79	0.80	0.00
1562027280	Proteasome subunit beta type-5	4.61	1	2	282	31.50	6.65	0.85	0.02
1561992339	Putative serine/threonine-protein phosphatase PP2A regulatory subunit	10.44	4	5	479	53.00	5.21	0.85	0.02
Lipid Metabolism									
1562029772	Ubiquitin-protein ligase E3C	0.87	1	2	1,032	117.50	6.76	0.78	0.01
1562030180	Fatty acid synthase	0.57	1	2	2,263	248.70	5.49	0.81	0.02

During blood sucking, the salivary gland of hematophagous parasites produces a cocktail of anti-hemostatic, anti-inflammatory, and immunomodulatory molecules that facilitate blood-meal acquisition. Saravanan et al. (2003) found that α_2-macroglobulin, which they consider to have an anticoagulant function, is highly expressed in tick salivary glands. In the present study, α_2-macroglobulin was significantly upregulated in isopods that had recently fed, which indicates that *T. chinensis* may also secrete anticoagulatory molecules during feeding. Moreover, Saurabh et al. (2011) found that fish macroglobulin was downregulated during *Argulus siamensis* parasitism. Similarly, we previously found that shrimp macroglobulin was downregulated during *T. chinensis* parasitism. Moreover, calreticulin, which functions in hematophagy in ticks through host immunosuppression or antihemostasis (Parizi et al., 2009), was also significantly upregulated after parasitism in the present study. Furthermore, calcineurin subunit B type 2 isoform X1, putative salivary alkaline phosphatase, insulin receptor substrate 2-B, PI-actitoxin-Aeq3a, and neurocalcin homolog isoform X3, which are similar to substances in the salivary glands of hematophagous parasites, were also upregulated in *T. chinensis* during feeding (Kim et al., 2015). However, the interaction of those proteins between parasites and hosts and the mechanisms of paralyzation and inhibition of inflammation remain unclear and require further study.

Anticlotting-related proteins are considered potential targets for the development of new drugs and vaccines to control and prevent ectoparasites such as ticks (Oleaga et al., 2017), mosquitos (Popova-Butler and Donald, 2009; Tetreau et al., 2012), *Schistosoma* (Delcroix et al., 2006), and sea louse (Carpio

TABLE 2 | Differentially expressed proteins involved in blood sucking, comparing the fed and unfed *Tachaea chinensis*.

Accession	Description	Coverage	Peptides	PSMs	AAs	MW (kDa)	Calc. pI	FC Fed/Unfed	*P*-value
BLOOD SUCKING									
427782987	Putative salivary alkaline phosphatase	1.68	1	1	1	1.0	535.00	0.45	6.60
1561973869	Barrier-to-autointegration factor	11.11	1	1	90	10.1	5.90	0.67	0.02
1067116995	Inorganic pyrophosphatase-like isoform X1	3.41	1	1	410	46.2	5.08	0.72	0.00
1067085871	Calcineurin subunit B type 2 isoform X1	4.69	1	1	213	23.5	4.97	0.75	0.02
1067070998	Neurocalcin homolog isoform X3	10.53	2	2	190	21.9	5.25	0.74	0.01
164632859	Alpha-2-macroglobulin, partial	3.85	2	3	571	61.7	4.94	0.75	0.00
1562026595	Calreticulin, partial	13.03	3	5	330	38.4	4.93	0.81	0.00
1202288454	Insulin receptor substrate 2-B, partial	2.35	1	1	426	46.2	6.38	0.82	0.01
1067101392	Mitogen-activated protein kinase 14B-like	4.08	1	1	392	44.0	7.30	0.82	0.03
1562031882	PI-actitoxin-Aeq3a	6.51	1	1	169	19.5	4.81	0.83	0.02
1562036618	Bleomycin hydrolase	4.76	1	1	252	29.0	6.64	0.85	0.04
1371956987	Peroxiredoxin, partial	9.65	1	1	114	12.4	5.48	1.20	0.03
1371959777	Galactose ABC transporter substrate-binding protein	3.26	1	1	337	37.1	5.03	1.50	0.00
HEAT SHOCK PROTEIN									
190014500	70 kDa heat shock protein	7.64	4	10	641	70.1	5.53	0.72	0.00
1561987640	Endoplasmin	3.99	3	5	803	92.1	5.02	0.77	0.00
1561990168	60 kDa heat shock protein, mitochondrial	14.19	8	13	571	60.5	5.41	0.81	0.01
1371970216	Heat shock protein HSP 90-alpha-like	7.49	5	7	708	82.0	5.05	0.83	0.00
1371965305	Stress-activated protein kinase JNK-like	3.14	1	1	509	57.2	7.40	0.83	0.04
1562029713	Putative heat shock protein HSP 90-alpha A4	10.86	5	8	488	55.7	5.08	0.83	0.00

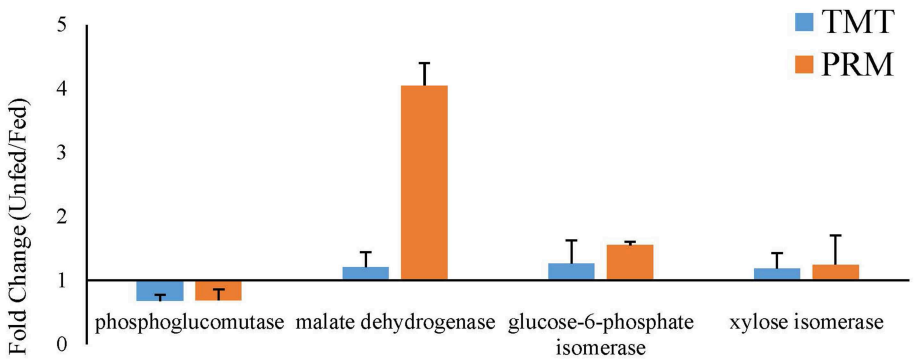

FIGURE 7 | Verification of the expression profiles of randomly selected significantly changed proteins comparing the fed and unfed *T. chinensis* groups, as determined by parallel reaction monitoring (PRM) and tandem mass tag (TMT) analysis. The data on the relative expression of proteins, for use in the TMT analysis, were obtained from **Tables 1**, **2**. The data on the relative expression of proteins for use in the PRM analysis were calculated relative to the expression of the relabeled peptide GISNEGQNASIK*.

et al., 2011, 2016). However, the hosts of these parasites are vertebrates, in which the composition of the coagulation system differs from that of invertebrates. In shrimps, the hemolymph clotting system comprises transglutaminase and clotting proteins and plays an important role in the innate immune response and prevention of blood loss during injury and wound healing (Maningas et al., 2013). Isopod parasites may inject anticoagulants or other compounds directly into the blood to obtain a blood meal (Nair and Nair, 1983; Manship et al., 2012), but the constituents of these compounds are still unclear. Here, we identified two protein disulfide-isomerase (PDI) proteins that participate in parasite–host cell interactions. PDI-specific antibodies may constitute part of the mucosal antibody repertoire, which is possibly involved in defense against parasites. The potential roles of those proteins for isopod parasite control will be investigated in our further study.

In conclusion, our results represent the first comparative proteomic study to detect key proteins from the whole body of fed and unfed *T. chinensis* isopod parasites. Owing to the lack of genomic data, we were able to identify only 888 proteins, and all were found in both stages. Differentially expressed proteins related to energy metabolism were upregulated in unfed individuals, particularly those involved in ATP generation. This may indicate that *T. chinensis* may

require considerable energy during its search for a host. We also found that similar to other hematophagous parasites, *T. chinensis* secretes antihemostatic, anti-inflammatory, and immunomodulatory molecules to facilitate blood meal acquisition. Our study provides valuable empirical data that will support future molecular research on isopod parasitization of crustaceans.

DATA AVAILABILITY STATEMENT

The raw data supporting the conclusions of this manuscript will be made available by the authors, without undue reservation, to any qualified researcher.

AUTHOR CONTRIBUTIONS

YL and QC designed the experiments. XinL and ZH generated biological samples. XinL, ZH, and WX performed the experiments. YL, XinL, and QC analyzed data. YL and WX performed statistic data analysis. YL and XiaL contributed reagents, materials and analysis tools. YL, XinL, ZH, and WX wrote the paper. All authors read and approved the final manuscript.

FUNDING

This work was supported by the earmarked fund for Modern Agro-industry Technology Research System (No. CARS-48), the National Natural Science Foundation of China (No. 31502190), and the Talent Introduction Program of Shenyang Agricultural University (Nos. 880416005 and 880417024).

ACKNOWLEDGMENTS

We thank Panjin Guanghe Fisheries Co., Ltd. for providing the shrimps.

SUPPLEMENTARY MATERIAL

The Supplementary Material for this article can be found online at: https://www.frontiersin.org/articles/10.3389/fcimb.2019.00350/full#supplementary-material

Figure S1 | Separation of proteins by SDS-PAGE from six unfed (A1, A2, and A3) and fed (B1, B2, and B3) *Tachaea chinensis*.

Figure S2 | Hierarchical clustering analysis of differentially expressed proteins in unfed (A1, A2, and A3) and fed (B1, B2, and B3) *Tachaea chinensis*.

Table S1 | Lists of proteins indented from *Tachaea chinensis*.

REFERENCES

Boonsriroj, H., Manalo, D. L., Kimitsuki, K., Shimatsu, T., Shiwa, N., Shinozaki, H., et al. (2015). A pathological study of the salivary glands of rabid dogs in the Philippines. *J. Vet. Med. Sci.* 78, 35–42. doi: 10.1292/jvms.15-0308

Carpio, Y., Basabe, L., Acosta, J., Rodríguez, A., Mendoza, A., Lisperger, A., et al. (2011). Novel gene isolated from *Caligus rogercresseyi*: a promising target for vaccine development against sea lice. *Vaccine* 29, 2810–2820. doi: 10.1016/j.vaccine.2011.01.109

Carpio, Y., Velazquez, J., Leal, Y., Herrera, N., García, C., Acosta, J., et al. (2016). Sea lice vaccine development based on an immunogenic peptide derived from the ribosomal protein P0. *Fish Shellfish Immunol.* 53, 64–64. doi: 10.1016/j.fsi.2016.03.061

Delcroix, M., Sajid, M., Caffrey, C. R., Lim, K.-C., Dvorak, J., Hsieh, I., et al. (2006). A multienzyme network functions in intestinal protein digestion by a platyhelminth parasite. *J. Biol. Chem.* 281, 39316–39329. doi: 10.1074/jbc.M607128200

Eliane, E., Maruyama, S. R., Kawahara, R., Fujita, A., Martins, L. A., Righi, A. A., et al. (2017). Analysis of the salivary gland transcriptome of unfed and partially fed *Amblyomma sculptum* ticks and descriptive proteome of the saliva. *Front. Cell. Infect. Microbiol.* 7:476. doi: 10.3389/fcimb.2017.00476

Garcia, G. R., Maruyama, S. R., Malardo, T., Zangirolamo, A. F., and Gardinassi, L. G. (2015). The biology of hematophagous arthropods addressed by molecular high-throughput approaches. *Austin J. Trop. Med. Hygiene* 1:1004.

Hajdusek, O., Síma, R., Ayllón, N., Jalovecká, M., Perner, J., De La Fuente, J., et al. (2013). Interaction of the tick immune system with transmitted pathogens. *Front. Cell. Infect. Microbiol.* 3:26. doi: 10.3389/fcimb.2013.00026

Hua, C. J., Li, W. X., Zhang, D., Zou, H., Li, M., Jakovlić, I., et al. (2018). Basal position of two new complete mitochondrial genomes of parasitic *Cymothoida* (*Crustacea*: *Isopoda*) challenges the monophyly of the suborder and phylogeny of the entire order. *Parasit. Vectors* 11:628. doi: 10.1186/s13071-018-3162-4

Jalovecka, M., Hajdusek, O., Sojka, D., Kopacek, P., and Malandrin, L. (2018). The complexity of piroplasms life cycles. *Front. Cell. Infect. Microbiol.* 8:248. doi: 10.3389/fcimb.2018.00248

Kim, T. K., Tirloni, L., Pinto, A. F., Moresco, J., Da Silva Vaz Junior, I., and Mulenga, A. (2016). *Ixodes scapularis* tick saliva proteins sequentially secreted every 24 h during blood feeding. *PLoS Negl. Trop. Dis.* 10:e0004323. doi: 10.1371/journal.pntd.0004323

Kim, Y. H., Slam, M. S., and You, M. J. (2015). Proteomic screening of atigenic proteins from the hard tick, *Haemaphysalis longicornis* (*Acari*: *Ixodidae*). *Korean J. Parasitol.* 53:85. doi: 10.3347/kjp.2015.53.1.85

Li, Y. D., Li, X., Xu, W. B., Han, Z. B., Zhao, Y. Y., Dong, J., et al. (2019). Comparative iTRAQ-based quantitative proteomic analysis of the Chinese grass shrimp (*Palaemonetes sinensis*) infected with the isopod parasite *Tachaea chinensis*. *Parasit. Vectors* 12:415. doi: 10.1186/s13071-019-3675-5

Li, Y. D., Xu, W. B., Li, X., Jiang, H. B., She, Q. X., Han, Z. B., et al. (2018). Comparative transcriptome analysis of Chinese grass shrimp (*Palaemonetes sinensis*) infected with isopod parasite *Tachaea chinensis*. *Fish Shellfish Immunol.* 82, 153–161. doi: 10.1016/j.fsi.2018.08.013

Lu, X., Zou, W., Peng, H., Shu, Q., Chen, W., Xie, J., et al. (2007). New records of two parasitic isopods in Peal River. *J. Fish. Sci. China* 14, 1023–1026.

Maningas, M. B. B., Hidehiro, K., and Ikuo, H. (2013). Molecular mechanisms of the shrimp clotting system. *Fish Shellfish Immunol.* 34, 968–972. doi: 10.1016/j.fsi.2012.09.018

Manship, B. M., Walker, A. J., Jones, L. A., and Davies, A. J. (2012). Blood feeding in juvenile *Paragnathia formica* (*Isopoda*: *Gnathiidae*): biochemical characterization of trypsin inhibitors, detection of anticoagulants, and molecular identification of fish hosts. *Parasitology* 139, 744–754. doi: 10.1017/S0031182011002320

Mcgowan, M. J., Homer, J. T., and Barker, R. W. (1982). Polyacrylamide gel electrophoresis of unfed, partially fed and gut tissues of *Amblyomma americanum* (L.). *Florida Entomol.* 65, 286–288. doi: 10.2307/3494293

Nagler, C., HyŽný, M., and Haug, J. T. (2017). 168 million years old "marine lice" and the evolution of parasitism within isopods. *BMC Evol. Biol.* 17:76. doi: 10.1186/s12862-017-0915-1

Nair, G. A., and Nair, N. B. (1983). Effect of infestation with the isopod, *Alitropus typus* M. Edwards (*Crustacea*: *Flabellifera*: Aegidae) on the haematological parameters of the host fish, *Channa striatus* (Bloch). *Aquaculture* 30, 11–19. doi: 10.1016/0044-8486(83)90147-3

Oleaga, A., Obolo-Mvoulouga, P., Manzano-Román, R., and Pérez-Sánchez, R. (2015). Midgut proteome of an argasid tick, *Ornithodoros erraticus*: a

comparison between unfed and engorged females. *Parasit. Vectors* 8:525. doi: 10.1186/s13071-015-1148-z

Oleaga, A., Obolo-Mvoulouga, P., Manzano-Román, R., and Pérez-Sánchez, R. (2017). A proteomic insight into the midgut proteome of *Ornithodoros moubata* females reveals novel information on blood digestion in argasid ticks. *Parasit. Vectors* 10:366. doi: 10.1186/s13071-017-2300-8

Parizi, L. F., Rech, H., Ferreira, C. A., Imamura, S., Ohashi, K., Onuma, M., et al. (2009). Comparative immunogenicity of *Haemaphysalis longicornis* and *Rhipicephalus* (Boophilus) *microplus* calreticulins. *Vet. Parasitol.* 164, 282–290. doi: 10.1016/j.vetpar.2009.05.023

Poore, G. C., and Bruce, N. L. (2012). Global diversity of marine isopods (except *Asellota* and crustacean symbionts). *PLoS ONE* 7:e43529. doi: 10.1371/annotation/3260cd00-89cf-4e08-ab25-07e0be598ab4

Popova-Butler, A., and Donald, H. D. (2009). Proteomic analysis of the mosquito *Aedes aegypti* midgut brush border membrane vesicles. *J. Insect Physiol.* 55, 264–272. doi: 10.1016/j.jinsphys.2008.12.008

Ribeiro, J. M. (1995). Blood-feeding arthropods: live syringes or invertebrate pharmacologists? *Infect. Agents Dis.* 4, 143–152.

Santiago, P. B., Araújo, C. N. D., Motta, F. N., Praça, Y. R., Charneau, S., Bastos, I. M. D., et al. (2017). Proteases of haematophagous arthropod vectors are involved in blood-feeding, yolk formation and immunity - a review. *Parasit. Vectors* 10:79. doi: 10.1186/s13071-017-2005-z

Saravanan, T., Weise, C., Sojka, D., and Kopáček, P. (2003). Molecular cloning, structure and bait region splice variants of α-macroglobulin from the soft tick. *Insect Biochem. Mol. Biol.* 33, 841–851. doi: 10.1016/S0965-1748(03)00083-3

Sarfati, M. (2005). Energy costs of blood digestion in a host-specific haematophagous parasite. *J. Exp. Biol.* 208, 2489–2496. doi: 10.1242/jeb.01676

Saurabh, S., Mohanty, B. R., and Sahoo, P. K. (2011). Expression of immune-related genes in rohu *Labeo rohita* (Hamilton) by experimental freshwater lice *Argulus siamensis* (Wilson) infection. *Vet. Parasitol.* 175, 119–128. doi: 10.1016/j.vetpar.2010.10.001

Shu, Q. T., Glanfield, A., Gobert, G. N., and Jones, M. K. (2010). Heme and blood-feeding parasites: friends or foes? *Parasit. Vectors* 3:108. doi: 10.1186/1756-3305-3-108

Simonetta, L., Martinis, M., and Ferrero, E. A. (2011). Ecological relevance of hemolymph total protein concentration in seven unrelated crustacean species from different habitats measured predictively by a density-salinity refractometer. *J. Mar. Biol.* 2011, 1–7. doi: 10.1155/2011/153654

Slovák, M., Hajnická, V., Labuda, M., and Fuchsberger, N. (2013). Comparison of the protein profiles of salivary gland extracts derived from three species of unfed and partially fed ixodid ticks analysed by SDS-PAGE. *Folia Parasitol.* 47, 67–71. doi: 10.14411/fp.2000.013

Smit, N. J., Bruce, N. L., and Hadfield, K. A. (2014). Global diversity of fish parasitic isopod crustaceans of the family *Cymothoidae*. *Int. J. Parasitol. Parasites Wildl.* 3, 188–197. doi: 10.1016/j.ijppaw.2014.03.004

Tetreau, G., Bayyareddy, K., Jones, C. M., Stalinski, R., Riaz, M. A., Paris, M., et al. (2012). Larval midgut modifications associated with Btiresistance in the yellow fever mosquito using proteomic and transcriptomic approaches. *BMC Genomics* 13:248. doi: 10.1186/1471-2164-13-248

Tirloni, L., Kim, T. K., Coutinho, M. L., Ali, A., Seixas, A., Termignoni, C., et al. (2016). The putative role of *Rhipicephalus microplus* salivary serpins in the tick-host relationship. *Insect Biochem. Mol. Biol.* 71, 12–28. doi: 10.1016/j.ibmb.2016.01.004

Tirloni, L., Kim, T. K., Pinto, A. F. M., Yates, J. R., Da Silva Vaz Junior, I., and Mulenga, A. (2017). Tick-host range adaptation: changes in protein profiles in unfed adult *Ixodes scapularis* and *Amblyomma americanum* saliva stimulated to feed on different hosts. *Front. Cell. Infect. Microbiol.* 7:517. doi: 10.3389/fcimb.2017.00517

Williams, J. D., and Boyko, C. B. (2012). The global diversity of parasitic isopods associated with crustacean hosts (*Isopoda*: Bopyroidea and Cryptoniscoidea). *PLoS ONE* 7:e35350. doi: 10.1371/journal.pone.0035350

Wilson, G. D. F. (2008). Global diversity of Isopod crustaceans (*Crustacea*; *Isopoda*) in freshwater. *Hydrobiologia* 595, 231–240. doi: 10.1007/s10750-007-9019-z

Xiao, C. F., Gao, J. H., Zhang, Y. X., Wang, Z., and Zhang, D. H. (2019). Quantitative proteomics of potato leaves infected with *Phytophthora infestans* provides insights into coordinated and altered protein expression during early and late disease stages. *Int. J. Mol. Sci.* 20:E136. doi: 10.3390/ijms20010136

Yu, X., Gong, H., Zhou, Y., Zhang, H., Cao, J., and Zhou, J. (2015). Differential sialotranscriptomes of unfed and fed *Rhipicephalus haemaphysaloides*, with particular regard to differentially expressed genes of cysteine proteases. *Parasit. Vectors* 8:597. doi: 10.1186/s13071-015-1213-7

Conflict of Interest: The authors declare that the research was conducted in the absence of any commercial or financial relationships that could be construed as a potential conflict of interest.

frontiers in Cellular and Infection Microbiology

ORIGINAL RESEARCH
published: 21 January 2020
doi: 10.3389/fcimb.2019.00477

Gene Expression in the Salivary Gland of *Rhipicephalus (Boophilus) microplus* Fed on Tick-Susceptible and Tick-Resistant Hosts

*Poliana Fernanda Giachetto[1], Rodrigo Casquero Cunha[2], Antônio Nhani Jr.[1], Marcos Valerio Garcia[3], Jesus Aparecido Ferro[4] and Renato Andreotti[3]**

[1] Embrapa Agricultural Informatics, Campinas, Brazil, [2] Bolsista do CNPq (157460/2018-5), Programa de Pós-Graduação em Biotecnologia, Universidade Federal de Pelotas, Pelotas, Brazil, [3] Embrapa Beef Cattle, Campo Grande, Brazil, [4] Department of Technology, São Paulo State University, Jaboticabal, Brazil

The success of cattle tick fixation largely depends on the secretion of substances that alter the immune response of the host. The majority of these substances are expressed by the parasite salivary gland and secreted in tick saliva. It is known that hosts can mount immune responses against ticks and bovine European breeds, and bovine industrial crossbreeds are more susceptible to infestations than are *Bos indicus* cattle. To identify candidates for the development of novel control strategies for the cattle tick *Rhipicephalus (Boophilus) microplus*, a salivary gland transcriptome analysis of engorged females fed on susceptible or resistant hosts was performed. Using RNA-Seq, transcriptomes were *de novo* assembled and produced a total of 235,451 contigs with 93.3% transcriptome completeness. Differential expression analysis identified 137 sequences as differentially expressed genes (DEGs) between ticks raised on tick-susceptible or tick-resistant cattle. DEGs predicted to be secreted proteins include innexins, which are transmembrane proteins that form gap junction channels; the transporters Na^+/dicarboxylate, Na^+/tricarboxylate, and phosphate transporter and a putative monocarboxylate transporter; a phosphoinositol 4-phosphate adaptor protein; a cysteine-rich protein containing a trypsin inhibitor-like (TIL) domain; a putative defense protein 3 containing a reeler domain; and an F-actin-uncapping protein LRRC16A with a CARMIL_C domain; these genes were upregulated in ticks fed on tick-susceptible cattle. DEGs predicted to be non-secreted proteins included a small heat shock protein and the negative elongation factor B-like, both acting in a coordinated manner to increase *HSP* transcript levels in the salivary glands of the ticks fed on tick-susceptible cattle; the 26S protease regulatory subunit 6B and another chaperone with similarity to calnexin, also upregulated in ticks fed on tick-susceptible cattle; an EF-hand calcium binding protein and a serine carboxypeptidase (*SCP*), both involved in the blood coagulation cascade and upregulated in ticks fed on tick-susceptible cattle; and two ribosomal proteins, the 60S acidic ribosomal protein P2 and the 60S ribosomal protein L19. These results help to characterize cattle tick salivary gland gene expression in tick-susceptible and tick-resistant hosts and suggest new putative targets for the control of tick infestations, as those genes involved in the mechanism of stress response during blood feeding.

Keywords: RNA-Seq, cattle tick, sialome, transcriptome, host-parasite interaction

OPEN ACCESS

Edited by:
Itabajara Silva Vaz Jr., Federal University of Rio Grande do Sul, Brazil

Reviewed by:
Iliano V. Coutinho-Abreu, National Institutes of Health (NIH), United States
Edvaldo Barros, Universidade Federal de Viçosa, Brazil

***Correspondence:**
Renato Andreotti
renato.andreotti@embrapa.br

Specialty section:
This article was submitted to Parasite and Host, a section of the journal Frontiers in Cellular and Infection Microbiology

Received: *01 October 2019*
Accepted: *24 December 2019*
Published: *21 January 2020*

Citation:
Giachetto PF, Cunha RC, Nhani A Jr, Garcia MV, Ferro JA and Andreotti R (2020) Gene Expression in the Salivary Gland of Rhipicephalus (Boophilus) microplus Fed on Tick-Susceptible and Tick-Resistant Hosts. Front. Cell. Infect. Microbiol. 9:477. doi: 10.3389/fcimb.2019.00477

INTRODUCTION

The cattle tick *R.* (*B.*) *microplus* limits the development of the cattle industry worldwide, causing production losses estimated at US $3.24 billion annually in Brazil alone (Grisi et al., 2014). The losses caused by ticks are caused primarily by their feeding in the host and by pathogens transmitted via saliva thereafter. To feed, the tick must attach to the skin of the cattle, introducing their hypostome. The success of the fixation of the tick depends on the secretion of cement substances and anticoagulants, which alter the immune response in the place of the bite but can also cause systemic effects (Mans and Neitz, 2004). In addition, the success of pathogen transmission depends on some tick molecules associated with this event (Ramamoorthi et al., 2005; Hovius et al., 2008). The majority of these substances are expressed by the salivary gland and may be secreted in the saliva.

The tick saliva contains a rich variety of pharmacologically bioactive molecules that support blood feeding. During coevolution, blood sucking ticks have adapted mechanisms to evade host detection and prevent blood coagulation by synthesizing an extensive array of molecules with anesthetic, immunosuppressive, vasodilatory, profibrinolytic, and anticoagulant properties (Mans and Neitz, 2004). Blood feeding triggers a heat shock response by arthropods, as demonstrated by the increased production of heat shock proteins in response to the increase in temperature and other stresses observed during blood meal by ticks, which has been considered a stressful event in multiple forms (Shahein et al., 2010; Benoit et al., 2011).

Gene transcripts, such as glutathione S-transferase and gamma-glutamyl transferase, can be found in salivary glands because they have physiological functions; one of these genes plays a central role in the detoxication of xenobiotic compounds (de Lima et al., 2002), such as insecticides (Nandi et al., 2015; Hernandez et al., 2018), and another of which is involved in the cross-cell membrane trafficking of amino acids and peptides and in glutathione metabolism, respectively (Mulenga and Erikson, 2011).

Many other transcripts that can code for non-secreted or secreted proteins with different physiological functions may be present in tick salivary glands. Examples of predicted non-secreted proteins are the following: calnexin, which plays a role in the quality control and assembly of proteins and glycoproteins in the endoplasmic reticulum (Williams, 2006); longistatin, which modulates biochemical reactions within the cell as the inflammatory response and has a role in anticoagulant action (Anisuzzaman et al., 2012); serine carboxypeptidase, implied to be involved in degrading hemoglobin to peptides and regulating the interaction with the host; β-N-acetyl hexosaminidases, which participates in the turnover of the chitin exoskeleton (Hogenkamp et al., 2008); leucine aminopeptidase, which belongs to a diverse group of the M17 family of Zn-metalloproteases (Maggioli et al., 2018), playing important roles in the host immune response, tick-tissue development, and pathogen transmission (Ali et al., 2015); ribosomal proteins, playing essential roles in cell growth and proliferation (Trainor and Merrill, 2014); phosphorylase kinase, a holoenzyme that activates glycogen phosphorylase (Brushia and Walsh, 1999); E3 ligase, promoting cullin neddylation, required for the regulation of NF-κB, which is crucial in immune response and apoptotic pathways (Cajee et al., 2012); and mucins, providing lubrication and protection to the epithelium (Hollingsworth and Swanson, 2004).

Among the salivary gland transcripts predicted to code for secreted proteins, the following genes may be observed: innexins, transmembrane proteins (Richards et al., 2015) that form gap junction channels and hemichannels in invertebrates, including arthropods (Güiza et al., 2018); Na^+/dicarboxylate, Na^+/tricarboxylate and phosphate transporter, which may play a role in osmoregulation with ion transport function (Hui et al., 2014); the phosphoinositol 4-phosphate adaptor protein, a component of a molecule complex that recruits proteins to the cell membrane (Choudhury et al., 2005), a transduction pathway in tick salivary glands (McSwain et al., 1989); monocarboxylate transporters that catalyze rapid transport of many monocarboxylates (Lew-Tabor et al., 2011), cysteine-rich proteins containing trypsin inhibitor-like (TIL) domain, belonging to the family that comprises chymotrypsin, elastase and trypsin inhibitors (Sasaki et al., 2008), which has been found ubiquitously in blood-feeding insect and tick sialomes (Karim and Adamson, 2012; Maruyama et al., 2017); BmSI-7, a trypsin inhibitor-like cysteine-rich domain family, which is involved in the inflammatory response and in injury caused by tick fixation on the bovines (Sasaki et al., 2008); defense proteins, such as defense protein 3 (Zhao et al., 2019), and ixodidin, a antimicrobial peptide (Fogaça et al., 2006), which are probably involved in the immune response in the tick; PIXR, a protein with a reeler domain, favoring the colonization of Borrelia burgdorferi in Ixodes scapularis gut (Narasimhan et al., 2017); and proteins involved in actin metabolism, such as the F-actin-uncapping protein LRRC16A isoform X2.

All of these compounds may play a role interacting on the interface of the tick-host relation and are crucial to the success of tick fixation and/or pathogen transmission. On this basis, knowledge of the transcripts that have been upregulated or downregulated in both tick-susceptible and tick-resistant cattle could guide the development of more consistent immunogens against ticks at the time when the use of vaccines has presented results with varied effects, and the type of antigen used interferes with the efficacy of the vaccine (Csordas et al., 2018). In the absence of a vaccine with these characteristics, only chemical control remains for cattle producers seeking to prevent tick infestations. In addition, the use of acaricides at higher concentrations and in association to overcome the resistance of the tick to the acaricides indicates a global crisis in tick control (Higa et al., 2019), and vaccine development is a promising alternative.

It has been known for many years that hosts can mount immune responses against ticks, and non-natural hosts can mount highly effective anti-tick immune responses, preventing successful tick fixation and halting the tick life cycle (Trager, 1939). In this way, bovine European breeds (*Bos taurus*) and their industrial crossbreeds are more susceptible to tick infestations than *B. indicus*. This resistance is associated with the immune systems of the hosts, since in the first infestation, the number

of ticks completing the cycle is similar in all races (Hewetson, 1972; Mattioli et al., 1993; Ghosh et al., 1999), and with the absence of transcripts of genes encoding enzymes producing volatile compounds, which may render the host less attractive to larvae (Franzin et al., 2017). Franzin et al. (2017) concluded that resistant hosts expose ticks to an earlier inflammatory response, which in ticks is associated with significantly lower expression of genes encoding salivary proteins that suppress host immunity, inflammation and coagulation. It means, at the same time, different levels of host immunity may affect the composition of tick saliva, contributing to these outcomes. The demonstration that immunosuppressive drugs eliminate this resistance reaffirmed the immune nature of this response (Bergman et al., 2000).

In this context, we aimed to differentiate the profile of salivary gland transcripts in ticks feeding on tick-resistant and tick-susceptible bovines to identify transcripts of genes encoding proteins with the potential to be used as immunogens for tick control.

MATERIALS AND METHODS

Ethics Statement

All experimental procedures were approved by Embrapa Beef Cattle's Ethics Committee on Animal Use according to Protocol 008/2014 and according to the requirements of the National Council for the Control of Animal Experimentation.

Cattle, Ticks, and Sample Collection

The trial for sample collection was conducted in Campo Grande, Mato Grosso do Sul, Brazil (20° 27′ S and 54° 37′ W, altitude of 530 m), at Embrapa Beef Cattle. The climate of this region is classified as rainy tropical savanna, characterized by irregular annual rainfall distribution, a well-defined dry period during the colder months, and a rainy period during the summer months.

Two weaned male cattle aged ∼8 months from two bovine genotypes were used: a tick-susceptible animal, Holstein (*Bos taurus taurus*), and a tick-resistant animal, crossbreed, resulting from the crossing of the previous susceptible breed with a tick-resistant breed, Nelore (*Bos taurus indicus*). The animals were kept in a *Brachiaria decumbens* pasture for a 4 months period for disinfestation and immunological memory loss, and they were later taken to individual stalls, where they received feed of sorghum silage (17 kg/animal/day), concentrate (1 kg/animal/day), and water *ad libitum* throughout the experimental period.

Ticks used in the experiment for artificial infestation were from a colony of *R.* (*B.*) *microplus* reared in the Laboratory of Tick Biology of Embrapa Beef Cattle. Engorged females from a stabled bovine were collected (21 days) placed in Petri dishes and incubated in a biological oxygen demand chamber (BOD) at a temperature of ∼28°C and humidity of ∼80%. After egg laying, eggs were collected and separated into 500-mg samples containing an equivalent of 10,000 larvae. Samples were placed in 10 ml syringes with the tips removed, sealed with cotton, and then placed again on BOD for egg incubation until larval hatching. Syringes containing non-fed larvae were used for artificial infestation of cattle. An infestation with 10,000 active larvae (12 days after hatching) was performed on the dorsum in each of the experimental animals—the tick-susceptible and tick-resistant cattle, which remained immobilized for a period of 3 h to avoid self-cleaning.

RNA Isolation and RNA-Seq

Semi-engorged adult salivary gland samples were dissected on ice and processed immediately. Three salivary gland samples were obtained for each of the bovine genotypes. In a total of six samples, each sample contained salivary glands collected from ∼10 ticks, which were used for RNA isolation following the TRIzol® reagent protocol (Life Technologies, Carlsbad, CA). The purity and amount of total RNA were assessed by electrophoresis in a 1.2% agarose gel stained with ethidium bromide and by spectrophotometry at 260 and 280 nm in a Nanodrop ND-1000 spectrophotometer (Thermo Fisher Scientific Inc., MA, USA). Total RNA quality and integrity were analyzed using an Agilent 2100 Bioanalyzer® (Agilent Technologies, Palo Alto, USA). RNA was stored at −70°C until further analysis.

Library preparation and next generation sequencing using the RNA-Seq technique were conducted at the Animal Biotechnology Laboratory of Luiz de Queiroz College of Agriculture, University of São Paulo (ESALQ-USP, Piracicaba, SP), following the stranded TruSeq RNA Sample Prep Kit protocol (Illumina, Inc., San Diego, CA, USA). The cDNA libraries were sequenced in the Illumina HiSeq 2500 System (Illumina, Inc., San Diego, CA, USA), generating 2 × 150 bp paired-end reads, according to the standard manufacturer protocol.

Bioinformatics Analysis

Data obtained by HiSeq 2500 sequencing were analyzed using the Real Time Analysis (Illumina) software, which makes the calls from the sequencing images, converting them into a FASTQ format. Evaluation of the sequencing reads was performed using FastQC v0.11.4 (http://www.bioinformatics.babraham.ac.uk/projects/fastqc/). Read sequences were subjected to adapter trimming and quality filtering using Trimmomatic (v0.35) (Bolger et al., 2014) with default parameters, except for a head crop of 15 bases and a read minimal length of 30 bases. Reads were also checked for foreign RNA contamination. A similarity search against the NR database (v04/18) using either blastx (v2.6.0) or DIAMOND (v0.9.17) (Buchfink et al., 2015) was performed to identify and filter hits to mammal and bacterial sequences above 50% identity and e-value ≤1e-20.

Trinity software (v2.6.6) (Grabherr et al., 2011) was used to *de novo* assembly of a reference transcriptome using all filtered samples, as described in https://github.com/trinityrnaseq/trinityrnaseq/wiki. Inchworm kmer coverage was set to 3, and contig minimal length was set to 300 bases. Assembly quality was accessed through mapping back each library to the *R.* (*B.*) *microplus* salivary gland reference transcriptome using Bowtie2 (v2.3.4) (Langmead and Salzberg, 2012) and Trinity scripts. Mapped contig sequences were recovered for each genotype to compose the transcriptomes.

TABLE 1 | Putative secreted proteins[a] transcribed in *R.* (*B.*) *microplus* salivary glands.

Putative secreted protein	e-value[b]	Similarity[c] (%)	LogFC	FDR	Taxonomy name[d]
Na^+/dicarboxylate, Na^+/tricarboxylate, and phosphate transporter, putative	0.0E0	82.81	0.96	2.3e−02	*Ixodes scapularis*
Beta-N-acetylhexosaminidase, putative	1.9E−160	67.95	2.34	2.4e−03	*Ixodes scapularis*
TPA_inf: hypothetical protein 384	3.5E−15	63.22	4.32	1.8e−02	*Amblyomma variegatum*
Acid methyltransferase, putative	1.1E−52	68.66	2.78	4.4e−02	*Ixodes scapularis*
Phosphoinositol 4-phosphate adaptor protein, putative	8.0E−71	78.47	−1.50	2e−02	*Ixodes scapularis*
Innexin, putative	4.7E−156	80.86	−3.35	4.8e−03	*Ixodes scapularis*
Monocarboxylate transporter 10-like	7.4E−122	68.14	1.37	2.4e−02	*Parasteatoda tepidariorum*
Secreted protein, putative	1.4E−8	56.06	4.13	4.2e−02	*Ixodes scapularis*
Putative defense protein 3	1.2E−14	49.98	1.80	4.5e−02	*Crassostrea gigas*
F-actin-uncapping protein LRRC16A isoform X2	0.0E0	3.44	−0.83	2e−03	*Limulus polyphemus*

[a] *Putative secreted proteins predicted by Min (2010) pipeline, using Phobius, WolfPsort, TMHMM, TargetP, and PS_SCAN.*
[b] *e-value from Blast result.*
[c] *Blast mean similarity.*
[d] *Blast hit taxonomy name. Log FC with negative signal means that transcripts are upregulated in ticks fed on resistant cattle.*

The completeness of the *R.* (*B.*) *microplus* salivary gland transcriptome was evaluated using BUSCO (Benchmarking Universal Single-Copy Orthologs) by comparing the transcriptome against a set of highly conserved single-copy orthologs of the known ancestral Arthropoda proteins (arthropoda_odb9, creation date: 2017-02-07, number of species: 60, number of BUSCOs: 1066) (Simão et al., 2015).

Differentially expressed genes (DEGs) between ticks fed on susceptible cattle and ticks fed on resistant cattle were identified by Trinity RSEM/edgeR differential expression analysis with FDR (False Discovery Rate) <0.05 and Fold Change ≥ 2. A preliminary similarity search, as described previously, was also performed in the DEG set of transcripts.

TransDecoder (v 5.0.0) (Haas et al., 2013) was used to obtain peptide ORFs from differentially expressed genes. Potential signal peptides and transmembrane domains were predicted from ORFs to identify secreted proteins according to the Min (2010) animal pipeline, which consists of filtering sequences that pass through Phobius (v 1.01), WolfPsort (v 0.02) TMHMM (v 2.0c) TargetP, and PS_SCAN tools.

To further investigate the biological functions of the DEGs, they were annotated to the Gene Ontology (GO) database for biological process (BP), molecular function (MF), and cellular component (CC) and to KEGG (Kyoto Encyclopedia of Genes and Genomes) for biological pathways using Blast2GO PRO (https://www.blast2go.com/). DEGs from the most represented GO terms and KEGG pathways were discussed further.

RESULTS

Gene Expression Profile and Secreted Proteins of Semi-engorged *R.* (*B.*) *microplus* Salivary Gland Fed on Tick-Susceptible and Tick-Resistant Cattle

Sialotranscriptomes from *R.* (*B.*) *microplus* fed on tick-susceptible (Holstein) and tick-resistant (Holstein × Nelore crossbreed) cattle were generated using RNA-Seq technology and *de novo* assembly. A total of 74,639,552 reads were obtained for ticks fed on Holstein cattle, and 63,013,658 reads were obtained for ticks fed on crossbreed cattle. Reads post-processing with Trimommatic resulted in a 99.9% recovery for the Holstein and crossbreed reads dataset, of which 92.53 and 92.79%, respectively, were realigned to the assembly with bowtie2. Trinity produced a total of 235,451 contigs with a mean length of 954 nt and a N50 of 1,624 nt. Completeness of the assembly, as evaluated using BUSCO, revealed that 93.3% of conserved genes across Arthropoda were present (994 out of 1,066). Complete and single-copy genes found (C) were 24.4%, complete and duplicated genes found (D) were 68.9%, fragmented genes found (F) were 5.0%, and genes missing (M) were 1.7%. To identify the function of the transcriptome-predicted genes, all 235,451 contigs were analyzed using Blast2GO PRO software, returning a total of 71,757 annotated transcripts with a sequence identity $\geq$50% and e-value $\leq$1e−10 (**Table 1**, **Supplementary Material**). Gene Ontology and KEGG categorizations of the annotated transcriptome are shown in **Figure 1**.

TransDecoder translation resulted in a total of 1,815 predicted ORFs, which were used for secreted protein identification. According to the pipeline proposed by Min (2010), a total of 20 ORFs were predicted as putative secreted proteins from the salivary glands (**Table 1**), corresponding to 15 candidate genes.

Differentially Expressed Genes Related to Cattle Resistance to Tick

The differential expression analysis identified 137 sequences as DEGs, corresponding to 126 candidate genes (**Figure 1**, **Table 2**, **Supplementary Material**). Gene Ontology analysis showed that the molecular functions most represented among DEGs upregulated in salivary glands from *R.* (*B.*) *microplus* fed on tick-susceptible and tick-resistant cattle were *ion binding* and *hydrolase activity*, while the most represented biological processes were the *nitrogen compound metabolic process* and the *cellular metabolic process* (**Figure 2** and **Table 2**).

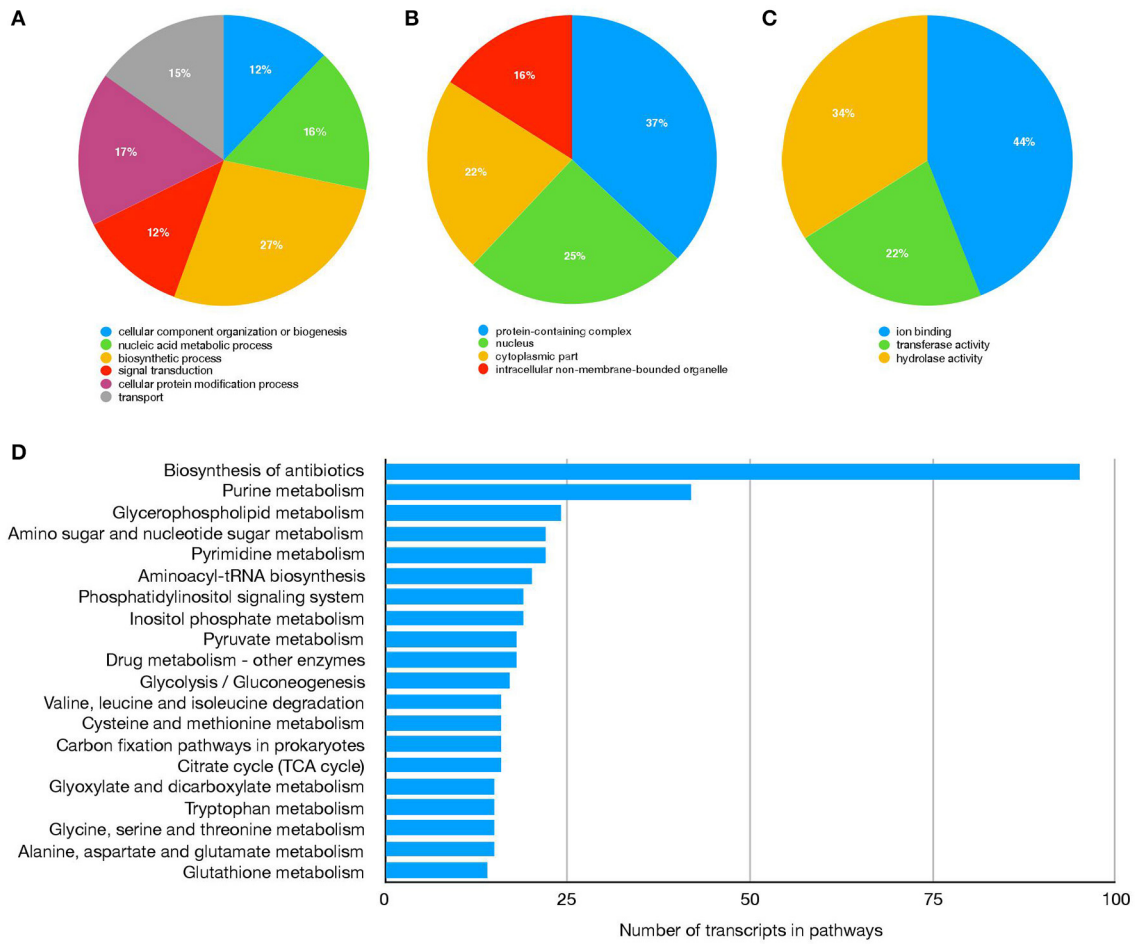

FIGURE 1 | *R.* (*B.*) *microplus* salivar gland transcriptome functional annotation. Transcripts distribution based on GO categories Biological process **(A)**, Cellular component **(B)**, and Molecular function **(C)**. Top 20 processes in KEGG pathways **(D)**.

DISCUSSION

DEGs Between Ticks Fed on Tick-Susceptible and Resistant Cattle

Blood feeding in arthropods is a stressful event in multiple forms and physiological targets. Energetic, thermal, osmotic and oxidative stresses are among the consequences of the rapid ingestion of large amounts of warm blood (Pereira et al., 2017). The large volumes of blood that arrives quickly to the midgut may increase the temperature of blood-feeding arthropods by up to 15°C in <1 min, and the thermal stress generated by the blood meal can trigger a heat shock response by arthropods, as demonstrated by the increased production of heat shock proteins (Benoit et al., 2011).

A transcript upregulated in ticks fed on tick-susceptible cattle showed similarity with the sequence of a small heat shock protein I gene cloned from salivary glands of *Rhipicephalus annulatus*—the RasHSPI (Hussein et al., 2014). The authors verified a strong immunogenic effect of the RasHSPI recombinant protein in rabbits, suggesting that it could be used as a potential protective antigen (Hussein et al., 2014). Previously, another sHSP also cloned from *R. annulatus* salivary glands, a RasHSPII, showed a role as a molecular chaperone, conferring protection at least or specifically to the tick salivary glands against the increase in temperature and other stresses observed during blood feeding by ticks (Shahein et al., 2010). Guilfoile and Packila (2004) verified an increase in the expression of a gene with similarity to a HSP70 in *I. scapularis* females and males throughout blood feeding and suggested that protein encoded by the gene may be required to stabilize tick proteins during ingestion of warm blood from the host or even when the parasite is in contact with the hot skin of the host. An increase in the expression of a small heat shock protein, HSP16, was also observed during the engorgement of *I. scapularis* females (Xu et al., 2005). According to Benoit et al. (2019), suppression of HSPs through RNA interference (RNAi) also leads to impaired digestion and subsequent egg production, indicating that prevention or repair of thermal-associated damage is critical to allow blood feeding arthropods to maximize egg production from a blood meal.

TABLE 2 | Differentially expressed genes (DEG) upregulated in salivary glands from ticks fed on susceptible-tick cattle (Holstein) and ticks fed on resistant-tick cattle (Holstein × Nelore crossbreed) from most represented molecular functions and biological process GO terms.

DEG	e-value[a]	Similarity[b] (%)	FC	FDR	SP	Taxonomy name[c]
UPREGULATED IN SALIVARY GLANDS FROM TICKS FED ON HOLSTEIN CATTLE						
Serine carboxypeptidase	4.5E−103	71.02	4.38	3.6e−05	N	*Haemaphysalis longicornis*
RNA-directed DNA polymerase from mobile element jockey-like	4.2E−126	51.45	0.88	4.7e−02	N	*Strongylocentrotus purpuratus*
Phosphorylase kinase, putative	0.0E0	81.17	0.95	4.8e−03	N	*Ixodes scapularis*
Conserved hypothetical protein	0.0	52.31	0.71	3.2e−02	Y	*Ixodes scapularis*
Neuroendocrine convertase 1	5.3E−245	83.98	1.59	3.6e−02	N	*Ixodes scapularis*
Negative elongation factor B-like	2.4E−128	80.98	1.90	1.5e−02	N	*Centruroides sculpturatus*
MAP kinase-activated protein kinase 3	1.0E−8	100.00	1.69	1.5e−03	N	*Ixodes scapularis*
Longistatin	1.5E−30	57.72	1.71	3.1e−02	N	*Haemaphysalis longicornis*
Leucine aminopeptidase	2.7E−242	90.63	3.52	1.2e−03	N	*Haemaphysalis longicornis*
Glycerol-3-phosphate dehydrogenase	6.9E−12	92.50	3.15	8e−03	N	*Ixodes scapularis*
Gamma-glutamyltransferase, putative 1[e]	6.8E−145	67.82	2.06	1.3e−02	N	*Ixodes scapularis*
Gamma-glutamyltransferase, putative 2[d]	4.7E−146	68.21	1.95	1.5e−02	N	*Ixodes scapularis*
Uncharacterized protein LOC111632264 isoform X1	6.4E−104	80.20	0.90	2.7e−02	N	*Centruroides sculpturatus*
Conserved hypothetical protein XP_002414744.1	2.5E−142	96.48	1.73	8.2e−03	N	*Ixodes scapularis*
Coagulation factor precursor putative	1.6E−53	69.47	2.74	4.1e−02	N	*Ixodes scapularis*
Calnexin	6.5E−118	92.70	2.98	2.9e−04	N	*Ixodes scapularis*
Bleomycin hydrolase	1.1E−82	41.18	1.85	1.6e−04	N	*Zootermopsis nevadensis*
Beta-N-acetylhexosaminidase, putative	1.9E−160	67.95	2.34	2.4e−03	Y	*Ixodes scapularis*
Hypothetical protein IscW_ISCW006057	5.3e−240	57.73	0.51	3e−02	N	*Ixodes scapularis*
Small heat shock protein I	4.7E−27	83.95%	3.71	1.4e−02	N	*Rhipicephalus annulatus*
Ribosomal protein P2	1.9E−24	98.48%	2.56	1e−02	N	*Haemaphysalis qinghaiensis*
RNA-directed DNA polymerase from mobile element jockey-like	4.2E−126	51.45	0.88	4.7e−02	N	*Strongylocentrotus purpuratus*
Pantothenate kinase PanK, putative	2.8E−203	92.23	1.79	4.1e−02	N	*Ixodes scapularis*
26S protease regulatory subunit 6B	3.9E−211	95.68	2.57	1.4e−02	N	*Pediculus humanus corporis*
UPREGULATED IN SALIVARY GLANDS FROM TICKS FED ON CROSSBREED CATTLE						
Conserved hypothetical protein	1.8E−98	87.45%	2.76	1.2e−03	N	*Ixodes scapularis*
Hypothetical protein IscW_ISCW000551	2.0E−202	50.26	0.65	2.8e−02	N	*Ixodes scapularis*
Pentatricopeptide repeat-containing protein, putative	8.7E−130	96.51	1.84	1e−02	N	*Ixodes scapularis*
Mucin-17-like isoform X3	2.0E−18	69.41	0.72	1.6e−02	N	*Limulus polyphemus*
Conserved hypothetical protein	1.9E−99	91.71%	2.13	1.3E−02	N	*Ixodes scapularis*
Fanconi anemia group I protein-like	4.9E−181	54.43%	0.58	3.2E−02	N	*Crassostrea virginica*
ATP synthase H+ transporting, mitochondrial F1 complex, delta subunit precursor	1.0E−68	94.58	3.69	4.5E−02	N	*Ixodes scapularis*
Ribosomal protein L19	2.0E−75	94.04%	3.39	4E−02	N	*Ixodes scapularis*

[a] *e-value from Blast result.*
[b] *Blast mean similarity.*
[c] *Blast hit taxonomy name.*
FC, fold change; FDR, false discovery rate; SP, predicted signal peptide that target proteins to be either secreted or to be a transmembrane protein; Y—signal peptide predicted, N—signal peptide not predicted.
[d,e] *Transcript isoforms.*

Recently, the role of an arthropod HSP70-like molecule in fibrinogenolysis during blood meal has been reported (Vora et al., 2017), as well as the protective effect of cellular protein integrity observed with the overexpression of genes from the heat shock protein family. In our results, in addition to an increase in heat shock gene expression observed in ticks fed on tick-susceptible cattle, downregulation of a transcript similar to the negative elongation factor B-like (*NELF*) was observed. Ghosh et al. (2011) found that *NELF* depletion in Drosophila, mediated by RNA interference, resulted in a delay in the dissociation of heat shock factors (HSF), the transcription factor that upregulates genes encoding heat shock proteins of the *HSP* genes during heat shock recovery. Thus, the observed increase in *HSP* transcript levels in the salivary gland of the ticks fed on tick-susceptible cattle may be related to the delay in the dissociation of the HSF from the *HSP* genes due to the downregulation of the *NELF*. This coordinated action may contribute to the success of the parasite in its interaction with the host.

Two isoforms of a transcript with similarity to an *I. scapularis* gamma-glutamyl transferase (*GGT*) were upregulated in ticks

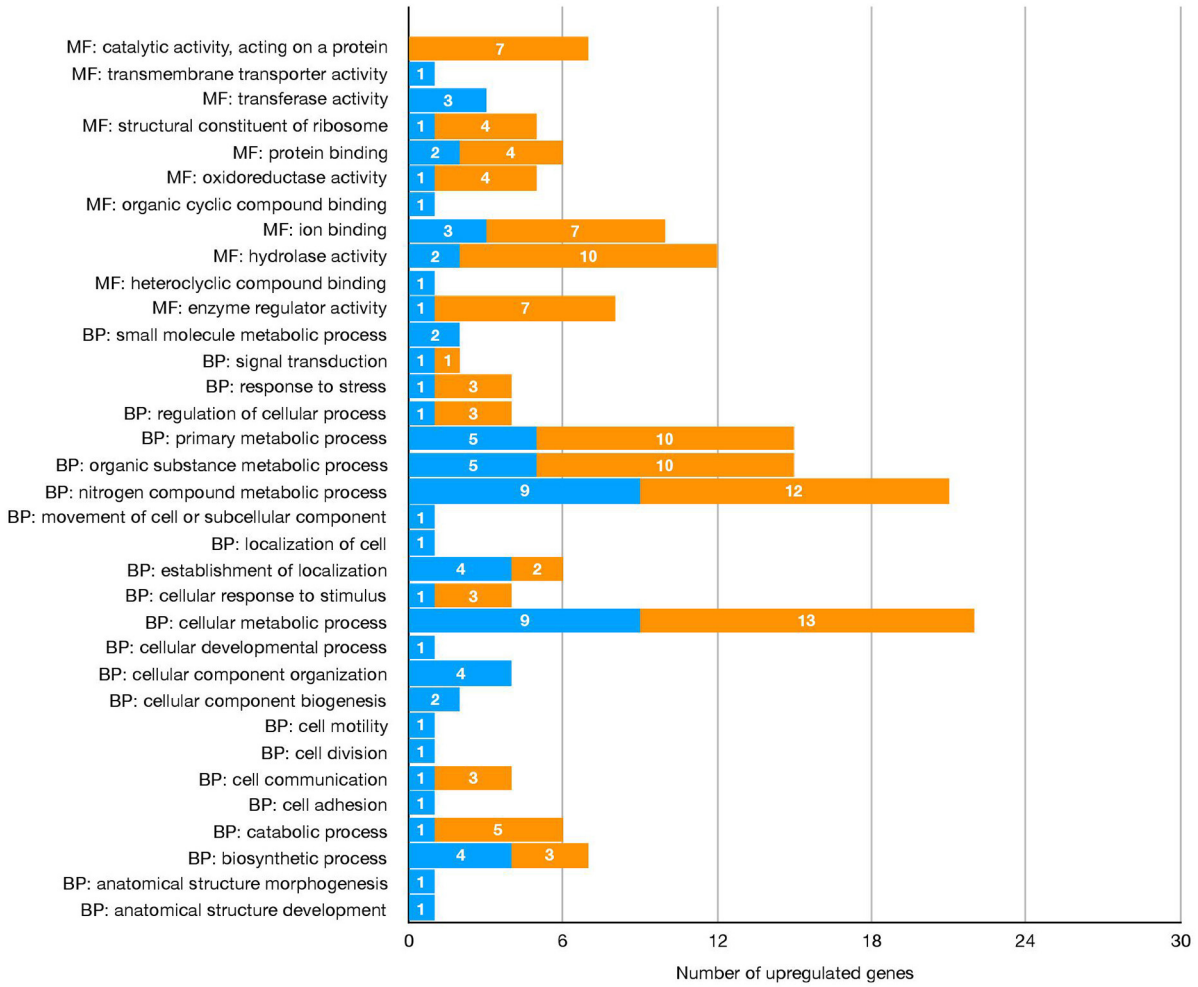

FIGURE 2 | Number of the differentially expressed genes upregulated in salivary glands of *R. (B.) microplus* fed on Holstein (susceptible) and crossbreed (resistant) cattle, based on GO categories Molecular function (MF) and Biological process (BP).

fed tick-susceptible cattle. GGT is an enzyme present in cell membranes and is involved in cross-cell-membrane trafficking of amino acids and peptides and in glutathione metabolism (Mulenga and Erikson, 2011). Glutathione S-transferases (GST) are proteins that belong to a multigene family and play a central role in the detoxification of xenobiotic compounds (de Lima et al., 2002), with increased expression levels being correlated with insecticide resistance in various organisms, including ticks (Nandi et al., 2015; Hernandez et al., 2018). GGT plays key roles in intracellular reduced glutathione (GSH) homeostasis by breaking down the extracellular molecule and providing cysteine for intracellular *de novo* synthesis of GSH (Accaoui et al., 2000; Zhang et al., 2005). Glutathione biosynthesis by GGT is important to maintain intracellular reduced glutathione and the cellular redox state. Additionally, during oxidative stress in rodents, GGT gene expression was increased, which is believed to constitute an adaptation to stress (Zhang et al., 2005). The authors also related that increased expression of GGT during oxidative stress facilitates GSH turnover, *de novo* GSH synthesis, and metabolism and detoxification of GSH conjugates, increasing cell resistance to subsequent stress. In *Haemaphysalis longicornis*, the analysis of two GSTs using real-time PCR showed that gene expression increases continuously in salivary glands and other organs of the tick as blood-feeding progresses until female engorgement, demonstrating the possible role of GSTs in coping with oxidative stress caused by blood-feeding (Hernandez et al., 2018).

The 26S proteasome, the heart of the ubiquitin-proteasome system, is a catalytic machine that cleaves most intracellular ubiquitinated proteins, maintaining cellular homeostasis by means of the recognition, unfolding, translocating and cleavage of protein substrates (Wang and Maldonado, 2006; Gallastegui and Groll, 2010). This proteasome is involved in the regulation of many crucial processes in the cell, such as the cell cycle, apoptosis, signal transduction, protein processing and immune and stress responses (Coux et al., 1996). In our study, the 26S protease regulatory subunit 6B was upregulated in salivary glands from ticks fed tick-susceptible cattle. An increase in the abundance of proteasome proteins was verified in *Trypanosoma cruzy* exposed to the antiparasitic benznidazole (Andrade

et al., 2008). In the small brown planthopper *Laodelphgax striatellus*, the vector of the rice stripe virus, an increase in the accumulation of the virus was observed after disrupting the 26S proteasome, indicating that the small brown planthopper 26S proteasome plays a role in defense against rice stripe virus infection by regulating virus accumulation (Xu et al., 2015). In vertebrates, another function associated with proteasome proteolytic activity, first suggested by Yang et al. (1992), is that the proteasome is also a proteolytic generator of antigenic peptides that can be presented by class I MHC molecules. A 26S proteasome non-ATPase regulatory subunit protein was characterized as an immunogenic enzyme in 24 h fed *I. scapularis* saliva (Lewis et al., 2015), and in *H. longicornis*, the increased expression of the 26S proteasome regulatory subunit protein indicated an increase in expression of the ubiquitin-proteasome system during salivary gland degeneration in engorged females, certainly as a consequence of the programmed cell death that salivary glands undergo after tick engorgement (Wang et al., 2019).

Another chaperone, a transcript with similarity to calnexin (*CNX*), was upregulated in ticks fed tick-susceptible cattle. Calnexin is a chaperone involved in the quality control of proteins, ensuring correct folding and assembly of many glycoproteins in the endoplasmic reticulum (Williams, 2006). The endoplasmic reticulum is a specialized organelle that plays essential and central functions in the cell, including protein folding assisted by a battery of molecular chaperones. Situations that reduce the protein folding capacity of the endoplasmic reticulum, which results in the accumulation and aggregation of unfolded proteins, cause a condition known as endoplasmic reticulum stress (Guérin et al., 2008). In *Schyzosaccharomyces pombe*, calnexin overexpression is involved in the induction of apoptosis triggered by endoplasmic reticulum stress (Guérin et al., 2008). In the midgut of the argasid tick *Ornithodoros moubata* female, a calnexin protein has been identified and determined to be involved with the stress responses associated with blood digestion (Oleaga et al., 2017). A calnexin transcript was upregulated in the *Ixodes ricinus*-derived cell line IRE/CTVM19 at day 2 post-infection with the flavivirus tick-borne encephalitis virus (TBEV), which may have an important role in the response of tick cells to virus infection (Weisheit et al., 2015). In *R.* (*B.*) *microplus*, calnexin was predicted as a transmembrane protein and has been suggested as a target for tick control strategies because it showed a higher VaxiJen score (0.91) than that predicted for Bm86 (0.77) in a study from Richards et al. (2015). Calnexin has also been suggested as a promising vaccine candidate against multiple fungal pathogens because it induces fungal antigen-specific $CD4^+$ T cell expansion and resistance to lethal challenge in mice with multiple fungal pathogens (Wüthrich et al., 2015).

The tick saliva contains a rich variety of pharmacologically bioactive molecules that support blood feeding. During coevolution, blood sucking ticks have adapted mechanisms to evade host detection and prevent blood coagulation by synthesizing an extensive array of molecules with anesthetic, immunosuppressive, vasodilatory, profibrinolytic, and anticoagulant properties (Mans and Neitz, 2004).

A transcript similar to longistatin, an EF-hand calcium binding protein, was overexpressed in ticks fed tick-susceptible cattle. The EF-hand calcium binding proteins modulate several crucial biochemical reactions within the cell and have a role in the blood clotting cascade, being secreted in some rare cases, as observed for the longistatin transcript identified by Anisuzzaman et al. (2012). The authors verified an overexpression of longistatin in salivary glands of the ixodide *H. longicornis* adults pre-engorged (96 h) and engorged (120 h) followed by an abrupt reduction in expression level with tick detachment, showing that longistatin clearly performs a vital function in the feeding process of the parasite through its anticoagulant action, resulting in fibrinogen hydrolysis and plasminogen activation. The post-transcriptional silencing of the longistatin gene in *H. longicornis* completely disrupted the ability of the parasite to form a blood pool and perform blood meals (Anisuzzaman et al., 2011).

In addition to the anticoagulant effect, longistatin has also been found to be able to modulate the inflammatory response of the host in a host-parasite interaction. The receptor for advanced glycation end products (RAGE) is highly expressed constitutively in different cell types of the skin and is responsible for immune activation mediation at inflammation sites. Anisuzzaman and Tsuji (2015) demonstrated that longistatin secreted in *H. longicornis* saliva binds to RAGE, modulating the host immune response and suppressing the inflammation associated with the lesion caused by the tick bite, thereby ensuring the successful acquisition of host blood. Immunization of mice with recombinant longistatin induced high levels of IgG protective antibodies against ticks, as well as reduced repletion of ticks by ∼54%, post-engorgement body weight by ∼11%, and nymph molting by ∼34% (Anisuzzaman et al., 2012). *H. longicornis* treated with dsRNA failed to form a blood pool necessary for the proper blood meal, which led to a reduced engorged tick weight (Anisuzzaman et al., 2011).

Other binding Ca^{++}-containing EF-hand motif molecules, similar to longistatin, have recently been identified from *Strongyloides venezuelensis*, the venestatin (Tsubokawa et al., 2017) and *Aedes aegypt*—the salivary factor LTRIN (Jin et al., 2018), which were upregulated promptly after larval invasion through the host's skin and during mosquito blood feeding, respectively.

A transcript similar to a serine carboxypeptidase (*SCP*) was upregulated in ticks fed on susceptible cattle compared to those fed on resistant cattle. SCPs are proteolytic enzymes that target serine in their catalytic activity and catalyze the hydrolysis of C-terminal residues in peptides and proteins (Anderson et al., 2008). In mammals, SCPs are involved in signaling events, such as the generation of bioactive peptides in the blood coagulation cascade (Turk, 2006), but little is known about SCPs in tick species. In *Ixodes ricinus*, enzymes as cathepsins B, C, and D, legumain, serine carboxypeptidase and leucine aminopeptidase were characterized as the main enzymes acting in the tick hemoglobinolytic system at midgut (Horn et al., 2009). Motobu et al. (2007) identified an *H. longicornis* SCP predominantly expressed in tick midgut upregulated in response to blood feeding, which has been described to play a role in hemoglobin degradation. SCPs were highly expressed in salivary glands

and viscera from fully engorged *Ixodes holocyclus* female ticks (Rodriguez-Valle et al., 2018). The secretory/excretory proteome of helminths parasites identified SCPs that are part of a protein complex that regulates parasite-host interaction (Morassutti et al., 2012). Radulović et al. (2014) identified SCPs transcribed in the salivary gland of *Amblyoma americanum* that could act to regulate the interaction with the host.

Insect cells usually express a number of β-N-acetylhexosaminidases, which are important in various developmental stages during their life cycle, primarily in the turnover of the chitin exoskeleton (Hogenkamp et al., 2008). According to You and Fujisaki (2009), molecules associated with molt act to protect organisms against pathogen invasion, on peritrophic membrane control and other functions necessary during blood feeding and molting in ticks and may be candidates for parasite control. In our results, a DEG similar to a β-N-acetylhexosaminidase and upregulated in ticks fed on tick-susceptible cattle was found in salivary glands. Del Pino et al. (1998) inoculated anti-β-N-acetylhexosaminidase antibodies obtained against the enzyme purified from larvae of *R.* (*B.*) *microplus* into fully engorged, adult females and verified a decrease in the reproductive efficiency of *R.* (*B.*) *microplus*. Chitin is a polysaccharide that consists predominantly of unbranched chains of N-acetylglucosamine and is present together with a protein matrix in the cuticle of arthropods, including *R.* (*B.*) *microplus* (Hackman, 1975). Ticks periodically shed their old cuticles and resynthesize new ones, a process that is mediated by the elaboration of chitinase in the molting fluid that accumulates between the old cuticle and the epidermis (You and Fujisaki, 2009). Female ticks of the Ixodidae family, in general, increase their mass up to 100-fold during the 7–10 days feeding period and synthesize sufficient endocuticle to thicken their cuticle by the end of the slow phase of engorgement (Flynn and Kaufman, 2015); thus, the inhibition of enzymes involved in chitin metabolism during morphogenesis might cause serious tick damage (Del Pino et al., 1998).

A transcript similar to leucine aminopeptidase (*LAP*) was upregulated in ticks fed tick-susceptible cattle. Leucine aminopeptidases belong to a diverse group of the M17 family of Zn-metalloproteases and preferentially cleave a leucine residue at the N-terminus of the proteins and peptides (Maggioli et al., 2018). Metalloproteases, which have been found in tick saliva, salivary gland, ovary and midgut, play an important role in inflammation, immunomodulation, fibrinolysis, blood protein digestion, nociception, vitellogenesis, remodeling of extracellular matrix, and pathogen transmission (Ali et al., 2015). Leucine aminopeptidases have been identified in the midgut and salivary glands of engorged *R.* (*B.*) *microplus* (Kerlin and Hughes, 1992) and in the cytosol of cells of the midgut, salivary glands type II acini and epidermal cells from *H. longicornis* (Hatta et al., 2006). Overexpression of the midgut enzyme has been observed during blood feeding in *H. longicornis*, where the disruption of the gene encoding LAP through RNAi significantly delayed onset of egg-laying and reduced egg oviposition, suggesting that HlLAP plays a role as a blood digestive enzyme and affects tick fecundity (Hatta et al., 2007). In sheep, immunization with a leucine aminopeptidase purified from *Fasciola hepatica* resulted in high levels of animal protection against the endoparasite (Piacenza et al., 1999).

Ribosomal proteins play essential roles in cell growth and proliferation through the ribosome biogenesis process to translate mRNAs into proteins (Trainor and Merrill, 2014), and the assembly of a functional ribosome is vital for successful protein synthesis. In our study, two transcripts with similarity to ribosomal proteins were found among the DEGs in the salivary gland of *R.* (*B.*) *microplus*. The first transcript, a 60S acidic ribosomal protein P2, was upregulated in the salivary glands of ticks feeding on tick-susceptible cattle.

Phosphoproteins P1 and P2 form a complex with P0 protein to raise the eukaryotic ribosomal stalk. A number of ribosome-associated proteins were identified in female tissues from *R.* (*B.*) *microplus*, including components of the 40S and ribosomal subunits, as well as the 29S and mitochondrial ribosomal subunits (Stutzer et al., 2013), and in the salivary gland immune-proteome of *A. americanum* (Radulović et al., 2014). In the salivary gland transcriptome of *Rhipicephalus appendiculatus*, most represented pathways were *ribosome*, *RNA transport*, *protein processing in endoplasmic reticulum*, and *spliceosome* (de Castro et al., 2016). Ribosomal P proteins seem to play an important role in diseases related to infections caused by intracellular protozoan parasites. Rodríguez-Mallon et al. (2015) identified an immunogenic region of ribosomal protein P0 from *Rhipicephalus* spp. ticks and a synthetic 20 amino acid peptide from this sequence showed an efficacy of 96% as a vaccine against *Rhipicephalus sanguineus* in an immunization experiment with rabbits.

The second transcript, with similarity to 60S ribosomal protein L19 (*RPL19*), was upregulated in ticks feeding on tick-resistant cattle. Despite the essential role of the ribosome in protein synthesis, RPL19 is predicted to have an extra-protein translational function, and its overexpression in cell culture activated the cellular signaling pathway of the UPR (unfolded protein response) (Hong et al., 2014). The UPR pathway is conserved from yeast to humans (Zhang et al., 2016) and activated in response to an overloading of unfolded or misfolded peptides, and its action can either have a protective effect, with the change of protein synthesis rate decreasing peptide load into the endoplasmic reticulum or inducing cell death with apoptotic characteristics (Kim et al., 2008; Hong et al., 2014). The RPL19 gene was upregulated in ticks fed tick-resistant cattle, which indicates that cell death was the main pathway activated to salivary gland cells during host-parasite interactions. In Jurkat cells, RPL19 protein expression was decreased by heat stress, although there was no significant change in mRNA expression (Zhang et al., 2016).

Phosphorylase kinase (*PhK*) is a holoenzyme that activates glycogen phosphorylase (Brushia and Walsh, 1999) which, in turn, catalyzes the hydrolysis of glycogen to generate glucose-1-phosphate. In ticks fed on tick-susceptible cattle, an upregulation in a transcript similar to *PhK* was observed.

Genes involved in stress response include molecular chaperones, such as members of the heat shock protein gene family, as already mentioned, in addition to antioxidative enzymes (e.g., catalase, superoxide dismutases, and glutathione-S-transferases) and enzymes of carbohydrate metabolism (e.g.,

glycogen phosphorylase and phosphofructokinase) (Barat et al., 2016). In mammals, glycogen metabolism is profoundly affected by stress, with glycogen content in peripheral tissues decreasing during stress because of increased glycogenolysis and decreased glycogen synthesis (Van Cromphaut, 2009). To date, few studies have investigated tick glycogen metabolism. However, in a study on arthropod thermal tolerance, a reduction in glycogen content was observed in *D. melanogaster* with a sudden increase in temperature from 25 to 41.2–41.3°C with a ramping rate of 0.1°C min^{-1} (Overgaard et al., 2012). As appears to have occurred with *HSPI* and *NELF* transcripts, the upregulation of *PHKA* in ticks feeding on tick-susceptible cattle may be related to the stress condition imposed by blood feeding.

A transcript that encodes a conserved hypothetical protein (XP_002414744.1) with cullin-binding and a UBA_DCNL2 domain was upregulated in ticks feeding on tick-susceptible cattle. This protein functions as an E3 ligase, promoting cullin neddylation by binding to cullins through conserved interaction surfaces on each protein (Kurz et al., 2008). Neddylation is a post-translational modification process analogous to ubiquitination, where neddylated proteins are modified through the closest relative to ubiquitin—NEDD8 protein, which attaches to a lysine residue of the cullin scaffold proteins (Sakata et al., 2007; Rabut and Peter, 2008). Neddylation is important for a number of biological processes and is required for the regulation of a multifunctional transcription factor, NF-κB, which is crucial in immune-response and apoptotic pathways (Cajee et al., 2012). The gene upregulation verified in ticks fed on tick-susceptible cattle in our study corroborates the role of pathways related to cellular proteolysis, as already mentioned in the case of upregulation of *HSP1*, *GGT*, and downregulation of *NELF*, in the maintenance of the susceptible host-tick interaction.

In vertebrates, mucins are abundant in the lungs and digestive tract, where they provide lubrication and protection of the epithelium against physical damage and pathogens (Hollingsworth and Swanson, 2004). Mucins are either secreted and gel-forming or attached to the membrane by special cleavable transmembrane domains (Syed et al., 2008). A mucin-like family has been identified in insects, and its family members are distributed in salivary glands, midgut, and Malpighian tubules (Barry et al., 1999; Syed et al., 2008; Hegedus et al., 2009). In our study, a transcript similar to a mucin-17-like isoform X3 was upregulated in ticks fed on crossbreed cattle. In the hemipteran *Nilaparvata lugens*, the rice brown planthopper (BPH), a mucin-like transcript, was upregulated when the insects were transferred from a susceptible rice variety to a resistant one (Huang et al., 2017). The authors suggested that the elevated mucin production might enable BPH to cope with the stress of the defense responses or help BPH to suppress the defenses of the resistant plant (Huang et al., 2017). An upregulation in a mucin-17-like isoform X3 transcript was also observed in *Diuraphis noxia* fed on an aphid-resistant wheat plant in comparison to non-resistant plants (Sinha et al., 2016). In mice immunized with *Anopheles gambiae* midgut-bound mucin cDNA, increased mortality was observed among mosquitoes fed immunized mice compared to those fed control mice (Foy et al., 2003).

Mucin and mucin-like proteins have been found in *R.* (*B.*) *microplus* (Maruyama et al., 2017) and the sialotranscriptomes of other tick species (Karim et al., 2011; Díaz-Martín et al., 2013; Radulović et al., 2014; Tan et al., 2015; Ong et al., 2016; Antunes et al., 2018), and they may function in tick feeding by coating the chitinous feeding mouthparts or the feeding lesion (Francischetti, 2010). In 1998, an antigen purified from *R.* (*B.*) *microplus* and named BMA7, exhibiting similarity to vertebrate mucins, induced partial immunity against tick infestation in cattle (Mckenna et al., 1998).

DEGs Predicted as Salivary Gland Secreted Proteins

Innexins are transmembrane proteins that form gap junction channels and hemichannels in invertebrates, including arthropods (Richards et al., 2015; Güiza et al., 2018). Gap junctions allow endocrine signals to be rapidly shared among adjacent cells within a tissue by mediating the direct transport of ions, small molecules, and second messengers between them (Phelan and Starich, 2001). Pharmacological inhibitors of gap junctions, such as carbenoxolone, mefloquine, and meclofenamic acids, have been cited as potential insecticides in arthropod vectors, such as *Aedes aegypti* (Calkins and Piermarini, 2015). In our study, a transcript similar to innexin was downregulated in the salivary glands of ticks fed on resistant cattle. A transcript with similarity to innexin was also expressed in the salivary glands of the female tick *A. americanum* during blood feeding (Aljamali et al., 2009) and in the proteome of the saliva of the tick *O. moubata* (Díaz-Martín et al., 2013).

The gene that encodes the predicted secreted protein Na^+/dicarboxylate, Na^+/tricarboxylate, and phosphate transporter, was upregulated in salivary glands of ticks fed on susceptible cattle. Analyzing transcriptome changes in *Eriocheir sinensis* larvae after desalination, Hui et al. (2014) identified transcripts of many genes involved in ion transport processes, including the Na^+/dicarboxylate, Na^+/tricarboxylate, and phosphate transporter, to which it was attributed a potential role in osmoregulation.

A protein predicted as secreted, the phosphoinositol 4-phosphate adaptor protein, was upregulated in ticks feeding on resistant cattle. Four phosphate-adaptor proteins 1 and 2 (FAPP1 and FAPP2) are proteins that localize to the trans-Golgi network (TGN) on nascent carriers and interact with phosphatidylinositol-4-phosphate and the small GTPase ADP-ribosylation factor (ARF) through their plekstrin homology domain (Godi et al., 2004). Phosphoinositol 4-phosphate adaptor proteins are involved in lipid transport (Oleaga et al., 2017) and control the formation and fission of post-Golgi vesicles and regulate secretory transport from the TGN to the plasma membrane, and displacement or knockdown of FAPPs inhibits cargo transfer to the plasma membrane (Godi et al., 2004). In *Ornithodoros moubata* ticks, phosphoinositol 4-phosphate adaptor protein transcripts were upregulated in the midgut after blood feeding in comparison with non-fed ticks (Oleaga et al., 2017). The phosphatidylinositol-4-phosphate, in turn, is a minor plasma membrane phospholipid component of a signal

transduction pathway in tick salivary glands (McSwain et al., 1989), a key regulator of membrane transport required for the formation of transport carriers from the TGN. ARF is a Ras-related GTP-binding protein that regulates the reversible binding of cytosolic coat proteins to Golgi membranes (Donaldson and Klausner, 1994).

A putative monocarboxylate transporter was identified on the *A. americanum* tick saliva immunoproteome from fed adult females (Radulović et al., 2014) and overexpressed in *R.* (*B.*) *microplus* engorged females treated with ubiquitin-63E dsRNA (Lew-Tabor et al., 2011). Monocarboxylate transporters catalyze rapid transport across the plasma membrane of many monocarboxylates, such as lactate and pyruvate (Lew-Tabor et al., 2011). A transcript similar to a monocarboxylate transporter, predicted as a secreted protein, was upregulated in ticks fed on tick-susceptible cattle.

A secreted cysteine-rich protein containing a trypsin inhibitor-like (TIL) domain was upregulated in the salivary glands of ticks feeding on tick-susceptible cattle. This family comprises chymotrypsin, elastase and trypsin inhibitors (Sasaki et al., 2008), although many extracellular proteins also contain multiple TIL domains (Wang et al., 2015). TIL domain-containing protein family members have been found ubiquitously in blood-feeding insect and tick sialomes (Karim and Adamson, 2012; Maruyama et al., 2017), and in fungal-pathogen interactions, members of this family are frequently associated with host adaptation or specialization (Schulze-Lefert and Panstruga, 2011).

In *R.* (*B.*) *microplus*, a member of this family, known as ixodidin, was purified from the hemocytes and characterized as an antimicrobial peptide, which affected the growth of *Micrococcus luteus* and *Escherichia coli* and presented inhibitory activity (Fogaça et al., 2006). BmSI-7, a protein from *R.* (*B.*) *microplus* belonging to the trypsin inhibitor-like cysteine-rich domain family showed strong inhibitory activity toward elastase, which participates in the inflammatory response and is involved in injury caused by tick fixation on bovines (Sasaki et al., 2008). A secreted cysteine-rich protein containing the TIL domain was upregulated in the proteome of fed *Amblyomma sculptum*, induced by blood feeding, compared with non-fed ticks (Esteves et al., 2017). In *R.* (*B.*) *microplus*, TIL domain-containing proteins were also upregulated in the fully engorged female proteome in comparison with partially engorged females (Tirloni et al., 2014).

A transcript similar to the putative defense protein 3 containing a reeler domain, predicted to be a secreted protein, was upregulated in ticks feeding on tick-susceptible cattle. A putative defense protein 3 was also upregulated in the proteome of a whitefly infected by two begomoviruses, the tomato yellow leaf curl virus (TYLCV) and the papaya leaf curl China virus (PaLCuCNV), as a defense response against the viruses (Zhao et al., 2019). Defense proteins with a reeler domain have been shown to have an important role in innate immune responses in a variety of insects (Bao et al., 2011; Arp et al., 2016). In *I. scapularis*, a predicted secreted protein with a reeler domain—PIXR—was induced upon feeding and upregulated in *B. burgdorferi*-infected tick guts, favoring colonization by the bacteria (Narasimhan et al., 2017).

In our results, a transcript similar to an F-actin-uncapping protein, LRRC16A isoform X2 (*LRCC16A*) with a CARMIL_C domain, a putative secreted protein, was upregulated in salivary glands from ticks feeding on tick-resistant cattle. Actins are the major constituents of the actin cytoskeleton and are essential for cell adhesion, migration, mechanosensing, and contractility in muscle and non-muscle tissues (Simiczyjew et al., 2017; Vedula and Kashina, 2018). Actin filaments grow and shrink by addition and loss, respectively, of actin monomers at the ends of filaments (Stark et al., 2017), and such regulation affects a wide range of cell processes, including development, differentiation, immunity, and inflammation (Marcos-Ramiro et al., 2014). Actin polymerization occurs primarily through elongation at the filament barbed end, and the elongation continues until the barbed end is capped by a capping protein (CP) (Yang et al., 2005). Regulation of barbed-end capping occurs by binding of the inhibitor factors to the filament, thereby protecting it from CP, by binding to CP and inhibiting its capping activity or by uncapping (Yang et al., 2005). CARMILs are multidomain proteins that regulate the actin-binding activity of CP binding directly to it and induce a conformational change that decreases its actin-capping activity (Stark et al., 2017).

Our results help to characterize cattle tick salivary gland gene expression in both susceptible and resistant hosts and suggest new putative targets for infestation control, as those genes involved in stress response mechanism during blood feeding. A possible coordinated regulation targeting a small heat shock protein and a negative elongation factor B-like genes, the latter expressed in order to maintain heat shock gene expression increased during blood feeding; along with upregulation of a 26S proteasome subunit and calnexin, other chaperone, shed light to the role of this mechanism in maintaining tick feeding. Other interactions, as the one described, are under analysis, and may evince important new targets to vaccines development.

DATA AVAILABILITY STATEMENT

The datasets generated for this study can be found in the NCBI SRA database under accessions SAMN13636118 and SAMN13636119 from BioProject PRJNA596777 (http://www.ncbi.nlm.nih.gov/bioproject/596777).

ETHICS STATEMENT

The animal study was reviewed and approved by Ethics Statement. All experimental procedures were approved by Embrapa Beef Cattle's Ethics Committee on Animal Use according to Protocol 008/2014; coordinated by Vanessa Felipe Souza. e-mail: vanessa.felipe@embrapa.br.

AUTHOR CONTRIBUTIONS

RA and RC conceived and designed the study. MG and RC were responsible for the tick rearing, cattle artificial infestation, tick collection, and RNA isolation. PG and AN performed the data analysis. PG, AN, and RA wrote the manuscript. JF critically

revised the manuscript. All authors edited and approved the final manuscript.

FUNDING

This work was supported by funds from the Brazilian Agricultural Research Corporation-Embrapa, grants 01.11.07.002.03.00.

ACKNOWLEDGMENTS

We thank the Foundation for Support to the Development of Education, Science and Technology of the State of Mato Grosso do Sul (FUNDECT/MS), the Government of the state of Mato Grosso do Sul, the Brazilian Federal Agency for Support and Evaluation of Graduate Education (Capes), the National Council for Scientific and Technological Development (CNPq), and Embrapa Bioinformatic Multi-user Laboratory (LMB) for providing support and computing resources.

SUPPLEMENTARY MATERIAL

The Supplementary Material for this article can be found online at: https://www.frontiersin.org/articles/10.3389/fcimb.2019.00477/full#supplementary-material

REFERENCES

Accaoui, M. J., Enoiu, M., Mergny, M., Masson, C., Dominici, S., Wellman, M., et al. (2000). Gamma-glutamyltranspeptidase-dependent glutathione catabolism results in activation of NF-kB. *Biochem. Biophys. Res. Commun.* 276, 1062–1067. doi: 10.1006/bbrc.2000.3585

Ali, A., Khan, S., Ali, I., Karim, S., da Silva Vaz, I. Jr., and Termignoni, C. (2015). Probing the functional role of tick metalloproteases. *Physiol. Entomol.* 40, 177–188. 10.1111/phen.12104 doi: 10.1111/phen.12104

Aljamali, M. N., Hern, L., Kupfer, D., Downard, S., So, S., Roe, B. A., et al. (2009). Transcriptome analysis of the salivary glands of the female tick *Amblyomma americanum* (Acari: Ixodidae). *Insect Mol. Biol.* 18, 129–154. doi: 10.1111/j.1365-2583.2009.00863.x

Anderson, J. M., Sonenshine, D. E., and Valenzuela, J. G. (2008). Exploring the mialome of ticks: an annotated catalogue of midgut transcripts from the hard tick, *Dermacentor variabilis* (Acari: Ixodidae). *BMC Genomics* 9:552. doi: 10.1186/1471-2164-9-552

Andrade, H. M., Murta, S. M., Chapeaurouge, A., Perales, J., Nirdé, P., and Romanha, A. J. (2008). Proteomic analysis of *Trypanosoma cruzi* resistance to benznidazole. *J. Proteome Res.* 7, 2357–2367. doi: 10.1021/pr700659m

Anisuzzaman, M., and Tsuji, N. (2015). Longistatin in tick-saliva targets RAGE. *Oncotarget* 6, 35133–35134. doi: 10.18632/oncotarget.6032

Anisuzzaman, M. K. I., Alim, M. A., Miyoshi, T., Hatta, T., Yamaji, K., Matsumoto, Y., et al. (2011). Longistatin, a plasminogen activator, is key to the availability of blood-meals for ixodid ticks. *PLoS Pathog.* 7:e1001312. doi: 10.1371/journal.ppat.1001312

Anisuzzaman, M. K. I., Alim, M. A., Miyoshi, T., Hatta, T., Yamaji, K., Matsumoto, Y., et al. (2012). Longistatin is an unconventional serine protease and induces protective immunity against tick infestation. *Mol. Biochem. Parasitol.* 182, 45–53. doi: 10.1016/j.molbiopara.2011.12.002

Antunes, S., Couto, J., Ferrolho, J., Rodrigues, F., Nobre, J., Santos, A. S., et al. (2018). *Rhipicephalus bursa* sialotranscriptomic response to blood feeding and *Babesia ovis* infection: identification of candidate protective antigens. *Front. Cell. Infect. Microbiol.* 8:116. doi: 10.3389/fcimb.2018.00116

Arp, A. P., Hunter, W. B., and Pelz-Stelinski, K. S. (2016). Annotation of the Asian citrus psyllid genome reveals a reduced innate immune system. *Front. Physiol.* 7:570. doi: 10.3389/fphys.2016.00570

Bao, Y. Y., Xue, J., Wu, W. J., Wang, Y., Lv, Z. Y., and Zhang, C. X. (2011). An immune-induced reeler protein is involved in the *Bombyx mori* melanization cascade. *Insect Biochem. Mol. Biol.* 41, 696–706. doi: 10.1016/j.ibmb.2011.05.001

Barat, A., Sahoo, P. K., Kumar, R., Goel, C., and Singh, A. K. (2016). Transcriptional response to heat shock in liver of snow trout (*Schizothorax richardsonii*)–a vulnerable Himalayan Cyprinid fish. *Funct. Integr. Genomics* 16, 203–213. doi: 10.1007/s10142-016-0477-0

Barry, M. K., Triplett, A. A., and Christensen, A. C. (1999). A peritrophin-like protein expressed in the embryonic tracheae of *Drosophila melanogaster*. *Insect Biochem. Mol. Biol.* 29, 319–327. doi: 10.1016/S0965-1748(99)00004-1

Benoit, J. B., Lazzari, C. R., Denlinger, D. L., and Lahondère, C. (2019). Thermoprotective adaptations are critical for arthropods feeding on warm-blooded hosts. *Curr. Opin. Insect Sci.* 34, 7–11. doi: 10.1016/j.cois.2019.02.003

Benoit, J. B., Lopez-Martinez, G., Patrick, K. R., Phillips, Z. P., Krause, T. B., and Denlinger, D. L. (2011). Drinking a hot blood meal elicits a protective heat shock response in mosquitoes. *PNAS* 108, 8026–8029. doi: 10.1073/pnas.1105195108

Bergman, D. K., Palmer, M. J., Caimano, M. J., Radolf, J. D., and Wikel, S. K. (2000). Isolation and molecular cloning of a secreted immunosuppressant protein from *Dermacentor andersoni* salivary gland. *J. Parasitol.* 86, 516–525. doi: 10.2307/3284866

Bolger, A. M., Lohse, M., and Usadel, B. (2014). Trimmomatic: a flexible trimmer for Illumina sequence data. *Bioinformatics* 30, 2114–2120. doi: 10.1093/bioinformatics/btu170

Brushia, R. J., and Walsh, D. A. (1999). Phosphorylase kinase: the complexity of its regulation is reflected in the complexity of its structure. *Front. Biosci.* 4, D618–D641. doi: 10.2741/Brushia

Buchfink, B., Xie, C., and Huson, D. H. (2015). Fast and sensitive protein alignment using DIAMOND. *Nat. Methods* 12, 59–60. doi: 10.1038/nmeth.3176

Cajee, U. F., Hull, R., and Ntwasa, M. (2012). Modification by ubiquitin-like proteins: significance in apoptosis and autophagy pathways. *Int. J. Mol. Sci.* 13, 11804–11831. doi: 10.3390/ijms130911804

Calkins, T. L., and Piermarini, P. M. (2015). Pharmacological and genetic evidence for gap junctions as potential new insecticide targets in the yellow fever mosquito, *Aedes aegypti*. *PLoS ONE* 10:e0137084. doi: 10.1371/journal.pone.0137084

Choudhury, R. R., Hyvola, N., and Lowe, M. (2005). Phosphoinositides and membrane traffic at the trans-Golgi network. *Biochem. Soc. Symp.* 72, 31–38. doi: 10.1042/bss0720031

Coux, O., Tanaka, K., and Goldberg, A. L. (1996). Structure and functions of the 20S and 26S proteasomes. *Annu. Rev. Biochem.* 65, 801–847. doi: 10.1146/annurev.bi.65.070196.004101

Csordas, B. G., Cunha, R. C., Garcia, M. V., da Silva, S. S., Leite, F. L., and Andreotti, R. (2018). Molecular characterization of the recombinant protein RmLTIBmCG-LTB: protective immunity against *Rhipicephalus* (*Boophilus*) *microplus*. *PLoS ONE* 13:e0191596. doi: 10.1371/journal.pone.0191596

de Castro, M. H., De Klerk, D., Pienaar, R., Latif, A. A., Rees, D. J. G., and Mans, B. J. (2016). *De novo* assembly and annotation of the salivary gland transcriptome of *Rhipicephalus appendiculatus* male and female ticks during blood feeding. *Ticks Tick Borne Dis.* 7, 536–548. doi: 10.1016/j.ttbdis.2016.01.014

de Lima, M. R., Ferreira, C. S., de Freitas, D. J., Valenzuela, J. G., and Masuda, A. (2002). Cloning and partial characterization of a *Boophilus microplus* (Acari: Ixodidae) glutathione S-transferase. *Insect Biochem. Mol. Biol.* 32, 747–754. doi: 10.1016/S0965-1748(01)00157-6

Del Pino, F. A., Brandelli, A., Gonzales, J. C., Henriques, J. A., and Dewes, H. (1998). Effect of antibodies against beta-N-acetylhexosaminidase on reproductive efficiency of the bovine tick *Boophilus microplus*. *Vet. Parasitol.* 79, 247–255. doi: 10.1016/S0304-4017(98)00154-X

Díaz-Martín, V., Manzano-Román, R., Valero, L., Oleaga, A., Encinas-Grandes, A., and Pérez-Sánchez, R. (2013). An insight into the proteome of the saliva of the argasid tick *Ornithodoros moubata* reveals important differences in saliva protein composition between the sexes. *J. Proteomics* 80, 216–235. doi: 10.1016/j.jprot.2013.01.015

Donaldson, J. G., and Klausner, R. D. (1994). ARF: a key regulatory switch in membrane traffic and organelle structure. *Curr. Opin. Cell. Biol.* 6, 527–532. doi: 10.1016/0955-0674(94)90072-8

Esteves, E., Maruyama, S. R., Kawahara, R., Fujita, A., Martins, L. A., Righi, A. A., et al. (2017). Analysis of the salivary gland transcriptome of unfed and partially fed *Amblyomma sculptum* ticks and descriptive proteome of the saliva. *Front. Cell. Infect. Microbiol.* 7:476. doi: 10.3389/fcimb.2017.00476

Flynn, P. C., and Kaufman, W. R. (2015). Mechanical properties of the cuticle of the tick *Amblyomma hebraeum* (Acari: Ixodidae). *J. Exp. Biol.* 218, 2806–2814. doi: 10.1242/jeb.123919

Fogaça, A. C., Almeida, I. C., Eberlin, M. N., Tanaka, A. S., Bulet, P., and Daffre, S. (2006). Ixodidin, a novel antimicrobial peptide from the hemocytes of the cattle tick *Boophilus microplus* with inhibitory activity against serine proteinases. *Peptides* 27, 667–674. doi: 10.1016/j.peptides.2005.07.013

Foy, B. D., Magalhaes, T., Injera, W. E., Sutherland, I., Devenport, M., Thanawastien, A., et al. (2003). Induction of mosquitocidal activity in mice immunized with *Anopheles gambiae* midgut cDNA. *Infect. Immun.* 71, 2032–2040. doi: 10.1128/IAI.71.4.2032-2040.2003

Francischetti, I. M. B. (2010). Platelet aggregation inhibitors from hematophagous animals. *Toxicon* 56, 1130–1144. doi: 10.1016/j.toxicon.2009.12.003

Franzin, A. M., Maruyama, S. R., Garcia, G. R., Oliveira, R. P., Ribeiro, J. M., Bishop, R., et al. (2017). Immune and biochemical responses in skin differ between bovine hosts genetically susceptible and resistant to the cattle tick *Rhipicephalus microplus*. *Parasit. Vectors* 10:51. doi: 10.1186/s13071-016-1945-z

Gallastegui, N., and Groll, M. (2010). The 26S proteasome: assembly and function of a destructive machine. *Trends Biochem. Sci.* 35, 634–642. doi: 10.1016/j.tibs.2010.05.005

Ghosh, S., Khan, M. H., and Ahmed, N. (1999). Cross-bred cattle protected against *Hyalomma anatolicum anatolicum* by larval antigens purified by immunoaffinity chromatography. *Trop. Anim. Health Prod.* 31, 263–273. doi: 10.1023/A:1005218821889

Ghosh, S. K. B., Missra, A., and Gilmour, D. S. (2011). Negative elongation factor accelerates the rate at which heat shock genes are shut off by facilitating dissociation of heat shock factor. *Mol. Cell. Biol.* 31, 4232–4243. doi: 10.1128/MCB.05930-11

Godi, A., Di Campli, A., Konstantakopoulos, A., Di Tullio, G., Alessi, D. R., Kular, G. S., et al. (2004). FAPPs control Golgi-to-cell-surface membrane traffic by binding to ARF and PtdIns (4) P. *Nat. Cell Biol.* 6, 393–404. doi: 10.1038/ncb1119

Grabherr, M. G., Haas, B. J., Yassour, M., Levin, J. Z., Thompson, D. A., et al. (2011). Full-length transcriptome assembly from RNA-Seq data without a reference genome. *Nat. Biotechnol.* 29, 644–652. doi: 10.1038/nbt.1883

Grisi, L., Leite, R. C., Martins, J. R. S., Barros, A. T. M., Andreotti, R., and Cançado, P. H. D., et al. (2014). Reassessment of the potential economic impact of cattle parasites in Brazil. *Rev. Bras. Parasitol. Vet.* 23, 150–156. doi: 10.1590/S1984-29612014042

Guérin, R., Arseneault, G., Dumont, S., and Rokeach, L. A. (2008). Calnexin is involved in apoptosis induced by endoplasmic reticulum stress in the fission yeast. *Mol. Biol. Cell* 19, 4404–4420. doi: 10.1091/mbc.e08-02-0188

Guilfoile, P. G., and Packila, M. (2004). Identification of four genes expressed by feeding, female *Ixodes scapularis* including three with sequence similarity to previously recognized genes. *Exp. Appl. Acarol.* 32, 103–110. doi: 10.1023/B:APPA.0000018197.63153.58

Güiza, J., Barria, I., Saez, J. C., and Vega, J. L. (2018). Innexins: expression, regulation and functions. *Front. Physiol.* 9:1414. doi: 10.3389/fphys.2018.01414

Haas, B. J., Papanicolaou, A., Yassour, M., Grabherr, M., Blood, P. D., Bowden, J., et al. (2013). *De novo* transcript sequence reconstruction from RNA-seq using the Trinity platform for reference generation and analysis. *Nat. Protoc.* 8, 1494–1512. doi: 10.1038/nprot.2013.084

Hackman, R. H. (1975). Expanding abdominal cuticle in the bug Rhodnius and the tick Boophilus. *J. Insect Physiol.* 21, 1613–1623. doi: 10.1016/0022-1910(75)90199-7

Hatta, T., Kazama, K., Miyoshi, T., Umemiya, R., Liao, M., Inoue, N., et al. (2006). Identification and characterisation of a leucine aminopeptidase from the hard tick *Haemaphysalis longicornis*. *Int. J. Parasitol.* 36, 1123–1132. doi: 10.1016/j.ijpara.2006.05.010

Hatta, T., Umemiya, R., Liao, M., Gong, H., Harnnoi, T., Tanaka, M., et al. (2007). RNA interference of cytosolic leucine aminopeptidase reduces fecundity in the hard tick, *Haemaphysalis longicornis*. *Parasitol. Res.* 100, 847–854. doi: 10.1007/s00436-006-0336-3

Hegedus, D., Erlandson, M., Gillott, C., and Toprak, U. (2009). New insights into peritrophic matrix synthesis, architecture, and function. *Annu. Rev. Entomol.* 54, 285–302. doi: 10.1146/annurev.ento.54.110807.090559

Hernandez, E. P., Kusakisako, K., Talactac, M. R., Galay, R. L., Hatta, T., Fujisaki, K., et al. (2018). Glutathione S-transferases play a role in the detoxification of flumethrin and chlorpyrifos in *Haemaphysalis longicornis*. *Parasit. Vectors* 11:460. doi: 10.1186/s13071-018-3044-9

Hewetson, R. W. (1972). The inheritance of resistance by cattle to cattle tick. *Aust. Vet. J.* 48, 299–303. doi: 10.1111/j.1751-0813.1972.tb05161.x

Higa, L. O. S., Garcia, M. V., Rodrigues, V. S., Bonatte, J. P., Piña, F. T. B., Barros, J. C., et al. (2019). Effects of cypermethrin, chlorpyrifos and piperonyl butoxide-based pour-on and spray acaricides on controlling the tick *Rhipicephalus microplus*. *Syst. Appl. Acarol.* 24, 278–286. doi: 10.11158/saa.24.2.10

Hogenkamp, D. G., Arakane, Y., Kramer, K. J., Muthukrishnan, S., and Beeman, R. W. (2008). Characterization and expression of the β-N-acetylhexosaminidase gene family of *Tribolium castaneum*. *Insect Biochem. Mol. Biol.* 38, 478–489. doi: 10.1016/j.ibmb.2007.08.002

Hollingsworth, M. A., and Swanson, B. J. (2004). Mucins in cancer: protection and control of the cell surface. *Nat. Rev. Cancer* 4, 45–60. doi: 10.1038/nrc1251

Hong, M., Kim, H., and Kim, I. (2014). Ribosomal protein L19 overexpression activates the unfolded protein response and sensitizes MCF7 breast cancer cells to endoplasmic reticulum stress-induced cell death. *Biochem. Biophys. Res. Commun.* 450, 673–678. doi: 10.1016/j.bbrc.2014.06.036

Horn, M., Nussbaumerová, M., Šanda, M., Kovárová, Z., and Srba, J., Franta, Z., et al. (2009). Hemoglobin digestion in blood-feeding ticks: mapping a multipeptidase pathway by functional proteomics. *Chem. Biol.* 16, 1053–1063. doi: 10.1016/j.chembiol.2009.09.009

Hovius, J. W. R., Levi, M., and Fikrig, E. (2008). Salivating for knowledge: potential pharmacological agents in tick saliva. *PLoS Med.* 5:e43. doi: 10.1371/journal.pmed.0050043

Huang, H. J., Liu, C. W., Xu, H. J., Bao, Y. Y., and Zhang, C. X. (2017). Mucin-like protein, a saliva component involved in brown planthopper virulence and host adaptation. *J. Insect Physiol.* 98, 223–230. doi: 10.1016/j.jinsphys.2017.01.012

Hui, M., Liu, Y., Song, C., Li, Y., Shi, G., and Cui, Z. (2014). Transcriptome changes in *Eriocheir sinensis megalopae* after desalination provide insights into osmoregulation and stress adaption in larvae. *PLoS ONE* 9:e114187. doi: 10.1371/journal.pone.0114187

Hussein, N. A., Shahein, Y. E., El-Hakim, A. E., Abouelella, A. M., Guneidy, R. A., and Hamed, R. R. (2014). Molecular cloning of Ra-sHSPI, a novel member of the HSP20 family from *Rhipicephalus annulatus* salivary glands. *Int. J. Biol. Macromol.* 67, 7–15. doi: 10.1016/j.ijbiomac.2014.02.057

Jin, L., Guo, X., Shen, C., Hao, X., Sun, P., Li, P., et al. (2018). Salivary factor LTRIN from *Aedes aegypti* facilitates the transmission of Zika virus by interfering with the lymphotoxin-β receptor. *Nat. Immunol.* 19, 342–353. doi: 10.1038/s41590-018-0063-9

Karim, S., and Adamson, S. W. (2012). "RNA interference in ticks: a functional genomics tool for the study of physiology," in *Advances in Insect Physiology*, ed E. L. Jockusch (London: Elsevier), 119–154. doi: 10.1016/B978-0-12-387680-5.00004-5

Karim, S., Singh, P., and Ribeiro, J. M. (2011). A deep insight into the sialotranscriptome of the gulf coast tick, *Amblyomma maculatum*. *PLoS ONE* 6:e28525. doi: 10.1371/journal.pone.0028525

Kerlin, R. L., and Hughes, S. (1992). Enzymes in saliva from four parasitic arthropods. *Med. Vet. Entomol.* 6, 121–126. doi: 10.1111/j.1365-2915.1992.tb00587.x

Kim, I., Xu, W., and Reed, J. C. (2008). Cell death and endoplasmic reticulum stress: disease relevance and therapeutic opportunities. *Nat. Rev. Drug Discov.* 7, 1013–1030. doi: 10.1038/nrd2755

Kurz, T., Chou, Y. C., Willems, A. R., Meyer-Schaller, N., Hecht, M. L., Tyers, M., et al. (2008). Dcn1 functions as a scaffold-type E3 ligase for cullin neddylation. *Mol. Cell* 29, 23–35. doi: 10.1016/j.molcel.2007.12.012

Langmead, B., and Salzberg, S. (2012). Fast gapped-read alignment with Bowtie 2. *Nat. Methods* 9, 357–359. doi: 10.1038/nmeth.1923

Lewis, L. A., Radulović, Ž. M., Kim, T. K., Porter, L. M., and Mulenga, A. (2015). Identification of 24 h *Ixodes scapularis* immunogenic tick saliva proteins. *Ticks Tick Borne Dis.* 6, 424–434. doi: 10.1016/j.ttbdis.2015.03.012

Lew-Tabor, A. E., Kurscheid, S., Barrero, R., Gondro, C., Moolhuijzen, P. M., Valle, M. R., et al. (2011). Gene expression evidence for off-target effects caused by RNA interference-mediated gene silencing of Ubiquitin-63E in the cattle tick *Rhipicephalus microplus*. *Int. J. Parasitol.* 41, 1001–1014. doi: 10.1016/j.ijpara.2011.05.003

Maggioli, G., Rinaldi, G., Giaudrone, I., Berasain, P., Tort, J. F., Brindley, P. J., et al. (2018). Expression, purification and characterization of two leucine aminopeptidases of the blood fluke, *Schistosoma mansoni*. *Mol. Biochem. Parasitol.* 219, 17–23. doi: 10.1016/j.molbiopara.2017.11.006

Mans, B. J., and Neitz, A. W. (2004). Adaptation of ticks to a blood-feeding environment: evolution from a functional perspective. *Insect Biochem. Mol. Biol.* 34, 1–17. doi: 10.1016/j.ibmb.2003.09.002

Marcos-Ramiro, B., García-Weber, D., and Millán, J. (2014). TNF-induced endothelial barrier disruption: beyond actin and Rho. *Thromb. Haemost.* 112, 1088–1102. doi: 10.1160/th14-04-0299

Maruyama, S. R., Garcia, G. R., Teixeira, F. R., Brandão, L. G., Anderson, J. M., Ribeiro, J. M., et al. (2017). Mining a differential sialotranscriptome of *Rhipicephalus microplus* guides antigen discovery to formulate a vaccine that reduces tick infestations. *Parasit. Vectors* 10:206. doi: 10.1186/s13071-017-2136-2

Mattioli, R. C., Bah, M., Faye, J., Kora, S., and Cassama, M. (1993). A comparison of field tick infestation on N'Dama, Zebu and N'Dama × Zebu crossbred cattle. *Vet. Parasitol.* 47, 139–148. doi: 10.1016/0304-4017(93)90184-O

Mckenna, R. V., Riding, G. A., Jarmey, J. M., Pearson, R. D., and Willadsen, P. (1998). Vaccination of cattle against the *Boophilus microplus* using a mucin-like membrane glycoprotein. *Parasite Immunol.* 20, 325–336. doi: 10.1046/j.1365-3024.1998.00149.x

McSwain, J. L., Tucker, J. S., Essenberg, R. C., and Sauer, J. R. (1989). Brain factor induced formation of inositol phosphates in tick salivary glands. *Insect Biochem.* 19, 343–349. doi: 10.1016/0020-1790(89)90038-3

Min, X. J. (2010). Evaluation of computational methods for secreted protein prediction in different eukaryotes. *J. Proteomics Bioinform.* 3, 143–147. doi: 10.4172/jpb.1000133

Morassutti, A. L., Levert, K., Pinto, P. M., da Silva, A. J., Wilkins, P., and Graeff-Teixeira, C. (2012). Characterization of *Angiostrongylus cantonensis* excretory–secretory proteins as potential diagnostic targets. *Exp. Parasitol.* 130, 26–31. doi: 10.1016/j.exppara.2011.10.003

Motobu, M., Tsuji, N., Miyoshi, T., Huang, X., Islam, M. K., Alim, M. A., et al. (2007). Molecular characterization of a blood-induced serine carboxypeptidase from the ixodid tick *Haemaphysalis longicornis*. *FEBS J.* 274, 3299–3312. doi: 10.1111/j.1742-4658.2007.05852.x

Mulenga, A., and Erikson, K. (2011). A snapshot of the *Ixodes scapularis* degradome. *Gene* 482, 78–93. doi: 10.1016/j.gene.2011.04.008

Nandi, A., Singh, H., and Singh, N. K. (2015). Esterase and glutathione S-transferase levels associated with synthetic pyrethroid resistance in *Hyalomma anatolicum* and *Rhipicephalus microplus* ticks from Punjab, India. *Exp. Appl. Acarol.* 66, 141–157. doi: 10.1007/s10493-015-9884-5

Narasimhan, S., Schuijt, T. J., Abraham, N. M., Rajeevan, N., Coumou, J., Graham, M., et al. (2017). Modulation of the tick gut milieu by a secreted tick protein favors *Borrelia burgdorferi* colonization. *Nat. Commun.* 8:184. doi: 10.1038/s41467-017-00208-0

Oleaga, A., Obolo-Mvoulouga, P., Manzano-Román, R., and Pérez-Sánchez, R. (2017). A proteomic insight into the midgut proteome of *Ornithodoros moubata* females reveals novel information on blood digestion in argasid ticks. *Parasit. Vectors* 10:366. doi: 10.1186/s13071-017-2300-8

Ong, C. T., Rodriguez-Valle, M., Barrero, R. A., Hunter, A., Bellgard, M. I., and Lew-Tabor, A. E. (2016). Exploring the transcriptomic data of the Australian paralysis tick, *Ixodes holocyclus*. *GSTF J. Vet. Sci.* 3. doi: 10.5176/2345-7880_3.1.14

Overgaard, J., Kristensen, T. N., and Sørensen, J. G. (2012). Validity of thermal ramping assays used to assess thermal tolerance in arthropods. *PLoS ONE* 7:e32758. doi: 10.1371/journal.pone.0032758

Pereira, M. H., Paim, R. M., Lahondère, C., and Lazzari, C. R. (2017). "Heat shock proteins and blood-feeding in arthropods," in *Heat Shock Proteins in Veterinary Medicine and Sciences*, eds A. A. A. Asea and P. Kaur (Cham: Springer), 349–359. doi: 10.1007/978-3-319-73377-7_13

Phelan, P., and Starich, T. A. (2001). Innexins get into the gap. *Bioessays* 23, 388–396. doi: 10.1002/bies.1057

Piacenza, L., Acosta, D., Basmadjian, I., Dalton, J. P., and Carmona, C. (1999). Vaccination with cathepsin L proteinases and with leucine aminopeptidase induces high levels of protection against fascioliasis in sheep. *Infect. Immun.* 67, 1954–1961.

Rabut, G., and Peter, M. (2008). Function and regulation of protein neddylation. *EMBO Rep.* 9, 969–976. doi: 10.1038/embor.2008.183

Radulović, Ž. M., Kim, T. K., Porter, L. M., Sze, S. H., Lewis, L., and Mulenga, A. (2014). A 24-48 h fed *Amblyomma americanum* tick saliva immuno-proteome. *BMC Genomics* 15:518. doi: 10.1186/1471-2164-15-518

Ramamoorthi, N., Narasimhan, S., Pal, U., Bao, F., Yang, X. F., Fish, D., et al. (2005). The Lyme disease agent exploits a tick protein to infect the mammalian host. *Nature* 436, 573–577. doi: 10.1038/nature03812

Richards, S. A., Stutzer, C., Bosman, A. M., and Maritz-Olivier, C. (2015). Transmembrane proteins–mining the cattle tick transcriptome. *Ticks Tick Borne Dis.* 6, 695–710. doi: 10.1016/j.ttbdis.2015.06.002

Rodríguez-Mallon, A., Encinosa, P. E., Méndez-Pérez, L., Bello, Y., Fernández, R. R., Garay, H., et al. (2015). High efficacy of a 20 amino acid peptide of the acidic ribosomal protein P0 against the cattle tick, *Rhipicephalus microplus*. *Ticks Tick Borne Dis.* 6, 530–537. doi: 10.1016/j.ttbdis.2015.04.007

Rodriguez-Valle, M., Moolhuijzen, P., Barrero, R. A., Ong, C. T., Busch, G., Karbanowicz, T., et al. (2018). Transcriptome and toxin family analysis of the paralysis tick, *Ixodes holocyclus*. *Int. J. Parasitol.* 48, 71–82. doi: 10.1016/j.ijpara.2017.07.007

Sakata, E., Yamaguchi, Y., Miyauchi, Y., Iwai, K., Chiba, T., Saeki, Y., et al. (2007). Direct interactions between NEDD8 and ubiquitin E2 conjugating enzymes upregulate cullin-based E3 ligase activity. *Nat. Struct. Mol. Biol.* 14, 167–168. doi: 10.1038/nsmb1191

Sasaki, S. D., de Lima, C. A., Lovato, D. V., Juliano, M. A., Torquato, R. J., and Tanaka, A. S. (2008). BmSI-7, a novel subtilisin inhibitor from *Boophilus microplus*, with activity toward Pr1 proteases from the fungus *Metarhizium anisopliae*. *Exp. Parasitol.* 118, 214–220. doi: 10.1016/j.exppara.2007.08.003

Schulze-Lefert, P., and Panstruga, R. (2011). A molecular evolutionary concept connecting nonhost resistance, pathogen host range, and pathogen speciation. *Trends Plant Sci.* 16, 117–125. doi: 10.1016/j.tplants.2011.01.001

Shahein, Y. E., El-Rahim, M. T. A., Hussein, N. A., Hamed, R. R., El-Hakim, A. E., and Barakat, M. M. (2010). Molecular cloning of a small heat shock protein (sHSPII) from the cattle tick *Rhipicephalus* (*Boophilus*) *annulatus* salivary gland. *Int. J. Biol. Macromol.* 47, 614–622. doi: 10.1016/j.ijbiomac.2010.08.006

Simão, F. A., Waterhouse, R. M., Ioannidis, P., Kriventseva, E. V., and Zdobnov, E. M. (2015). BUSCO: assessing genome assembly and annotation completeness with single-copy orthologs. *Bioinformatics* 31, 3210–3212. doi: 10.1093/bioinformatics/btv351

Simiczyjew, A., Mazur, A. J., Dratkiewicz, E., and Nowak, D. (2017). Involvement of β-and γ-actin isoforms in actin cytoskeleton organization and migration abilities of bleb-forming human colon cancer cells. *PLoS ONE* 12:e0173709. doi: 10.1371/journal.pone.0173709

Sinha, D. K., Chandran, P., Timm, A. E., Aguirre-Rojas, L., and Smith, C. M. (2016). Virulent *Diuraphis noxia* aphids over-express calcium signaling proteins to overcome defenses of aphid-resistant wheat plants. *PLoS ONE* 11:e0146809. doi: 10.1371/journal.pone.0146809

Stark, B. C., Lanier, M. H., and Cooper, J. A. (2017). CARMIL family proteins as multidomain regulators of actin-based motility. *Mol. Biol. Cell* 28, 1713–1723. doi: 10.1091/mbc.e17-01-0019

Stutzer, C., van Zyl, W. A., Olivier, N. A., Richards, S., and Maritz-Olivier, C. (2013). Gene expression profiling of adult female tissues in feeding *Rhipicephalus microplus* cattle ticks. *Int. J. Parasitol.* 43, 541–554. doi: 10.1016/j.ijpara.2013.01.009

Syed, Z. A., Härd, T., Uv, A., and van Dijk-Härd, I. F. (2008). A potential role for Drosophila mucins in development and physiology. *PLoS ONE* 3:e3041. doi: 10.1371/journal.pone.0003041

Tan, A. W., Francischetti, I. M., Slovak, M., Kini, R. M., and Ribeiro, J. M. (2015). Sexual differences in the sialomes of the zebra tick, *Rhipicephalus pulchellus*. *J. Proteom* 117, 120–144. doi: 10.1016/j.jprot.2014.12.014

Tirloni, L., Reck, J., Terra, R. M. S., Martins, J. R., Mulenga, A., Sherman, N. E., et al. (2014). Proteomic analysis of cattle tick *Rhipicephalus (Boophilus) microplus* saliva: a comparison between partially and fully engorged females. *PLoS ONE* 9:e94831. doi: 10.1371/journal.pone.0094831

Trager, W. (1939). Acquired immunity to ticks. *J. Parasitol.* 25, 57–81. doi: 10.2307/3272160

Trainor, P. A., and Merrill, A. E. (2014). Ribosome biogenesis in skeletal development and the pathogenesis of skeletal disorders. *Biochim. Biophys. Acta Mol. Basis Dis.* 1842, 769–778. doi: 10.1016/j.bbadis.2013.11.010

Tsubokawa, D., Hatta, T., Kikuchi, T., Maeda, H., Mikami, F., Alim, M. A., et al. (2017). Venestatin, a Ca^{++}-binding protein from the parasitic nematode *Strongyloides venezuelensis*, is involved in the larval migration process. *Int. J. Parasitol.* 47, 501–509. doi: 10.1016/j.ijpara.2017.01.008

Turk, B. (2006). Targeting proteases: successes, failures and future prospects. *Nat. Rev. Drug Discov.* 5, 785–799. doi: 10.1038/nrd2092

Van Cromphaut, S. J. (2009). Hyperglycaemia as part of the stress response: the underlying mechanisms. *Best Pract. Res. Clin. Anaesthesiol.* 23, 375–386. doi: 10.1016/j.bpa.2009.08.005

Vedula, P., and Kashina, A. (2018). The makings of the 'actin code': regulation of actin's biological function at the amino acid and nucleotide level. *J. Cell Sci.* 131:jcs215509. doi: 10.1242/jcs.215509

Vora, A., Taank, V., Dutta, S. M., Anderson, J. F., Fish, D., Sonenshine, D. E., et al. (2017). Ticks elicit variable fibrinogenolytic activities upon feeding on hosts with different immune backgrounds. *Sci. Rep.* 7:44593. doi: 10.1038/srep44593

Wang, H., Zhang, X., Wang, X., Wang, M., Yang, X., Han, X., et al. (2019). Comprehensive analysis of the global protein changes that occur during salivary gland degeneration in female ixodid ticks *Haemaphysalis longicornis*. *Front. Physiol.* 9:1943. doi: 10.3389/fphys.2018.01943

Wang, J., and Maldonado, M. A. (2006). The ubiquitin-proteasome system and its role in inflammatory and autoimmune diseases. *Cell Mol. Immunol.* 3, 255–261.

Wang, X., Jiang, W., Kang, J., Liu, Q., and Nie, M. (2015). Knockdown of RhoA expression alters ovarian cancer biological behavior *in vitro* and in nude mice. *Oncol. Rep.* 34, 891–899. doi: 10.3892/or.2015.4009

Weisheit, S., Villar, M., Tykalová, H., Popara, M., Loecherbach, J., et al. (2015). *Ixodes scapularis* and *Ixodes ricinus* tick cell lines respond to infection with tick-borne encephalitis virus: transcriptomic and proteomic analysis. *Parasit. Vectors* 8:599. doi: 10.1186/s13071-015-1210-x

Williams, D. B. (2006). Beyond lectins: the calnexin/calreticulin chaperone system of the endoplasmic reticulum. *J. Cell Sci.* 119, 615–623. doi: 10.1242/jcs.02856

Wüthrich, M., Brandhorst, T. T., Sullivan, T. D., Filutowicz, H., Sterkel, A., Stewart, D., et al. (2015). Calnexin induces expansion of antigen-specific $CD4^+$ T cells that confer immunity to fungal ascomycetes via conserved epitopes. *Cell Host Microbe* 17, 452–465. doi: 10.1016/j.chom.2015.02.009

Xu, Y., Bruno, J. F., and Luft, B. J. (2005). Identification of novel tick salivary gland proteins for vaccine development. *Biochem. Biophys. Res. Commun.* 326, 901–904. doi: 10.1016/j.bbrc.2004.11.127

Xu, Y., Wu, J., Fu, S., Li, C., Zhu, Z. R., and Zhou, X. (2015). Rice stripe tenuivirus nonstructural protein 3 hijacks the 26S proteasome of the small brown planthopper via direct interaction with regulatory particle non-ATPase subunit 3. *J. Virol.* 89, 4296–4310. doi: 10.1128/JVI.03055-14

Yang, C., Pring, M., Wear, M. A., Huang, M., Cooper, J. A., Svitkina, T. M., et al. (2005). Mammalian CARMIL inhibits actin filament capping by capping protein. *Dev. Cell* 9, 209–221. doi: 10.1016/j.devcel.2005.06.008

Yang, Y., Waters, J. B., Frueh, K., and Peterson, P. A. (1992). Proteasomes are regulated by interferon gamma: implications for antigen processing. *Proc. Natl. Acad. Sci. U.S.A.* 89, 4928–4932. doi: 10.1073/pnas.89.11.4928

You, M., and Fujisaki, K. (2009). Vaccination effects of recombinant chitinase protein from the hard tick *Haemaphysalis longicornis* (Acari: Ixodidae). *J. Vet. Med. Sci.* 71, 709–712. doi: 10.1292/jvms.71.709

Zhang, H., Forman, H. J., and Choi, J. (2005). Gamma-glutamyl transpeptidase in glutathione biosynthesis. *Methods Enzymol.* 401, 468–483. doi: 10.1016/S0076-6879(05)01028-1

Zhang, X., Kuramitsu, Y., Ma, A., Zhang, H., and Nakamura, K. (2016). Endoplasmic reticulium protein profiling of heat-stressed Jurkat cells by one dimensional electrophoresis and liquid chromatography tandem mass spectrometry. *Cytotechnology* 68, 1103–1113. doi: 10.1007/s10616-015-9867-8

Zhao, J., Chi, Y., Zhang, X. J., Lei, T., Wang, X. W., and Liu, S. S. (2019). Comparative proteomic analysis providesnew insight into differential transmission of two begomoviruses by a whitefly. *Virol. J.* 16:32. doi: 10.1186/s12985-019-1138-4

Conflict of Interest: The authors declare that the research was conducted in the absence of any commercial or financial relationships that could be construed as a potential conflict of interest.

frontiers in Cellular and Infection Microbiology

ORIGINAL RESEARCH
published: 28 January 2020
doi: 10.3389/fcimb.2020.00007

A Peroxiredoxin From the *Haemaphysalis longicornis* Tick Affects Langat Virus Replication in a Hamster Cell Line

Kodai Kusakisako[1,2†], *Haruki Morokuma*[2†], *Melbourne Rio Talactac*[3], *Emmanuel Pacia Hernandez*[2,4], *Kentaro Yoshii*[5] *and Tetsuya Tanaka*[2,4*]

[1] *Laboratory of Parasitology, Department of Disease Control, Graduate School of Veterinary Medicine, Hokkaido University, Sapporo, Japan,* [2] *Laboratory of Infectious Diseases, Joint Faculty of Veterinary Medicine, Kagoshima University, Kagoshima, Japan,* [3] *Department of Clinical and Population Health, College of Veterinary Medicine and Biomedical Sciences, Cavite State University, Indang, Philippines,* [4] *Department of Pathological and Preventive Veterinary Science, The United Graduate School of Veterinary Science, Yamaguchi University, Yamaguchi, Japan,* [5] *Laboratory of Public Health, Faculty of Veterinary Medicine, Hokkaido University, Sapporo, Japan*

OPEN ACCESS

Edited by:
Lucas Tirloni, National Institute of Allergy and Infectious Diseases (NIAID), United States

Reviewed by:
Jeff Grabowski, Rocky Mountain Laboratories (NIAID), United States
Meghan Hermance, Upstate Medical University, United States

***Correspondence:**
Tetsuya Tanaka
k6199431@kadai.jp

[†] *These authors have contributed equally to this work*

Specialty section:
This article was submitted to Parasite and Host, a section of the journal Frontiers in Cellular and Infection Microbiology

Received: *05 October 2019*
Accepted: *09 January 2020*
Published: *28 January 2020*

Citation:
Kusakisako K, Morokuma H, Talactac MR, Hernandez EP, Yoshii K and Tanaka T (2020) A Peroxiredoxin From the Haemaphysalis longicornis Tick Affects Langat Virus Replication in a Hamster Cell Line. Front. Cell. Infect. Microbiol. 10:7. doi: 10.3389/fcimb.2020.00007

Ticks are hematophagous arthropods, and their blood feeding on vertebrate hosts is essential for their development. The vertebrate blood contains high levels of free iron that can react with oxygen in ticks, resulting in the production of hydrogen peroxide (H_2O_2), one of the reactive oxygen species. Peroxiredoxins (Prxs), H_2O_2-scavenging enzymes, take on an important role in the ticks' oxidative stress coping mechanism. Ticks also transmit several disease-causing pathogens, including tick-borne encephalitis virus (TBEV), in animals and humans. Therefore, the control of ticks and tick-borne pathogens is a key issue that needs to be addressed. Infection with an arthropod-borne flavivirus is known to induce oxidative stress in insect cells. We hypothesize that vector-derived Prxs could have an effect on the infection and/or replication of flaviviruses in the hosts, since ticks Prxs are possibly transmitted from ticks to their hosts. In this study, we established stable strains of baby hamster kidney (BHK) cells expressing two types of H_2O_2-scavenging Prxs from the hard tick *Haemaphysalis longicornis* (BHK-HlPrx and BHK-HlPrx2 cells). Although the infection of TBEV surrogate Langat virus (LGTV) did not induce H_2O_2 production in normal BHK cells, the mortality rate and the virus titer of LGTV infected BHK-HlPrx cells increased. In addition, HlPrx proteins in BHK cells can facilitate LGTV replication in cells, while HlPrx2 proteins in BHK cells cannot. The results also demonstrated that this facilitation of LGTV replication by the 1-Cys Prx in the BHK cells is not by scavenging H_2O_2 but by an unknown mechanism. In order to understand this mechanism, more studies using tick-derived cells and ticks are necessary.

Keywords: tick, peroxiredoxins, tick-derived molecule in the host, host–virus interaction, langat virus

INTRODUCTION

Ticks are obligate hematophagous ectoparasites and require blood feeding throughout their life cycle, except in the egg stage. The process from blood-feeding to blood-digestion lead to providing nutrition to ticks and activating tick life cycles including development, molting, and embryogenesis (Grandjean, 1983). Ticks feed on vertebrate blood that contains high levels of iron, like heme,

and ferrous iron (Galay et al., 2014). In addition, ticks concentrate host-derived blood with iron, leading to a high concentration of iron in ticks. The concentrated iron can react with oxygen in the tick's body, resulting in high levels of reactive oxygen species (ROS), including hydrogen peroxide (H_2O_2) (Citelli et al., 2007; Galay et al., 2015). A high concentration of H_2O_2 causes oxidative damage to biopolymers, such as membrane lipids, nucleic acids, and proteins, leading to harmful effects on aerobic organisms (Robinson et al., 2010). Ticks have antioxidant enzymes that scavenge H_2O_2, like peroxiredoxins (Prxs) (Tsuji et al., 2001; Kusakisako et al., 2016a), catalases (Kumar et al., 2016), and selenoproteins (Adamson et al., 2014). Reports have demonstrated that the knockdown of these H_2O_2-scavenging enzyme genes has an inhibition effect on tick blood feeding and/or reproduction (Adamson et al., 2014; Kumar et al., 2016; Kusakisako et al., 2016a). Therefore, the antioxidant enzymes controlling the H_2O_2 concentration in ticks can be considered to be important in tick blood feeding and reproduction (Kusakisako et al., 2018a).

On the other hand, ticks are vectors of pathogens with economic importance to humans and animals, such as viruses, protozoa, and bacteria (Hoogstraal, 1985). H_2O_2-scavenging enzymes, such as Prxs, catalases, and selenoproteins, also have been analyzed in ticks to comprehend the interaction between the antioxidant enzymes and tick-borne pathogens (Narasimhan et al., 2007; Budachetri et al., 2017a,b). A Prx homologous protein (Salp25D) derived from the salivary glands of an *Ixodes scapularis* tick facilitates *Borrelia* to escape from neutrophil oxidation in the vertebrate host, resulting in successful transmission of the parasites from tick to host (Narasimhan et al., 2007). In addition, silencing of the *catalase* gene and inhibition of that protein resulted to the low transmission of *Rickettsia parkeri* to eggs of *Amblyomma maculatum* ticks (Budachetri et al., 2017b). Furthermore, the gene silencing of a selenocysteine insertion sequence (SECIS) binding protein (*SBP2*), involved in selenoprotein synthesis, significantly diminished the transovarial transmission of *R. parkeri* parasites to eggs in *A. maculatum* ticks (Budachetri et al., 2017a). Thus, these enzymes are also important to the vector competency of ticks with regard to horizontal transmission and transovarial transmission (Kusakisako et al., 2018a; Hernandez et al., 2019).

Tick-borne flaviviruses (TBFVs) induce considerable disease and death worldwide. Infections are characterized by mild to severe neurological symptoms, like meningitis and encephalitis (Weber et al., 2014; Mlera et al., 2015). In Europe, Russia, and Far East, including Japan, tick-borne encephalitis virus (TBEV) is considered one of the most medically important arboviruses, with 10,000 to 15,000 cases recorded each year (Lindquist and Vapalahti, 2008; Weber et al., 2014). Since most TBFVs require at least a biosafety level 3 (BSL3) containment facility, use of Langat virus (LGTV), a TBFV of low neurovirulence, provides a convenient BSL2 model of TBEV and other highly pathogenic TBFVs (Mlera et al., 2015). The Dengue virus, a known mosquito-borne flavivirus, requires the *catalase* gene to invade the mosquito midgut (Oliveira et al., 2017). Furthermore, some reports have demonstrated that mammalian cells which were infected with some arbovirus, such as Togaviridae, or expressing nonstructural proteins derived from TBEV were induced the production of ROS (Kuzmenko et al., 2016; Camini et al., 2017). These reports suggest that the H_2O_2-scavenging enzymes could also be important in the vector competency of arthropod-borne viruses.

Among these H_2O_2-scavenging enzymes in ticks, Prxs have been well-characterized in tick biology and in relationship to tick pathogens (Tsuji et al., 2001; Narasimhan et al., 2007; Kusakisako et al., 2016a, 2018a,b). Furthermore, Narasimhan et al. (2007) demonstrated that one tick Prx facilitate the transmission of pathogen from ticks to their host. Therefore, we considered that tick Prxs could be important for the interaction between ticks and tick-borne pathogens in the host. In this study, we established tick Prxs–expressing mammalian cells and investigated the interaction between tick-derived Prxs and LGTV infection in the mammalian cells.

MATERIALS AND METHODS

Cell Culture and Virus

Baby hamster kidney (BHK-21) cells (ATCC CCL-10) were maintained in Eagle's minimum essential medium (EMEM) (Wako Pure Chemical Industries, Ltd., Osaka, Japan) containing 5% fetal bovine serum (FBS) (Equitech-Bio, Kerrville, TX, USA) and 1% antibiotic/antimycotic (Nacalai Tesque, Kyoto, Japan). The cells were maintained at 37°C under 5% CO_2 until use.

The LGTV TP21 used in this study was amplified in BHK cells, and the virus stock titer was determined via focus forming assay as previously described (Talactac et al., 2016). The virus stock was aliquoted and stored at −80°C until use.

Construction of *Haemaphysalis longicornis* Tick-Derived Prx Gene Expression Vectors Using the *H. longicornis actin* (*HlAct*) Promoter Region

Prxs can be classified into two groups in accordance with the presence of one or two conserved cysteines, 1-Cys or 2-Cys Prxs (Hall et al., 2011). In hard ticks, especially *H. longicornis*, some previous reports on tick Prxs have focused on 1-Cys Prx (HlPrx) (Tsuji et al., 2001), and 2-Cys Prx (HlPrx2) (Kusakisako et al., 2016a,b).

To construct *H. longicornis* tick-derived Prx (*HlPrx* and *HlPrx2*) gene expression vectors using an *HlAct* promoter region, the human phosphoglycerate kinase (PGK) promoter of the pmirGLO plasmid (Promega, Madison, WI, USA) was replaced with an *HlAct* promoter region as previously described (Kusakisako et al., 2018b), with some modifications. The reason we constructed the gene expression vectors using a tick-derived promoter was that tick-derived molecules were considered to be compatible with the tick-derived promoter for foreign protein expression in the host cells. The pmirGLO vector was double digested using *Bgl*II and *Xho*I, and the PGK promoter and luciferase sequence were removed from the pmirGLO plasmid (pmirGLO-no pro-no Luc). The plasmid was purified using the NucleoSpin® Gel PCR Clean-up Kit (Macherey-Nagel, Düren, Germany). The *HlAct* promoter region or *HlPrx* and

TABLE 1 | Oligonucleotide primer sequences used for the construction of plasmids.

Primer	Sequence (5′→ 3′)
pmirGLO-*Bgl* II-*HlAct*-F	AGAGGATCGAGATCTGGCTTCGGACGAAGGCC
pmirGLO-*HlAct*-Kozak-FLAG-R	CTTGTCGTCGTCGTCCTTGTAGTCCATGTTGACTGT TTAGCTGCA
FLAG-HlPrx-F	ATGGACTACAAGGACGACGACGACAAGGGCGGC GGCATGCCTCCC
HlPrx-*Xho* I-R	GACTCTAGACTCGAGCTAATCCATGGTGGTGCGAAG GTAC
FLAG-HlPrx2-F	ATGGACTACAAGGACGACGACGACAAGGGCGGC GGCATGGACGTG
HlPrx2-*Xho* I-R	GACTCTAGACTCGAGCTATTGTTTGGCGAAGTAGGCC

Underlines denote the restriction enzyme recognition site that was included in its primer name. A double underline denotes the estimated Kozak consensus sequence in Haemaphysalis longicornis. Broken underlines denote the spacer sequence.

HlPrx2 genes with a FLAG-tag were amplified by polymerase chain reaction (PCR) using KOD-Plus-Neo (Toyobo, Osaka, Japan) with pmirGLO-*Bgl* II-*HlAct*-F and pmirGLO-*HlAct*-kozak-FLAG-R primers for the *HlAct* promoter region, FLAG-HlPrx-F and HlPrx-*Xho* I-R primers for the *HlPrx* gene, and FLAG-HlPrx2-F and HlPrx2-*Xho* I-R primers for the *HlPrx2* gene (**Table 1**). These PCR products were purified using the NucleoSpin® Gel PCR Clean-up Kit (Macherey-Nagel). The pmirGLO-no pro-no Luc plasmid and the purified PCR products were mixed with a 5× Infusion Enzyme (Takara, Shiga, Japan) and incubated at 50°C for 15 min. The pmirGLO-*HlAct* pro-*HlPrx* and pmirGLO-*HlAct* pro-*HlPrx2* plasmids were transformed into an *Escherichia coli* stellar strain, and the plasmid was then increased and purified using the Qiagen® Plasmid Midi Kit (Qiagen, Hilden, Germany) as previously described (Kusakisako et al., 2018b).

Transfection of Plasmid Vectors Into BHK Cells and Establishment of HlPrx-Expressed BHK Cells Using Antibiotic G418

BHK cells were seeded in a 6-well plate at 2 ml/well of 1.5×10^5 cells/ml and incubated at 37°C overnight. The plasmid vector (6 μg/well), 120 μl of Opti-MEM (Gibco, Grand Island, NY, USA), and 12 μl of HilyMax (Dojindo, Kumamoto, Japan) were mixed and incubated at room temperature (RT) for 15 min. Then the incubated mixture was added to the culture medium in each well, and the cells were incubated at 37°C for 16 h. After 16 h, 2 ml of the medium was added to each well, and the cells were further incubated for 32 h.

After transfection of the HlPrx-expressed plasmids to BHK cells, the supernatant was removed, and the medium with 1 mg/ml G-418 Sulfate Solution (Geneticin, Wako Pure Chemical Industries, Ltd.) was added every third day until the cells were confluent (around 10 days). G418 was used for the drug selection, since the pmirGLO plasmid originally has a G418-resistant gene. The confluent cells were transferred into a 96-well plate at 0.1 ml/well of 8 cells/ml and incubated at 37°C for 3 days. After 3 days, 0.1 ml of the medium with 0.3 mg/ml G418 was added to each well. The supernatant was replaced, and the medium containing 0.3 mg/ml G418 was replaced every third day until the single cell was colonized. The single-cell colony was transferred to a larger culture plate and flask. Finally, the drug-selected and HlPrx-expressing BHK cells (BHK-HlPrx and BHK-HlPrx2, respectively) were obtained. In addition, BHK cells used as a control cells following experiments did not go through the transfection process as described above.

Protein Extraction and Western Blotting

To confirm the FLAG-tagged HlPrx and HlPrx2 proteins in BHK cells, immunostaining was performed. The obtained BHK cells were collected and suspended in phosphate buffered saline (PBS) and sonicated for 6 min at 45 kHz using a VS-100III ultrasonic cleaner (AS ONE Corporation, Osaka, Japan) and then centrifuged at 22,140 ×*g*. The supernatant was resolved in SDS-polyacrylamide gel electrophoresis (SDS-PAGE) gel under reducing conditions. After SDS-PAGE, the proteins were transferred onto a polyvinylidene difluoride (PVDF) membrane (Immobilon®-P, Millipore, Danvers, MA, USA). The membranes were blocked for 1 h at RT with 0.3% skim milk in PBS containing 0.05% Tween 20 (PBS-T, blocking solution); they were incubated with 1:1,000 dilutions of Anti-DDDDK-tag pAb (rabbit, MBL, Nagoya, Japan) against FLAG-tagged HlPrx; and HlPrx2 proteins in a blocking solution at 4°C overnight. For loading control, α-tubulin was detected using a monoclonal anti-α-tubulin antibody (mouse, Sigma-Aldrich, St. Louis, MO, USA). After washing three times in PBS-T, the membranes were incubated with a 1:50,000 dilution of horseradish peroxidase (HRP)-conjugated goat anti-rabbit or anti-mouse immunoglobulins (Dako, Glostrup, Denmark) in a blocking solution at RT for 1 h. After washing three times in PBS-T, bands were detected using Amersham™ ECL™ Prime Western Blotting Detection Reagent (GE Healthcare, Buckinghamshire, UK) and viewed using FluorChem® FC2 software (Alpha Innotech, San Leandro, CA, USA).

Detection of H_2O_2 Using BES-H_2O_2-Ac in BHK Cells

The intracellular H_2O_2 detection in BHK cells was performed using BES-H_2O_2-Ac (Wako Pure Chemical Industries, Ltd.) as previously described (Kusakisako et al., 2018b), with some modifications. BHK, BHK-HlPrx, and BHK-HlPrx2 cells were seeded in a 24-well plate at 500 μl/well of 1.5×10^5 cells/ml and incubated overnight at 37°C. After removing the supernatants, the cells were washed with 500 μl of PBS in each well. After washing the cells, the supernatants were replaced with 5 μM BES-H_2O_2-Ac and 1 μM Hoechst 33342 (Dojindo) in a culture medium without FBS and incubated at 37°C for 30 min. The cells were washed again with PBS, and then the supernatants were replaced with 0.05% H_2O_2 in a culture medium and incubated at 37°C for 30 min. After exposure to H_2O_2, the cells were washed with PBS, and the supernatants were replaced with the culture medium. The cells were observed under a fluorescent microscope (IX71, Olympus, Tokyo, Japan). Furthermore, to measure the

fluorescence intensities of H_2O_2 in the cells, the cells were collected using 120 μl of 0.25% Trypsin-EDTA solution (Wako Pure Chemical Industries, Ltd.). The collected cells (100 μl) were transferred to a 96-well plate to measure their fluorescence. Fluorescence was detected using a microplate reader (SH-9000Lab, Corona Electric, Ibaraki, Japan) with excitation at 480 nm and emission at 535 nm for BES-H_2O_2-Ac and with excitation at 352 nm and emission at 461 nm for Hoechst 33342.

Cell Survival Assays After the H_2O_2 Treatment of BHK Cells

After H_2O_2 treatment, the BHK cells (20 μl) were used for *in vitro* cell survival assay (Strober, 2001). The cells were mixed with 20 μl of Trypan blue (Nacalai Tesque). Then the ratio between the surviving and dead Trypan blue–stained cells was determined using a hemocytometer.

Cell Survival Assays After LGTV Infected BHK Cells

To measure the cell survival rate of the LGTV-infected BHK cells and the BHK-HlPrx and BHK-HlPrx2 cells, the normal BHK, BHK-HlPrx, and BHK-HlPrx2 cells were seeded in a 24-well plate at 500 μl/well of 4.0×10^5 cells/ml and incubated overnight at 37°C. The supernatants were replaced with a culture medium containing 0.01 multiplicity of infection (MOI) of LGTV and incubated for 1 h at 37°C. For each assay, cells were either infected with LGTV or were mock-infected with control medium. The cells were washed with PBS to remove the unabsorbed viruses. Then the plates were incubated at 37°C for 3 days. To collect the dead cells during this experiment, the supernatants were collected and centrifuged at 100 ×*g*. The supernatants for the measurement of virus titers were collected in new tubes and stored at −30°C until use. The live cells attached to the plate were collected using 100 μl of 0.25% Trypsin-EDTA (Wako Pure Chemical Industries, Ltd.). Finally, the centrifuged detached cells and the collected attached cells were mixed. The counting of the live and dead cells was performed as mentioned above.

Titration of LGTV in the Supernatant Using a Focus Forming Assay

The LGTV used in this study was amplified in BHK, BHK-HlPrx, and BHK-HlPrx2 cells, and the virus titers were determined by focus forming assay as previously described (Talactac et al., 2016). Briefly, serial 10-fold dilutions of the cultured supernatants were plated on 4.0×10^5 cells/well of BHK cells in 24-well plates and incubated at 37°C for 1 h. After washing with PBS, the infected cells were overlaid with 1.5% methylcellulose containing modified Eagle's medium (MEM) (Gibco) with 1% FBS and 1% antibiotic/antimycotic and incubated at 37°C for 4 days. The supernatants were removed, and the cells were fixed by a 4% paraformaldehyde phosphate buffer solution (pH 7.4) at RT for 30 min. The fixed cells were blocked by 5% skim milk in PBS at RT for 1 h. After washing with PBS, viral foci were detected by a primary antibody against Langat virus in mice (1:1,000 dilution), followed by Alexa Fluor® 594 goat antimouse IgG (1:1,000 dilution, Invitrogen, Carlsbad, CA, USA). For taking photos, we decided the maximum exposure time using the LGTV uninfected BHK cells, and then, the photos of the experimental groups were taken under the maximum exposure time. The foci were counted using a fluorescence microscope (IX71, Olympus), and the virus titers of the cultured supernatant derived from BHK, BHK-HlPrx, and BHK-HlPrx2 cells were expressed as focus-forming unit (FFU) per milliliter (FFU/ml).

Statistical Analysis

All experiments were done at least three times. The results are shown as average ± standard deviation (SD). A one-way ANOVA test was applied to the obtained data, and statistically significant differences ($p < 0.001$) in each group were demonstrated. For pair comparisons within groups, Tukey's test was applied. In contrast, the statistical comparison between two groups of the same cells was analyzed using Welch's *t*-test. $P < 0.05$ was considered to be a statistically significant difference.

RESULTS

Detection of FLAG-Tagged HlPrxs in Transfected BHK Cells Using Western Blotting

To detect FLAG-tagged HlPrx and HlPrx2 in the transfected BHK cells (BHK-HlPrx and BHK-HlPrx2 cells), Western blotting was performed using an anti-FLAG-tag antibody as a primary antibody. Western blotting demonstrated that the FLAG-tagged HlPrx and HlPrx2 in BHK cells were detected with molecular weights of 25.7 kDa (white arrowhead) and 23.5 kDa (black arrowhead), respectively (**Figure 1**). On the other hand, in the normal BHK cells, FLAG-tagged HlPrxs were not detected. These results demonstrated that the HlPrx- or HlPrx2-expressing plasmid-transfected BHK cell lines (BHK-HlPrx and BHK-HlPrx2 cells) expressed a certain Prx protein in the cells.

Antioxidant Activity of BHK-HlPrx and BHK-HlPrx2 Cells Against H_2O_2 Exposure

To evaluate the antioxidant activity of BHK-HlPrx and BHK-HlPrx2 cells against H_2O_2, the detection of intracellular H_2O_2 in the BHK cells was conducted using a BES-H_2O_2-Ac probe. The BHK cells were incubated with 5 μM BES-H_2O_2-Ac and 1 μM Hoechst 33342, and then the cells were exposed to 0.05% H_2O_2. The cells were observed under fluorescence microscopy, while the fluorescent intensities in BHK cells were measured using the microplate reader. Fluorescent microscopy revealed that the fluorescence of the intracellular H_2O_2 in the BHK-HlPrx and BHK-HlPrx2 cells was of lower intensity than that in BHK cells (**Figure 2A**, H_2O_2), even though without the addition of external H_2O_2, the H_2O_2 fluorescence in the BHK-HlPrx and BHK-HlPrx2 cells seemed to be weaker than that in the BHK cells (**Figure 2B**, Normal). In addition, the microplate reader fluorescence intensity measurement showed that the intracellular H_2O_2 in the BHK-HlPrx and BHK-HlPrx2 cells had significantly lower relative intensities as compared with the BHK cells in both the normal and H_2O_2-exposed states (**Figure 2B**). In each

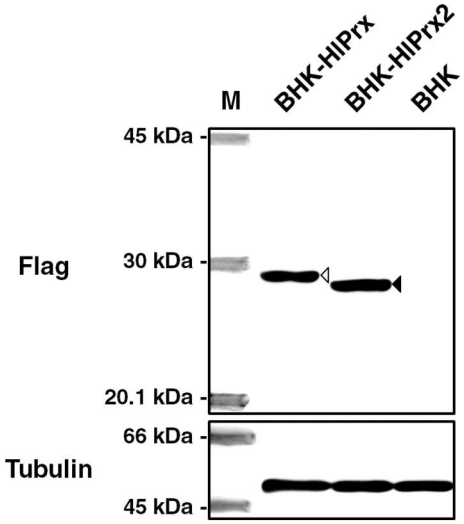

FIGURE 1 | Detection of FLAG-tagged HlPrxs in transfected BHK cells using Western blotting. The left column indicates the specific antibody against FLAG-tagged HlPrx and HlPrx2 proteins or α-tubulin in BHK cells. The upper rows show the BHK cell lines. The white arrowhead indicates the FLAG-tagged HlPrx protein (∼25.7 kDa), while the black arrowhead indicates the FLAG-tagged HlPrx2 protein (∼23.5 kDa). The α-tubulin protein served as a loading control. M, molecular weight Marker; BHK-HlPrx, *Haemaphysalis longicornis* 1-Cys peroxiredoxin-expressing baby hamster kidney cells; BHK-HlPrx2, *H. longicornis* 2-Cys peroxiredoxin-expressing baby hamster kidney cells.

cell line, the fluorescence intensities of H_2O_2 in the BHK cells significantly increased with exposure to 0.05% H_2O_2 (**Figure 2B**, Normal vs. H_2O_2).

To evaluate the mortality rate among three cell lines cultured with or without H_2O_2, Trypan blue assays were conducted. The Trypan blue assays revealed that the mortality rate of BHK-HlPrx2 cells was significantly lower than that of BHK cells under the H_2O_2 treatment (**Figure 2C**, H_2O_2). In addition, the mortality rate of BHK-HlPrx and BHK cells in the H_2O_2-exposed state was significantly higher than in the normal state (**Figure 2C**). These results suggested that HlPrxs decrease the H_2O_2 concentration in the host cells, and HlPrx2 might have a higher antioxidant activity than HlPrx, resulting in a decreased mortality rate in BHK-HlPrx2 cells.

Interaction Between Tick Prxs and LGTV in BHK Cells

To evaluate the effects of LGTV infection on the mortality rate of BHK-HlPrx and BHK-HlPrx2 cells, Trypan blue assays were conducted after the BHK cell lines were infected with LGTV. Before conducting Trypan blue assays in these BHK cell lines, we confirmed whether the concentration of H_2O_2 will increase in BHK cells due to LGTV infection. First, we observed BHK cells infected with LGTV and treated with BES-H_2O_2-Ac and Hoechst 33342 under fluorescence microscopy. The fluorescence microscopy indicated that LGTV infection did not induce H_2O_2 production in LGTV-infected or the normal-state BHK cells (**Supplementary Figure 1A**). In addition, we evaluated the H_2O_2 fluorescence intensities in BHK cells using a microplate reader. We did not observe any difference in H_2O_2-specific fluorescent intensity between the normal state and LGTV-infected BHK cells (**Supplementary Figure 1B**). These results indicated that LGTV infection of BHK cells might not influence the concentration of H_2O_2. Therefore, we considered that the LGTV-infection also may not influence H_2O_2 concentrations in BHK-HlPrx and BHK-HlPrx2 cells. Next we conducted Trypan blue assays to evaluate the effects of LGTV infection on the mortality rate of BHK cell lines. The assays revealed that LGTV infection of the BHK cell lines significantly increased the mortality rate in all cell lines (**Figure 3A**). Although the mortality rate in BHK-HlPrx cells was significantly increased (142.7%) as compared with BHK cells, the mortality rate in BHK-HlPrx2 cells was significantly decreased (55.6%) as compared with BHK cells (**Figure 3A**, LGTV-infected; **Supplementary Table 1**).

Moreover, to compare the LGTV replication among BHK-HlPrx, BHK-HlPrx2, and BHK cells, the virus titers of the culture supernatants were measured. First, the LGTV-derived proteins were observed under a fluorescent microscope using anti-LGTV mouse antiserum. The fluorescence microscopy revealed that LGTV-derived fluorescence was detected in all culture supernatants, and more fluorescent foci were observed in the BHK-HlPrx compared to BHK-HlPrx2 or normal BHK cells (**Figure 3B**). In addition, when the virus titers were measured in the culture supernatants, a significantly higher virus titer was detected in the supernatant of BHK-HlPrx cells than in the supernatants of BHK-HlPrx2 and BHK cells (**Figure 3C**; **Supplementary Table 1**). However, the virus titer in the supernatant of BHK-H1Prx2 cells was not significantly different from the virus titer in the supernatant of BHK cells, although the cell mortality rate in BHK-HlPrx2 cells was significantly lower than the one in BHK cells (**Figure 3**). These results indicated that the HlPrx protein in BHK cells increases LGTV replication, leading to a higher mortality rate in BHK-HlPrx cells.

DISCUSSION

H_2O_2-scavenging enzymes in ticks, like Prxs, catalases, and selenoproteins, have been investigated to comprehend not only their antioxidant effects in ticks (Adamson et al., 2014; Kumar et al., 2016; Kusakisako et al., 2016a), but also their interactions with tick-borne pathogens (Narasimhan et al., 2007; Budachetri et al., 2017a,b). In *I. scapularis* ticks, 1-Cys Prx (Salp25D) is important for *B. burgdorferi* transmission from ticks to the host to protect *Borrelia* from neutrophil oxidation in the host (Narasimhan et al., 2007). In *I. ricinus* ticks, two Prx-homologous genes were strongly induced in the hemolymph during *B. burgdorferi* infection (Rudenko et al., 2005). In addition, the obstruction of the catalase functions or knockdown of the *SBP2* gene related to selenoprotein synthesis in *A. maculatum* resulted in the low transmission of *R. parkeri* to tick eggs (Budachetri et al., 2017a,b). Thus, these enzymes affect the transmission of

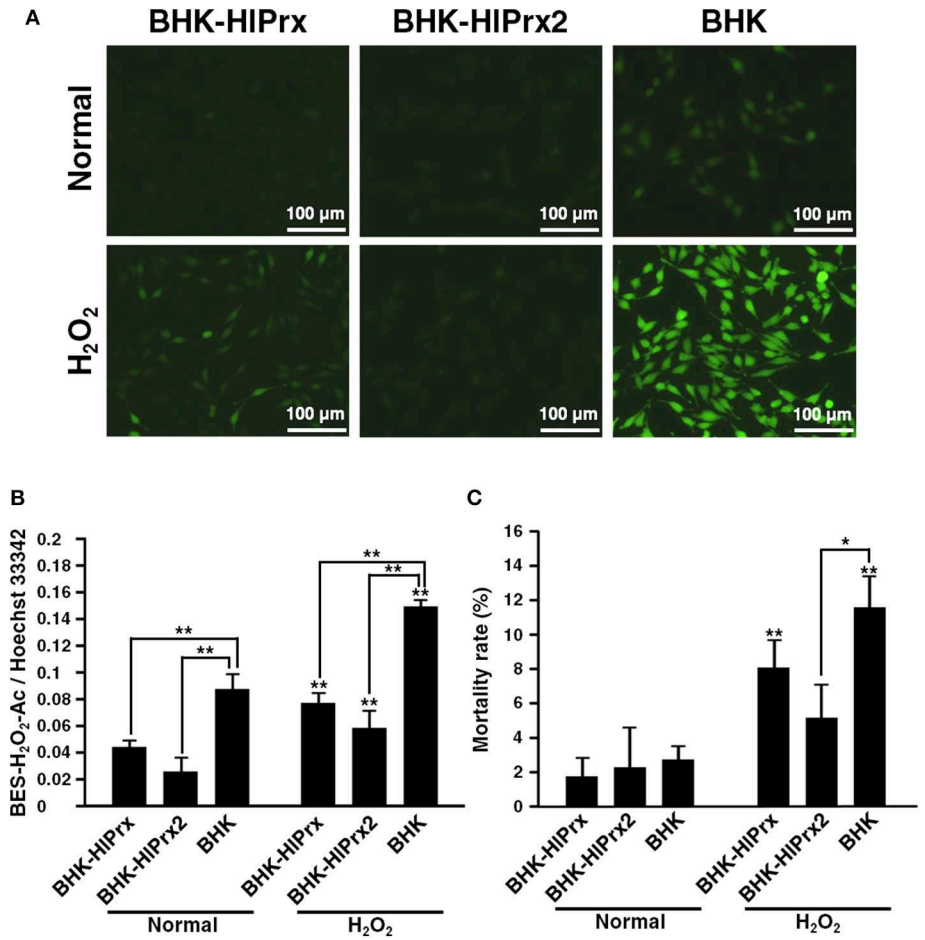

FIGURE 2 | Antioxidant activity of BHK-HIPrx and BHK-HIPrx2 cells against H_2O_2 exposure. **(A)** The fluorescence of the BES-H_2O_2-Ac probe in BHK-HIPrx, BHK-HIPrx2, and BHK cells was observed under a fluorescence microscope after H_2O_2 treatment. The left column indicates the treatment of the cells. Scale bars: 100 μm. **(B)** Graph of the fluorescence intensities of the BES-H_2O_2-Ac probe in the BHK cell lines after exposure to 0.05% H_2O_2 for 30 min. The intensities are shown as the ratio of BES-H_2O_2-Ac/Hoechst 33342 intensities. **(C)** Graph of the mortality rate in BHK cell lines after exposure to 0.05% H_2O_2 for 30 min. In the **(B,C)** graph, the results are shown as average ± standard deviation (SD). Data were analyzed using Tukey's test in the same state as indicated by the line with asterisks and Welch's *t*-test in the same BHK cell line as indicated by the line with asterisks above error bars in the H_2O_2-treated state. $^*P < 0.05$ and $^{**}P < 0.01$ indicate significant differences. Normal, normal cultured state; H_2O_2, 0.05% H_2O_2-treated state; BHK-HIPrx, *H. longicornis* 1-Cys peroxiredoxin-expressing baby hamster kidney cells; BHK-HIPrx2, *H. longicornis* 2-Cys peroxiredoxin-expressing baby hamster kidney cells.

tick-borne pathogens from ticks to hosts or from adult female ticks to their eggs.

In the present study, we utilized *H. longicornis* tick-derived Prxs-expressing BHK cell lines. The BHK cells themselves have four BHK cells-derived Prxs (**Supplementary Table 2**). Therefore, both the *H. longicornis* tick-derived Prx and BHK-cells derived Prxs are present within the cells, but on this study, we focused on the Prxs derived from *H. longicornis* ticks. Prxs can be divided into two groups (1-Cys and 2-Cys Prxs) based on the presence of one or two conserved cysteines (Hall et al., 2011). In general, 2-Cys Prxs have two conserved cysteines, peroxidatic and resolving ones (Hofmann et al., 2002). The peroxidatic cysteine reacts with and detoxifies H_2O_2. Then the post-reaction peroxidatic cysteine reacts with another Prx's resolving cysteine, and the two Prxs form homodimers via intermolecular disulfide bonds. These disulfide bonds are resolved by thioredoxins, and the reduced 2-Cys Prxs become active forms (Lu and Holmgren, 2014). On the other hand, 1-Cys Prxs contain only the peroxidatic cysteine without a resolving cysteine (Choi et al., 1998). The mechanism of 1-Cys Prxs is considered to react with and detoxify H_2O_2 as one molecule. Then the post-reaction peroxidatic cysteine is reduced by a hydrogen donor such as glutathione, and finally the enzyme is recycled (Wood et al., 2003). In addition, mammal Prxs are classified into six subgroups (Prx I to Prx VI) in accordance with the localization within the cells: Prx I and Prx II are localized in the cytosol, Prx III in mitochondria, Prx IV in the extracellular space, Prx V in mitochondria and peroxisomes, and Prx VI in the cytosol (Rhee et al., 2005). Prx I to Prx V are 2-Cys Prxs, and Prx VI is a 1-Cys Prx (Rhee et al., 2005). The tick Prxs used in this study were

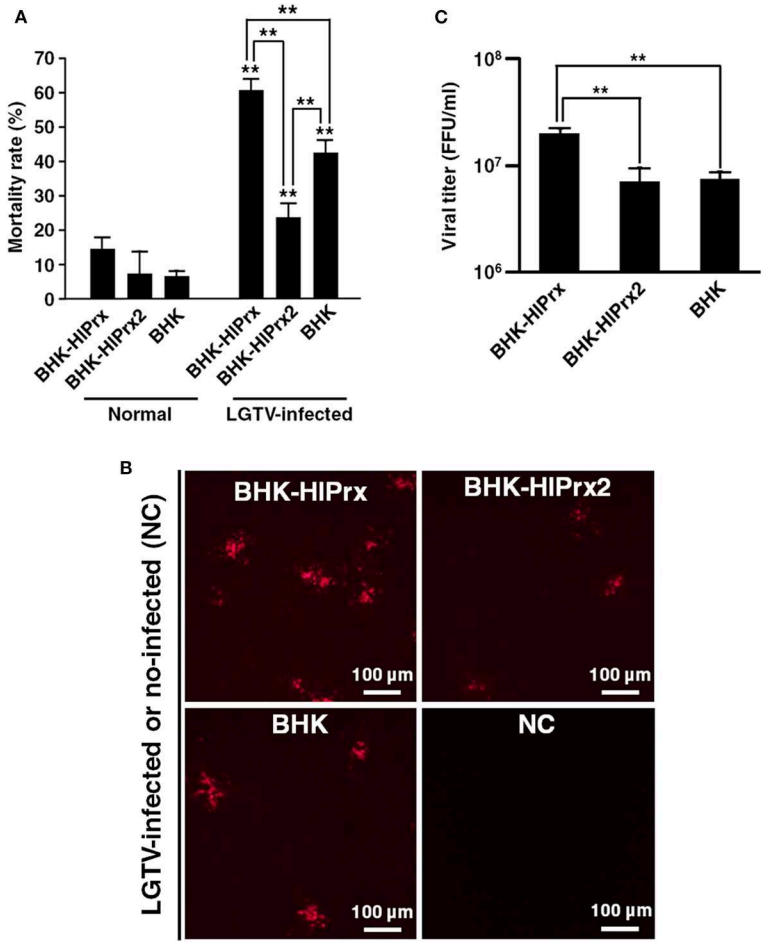

FIGURE 3 | Interaction between tick Prxs and LGTV in BHK cells. **(A)** Graph of the mortality rate in BHK cell lines after infection with LGTV. **(B)** Observation of LGTV in BHK cell lines under fluorescent microscopy using anti-LGTV mouse antisera. Scale bars: 100 μm. NC, Negative Control for a baseline fluorescence. **(C)** Graph of the viral titers in cultured supernatants from the BHK cell lines infected with LGTV. Viral titers represented as foci-forming-unit (FFU)/ml. In the **(A,C)** graph, the results are shown as average ± standard deviation (SD). Data were analyzed using Tukey's test in the same state as described line with asterisks and Welch's *t*-test in the same BHK cell line as described asterisks above error bars in H_2O_2 treated state. $^{**}P < 0.01$ indicate significant differences. Normal, normal cultured state; LGTV-infected, the cell lines infected with Langat virus; BHK-HlPrx, *H. longicornis* 1-Cys peroxiredoxin-expressing baby hamster kidney cells; BHK-HlPrx2, *H. longicornis* 2-Cys peroxiredoxin-expressing baby hamster kidney cells.

1-Cys Prx (HlPrx) and 2-Cys Prx (HlPrx2). HlPrx was classified as Prx VI, and the identity with BHK cell-derived Prx VI, a 1-Cys Prx, was 62.8%, with 97% coverage against the Prx VI of BHK cells (**Supplementary Table 2**). HlPrx2 could be classified as Prx II, since the localization within tick hemocytes, a cell in tick hemolymph, is the cytosol (Kusakisako et al., 2016b) and the full length of the amino acid sequence is almost the same between HlPrx2 and Prx II (**Supplementary Table 2**). The identity with BHK cell-derived Prx II was 75.3%, with 96% coverage against the Prx II of BHK cells (**Supplementary Table 1**). In addition, the identity between HlPrx and HlPrx2 was 30.4%, with 75% coverage (**Supplementary Table 2**). These results suggested that HlPrx and HlPrx2 proteins expressed in the BHK-HlPrx or BHK-HlPrx2 cell lines would localize to the cytosol of the cells, and the functions against the cells might be different.

In this study, we were interested in the associated effects on the pathogen within the host cell in the presence of Prxs. We initially confirmed the biological activity of the expressed HlPrx and HlPrx2 proteins in the established BHK cell lines through the antioxidant activity against H_2O_2. The results (**Figures 1**, **2**) demonstrated that the HlPrx and HlPrx2 proteins expressed in the established cell lines (BHK-HlPrx and BHK-HlPrx2 cells) had antioxidant activity through scavenging H_2O_2. The survival rate of the BHK-HlPrx2 cell line was higher than that of the other cell lines (**Figure 2C**). The HlPrx2 protein was reported to play an important role in the antioxidant activity in tick blood feeding and oviposition by controlling the H_2O_2 concentration in ticks (Kusakisako et al., 2016b). In addition, tick Prxs would transfer to their host body during tick blood feeding (Tsuji et al., 2001; Narasimhan et al., 2007; Tirloni et al., 2015; Kim et al., 2016). Therefore, the present study, together with other notable reports,

indicates that the established cell lines (BHK-HlPrx and BHK-HlPrx2 cells) could be a model environment in which the tick-derived proteins interacted with tick-transmitted pathogens in the host cell.

To evaluate the interaction between BHK cells and LGTV on H_2O_2 induction in the host cells, we observed the fluorescence and amount of H_2O_2 in BHK cells infected with LGTV. However, there was no significant difference in the fluorescence and amount of H_2O_2 between the normal state and LGTV-infected BHK cells (**Supplementary Figure 1**). This suggested that LGTV infection does not induce H_2O_2 in BHK cells. On the other hand, it has been reported that a human liver-derived cell line infected with Togavirus, an arbovirus, were induced the production of ROS (Camini et al., 2017). Furthermore, Kuzmenko et al. (2016) reported that ROS induction was observed when non-structural proteins of TBEV were expressed in a human kidney-derived cell line. In other viruses, such as influenza A and lymphocytic choriomeningitis, infection of the host induced ROS production in granulocytes, including neutrophils (Akaike et al., 1996; Lang et al., 2013). These reports showed that the ROS production was induced by virus infections in cell lines, including the immune cells, such as neutrophils. In the present study, ROS induction was not observed in BHK cells infected with LGTV. It could be that LGTV did not stimulate ROS production in BHK cells or that the stimulation of ROS production in BHK cells by LGTV occurred minimally. Therefore, it is expected that further evaluation of the interaction between the viral infection and HlPrxs protein is possible by using the immune cells, such as neutrophils and macrophages, in which the induction of ROS production by viral infection has been reported.

Interestingly, our experiments demonstrated that the mortality rate of the LGTV-infected BHK-HlPrx cells and the virus titer of the culture supernatant from those cells increased, even though LGTV infection did not induce the production of H_2O_2 in the virus-infected BHK-HlPrx cells (**Figure 3**; **Supplementary Figure 1**). These results suggested that an unknown mechanism in HlPrx promotes the growth of LGTV in BHK-HlPrx cells. In general, flaviviruses replicate on the endoplasmic reticulum (ER), including the lysosome, after invading the target cells (Okamoto et al., 2017). 1-Cys Prx in mammalian cells is known to be localized in the cytoplasm and lysosome (Fisher, 2017), and thus, 1-Cys Prx would be abundant in the ER that produces lysosome. In addition, cyclophilin A, one of the immunophilins, facilitates the replication of flaviviruses to interact with virus-derived non-structural proteins (Qing et al., 2009), and cyclophilin A would be related to 1-Cys Prx (Prx VI) (Ishii et al., 2012). These reports suggested the possibility that 1-Cys Prx affects the replication of flaviviruses on the ER. On the other hand, LGTV infection is known to be involved in the apoptosis control system through the upregulation of caspase-3 and -7 in human embryonic kidney (HEK) 293T cells (Mlera et al., 2016). Dengue fever virus (DENV) infection was also reported to induce mitochondria-mediated apoptosis in BHK cells and Vero cells derived from a monkey kidney (Nasirudeen et al., 2008). In addition, the ER stress due to infection with the Japanese encephalitis virus (JEV) promoted apoptosis in BHK cells (Huang et al., 2016). Flavivirus-related apoptosis is often induced by virus-derived proteins, such as capsid proteins and non-structural proteins (Bhuvanakantham et al., 2010). These reports and our results suggest that the promotion of LGTV replication in BHK-HlPrx cells led to the induction of apoptosis of the infected cells and a higher mortality rate among the experimental cell lines.

In BHK-HlPrx2 cells, the mortality due to LGTV infection significantly decreased as compared to normal BHK cells, while the virus titer from the culture supernatant did not increase (**Figure 3**). The HlPrx2 protein in ticks is considered to be important for tick survival and development through the control of H_2O_2 concentration during and after blood feeding (Kusakisako et al., 2016b). However, the H_2O_2 concentration in BHK cells, including the BHK-HlPrx and BHK-HlPrx2 cell lines, would not increase (**Supplementary Figure 1**). In ticks, the HlPrx2 protein localizes inside the cell and tissue membranes using immunostaining (Kusakisako et al., 2016b). In addition, HlPrx2 proteins can become a hexamer with a chaperon activity (Moon et al., 2005; Hall et al., 2011; König et al., 2013; Kusakisako et al., 2016b), which would lead to protection of the membrane from damage, including oxidative stress and viral infection. Therefore, we concluded that the HlPrx2 protein in the BHK-HlPrx2 cell line acted to maintain homeostasis in the BHK cells, resulting in lower mortality of the BHK-HlPrx2 cells infected with LGTV in comparison with the BHK cells infected with LGTV. These results and reports also suggested that HlPrx2 proteins have a low possibility of being related to LGTV replication in the BHK cells.

Chen et al. (2018) reported that DENV replicates and induces ROS production in a mosquito-derived cell line without a cytopathic effect (CPE), while the infection of a mammalian cell line leads to cell death. Likewise, although LGTV infection of BHK cells induced CPE in the cells at Day 3 after inoculation, LGTV could replicate in an *I. scapularis* tick cell line (ISE6) without inducing CPE in the cells (Mlera et al., 2016). Additionally, many immune-associated pathways in *I. scapularis*/*I. ricinus* cells are observed with protein expression changes following TBFV infection (Weisheit et al., 2015; Grabowski et al., 2016). These reports and the results from this study indicate that LGTV infection of mammalian cells and tick cells would produce different reactions with different immune responses; thus, we should consider similar experiments using ISE6 cells infected with LGTV to evaluate the interaction between tick-derived Prxs and LGTV in tick cells. It would also be of interest and could be a subject of future studies if the same result could be observed if a more virulent TBFV such as TBEV is infected on both mammalian and tick cells.

As the purpose of this study was evaluation of the interaction between LGTV infection and HlPrxs, which are tick-derived molecules, we established the HlPrxs expressing BHK cell lines and investigated the effects of LGTV infection of these cell lines. The virus replication of LGTV and the cell mortality of BHK cell lines infected with LGTV were evaluated using the tick-derived molecules expressing BHK cells (BHK-HlPrx and BHK-HlPrx2 cells). These results suggest that LGTV might utilize the tick Prxs to facilitate replication in the host cells. This study is

considered to be an important model to elucidate the interaction between tick-derived molecules and tick-borne pathogens in the host.

DATA AVAILABILITY STATEMENT

All datasets generated for this study are included in the article/**Supplementary Material**.

AUTHOR CONTRIBUTIONS

KK, HM, and TT designed the study and interpreted the data. KK and HM collected the data and wrote the manuscript. KK, HM, MT, EH, KY, and TT analyzed the data. MT, EH, KY, and TT revised and approved the manuscript.

FUNDING

This study was funded by the Japan Society for the Promotion of Science (JSPS) KAKENHI Grant Numbers 16J08221, 16H05028, 17K19328, and 17H03910, and the Takeda Science Foundation. KK was supported by a Grant-in-Aid for JSPS fellows.

SUPPLEMENTARY MATERIAL

The Supplementary Material for this article can be found online at: https://www.frontiersin.org/articles/10.3389/fcimb.2020.00007/full#supplementary-material

Supplementary Figure 1 | Evaluation of the effects of LGTV infection on H_2O_2 concentration in BHK cells. **(A)** Observation of H_2O_2 in BHK cells infected with LGTV under fluorescent microscopy using BES-H_2O_2-Ac. Scale bars: 100 μm. **(B)** Graph of the fluorescence intensities of the BES-H_2O_2-Ac probe in BHK cells infected with LGTV. The fluorescent intensities are shown as the ratio of BES-H_2O_2-Ac/Hoechst 33342 intensities. Data were analyzed using Tukey's test. $^{**}P < 0.01$ indicates significant differences. Normal, normal cultured state as a negative control; LGTV-infected, BHK cells infected with Langat virus; H_2O_2, 0.05% H_2O_2-treated state as a positive control.

Supplementary Table 1 | Summary of the results on mortality rate and viral titer in BHK cell lines infected with LGTV.

Supplementary Table 2 | Comparison of Prxs derived from H. Longicornis ticks and BHK cells on amino acid sequences.

REFERENCES

Adamson, S., Browning, R., Singh, P., Nobles, S., Villarreal, A., and Karim, S. (2014). Transcriptional activation of antioxidants may compensate for selenoprotein deficiencies in *Amblyomma maculatum* (Acari: Ixodidae) injected with selK- or selM-dsRNA. *Insect Mol. Biol.* 23, 497–510. doi: 10.1111/imb.12098

Akaike, T., Noguchi, Y., Ijiri, S., Setoguchi, K., Suga, M., Zheng, Y. M., et al. (1996). Pathogenesis of influenza virus-induced pneumonia: involvement of both nitric oxide and oxygen radicals. *Proc. Natl. Acad. Sci. U.S.A.* 93, 2448–2453. doi: 10.1073/pnas.93.6.2448

Bhuvanakantham, R., Cheong, Y. K., and Ng, M. L. (2010). West Nile virus capsid protein interaction with importin and HDM2 protein is regulated by protein kinase C-mediated phosphorylation. *Microbes Infect.* 12, 615–625. doi: 10.1016/j.micinf.2010.04.005

Budachetri, K., Crispell, G., and Karim, S. (2017a). *Amblyomma maculatum* SECIS binding protein 2 and putative selenoprotein P are indispensable for pathogen replication and tick fecundity. *Insect Biochem. Mol. Biol.* 88, 37–47. doi: 10.1016/j.ibmb.2017.07.006

Budachetri, K., Kumar, D., and Karim, S. (2017b). Catalase is a determinant of the colonization and transovarial transmission of *Rickettsia parkeri* in the Gulf Coast tick *Amblyomma maculatum*. *Insect Mol. Biol.* 26, 414–419. doi: 10.1111/imb.12304

Camini, F. C., da Silva Caetano, C. C., Almeida, L. T., da Costa Guerra, J. F., de Mello Silva, B., de Queiroz Silva, S., et al. (2017). Oxidative stress in Mayaro virus infection. *Virus Res.* 236, 1–8. doi: 10.1016/j.virusres.2017.04.017

Chen, T. H., Wu, Y. J., Hou, J. N., Chiang, Y. H., Cheng, C. C., Sifiyatun, E., et al. (2018). A novel p53 paralogue mediates antioxidant defense of mosquito cells to survive dengue virus replication. *Virology* 519, 156–169. doi: 10.1016/j.virol.2018.04.011

Choi, H. J., Kang, S. W., Yang, C. H., Rhee, S. G., and Ryu, S. E. (1998). Crystal structure of a novel human peroxidase enzyme at 2.0 A resolution. *Nat. Struct. Biol.* 5, 400–406. doi: 10.1038/nsb0598-400

Citelli, M., Lara, F. A., da Silva, V. I. J., and Oliveira, P. L. (2007). Oxidative stress impairs heme detoxification in the midgut of the cattle tick, *Rhipicephalus* (*Boophilus*) *microplus*. *Mol. Biochem. Parasitol.* 151, 81–88. doi: 10.1016/j.molbiopara.2006.10.008

Fisher, A. B. (2017). Peroxiredoxin 6 in the repair of peroxidized cell membranes and cell signaling. *Arch. Biochem. Biophys.* 617, 68–83. doi: 10.1016/j.abb.2016.12.003

Galay, R. L., Umemiya-Shirafuji, R., Bacolod, E. T., Maeda, H., Kusakisako, K., Koyama, J., et al. (2014). Two kinds of ferritin protect ixodid ticks from iron overload and consequent oxidative stress. *PLoS ONE* 9:e90661. doi: 10.1371/journal.pone.0090661

Galay, R. L., Umemiya-Shirafuji, R., Mochizuki, M., Fujisaki, K., and Tanaka, T. (2015). Iron metabolism in hard ticks (Acari: Ixodidae): The antidote to their toxic diet. *Parasit. Int.* 64, 182–189. doi: 10.1016/j.parint.2014.12.005

Grabowski, J. M., Perera, R., Roumani, A. M., Hedrick, V. E., Inerowicz, H. D., Hill, C. A., et al. (2016). Changes in the proteome of langat-infected *Ixodes scapularis* ISE6 cells: metabolic pathways associated with flavivirus infection. *PLoS Negl. Trop. Dis.* 10:e0004180. doi: 10.1371/journal.pntd.0004180

Grandjean, O. (1983). Blood digestion in *Ornithodorus moubata* Murray sensu stricto Walton females (Ixodoidea: Argasidae) II. Modifications of midgut cells related to the digestive cycle and to the triggering action of mating. *Ann. Parasitol. Hum. Comp.* 58, 493–514. doi: 10.1051/parasite/1983585493

Hall, A., Nelson, K., Poole, L. B., and Karplus, P. A. (2011). Structure-based insights into the catalytic power and conformational dexterity of peroxiredoxins. *Antioxid. Redox Signal.* 15, 795–815, doi: 10.1089/ars.2010.3624

Hernandez, E. P., Talactac, M. R., Fujisaki, K., and Tanaka, T. (2019). The case for oxidative stress molecule involvement in the tick-pathogen interactions -an omics approach. *Dev. Comp. Immunol.* 100:103409. doi: 10.1016/j.dci.2019.103409

Hofmann, B., Hecht, H.-J., and Flohé, L. (2002). Peroxiredoxins. *Biol. Chem.* 383, 347–364. doi: 10.1515/BC.2002.040

Hoogstraal, H. (1985). Argasid and nuttalliellid ticks as parasites and vectors. *Adv. Parasitol.* 24, 135–238. doi: 10.1016/S0065-308X(08)60563-1

Huang, M., Xu, A., Wu, X., Zhang, Y., Guo, Y., Guo, F., et al. (2016). Japanese encephalitis virus induces apoptosis by the IRE1/JNK pathway of ER stress response in BHK-21 cells. *Arch. Virol.* 161, 699–703. doi: 10.1007/s00705-015-2715-5

Ishii, T., Warabi, E., and Yanagawa, T. (2012). Novel roles of peroxiredoxins in inflammation, cancer and innate immunity. *J. Clin. Biochem. Nutr.* 50, 91–105. doi: 10.3164/jcbn.11-109

Kim, T. K., Tirloni, L., Pinto, A. F., Moresco, J., Yates, J. R. III, da Silva Vaz, I., et al. (2016). *Ixodes scapularis* tick saliva proteins sequentially secreted every 24 h during blood feeding. *PLoS Negl. Trop. Dis.* 10:e0004323. doi: 10.1371/journal.pntd.0004323

König, J., Galliardt, H., Jütte, P., Schäper, S., Dittmann, L., and Dietz, K. J. (2013). The conformational bases for the two functionalities of 2-cysteine peroxiredoxins as peroxidase and chaperone. *J. Exp. Bot.* 64, 3483–3497. doi: 10.1093/jxb/ert184

Kumar, D., Budachetri, K., Meyers, V. C., and Karim, S. (2016). Assessment of tick antioxidant responses to exogenous oxidative stressors and insight into the role of catalase in the reproductive fitness of the Gulf Coast tick, *Amblyomma maculatum*. *Insect Mol. Biol.* 25, 283–294. doi: 10.1111/imb.12218

Kusakisako, K., Fujisaki, K., and Tanaka, T. (2018a). The multiple roles of peroxiredoxins in tick blood feeding. *Exp. Appl. Acarol.* 75, 269–280. doi: 10.1007/s10493-018-0273-8

Kusakisako, K., Galay, R. L., Umemiya-Shirafuji, R., Hernandez, E. P., Maeda, H., Talactac, M. R., et al. (2016b). 2-Cys peroxiredoxin is required in successful blood-feeding, reproduction, and antioxidant response in the hard tick *Haemaphysalis longicornis*. *Parasit. Vectors* 9:457. doi: 10.1186/s13071-016-1748-2

Kusakisako, K., Ido, A., Masatani, T., Morokuma, H., Hernandez, E. P., Talactac, M. R., et al. (2018b). Transcriptional activities of two newly identified *Haemaphysalis longicornis* tick-derived promoter regions in the *Ixodes scapularis* tick cell line (ISE6). *Insect Mol. Biol.* 27, 590–602. doi: 10.1111/imb.12497

Kusakisako, K., Masatani, T., Miyata, T., Galay, R. L., Maeda, H., Talactac, M. R., et al. (2016a). Functional analysis of recombinant 2-Cys peroxiredoxin from the hard tick *Haemaphysalis longicornis*. *Insect Mol. Biol.* 25, 16–23. doi: 10.1111/imb.12193

Kuzmenko, Y. V., Smirnova, O. A., Ivanov, A. V., Starodubova, E. S., and Karpov, V. L. (2016). Nonstructural protein 1 of tick-borne encephalitis virus induces oxidative stress and activates antioxidant defense by the Nrf2/ARE pathway. *Intervirology* 59, 111–117. doi: 10.1159/000452160

Lang, P. A., Xu, H. C., Grusdat, M., McIlwain, D. R., Pandyra, A. A., Harris, I. S., et al. (2013). Reactive oxygen species delay control of lymphocytic choriomeningitis virus. *Cell Death Differ.* 20, 649–658. doi: 10.1038/cdd.2012.167

Lindquist, L., and Vapalahti, O. (2008). Tick-borne encephalitis. *Lancet* 371, 1861–1871. doi: 10.1016/S0140-6736(08)60800-4

Lu, J., and Holmgren, A. (2014). The thioredoxin antioxidant system. *Free Radic. Biol. Med.* 66, 75–87. doi: 10.1016/j.freeradbiomed.2013.07.036

Mlera, L., Melik, W., Offerdahl, D. K., Dahlstrom, E., Porcella, S. F., and Bloom, M. E. (2016). Analysis of the langat virus genome in persistent infection of an *Ixodes scapularis* cell line. *Viruses* 8:E252. doi: 10.3390/v8090252

Mlera, L., Offerdahl, D. K., Martens, C., Porcella, S. F., Melik, W., and Bloom, M. E. (2015). Development of a model system for tick-borne flavivirus persistence in HEK 293T cells. *MBio* 6:e00614. doi: 10.1128/mBio.00614-15

Moon, J. C., Hah, Y. S., Kim, W. Y., Jung, B. G., Jang, H. H., Lee, J. R., et al. (2005). Oxidative stress-dependent structural and functional switching of a human 2-Cys peroxiredoxin isotype II that enhances HeLa cell resistance to H_2O_2-induced cell death. *J. Biol. Chem.* 280, 28775–28784. doi: 10.1074/jbc.M505362200

Narasimhan, S., Sukumaran, B., Bozdogan, U., Thomas, V., Liang, X., DePonte, K., et al. (2007). A tick antioxidant facilitates the Lyme disease agent's successful migration from the mammalian host to the arthropod vector. *Cell Host Microbe* 2, 7–18. doi: 10.1016/j.chom.2007.06.001

Nasirudeen, A. M., Wang, L., and Liu, D. X. (2008). Induction of p53-dependent and mitochondria-mediated cell death pathway by dengue virus infection of human and animal cells. *Microbes Infect.* 10, 1124–1132. doi: 10.1016/j.micinf.2008.06.005

Okamoto, T., Suzuki, T., Kusakabe, S., Tokunaga, M., Hirano, J., Miyata, Y., et al. (2017). Regulation of apoptosis during Flavivirus infection. *Viruses* 9:243. doi: 10.3390/v9090243

Oliveira, J. H. M., Talyuli, O. A. C., Goncalves, R. L. S., Paiva-Silva, G. O., Sorgine, M. H. F., Alvarenga, P. H., et al. (2017). Catalase protects *Aedes aegypti* from oxidative stress and increases midgut infection prevalence of Dengue but not Zika. *PLoS Negl. Trop. Dis.* 11:e0005525. doi: 10.1371/journal.pntd.0005525

Qing, M., Yang, F., Zhang, B., Zou, G., Robida, J. M., Yuan, Z., et al. (2009). Cyclosporine inhibits flavivirus replication through blocking the interaction between host cyclophilins and viral NS5 protein. *Antimicrobial Agents Chemother.* 53, 3226–3235. doi: 10.1128/AAC.00189-09

Rhee, S. G., Chae, H. Z., and Kim, K. (2005). Peroxiredoxins: a historical overview and speculative preview of novel mechanisms and emerging concepts in cell signaling. *Free Radic. Biol. Med.* 38, 1543–1552. doi: 10.1016/j.freeradbiomed.2005.02.026

Robinson, M. W., Hutchinson, A. T., Dalton, J. P., and Donnelly, S. (2010). Peroxiredoxin: a central player in immune modulation. *Parasite. Immunol.* 32, 305–313. doi: 10.1111/j.1365-3024.2010.01201.x

Rudenko, N., Golovchenko, M., Edwards, M. J., and Grubhoffer, L. (2005). Differential expression of *Ixodes ricinus* tick genes induced by blood feeding or *Borrelia burgdorferi* infection. *J. Med. Entomol.* 42, 36–41. doi: 10.1093/jmedent/42.1.36

Strober, W. (2001). Trypan blue exclusion test of cell viability. *Curr. Protoc. Immunol. Appendix* 3:Appendix 3B. doi: 10.1002/0471142735.ima03bs21

Talactac, M. R., Yoshii, K., Maeda, H., Kusakisako, K., Hernandez, E. P., Tsuji, N., et al. (2016). Virucidal activity of *Haemaphysalis longicornis* longicin P4 peptide against tick-borne encephalitis virus surrogate Langat virus. *Parasit. Vectors* 9:59. doi: 10.1186/s13071-016-1344-5

Tirloni, L., Islam, M. S., Kim, T. K., Diedrich, J. K., Yates, J. R III, Pinto, A. F., et al. (2015). Saliva from nymph and adult females of *Haemaphysalis longicornis*: a proteomic study. *Parasit. Vectors* 8:338. doi: 10.1186/s13071-015-0918-y

Tsuji, N., Kamio, T., Isobe, T., and Fujisaki, K. (2001). Molecular characterization of a peroxiredoxin from the hard tick *Haemaphysalis longicornis*. *Insect Mol. Biol.* 10, 121–129. doi: 10.1046/j.1365-2583.2001.00246.x

Weber, E., Finsterbusch, K., Lindquist, R., Nair, S., Lienenklaus, S., Gekara, N. O., et al. (2014). Type I interferon protects mice from fatal neurotropic infection with Langat virus by systemic and local antiviral responses. *J. Virol.* 88, 12202–12212. doi: 10.1128/JVI.01215-14

Weisheit, S., Villar, M., Tykalová, H., Popara, M., Loecherbach, J., Watson, M., et al. (2015). *Ixodes scapularis* and *Ixodes ricinus* tick cell lines respond to infection with tick-borne encephalitis virus: transcriptomic and proteomic analysis. *Parasit. Vectors* 8:599. doi: 10.1186/s13071-015-1210-x

Wood, Z. A., Schröder, E., Robin Harris, J., and Poole, L. B. (2003). Structure, mechanism and regulation of peroxiredoxins. *Trends Biochem. Sci.* 28, 32–40. doi: 10.1016/S0968-0004(02)00003-8

Conflict of Interest: The authors declare that the research was conducted in the absence of any commercial or financial relationships that could be construed as a potential conflict of interest.

frontiers in Cellular and Infection Microbiology

ORIGINAL RESEARCH
published: 10 March 2020
doi: 10.3389/fcimb.2020.00093

Ovary Proteome Analysis Reveals RH36 Regulates Reproduction via Vitellin Uptake Mediated by HSP70 Protein in Hard Ticks

Fangfang Wang[1,2], *Yanan Wang*[1], *Guanghua Wang*[1], *Houshuang Zhang*[1], *Ceyan Kuang*[1], *Yongzhi Zhou*[1], *Jie Cao*[1] *and Jinlin Zhou*[1]*

[1] *Key Laboratory of Animal Parasitology of Ministry of Agriculture, Shanghai Veterinary Research Institute, Chinese Academy of Agricultural Sciences, Shanghai, China,* [2] *College of Life Science and Food Engineering, Hebei University of Engineering, Handan, China*

OPEN ACCESS

Edited by:
Lucas Tirloni, National Institute of Allergy and Infectious Diseases (NIAID), United States

Reviewed by:
Camila Fernanda Waltero Orjuela, Federal University of Rio de Janeiro, Brazil
Marina Amaral Xavier, Federal University of Rio Grande Do Sul, Brazil

***Correspondence:**
Jinlin Zhou
jinlinzhou@shvri.ac.cn

Specialty section:
This article was submitted to Parasite and Host, a section of the journal Frontiers in Cellular and Infection Microbiology

Received: *02 November 2019*
Accepted: *21 February 2020*
Published: *10 March 2020*

Citation:
Wang F, Wang Y, Wang G, Zhang H, Kuang C, Zhou Y, Cao J and Zhou J (2020) Ovary Proteome Analysis Reveals RH36 Regulates Reproduction via Vitellin Uptake Mediated by HSP70 Protein in Hard Ticks. Front. Cell. Infect. Microbiol. 10:93. doi: 10.3389/fcimb.2020.00093

Ticks are blood-sucking vector arthropods, which play an important role in transmitting pathogens between humans and animals. RH36 is an immunomodulatory protein expressed in the salivary glands, but not other organs, of partially fed *Rhipicephalus haemaphysaloides* ticks, and it reaches its peak on the day of tick engorgement. RH36 gene silencing inhibited tick blood feeding and induced a significant decrease in tick oviposition, indicating that another function of immunosuppressor RH36 was regulating tick reproduction. Why did RH36 protein expressed uniquely in the salivary gland regulate tick reproduction? RH36 regulated positively the expression of vitellogenin in ovary, which indicated RH36 protein played an important role in the integration of nutrition and reproduction. According to proteomic analysis, heat shock protein 70 (HSP70) was significantly down-regulated in the immature ovary of post-engorged ticks. In addition, gene silencing of HSP70 not only inhibited tick blood-sucking and the expression of vitellogenin, but also increased tick death rate. These results suggested RH36 affected tick vitellogenin uptake and then regulated ovary cell maturation by modulating the expression of HSP70 protein, and finally controlled tick oviposition.

Keywords: ***Rhipicephalus haemaphysaloides*, RH36, vitellogenesis, RNA interference, HSP70 protein**

INTRODUCTION

Ticks transmit a wide range of zoonosis, such as tick-borne encephalitis (Grabowski et al., 2017), Lyme disease (Ehrmann et al., 2018), tick-borne spotted fever (Han et al., 2018), anaplasmosis (Parola and Raoult, 2001; Eisen and Eisen, 2018), and babesiosis (Kotal et al., 2015). These pathogens are transmitted via tick saliva to their vertebrate host when ticks feed on host. Transovarial transmission from adult female tick to its offspring may also occur in some tick species and tick-borne diseases (Danielova et al., 2002; Harris et al., 2017; Umemiya-Shirafuji et al., 2017; Jongejan et al., 2018; Moore et al., 2018). Tick salivary glands secrete immunosuppressant proteins including P36 protein that regulate the host immune system during blood feeding (Bergman et al., 2000; Alarcon-Chaidez et al., 2003; Konnai et al., 2009; Anatriello et al., 2010; Wang et al., 2017). Although P36 homolog proteins from Ixodid ticks are not highly conserved, all ticks share the same key site and structural features with conserved region "IDKGMLSPF". Based on 3D structures of P36 from *Dermacentor andersoni*, a predicted conserved antigenic region was identified, located

within the exposed loop with a potential of binding immunomodulating ligands, including glycerol and lactose (Oyugi et al., 2018). In our previous study, we found that RH36 from *Rhipicephalus haemaphysaloides*, P36 homolog, suppressed the T-lymphocyte mitogen-driven proliferation of splenocytes *in vitro* and *in vivo*, as well as the expression of several cytokines, including IL-2, IL-12, and TNF-α (Wang et al., 2017). P36 homologs expressed mainly in the salivary glands of partially fed ticks (Alarcon-Chaidez et al., 2003; Konnai et al., 2009) and RH36 protein production correlated with blood-feeding success and oviposition (Wang et al., 2017). Little information is known about the expression and interaction of RH36 molecules in the salivary glands and reproductive organs, including the ovary, while the mechanism by which the RH36 gene regulates ovary development is also unknown.

Ticks with a huge reproductive capacity produce hundreds of eggs, while the key of egg maturation is vitellogenesis, a process in which massive amounts of vitellin (Vn) precursors (vitellogenin, Vg) are expressed in fat bodies and midguts, and then secreted into hemolymph, and subsequently accumulated by developing oocytes via vitellogenin receptor-mediated clathrin-dependent endocytosis (Rosell and Coons, 1992; Esmeralda Parra-Peralbo, 2011; Khalil et al., 2011). After blood feeding, tick vitellogenesis is activated by a cooperative action of nutritional amino acid/target of rapamycin/S6 kinase (AA/TOR/S6K) (Umemiya-Shirafuji et al., 2012) and steroid hormone (20-hydroxyecdysone, 20E) pathways, closely correlated with mating (Thompson et al., 2005). In addition, heme and iron metabolism during tick blood feeding are essential for tick reproduction and egg fertility (Hajdusek et al., 2009; Galay et al., 2013; Perner et al., 2016). Genome and proteomics analyses of the parasitic processes seem to be unique in ticks, including prolonged feeding, new methods of hemoglobin digestion, heme detoxification, vitellogenesis and transmission of pathogens (Gulia-Nuss et al., 2016; Barrero et al., 2017). We hypothesized that the RH36 molecules participated in the integration between reproduction and nutrition and investigated the mechanism of RH36 in oviposition by proteomics analyses.

The significance of our study is revelation of the molecular mechanism of immunosuppressor RH36 modulating ovary development and oviposition in *R. haemaphysaloides* ticks. The main hypothesis addressed in this study was that RH36 may regulate tick vitellogenesis, while heat shock protein 70 (HSP70) was found to be down-regulated in the RH36 gene-silenced ticks by proteomic analysis, which regulated tick blood feeding and the expression of vitellogenin. This study illustrates the critical function of RH36 in the process of ovary development and tick reproduction, which are required for blood meal completion.

MATERIALS AND METHODS

Ethics Statement

The protocols (shvri-ra-2017070578) were approved by the Institutional Animal Care and Use Committee of the Shanghai Veterinary Research Institute, and authorized by the Animal Ethical Committee of Shanghai Veterinary Research Institute.

Ticks and Sample Preparation

Ticks were obtained from a colony of *R. haemaphysaloides* maintained on the ears of New Zealand white rabbits at Shanghai Veterinary Research Institute, CAAS. Off-host ticks were kept in an incubator at 25°C and 95% humidity. To detect dynamic expression of RH36 and other proteins, midguts, salivary glands, ovaries, hemolymph, and fat bodies were dissected from unfed female ticks, 5-day-fed female ticks, 7-day-fed female ticks, engorging ticks and ticks on day 3 or 10 after engorgement. Furthermore, unfed female adult ticks ($N = 80$ females per group, three replicates) were microinjected with RH36 and luciferase double-stranded RNA (dsRNA), respectively, as described previously (Wang et al., 2017). Two individual five-day fed female ticks from each group were collected to characterize RH36 mRNA levels after RH36 RNA interference (RNAi). Blood-feeding ticks from RH36 or luciferase gene silencing groups (14 ticks per group) were removed from rabbits at 5 (indicated by RF5 and LF5, respectively) or 7 days (indicated by RF7 and LF7). Engorged ticks (14 ticks per group) were also collected from RH36 or luciferase gene silencing groups at day 0 (denoted by RE0 and LE0), day 3 (denoted by RE3 and LE3), day 7 (denoted by RE7 and LE7) and day 10 (denoted by RE10 and LE10) after engorgement. The ovaries, hemolymph, fat bodies and salivary glands were dissected from 7 ticks per group for RNA or protein extraction and washed in PBS to remove hemolymph -related cells.

Total RNA was extracted from ovaries using TRIZOL (Invitrogen, Carlsbad, CA, USA) according to the manufacturer's instructions. Total RNA quality was evaluated using Agilent 2100 Bioanalyzer RNA Nano Chip (Agilent Technologies, Santa Clara, CA, USA). Tick ovaries with SDT buffer (containing 4% SDS, 100 mM DTT and 100 mM Tris-HCl, pH 7.6) and quartz sand (another 1/4 inch ceramic bead MP 6540-424 for tissue samples) were homogenized by MP homogenizer (24 × 2, 6.0M/S, 60s, twice) and subsequently sonicated and boiled for 15 min. After it was centrifuged at 10,000 rpm for 20 min, the supernatant was filtered with 0.22 μm filters. Total protein was also extracted from tick salivary glands, fat bodies and hemolymph according to the above instruction, respectively. The filtrate was quantified with the BCA Protein Assay Kit (Bio-Rad, USA). These RNA and protein samples were stored at −80°C until use.

Antibody Against RH36 Preparation and Expression Level of RH36 Protein by Western Blot

The B cell linear epitope of RH36 protein was predicted using the Immune Epitope Database (IEDB) of http://tools.iedb.org/bcell/result/. The peptide (LTDDYWKQGEHPSGEYPIS) was selected randomly and synthesized with peptide purify of at least 95% and coupled with KLH by GL Biochem (Shanghai, China), and emulsified with an equal volume of Freund's complete adjuvant (Sigma-Aldrich, St. Louis, MO, USA) used to intraperitoneally inject Balb/c mice. Two booster injections of RH36 peptide were given with the same procedure but using Freund's incomplete adjuvant. One week after the final immunization, sera were collected following centrifugation. Antibodies against RH36 peptides were used to detect expression levels by Western

blot. According to standard techniques, total proteins were separated on a 12% SDS-PAGE gel and transferred to PVDF membranes (0.45 μm, Millipore, Billerica, MA, USA), and the membranes were immunoblotted with RH36 antibody (1:200). The monoclonal antibody of β-actin against mouse (Proteintech, Rosemont, USA, Cat. No. 60008-1-Ig) was used as the control. IgG goat anti-mouse or goat anti-rabbit antibodies conjugated with HRP were used for secondary antibodies (1:8,000, Bethyl Laboratories, Inc., Montgomery, Texas, USA). The membranes were visualized using automatic chemiluminescence image analysis system (Tanon-5200, Tanon Science & Technology Co., Ltd, Shanghai, China). Densitometry used to analyze indicated protein bands was determined by Image J (NIH), normalized with the control (Schneider et al., 2012).

Antibody Against Vitellin Preparation and Expression Level of Vitellin Protein by Western Blot

Crude eggs were homogenized and subsequently centrifuged at 10,000 rpm for 20 min, the supernatant was applied onto a Sepharose CL-4B gel filtration column and diethyl-amino-ethyl (DEAE)-cellulose column in turn (Yang et al., 2015). Polyclonal antibody and monoclonal antibody against vitellin was generated from Balb/c mice (Wang et al., 2017). Splenocytes from immunized mice were fused to myeloma cells, SP2/0, using polyethylene glycol. Hybridomas were selected in HAT medium and the hybridoma culture supernatants were screened by enzyme-linked immunosorbent assay (ELISA) in 96-microtiter plates and Western blot (Yang et al., 2015).

Expression of vitellin was detected in the ovaries, hemolymph, fat bodies and salivary glands by Western blot according to the above description. The monoclonal antibodies of β-actin (Proteintech, Cat. No. 60008-1-Ig) and GAPDH (Proteintech, Cat. No. 60004-1-Ig) against mouse were used as the control. The bands were visualized using automatic chemiluminescence image analysis system (Tanon-5200, Tanon Science & Technology Co., Ltd., Shanghai, China). Heat shock protein 70 rabbit antibody (HSP70, Cell Signaling Technology, Boston, USA, Cat. No. 3177) was also used to detect the protein expression level in the different organs during different blood-feeding ticks by Western blot. The anti-GAPDH antibody against rabbit (Cell Signaling Technology, Cat. No. 2118) was used as the control.

Immunofluorescence Assays (IFA)

For immunofluorescence, ovaries were obtained from adult female ticks at 10 days after engorgement as described above, fixed with 4% paraformaldehyde in 0.2 M sodium cacodylate buffer, and dehydrated in a graded series of ethanol and

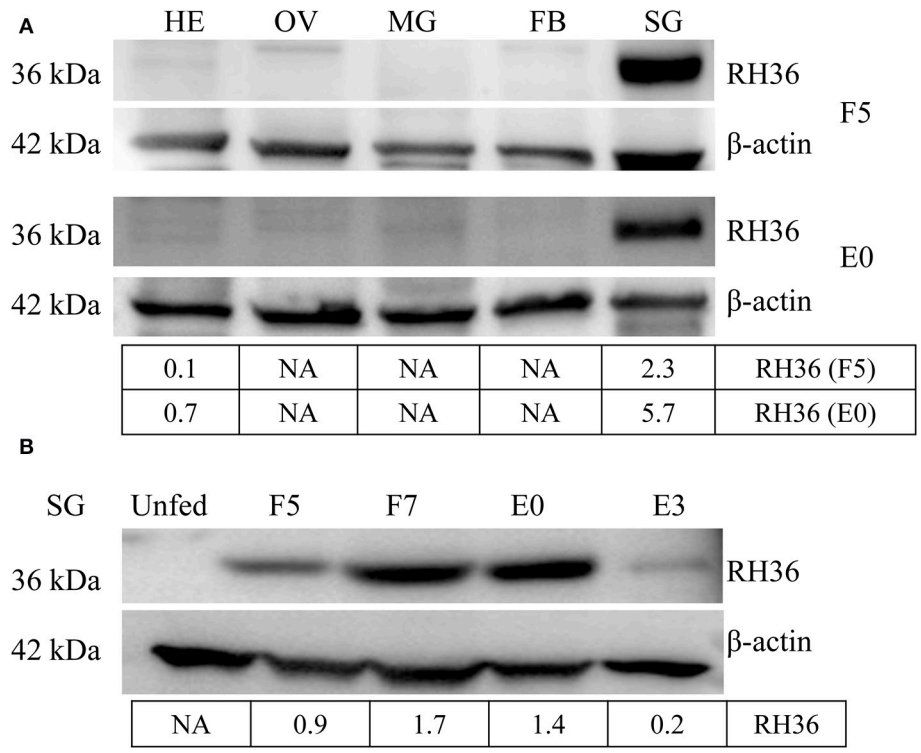

FIGURE 1 | RH36 is expressed uniquely in the salivary gland and expressed higher in 7-day-fed ticks and engorged ticks. Expression level of RH36 was detected at different organs from 5-day-fed ticks (upper panel, **A**) and engorged ticks (lower panel, **A**), and different development stages **(B)** using polyclonal antibody prepared by KLH binding RH36 polypeptide. Density analysis shows RH36 protein is induced by feeding and expressed characteristically in salivary glands. The protein level of RH36 was normalized to β-actin. FB, fat body; HE, hemolymph; OV, ovary; SG, salivary gland; MG, midgut; F5, at day 5 for blood feeding; F7, at day 7 for blood feeding; E0, on the day of engorgement; E3, at 3 days post-engorgement.

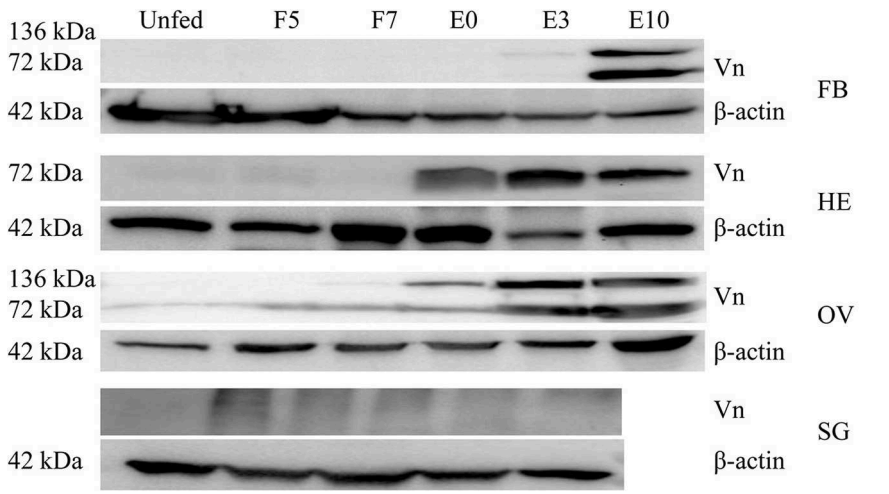

NA	NA	NA	NA	0.05	0.7	Vn (136 kDa, FB)
NA	NA	NA	2.0	3.5	1.5	Vn (72 kDa, HE)
NA	NA	0.03	0.4	0.8	0.5	Vn (136 kDa, OV)
NA	NA	NA	NA	NA		Vn (SG)

FIGURE 2 | Vitellin expression is induced by blood feeding. Except for salivary gland, vitellin protein was expressed highly in fat body, hemolymph, ovary at different engorgement statuses by Western blot. The intensities of vitellin protein bands (136 and 72 kDa) were determined, normalized to β-actin. Vn, Vitellin; FB, fat body; HE, hemolymph; OV, ovary; SG, salivary gland; UF, unfed; F5, at day 5 for blood feeding; F7, at day 7 for blood feeding; E0, on the day of engorgement; E3, at 3 days post-engorgement; E10, at day 10 after engorgement.

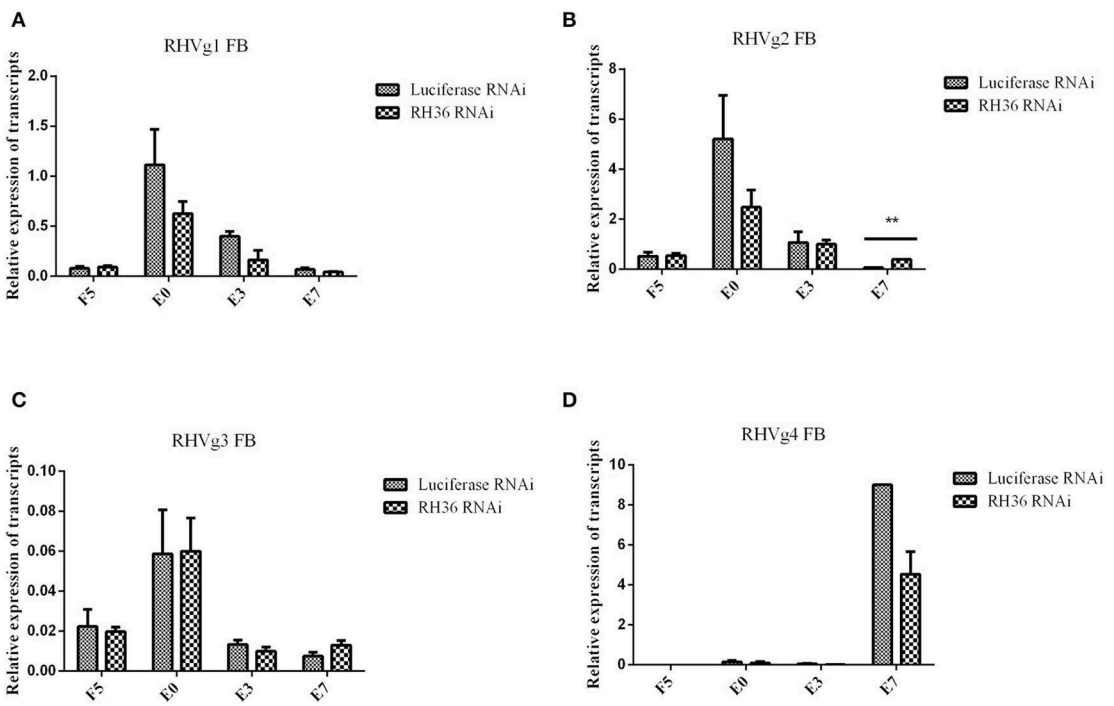

FIGURE 3 | Expression of RHVg mRNA in fat body of female ticks is not affected after RH36 gene silencing. Transcript levels of RHVg1 **(A)**, RHVg2 **(B)**, RHVg3 **(C)**, and RHVg4 **(D)** were detected in the fat body of 5-day-fed ticks, engorgement ticks, 3 day post-engorgement ticks and 7 day post-engorged ticks by real-time quantitative PCR. The data were normalized to tick elongation factor 1α and gene-specific standards were the respective plasmids. RHVg2 mRNA was up-regulated significantly at 7 day post-engorgement ($p < 0.01$), but there was no difference for other RHVg genes. ** means highly statistical significance that p-values less than 0.01. FB, fat body; F5, at day 5 for blood feeding; E0, on the day of engorgement; E3, at 3 days post-engorgement; E7, at 7 days after engorgement.

embedded in paraffin. Sections (4 μm) were prepared and mounted on glass slides. Paraffin was removed from the sections with xylene and the sections were hydrated by successive 5-min washes with a graded series of 100, 80, 75, and 65% ethanol. The slides were treated with EDTA antigen repair buffer for 30 min at 37°C, washed with PBST and incubated with 2% bovine serum albumin (BSA; Sigma-Aldrich) in PBST for 30 min at room temperature. The slides were then incubated for 14 h at 4°C with primary antibodies against vitellin diluted 1:5–1:200 in 2% BSA mixture and developed for 30 min with goat-anti-mouse IgG conjugated with FITC (Sigma-Aldrich) (diluted 1:500 in 2% BSA mixture) after 3 washes in PBST buffer. The slides were incubated for 20 min with DAPI (1:200, 2% BSA dilution) after 3 washes in PBST buffer and mounted in Fluoromount Aqueous Mounting Medium (Sigma-Aldrich). Samples were observed and photographed with 10X objective, 1.0X zoom and the excitation of 488 nm (FITC) and 405 nm (DAPI) under a Zeiss inverted fluorescence microscope (Zeiss, Germany).

Proteomic Data Collection and Bioinformatics Analysis

Quantitative proteomic analysis by tandem mass tag (TMT) technology was performed by Shanghai Applied Protein Technology (APT, Shanghai, China). Each 100 μg peptide

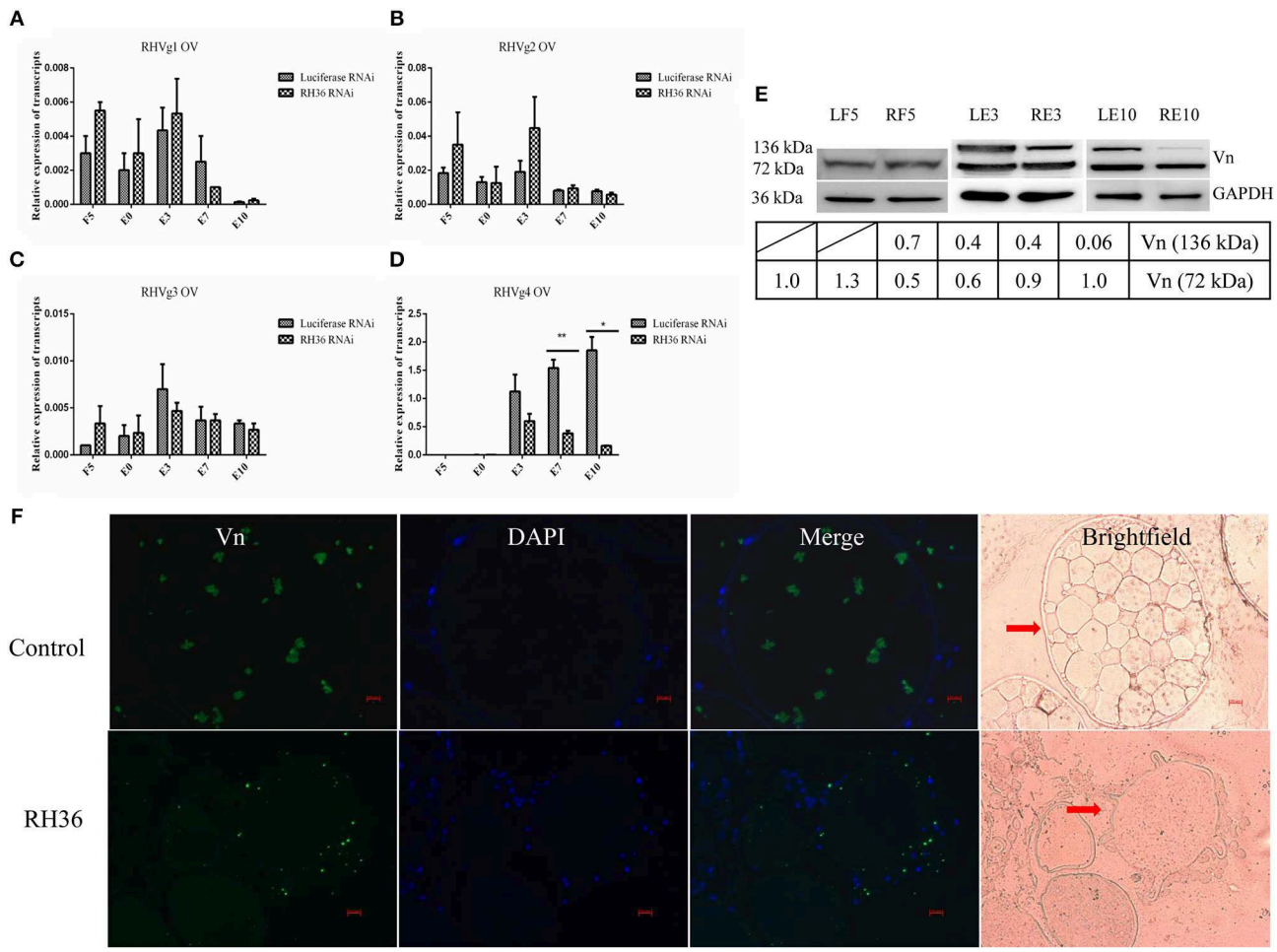

FIGURE 4 | RH36 is involved in expression and/or processing of RHVg genes and vitellin protein after engorgement. Transcript level of RHVg1 **(A)**, RHVg2 **(B)**, RHVg3 **(C)**, RHVg4 **(D)** genes was tested in the ovaries of adult ticks at 5 days blood feeding, engorgement, 3 days post-engorgement, 7 days post-engorgement and 10 days post-engorgement by real-time quantitative PCR, which shows RHVg4 gene is observably down-regulated at 7 days post-engorgement ($p < 0.01$) and 10 days post-engorgement ($p < 0.05$). ** means highly statistical significance that P-values less than 0.01. * means statistical significance that p-values less than 0.05. The data were normalized to tick elongation factor 1α and gene-specific standards were the respective plasmids. Protein level of vitellin reduced in the ovaries at 3 days post-engorgement and 10 days post-engorgement by Western blot **(E)**. The intensities of vitellin protein bands (136 and 72 kDa) were normalized to GAPDH. RH36 regulates tick ovary development by reducing vitellin uptake in oocytes using immunofluorescence assay **(F)**. Tick ovaries were collected at 10 days after engorgement from RH36 and luciferase (as control) RNAi groups and stained with mouse anti-vitellin antibodies. Vitellin was observed in green fluorescent and DNA was stained with DAPI (blue fluorescent). Scale bar: 20 μm. LF5, 5-day-fed ticks from luciferase RNAi groups; RF5, 5-day-fed ticks from RH36 RNAi groups; E0, on the day of engorgement; LE3, 3 days post-engorgement ticks from luciferase RNAi groups; RE3, 3 days post-engorgement ticks from RH36 RNAi groups; E7, at day 7 after engorgement; LE10, 10 days post-engorgement ticks from luciferase RNAi groups; RE10, 10 days post-engorgement ticks from RH36 RNAi groups; Vn, Vitellin; OV, ovary, arrows point to oocytes.

mixture digested with trypsin (Promega, Madison, WI, USA) was labeled using TMT reagent (Thermo Fisher Scientific, Waltham, MA, USA) according to the manufacturer's instructions. The 6-plex TMT Labeling were fractionated into 15 strong cation exchange (SCX). LC-MS/MS analysis (1H) was performed on a Q Exactive mass spectrometer (Thermo Fisher Scientific) that was coupled to Easy nLC (Proxeon Biosystems, now Thermo Fisher Scientific) for 60 min. The mass spectrometer was operated in positive ion mode. MS data was acquired using a data-dependent top 10 method dynamically choosing the most abundant precursor ions from the survey scan (300–1,800 m/z) for HCD fragmentation. Automatic gain control (AGC) target was set to 3e6, and maximum inject time to 10 ms. Dynamic exclusion duration was 40.0 s. Survey scans were acquired at a resolution of 70,000 at m/z 200 and resolution for HCD spectra was set to 17,500 at m/z 200 and isolation width was 2 m/z. Normalized collision energy was 30 eV and the underfill ratio, which specifies the minimum percentage of the target value likely to be reached at maximum fill time, was defined as 0.1%. The instrument was run with peptide recognition mode enabled. And results were compared to a Uniprot database containing all sequences from Ixodidae (January 1, 2017) using MASCOT engine (Matrix Science, London, UK; version 2.2) embedded into Proteome Discoverer 1.4. The MASCOT identified parameters were set in **Supplementary Table 1**. Peptide identification was validated using false discovery rate (FDR $\leq$ 0.01). The standard of screening differentially expressed proteins was Fold change $>$1.2 and a P-value $<$ 0.05 was considered statistically significant.

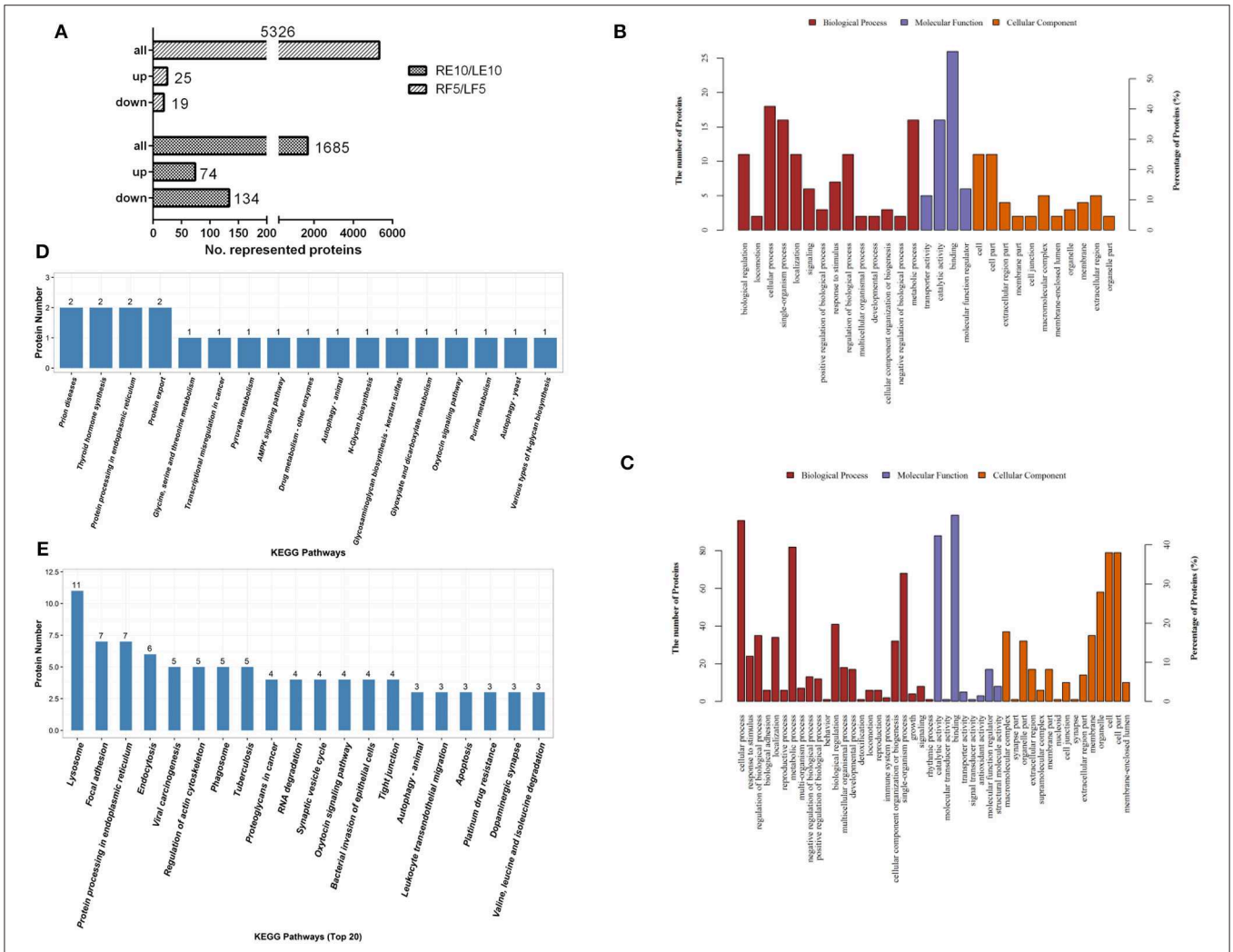

FIGURE 5 | Vitellogenin and HSP70 were expressed differentially in the ovary proteomic analyses. Twelve tick ovary samples were collected from RH36 or luciferase gene-silenced adult ticks at 5 days blood feeding and 10 days post-engorgement and analyzed using TMT technology. Number of total proteins and differentially-expressed proteins were obtained from ovary samples of adult ticks **(A)**. Differentially expressed proteins mainly involved in cellular process, developmental process and metabolic process with function of lipid transporter activity, catalytic activity and binding in the 5-day-fed tick ovaries **(B)** and 10-day post-engorged tick ovaries **(C)** by GO analysis, in which vitellogenin and HSP70 involved in protein export and protein processing in endoplasmic reticulum using KEGG enrichment analysis, respectively **(D)**. Differentially expressed proteins in the 10-day post-engorged tick ovaries chiefly participate in focal adhesion, endocytosis and protein processing in endoplasmic reticulum using KEGG enrichment analysis **(E)**.

Sequences of differentially expressed proteins were also searched using blastp tool against the online Kyoto Encyclopedia of Genes and Genomes (KEGG) database (http://geneontology.org/) and were subsequently mapped to pathways in KEGG. GO and KEGG pathway enrichment analysis were applied based on the Fisher's exact test. All assays were performed in three replicates.

RNA Sequencing and Analysis

After total RNA was treated with DNase I, mRNA was enriched by oligo (dT) with beads and fragmented into fragments of 100–400 bp. First-strand cDNA was synthesized from the mRNA fragments. And second-strand cDNA was then synthesized using DNA polymerase I and RNaseH. Short fragments were purified, end-repaired, connected with signal nucleotide A (adenine) addition and ligated with library-specific adaptors. The cDNA library was constructed and tested in qualification by Agilent 2100 Bioanalyzer and ABI StepOnePlus Real-Time PCR System, and then sequenced using Illumina HiSeq 4000.

Tick ovary transcriptome *de novo* assembly was performed by Beijing Genomics Institute (BGI, Shenzhen, China). After sequencing, low-quality, adaptor-polluted and high content of unknown base (N) reads were filtered to get clean reads. Clean reads were assembled by Trinity assembles software to obtain high-quality contigs (Yu et al., 2015). T gicl was used to perform clustering and eliminate redundant data in the assembled transcripts to obtain unique genes. Subsequently, expression analysis, heterozygous SNP detection, and functional annotation were performed. Differentially expression genes (DEGs) were further analyzed with gene ontology functional enrichment and KEGG pathway functional enrichment. The false discovery rate (FDR $\leq$ 0.001) was used to determine the threshold *P* value in multiple tests. Results were the mean of three replicates.

HSP70 RNA Interference (RNAi) for Gene Knockdown in Ticks

The dsRNA was synthesized using the T7 RiboMAX™ RNAi System (Promega, Madison, WI, USA) according to the manufacturer's recommendations. Oligonucleotide primers containing T7 promoter sequences (in italics at 5′-end) were listed in **Supplementary Table 2**. A dsRNA targeting luciferase used as a negative control was subjected to the same PCR amplification protocol using luciferase-specific primers (Yu et al., 2013). These dsRNA were maintained at −80°C until use. Unfed adult ticks ($N = 50$ females per group, two independent groups) were microinjected with 0.5 μL HSP70 dsRNA (about 1 μg RNA) at the base of the fourth right leg of the ventral surface of ticks. Control ticks were microinjected with unrelated luciferase dsRNA. After microinjection, ticks were maintained in an incubator at 25°C and 95% humidity for 24 h and then allowed to feed on rabbits' ears. Four female ticks per group were collected at 5 days of blood feeding for RNA and protein extraction to characterize gene knockdown by real-time quantitative PCR and Western blot with respect to luciferase control. Remaining ticks were allowed to feed until engorgement, which tick mortality, engorgement rate and engorgement weight was determined in individual engorged female ticks.

TABLE 1 | List of heat shock 70 kDa protein in the tick ovaries transcriptome.

Unigenes	Subject_id	Gene Name	Species	Identity	Align length	Miss_match	E_value	Score
Unigene10768_All	ACA84007.1	Heat shock 70 kDa protein 5	*Haemaphysalis longicornis*	100	21	0	1.01E-11	45.4394
CL2077.Contig1_All	ACA84007.1	Heat shock 70 kDa protein 5	*Haemaphysalis longicornis*	97.51	401	10	0	761.14
Unigene11678_All	XP_013782730.1	Heat shock 70 kDa protein 4-like	*Limulus polyphemus*	53.91	831	383	0	869.766
Unigene13971_All	P19120.2	Heat shock 70 kDa protein 8	*Bos taurus*	93.68	174	11	3.24E-86	321.627
Unigene16158_All	XP_012264348.1	Heat shock 70 kDa protein cognate 5	*Athalia rosae*	79.97	694	139	0	1061.21
Unigene18598_All	XP_001012263.1	Heat shock 70 kDa protein	*Tetrahymena thermophila*	76	75	18	6.00E-24	114.39
Unigene19775_All	XP_007453496.1	Heat shock 70 kDa protein	*Lipotes vexillifer*	61.64	219	84	3.08E-68	263.462
Unigene23136_All	XP_013788178.1	Heat shock 70 kDa protein 12A-like	*Limulus polyphemus*	72.4	616	170	0	920.613
Unigene48580_All	AIS39468.1	Heat shock 70 kDa protein	*Haemaphysalis flava*	100	20	0	2.31E-10	45.4394
Unigene48580_All	DAA34432.1	Heat shock 70 kDa protein	*Amblyomma variegatum*	95	20	1	5.35E-10	41.5874
Unigene56143_All	XP_010125825.1	Heat shock 70 kDa protein	*Chlamydotis macqueenii*	88.61	79	9	3.87E-34	148.288
CL434.Contig1_All	XP_014239635.1	Major heat shock 70 kDa protein Ba-like	*Cimex lectularius*	78.74	635	135	0	1012.29
CL2742.Contig1_All	XP_013778668.1	Heat shock 70 kDa protein cognate 4	*Limulus polyphemus*	89.68	649	67	0	1162.52

Determination of Tick mRNA Levels by Real-time Quantitative PCR

The primers and amplicon length of target genes used for real-time quantitative PCR are listed in **Supplementary Table 3**. The first-stranded cDNA was synthesized from 1 μg RNAs with the PrimeScript RT reagent kit (Perfect Real Time) (Takara, Shiga, Japan) in the following program: 37°C for 15 min, 85°C for 7 s, and finally 4°C. Quantitative real-time PCR was performed using SYBR Premix Ex Taq (Takara, Japan) with QuantStudio 5 (ABI, Waltham, USA) in 20 μL reaction mixtures including 0.4 μL ROX Dye II. The reactions were incubated for 30 s at 95°C, followed by 40 cycles at 95°C for 5 s, 60°C for 34 s, and analysis of a melting curve. Tick elongation factor 1α (ELF1α) was used as an internal control because of its stability in *R. microplus* and *R. appendiculatus* ticks (Nijhof et al., 2009). All reactions were performed in triplicate. The $2^{-\Delta Ct}$ method was used to calculate relative expression levels.

Statistical Analysis

The body weights of engorged ticks were expressed as the mean ± standard error of mean (SEM) and analyzed using Student *t*-test. Differences in the attachment rate, engorgement rate, and death rate of ticks in different groups were tested using the Chi-square test. Significance of quantitative real-time PCR results was expressed as means ± SEM and determined with the one-way analysis of variance (ANOVA), and statistical analysis was conducted using software SPSS version 20.0. $P < 0.05$ and 0.01 were considered to be statistically significant (*) and extremely significant (**), respectively.

RESULTS

The Immunomodulatory Protein RH36 Regulated the Complex Changes of Vitellin

RH36 protein was expressed exclusively in the salivary glands, not in the midguts, ovaries or fat bodies of 5-day-fed ticks and engorged ticks (**Figure 1A**). Additionally, RH36 protein was expressed at higher levels in 7-day-fed and saturated ticks and subsequently decreased after engorgement, which was highly consistent with the time of tick ovarian development (**Figure 1B**). To confirm our hypothesis that RH36 modulating tick ovary development via vitellogenesis, four vitellogenin genes (named RHVg1, RHVg2, RHVg3, and RHVg4, respectively) were cloned from ovarian transcriptome from the post-engorgement *R. haemaphysaloides* female ticks (**Supplementary Figure 1**). These sequences are highly homologous in *Haemaphysalis longicornis* and *Dermacentor variabilis* (**Supplementary Figure 2**). RHVg1, RHVg2, RHVg3, RHVg4 sequences were

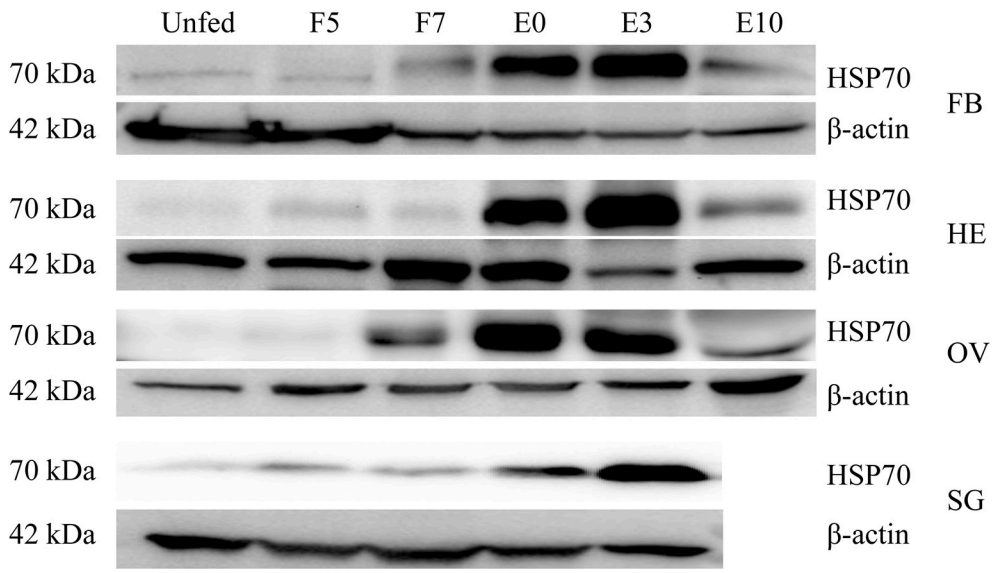

0.1	0.1	0.5	1.6	2.1	0.8	HSP70 (FB)
0.2	0.5	0.3	2.2	3.3	1.3	HSP70 (HE)
0.1	0.2	1.4	2.1	1.3	0.4	HSP70 (OV)
0.2	0.6	0.5	0.9	1.6		HSP70 (SG)

FIGURE 6 | HSP70 protein was widely distributed in a variety of organs and accelerated by blood feeding. HSP70 protein was expressed widely in fat body, hemolymph, ovary and salivary gland of adult ticks at 5 days blood feeding, 7 days blood feeding, engorgement, 3 days post-engorgement and 10 days post-engorgement by Western blot. The intensities of HSP70 protein were determined and normalized to β-actin. β-actin bands were used in the previous **Figure 2**. FB, fat body; HE, hemolymph; OV, ovary; SG, salivary gland; UF, unfed; F5, at day 5 for blood feeding; F7, at day 7 for blood feeding; E0, on the day of engorgement; E3, at 3 days post-engorgement; E10, at day 10 after engorgement.

available in the GenBank databases under the accession numbers: MK584634, MK584635, MK584636, MK584637, respectively. In addition, RHVg1 (**Supplementary Figure 3A**), RHVg2 (**Supplementary Figure 3B**) and RHVg3 (**Supplementary Figure 3C**) genes were widely distributed in the different development stages of ticks and RHVg4 (**Supplementary Figure 3D**) was detected only in engorged adults not larvae and nymphs by real-time quantitative PCR and semi-quantitative PCR (**Supplementary Figure 3E**). What's more, RHVg2 and RHVg4 was expressed in the fat body and ovary of engorged adult ticks, respectively (**Supplementary Figure 3F**).

Vitellin was purified from crude egg extraction by gel filtration (Sepharose CL-4B) and ion exchange chromatography on DEAE-cellulose and identified by possible polypeptide bands with molecular weights of 43.0, 47.3, 64.4, 72.6, 79, 85.9, 94, 102.3, 108.7, 136.5, and 161.5 kDa, respectively (**Supplementary Figure 4A**), in which two polypeptides (136.5, 72.7 kDa) were identified by LC-MS/MS (**Supplementary Tables 4**, **5**). Monoclonal antibodies were generated and had specific immunological reaction with two polypeptides (136.5, 72.7 kDa) of vitellin (**Supplementary Figure 4B**). Vitellin proteins were highly expressed in fat body, hemolymph and ovary of adult ticks after engorgement (**Figure 2**).

After RH36 gene silencing, there was no difference for four vitellogenin genes in the fat body of adult ticks (**Figures 3A,C,D**). There was one exception: RHVg2 gene

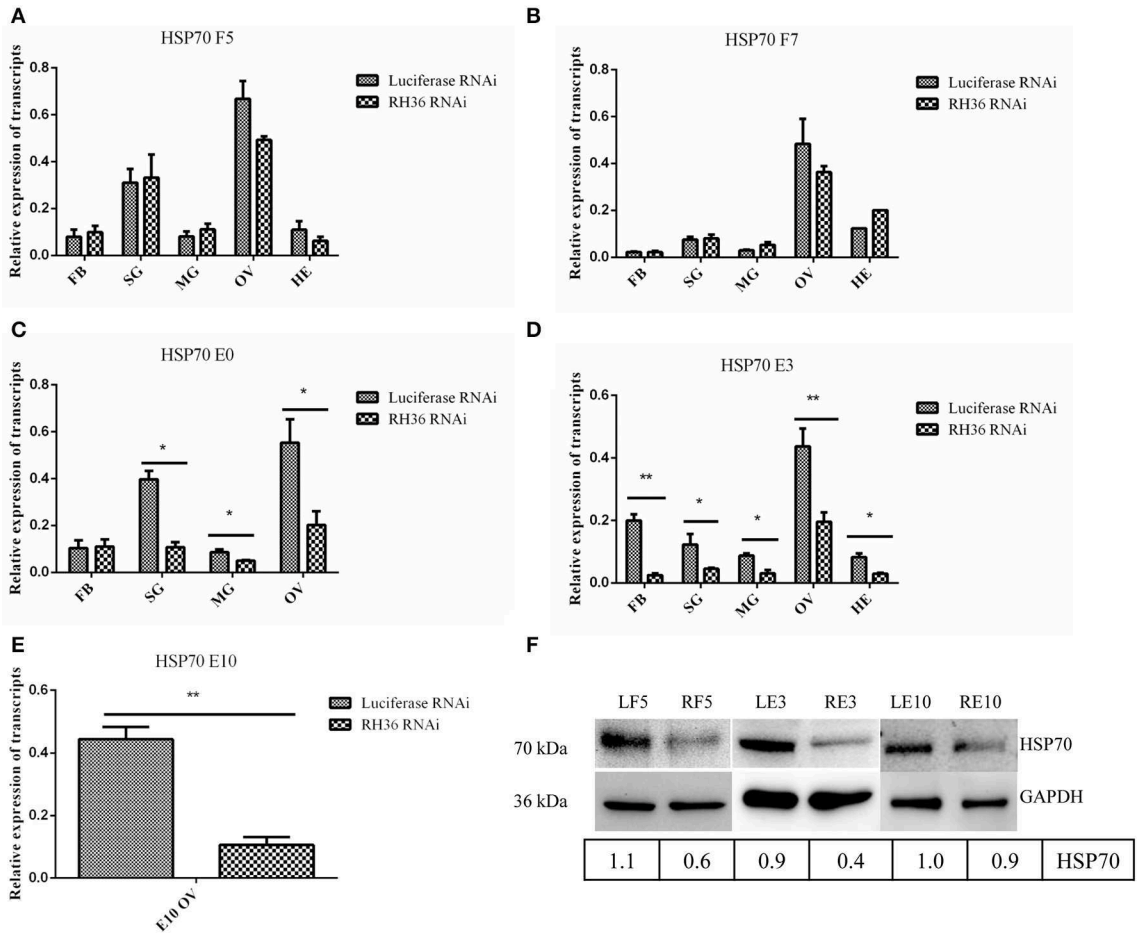

FIGURE 7 | RH36 gene silencing inhibits expression of HSP70 protein after engorgement. Transcript level of HSP70 was detected in the fat body, salivary gland, midgut, ovaries and hemolymph at 5 days blood feeding **(A)**, 7 days blood feeding **(B)**, engorgement **(C)**, 3 days post-engorgement **(D)**, and 10 days post-engorgement **(E)** by real-time quantitative PCR, results show HSP70 gene is observably down-regulated in the different organs at engorgement, 3 days post-engorgement and 10 days post-engorgement ($p < 0.05$ or $p < 0.01$). The data were normalized to tick elongation factor 1α and gene-specific standard was the HSP70 plasmid including open reading frame. ** means highly statistical significance that P-values less than 0.01. * means statistical significance that *p*-values less than 0.05. Protein level of HSP70 reduced in the ovaries at 5 days blood feeding, 3 days post-engorgement and 10 days post-engorgement by Western blot **(F)**. The intensities of HSP70 were normalized to GAPDH. GAPDH bands appeared in the previous **Figure 4**. GAPDH bands were re-used due to LF5, 5-day-fed ticks from luciferase RNAi groups; RF5, 5-day-fed ticks from RH36 RNAi groups; F7, at day 7 for blood-feeding; E0, on the day of engorgement; LE3, 3 days post-engorgement ticks from luciferase RNAi groups; RE3, 3 days post-engorgement ticks from RH36 RNAi groups; LE10, 10 days post-engorgement ticks from luciferase RNAi groups; RE10, 10 days post-engorgement ticks from RH36 RNAi groups; FB, fat body; HE, hemolymph; OV, ovary; MG, midgut; SG, salivary gland.

was up-regulated significantly at 7 days after engorgement ($p < 0.01$, **Figure 3B**). In the ovaries, although there was no difference in the transcript level of RHVg1 (**Figure 4A**), RHVg2 (**Figure 4B**) and RHVg3 (**Figure 4C**) genes from blood feeding to post-engorgement, RHVg4 gene was down-regulated significantly at 7 days or 10 days post engorgement ($p < 0.01$, **Figure 4D**). In addition, vitellin (the band of 136 kDa) protein decreased in the ovary of adult ticks at 3 or 10 days after engorgement, but not at 5 days of blood feeding (**Figure 4E**). Compared to mature oocytes from luciferase gene-silenced adult ticks, immunofluorescence showed that vitellin protein was less expressed in the cytoplasm of immature oocytes in response to RH36 gene-silencing (**Figure 4F**).

The Importance of HSP70 in the Ovary Development in Response to RH36 Depletion

To identify which proteins regulate ovary development, ovaries from adult female ticks at 5 days blood feeding and 10 days post-engorgement were selected to conduct TMT proteomics analysis. Because of significant difference in total proteins found in ovaries between blood feeding and post-engorgement (**Supplementary Figure 5**), the TMT Mass-Tagging mass spectrometric (2, 6-plex) results were analyzed using MASCOT engine version 2.2. Ovary proteomics analysis resulted in the identification of 5,326 and 1,685 unique proteins in ticks at 5 days feeding and 10 days post-engorgement respectively. In the 5-day-fed ovaries, there were 44 proteins statistically significant ($p < 0.05$ and fold change > 1.2). Among these proteins, 25 and 19 proteins were up- and down-regulated, respectively (**Figure 5A** and **Supplementary Table 6**). In the day 10 post-engorgement ovaries, RH36 gene knockdown resulted in 208 proteins with statistically significant production differentiation ($p < 0.05$ and fold change > 1.2). Among these proteins, 74 were up-regulated and 134 were down-regulated (**Figure 5A** and **Supplementary Table 7**). According to GO and KEGG analyses, differentially expressed proteins mainly correlated with cellular process, developmental process and metabolic process with function of lipid transporter activity, catalytic activity and binding in the ovaries at 5 days feeding (**Figure 5B**) and 10 days post-engorgement

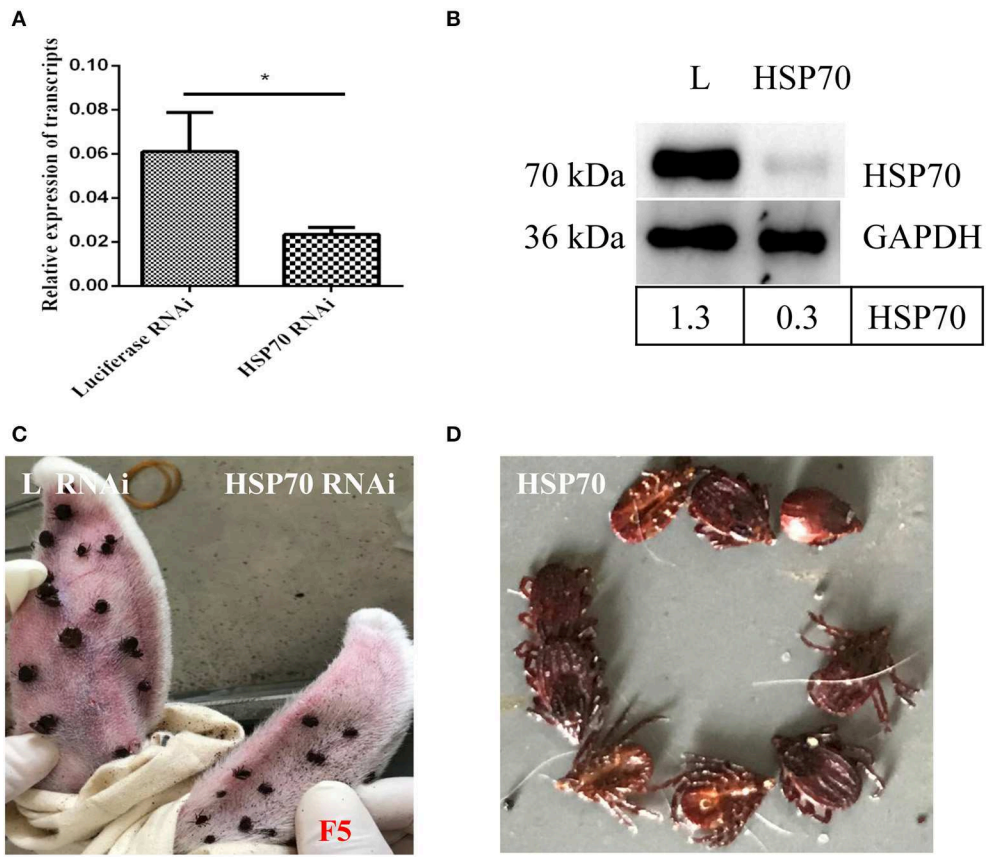

FIGURE 8 | Effect of HSP70 gene knockdown on tick blood feeding. Relative expression level of HSP70 was determined by real-time quantitative PCR **(A)** and Western blot **(B)** after interference with HSP70 dsRNA vs. luciferase dsRNA. The data were normalized to tick elongation factor 1α and gene-specific standard was the HSP70 plasmid. * means statistical significance that *p*-values less than 0.05. Tick attachment was observed at 5 days blood feeding **(C,D)**. It shows HSP70 gene-knocked down inhibits blood feeding and increases tick death. F5, 5-day-fed ticks; L, luciferase RNAi groups.

TABLE 2 | Effect of HSP70 gene knockdown on tick blood feeding and death rate.

Groups	48 h attachment rate (%)[a]	Engorgement rate (%)[a]	Engorged body weight (mg)[b]	Death rate (%)[a]
HSP70	52.22 (47/90)	2.56 (2/78)	208.95±201.53 (2 ticks)	97.44 (76/78)
L	88.89 (80/90)	80.39 (41/51)	324.45±85.24	19.61 (10/51)

[a] *Significantly different using the chi-square test.*
[b] *Significantly different using Student's t-test.*

(**Figure 5C**), in which vitellogenin (**Supplementary Figure 6A**) and HSP70 (**Supplementary Figure 6B**) involved in protein export and protein processing in endoplasmic reticulum, respectively (**Figures 5D,E**).

RH36 Gene Regulated the Expression of HSP70 Protein

Since HSP70 protein was very important in tick blood-sucking and ovary maturation, we obtained HSP70 gene sequence (GenBank accession numbers: MK584638) from the ovary transcriptome (**Table 1**) and found that the open reading frame (ORF) of HSP70 was 1,980 bp long, encoding a deduced protein with 660 amino acids in length, a predicted molecular mass of 72.5 kDa and a pI of 5.32. It was also found that HSP70 protein included three signature sequences and the extreme C-terminal endoplasmic reticulum targeting sequence (KDEL, **Supplementary Figure 7A**). As shown in **Supplementary Figure 7B**, HSP70 from *R. haemaphysaloides* was highly conserved with over 83% identity in arthropods and mammals, in which it was highly homologous in *Haemaphysalis flava* and *Ixodes scapularis* with the identity of 96.21 and 91.06%, respectively. HSP70 protein was widely distributed in the hemolymph, ovary, salivary gland and fat body of post-engorgement ticks, with highest levels in the ovary at 7 days blood feeding and in the circulating hemolymph at 3 days post-engorgement (**Figure 6**).

After RH36 gene knocking down, there was no difference for HSP70 gene expression in the fat body, salivary gland, midgut, ovary and hemolymph of 5-day-fed and 7-day-fed adult ticks (**Figures 7A,B**, respectively). On the day of engorgement, HSP70 gene was down-regulated significantly in the ovary, midgut and salivary gland of adult ticks ($p < 0.05$, **Figure 7C**), coinciding with RH36 down-regulation expression. At 3 days post-engorgement, HSP70 gene also decreased markedly in the fat body, ovary, midgut, salivary gland, and hemolymph of adult ticks ($p < 0.05$, **Figure 7D**). In addition, HSP70 gene expression reduced observably in the ovary of adult ticks at 10 days post-engorgement ($p < 0.01$, **Figure 7E**). From tick blood-sucking to engorgement, HSP70 protein level decreased in the ovaries of adult ticks from RH36 RNAi groups by Western blot (**Figure 7F**). These results suggested that RH36 promoted expression of HSP70 protein in the post-engorged adult ticks.

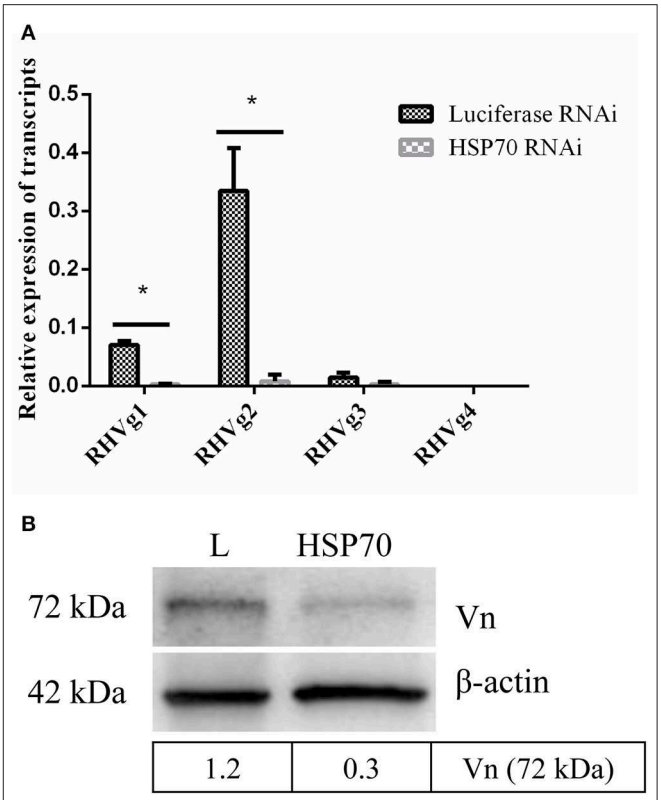

FIGURE 9 | HSP70 gene silencing down regulates expression of Vg and vitellin. RHVg1 and RHVg2 genes decreased significantly in 5-day-fed ticks by real-time quantitative PCR (**A**, $p < 0.05$). ELFIa gene served as the endogenous control. Every group has three biological repeats and each repeat is three times. Data are calculated with $2^{-\Delta CT}$. Gene-specific standards were the respective plasmid of RHVg genes. Meanwhile, vitellin protein was down-regulated dramatically at 5 days blood feeding using Western blot (**B**, $p < 0.05$). The intensities of vitellin protein bands (72 kDa) were determined, normalizing to β-actin. * means statistical significance that *p*-values less than 0.05. L, luciferase RNA interference, Vn, Vitellin.

Impacts of HSP70 Gene Knockdown on Tick Blood Feeding

HSP70 mRNA decreased by 73.86% (**Figure 8A**) and HSP70 protein was significantly down-regulated after microinjecting HSP70 dsRNA ($p < 0.05$, **Figure 8B**). After HSP70 gene silencing, mean of 48 h attachment rate and average engorgement rate was 52.22 and 2.56%, respectively. Meanwhile, these parameters showed 88.89 and 80.39% in the luciferase RNAi groups, respectively, which revealed that down-regulation of HSP70 gene decreased tick blood feeding and engorgement rate (**Table 2**). Although ticks attached to rabbit ears after HSP70 gene silencing (**Figure 8C**), the engorged body weight of ticks decreased and death rate increased compared to the luciferase RNAi groups ($p < 0.05$, **Table 2** and **Figure 8D**), which shows that HSP70 gene facilitates abundance of tick blood feeding and protects ticks from death. After HSP70 gene knockdown, two vitellogenins (RHVg1 and RHVg2, **Figure 9A**) and vitellin (**Figure 9B**) were observably

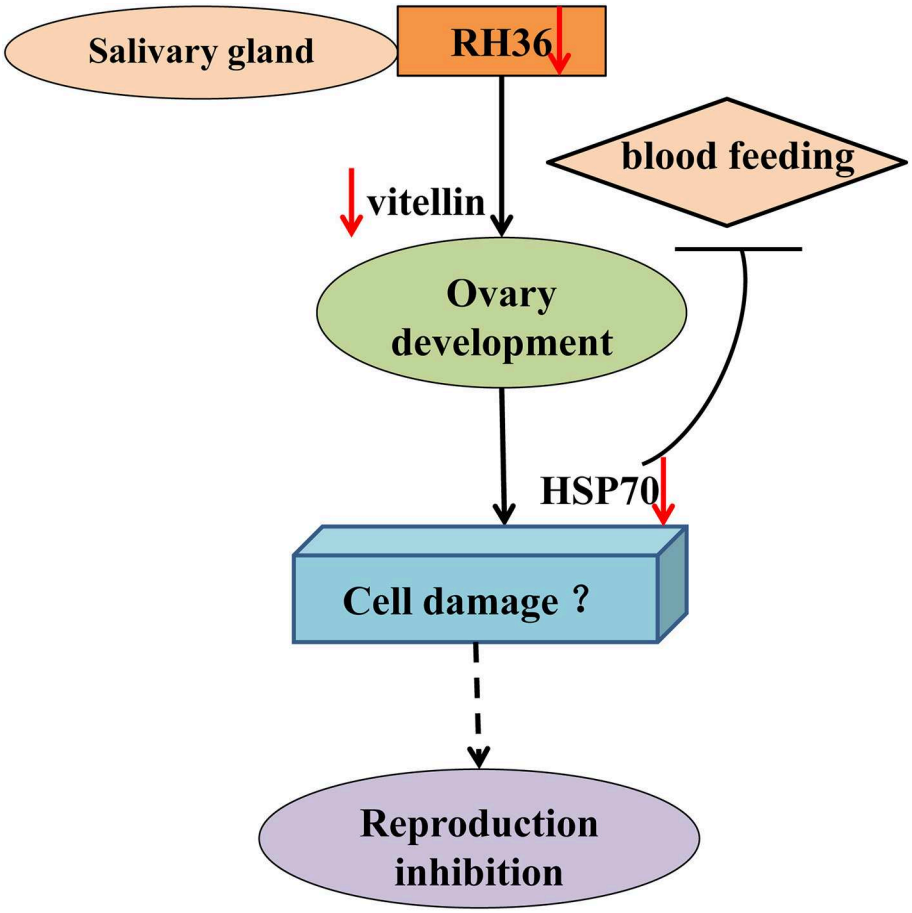

FIGURE 10 | Model of RH36 regulated tick oviposition via nutrition uptake. RH36 expressed-uniquely in salivary gland regulates tick blood feeding and ovary development by inhibiting vitellin uptake mediated by HSP70 protein using real-time quantitative PCR and Western blot. In addition, HSP70 gene silencing considerably increased tick death rate during blood feeding but it is still to be further studied that RH36 gene regulates tick oviposition by accelerating cell damage via HSP70.

down-regulated ($p < 0.05$), indicating that HSP70 protein regulated expression of vitellogenin proteins via promoting tick blood feeding.

RH36 Gene Played an Important Role in the Integration of Nutrition Uptake and Reproduction

As shown in **Figure 10**, RH36 gene expressed-uniquely in salivary gland controlled tick blood feeding and modulated tick ovary development and oviposition by regulating the expression of vitellin in ovary, while HSP70 protein was down-regulated significantly in the ovaries of post-engorged ticks after RH36 gene silencing by real-time quantitative PCR and Western blot ($p < 0.05$). HSP70 gene positively modulated tick blood feeding and ovary development via nutrition uptake. Therefore, we speculated that RH36 gene silencing hindered tick blood feeding and oocytes maturity by inhibiting vitellin uptake mediated by HSP70 protein. In addition, HSP70 gene silencing considerably increased tick death rate during blood feeding.

DISCUSSION

RH36 not only is an immunomodulatory protein that suppressed the proliferation of splenocytes and expression of several cytokines such as IL-2, IL-12, and TNF-α, but also modulates blood feeding and oviposition in hard ticks (Wang et al., 2017). Moreover, RH36 was induced by blood feeding and expressed specifically in salivary glands, but not in other organs such as ovary and hemolymph (**Figure 1**). How did RH36 regulate tick ovary development indirectly? We speculated that RH36 was involved in the integration of nutrition and reproduction in ticks, in which vitellogenin is critical to tick ovary maturation since it serves as the nutritional source for tick survivability and reproduction (Xavier et al., 2018). Vitellogenin and vitellin are structurally, biochemically and immunologically similar in the majority of insects, including ticks, which results in McAb against vitellin recognized vitellogenins (Kaufman, 2004; Yang et al., 2015). Four vitellogenin genes (**Supplementary Figure 1**) and McAb against vitellin (**Figure 4**) were obtained to test the dynamics

of vitellogenesis. Vitellogenin genes were widely distributed in fat body, midgut, hemolymph and ovaries of fed and engorged adult ticks (**Figure 2** and **Supplementary Figure 3**). It is reported that vitellogenin is synthesized in the fat body and midgut of female ticks after mating and transported through the hemolymph, captured by surface receptors called vitellogenin receptors (VgRs), and endocytosed into developing oocytes within the ovaries (Rosell and Coons, 1992; Khalil et al., 2011; Mitchell et al., 2019). RH36 gene did not regulate transcripts of RHVg1, RHVg3, and RHVg4 genes in the fat body of adult ticks (**Figures 3A,C,D**), but RHVg2 gene in fat body was up-regulated at 7 days post-engorgement (**Figure 3B**), which may be stimulated by down-regulation of vitellin protein in the ovaries of 7-day-engorged ticks (**Figure 4D**). RHVg4 gene and vitellin protein decreased significantly in the post-engorged ovaries after RH36 gene silencing ($p < 0.05$, **Figures 4A–E**), and vitellin protein was less expressed in the cytoplasm of immature oocytes compared to mature oocytes at 10 days after engorgement (**Figure 4F**), which suggested RH36 gene silencing attenuated vitellin expression in ovaries at post-engorgement. Due to the absence of available genome for *Rhipicephalus haemaphysaloides* ticks, some ovarian-specific proteins may be lost by searching Ixodidae database resulting in less proteins correlating with reproductive process in proteomic analysis (**Figure 5C**). Differentially-expressed proteins relating to endocytosis played an important role in vitellogenesis (**Figures 5C,E**). It is suggested that RH36 may modulate vitellin uptake via endocytosis. Clathrin heavy chain involved in endocytic pathway regulates expression of vitellogenin in *R. haemaphysaloides* (Kuang et al., 2020). Vitellin is a hemoglycolipoprotein consisting of many bands (James and Oliver, 1997; Yang et al., 2015). Similarly, there were 11 polypeptides of vitellin identified by proteomic analysis in the *R. haemaphysaloides* ticks and vitellin antibody in this study recognized two bands of 136 and 72 kDa (**Supplementary Figure 4**) that is different from the peptides of vitellogenin in ovary proteomics analysis (**Supplementary Tables 4**, **5**), resulting in inconsistent phenomenon.

The ovarian transcriptome from post-engorged *R. haemaphysaloides* females was analyzed and revealed that the transcripts related to lipid metabolism and other metabolisms were differentially expressed. These transcripts may play an important role in ovary development after tick engorgement. The metabolism processes could be involved in the increase of fat body cells observing in the vitellogenesis/oogenesis processes (Denardi et al., 2009). In addition, the abundance of metabolic transcripts could be related to changes in the reproductive tissues during the oogenesis/vitellogenesis processes, such as ovary size growth and oocyte maturation (Moreira et al., 2017), which is consistent with the result that RH36 gene silencing affects tick ovary development and oocytes maturity (Wang et al., 2017).

In the ovary proteomic analysis of ticks fed for 5 days, HSP70 was a typical stress protein in response to micro-injection of RH36 dsRNA (Villar et al., 2010). In the 10 days post-engorged ovary, HSP70 was inhibited significantly after RH36 gene silencing ($p < 0.05$, **Figures 5A**, **7**) and related closely to protein processing in endoplasmic reticulum (**Figure 5E**). Recent work has shown that heat shock proteins are secreted to the cell exterior partially in response to stress, we hypothesize that RH36 may modulate ovary development indirectly via mediator HSP70 protein. On the one hand, HSP-70 like protein in salivary gland of ticks participates in variable fibrinogenolysis and accelerates engorged quantity upon blood feeding (Vora et al., 2017), immunomodulatory protein RH36 may be dependent on HSP70 protein to modulate tick blood feeding and nutrient supply (Wang et al., 2017). On the other hand, HSP70, as a endoplasmic reticulum chaperone, exhibits both pro-inflammatory and anti-inflammatory properties, depending on the context in which they encounter responding immune cells (Pockley and Henderson, 2018). HSP70 may have a synergistic effect with RH36 protein in salivary gland of adult ticks. However, the mechanism of HSP70 gene regulating tick oocytes development was still to be further identified. Furthermore, it is still unknown that RH36 gene regulates tick oviposition by accelerating cell death via HSP70.

After HSP70 gene silencing, the mean of 48 h attachment rate, average engorgement rate and expression of vitellin significantly decreased ($p < 0.05$, **Table 2** and **Figure 9**). This indicates that the down-regulation of HSP70 gene decreases tick blood feeding and nutrition uptake. In ticks, blood feeding triggered salivary gland degeneration (L'Amoreaux et al., 2003) and ovary maturation (Friesen and Kaufman, 2009), suggesting vitellin protein reduced by HSP70 gene silencing inhibits tick ovary development. Starvation activates cell apoptosis and increases tick death. Consistent with this, HSP70 gene silencing dramatically increased tick death rate (**Table 2** and **Figure 8**). We speculated that nutrition deficiency accelerated HSP70-mediated cell damage in ticks (**Figure 10**). The expression of HSP with antioxidant activity extends lifespan via regulating the downstream protein autophagy-related gene 7 (Morrow et al., 2004; Liao et al., 2008; Chen et al., 2012; Sarup et al., 2014; Vos et al., 2016), while HSP depletion reduces the number of viviparous offspring and simultaneously increases the number of premature nymphs, suggesting an unexpected role in aphid embryogenesis and eclosion (Will et al., 2017). Therefore, it is suggested that RH36 gene regulates vitellogenin uptake via HSP70 protein and extends lifespan of ovary to improve oviposition rate.

DATA AVAILABILITY STATEMENT

The Transcriptome Shotgun Assembly project has been deposited at DDBJ/EMBL/GenBank under the accession GIJA00000000.

ETHICS STATEMENT

The animal study was reviewed and approved by the Institutional Animal Care and Use Committee of the Shanghai Veterinary

Research Institute, and authorized by the Animal Ethical Committee of Shanghai Veterinary Research Institute.

AUTHOR CONTRIBUTIONS

FW planned the experiments and wrote the paper. FW, YW, GW, and CK performed the experiments. FW, HZ, and JZ analyzed the data. JC and YZ contributed to the reagents or ticks.

FUNDING

This study was supported by the National Natural Science Foundation of China (NSFC; grant No. 31572512).

ACKNOWLEDGMENTS

We would like to thank Beijing Genomics Institute (BGI, Shenzhen, China) for helping with RNA sequencing and Shanghai Applied Protein Technology (APT, shanghai, China) for helping with quantitative proteomic analysis.

SUPPLEMENTARY MATERIAL

The Supplementary Material for this article can be found online at: https://www.frontiersin.org/articles/10.3389/fcimb.2020.00093/full#supplementary-material

REFERENCES

Alarcon-Chaidez, F. J., Muller-Doblies, U. U., and Wikel, S. (2003). Characterization of a recombinant immunomodulatory protein from the salivary glands of *Dermacentor andersoni*. *Parasite Immunol.* 25, 69–77. doi: 10.1046/j.1365-3024.2003.00609.x

Anatriello, E., Ribeiro, J. M., De Miranda-Santos, I. K., Brandao, L. G., Anderson, J. M., Valenzuela, J. G., et al. (2010). An insight into the sialotranscriptome of the brown dog tick, *Rhipicephalus sanguineus*. *BMC Genomics* 11:450. doi: 10.1186/1471-2164-11-450

Barrero, R. A., Guerrero, F. D., Black, M., Mccooke, J., Chapman, B., Schilkey, F., et al. (2017). Gene-enriched draft genome of the cattle tick *Rhipicephalus microplus*: assembly by the hybrid Pacific Biosciences/Illumina approach enabled analysis of the highly repetitive genome. *Int. J. Parasitol.* 47, 569–583. doi: 10.1016/j.ijpara.2017.03.007

Bergman, D. K., Palmer, M. J., Caimano, M. J., Radolf, J. D., and Wikel, S. K. (2000). Isolation and molecular cloning of a secreted immunosuppressant protein from *Dermacentor andersoni* salivary gland. *J. Parasitol.* 86, 516–525. doi: 10.1645/0022-3395(2000)086[0516:IAMCOA]2.0.CO;2

Chen, S. F., Kang, M. L., Chen, Y. C., Tang, H. W., Huang, C. W., Li, W. H., et al. (2012). Autophagy-related gene 7 is downstream of heat shock protein 27 in the regulation of eye morphology, polyglutamine toxicity, and lifespan in *Drosophila*. *J. Biomed. Sci.* 19:52. doi: 10.1186/1423-0127-19-52

Danielova, V., Holubova, J., Pejcoch, M., and Daniel, M. (2002). Potential significance of transovarial transmission in the circulation of tick-borne encephalitis virus. *Folia Parasitol.* 49, 323–325. doi: 10.14411/fp.2002.060

Denardi, S. E., Bechara, G. H., and Camargo-Mathias, M. I. (2009). Fat body cells of *Amblyomma cajennense* partially engorged females (Acari: Ixodidae) and their role on vitellogenesis process. *Exp. Parasitol.* 121, 213–218. doi: 10.1016/j.exppara.2008.10.019

Ehrmann, S., Ruyts, S. C., Scherer-Lorenzen, M., Bauhus, J., Brunet, J., Cousins, S., et al. (2018). Habitat properties are key drivers of *Borrelia burgdorferi* (s.l.) prevalence in Ixodes ricinus populations of deciduous forest fragments. *Parasit. Vectors.* 11:23. doi: 10.1186/s13071-017-2590-x

Eisen, R. J., and Eisen, L. (2018). The blacklegged tick, *Ixodes scapularis*: an increasing public health concern. *Trends Parasitol.* 34, 295–309. doi: 10.1016/j.pt.2017.12.006

Esmeralda Parra-Peralbo, J. C. (2011). *Drosophila* lipophorin receptors mediate the uptake of neutral lipids in oocytes and imaginal disc cells by an endocytosis-independent mechanism. *PLoS Genet.* 7:e1001297. doi: 10.1371/journal.pgen.1001297

Friesen, K. J., and Kaufman, W. R. (2009). Salivary gland degeneration and vitellogenesis in the ixodid tick *Amblyomma hebraeum*: surpassing a critical weight is the prerequisite and detachment from the host is the trigger. *J. Insect Physiol.* 55, 936–942. doi: 10.1016/j.jinsphys.2009.06.007

Galay, R. L., Aung, K. M., Umemiya-Shirafuji, R., Maeda, H., Matsuo, T., Kawaguchi, H., et al. (2013). Multiple ferritins are vital to successful blood feeding and reproduction of the hard tick *Haemaphysalis longicornis*. *J. Exp. Biol.* 216, 1905–1915. doi: 10.1242/jeb.081240

Grabowski, J. M., Tsetsarkin, K. A., Long, D., Scott, D. P., Rosenke, R., Schwan, T. G., et al. (2017). Flavivirus infection of *Ixodes scapularis* (black-legged tick) *ex vivo* organotypic cultures and applications for disease control. *MBio* 8, e01255–e01217. doi: 10.1128/mBio.01255-17

Gulia-Nuss, M., Nuss, A. B., Meyer, J. M., Sonenshine, D. E., Roe, R. M., Waterhouse, R. M., et al. (2016). Genomic insights into the *Ixodes scapularis* tick vector of Lyme disease. *Nat. Commun.* 7, 1569–1576. doi: 10.1038/ncomms10507

Hajdusek, O., Sojka, D., Kopacek, P., Buresova, V., Franta, Z., Sauman, I., et al. (2009). Knockdown of proteins involved in iron metabolism limits tick reproduction and development. *Proc. Natl. Acad. Sci. U.S.A.* 106, 1033–1038. doi: 10.1073/pnas.0807961106

Han, R., Yang, J., Niu, Q., Liu, Z., Chen, Z., Kan, W., et al. (2018). Molecular prevalence of spotted fever group rickettsiae in ticks from Qinghai province, northwestern China. *Infect. Genet. Evol.* 57, 1–7. doi: 10.1016/j.meegid.2017.10.025

Harris, E. K., Verhoeve, V. I., Banajee, K. H., Macaluso, J. A., Azad, A. F., and Macaluso, K. R. (2017). Comparative vertical transmission of Rickettsia by *Dermacentor variabilis* and *Amblyomma maculatum*. *Ticks Tick Borne Dis.* 8, 598–604. doi: 10.1016/j.ttbdis.2017.04.003

James, A. M., and Oliver, J. H. Jr. (1997). Purification and partial characterization of vitellin from the black-legged tick, *Ixodes scapularis*. *Insect Biochem. Mol. Biol.* 27, 639–649. doi: 10.1016/S0965-1748(97)00038-6

Jongejan, F., Su, B. L., Yang, H. J., Berger, L., Bevers, J., Liu, P. C., et al. (2018). Molecular evidence for the transovarial passage of *Babesia gibsoni* in *Haemaphysalis hystricis* (Acari: Ixodidae) ticks from Taiwan: a novel vector for canine babesiosis. *Parasit. Vectors.* 11:134. doi: 10.1186/s13071-018-2722-y

Kaufman, W. R. (2004). Assuring paternity in a promiscuous world: are there lessons for ticks among the insects? *Parasitology* 129, 145–160. doi: 10.1017/S0031182004004846

Khalil, S. M., Donohue, K. V., Thompson, D. M., Jeffers, L. A., Ananthapadmanaban, U., Sonenshine, D. E., et al. (2011). Full-length sequence, regulation and developmental studies of a second vitellogenin gene from the American dog tick, *Dermacentor variabilis*. *J. Insect Physiol.* 57, 400–408. doi: 10.1016/j.jinsphys.2010.12.008

Konnai, S., Nakajima, C., Imamura, S., Yamada, S., Nishikado, H., Kodama, M., et al. (2009). Suppression of cell proliferation and cytokine expression by HL-p36, a tick salivary gland-derived protein of *Haemaphysalis longicornis*. *Immunology* 126, 209–219. doi: 10.1111/j.1365-2567.2008.02890.x

Kotal, J., Langhansova, H., Lieskovska, J., Andersen, J. F., Francischetti, I. M., Chavakis, T., et al. (2015). Modulation of host immunity by tick saliva. *J. Proteomics* 128, 58–68. doi: 10.1016/j.jprot.2015.07.005

Kuang, C., Wang, F., Zhou, Y., Cao, J., Zhang, H., Gong, H., et al. (2020). Molecular characterization of clathrin heavy chain (Chc) in Rhipicephalus haemaphysaloides and its effect on vitellogenin (Vg) expression via the clathrin-mediated endocytic pathway. *Exp. Appl. Acarol.* 80, 71–89. doi: 10.1007/s10493-019-00438-5

L'Amoreaux, W. J., Junaid, L., and Trevidi, S. (2003). Morphological evidence that salivary gland degeneration in the American dog tick, *Dermacentor variabilis* (Say), involves programmed cell death. *Tissue Cell* 35, 95–99. doi: 10.1016/S0040-8166(02)00109-X

Liao, P. C., Lin, H. Y., Yuh, C. H., Yu, L. K., and Wang, H. D. (2008). The effect of neuronal expression of heat shock proteins 26 and 27 on lifespan, neurodegeneration, and apoptosis in *Drosophila*. *Biochem. Biophys. Res. Commun.* 376, 637–641. doi: 10.1016/j.bbrc.2008.08.161

Mitchell, R. D, III, Sonenshine, D. E., and Perez De Leon, A. A. (2019). Vitellogenin receptor as a target for tick control: a mini-review. *Front. Physiol.* 10:618. doi: 10.3389/fphys.2019.00618

Moore, T. C., Pulscher, L. A., Caddell, L., Von Fricken, M. E., Anderson, B. D., Gonchigoo, B., et al. (2018). Evidence for transovarial transmission of tick-borne rickettsiae circulating in Northern Mongolia. *PLoS Negl. Trop. Dis.* 12:e0006696. doi: 10.1371/journal.pntd.0006696

Moreira, H. N. S., Barcelos, R. M., Vidigal, P. M. P., Klein, R. C., Montandon, C. E., Maciel, T. E. F., et al. (2017). A deep insight into the whole transcriptome of midguts, ovaries and salivary glands of the *Amblyomma sculptum* tick. *Parasitol. Int.* 66, 64–73. doi: 10.1016/j.parint.2016.10.011

Morrow, G., Battistini, S., Zhang, P., and Tanguay, R. M. (2004). Decreased lifespan in the absence of expression of the mitochondrial small heat shock protein Hsp22 in *Drosophila. J. Biol. Chem.* 279, 43382–43385. doi: 10.1074/jbc.C400357200

Nijhof, A. M., Balk, J. A., Postigo, M., and Jongejan, F. (2009). Selection of reference genes for quantitative REAL-TIME PCR studies in *Rhipicephalus (Boophilus) microplus* and *Rhipicephalus appendiculatus* ticks and determination of the expression profile of Bm86. *BMC Mol. Biol.* 10:112. doi: 10.1186/1471-2199-10-112

Oyugi, M. O., Kinyua, J. K., Magiri, E. N., Kigoni, M. W., Costa, E. P., and Githaka, N. W. (2018). *In silico* characterization and structural modeling of *Dermacentor andersoni* p36 immunosuppressive protein. *Adv. Bioinformatics*. 2018:7963401. doi: 10.1155/2018/7963401

Parola, P., and Raoult, D. (2001). Ticks and tickborne bacterial diseases in humans: an emerging infectious threat. *Clin. Infect. Dis.* 32, 897–928. doi: 10.1086/319347

Perner, J., Sobotka, R., Sima, R., Konvickova, J., Sojka, D., Oliveira, P. L., et al. (2016). Acquisition of exogenous haem is essential for tick reproduction. *Elife*. 5:e12318. doi: 10.7554/eLife.12318

Pockley, A. G., and Henderson, B. (2018). Extracellular cell stress (heat shock) proteins-immune responses and disease: an overview. *Philos. Trans. R. Soc. Lond. B. Biol. Sci.* 373: 20160522. doi: 10.1098/rstb.2016.0522

Rosell, R., and Coons, L. B. (1992). The role of the fat body, midgut and ovary in vitellogenin production and vitellogenesis in the female tick, *Dermacentor variabilis*. *Int. J. Parasitol.* 22, 341–349. doi: 10.1016/S0020-7519(05)80012-8

Sarup, P., Sorensen, P., and Loeschcke, V. (2014). The long-term effects of a life-prolonging heat treatment on the *Drosophila melanogaster* transcriptome suggest that heat shock proteins extend lifespan. *Exp. Gerontol.* 50, 34–39. doi: 10.1016/j.exger.2013.11.017

Schneider, C. A., Rasband, W. S., and Eliceiri, K. W. (2012). NIH Image to ImageJ: 25 years of image analysis. *Nat. Methods*. 9, 671–675. doi: 10.1038/nmeth.2089

Thompson, D. M., Khalil, S. M., Jeffers, L. A., Ananthapadmanaban, U., Sonenshine, D. E., Mitchell, R. D., et al. (2005). *In vivo* role of 20-hydroxyecdysone in the regulation of the vitellogenin mRNA and egg development in the American dog tick, *Dermacentor variabilis* (Say). *J. Insect Physiol.* 51, 1105–1116. doi: 10.1016/j.jinsphys.2005.05.011

Umemiya-Shirafuji, R., Boldbaatar, D., Liao, M., Battur, B., Rahman, M. M., Kuboki, T., et al. (2012). Target of rapamycin (TOR) controls vitellogenesis via activation of the S6 kinase in the fat body of the tick, *Haemaphysalis longicornis*. *Int. J. Parasitol.* 42, 991–998. doi: 10.1016/j.ijpara.2012.08.002

Umemiya-Shirafuji, R., Hatta, T., Okubo, K., Sato, M., Maeda, H., Kume, A., et al. (2017). Transovarial persistence of Babesia ovata DNA in a hard tick, *Haemaphysalis longicornis*, in a semi-artificial mouse skin membrane feeding system. *Acta Parasitol.* 62, 836–841. doi: 10.1515/ap-2017-0100

Villar, M., Ayllon, N., Busby, A. T., Galindo, R. C., Blouin, E. F., Kocan, K. M., et al. (2010). Expression of heat shock and other stress response proteins in ticks and cultured tick cells in response to *Anaplasma* spp. *infection and heat shock. Int. J. Proteomics* 2010:657261. doi: 10.1155/2010/657261

Vora, A., Taank, V., Dutta, S. M., Anderson, J. F., Fish, D., Sonenshine, D. E., et al. (2017). Ticks elicit variable fibrinogenolytic activities upon feeding on hosts with different immune backgrounds. *Sci. Rep.* 7:44593. doi: 10.1038/srep44593

Vos, M. J., Carra, S., Kanon, B., Bosveld, F., Klauke, K., Sibon, O. C., et al. (2016). Specific protein homeostatic functions of small heat-shock proteins increase lifespan. *Aging Cell* 15, 217–226. doi: 10.1111/acel.12422

Wang, F., Lu, X., Guo, F., Gong, H., Zhang, H., Zhou, Y., et al. (2017). The immunomodulatory protein RH36 is relating to blood-feeding success and oviposition in hard ticks. *Vet. Parasitol.* 240, 49–59. doi: 10.1016/j.vetpar.2017.03.017

Will, T., Schmidtberg, H., Skaljac, M., and Vilcinskas, A. (2017). Heat shock protein 83 plays pleiotropic roles in embryogenesis, longevity, and fecundity of the pea aphid *Acyrthosiphon pisum*. *Dev. Genes Evol.* 227, 1–9. doi: 10.1007/s00427-016-0564-1

Xavier, M. A., Tirloni, L., Pinto, A. F. M., Diedrich, J. K., Yates, J. R., Mulenga, A., et al. (2018). A proteomic insight into vitellogenesis during tick ovary *maturation. Sci. Rep.* 8:4698. doi: 10.1038/s41598-018-23090-2

Yang, X., Yu, Z., He, Y., Xu, X., Gao, Z., Wang, H., et al. (2015). Purification of vitellin and dynamics of vitellogenesis in the parthenogenetic tick *Haemaphysalis longicornis* (Acari: Ixodidae). *Exp. Appl. Acarol.* 65, 377–388. doi: 10.1007/s10493-014-9866-z

Yu, X., Gong, H., Zhou, Y., Zhang, H., Cao, J., and Zhou, J. (2015). Differential sialotranscriptomes of unfed and fed *Rhipicephalus haemaphysaloides*, with particular regard to differentially expressed genes of cysteine proteases. *Parasit. Vectors* 8:597. doi: 10.1186/s13071-015-1213-7

Yu, Y., Cao, J., Zhou, Y., Zhang, H., and Zhou, J. (2013). Isolation and characterization of two novel serpins from the tick Rhipicephalus haemaphysaloides. *Ticks Tick Borne Dis.* 4, 297–303.

Conflict of Interest: The authors declare that the research was conducted in the absence of any commercial or financial relationships that could be construed as a potential conflict of interest.

frontiers in Cellular and Infection Microbiology

ORIGINAL RESEARCH
published: 10 March 2020
doi: 10.3389/fcimb.2020.00078

Allergic Reactions and Immunity in Response to Tick Salivary Biogenic Substances and Red Meat Consumption in the Zebrafish Model

Marinela Contreras[1†], Iván Pacheco[1†], Pilar Alberdi[1], Sandra Díaz-Sánchez[1], Sara Artigas-Jerónimo[1], Lourdes Mateos-Hernández[1,2], Margarita Villar[1], Alejandro Cabezas-Cruz[2] and José de la Fuente[1,3]*

[1] SaBio, Instituto de Investigación en Recursos Cinegéticos IREC-CSIC-UCLM-JCCM, Ciudad Real, Spain, [2] UMR BIPAR, INRA, ANSES, Ecole Nationale Vétérinaire d'Alfort, Université Paris-Est, Maisons-Alfort, France, [3] Department of Veterinary Pathobiology, Center for Veterinary Health Sciences, Oklahoma State University, Stillwater, OK, United States

OPEN ACCESS

Edited by:
Itabajara Silva Vaz Jr., Federal University of Rio Grande Do Sul, Brazil

Reviewed by:
Alexandre F. Marques, Federal University of Minas Gerais, Brazil
Sheryl Anne Van Nunen, Royal North Shore Hospital, Australia

***Correspondence:**
José de la Fuente
jose_delafuente@yahoo.com

[†]These authors have contributed equally to this work

Specialty section:
This article was submitted to Parasite and Host, a section of the journal Frontiers in Cellular and Infection Microbiology

Received: *13 January 2020*
Accepted: *17 February 2020*
Published: *10 March 2020*

Citation:
Contreras M, Pacheco I, Alberdi P, Díaz-Sánchez S, Artigas-Jerónimo S, Mateos-Hernández L, Villar M, Cabezas-Cruz A and de la Fuente J (2020) Allergic Reactions and Immunity in Response to Tick Salivary Biogenic Substances and Red Meat Consumption in the Zebrafish Model. Front. Cell. Infect. Microbiol. 10:78. doi: 10.3389/fcimb.2020.00078

Ticks are arthropod ectoparasite vectors of pathogens and the cause of allergic reactions affecting human health worldwide. In humans, tick bites can induce high levels of immunoglobulin E antibodies against the carbohydrate Galα1-3Galβ1-(3)4GlcNAc-R (α-Gal) present in glycoproteins and glycolipids from tick saliva that mediate anaphylactic reactions known as the alpha-Gal syndrome (AGS) or red meat allergy. In this study, a new animal model was developed using zebrafish for the study of allergic reactions and the immune mechanisms in response to tick salivary biogenic substances and red meat consumption. The results showed allergic hemorrhagic anaphylactic-type reactions and abnormal behavior patterns likely in response to tick salivary toxic and anticoagulant biogenic compounds different from α-Gal. However, the results showed that only zebrafish previously exposed to tick saliva developed allergic reactions to red meat consumption with rapid desensitization and tolerance. These allergic reactions were associated with tissue-specific Toll-like receptor-mediated responses in types 1 and 2 T helper cells (T_H1 and T_H2) with a possible role for basophils in response to tick saliva. These results support previously proposed immune mechanisms triggering the AGS and provided evidence for new mechanisms also potentially involved in the AGS. These results support the use of the zebrafish animal model for the study of the AGS and other tick-borne allergies.

Keywords: alpha gal, alpha gal syndrome, tick, zebrafish, allergy

INTRODUCTION

Arthropod ectoparasites are a growing burden worldwide (Stutzer et al., 2018). Local allergic reactions to the bite of arthropod ectoparasites such as mosquitoes, ticks, fleas, mites, and lice are common, but in some cases large local and anaphylactic reactions are possible (Lee et al., 2016; Mihara, 2017; Stringer et al., 2017; Haddad et al., 2018; Ha et al., 2019).

Ticks are vectors of pathogens affecting human and animal health worldwide (de la Fuente et al., 2008, 2017). Tick saliva contains multiple biomolecules such as proteins and lipids that facilitate feeding while counteracting host defense responses, properties that also lead to possible

application of these molecules in therapeutic interventions (Chmelar et al., 2019). However, tick bites themselves can induce a spectrum of inflammatory reactions in response to toxic and anticoagulant biogenic substances present in tick saliva and/or mouthpart penetration such as coagulative necrosis producing firm papules, tick paralysis, intense pruritus, tick bite alopecia, cutaneous lymphoid hyperplasia, and cell histiocytosis (Mihara, 2017; Stringer et al., 2017; Haddad et al., 2018; Ha et al., 2019). Additionally, tick bites can induce in humans high levels of immunoglobulin E (IgE) antibodies against the carbohydrate Galα1-3Galβ1-(3)4GlcNAc-R (α-Gal) present in glycoproteins and glycolipids from tick saliva that mediate delayed anaphylaxis to red meat consumption, and immediate anaphylaxis to tick bites, xenotransplantation, and certain drugs such as cetuximab (Mateos-Hernández et al., 2017; Hilger et al., 2019). These anaphylactic reactions are known as the alpha-Gal syndrome (AGS) or red meat allergy and are now the focus of recent investigations (Commins et al., 2009; Van Nunen et al., 2009; Platts-Mills et al., 2015; Steinke et al., 2015; Galili, 2018; Cabezas-Cruz et al., 2019; de la Fuente et al., 2019; Hilger et al., 2019).

Recently, C57BL/6 α1,3-galactosyltransferase-knockout (α1,3-GalT-KO) mice that like humans do not synthesize α-Gal have been used as a model to characterize the percutaneous sensitization to α-Gal and *Amblyomma sculptum* tick saliva (Araujo et al., 2016) and the IgE-mediated immune response to cutaneous exposure to *Amblyomma americanum* tick proteins (Chandrasekhar et al., 2019). Additionally, this animal model has been used to study the antibody response to the carbohydrate α-Gal and its potential for the control of infectious diseases caused by pathogens with this modification on their surface (Yilmaz et al., 2014; Cabezas-Cruz et al., 2016; Iniguez et al., 2017; Moura et al., 2017; Portillo et al., 2019). In this context, various fish species constitute models for investigating human diseases (Schartl, 2014), and zebrafish (*Danio rerio* Hamilton 1822) is a relevant animal model for research in genetics, developmental biology, toxicology, oncology, immunology, and allergy (Huang et al., 2018).

In this study, we have developed a new zebrafish animal model for the study of tick-borne allergies caused by biogenic substances present in tick saliva. First, we showed that as occurs in humans, zebrafish do not have α-Gal in their tissues and produce anti–α-Gal IgM antibodies likely in response to bacteria with this modification present in the gut microbiota. Then, an experiment was conducted to evaluate the effect of tick saliva and the salivary components α-Gal and prostaglandin E_2 (PGE_2) alone and in combination with red meat consumption on zebrafish allergic response and survival. The results showed that some zebrafish develop hemorrhagic anaphylactic-type reactions provoking deaths in response to tick saliva, but only fish previously exposed to tick saliva develop allergic reactions to red meat consumption with rapid desensitization and tolerance. The immunity in response to tick saliva and red meat consumption showed tissue-specific differences and suggested immune mechanisms triggering the AGS. Taken together, these results identified allergic reactions and immune mechanisms in response to tick saliva and red meat consumption and provided a new animal model for the study of the AGS and other tick-borne allergies.

MATERIALS AND METHODS

Ethics Statement

Animal experiments were conducted in strict accordance with the recommendations of the European Guide for the Care and Use of Laboratory Animals. Animals were housed and experiments conducted at experimental facility (IREC, Ciudad Real, Spain) with the approval and supervision of the Ethics Committee on Animal Experimentation of the University of Castilla La Mancha (PR-2018-06-13) and the Counseling of Agriculture, Environment and Rural Development of Castilla La Mancha (ES130340000218).

Zebrafish

Wild-type adult (6–8 months old) AB male and female zebrafish were kindly provided by Dr. Juan Galcerán Sáez from the Instituto de Neurociencias (IN-CSIC-UMH, Sant Joan d'Alacant, Alicante, Spain). These zebrafish were certified by Biosait Europe S.L. (Barcelona, Spain; https://biosait.com) as free of major fish pathogens such as *Mycobacterium* spp., *Pseudoloma neurophilia*, *Pseudocapillaria tomentosa*, and zebrafish retroviruses. The zebrafish were maintained in a flow-through water system at 27°C with a light–dark cycle of 14/10 h and fed twice daily with dry fish feed. For bacterial microbiota studies, 15 freshwater zebrafish adults were also included purchased from a pet store in Ciudad Real, Spain, and used immediately for analysis in the laboratory.

Zebrafish Feeds and Feeding

Zebrafish were fed before and throughout the experiment twice daily at 9:30 a.m. and 1:30 p.m. Before the beginning of the experiment and up to day 2, all fish were fed with fish feed (Premium food tropical fish, DAPC, Valladolid, Spain; 50–70 μg/fish). On day 2, each experimental group was divided into two subgroups. One subgroup continued to be fed with fish feed at the same regimen, and the second subgroup was fed with dog food (Classic red, ACANA; Champion Petfoods LP, Edmonton, Alberta, Canada; 150–200 μg/fish). The fish feed contains cereals, fish and fish byproducts, soya, yeast, crustaceans, and algae. The dog food is composed of lamb meat meal (23%), steel-cut oats (22%), fresh ranch-raised beef (5%), fresh Yorkshire pork (5%), lamb fat (5%), whole red lentils, whole green peas, whole green lentils, raw grass-fed lamb (4%), whole oats, fresh beef liver (2%), pork meat meal (2%), herring oil (2%), fresh pork liver (2%), whole garbanzo beans, whole yellow peas, sun-cured alfalfa, lentil fiber, fresh beef tripe (1%), dried brown kelp, fresh pumpkin, fresh butternut squash, fresh parsnips, fresh green kale, fresh spinach, fresh carrots, fresh Red Delicious apples, fresh Bartlett pears, freeze-dried beef liver (0.1%), fresh cranberries, fresh blueberries, chicory root, turmeric root, milk thistle, burdock root, lavender, marshmallow root, and rosehips.

Tick Saliva and Salivary Biogenic Components

Rhipicephalus sanguineus (Latreille 1806) female ticks were collected in an animal shelter at Ciudad Real, Spain, while feeding on naturally infested dogs. Ticks were collected at different

feeding times for saliva collection as previously described but using pilocarpine hydrochloride (Poole et al., 2013). Partially fed ticks were inoculated with 5 μL of a 2% (wt/vol) solution of pilocarpine hydrochloride in phosphate-buffered saline (PBS), pH 7.4 (Sigma-Aldrich, St. Louis, MO, USA), into the hemocoel using a 50-μL syringe with a 0.33-mm needle (Hamilton Bonaduz AG, Bonaduz, Switzerland). Saliva was harvested using a micropipette, kept on ice, pooled, and stored at −80°C. Saliva protein concentration (1.96 μg/mL) was determined using a BCA Protein Assay Kit (Thermo Fisher Scientific, Waltham, MA, USA) following manufacturer's recommendations. Prostaglandin E_2 was obtained from Sigma-Aldrich. The bovine serum albumin (BSA) coated with α-Gal (thereafter named α-Gal) was obtained from Dextra (NGP0203 Gala1-3Gal-BSA 3 atom spacer; Shinfield, UK).

Protein Extracts From Zebrafish Tissues and Feeds, Human HL60 Cells, Pork Kidney, and Tick Salivary Glands

Zebrafish, HL60 Cells, and Pork Kidney

Wild-type adult AB zebrafish ($N = 5$; three females and two males) were dissected and muscle, liver/kidney, and gut collected for protein extraction. Human promyelocytic leukemia HL60 cells (ATCC CCL-240; α-Gal negative) were cultured in RPMI 1640 medium supplemented with 10% heat-inactivated fetal calf serum, 2 mM L-glutamine, and 25 mM HEPES buffer as previously described (de la Fuente et al., 2005). Pork (*Sus scrofa*) kidney (1 g; α-Gal positive) was obtained from a slaughterhouse at Ciudad Real, Spain. All samples were homogenized in lysis buffer (7 M urea, 2 M thiourea, 2% 3-[(3-cholamidopropyl)dimethylammonio]-1-propanesulfonate, CHAPS) supplemented with complete mini protease inhibitor cocktail (Roche, Basel, Switzerland). Samples were boiled for 2 min, mixed in a thermocycler for 1 h, and sonicated for 1 min in an ultrasonic cooled bath followed by 10-s vortex. After three cycles of sonication vortex, the homogenate was centrifuged at 200 g for 5 min at 4°C, and the supernatant was quantified using an RC DC protein assay (BioRad, Hercules, CA, USA) with BSA as standard. This methodology has been previously shown to preserve the presence of the α-Gal epitope in extracted proteins (Lima-Barbero et al., 2019).

Tick Salivary Glands, Dog Food, and Fish Feed

Salivary glands were dissected from unfed and partially fed *R. sanguineus* female ticks and pooled for analysis ($N = 10$ per pool). Dog food and fish feed were pooled (1 μg per sample) for analysis. Samples were pooled in 500 μL lysis buffer (PBS, 1% Triton X-100) supplemented with complete protease inhibitor mixture (Roche) and homogenized by passing through a needle (27-gauge). Samples were sonicated for 1 min in an ultrasonic cooled bath, followed by vortexing for 10 s. After three cycles of sonication vortex, total protein extracts were centrifuged at 200 g for 5 min to remove debris. The supernatants were collected, and protein concentration was determined using the BCA Protein Assay (Life Technologies, Carlsbad, CA) with BSA as standard following the manufacturer's recommendations.

Determination of α-Gal Content by Enzyme-Linked Immunosorbent Assay

The α-Gal levels were determined by enzyme-linked immunosorbent assay (ELISA) in zebrafish proteins from different organs, *R. sanguineus* saliva and salivary gland proteins, fish feed, and dog food in comparison with pork kidney (α-Gal–positive control) and human HL60 cells (α-Gal–negative control). Plates were coated with 100 ng proteins per well from different samples in carbonate/bicarbonate buffer incubated overnight at 4°C, following five washes with PBS containing 0.05% Tween 20 (PBST). Unspecific unions were blocked with 1% human serum albumin (HSA; Sigma-Aldrich) and the α-Gal epitope monoclonal antibodies (M86; Enzo Life Sciences, Farmingdale, NY, USA) were added at 1:50 dilution in PBS and incubated for 1 h at 37°C followed by five washes with PBST. Finally, anti–mouse IgM (μ-chain specific)–peroxidase antibody produced in goat (Sigma-Aldrich) was added at 1:2,000 dilution in PBS. Reactions were visualized by adding 100 μL of 3,3′,5,5-tetramethylbenzidine (TMB; Promega, Madison, WI, USA) and incubated for 20 min in the dark at room temperature (RT). The optical density (OD) was measured at 450 nm with an ELISA reader. The average value of the blanks (wells without sample proteins; $N = 5$) was subtracted from all reads, and the average of nine replicates for each sample was used for analysis. A calibration curve with 0.0 to 1.0 ng α-Gal and OD values at 450 nm was constructed using Microsoft Excel for Mac (v. 16.26) to convert ELISA reader values to α-Gal content per sample ($R^2 = 0.992$; **Supplementary Figure 5A**). To further validate the calibration curve, a correlation was constructed between 0.0 to 3.5 ng α-Gal and 0.0 to 1.0 μg tick salivary gland proteins using Microsoft Excel for Mac (v. 16.26) ($R^2 = 0.992$; **Supplementary Figure 5B**). The results (average ± SD of α-Gal/1 μg protein) were compared between samples and negative or positive controls by Student *t*-test with unequal variance ($p < 0.05$, $N = 3$–5 biological replicates).

Characterization of α-Gal–Positive Bacteria Zebrafish Gut Microbiota

The study was performed using wild-type adult AB and pet store adult female and male zebrafish ($N = 5$ for each fish group; three females and two males). The microbiota was sampled as previously described (Cantas et al., 2012). Briefly, the ventral belly surface of freshly euthanized fish was opened with sterilized micro–surgical blade and forceps under a light source. The intestinal system was transferred to 1.5-mL tubes containing 200 μL sterile PBS. The intestines were homogenized with a motorized pestle, and disposable plastic loops were used to streak on 5% chicken (α-Gal negative) (Parmentier et al., 2008) blood agar (Rockland Immunochemicals Inc., Pottstown, PA, USA) and tryptic soy agar (Sigma-Aldrich) bacteriological plates for isolation of aerobic and anaerobic bacteria, respectively, following four serial dilutions. The plates were incubated at 28°C and followed by inspections every day for up to 1 week. Bacterial colonies were morphologically classified as aerobic types I (circular, pink, raised punctiform colonies), II (circular, diameter ≤5 mm, creamy white, raised colonies),

III (irregular, dry white, flat colonies), and anaerobic types Ib (circular, diameter ≤5 mm, creamy white, raised colonies) and IIb (circular, white, raised, punctiform colonies). Bacteria isolated from the zebrafish gut microbiota were washed in PBS, fixed, and permeabilized with the Intracell fixation and permeabilization kit (Immunostep, Salamanca, Spain) following manufacturer recommendations. The cells were incubated with 3% HSA (Sigma-Aldrich) in PBS for 1 h at RT. Then, cells were incubated for 14 h at 4°C with the anti–α-Gal monoclonal antibody (M86; Enzo Life Sciences) diluted 1:50 in 3% HSA/PBS. Fluorescein isothiocyanate (FITC) goat anti–mouse IgM (Abcam, Cambridge, UK)–labeled antibody diluted 1:200 in 3% HSA/PBS was used as a secondary antibody and incubated for 1 h at RT. The *Escherichia coli* O86:B7 (ATCC 12701) and BL21 (DE3) cells were included as positive and negative α-Gal controls, respectively (Cabezas-Cruz et al., 2017c). Samples were analyzed on a FACScalibur flow cytometer equipped with CellQuest Pro software (BD BioSciences, Madrid, Spain). The viable cell population was gated according to forward-scatter and side-scatter parameters. The mean fluorescence intensity (MFI) was determined by flow cytometry, and the geometric mean compared between aerobic and anaerobic bacteria by Student *t*-test with unequal variance ($p = 0.05$, $N = 5$ biological replicates).

Zebrafish Treatment With Tick Saliva and Salivary Biogenic Components

The first trial (Experiment 1) was designed and performed to evaluate the allergic reactions and immune response in zebrafish treated with tick saliva and salivary components and in response to red meat consumption (**Figure 3A**). Adult zebrafish were randomly distributed into five gender-balanced groups (tick saliva, α-Gal, PGE_2, α-Gal + PGE_2, PBS) (**Figure 3A**, **Table 1**). Fish were intramuscularly injected at days 1, 3, and 8 with a Monoject insulin syringe fitted with a 1-cm, 29-gauge needle at the muscle close to the caudal fin with 2.5 μL *R. sanguineus* saliva in 10 μL PBS (tick saliva), 5 μg α-Gal in 10 μL PBS (α-Gal), 350 pg PGE_2 in 10 μL PBS (PGE_2), 5 μg α-Gal and 350 pg PGE_2 in 10 μL PBS (α-Gal + PGE_2), and 10 μL PBS (PBS). On day 2, each experimental group was randomly divided into two subgroups allocated in two separate water tanks and continued to be fed with fish feed or changed to dog food until the end of the experiment at day 14 when all surviving fish were euthanized (**Figure 3A**, **Table 1**). Zebrafish local allergic reactions and behavior were examined immediately after treatment or feed change and followed daily until the end of the experiment at day 14. After fish death or euthanize, serum was collected from each animal to determine anti–α-Gal and antitick salivary gland protein IgM antibody titers. Fish were then divided into two longitudinal halves. One-half was used to dissect intestine and kidney for RNA extraction to characterize the mRNA levels for selected immune response markers–correlates of allergy. The second half was used for histochemical characterization of local basophils. Accumulated zebrafish survival was analyzed by a Cox proportional survival regression test (http://statpages.info/prophaz.html) ($p = 0.05$; N = 7–9 biological replicates). Accumulated zebrafish allergy was analyzed by a one-way analysis of variance (ANOVA) test (https://www.socscistatistics.com/tests/anova/default2.aspx) ($p = 0.05$; N = 7–9 biological replicates). The risk of allergic reactions was analyzed in female and male zebrafish by McNemar test (https://www.graphpad.com/quickcalcs/McNemar1.cfm) ($p = 0.05$; $N = 7$–9).

A second trial (Experiment 2) was conducted with 10 zebrafish per group and treated with tick saliva and PBS control (**Figure 3B**). Experiment 2 was conducted to inject fish with less amount of tick saliva than in Experiment 1 (1 μL instead of 2.5 μL *R. sanguineus* saliva) to reduce response to toxic and anticoagulant biogenic compounds different from α-Gal and PGE_2 present in tick saliva and to better monitor the incidence of allergic reactions, abnormal behavior patterns, and feeding during the experiment. As in Experiment 1, adult zebrafish were randomly distributed into two gender-balanced groups (tick saliva PBS) (**Figure 3B**). Fish were intramuscularly injected at days 1, 3, and 8 as in Experiment 1 with 1 μL *R. sanguineus* saliva in 10 μL PBS (tick saliva) and 10 μL PBS (PBS) as control. On day 2, each experimental group was randomly divided into two subgroups ($N = 5$ each) allocated in two separate water tanks and continued to be fed with fish feed or changed to dog food until the end of the experiment at day 10 when all surviving fish were euthanized (**Figure 3B**). Zebrafish local allergic reactions and behavior were examined immediately after treatment or feed change and followed daily until the end of the experiment at day 10. After fish were euthanized, serum was collected from each animal to determine anti–α-Gal IgM antibody titers. The percent of zebrafish affected by allergic reactions and abnormal behavior and feeding on each group fed with fish feed or dog food was compare between saliva-treated and PBS-treated control fish by a one-way ANOVA test (https://www.socscistatistics.com/tests/anova/default2.aspx) ($p = 0.05$; $N = 4$–5 biological replicates).

Anti–α-Gal IgM Antibody Titers in Zebrafish

For ELISA, high-absorption-capacity polystyrene microtiter plates were coated with 100 ng of α-Gal per well in carbonate–bicarbonate buffer (Sigma-Aldrich). After an overnight incubation at 4°C, coated plates were washed one time with 100 μL/well PBST (Sigma-Aldrich) and then blocked with 100 μL/well of 1% HSA (Sigma-Aldrich) for 1 h at RT. Serum peritoneal fluid samples were diluted (1:100, vol/vol) in blocking solution, and 100 μL/well was added into the wells of the antigen-coated plates and incubated for 1.5 h at 37°C. Plates were washed three times with PBST, and 100 μL/well of species-specific rabbit anti–zebrafish IgM antibodies diluted (1:1,000, vol/vol) in blocking solution was added and incubated for 1 h at RT. Plates were washed three times with 300 μL/well of PBST. A goat anti–rabbit IgG-peroxidase conjugate (Sigma-Aldrich) was added, diluted 1:3,000 in blocking solution, and incubated for 1 h at RT. After four washes with 100 μL/well of PBST, 100 μL/well of TMB (Promega) was added and incubated for 15 min at RT. Finally, the reaction was stopped with 50 μL/well of 2 N H_2SO_4, and the OD was measured in a spectrophotometer at 450 nm. The OD at 450 nm was compared between fish treated with saliva, α-Gal, PGE_2, or α-Gal + PGE_2, and the PBS-treated control group by Student *t* test with unequal variance ($p = 0.005$; $N = 7$–9). A Spearman ρ correlation analysis (https://

TABLE 1 | Experiment 1 design and records of zebrafish allergies and deaths.

Group	Fish No.	Gender	Feed	Day													
				1[a]	2[b]	3[a]	4	5	6	7	8[a]	9	10	11	12	13	14
Saliva	26-1	Female	Fish	A	D						Dead						
	26-2	Female	Fish	A	D						Dead						
	26-3	Female	Fish	A	D						Dead						
	26-4	Female	Fish	—	—	—	—	—	—	—	—	—	—	—	—	—	E
	26-5	Male	Fish	—	—	—	—	—	—	—	—	—	—	—	—	—	E
	26-6	Male	Fish	—	—	—	—	—	—	—	—	—	—	—	—	—	E
	14-7	Female	Dog	—	—	A	A	—	—	—	—	—	—	—	—	—	E
	14-8	Male	Dog	—	—	A	A	—	—	—	—	—	—	—	—	—	E
	14-9	Female	Dog	—	—	A	A	—	—	—	—	—	—	—	—	—	E
α-Gal	27-1	Male	Fish	—	—	—	—	—	—	—	—	—	—	—	—	—	E
	27-2	Female	Fish	—	—	—	—	—	—	—	—	—	—	—	—	—	E
	27-3	Female	Fish	—	—	—	—	—	—	—	—	—	—	—	—	—	E
	27-4	Male	Fish	—	—	—	—	—	—	—	—	—	—	—	—	—	E
	15-5	Male	Dog	—	—	—	—	—	—	—	—	—	—	—	—	—	E
	15-5	Male	Dog	—	—	—	—	—	—	—	—	—	—	—	—	—	E
	15-7	Female	Dog	—	—	—	—	—	—	—	—	—	—	—	—	—	E
PGE_2	28-1	Female	Fish	—	—	—	—	—	—	D				Dead			
	28-2	Female	Fish	—	—	—	—	—	—	—	—	—	—	—	—	—	E
	28-3	Male	Fish	—	—	—	—	—	—	—	—	—	—	—	—	—	E
	28-4	Male	Fish	—	—	—	—	—	—	—	—	—	—	—	—	—	E
	16-5	Female	Dog	—	—	—	—	—	—	—	—	—	—	—	—	—	E
	16-6	Male	Dog	—	—	—	—	—	—	—	—	—	—	—	—	—	E
	16-7	Male	Dog	—	—	—	—	—	—	—	—	—	—	—	—	—	E
α-Gal + PGE_2	29-1	Female	Fish	AD							Dead						
	29-2	Male	Fish	—	—	—	—	—	—	—	—	—	—	—	—	—	E
	29-3	Male	Fish	—	—	—	—	—	—	—	—	—	—	—	—	—	E
	29-4	Female	Fish	—	—	—	—	—	—	—	—	—	—	—	—	—	E
	29-5	Male	Fish	—	—	—	—	—	—	—	—	—	—	—	—	—	E
	17-6	Male	Dog	—	—	—	—	—	—	—	—	—	—	—	—	—	E
	17-7	Male	Dog	—	—	—	—	—	—	—	—	—	—	—	—	—	E
	17-8	Female	Dog	Disappeared from the tank													
PBS	30-1	Female	Fish	—	—						Died from injection						
	30-2	Female	Fish	—	—	—	—	—	—	—	—	—	—	—	—	—	E
	30-3	Male	Fish	—	—	—	—	—	—	—	—	—	—	—	—	—	E
	30-4	Male	Fish	—	—	—	—	—	—	—	—	—	—	—	—	—	E
	18-5	Female	Dog	—	—	—	—	—	—	—	—	—	—	—	—	—	E
	18-6	Male	Dog	—	—	—	—	—	—	—	—	—	—	—	—	—	E
	18-7	Male	Dog	—	—	—	—	—	—	—	—	—	—	—	—	—	E

[a] *Treatments according to the experimental group were done at days 1, 3, and 8.*

[b] *Feed change (fish feed to dog food for some animals) occurred at day 2. The appearance of allergic reactions (A) and death due to allergic reactions (D) were recorded. The absence of allergic reactions and deaths are represented with a dash (—). All surviving fish were euthanized (E) at the end of the experiment.*

www.socscistatistics.com/tests/spearman/Default2.aspx) was performed between anti–α-Gal IgM antibody levels and allergic reactions to tick saliva rated as 10 for fish with allergic reactions and death (AD), 8 for fish with allergic reactions only (A), and 0 for fish without reactions (NR), $\rho = 0.179$, two-tailed $p = 0.283$.

Anti-tick Salivary Gland Proteins IgM Antibody Titers in Zebrafish

Proteins were extracted from *R. sanguineus* salivary glands as described above. For ELISA, high-absorption-capacity polystyrene microtiter plates were coated with 100 ng of protein extracts of salivary glands per well in carbonate–bicarbonate buffer (Sigma-Aldrich). After an overnight incubation at 4°C, coated plates were washed one time with 100 μL/well PBST (Sigma-Aldrich) and then blocked with 100 μL /well of 2% BSA (Sigma-Aldrich) for 1 h at RT. Serum peritoneal fluid samples were diluted (1:100, vol/vol) in blocking solution, and 100 μL/well was added into the wells of the antigen-coated plates and incubated for 1.5 h at 37°C. Plates were washed three times with PBST and 100 μL/well of species-specific rabbit anti–zebrafish IgM antibodies diluted (1:2,000, vol/vol) in blocking solution were added and incubated for 1 h at RT. Plates were washed three times with 100 μL/well of PBST. A goat anti–rabbit IgG–horseradish peroxidase conjugate (Sigma-Aldrich) was added diluted 1:3,000 in blocking solution and incubated for 1 h at RT. After four washes with 100 μL/well of PBST, 100 μL/well of TMB solution (Promega) was added and incubated for 10 min at RT. Finally, the reaction was stopped with 50 μL/well of 2 N H_2SO_4 and the OD measured in a spectrophotometer at 450 nm. A Student *t*-test with unequal variance was used to compare the OD at 450 nm of IgM antibody titers against tick salivary gland proteins between fish treated with saliva, α-Gal, PGE_2, or α-Gal + PGE_2, and the PBS-treated control group ($p = 0.05$; $N = 7$–9) and between zebrafish fed with fish feed or dog food ($p = 0.05$; $N = 3$–6).

Expression of Selected Immune Response Markers by Quantitative Reverse Transcription–Polymerase Chain Reaction

Total RNA was extracted from zebrafish intestine and kidney samples using the AllPrep DNA/RNA/Protein (Qiagen, Hilden, Germany). The expression of selected zebrafish immune response and food allergy markers (Lu et al., 2008; Huang et al., 2018) *akirin 2* (*akr2*), *complement component c3a* (*c3a*), *interleukin 1-beta* (*il1b*), *interleukin* 4 (*il4*), *nuclear factor interleukin 3 regulated* (*nfil3*), *Toll-like receptor 4b* (*tlr4b*), *interferon-induced GTP-binding protein MxA* (*mxa*), *interferon* (*ifn*), and *MYD88 innate immune signal transduction adaptor* (*myd88*) was analyzed by quantitative reverse transcription–polymerase chain reaction (qRT-PCR) with gene-specific primers (**Supplementary Table 1**) using the KAPA SYBR FAST one-step universal kit (Sigma-Aldrich) in the Rotor-Gene Q (Qiagen) thermocycler following manufacturer's recommendations. A dissociation curve was run at the end of the reactions to ensure that only one amplicon was formed and that the amplicon denatured consistently in the same temperature range for every sample (Ririe et al., 1997). The mRNA Ct values were normalized against *D. rerio glyceraldehyde-3-phosphate dehydrogenase* (*gapdh*) using the genNormddCT method (Livak and Schmittgen, 2001). The normalized Ct values were compared between fish treated with saliva, α-Gal, PGE_2, or α-Gal + PGE_2, and the PBS-treated control group and between fish treated with saliva presenting anaphylactic-type reactions and dead on day 2 and fish without reactions by Student *t*-test with unequal variance ($p = 0.005$; $N = 3$–6).

Histochemistry of Local Granulocytes in Zebrafish

Euthanized fish at day 14 were sagittal sectioned and then immediately fixed in 10% neutral buffered formalin for 24 h at 21°C, dehydrated in a graded series of ethanol, immersed in xylol, and embedded in paraffin wax using an automatic processor. Sections were cut at 4 mm and stained with hematoxylin and eosin (Sigma-Aldrich) following manufacturer's instructions and standard procedures (Bennett et al., 2001). Stained tissue sections were examined by light microscopy to count granulocytes (three sections of 40 mm^2 each per fish) and photographed at 40× and 100× magnifications. The average counts of granulocytes were compared between fish treated with tick saliva, α-Gal, or PGE_2 α-Gal + PGE_2, and PBS-treated controls and between fish fed on dog food or fish feed for each treatment by Student *t*-test with unequal variance ($p = 0.05$; $N = 3$–6).

RESULTS

Zebrafish Do Not Produce α-Gal and Have Natural Anti–α-Gal Antibodies in Response to Bacteria in the Gut Microbiota

This study was designed to evaluate the allergic reactions and immunity in response to tick saliva and salivary biogenic substances such as α-Gal and PEG_2 and red meat consumption in the zebrafish model.

Herein we first characterized the α-Gal content in fish tissues (**Figure 1A**). The results showed that only zebrafish gut had α-Gal levels higher than the human HL60 α-Gal–negative control cells, and all zebrafish tissues had significantly lower α-Gal levels than the pork kidney α-Gal–positive control (**Figure 1A**). Then, the presence of α-Gal was characterized in bacteria from the gut microbiota of laboratory wild-type AB and pet store zebrafish (**Figures 1B–D**). Identified anaerobic and aerobic gut bacteria had α-Gal levels higher than the *E. coli*—negative and—positive controls (**Figure 1B**), with higher levels in aerobic than in anaerobic bacteria (**Figure 1C**). A total of five morphologically different bacterial colonies were isolated in both fish groups with α-Gal content higher than the *E. coli*-negative control (**Figure 1D**). These results were similar to those described in humans (Galili, 2018) and suggested that natural anti–α-Gal IgM antibody levels in untreated zebrafish are produced in response to gut bacterial microbiota (PBS-treated group; **Figure 2A**).

Additionally, zebrafish treated with tick saliva, α-Gal, and α-Gal+PGE_2 developed IgM antibodies against α-Gal that showed higher levels than in fish treated with PGE_2 or PBS (**Figure 2A**). Zebrafish treated with tick saliva, α-Gal, PGE_2, and

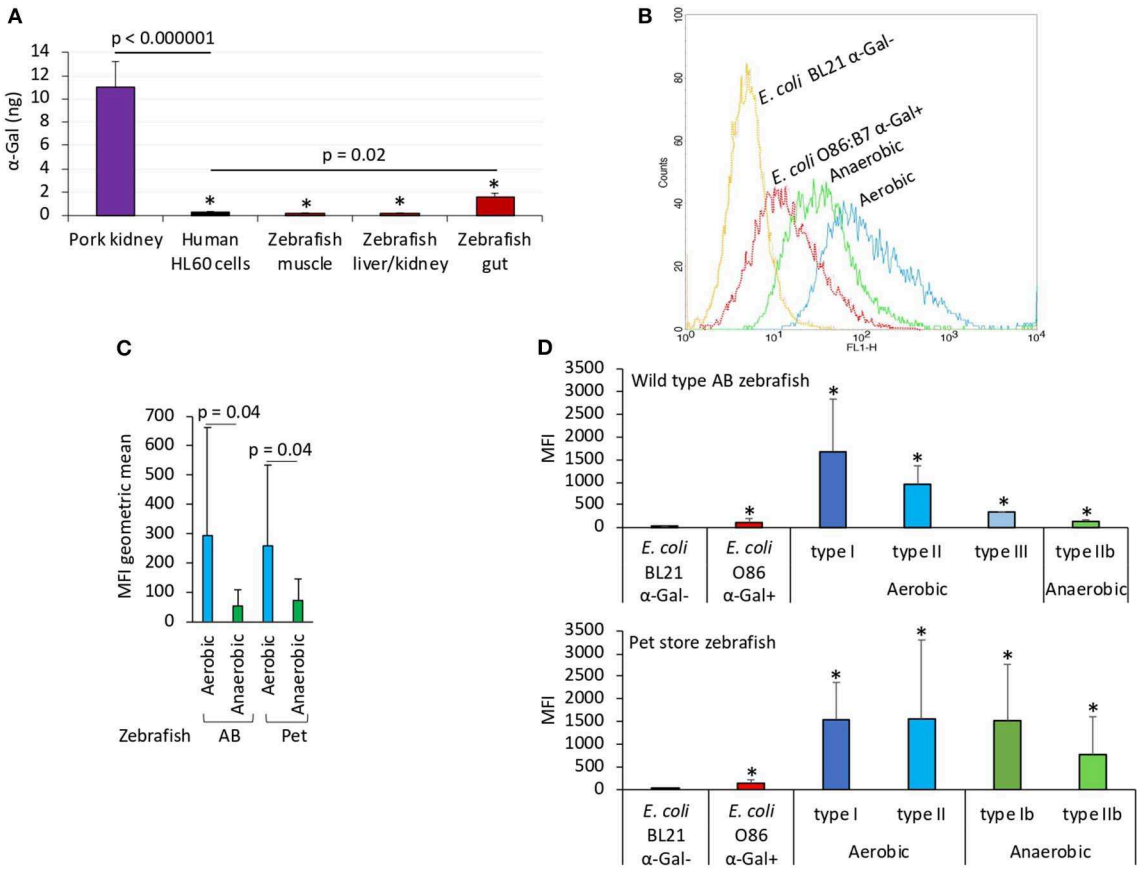

FIGURE 1 | The α-Gal content is similar in humans and zebrafish. The α-Gal content was determined in zebrafish tissues and gut bacterial microbiota and in *R. sanguineus* salivary glands. **(A)** The α-Gal levels were determined by ELISA in zebrafish muscle, liver/kidney, and gut and in comparison with pork kidney (α-Gal positive) and human HL60 cells (α-Gal negative) as positive and negative controls, respectively. The results were converted to α-Gal content per sample using a calibration curve ($R^2 = 0.992$; **Supplementary Figure 5A**) and compared between all samples and negative (lines) or positive (*$p <$ 1E-8) controls by Student *t*-test with unequal variance ($p < 0.05$, $N = 5$ biological replicates). **(B)** Flow cytometry showing the presence of α-Gal on the surface of aerobic and anaerobic bacteria isolated from zebrafish gut microbiota. *Escherichia coli* O86:B7 and BL21 (DE3) strains were included as positive and negative controls for α-Gal, respectively. For flow cytometry, cells were stained with *Bandeiraea simplicifolia* I-isolectin B4–FITC to visualize α-Gal, and the viable cell population was gated according to forward-scatter and side-scatter parameters. **(C)** The MFI was determined by flow cytometry, and the geometric mean ± SD compared between aerobic and anaerobic bacteria by Student *t*-test with unequal variance ($p = 0.05$, $N = 5$ biological replicates). **(D)** Distribution of the MFI among aerobic and anaerobic type bacteria in wild-type AB and pet store zebrafish and in comparison with *E. coli* O86:B7 and BL21 (DE3)–positive and –negative controls for α-Gal, respectively. The results (average ± SD) were compared between all samples and negative control by Student *t*-test with unequal variance (*$p < 0.05$, $N = 5$ biological replicates).

α-Gal+PGE_2 but not PBS also developed IgM antibodies against proteins present in tick salivary glands (**Figure 2B**). Salivary gland proteins in both unfed and partially fed ticks and in tick saliva showed the presence of α-Gal (**Figure 2C**), thus suggesting that *R. sanguineus* synthesize α-Gal and explaining the anti–α-Gal IgM antibody titers in zebrafish treated with tick saliva (**Figure 2A**). As expected, because of the presence of PGE_2 in tick saliva and salivary glands, zebrafish treated with PGE_2 developed antibodies against salivary gland proteins (**Figure 2B**) but not against α-Gal (**Figure 2A**). Finally, a tendency was observed toward higher IgM titers against tick salivary gland proteins in fish fed with dog food when compared to those fed with fish feed (**Supplementary Figure 1**).

Taken together, these results evidenced similarities in α-Gal content and anti–α-Gal antibody response in zebrafish and humans, suggesting that zebrafish may be evaluated like an animal model for the study of tick-borne allergies produced by salivary biogenic components.

Zebrafish Develop Hemorrhagic Anaphylactic-Type Reactions and Abnormal Behavior Patterns in Response to Tick Saliva

The study was designed with two experiments to characterize the allergic response in zebrafish exposed to tick saliva and salivary biogenic components such as α-Gal and PGE_2 (**Figures 3A,B**). In Experiment 1 (**Figure 3A**), zebrafish were injected with 2.5 μL tick saliva and biogenic substances α-Gal and PGE_2 to evaluate the allergic reactions and immune response in fish feeding on fish feed or dog food. Experiment 2 (**Figure 3B**) was then conducted to inject fish with less

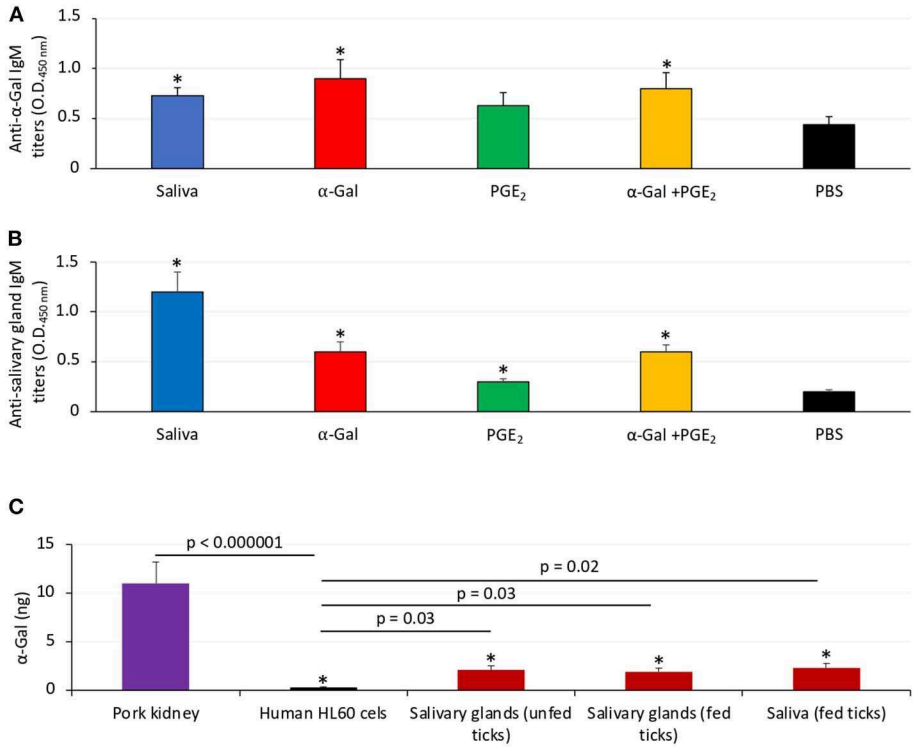

FIGURE 2 | Zebrafish develop antibodies against tick α-Gal and proteins. **(A)** The IgM antibody titers against α-Gal were determined by ELISA, represented as the average ± SD OD at 450 nm and compared between fish treated with saliva, α-Gal, PGE_2, or α-Gal + PGE_2, and the PBS-treated control group by Student *t*-test with unequal variance (*$p < 0.005$; $N = 7–9$). **(B)** The IgM antibody titers against tick salivary gland proteins were determined by ELISA, represented as the average ± SD OD at 450 nm and compared between fish treated with saliva, α-Gal, PGE_2, or α-Gal + PGE_2 and the PBS-treated control group by Student *t*-test with unequal variance (*$p < 0.001$; $N = 7–9$). **(C)** The α-Gal levels were determined by ELISA in salivary glands from unfed and partially fed ticks and saliva from fed ticks in comparison with pork kidney (α-Gal positive) and human HL60 cells (α-Gal negative) as positive and negative controls, respectively. The results were converted to α-Gal content per sample using a calibration curve ($R^2 = 0.992$; **Supplementary Figure 5A**) and compared between all samples and negative (lines) or positive (*$p <$ 1E-8) controls by Student *t*-test with unequal variance ($p < 0.05$, $N = 3$ biological replicates).

tick saliva than in Experiment 1 (1 μL instead of 2.5 μL *R. sanguineus* saliva) to reduce responses to toxic and anticoagulant biogenic compounds different from α-Gal and PGE_2 present in tick saliva and to better monitor the incidence of allergic reactions, abnormal behavior patterns, and feeding during the experiment.

In Experiment 1, the results showed that the incidence of allergic reactions was statistically significant in zebrafish treated with tick saliva (six animals; 66%) but not in fish treated with α-Gal, PGE_2, α-Gal + PGE_2, and PBS (**Figure 4A**, **Table 1**). In three animals treated with tick saliva (33%) and before food change, these reactions resulted in death that significantly affected fish survival rate (**Figure 4B**, **Table 1**). Although not statistically significant, one fish treated with α-Gal + PGE_2 also developed allergy and died at day 1 (**Figures 4A–C**, **Table 1**). The results showed that zebrafish response to tick saliva was characterized by hemorrhagic anaphylactic-type reactions appearing 3 to 5 h posttreatment (hpt) with hemorrhage affecting various organs (**Figure 4D**). Although allergy was more prevalent in female than male zebrafish, the analysis by McNemar test of the risk of developing allergic reactions in response to tick saliva did not show a significant association in female ($p = 0.07$) and male ($p = 1.00$) zebrafish.

Abnormal behavior patterns in Experiment 1 consisted of low mobility, permanence at the bottom of the water tank, and zigzag-type swimming (**Supplementary Figures 2A–F**). Low mobility and permanence at the bottom of the water tank were shown in three zebrafish injected with tick saliva (**Supplementary Figure 2A**), one zebrafish injected with α-Gal (**Supplementary Figure 2C**), and one zebrafish injected with α-Gal + PGE_2 (**Supplementary Figure 2E**). Normal behavior patterns were seen in all zebrafish injected with PGE_2 and PBS (**Supplementary Figures 2D,F**).

These results provided evidence to support that zebrafish develop delayed hemorrhagic anaphylactic-type reactions affecting survival and behavior in response to tick saliva.

Zebrafish Develop Allergic Reactions and Abnormal Behavior Patterns in Response to Red Meat Consumption After Exposure to Tick Saliva

The results of the Experiment 1 (**Figure 3A**) showed that zebrafish develop delayed hemorrhagic anaphylactic-type reactions and abnormal behavior patterns primarily in response to tick saliva resulting in deaths for 33% of the animals

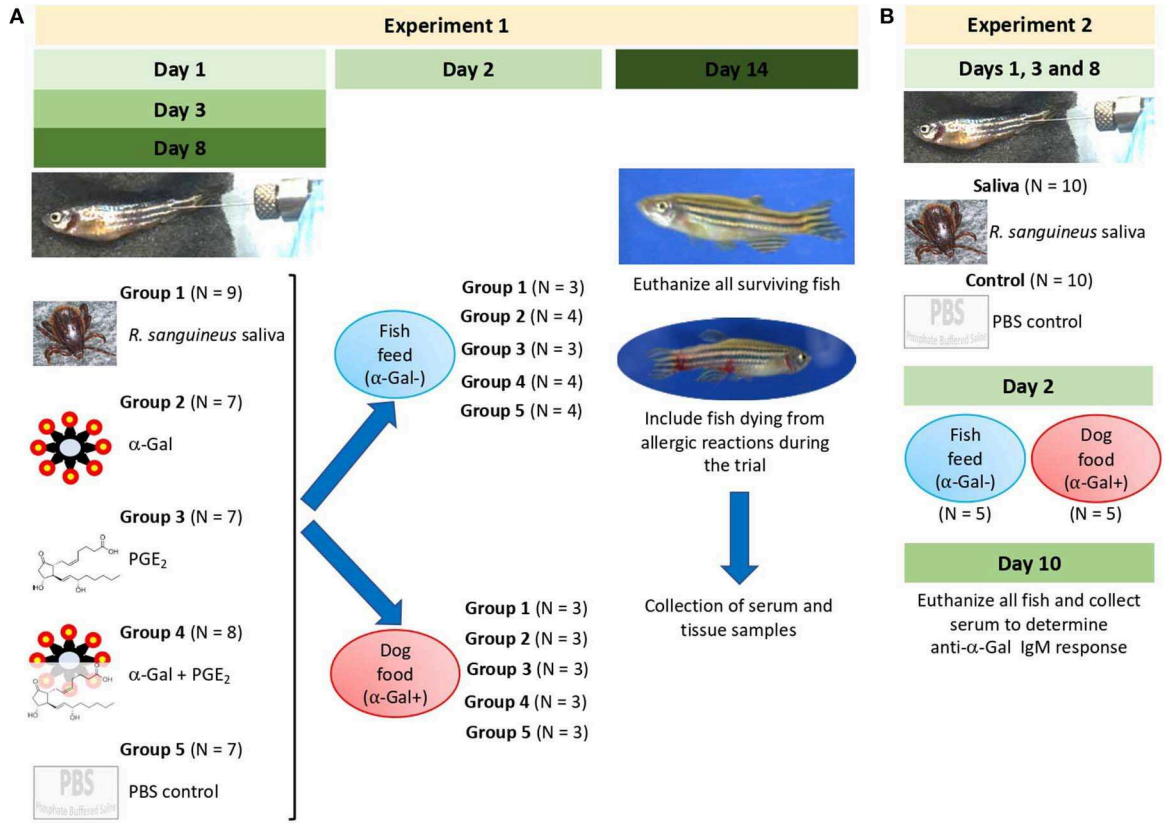

FIGURE 3 | Experimental design. Experiments were designed and performed to evaluate the allergic reactions and immune response in zebrafish treated with tick saliva and salivary components and in response to red meat consumption. **(A)** In Experiment 1, zebrafish were injected with 2.5 μL tick saliva and biogenic substances α-Gal and PGE_2 to evaluate the allergic reactions and immune response in fish feeding on fish feed or dog food. Serum and tissue samples were collected to determine anti–α-Gal IgM response, intestine and kidney for qRT-PCR analysis of immune response markers, and half fish for histochemical characterization of local granulocytes. **(B)** Experiment 2 was conducted to inject fish with less amount of tick saliva than in Experiment 1 (1 μL instead of 2.5 μL *R. sanguineus* saliva) to reduce response to toxic and anticoagulant biogenic compounds different from α-Gal and PGE_2 present in tick saliva and to better monitor the incidence of allergic reactions, abnormal behavior patterns, and feeding during the experiment. Zebrafish local allergic reactions and behavior were examined immediately after treatment or feed change and followed daily until the end of the experiment at day 14 (Experiment 1) or day 10 (Experiment 2). Fish and tick representative images are shown.

(**Figures 5A,B**). However, anaphylaxis to consumption of red meat with high α-Gal content is one of the symptoms of the AGS.

To address this sign of the AGS, zebrafish on each treatment group in Experiment 1 and without reactions in response to first treatment with tick saliva on day 1 were split into two subgroups on day 2 (**Figures 3A**, **5A**, **Table 1**). One subgroup continued to feed on fish feed without α-Gal, whereas the other was fed with dog food containing α-Gal (**Figure 6A**), and both were treated again with tick saliva on day 3 (**Figures 3A**, **5A**, **Table 1**). All zebrafish feeding on fish feed did not develop any visible reaction to tick saliva injected on day 3 (**Figure 5A**, **Table 1**). However, zebrafish fed with dog food and treated with tick saliva on day 3 did develop delayed (3–5 hpt) hemorrhagic anaphylactic-type reactions that lasted for 48 h (**Figures 5A,B**, **Table 1**). An abnormal zig-zag type swimming was also observed at day 3 in fish No. 14-8 injected with tick saliva and fed with dog food (**Supplementary Figures 2B, 3**). These fish recovered from allergic reactions after 48 h and as animals fed on fish feed did not develop any reactions when treated again with tick saliva on day 8 (**Figure 5A**). Although a tendency was observed toward a positive correlation between allergic reactions to tick saliva and anti–α-Gal IgM antibody levels, the correlation was not significant (**Figure 6B**). However, all fish developing anaphylactic-type reactions had IgM antibody levels higher than 0.6 OD at 450 nm (**Figure 5C**).

To gain additional information on the zebrafish allergic reactions and abnormal behavior patterns in response to red meat consumption after exposure to tick saliva, Experiment 2 was conducted (**Figure 3B**). One fish died on each group on day 5 but for reasons not related to the treatments. Although fish were injected with less tick saliva than in Experiment 1, the anti–α-Gal IgM antibody levels were higher than in PBS-treated controls (**Figure 7A**). Furthermore, in fish treated with tick saliva but not in controls, the anti–α-Gal IgM antibody levels were higher in fish fed on dog food than in those fed with fish feed (**Figure 7A**). The analysis of the fish affected by hemorrhagic-type allergic reactions and abnormal behavior and feeding showed that the percentage of affected fish with allergic reactions was higher

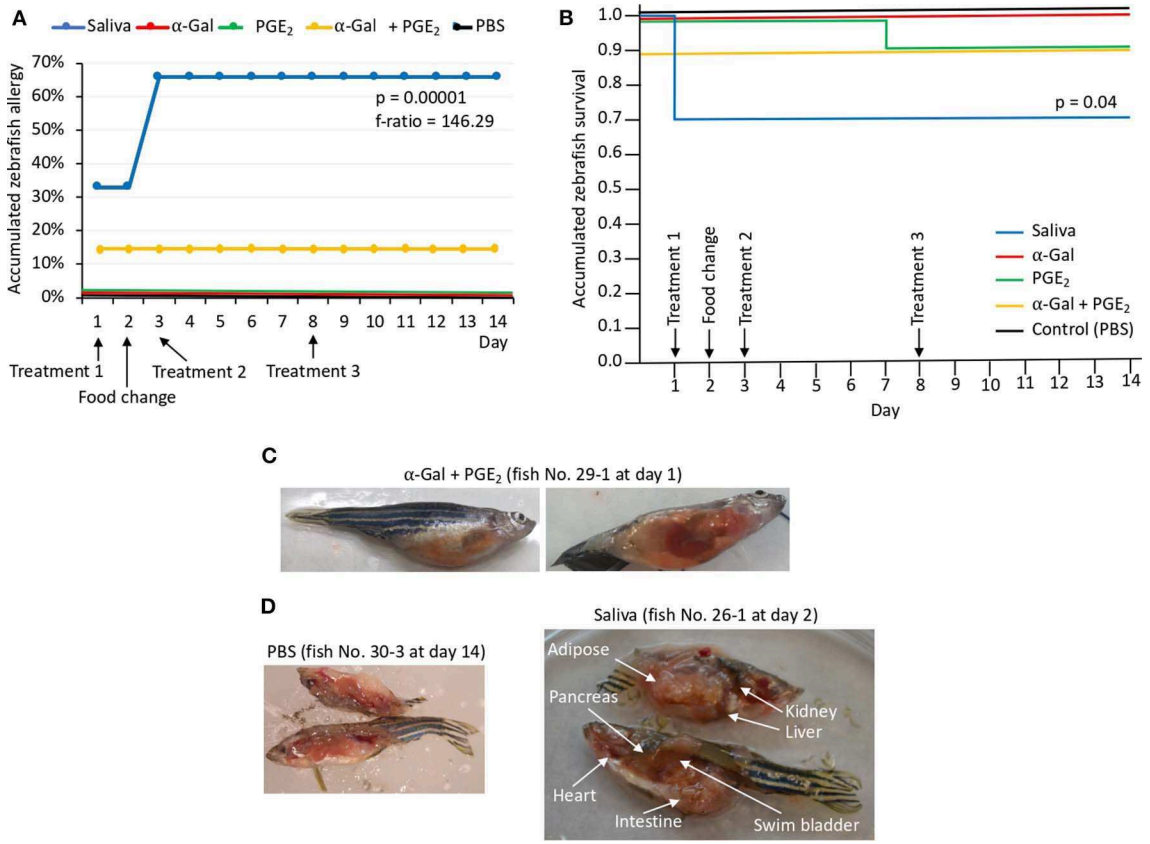

FIGURE 4 | Zebrafish injected with tick saliva develop hemorrhagic anaphylactic-type reactions (Experiment 1). **(A)** Accumulated zebrafish allergy was compared between different groups by a one-way ANOVA test ($p < 0.05$; $N = 7$–9 biological replicates). **(B)** Accumulated zebrafish survival in the different groups was compared by a Cox proportional survival regression test ($p < 0.05$; $N = 7$–9 biological replicates). **(C)** Signs of hemorrhagic anaphylactic-type reactions in zebrafish 29-1 injected with α-Gal + PGE_2. Fish No. 29-1 died on day 1. **(D)** Representative comparison between necropsied control fish No. 30-1 injected with PBS and fish No. 26-1 injected with tick saliva. Evidence of hemorrhage is shown in organs of a saliva-injected fish.

in saliva-treated than in PBS-treated controls fed with either fish or dog food (**Figure 7B**). However, these reactions appeared after third treatment with tick saliva only in fish fed on dog food (**Figure 7B**). Abnormal behavior patterns and feeding were higher in saliva-treated fish than in controls only when feeding on dog food (**Figure 7B**).

These results showed that zebrafish treated with tick saliva develop hemorrhagic-type allergic reactions with abnormal behavior patterns with higher incidence in fish fed with α-Gal–positive dog food than with α-Gal–negative fish feed. Once recovered from allergic reactions, fish continuing feeding on dog food became tolerant to tick saliva. A risk factor associated with anti–α-Gal IgM antibody levels was also identified.

Allergic Reactions to Tick Saliva and Red Meat Consumption in Zebrafish Are Associated With Different Tissue-Specific Immune Response Mechanisms

The expressions of selected immune response and food allergy markers were characterized in Experiment 1 using the kidney and intestine involved in both innate and adaptive fish immunity. Different immune responses were observed in zebrafish kidney and intestine and between fish fed on dog food and fish feed (**Figures 8A,B**). In the kidney of zebrafish fed on dog food but not on fish feed, except for *c3a*, all genes were downregulated in response to tick saliva when compared to PBS-treated controls (**Figures 8A,B**). However, in the intestine of fish fed on dog food all genes except for *myd88*, *akr2*, and *il1b* were upregulated in response to tick saliva but not to other treatments (**Figures 8A,B**). In response to α-Gal or PGE_2 but not to the combined α-Gal + PGE_2, various genes were downregulated in the kidney of zebrafish fed on dog food (**Figures 8A,B**). Minor or no changes in gene expression were observed in the kidney and intestine of fish fed on fish feed and treated with tick saliva, α-Gal, PGE_2, or α-Gal + PGE_2 when compared to PBS controls (**Figures 8A,B**).

The analysis of granulocytes in zebrafish tissue sections collected in Experiment 1 identified the presence of these cells mainly in the skeletal muscle (**Figure 9A** and **Supplementary Figure 4**). The results showed a higher number ($p = 0.00000002$) of granulocytes and granulocyte agglomerations in zebrafish treated with tick saliva (8.8 ± 0.8) when compared to fish treated with α-Gal (2.7 ± 0.8),

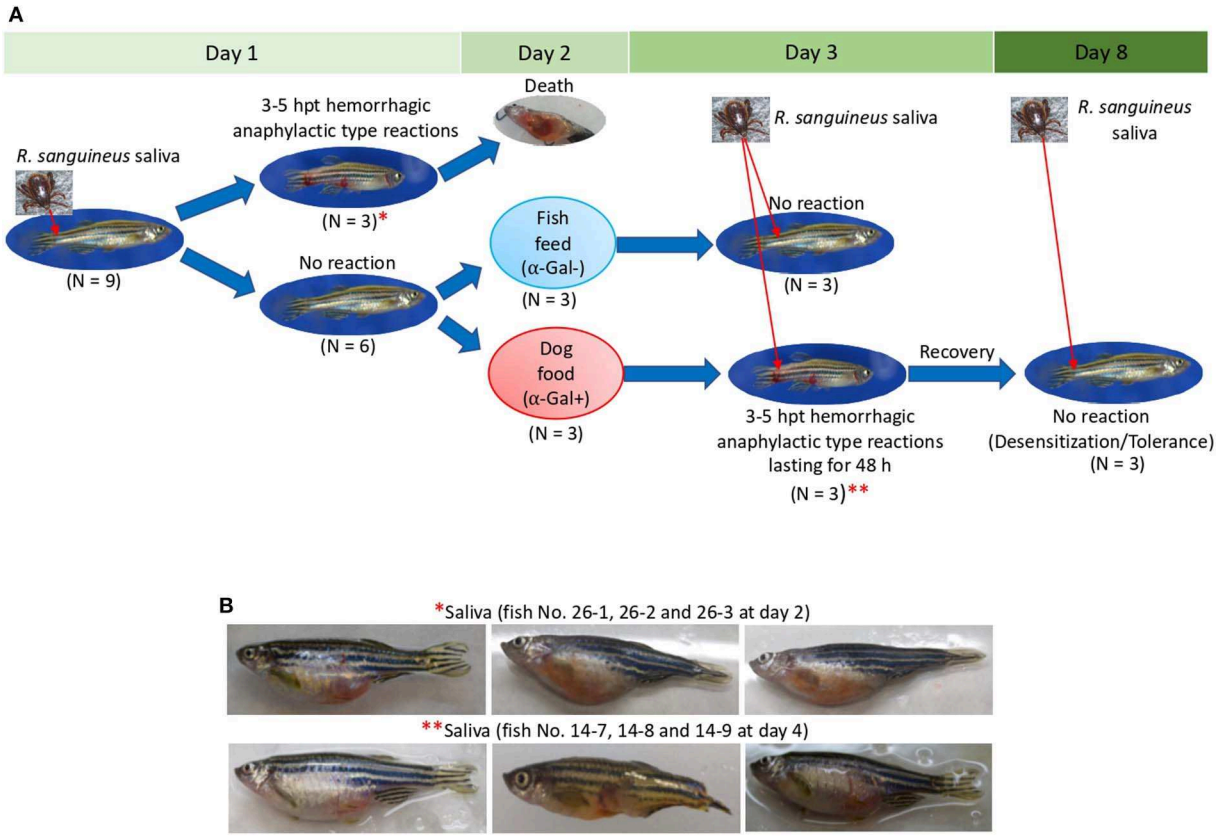

FIGURE 5 | Zebrafish injected with tick saliva and fed with red meat develop hemorrhagic anaphylactic-type reactions and desensitization (Experiment 1). **(A)** In the zebrafish model, 33% of animals treated with tick saliva on day 1 developed hemorrhagic anaphylactic-type allergic reactions 3–5 hpt and died. Furthermore, 100% of fish fed with dog food, but none of the fish that continued feeding on fish feed at day 2, developed allergy to tick saliva injected on day 3. Once recovered from anaphylactic-type reactions, all fish were desensitized and became tolerant to tick saliva injected on day 8. **(B)** Signs of hemorrhagic anaphylactic-type reactions in zebrafish No. 26-1, 26-2, and 26-3 injected with tick saliva and dying at day 2 before food change. After food change, only fish No. 14-7, 14-8, and 14-9 feeding on dog food developed anaphylactic-type reactions. Asterisks in red connect representative fish images in **(A)** with results in **(B)**.

PGE_2 (3.2 ± 0.8), α-Gal + PGE_2 (3.2 ± 1.0), or PBS (2.3 ± 0.6) (**Figures 9A,B**, **Supplementary Figure 4**). No differences were observed between fish fed on fish feed or dog food for each treatment (**Supplementary Figure 4**). At a higher magnification, the structure of the granulocytes showed characteristics of fish basophils/eosinophils such as a highly granular cytoplasm with large and spherical granules (**Figure 9C**).

Finally, of the selected zebrafish immune response and food allergy markers, only the expression of *il1b* was significantly higher in the intestine of zebrafish treated with tick saliva and presenting anaphylactic-type reactions and death when compared to fish without reactions on day 2 (**Figure 9D**).

These results suggested that tick salivary biogenic components different from or in combination with α-Gal and PGE_2 are essential for the modulation of zebrafish immune response to tick saliva and red meat consumption in both kidney and intestine but affecting different tissue-specific mechanisms. The results also suggested a role for basophils/eosinophils in zebrafish response to tick saliva.

DISCUSSION

Tick saliva contains biogenic substances including proteins, lipids, and other biomolecules such as PGE_2 and α-Gal that modulate multiple biological processes affecting ectoparasite feeding and pathogen infection and transmission (Oliveira et al., 2011; Poole et al., 2013; Chmelar et al., 2019). These molecules may also affect host immune response leading to allergic diseases such as the AGS (Araujo et al., 2016; Cabezas-Cruz et al., 2017c, 2019; Chandrasekhar et al., 2019; Hilger et al., 2019). In this study, we focused on the brown dog tick *R. sanguineus* based on the worldwide distribution of this tick species as a major dog ectoparasite, the risk it poses for urban populations, its role in the transmission of pathogens such as *Rickettsia rickettsii* causing Rocky Mountain spotted fever and the cause of anaphylactic reactions to tick bite, and its phylogenetically close relationship with tick species such as *Rhipicephalus bursa* and *Rhipicephalus microplus* previously shown to contain α-Gal–modified proteins (Valls et al., 2007; Uspensky, 2014; de la Fuente et al., 2017; Mateos-Hernández et al., 2017).

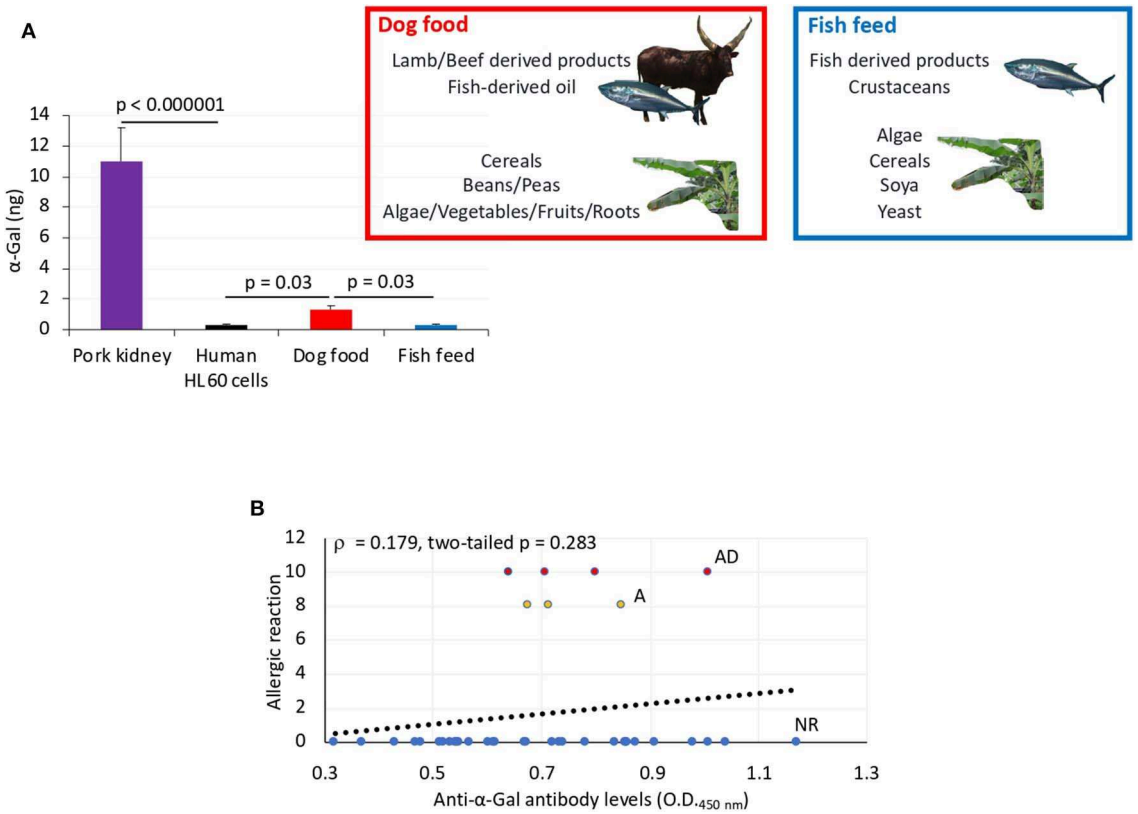

FIGURE 6 | α-Gal levels in dog food and fish feed and correlation analysis between anti–α-Gal IgM antibody levels and allergic reactions to tick saliva. **(A)** The α-Gal levels were determined by ELISA in fish feed and dog food and in comparison with pork kidney (α-Gal positive) and human HL60 cells (α-Gal negative) as positive and negative controls, respectively. The results were converted to α-Gal content per sample using a calibration curve ($R^2 = 0.992$; **Supplementary Figure 5A**) and compared between samples and negative control and between dog food and fish feed by Student *t*-test with unequal variance ($p < 0.05$, $N = 3$ biological replicates). The main components of dog food and fish feed are shown. Only dog food contains α-Gal–positive animal-derived products. **(B)** Spearman ρ correlation analysis between anti–α-Gal IgM antibody levels and allergic reactions to tick saliva in Experiment 1 rated as 10 for fish with allergic reactions and death (AD), 8 for fish with allergic reactions only (A), and 0 for fish without reactions (NR). Correlation rank coefficient (ρ) and *p*-value are shown.

Humans evolved with the inactivation of the α1,3-GalT gene, which resulted in the recognition of the carbohydrate α-Gal as a non–self-antigen, thus inducing the production of high antibody titers against this molecule (Galili, 2018). This evolutionary trait benefits humans by providing immunity to pathogens containing α-Gal in the surface while increasing the risks of developing the AGS triggered by the IgE antibody response against α-Gal present in glycoproteins and glycolipids from tick saliva and tissues of non-catarrhine mammals (Commins et al., 2009; Van Nunen et al., 2009; Platts-Mills et al., 2015; Steinke et al., 2015; Galili, 2018; Cabezas-Cruz et al., 2019; de la Fuente et al., 2019; Hilger et al., 2019; Román-Carrasco et al., 2019; Park et al., 2020). The AGS is characterized by delayed anaphylaxis to red meat consumption and immediate anaphylaxis to tick bites, xenotransplantation, and certain drugs such as cetuximab (Mateos-Hernández et al., 2017; Hilger et al., 2019). Despite recent advances in the study of the AGS (Commins et al., 2009; Van Nunen et al., 2009; Platts-Mills et al., 2015; Steinke et al., 2015; Mateos-Hernández et al., 2017; Galili, 2018; Cabezas-Cruz et al., 2019; de la Fuente et al., 2019; Hilger et al., 2019), the immune-mediated mechanisms induced by tick bites and leading to the AGS have been only partially characterized in α1,3-GalT-KO mice (Araujo et al., 2016; Chandrasekhar et al., 2019). The development of new animal models for tick-borne allergies such as the AGS would contribute to these studies.

Considering that zebrafish are evolutionarily naive to tick saliva as they are not naturally exposed to ticks, the observed allergic hemorrhagic anaphylactic-type reactions and abnormal behavior patterns may occur in response to toxic and anticoagulant biogenic compounds different from α-Gal and PGE_2 present in tick saliva (Francischetti et al., 2009; Aleman and Wolberg, 2013; Mihara, 2017; Stringer et al., 2017; Haddad et al., 2018). For example, although uncommon, episodic hemorrhage has been described in humans during honeybee venom anaphylaxis (Mingomataj and Bakiri, 2012). This episodic hemorrhage has been associated with honeybee venom components that interfere with complement cleavage and bradykinin release, thus affecting coagulation, thrombolysis, hemolysis, and smooth muscle tone. Additionally, infestations by sea lice of the family Caligidae such as *Lepeophtheirus* and *Caligus*

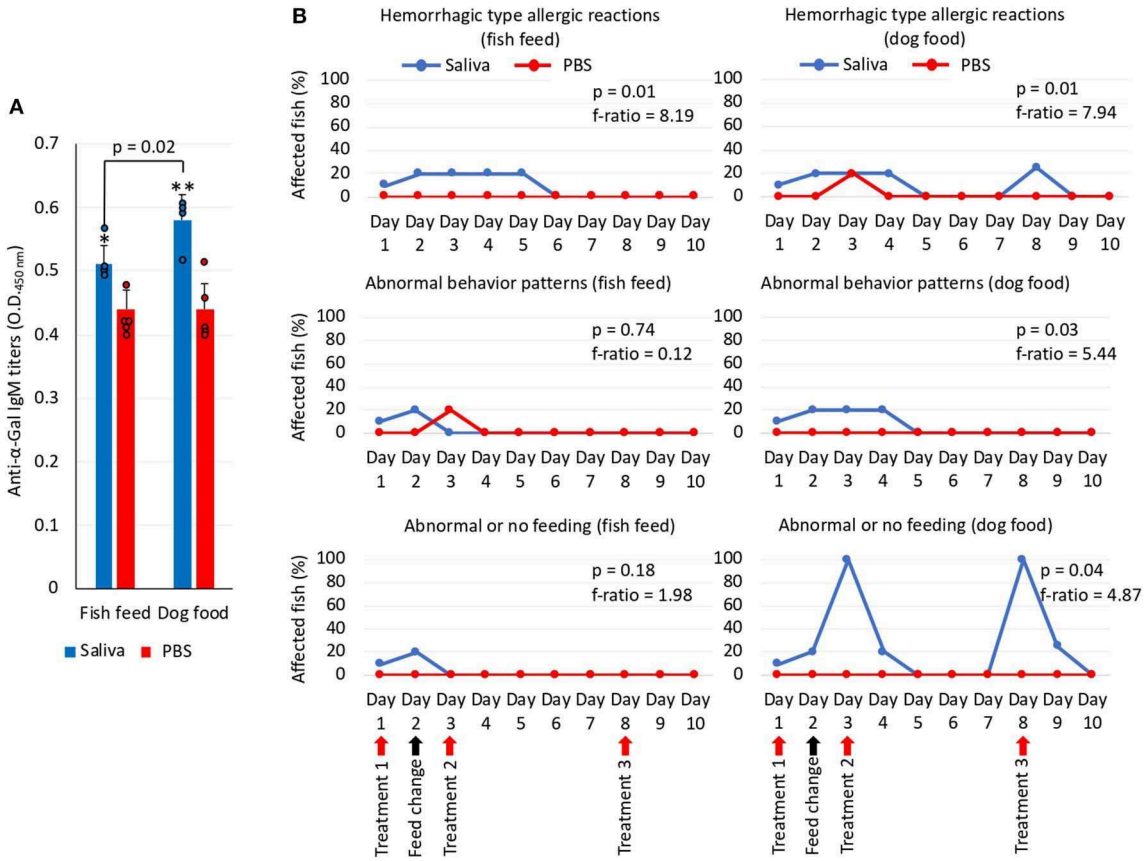

FIGURE 7 | Zebrafish injected with tick saliva and fed with red meat develop allergic reactions and abnormal behavior and feeding patterns (Experiment 2). **(A)** The IgM antibody titers against α-Gal were determined by ELISA, represented as the average ± SD OD at 450 nm and compared between fish treated with tick saliva and the PBS-treated control group and between fish fed on fish feed or dog food Student *t*-test ($^{*}p = 0.003$, $^{**}p = 0.0008$; $N = 4$–5 biological replicates with individual values shown). **(B)** Zebrafish local allergic reactions and behavior were examined immediately after treatment or feed change and followed daily until the end of the experiment at day 10. The percent of zebrafish affected by allergic reactions and abnormal behavior and feeding on each group fed with fish feed or dog food was compared between saliva-treated and PBS-treated control fish by a one-way ANOVA test (https://www.socscistatistics.com/tests/anova/default2.aspx) ($p = 0.05$; $N = 4$–5 biological replicates).

species affect fish behavior and cause abrasion-like lesions at their attachment and feeding sites by changing mucus consistency and damaging the epithelium, which results in loss of blood and fluids and cortisol release (Fast, 2014; Øverli et al., 2014). Some species of fish will spend more time lying on the bottom of the tank when they become stressed, which will also reduce eating (Kalueff et al., 2013). Zigzagging is also a behavior associated with fish stress (Kalueff et al., 2013).

Anaphylactic-type reactions have been previously described in channel catfish (*Ictalurus punctatus* Refinesque) and goldfish (*Carassius auratus* L.) following immunization and challenge with solubilized protozoa (*Tetrahymena pyriformis*) and human serum proteins, respectively, but not when challenged with the heterologous BSA antigen (Goven et al., 1980). The fishes sensitized and challenged with homologous antigens showed abnormal behavior patterns consisting of disorientation, breading problems, and increased defecation. Severe respiratory distress resulted in 33% death of treated catfish. The authors concluded that type I hypersensitivity reactions were the cause of observed anaphylaxis, a mechanism currently defined as type 2 T helper (T_H2) immunity that has been proposed to be associated with the AGS (Wilson et al., 2017; Cabezas-Cruz et al., 2019; Chandrasekhar et al., 2019). In our study, the potential role of BSA present in in the α-Gal–coated particles in the observed allergic reactions when administered to zebrafish was discarded because as previously described (Goven et al., 1980), fish were not previously exposed to BSA, and BSA was likely not present in the tick saliva. Although fish were intramuscularly injected with tick salivary biogenic substances, part of the injected liquid remained subcutaneous, which would better resemble tick bites.

The effect of red meat consumption in the form of dog food containing α-Gal in zebrafish previously treated with tick saliva and normally fed with fish feed free of α-Gal is relevant for the study of the AGS. Dog feed was used because it contains fish- and plant-derived components also present in fish food, and it is registered for animal use. Both fish feed and dog food contained plant-derived compounds together for either fish or animal (red meat) products, thus making it difficult to assign the observed

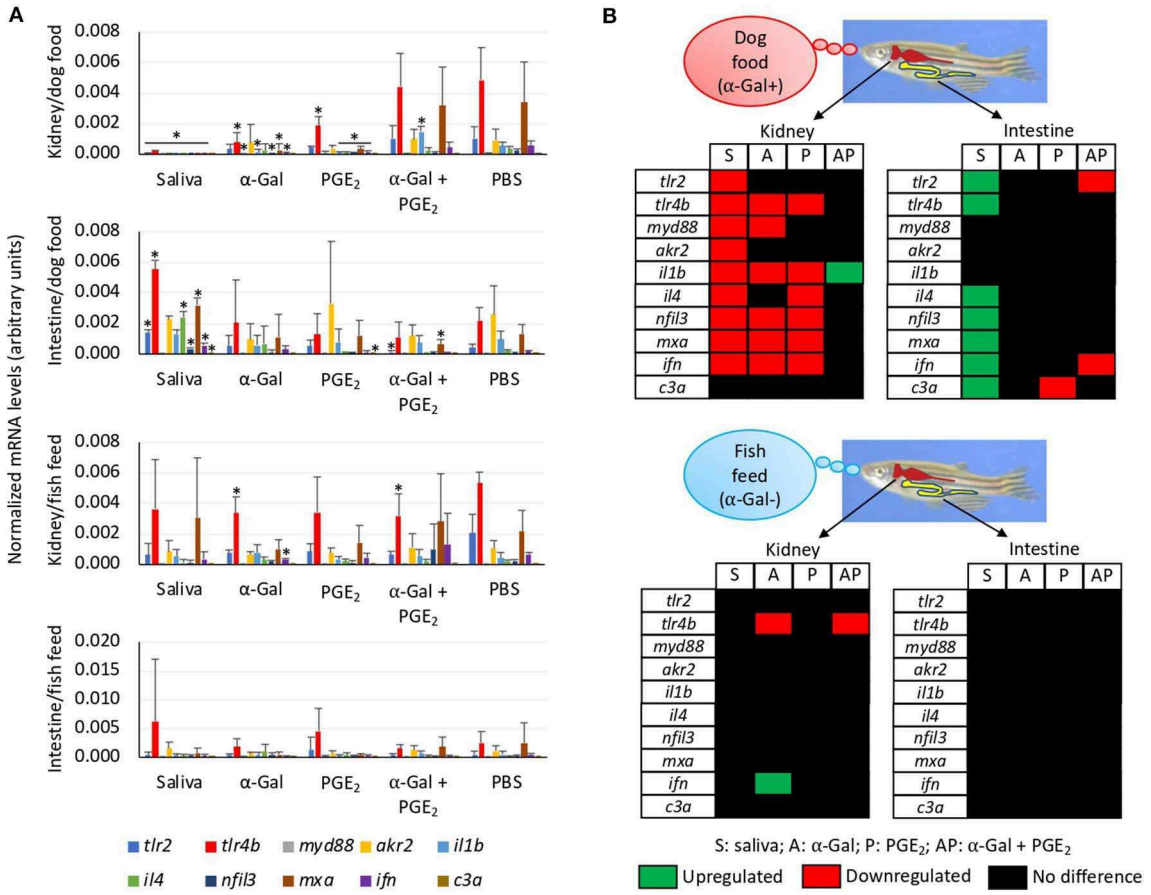

FIGURE 8 | Tissue-specific differences in the immune response of zebrafish injected with tick saliva and fed with red meat (Experiment 1). **(A)** The expression of selected immune response and food allergy markers was analyzed by qRT-PCR in the kidney and intestine of zebrafish fed on dog food or fish feed. The mRNA Ct values were normalized against *D. rerio gapdh*, presented as average ± SD, and compared between fish treated with saliva, α-Gal, PGE_2, or α-Gal + PGE_2, and the PBS-treated control group by Student *t*-test with unequal variance (*$p < 0.05$; $N = 3$–6). **(B)** Representation of differential gene expression with respect to PBS-treated controls in the kidney and intestine of zebrafish fed on dog food or fish feed. Data were obtained from the analysis described in **(A)**.

reactions to other compounds present in dog food. We did not add α-Gal to fish feed because it is possible that the immune response to α-Gal depends on the way this molecule is presented on proteins or lipids and not only the carbohydrate by itself. For still unknown reasons and despite identified risk factors such as gender, pollen allergy, bronchial asthma, pet keeping, age, blood group, and lifestyle (Cabezas-Cruz et al., 2017a,b, 2019), only a fraction of the humans exposed to tick bites develop the AGS, and cases of mammalian meat desensitization have been recently reported (Yucel et al., 2019). Despite the limitations associated with the low number of fish included on each treatment, in the zebrafish model 33% (Experiment 1) and 20% (Experiment 2) of the animals treated with tick saliva developed allergic reactions with no reactions in control fish. However, when fed with dog food, 100% of the animals in both experiments presented allergic reactions including abnormal behavior or feeding after treatment with tick saliva. Furthermore, once recovered from anaphylactic-type reactions, fish became tolerant to tick saliva by still unknown mechanisms. Differences in the presentations of allergic reactions between Experiments 1 and 2 may be due to the amount of tick saliva injected in fish (2.5 μL in Experiment 1 vs. 1 μL in Experiment 2). These results suggested a role for red meat consumption in the allergic reactions to tick saliva in zebrafish and in a rapid desensitization process to become tolerant to tick saliva.

In humans, anti–α-Gal IgE antibody levels (≥0.35 kU/L) have been identified like a risk factor for the development of the AGS (Commins et al., 2009; Van Nunen et al., 2009; Platts-Mills et al., 2015; Steinke et al., 2015; Galili, 2018; Cabezas-Cruz et al., 2019; de la Fuente et al., 2019; Hilger et al., 2019). Recently and albeit that cofactors are influential in the expression of mammalian meat allergy (Platts-Mills et al., 2020), Mabelane et al. (2018) reported that anti–α-Gal IgE antibody levels higher than 5.5 kU/L are an indicator of AGS with 95% confidence. Herein we showed that zebrafish as humans do not synthesize α-Gal and produce natural anti–α-Gal IgM antibodies in response to gut bacterial microbiota. However, in zebrafish, a significant correlation was not observed between anti–α-Gal IgM antibody

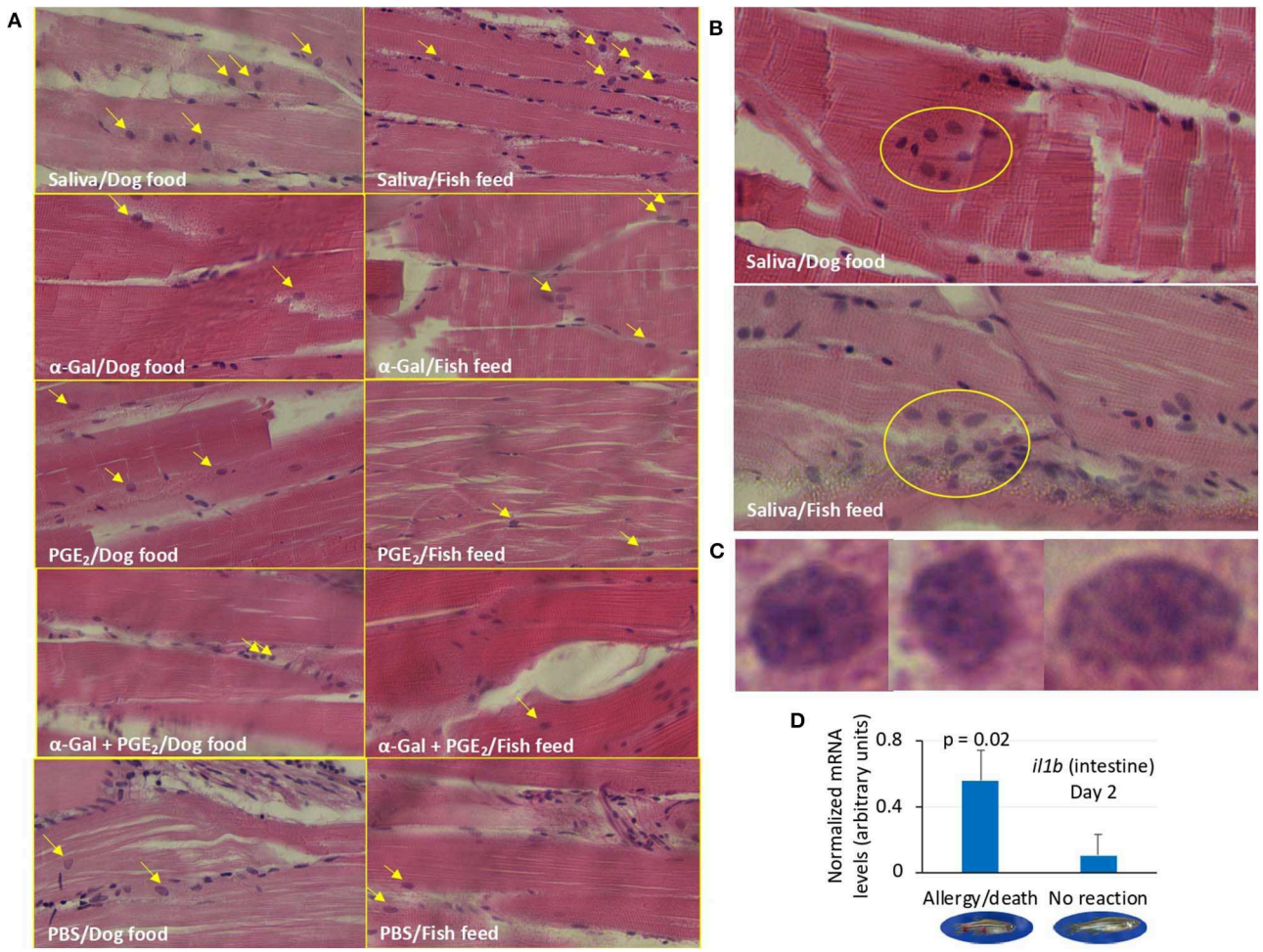

FIGURE 9 | Granulocyte profile in zebrafish (Experiment 1). **(A)** Representative images of granulocytes detected in tissue sections stained with hematoxylin and eosin of zebrafish treated with saliva, α-Gal, PGE_2, or α-Gal + PGE_2, or the PBS control and fed with dog food or fish feed. The fields were randomly chosen, and granulocytes are indicated with arrows. The average counts of granulocytes were compared between fish treated with tick saliva, α-Gal, or PGE_2 α-Gal + PGE_2, and PBS-treated controls and between fish fed on dog food or fish feed for each treatment by Student *t*-test with unequal variance ($p < 0.05$; $N = 3$–6; **Supplementary Figure 4**). Most granulocytes were observed in the skeletal muscle. Magnification ×40. **(B)** Representative images of granulocytes agglomerations only detected in zebrafish treated with tick saliva. Magnification ×40. **(C)** Selected images for identified granulocytes showing characteristics of basophils/eosinophils. Magnification ×100. **(D)** The expression of selected immune response and food allergy markers was analyzed by qRT-PCR in the kidney and intestine of zebrafish treated with saliva and presenting anaphylactic-type reactions and death on day 2, and fish without reactions and normalized mRNA Ct values (average ± SD) were compared by Student *t*-test with unequal variance ($p < 0.05$; $N = 3$–6). Only *il1b* gene in the intestine showed significant differences.

levels and allergic reactions to tick saliva, but IgM antibody levels higher than 0.6 OD at 450 nm were identified as a risk factor for developing anaphylactic-type reactions to tick saliva and red meat consumption. Nevertheless, these results may be affected by the fact that the antibody levels in zebrafish dying from anaphylactic-type reactions were determined on day 2 after a single treatment with tick saliva, whereas most fish were treated three times and sera collected on day 14 for analysis.

To identify the possible immune mechanisms associated with allergic reactions observed in zebrafish in response to tick saliva and red meat consumption, selected immune response and food allergy markers involved in T_H1 and T_H2 cell–mediated responses (Lu et al., 2008; Huang et al., 2018) were characterized in the kidney and intestine involved in both innate and adaptive fish immunity (Liu et al., 2015; Brugman, 2016; Martins et al., 2019). The $CD4^+$ T cells or T helper cells develop into T_H1 and T_H2 cells (**Figure 10A**). While type 1 T helper (T_H1) cells produce interferon (IFN), interelukin 1 (IL-1), and Mxa, among other proteins, for cell-mediated immunity and macrophage-dependent protective responses, T_H2 cells produce IL-1, IL-4, and other cytokines to induce antibody-mediated adaptive immune response and inhibition of several macrophage functions (Romagnani, 1999). Other cytokines such as IL-3 and regulated factors (NFIL-3) are produced by both T_H1 and T_H2 cells (Romagnani, 1999). Additionally, T_H1 cells are involved in the pathogenesis of organ-specific autoimmune disorders, whereas T_H2 mediates allergen-specific responses (Romagnani, 1999).

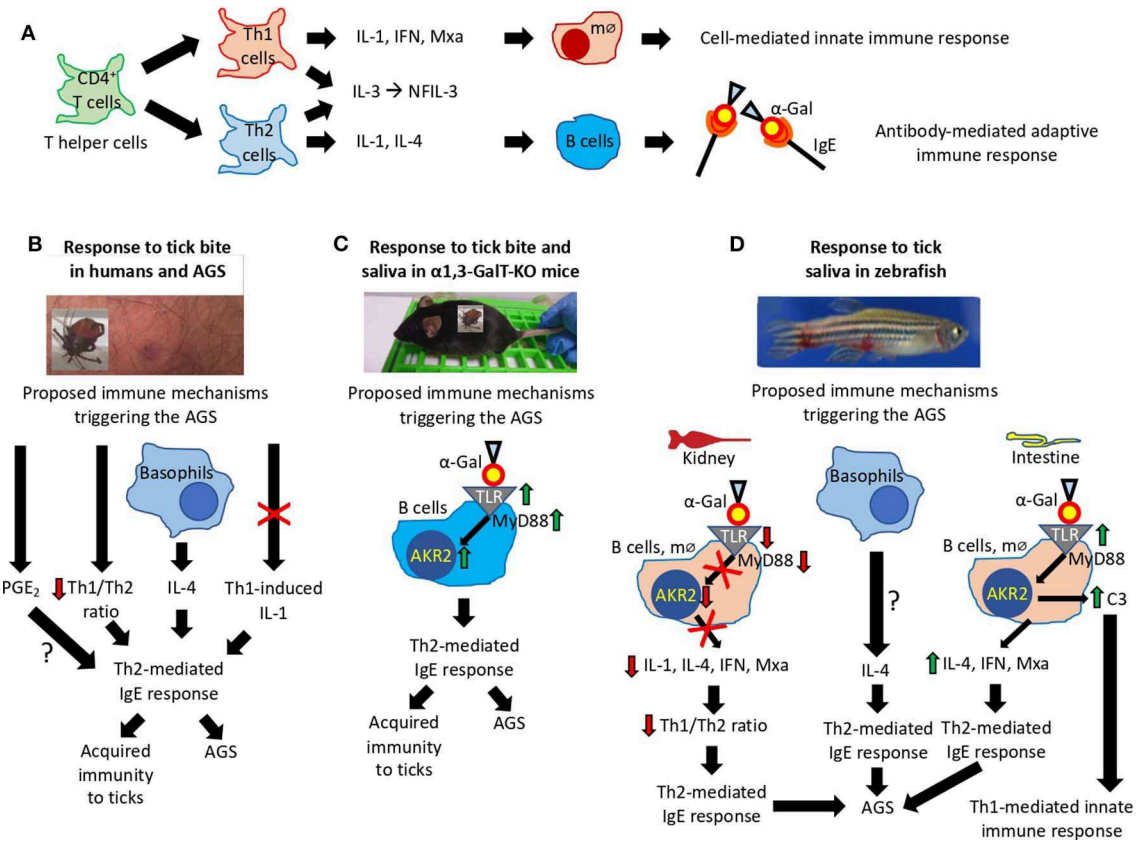

FIGURE 10 | Proposed mechanisms triggering the AGS. **(A)** Mechanisms mediated by $CD4^+$ T cells or T helper (T_H) cells that develop into T_H1 and T_H2 cells regulating cell-mediated and antibody-mediated innate and adaptive immune responses, respectively. **(B–D)** Immune mechanisms triggering the AGS that have been proposed based on existing evidence in **(B)** humans, **(C)** α1,3-GalT-KO mice, and **(D)** our zebrafish animal model. The interrogation marks (?) represent mechanisms that need additional evidence to be sustained.

In humans, the AGS has been proposed to be associated with tick saliva–induced inhibition of T_H1-induced production of IL-1, basophil-mediated production of IL-4, decrease in T_H1/T_H2 ratio, and PGE_2-induced antibody class switching, all resulting in the induction of T_H2-mediated IgE response against α-Gal (Cabezas-Cruz et al., 2019; Kageyama et al., 2019) (**Figure 10B**). As recently concluded by Kageyama et al. (2019), repeated tick bites promote basophil recruitment and attract T_H2 cells to the skin, which results in a proper cytokine milieu to enhance IgE antibody levels against tick proteins and α-Gal to facilitate acquired immunity to ticks and the AGS.

In the α1,3-GalT-KO mouse model, the induction of α-Gal–specific IgE antibodies following tick feeding and in response to subcutaneous injection of tick saliva was proposed to be associated with the salivary proteins modified with α-Gal–like antigens that might modulate host immune response toward anti–α-Gal IgE antibodies (Araujo et al., 2016). However, recently Román-Carrasco et al. (2019) provided evidence supporting that glycolipids but not glycoproteins containing α-Gal were able to cross the intestinal monolayer and trigger an allergic reaction such as the AGS. To characterize the immune mechanisms leading to production of IgE antibodies and allergic reactions in response to tick bites and red meat consumption, Chandrasekhar et al. (2019) showed in the α1,3-GalT-KO mouse model that the induction of IgE responses was dependent on $CD4^+$ T cells and the expression of the B cell-intrinsic MyD88 adaptor for inflammatory Toll-like receptor (TLR) and IL-1 signaling pathways leading, among others, to the activation of the Akr2/nuclear factor κB (NF-κB) (Deguine and Barton, 2014) (**Figure 10C**).

The results reported here in the zebrafish model support some of the previously proposed immune mechanisms triggering the AGS and provided evidence for different tissue-specific mechanisms also potentially involved in the AGS (**Figure 10D**). While in zebrafish kidney α-Gal–containing glycolipids and glycoproteins may antagonize TLR-mediated response to promote T_H2-mediated IgE response to α-Gal, in the intestine a mechanism similar to that proposed in humans and mouse model may trigger AGS through activation of TLR by α-Gal leading to production of proinflammatory cytokines and anti–α-Gal IgE response. As proposed for humans in response to tick saliva, basophils in zebrafish may be also recruited to attract T_H2 cells producing IL-4 to the muscle inducing T_H2-mediated IgE response to α-Gal. Basophils/eosinophils have been described in zebrafish and other fish species, but the functional role of these cells in immune response and allergy has not been previously

characterized (Ainsworth, 1992; Bennett et al., 2001). The fact that *il1b* was the only gene upregulated in zebrafish suffering and dying of hemorrhagic anaphylactic-type reactions in response to tick saliva on day 2 and the regulation of this gene after red meat consumption suggesting a key role for this cytokine, which has been previously shown to promote adhesion of basophils, eosinophils, and neutrophils to human vascular endothelial cells (Bochner et al., 1991). Although a role for PGE_2 during AGS has been proposed in humans (Cabezas-Cruz et al., 2017c), in the zebrafish model we did not find a correlation between this prostaglandin and the allergic response to tick saliva.

Based on the evidence obtained from studies in humans and the mouse and zebrafish animal models, the proposed mechanisms triggering the AGS involve TLR-mediated responses in both T_H1 and T_H2 cells with a role for basophils in this process (**Figures 10B–D**). The TLRs play a role in immune response by initiating signaling cascades that result in the recruitment of signaling adaptors such as MyD88 to trigger the formation of supramolecular organizing centers that coordinate various cellular responses such as translocation of Akr2/NF-κB and the activation of immune cells leading to the expression of proinflammatory cytokines and IFNs (Rosadini and Kagan, 2015). Pathogen-derived glycoproteins and glycolipids interact with TLRs with different outcomes. The TLR4 sensors bacterial lipopolysaccharides that activate the MyD88-dependent pathway resulting in Akr2/NF-κB activation leading to the production of IFN and proinflammatory cytokines (Perrin-Cocon et al., 2017). However, pathogen-derived glycolipids and glycoproteins can antagonize TLR-mediated response to interfere with cellular immune response (Hajishengallis and Lambris, 2011; Cochet et al., 2019). Basophil levels increase and infiltrate lesions after tick infestations contributing to acquired immunity and secretion of the histamine-repellent factor in tick-resistant animals (Karasuyama et al., 2018b; Tabakawa et al., 2018). Basophils have been also shown to activate T_H2 IL-4–mediated responses (Karasuyama et al., 2018a), which may lead to acquired immunity to ticks and the high anti–α-Gal IgE antibody levels associated with the AGS (Kageyama et al., 2019). Additionally, basophils may attract T_H2 cells to the tick bite site to induce intrinsic T_H2 immunity-promoting adjuvant function of tick salivary components to enhance IgE response to α-Gal–containing tick proteins causing the AGS (Hilger et al., 2019; Kageyama et al., 2019).

CONCLUSIONS

In this study, a new animal model was developed using zebrafish for the study of allergic reactions in response to tick salivary biogenic substances and red meat consumption. The observed allergic hemorrhagic anaphylactic-type reactions and abnormal behavior patterns may occur in response to toxic and anticoagulant biogenic compounds different from α-Gal present in tick saliva. Furthermore, host-derived and not only tick-derived molecules with α-Gal may be involved in the AGS (Platts-Mills et al., 2020). However, the results showed that only zebrafish previously exposed to tick saliva and fed on dog food developed hemorrhagic anaphylactic-type allergic reactions and/or abnormal behavior or feeding patterns with rapid desensitization and tolerance. These allergic reactions were associated with tissue-specific TLR-mediated responses in T_H1 and T_H2 cells with a possible role for basophils in the immune response to tick saliva. The results obtained in this proof-of-concept study support some of the previously proposed immune mechanisms triggering the AGS in humans and the α1,3-GalT-KO mouse model and provided evidence for different tissue-specific mechanisms also potentially involved in the AGS. These results support the use of the zebrafish animal model for the study of the AGS and other tick-borne allergies.

DATA AVAILABILITY STATEMENT

All datasets generated for this study are included in the article/**Supplementary Material**.

ETHICS STATEMENT

The animal study was reviewed and approved by Ethics Committee on Animal Experimentation of the University of Castilla La Mancha (PR-2018-06-13) and the Counseling of Agriculture, Environment and Rural Development of Castilla La Mancha (ES130340000218).

AUTHOR CONTRIBUTIONS

JF and AC-C: conceptualization. JF: methodology, writing-original draft preparation, visualization, supervision, and project administration. MC, IP, and LM-H: validation. MC and JF: formal analysis. MC, IP, PA, SD-S, SA-J, LM-H, and MV: investigation. JF, MC, PA, SA-J, and AC-C: writing-review and editing. JF and MV: funding acquisition.

FUNDING

This study was funded by the Consejería de Educación, Cultura y Deportes, JCCM, Spain, project CCM17-PIC-036 (SBPLY/17/180501/000185). MV was supported by the University of Castilla La Mancha, Spain.

ACKNOWLEDGMENTS

We thank Gabriela de la Fuente (Sabiotec spin-off S.L., Spain) for assistance with collection of *R. sanguineus* ticks, Almudena González García (IREC, Spain) for technical assistance with the fish experimental facility, Francisca Talavera for technical assistance with histochemical analyses and Juan Galcerán Sáez (IN-CSIC-UMH, Spain) for providing zebrafish.

SUPPLEMENTARY MATERIAL

The Supplementary Material for this article can be found online at: https://www.frontiersin.org/articles/10.3389/fcimb.2020.00078/full#supplementary-material

REFERENCES

Ainsworth, A. J. (1992). Fish granulocytes: morphology, distribution, and function. *Annu. Rev. Fish Dis.* 2, 123–148.

Aleman, M. M., and Wolberg, A. S. (2013). Tick spit shines a light on the initiation of coagulation. *Circulation* 128, 203–205. doi: 10.1161/CIRCULATIONAHA.113.003800

Araujo, R. N., Franco, P. F., Rodrigues, H., Santos, L. C. B., McKay, C. S., Sanhueza, C. A., et al. (2016). *Amblyomma sculptum* tick saliva: alpha-Gal identification, antibody response and possible association with red meat allergy in Brazil. *Int. J. Parasitol.* 46, 213–220. doi: 10.1016/j.ijpara.2015.12.005

Bennett, C. M., Kanki, J. P., Rhodes, J., Liu, T. X., Paw, B. H., Kieran, M. W., et al. (2001). Myelopoiesis in the zebrafish, *Danio rerio*. *Blood*. 98, 643–651. doi: 10.1182/blood.v98.3.643

Bochner, B. S., Luscinskas, F. W., Gimbrone, M. A. Jr, Newman, W., Sterbinsky, S. A., Derse-Anthony, C. P., et al. (1991). Adhesion of human basophils, eosinophils, and neutrophils to interleukin 1-activated human vascular endothelial cells: contributions of endothelial cell adhesion molecules. *J. Exp. Med.* 173, 1553–1557. doi: 10.1084/jem.173.6.1553

Brugman, S. (2016). The zebrafish as a model to study intestinal inflammation. *Dev. Comp. Immunol.* 64, 82–92. doi: 10.1016/j.dci.2016.02.020

Cabezas-Cruz, A., de la Fuente, J., Fischer, J., Hebsaker, J., Lupberger, E., Blumenstock, G., et al. (2017a). Prevalence of type I sensitization to alpha-gal in forest service employees and hunters: Is the blood type an overlooked risk factor in epidemiological studies of the α-Gal syndrome? *Allergy* 72, 2044–2047. doi: 10.1111/all.13206

Cabezas-Cruz, A., Hodžić, A., Román-Carrasco, P., Mateos-Hernández, L., Duscher, G. G., Sinha, D. K., et al. (2019). Environmental and molecular drivers of the α-Gal syndrome. *Front. Immunol.* 10:1210. doi: 10.3389/fimmu.2019.01210

Cabezas-Cruz, A., Mateos-Hernández, L., Alberdi, P., Villar, M., Riveau, G., Hermann, E., et al. (2017b). Effect of blood type on anti-α-Gal immunity and the incidence of infectious diseases. *Exp. Mol. Med.* 49:e301. doi: 10.1038/emm.2016.164

Cabezas-Cruz, A., Mateos-Hernández, L., Chmelar, J., Villar, M., and de la Fuente, J. (2017c). Salivary prostaglandin E2: role in tick-induced allergy to red meat. *Trends Parasitol.* 33, 495–498. doi: 10.1016/j.pt.2017.03.004

Cabezas-Cruz, A., Valdés, J. J., and de la Fuente, J. (2016). Control of vector-borne infectious diseases by human immunity against α-Gal. *Expert Rev. Vaccines* 15, 953–955. doi: 10.1080/14760584.2016.1181547

Cantas, L., Sørby, J. R., Aleström, P., and Sørum, H. (2012). Culturable gut microbiota in zebrafish. *Zebrafish* 9, 26–37. doi: 10.1089/zeb.2011.0712

Chandrasekhar, J. L., Cox, K. M., Loo, W. M., Qiao, H., Tung, K. S., and Erickson, L. D. (2019). Cutaneous exposure to clinically relevant Lone Star ticks promotes IgE production and hypersensitivity through CD4+ T Cell- and MyD88-dependent pathways in mice. *J. Immunol.* 203, 813–824. doi: 10.4049/jimmunol.1801156

Chmelar, J., Kotál, J., Kovaříková, A., and Kotsyfakis, M. (2019). The use of tick salivary proteins as novel therapeutics. *Front. Physiol.* 10:812. doi: 10.3389/fphys.2019.00812

Cochet, F., Facchini, F. A., Zaffaroni, L., Billod, J. M., Coelho, H., Holgado, A., et al. (2019). Novel carboxylate-based glycolipids: TLR4 antagonism, MD-2 binding and self-assembly properties. *Sci. Rep.* 9:919. doi: 10.1038/s41598-018-37421-w

Commins, S. P., Satinover, S. M., Hosen, J., Mozena, J., Borish, L., Lewis, B. D., et al. (2009). Delayed anaphylaxis, angioedema, or urticaria after consumption of red meat in patients with IgE antibodies specific for galactose-alpha-1,3-galactose. *J. Allergy Clin. Immunol.* 123, 426–433. doi: 10.1016/j.jaci.2008.10.052

de la Fuente, J., Antunes, S., Bonnet, S., Cabezas-Cruz, A., Domingos, A., Estrada-Peña, A., et al. (2017). Tick-pathogen interactions and vector competence: identification of molecular drivers for tick-borne diseases. *Front. Cell. Infect. Microbiol.* 7:114. doi: 10.3389/fcimb.2017.00114

de la Fuente, J., Ayoubi, P., Blouin, E. F., Almazán, C., Naranjo, V., and Kocan, K. M. (2005). Gene expression profiling of human promyelocytic cells in response to infection with *Anaplasma phagocytophilum*. *Cell. Microbiol.* 7, 549–559. doi: 10.1111/j.1462-5822.2004.00485.x

de la Fuente, J., Estrada-Pena, A., Venzal, J. M., Kocan, K. M., and Sonenshine, D. E. (2008). Overview: ticks as vectors of pathogens that cause disease in humans and animals. *Front. Biosci.* 13, 6938–6946. doi: 10.2741/3200

de la Fuente, J., Pacheco, I., Villar, M., and Cabezas-Cruz, A. (2019). The alpha-Gal syndrome: new insights into the tick-host conflict and cooperation. *Parasit. Vectors* 12:154. doi: 10.1186/s13071-019-3413-z

Deguine, J., and Barton, G. M. (2014). MyD88: a central player in innate immune signaling. *F1000Prime Rep.* 6:97. doi: 10.12703/P6-97

Fast, M. D. (2014). Fish immune responses to parasitic copepod (namely sea lice) infection. *Dev. Comp. Immunol.* 43, 300–312. doi: 10.1016/j.dci.2013.08.019

Francischetti, I. M., Sa-Nunes, A., Mans, B. J., Santos, I. M., and Ribeiro, J. M. (2009). The role of saliva in tick feeding. *Front. Biosci.* 14, 2051–2088. doi: 10.2741/3363

Galili, U. (2018). Evolution in primates by "Catastrophic-selection" interplay between enveloped virus epidemics, mutated genes of enzymes synthesizing carbohydrate antigens, and natural anticarbohydrate antibodies. *Am. J. Phys. Anthropol.* 168, 352–363. doi: 10.1002/ajpa.23745

Goven, B. A., Dawe, D. L., and Gratzek, J. B. (1980). *In vivo* and *in vitro* anaphylactic type reactions in fish. *Dev. Comp. Immunol.* 4, 55–64.

Ha, K., Lewis, K., Patel, V., and Grinceri, J. (2019). A case of tick-borne paralysis in a traveling patient. *Case Rep. Neurol. Med.* 2019:3934696. doi: 10.1155/2019/3934696

Haddad, V. Jr, Haddad, M. R., Santos, M., and Cardoso, J. L. C. (2018). Skin manifestations of tick bites in humans. *An. Bras. Dermatol.* 93, 251–255. doi: 10.1590/abd1806-4841.20186378

Hajishengallis, G., and Lambris, J. D. (2011). Microbial manipulation of receptor crosstalk in innate immunity. *Nat. Rev. Immunol.* 11, 187–200. doi: 10.1038/nri2918

Hilger, C., Fischer, J., Wölbing, F., and Biedermann, T. (2019). Role and mechanism of galactose-alpha-1,3-galactose in the elicitation of delayed anaphylactic reactions to red meat. *Curr. Allergy Asthma Rep.* 19:3. doi: 10.1007/s11882-019-0835-9

Huang, J., Liu, C., Wang, Y., Wang, C., Xie, M., Qian, Y., et al. (2018). Application of *in vitro* and *in vivo* models in the study of food allergy. *Food Sci. Hum. Wellness* 7, 235–243. doi: 10.1016/j.fshw.2018.10.002

Iniguez, E., Schocker, N. S., Subramaniam, K., Portillo, S., Montoya, A. L., Al-Salem, W. S., et al. (2017). An α-Gal-containing neoglycoprotein-based vaccine partially protects against murine cutaneous leishmaniasis caused by *Leishmania major*. *PLoS Negl. Trop. Dis.* 11:e0006039. doi: 10.1371/journal.pntd.0006039

Kageyama, R., Fujiyama, T., Satoh, T., Keneko, Y., Kitano, S., Tokura, Y., et al. (2019). The contribution made by skin-infiltrating basophils to the development of alpha gal syndrome. *Allergy*. 74, 1805–1807. doi: 10.1111/all.13794

Kalueff, A. V., Gebhardt, M., Stewart, A. M., Cachat, J. M., Brimmer, M., Chawla, J. S., et al. (2013). Towards a comprehensive catalog of Zebrafish Behavior 1.0 and Beyond. *Zebrafish* 10, 70–86. doi: 10.1089/zeb.2012.0861

Karasuyama, H., Miyake, K., Yoshikawa, S., Kawano, Y., and Yamanishi, Y. (2018a). How do basophils contribute to Th2 cell differentiation and allergic responses? *Int. Immunol.* 30, 391–396. doi: 10.1093/intimm/dxy026

Karasuyama, H., Tabakawa, Y., Ohta, T., Wada, T., and Yoshikawa, S. (2018b). Crucial role for basophils in acquired protective immunity to tick infestation. *Front. Physiol.* 9:1769. doi: 10.3389/fphys.2018.01769

Lee, H., Halverson, S., and Mackey, R. (2016). Insect allergy. *Prim. Care* 43, 417–431. doi: 10.1016/j.pop.2016.04.010

Lima-Barbero, J. F., Sánchez, M. S., Cabezas-Cruz, A., Mateos-Hernández, L., Contreras, M., Fernández de Mera, I. G. F., et al. (2019). Clinical gamasoidosis and antibody response in two patients infested with *Ornithonyssus bursa* (Acari: Gamasida: Macronyssidae). *Exp. Appl. Acarol.* 78, 555–564. doi: 10.1007/s10493-019-00408-x

Liu, X., Wu, H., Liu, Q., Wang, Q., Xiao, J., Chang, X., et al. (2015). Profiling immune response in zebrafish intestine, skin, spleen and kidney bath-vaccinated with a live attenuated *Vibrio anguillarum* vaccine. *Fish Shellfish Immunol.* 45, 342–345. doi: 10.1016/j.fsi.2015.04.028

Livak, K. J., and Schmittgen, T. D. (2001). Analysis of relative gene expression data using real-time quantitative PCR and the 2(-Delta Delta C(T)) Method. *Methods* 25, 402–408. doi: 10.1006/meth.2001.1262

Lu, M. W., Chao, Y. M., Guo, T. C., Santi, N., Evensen, O., Kasani, S. K., et al. (2008). The interferon response is involved in nervous necrosis virus acute and persistent infection in zebrafish infection model. *Mol. Immunol.* 45, 1146–1152. doi: 10.1016/j.molimm.2007.07.018

Mabelane, T., Basera, W., Botha, M., Thomas, H. F., Ramjith, J., and Levin, M. E. (2018). Predictive values of alpha-gal IgE levels and alpha-gal IgE: total IgE ratio and oral food challenge-proven meat allergy in a population with a high prevalence of reported red meat allergy. *Pediatr. Allergy Immunol*. 29, 841–849. doi: 10.1111/pai.12969

Martins, R. R., Ellis, P. S., MacDonald, R. B., Richardson, R. J., and Henriques, C. M. (2019). Resident immunity in tissue repair and maintenance: the zebrafish model coming of age. *Front. Cell. Dev. Biol*. 7:12. doi: 10.3389/fcell.2019.00012

Mateos-Hernández, L., Villar, M., Moral, A., Rodríguez, C. G., Arias, T. A., de la Osa, V., et al. (2017). Tick-host conflict: immunoglobulin E antibodies to tick proteins in patients with anaphylaxis to tick bite. *Oncotarget* 8, 20630–20644. doi: 10.18632/oncotarget.15243

Mihara, M. (2017). Histopathologic study of the human skin in the early stage after a tick bite: a special reference to cutaneous tissue reaction to the cement substance of tick saliva. *Yonago Acta Med*. 60, 186–199. doi: 10.33160/yam.2017.09.009

Mingomataj, E. C., and Bakiri, A. H. (2012). Episodic hemorrhage during honeybee venom anaphylaxis: potential mechanisms. *J. Investig. Allergol. Clin. Immunol*. 22, 237–244.

Moura, A. P. V., Santos, L. C. B., Brito, C. R. N., Valencia, E., Junqueira, C., Filho, A. A. P., et al. (2017). Virus-like particle display of the α-Gal carbohydrate for vaccination against *Leishmania* infection. *ACS Cent Sci*. 3, 1026–1031. doi: 10.1021/acscentsci.7b00311

Oliveira, C. J., Sá-Nunes, A., Francischetti, I. M., Carregaro, V., Anatriello, E., Silva, J. S., et al. (2011). Deconstructing tick saliva: non-protein molecules with potent immunomodulatory properties. *J. Biol. Chem*. 286, 10960–10969. doi: 10.1074/jbc.M110.205047

Øverli, Ø., Nordgreen, J, Mejdell, C. M., Janczak, A. M., Kittilsen, S., Johansen, I. B., et al. (2014). Ectoparasitic sea lice (*Lepeophtheirus salmonis*) affect behavior and brain serotonergic activity in Atlantic salmon (*Salmo salar* L.): perspectives on animal welfare. *Physiol. Behav*. 132, 44–50. doi: 10.1016/j.physbeh.2014.04.031

Park, Y., Kim, D., Boorgula, G. D., De Schutter, K., Smagghe, G., Šimo, L., et al. (2020). Alpha-gal and cross-reactive carbohydrate determinants in the N-glycans of salivary glands in the lone star tick, *Amblyomma americanum*. *Vaccines* 8:E18. doi: 10.3390/vaccines8010018

Parmentier, H. K., De Vries Reilingh, G., and Lammers, A. (2008). Decreased specific antibody responses to alpha-Gal-conjugated antigen in animals with preexisting high levels of natural antibodies binding alpha-Gal residues. *Poult. Sci*. 87, 918–926. doi: 10.3382/ps.2007-00487

Perrin-Cocon, L., Aublin-Gex, A., Sestito, S. E., Shirey, K. A., Patel, M. C., André, P., et al. (2017). TLR4 antagonist FP7 inhibits LPS-induced cytokine production and glycolytic reprogramming in dendritic cells, and protects mice from lethal influenza infection. *Sci. Rep*. 7:40791. doi: 10.1038/srep40791

Platts-Mills, T. A., Schuyler, A. J., Tripathi, A., and Commins, S. P. (2015). Anaphylaxis to the carbohydrate side chain alpha-gal. *Immunol. Allergy Clin. North Am*. 35, 247–260. doi: 10.1016/j.iac.2015.01.009

Platts-Mills, T. A. E., Commins, S. P., Biedermann, T., et al. (2020). On the cause and consequences of IgE to galactose-α-1,3-galactose: a Report from the National Institute of Allergy and Infectious Disease Workshop on Understanding IgE-Mediated Mammalian Meat Allergy. *J. Allergy Clin. Immunol*. doi: 10.1016/j.jaci.2020.01.047. [Epub ahead of print].

Poole, N. M., Mamidanna, G., Smith, R. A., Coons, L. B., and Cole, J. A. (2013). Prostaglandin E2 in tick saliva regulates macrophage cell migration and cytokine profile. *Parasit. Vectors* 6:261. doi: 10.1186/1756-3305-6-261

Portillo, S., Zepeda, B. G., Iniguez, E., Olivas, J. J., Karimi, N. H., Moreira, O. C., et al. (2019). A prophylactic α-Gal-based glycovaccine effectively protects against murine acute Chagas disease. *NPJ Vaccines* 4:13. doi: 10.1038/s41541-019-0107-7

Ririe, K. M., Rasmussen, R. P., and Wittwer, C. T. (1997). Product differentiation by analysis of DNA melting curves during the polymerase chain reaction. *Anal. Biochem*. 245, 154–160.

Romagnani, S. (1999). Th1/Th2 cells. *Inflamm. Bowel Dis*. 5, 285–294.

Román-Carrasco, P., Lieder, B., Somoza, V., Ponce, M., Szépfalusi, Z., Martin, D., et al. (2019). Only aGal bound to lipids, but not to proteins, is transported across enterocytes as an IgE reactive molecule that can induce effector cell activation. *Allergy* 74, 1956–1968. doi: 10.1111/all.13873

Rosadini, C. V., and Kagan, J. C. (2015). Microbial strategies for antagonizing Toll-like-Receptor signal transduction. *Curr. Opin. Immunol*. 32, 61–70. doi: 10.1016/j.coi.2014.12.011

Schartl, M. (2014). Beyond the zebrafish: diverse fish species for modeling human disease. *Dis. Model. Mech*. 7, 181–192. doi: 10.1242/dmm.012245

Steinke, J. W., Platts-Mills, T. A., and Commins, S. P. (2015). The alpha-gal story: lessons learned from connecting the dots. *J. Allergy Clin. Immunol*. 135, 589–596. doi: 10.1016/j.jaci.2014.12.1947

Stringer, T., Ghazi, E., Alvarez Del Manzano, G., Beasley, J., Brinster, N., and Oza, V. S. (2017). Tick bite mimicking indeterminate cell histiocytosis. *Pediatr. Dermatol*. 34, e347–e348. doi: 10.1111/pde.13291

Stutzer, C., Richards, S. A., Ferreira, M., Baron, S., and Maritz-Olivier, C. (2018). Metazoan parasite vaccines: present status and future prospects. *Front. Cell. Infect. Microbiol*. 8:67. doi: 10.3389/fcimb.2018.00067

Tabakawa, Y., Ohta, T., Yoshikawa, S., Robinson, E. J., Yamaji, K., Ishiwata, K., et al. (2018). Histamine released from skin-infiltrating basophils but not mast cells is crucial for acquired tick resistance in mice. *Front. Immunol*. 9:1540. doi: 10.3389/fimmu.2018.01540

Uspensky, I. (2014). Tick pests and vectors (Acari: Ixodoidea) in European towns: introduction, persistence and management. *Ticks Tick Borne Dis*. 5, 41–47. doi: 10.1016/j.ttbdis.2013.07.011

Valls, A., Pineda, F., Belver, M., Caballero, T., and López Serrano, M. C. (2007). Anaphylactic shock caused by tick (*Rhipicephalus sanguineous*). *J. Investig. Allergol. Clin. Immunol*. 17, 279–280.

Van Nunen, S. A., O'Connor, K. S., Clarke, L. R., Boyle, R. X., and Fernando, S. L. (2009). An association between tick bite reactions and red meat allergy in humans. *Med. J. Aust*. 190:510–511. doi: 10.5694/j.1326-5377.2009.tb02533.x

Wilson, J. M., Schuyler, A. J., Schroeder, N., and Platts-Mills, T. A. (2017). Galactose-α-1,3-Galactose: atypical food allergen or model IgE hypersensitivity? *Curr. Allergy Asthma Rep*. 17:8. doi: 10.1007/s11882-017-0672-7

Yilmaz, B., Portugal, S., Tran, T. M., Gozzelino, R., Ramos, S., Gomes, J., et al. (2014). Gut microbiota elicits a protective immune response against malaria transmission. *Cell* 159, 1277–1289. doi: 10.1016/j.cell.2014.10.053

Yucel, E., Sipahi Cimen, S., Varol, S., Suleyman, A., Ozdemir, C., and Tamay, Z. U. (2019). Red-meat desensitization in a child with delayed anaphylaxis due to alpha-Gal allergy. *Pediatr. Allergy Immunol*. 30, 771–773. doi: 10.1111/pai.13092

Conflict of Interest: The authors declare that the research was conducted in the absence of any commercial or financial relationships that could be construed as a potential conflict of interest.

frontiers in Cellular and Infection Microbiology

BRIEF RESEARCH REPORT
published: 28 April 2020
doi: 10.3389/fcimb.2020.00172

Utilization of RNA *in situ* Hybridization to Understand the Cellular Localization of Powassan Virus RNA at the Tick-Virus-Host Interface

Meghan E. Hermance [1,2,3] *and Saravanan Thangamani* [1,2,3]*

[1] SUNY Center for Environmental Health and Medicine, SUNY Upstate Medical University, Syracuse, NY, United States,
[2] Institute for Global Health and Translational Science, SUNY Upstate Medical University, Syracuse, NY, United States,
[3] Department of Microbiology and Immunology, SUNY Upstate Medical University, Syracuse, NY, United States

Skin is the interface between an attached, feeding tick and a host; consequently, it is the first line of defense against invading pathogenic microorganisms that are delivered to a vertebrate host together with tick saliva. Central to the successful transmission of a tick-borne pathogen are complex interactions between the host immune response and early tick-mediated immunomodulation, all of which initially occur at the skin interface. The focus of this work was to demonstrate the use of RNA *in situ* hybridization (RNA ISH) as a tool for understanding the cellular localization of viral RNA at the feeding site of Powassan virus (POWV)-infected *Ixodes scapularis* ticks. Intense positive staining for POWV RNA was frequently detected in dermal foci and occasionally detected in hypodermal foci after 24 h of POWV-infected tick feeding. Additionally, duplex chromogenic RNA ISH staining demonstrated co-localization of POWV RNA with *Mus musculus* F4/80 RNA, CD11c RNA, vimentin RNA, Krt14 RNA, and CD3ε RNA at the feeding site of POWV-infected ticks. In future studies, RNA ISH can be used to validate transcriptomic analyses conducted at the tick-virus-host cutaneous interface and will provide cellular resolution for specific gene signatures temporally expressed during infected tick feeding. Such a systems biology approach will help create a more refined understanding of the cellular and molecular interactions influencing virus transmission at the cutaneous interface.

Keywords: Powassan virus, tick-virus-host interface, skin, RNA *in situ* hybridization, tick feeding

OPEN ACCESS

Edited by:
Eric Calvo,
National Institutes of Health (NIH),
United States

Reviewed by:
Jeff Grabowski,
Rocky Mountain Laboratories (NIAID),
United States
Travis Bourret,
Creighton University, United States

***Correspondence:**
Saravanan Thangamani
thangams@upstate.edu

Specialty section:
This article was submitted to Parasite and Host, a section of the journal Frontiers in Cellular and Infection Microbiology

Received: *28 January 2020*
Accepted: *31 March 2020*
Published: *28 April 2020*

Citation:
Hermance ME and Thangamani S (2020) Utilization of RNA in situ Hybridization to Understand the Cellular Localization of Powassan Virus RNA at the Tick-Virus-Host Interface. Front. Cell. Infect. Microbiol. 10:172. doi: 10.3389/fcimb.2020.00172

INTRODUCTION

Mammalian skin serves as a mechanical and immunological barrier to protect the host from injury and infection (Pasparakis et al., 2014). This complex organ consists of an intricate network of epithelial cells, stromal cells, resident immune cells, migratory immune cells, blood and lymphatic vessels, peripheral nerves, and soluble mediators of the immune response (Wikel, 2013; Pasparakis et al., 2014; Nguyen and Soulika, 2019). Ticks are obligate blood-feeding ectoparasites of vertebrates and they require a blood meal at every active life stage. To acquire its necessary blood meal, an ixodid tick must remain attached to the skin of a vertebrate host and complete its multi-day feeding process without being deterred by the complex and redundant host cutaneous defense mechanisms.

Successful tick feeding is enabled by the complex repertoire of bioactive factors in tick saliva, which can modulate host hemostasis, pain and itch responses, wound healing, and innate and adaptive immunity (Ribeiro et al., 2006; Kazimírová et al., 2017; Hermance and Thangamani, 2018; Wikel, 2018). Tick saliva is composed is of hundreds of proteins and short non-coding regulatory RNAs that are differentially expressed throughout the process of tick feeding (Ribeiro et al., 2006; Chmelar et al., 2016; Hermance et al., 2019). Studies have demonstrated that a variety of tick salivary proteins, as well as some non-proteinaceous molecules, can modulate the cutaneous immune defenses of the host (Ribeiro et al., 2006; Oliveira et al., 2011; Kazimírová et al., 2017).

Skin is the first mammalian organ that a tick-borne pathogen and tick salivary factors encounter during their journey from the infected tick salivary glands to the host. With respect to several tick-borne flaviviruses (TBFVs), an infected *Ixodes* species tick can transmit virus to the host on which it feeds in as little as a few minutes to several hours of feeding (Alekseev et al., 1996; Ebel and Kramer, 2004; Hermance and Thangamani, 2018). The rapid transmission of a TBFV from tick salivary glands to host underscores the importance of investigating the initial immunomodulatory events that occur at the cutaneous interface where a tick first delivers virus. *In vivo* models (infected ticks fed on small mammals) are valuable tools for studying the early host immune response to infected tick feeding. Using such models, transcriptional profiling and histopathological analyses conducted at the tick feeding site comprehensively illustrate how TBFV-infected tick feeding temporally influences the host cutaneous immune response. Comparative transcriptional analyses of TBFV-infected vs. uninfected tick feeding sites reveal significant up-regulation of transcripts related to the recruitment, migration, and accumulation of immune cells after the first 1–3 h of infected tick feeding (Hermance and Thangamani, 2014; Thangamani et al., 2017). Early cutaneous changes at the *in vivo* flavivirus-tick-host interface have been further illuminated with histopathological analyses. Until recently, these analyses have relied on immunohistochemical detection of viral antigen and specific cell markers at the tick feeding site. Specifically, Powassan virus (POWV) antigen was detected in fibroblasts and macrophages via immunofluorescence (Hermance et al., 2016), and Tick-borne encephalitis virus (TBEV) antigen was detected in fibroblasts and mononuclear phagocytes via immunohistochemistry (Thangamani et al., 2017). The present work is the first to demonstrate use of RNA *in situ* hybridization (RNA ISH) for precise localization of *Mus musculus*-specific F4/80, CD11c, vimentin, keratin 14, CD3ε, and CD49b RNAs at the tick feeding site, and to detect the distribution of POWV RNA at the skin site of POWV-infected *Ixodes scapularis* feeding. Simultaneous visualization POWV RNA with *Mus musculus*-specific mRNA targets is also demonstrated. Ultimately, a systems biology approach enables analyses of the complex interplay between tick-host-virus at the skin interface, and RNA ISH can be incorporated as a tool to visualize and validate cellular and molecular interactions occurring within the infected tick feeding site.

METHODS

Cells and Viruses

African green monkey kidney (VeroE6) cells were purchased from the American Type Culture Collection (ATCC) and maintained in culture with Modified Eagle's Medium (MEM) supplemented with 10% fetal bovine serum (FBS), 1% non-essential amino acids, and a 1% antibiotic mixture of penicillin/streptomycin incubated at 37°C with 5% CO_2. The World Reference Center for Emerging Viruses and Arboviruses at UTMB provided stock of the POWV (LB strain), which had previously been passaged 7 times in suckling mice brains. The stock was then passaged 5 times on VeroE6 cells. Stock virus titers were determined by focus-forming immunoassay as described previously (Rossi et al., 2012). Next Generation Sequencing demonstrated that the consensus nucleotide sequence of the POWV genome was 99.98% identical to the POWV LB strain. Two nucleotide sequence differences were observed between our POWV stock and that of the POWV LB strain (NCBI Reference Sequence: NC_003687.1), which resulted in the following amino acid sequence difference in: E (Q442R).

Synchronous Infection of Ticks

POWV-infected *I. scapularis* nymphs were generated in the laboratory via synchronous infection, a technique that has been previously validated in our laboratory for virus infection of *I. scapularis* nymphs (Hermance and Thangamani, 2014; Hermance et al., 2016). Three days prior to synchronous infection, uninfected *I. scapularis* nymphs were stored in a 26°C environmental chamber at ∼60% relative humidity for dehydration and desiccation. Ticks were then submerged in 1.5×10^7 FFU/mL of POWV LB strain at 34°C for 45 min with gentle mixing every 10 min. Ticks were mock-infected in the same manner with DMEM media. Infected and mock-infected ticks were washed two times with sterile PBS and then dried of excess moisture using sterile filter paper. All ticks were transferred to glass vials and stored inside a desiccator for 4 weeks at 26°C and ∼90% relative humidity to allow extrinsic incubation of POWV.

Tick Infestation on Mice

Four weeks after synchronous infection, ticks were infested on mice as previously described (Hermance and Thangamani, 2014; Hermance et al., 2016). Briefly, tick containment capsules were fashioned from 2 mL cryotubes by cutting off the base of the tube, leaving approximately 5 mm of remaining tube and the screw cap lid intact. Tensoplast athletic tape (BSN Medical) was fitted around the perimeter of the base of the tube with approximately 1 cm of tape width around the edge of the capsule. Holes were punctured in the lid of the capsule with a 28-gauge needle to enable air-flow within the capsule during tick feeding. Mice were anesthetized with isoflurane for the capsule attachment process. The dorsum and lateral sides of each mouse was shaved with a size 40 electric razor blade. Livestock Tag Cement (Nasco) was applied to the adhesive side of the 1 cm athletic tape that was fitted around the edge of the capsule, and school glue was applied

in a ring along the inner base of the capsule. Capsules were adhered to the center of the mouse dorsum 1 day prior to tick infestation. Capsule integrity was checked before and during the tick infestations.

One day after capsule attachment, a single *I. scapularis* nymph was placed inside each capsule. The screw-cap capsule lids were secured with a thin piece of masking tape. Ticks were fed on mice for 24 h. At 24 h after tick attachment (hours post-infection, hpi), mice were euthanized by CO_2 inhalation followed by cervical dislocation. Immediately following euthanasia, 4 mm skin punch biopsies were harvested, including the attached ticks.

Histology and RNA *in situ* Hybridization

Each skin plus tick biopsy was formalin-fixed for a minimum of 48 h in 10% neutral buffered formalin at room temperature. Tick legs were snipped prior to fixation to expedite formalin penetration into the tick body cavity. The biopsy samples were treated with Decal (StatLab) for 2 h at room temperature, thoroughly washed with DI water, and returned to formalin. The biopsies were then dehydrated with a standard ethanol series followed by xylene. Paraffin embedding of each biopsy was performed at an orientation that, upon sectioning, would produce a cross-section of the mouse skin and a longitudinal section of the tick mouthparts and body (Hermance et al., 2016). Formalin-fixed paraffin-embedded (FFPE) biopsies were sectioned at 5 µm thickness and sections were mounted on Superfrost Plus slides (Fisher Scientific). Slides were dried at 34°C for 48 h and then stored at room temperature in plastic bags with desiccants.

RNA ISH was performed with the RNAscope™ platform (Advanced Cell Diagnostics), including the RNAscope 2.5 Duplex reagent kit, RNAscope probes, and the RNAscope HybEZ hybridization system. RNA ISH was performed manually with a RNAscope 2.5 HD duplex chromogenic assay (Advanced Cell Diagnostics) in accordance with the manufacturer's recommendations for FFPE tissue. The FFPE tissue sections were incubated at 60°C for 1 h and deparaffinized in xylene. Endogenous peroxidases were quenched with H_2O_2 for 10 min at room temperature. Pretreatment times of the tissue sections were optimized so the delicate skin and brittle tick tissue would not lift off the slide during boiling or be damaged during protease digestion; therefore, slides underwent target retrieval for 15 min in RNAscope Target Retrieval Reagent at 98°C. Slides were then incubated for 15 min in RNAscope Protease Plus reagent at 40°C with constant humidity and temperature maintained by the RNAscope HybEZ hybridization system. RNA probes hybridizing to POWV positive-sense RNA (ACD Cat. # 415641),

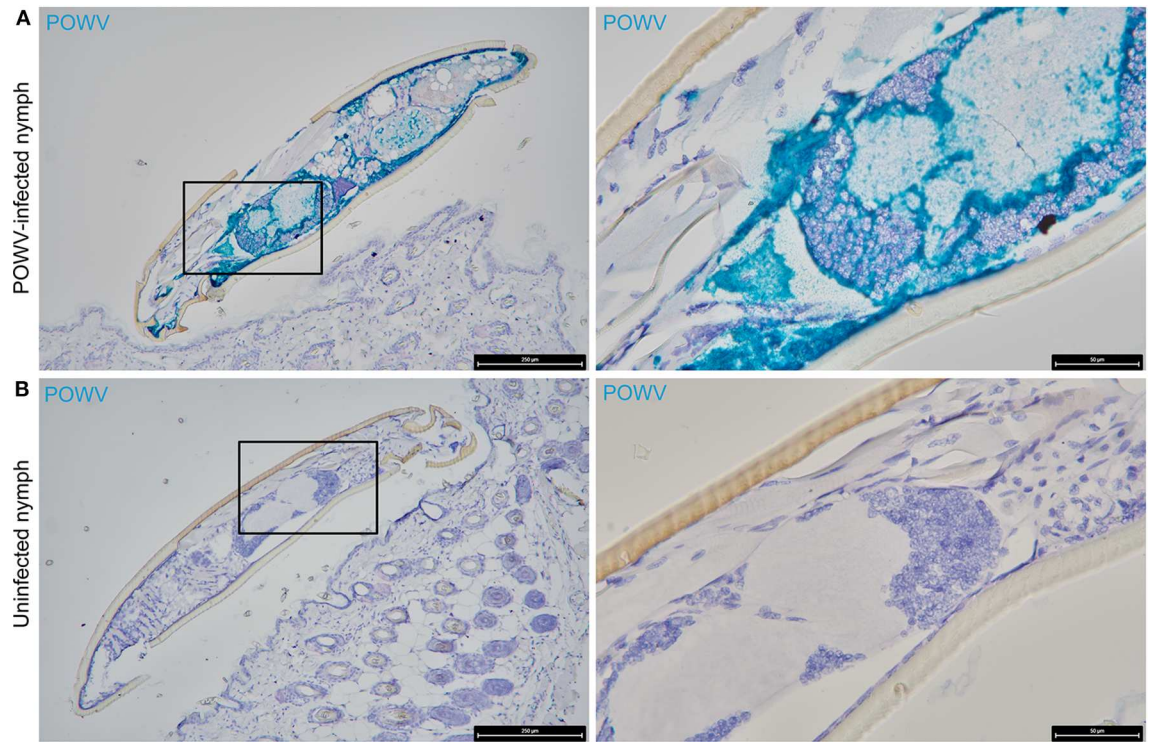

FIGURE 1 | Distribution of POWV RNA in the POWV-infected *Ixodes scapularis* nymph body. **(A)** POWV-infected *I. scapularis* nymph feeding on *M. musculus* skin for 6 h. **(B)** Mock-infected *I. scapularis* nymph feeding on *M. musculus* skin for 6 h. POWV RNA is detected with HRP-based green chromogen and *M. musculus* F4/80 RNA is detected with AP-based red chromogen. For rows **(A,B)**, magnification is x10 and x40 from left to right. Black boxes on the left image panels indicate magnified regions shown in the right panels.

Mus musculus F4/80 RNA (Cat. # 460651-C2), *M. musculus* CD11c RNA (Cat. # 311501-C2), *M. musculus* vimentin RNA (Cat. # 457961-C2), *M. musculus* keratin 14 RNA (Cat. # 422521-C2), *M. musculus* CD3ε RNA (Cat. # 314721-C2), *M. musculus* CD49b RNA (Cat. # 441081-C2), positive control *M. musculus* ubiquitin C (Ubc) RNA (Cat. # 310771), positive control *M. musculus* Polr2a RNA (Cat. # 312471-C2), and positive control *M. musculus* Ppib RNA (Cat. # 321651) were hybridized to the tissues for 2 h at 40°C. All remaining steps of signal amplification and detection were conducted as recommended by the RNAscope 2.5 HD duplex detection kit user manual. Horseradish peroxidase (HRP)-based green and alkaline phosphatase (AP)-based red chromogenic substrates were used for signal detection. Slides were counterstained with Gill's Hematoxylin I (diluted 1:1 in DI water) for 30 s, briefly washed in tap water, air dried for 45 min at 60°C, and cover-slipped using VectaMount (Vector Laboratories) reagent. Tissue sections were examined under a standard light microscope.

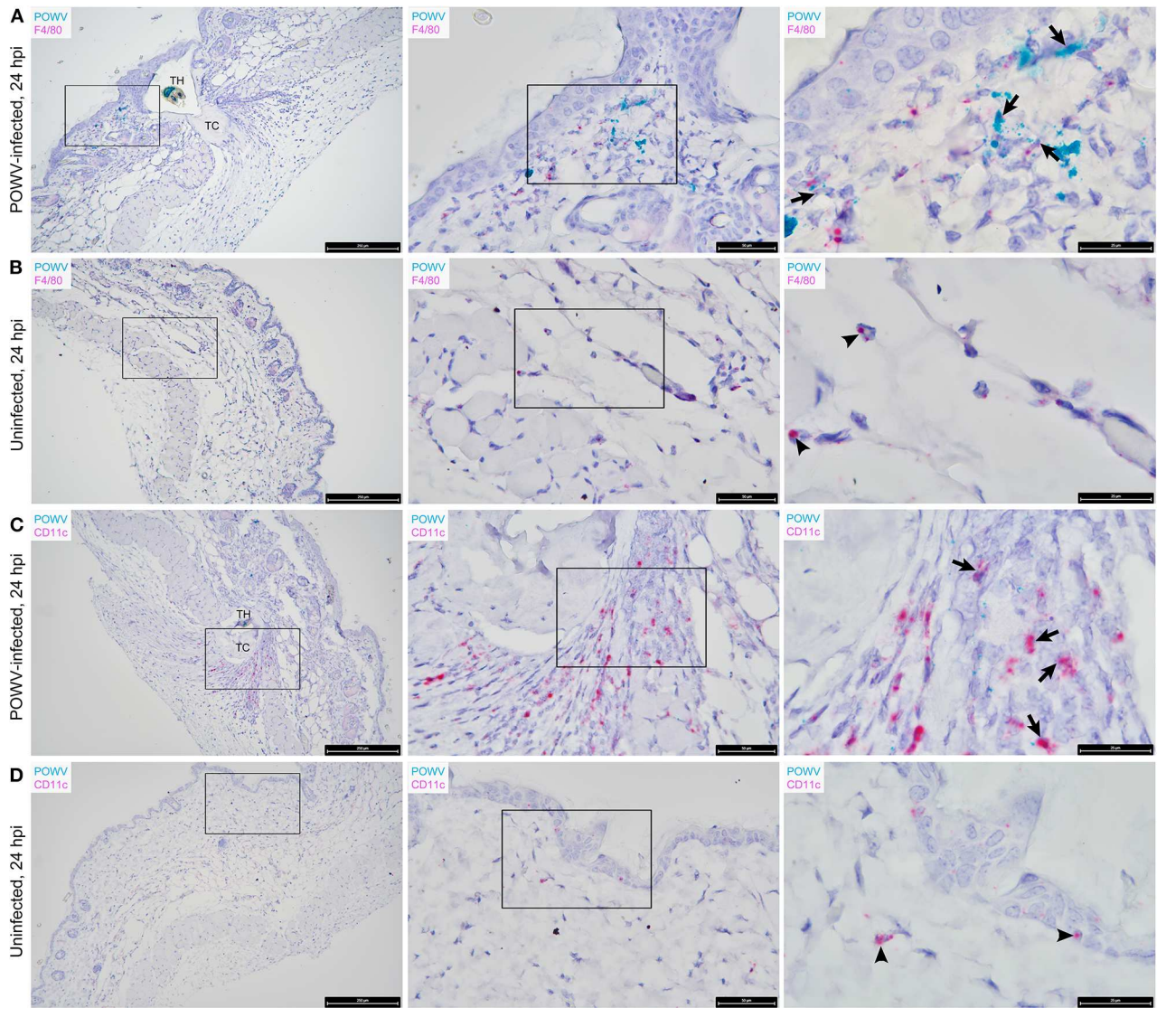

FIGURE 2 | Distribution of POWV RNA, *Mus musculus* F4/80 RNA, and *M. musculus* CD11c RNA in the *Ixodes scapularis* nymph feeding site at 24 h post-tick attachment. **(A)** POWV-infected nymph feeding site showing POWV RNA (green signal) and *M. musculus* F4/80 RNA (red signal). Arrows indicate cells with co-localization of both RNA targets. **(B)** Mock-infected nymph feeding site with only *M. musculus* F4/80 RNA (red signal) detected. Arrowheads indicate cells with positive F4/80 RNA signal. **(C)** POWV-infected nymph feeding site showing POWV RNA (green signal) and *M. musculus* CD11c RNA (red signal). Arrows indicate cells with co-localization of both RNA targets. **(D)** Mock-infected nymph feeding site with only *M. musculus* CD11c RNA (red signal) detected. Arrowheads indicate cells with positive CD11c RNA signal. For rows **(A–D)**, magnification is x10, x40, x100 from left to right. Each black box indicates the magnified region shown in the adjacent right panel. TH, tick hypostome; TC, tick cement.

RESULTS AND DISCUSSION

The RNAscope™ platform (Advanced Cell Diagnostics) used in this study reveals positive RNA signals as punctate staining, and previous work demonstrated that each punctate dot represents a single mRNA transcript (Wang et al., 2012). Probes targeting the endogenous *M. musculus* housekeeping genes, ubiquitin C (Ubc), Ppib, and Polr2a, were used as positive controls to assess mouse skin biopsies with attached ticks for RNA integrity and to serve as technical assay controls for the RNA ISH procedures. Endogenously expressed Ubc RNA was detected with HRP-based green chromogen in a punctate staining pattern and was moderately to highly expressed (>20 transcript copies per cell) in many *M. musculus* skin cells (**Figure S1A**). The Polr2a probe was used as a rigorous positive control for low copy mRNA (1–5 transcript copies per cell). Polr2a signal was detected with AP-based red chromogen, and as expected, was lowly expressed in *M. musculus* skin (**Figures S1A,B**). The Ppib housekeeping gene was used as a positive control for moderately expressed RNA targets (6–20 transcript copies per cell) (**Figure S1B**). The attached *I. scapularis* tick body in these tissue sections served as an internal negative control because the *M. musculus* Ubc, Polr2a,

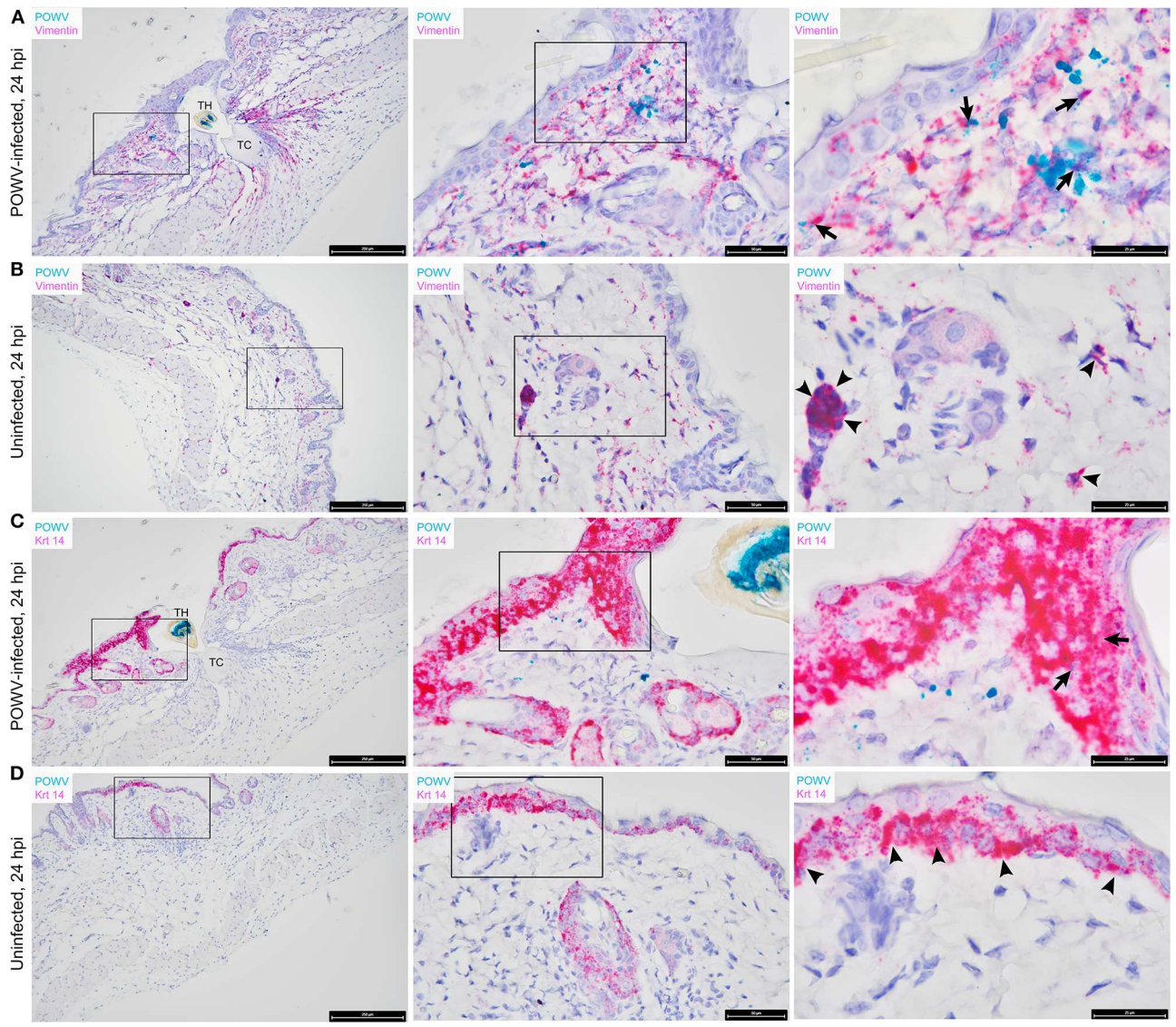

FIGURE 3 | Distribution of POWV RNA, *Mus musculus* vimentin RNA, and *M. musculus* keratin 14 (Krt 14) RNA in the *Ixodes scapularis* nymph feeding site at 24 h post-tick attachment. **(A)** POWV-infected nymph feeding site showing POWV RNA (green signal) and *M. musculus* vimentin RNA (red signal). Arrows indicate cells with co-localization of both RNA targets. **(B)** Mock-infected nymph feeding site with only *M. musculus* vimentin RNA (red signal) detected. Arrowheads indicate cells with positive vimentin RNA signal. **(C)** POWV-infected nymph feeding site showing POWV RNA (green signal) and *M. musculus* Krt 14 RNA (red signal). Arrows indicate cells with co-localization of both RNA targets. **(D)** Mock-infected nymph feeding site with only *M. musculus* Krt 14 RNA (red signal) detected. Arrowheads indicate cells with positive Krt 14 RNA signal. For rows **(A–D)**, magnification is x10, x40, x100 from left to right. Each black box indicates the magnified region shown in the adjacent right panel. TH, tick hypostome; TC, tick cement.

and Ppib probes did not bind to the tick tissue and only bound to the *M. musculus* skin, demonstrating probe specificity.

POWV RNA was detected via HRP-based green chromogen in the cross-section of POWV-infected *I. scapularis* nymphs but not in mock-infected nymphs (**Figure 1**). In the cross-sections of mock-infected nymphs, only the hematoxylin counterstain was visible (**Figure 1B**). In addition to the POWV RNA probe, the *M. musculus* F4/80 RNA probe was simultaneously hybridized to these skin plus nymph tissue sections, and duplex chromogenic detection of RNA targets was performed. No F4/80 RNA signal was detected via AP-based red chromogen in the tick bodies, demonstrating target-specificity of the *M. musculus* F4/80 RNA probe.

The main focus of this work was to demonstrate the use of RNA ISH technology as a tool for detecting the distribution of POWV RNA at the cutaneous feeding site of an infected tick while identifying co-localization of the POWV RNA signal with secondary mammalian-specific RNA targets of interest. In this study, POWV RNA was routinely detected with HRP-based green chromogen at the feeding site of POWV-infected *I. scapularis* nymphs that were fed on mice for 24 h (**Figures 2–4**). Intense viral RNA staining was often focally detected in the

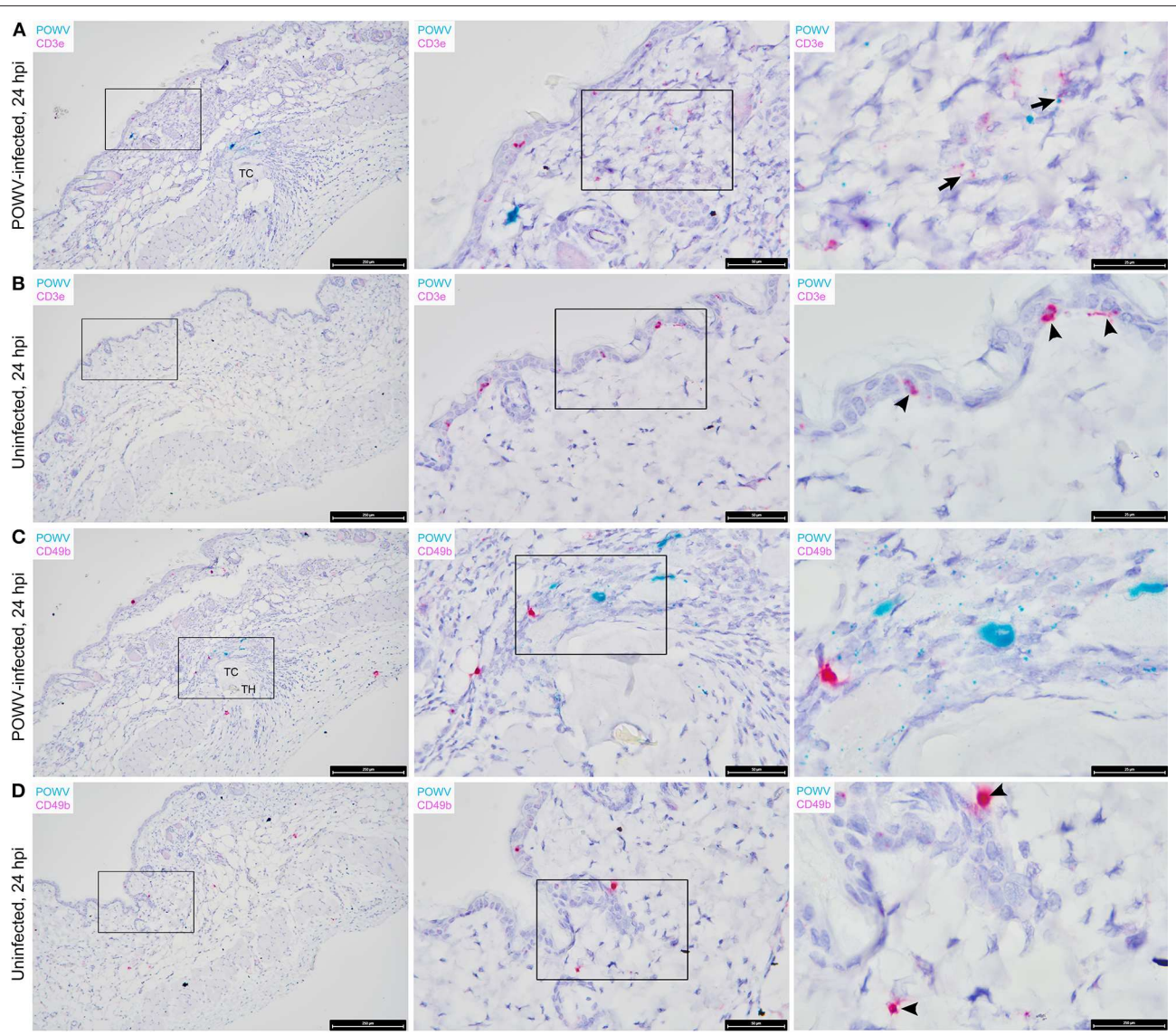

FIGURE 4 | Distribution of POWV RNA, *Mus musculus* CD3ε RNA, and *M. musculus* CD49b RNA in the *Ixodes scapularis* nymph feeding site at 24 h post-tick attachment. **(A)** POWV-infected nymph feeding site showing POWV RNA (green signal) and *M. musculus* CD3ε RNA (red signal). Arrows indicate cells with co-localization of both RNA targets. **(B)** Mock-infected nymph feeding site with only *M. musculus* CD3ε RNA (red signal) detected. Arrowheads indicate cells with positive CD3ε RNA signal. **(C)** POWV-infected nymph feeding site showing POWV RNA (green signal) and *M. musculus* CD49b (red signal). No arrows are present because POWV RNA and CD49b RNA signals did not co-localize in this tick feeding site. **(D)** Mock-infected nymph feeding site with only *M. musculus* CD49b (red signal) detected. Arrowheads indicate cells with positive CD3ε RNA signal. For rows **(A–D)**, magnification is x10, x40, x100 from left to right. Each black box indicates the magnified region shown in the adjacent right panel. TH, tick hypostome; TC, tick cement.

dermis (**Figures 2A,C**, **3A,C**, **4A,C**), and in some sections, intense POWV RNA signal was also detected in hypodermal foci (**Figures 4A,C**). Positive staining for POWV RNA in the epidermis was less common and weaker overall than the POWV RNA signals in the dermis (**Figures 2A**, **3A,C**). The epidermis is the thinnest layer of murine skin, and nymphal tick mouthparts penetrate well-beyond the epidermis, reaching the dermal, and hypodermal layers of skin; therefore, it is not surprising that we detected less POWV RNA in the epidermis than the dermis. For skin cross-sections that include portions of POWV-infected tick mouthparts, POWV RNA was frequently identified within the bounds of the tick mouthparts (**Figures 2A,C**, **3A,C**).

We previously used the F4/80 antigen as an immunohistochemical marker for macrophages at the skin feeding site of POWV-infected ticks and demonstrated that macrophages contained POWV antigen (Hermance et al., 2016). In this study, we sought to detect F4/80 transcript expression within tissue context during POWV-infected tick feeding. POWV RNA and *M. musculus* F4/80 RNA probes were hybridized to the POWV-infected and mock-infected *I. scapularis* nymph feeding sites (**Figures 2A,B**). F4/80 RNA was detected with AP-based red chromogen in both the POWV-infected and mock-infected nymph feeding sites, and the F4/80 RNA signal was scattered throughout the dermis and hypodermis of these sections. Additionally, in the POWV-infected nymph feeding site, multiple F4/80-positive RNA signals were detected in the hypodermis and sub-muscular layer adjacent to the tick cement deposits and were likely expressed by the mononuclear cells infiltrating the tick feeding site (**Figure 2A**). Co-localization of POWV RNA with F4/80 RNA was detected in in the dermis of the POWV-infected tick feeding site (**Figure 2A**); however, as expected, co-localization of POWV and F4/80 RNA signals was not detected in the mock-infected tick feeding site (**Figure 2B**).

The distribution of POWV RNA and *M. musculus* CD11c RNA in the tick feeding sites was detected via HRP-based green chromogen and AP-based red chromogen, respectively (**Figures 2C,D**). CD11c RNA signals were detected in the epidermis, dermis, hypodermis, and sub-muscular layer of the *I. scapularis* feeding sites. Epidermal cells with CD11c-positive RNA signal are likely Langerhans cells, which are the main dendritic cell subpopulation in the epidermis (Kazimírová et al., 2017). In the present study, cells in which POWV RNA co-localized with CD11c RNA were located in the hypodermal and sub-muscular regions adjacent to the cement deposited by the feeding POWV-infected nymph (**Figure 2C**). These compartments of the skin included multiple cells with CD11c-positive RNA signal, which can likely be attributed to mononuclear phagocyte infiltrates recruited to the *I. scapularis* feeding site. Although we did not detect co-localization of POWV RNA with CD11c RNA in epidermal cells, our findings do not preclude Langerhans cells as putative cell targets of POWV infection at the tick feeding site. A previous study detected TBEV antigen in Langerhans cells emigrating from skin explants harvested at the feeding site of TBEV-infected ticks, suggesting that Langerhans cells are early cutaneous cell targets of TBEV infection and that they serve as vehicles for virus dissemination to skin-draining lymph nodes (Labuda et al., 1996). Furthermore, Langerhans cell migration to draining lymph nodes has been demonstrated in response to cutaneous infection with live West Nile virus (Johnston et al., 2000). Therefore, it is possible that some of the hypodermal and sub-muscular cells in this study that displayed co-localized POWV and CD11c RNA signals were Langerhans cells or dermal dendritic cells migrating from the tick feeding site to the lymphatic system.

Vimentin transcript expression was characterized *in situ* in the presence of POWV-infected vs. uninfected *I. scapularis* nymph feeding. *M. musculus* vimentin RNA was detected throughout the epidermis, dermis, hypodermis, and sub-muscular layers of the skin (**Figures 3A,B**). The vimentin gene encodes a type III intermediate filament protein which participates in numerous cellular functions, including cell adhesion, migration, differentiation, cytoskeletal rearrangements, and wound healing (Cheng et al., 2016). The most intense staining for vimentin RNA was detected near the feeding lesion of the tick where the tissue architecture, including the sub-muscular layer, had the appearance of streaming toward the tick mouthparts (**Figures 3A,B**). Previous studies conducted at the 24-h feeding site of uninfected and POWV-infected *I. scapularis* nymphs demonstrated upregulated gene ontology clusters related to cytoskeletal arrangements and histopathological changes related to wound healing (Heinze et al., 2012; Hermance et al., 2016); therefore, increased vimentin transcript expression in sites adjacent to the tick feeding lesion after 24 h of tick feeding was anticipated in these samples. Furthermore, RNA ISH revealed co-localization of POWV RNA with vimentin RNA (**Figure 3A**), supporting previous immunohistochemical

TABLE 1 | Summary of RNA ISH findings at the POWV-infected *Ixodes scapularis* nymph feeding site.

***M. musculus* target transcript**	**Location of target transcript in the skin**	***M. musculus* cells expressing this target transcript**	**Co-localization of target transcript with POWV RNA?**
F4/80	Dermis, hypodermis, sub-muscular layer	Macrophages, monocytes	Yes
CD11c	Epidermis, dermis, hypodermis, sub-muscular layer	Dendritic cells, Langerhans cells, macrophages, NK cells	Yes
Vimentin	Epidermis, dermis, hypodermis, sub-muscular layer	Mesenchymal cells	Yes
Keratin 14	Epidermis, hair follicles	Keratinocytes	Yes
CD3ε	Epidermis, dermis	T cells	Yes
CD49b	Epidermis, dermis, hypodermis, sub-muscular layer	Lymphocytes	No

findings where POWV and vimentin antigens co-localized at the POWV-infected tick feeding site (Hermance et al., 2016).

The distribution of *M. musculus* Keratin 14 (Krt14) RNA was characterized at the tick feeding site via RNA ISH. Krt14 is expressed in the basal layer of the epidermis and in hair follicles, and it is a prototypic marker of proliferative basal keratinocytes (Coulombe et al., 1989; Alam et al., 2011; Wang et al., 2016). The mouse skin biopsies included in this study displayed Krt14-positive RNA signals in the epidermis and hair follicles (**Figures 3C,D**). Here, several punctate dots of POWV RNA signal co-localized with Krt14 RNA in the epidermis of the POWV-infected tick feeding site (**Figure 3C**). This suggests that keratinocytes are early cutaneous cell targets of POWV infection at the tick feeding site. Previous reports have implicated keratinocytes as initial cell targets of flavivirus infection *in vivo*, which supports our findings (Labuda et al., 1996; Lim et al., 2011; Hamel et al., 2015). Additionally, *M. musculus* CD3ε RNA and CD49b RNA were also detected in the POWV-infected and mock-infected nymph feeding sites (**Figure 4**). The CD3ε-positive RNA staining was detected focally in the epidermis and dermis (**Figures 4A,B**), while foci of CD49b RNA were identified in all layers of the skin biopsies taken at the tick feeding sites (**Figures 4C,D**). POWV RNA co-localized with CD3ε RNA but not with CD49b RNA at the 24-h feeding site of the POWV-infected *I. scapularis* nymph (**Figure 4A**).

Identification of mammalian immune cells that are early targets of TBFV infection at the cutaneous interface contributes to our overall understanding of virus pathogenesis in the mammalian host. The present study adds knowledge to this realm via RNA ISH detection of POWV RNA and mammalian-specific RNAs at the tick feeding site, and the findings are summarized in **Table 1**. Although co-localization of POWV RNA and mammalian RNA targets suggests that a cell is infected with POWV, this does not confirm whether viral proteins co-localize with the mammal-specific protein or that the mammalian-specific transcript is involved in the lifecycle of POWV. A limitation of this study is that the RNA signals were not quantified. The development of a digital analysis program that could quantify individual RNA signals, as well as the relative degree of signal co-localization between two transcripts, would be an asset for future studies of this nature. Furthermore, this study detected POWV lineage I RNA at the feeding site of *I. scapularis* nymphs; however, results could vary for ticks infected with POWV lineage II, otherwise known as deer tick virus. Viral RNA distribution patterns at the cutaneous feeding site of a deer tick virus-infected tick could be different from that of a POWV-infected tick. Future studies investigating differences in the viral RNA distribution between both virus genotypes would be beneficial.

CONCLUSION

In summary, the present study is the first to demonstrate the use of RNA ISH technology for precise cellular localization of viral RNA at the tick feeding site. This technology can be applied to studies with other vector-borne pathogens to investigate cellular localization of pathogen RNA and the potential immune responses occurring at the vector-pathogen-host interface. Here, we detected the distribution of POWV RNA at the feeding site of POWV-infected *I. scapularis* nymphs and detected co-localization of POWV RNA with *M. musculus* F4/80 RNA, CD11c RNA, vimentin RNA, Krt14 RNA, and CD3ε RNA. In future studies, RNA ISH can serve as a validation tool for transcriptomic analyses investigating the host cutaneous immune response during infected tick feeding. This technology will also enable us to map specific gene expression signals to individual cells or compartments within the infected tick feeding site. Using RNA ISH to acquire cellular resolution for specific gene expression patterns will improve our understanding of the cellular and molecular interactions occurring at the tick-virus-host interface.

DATA AVAILABILITY STATEMENT

All datasets generated for this study are included in the article/**Supplementary Material**.

ETHICS STATEMENT

All experiments involving mice were conducted in arthropod containment biosafety level 3 (ACL-3) facilities in strict accordance with an animal use protocol approved by the University of Texas Medical Branch (UTMB) Institutional Animal Care and Use Committee (IACUC: # 0907054).

AUTHOR CONTRIBUTIONS

MH and ST designed the experiments and analyzed the data. ST provided reagents and materials, and critically read and revised the manuscript. MH performed the experiments and drafted the manuscript.

FUNDING

This study described in this manuscript was funded by grant to ST from the National Institutes of Health, R01AI127771.

ACKNOWLEDGMENTS

The authors would like to acknowledge Ms. Nicole Hausser for her help with tick colony maintenance.

SUPPLEMENTARY MATERIAL

The Supplementary Material for this article can be found online at: https://www.frontiersin.org/articles/10.3389/fcimb.2020.00172/full#supplementary-material

Figure S1 | Positive controls for RNA ISH of skin sections. **(A)** *I. scapularis* nymph feeding site where *M. musculus* ubiquitin (Ubc) RNA is detected with an HRP-based green chromogen and Polr2a RNA is detected with an AP-based red signal. **(B)** *I. scapularis* nymph feeding site where *M. musculus* Ppib RNA is detected with an HRP-based green chromogen and Polr2a RNA is detected with an AP-based red signal. For rows **(A,B)**, magnification is x10, x40 from left to right. Black boxes on the left image panels indicate magnified regions shown in the right panels.

REFERENCES

Alam, H., Sehgal, L., Kundu, S. T., Dalal, S. N., and Vaidya, M. M. (2011). Novel function of keratins 5 and 14 in proliferation and differentiation of stratified epithelial cells. *Mol. Biol. Cell*. 22, 4068–4078. doi: 10.1091/mbc.E10-08-0703

Alekseev, A. N., Burenkova, L. A., Vasilieva, I. S., Dubinina, H. V., and Chunikhin, S. P. (1996). Preliminary studies on virus and spirochete accumulation in the cement plug of ixodid ticks. *Exp. Appl. Acarol*. 20, 713–723. doi: 10.1007/bf00051556

Cheng, F., Shen, Y., Mohanasundaram, P., Lindström, M., Ivaska, J., Ny, T., et al. (2016). Vimentin coordinates fibroblast proliferation and keratinocyte differentiation in wound healing via TGF-β-Slug signaling. *Proc. Natl. Acad. Sci. U.S.A.* 113, e4320–e4327. doi: 10.1073/pnas.1519197113

Chmelar, J., Kotál, J., Karim, S., Kopacek, P., Francischetti, I. M. B., Pedra, J. H. F., et al. (2016). Sialomes and mialomes: a systems-biology view of tick tissues and tick-host interactions. *Trends Parasitol*. 32, 242–254. doi: 10.1016/j.pt.2015.10.002

Coulombe, P. A., Kopan, R., and Fuchs, E. (1989). Expression of keratin K14 in the epidermis and hair follicle: insights into complex programs of differentiation. *J. Cell Biol*. 109, 2295–2312. doi: 10.1083/jcb.109.5.2295

Ebel, G. D., and Kramer, L. D. (2004). Short report: duration of tick attachment required for transmission of powassan virus by deer ticks. *Am. J. Trop. Med. Hyg*. 71, 268–271. doi: 10.4269/ajtmh.2004.71.3.0700268

Hamel, R., Dejarnac, O., Wichit, S., Ekchariyawat, P., Neyret, A., Luplertlop, N., et al. (2015). Biology of zika virus infection in human skin cells. *J. Virol*. 89, 8880–8896. doi: 10.1128/JVI.00354-15

Heinze, D. M., Carmical, J. R., Aronson, J. F., and Thangamani, S. (2012). Early immunologic events at the tick-host interface. *PLoS ONE* 7:e47301. doi: 10.1371/journal.pone.0047301

Hermance, M. E., Santos, R. I., Kelly, B. C., Valbuena, G., and Thangamani, S. (2016). Immune cell targets of infection at the tick-skin interface during powassan virus transmission. *PLoS ONE* 11:e0155889. doi: 10.1371/journal.pone.0155889

Hermance, M. E., and Thangamani, S. (2014). Proinflammatory cytokines and chemokines at the skin interface during Powassan virus transmission. *J. Invest. Dermatol*. 134, 2280–2283. doi: 10.1038/jid.2014.150

Hermance, M. E., and Thangamani, S. (2018). Tick-virus-host interactions at the cutaneous interface: the nidus of flavivirus transmission. *Viruses* 10:362. doi: 10.3390/v10070362

Hermance, M. E., Widen, S. G., Wood, T. G., and Thangamani, S. (2019). Ixodes scapularis salivary gland microRNAs are differentially expressed during Powassan virus transmission. *Sci. Rep*. 9:13110. doi: 10.1038/s41598-019-49572-5

Johnston, L. J., Halliday, G. M., and King, N. J. (2000). Langerhans cells migrate to local lymph nodes following cutaneous infection with an arbovirus. *J. Invest. Dermatol*. 114, 560–568. doi: 10.1046/j.1523-1747.2000.00904.x

Kazimírová, M., Thangamani, S., Bartíková, P., Hermance, M., Holíková, V., Štibrániová, I., et al. (2017). Tick-borne viruses and biological processes at the tick-host-virus interface. *Front. Cell. Infect. Microbiol.* 7:339. doi: 10.3389/fcimb.2017.00339

Labuda, M., Austyn, J. M., Zuffova, E., Kozuch, O., Fuchsberger, N., Lysy, J., et al. (1996). Importance of localized skin infection in tick-borne encephalitis virus transmission. *Virology*. 219, 357–366. doi: 10.1006/viro.1996.0261

Lim, P. Y., Behr, M. J., Chadwick, C. M., Shi, P. Y., and Bernard, K. A. (2011). Keratinocytes are cell targets of West Nile virus *in vivo*. *J. Virol*. 85, 5197–5201. doi: 10.1128/JVI.02692-10

Nguyen, A. V., and Soulika, A. M. (2019). The dynamics of the skin's immune system. *Int. J. Mol. Sci.* 20:e1811. doi: 10.3390/ijms20081811

Oliveira, C. J., Sá-Nunes, A., Francischetti, I. M., Carregaro, V., Anatriello, E., Silva, J. S. et al. (2011). Deconstructing tick saliva: non-protein molecules with potent immunomodulatory properties. *J. Biol. Chem*. 286, 10960–10969. doi: 10.1074/jbc.M110.205047

Pasparakis, M., Haase, I., and Nestle, F. O. (2014). Mechanisms regulating skin immunity and inflammation. *Nat. Rev. Immunol*. 14, 289–301. doi: 10.1038/nri3646

Ribeiro, J. M., Alarcon-Chaidez, F., Francischetti, I. M., Mans, B. J., Mather, T. N., Valenzuela, J. G., et al. (2006). An annotated catalog of salivary gland transcripts from ixodes scapularis ticks. *Insect. Biochem. Mol. Biol*. 36, 111–129. doi: 10.1016/j.ibmb.2005.11.005

Rossi, S. L., Nasar, F., Cardosa, J., Mayer, S. V., Tesh, R. B., Hanley, K. A., et al. (2012). Genetic and phenotypic characterization of sylvatic dengue virus type 4 strains. *Virology* 423, 58–67. doi: 10.1016/j.virol.2011.11.018

Thangamani, S., Hermance, M. E., Santos, R. I., Slovak, M., Heinze, D., Widen, S. G., et al. (2017). Transcriptional immunoprofiling at the tick-virus-host interface during early stages of tick-borne encephalitis virus transmission. *Front. Cell. Infect. Microbiol.* 7:494. doi: 10.3389/fcimb.2017.00494

Wang, F., Flanagan, J., Su, N., Wang, L. C., Bui, S., Nielson, A., et al. (2012). RNAscope: a novel *in situ* RNA analysis platform for formalin-fixed, paraffin-embedded tissues. *J. Mol. Diagn.* 14, 22–29. doi: 10.1016/j.jmoldx.2011.08.002

Wang, F., Zieman, A., and Coulombe, P. A. (2016). Skin keratins. *Methods Enzymol.* 568, 303–350. doi: 10.1016/bs.mie.2015.09.032

Wikel, S. K. (2013). Ticks and tick-borne pathogens at the cutaneous interface: host defenses, tick countermeasures, and a suitable environment for pathogen establishment. *Front. Microbiol.* 4:337. doi: 10.3389/fmicb.2013.00337

Wikel, S. K. (2018). Tick-host-pathogen systems immunobiology: an interactive trio. *Front. Biosci*. 23, 265–283. doi: 10.2741/4590

Conflict of Interest: The authors declare that the research was conducted in the absence of any commercial or financial relationships that could be construed as a potential conflict of interest.

frontiers in Cellular and Infection Microbiology

ORIGINAL RESEARCH
published: 24 July 2020
doi: 10.3389/fcimb.2020.00374

TickSialoFam (TSFam): A Database That Helps to Classify Tick Salivary Proteins, a Review on Tick Salivary Protein Function and Evolution, With Considerations on the Tick Sialome Switching Phenomenon

José M. C. Ribeiro[1]* *and Ben J. Mans*[2,3,4]

[1] Section of Vector Biology, Laboratory of Malaria and Vector Research, National Institute of Allergy and Infectious Diseases, Rockville, MD, United States, [2] Epidemiology, Parasites and Vectors, Agricultural Research Council - Onderstepoort Veterinary Research, Pretoria, South Africa, [3] The Department of Veterinary Tropical Diseases, University of Pretoria, Pretoria, South Africa, [4] Department of Life and Consumer Sciences, University of South Africa, Pretoria, South Africa

OPEN ACCESS

Edited by:
Brice Rotureau,
Institut Pasteur, France

Reviewed by:
Jindrich Chmelar,
University of South Bohemia in Ceské Budějovice, Czechia
Daniel Sojka,
Institute of Parasitology (ASCR), Czechia
James Jason Valdes,
Institute of Parasitology (ASCR), Czechia

***Correspondence:**
José M. C. Ribeiro
jribeiro@niaid.nih.gov

Specialty section:
This article was submitted to Parasite and Host, a section of the journal Frontiers in Cellular and Infection Microbiology

Received: 28 March 2020
Accepted: 17 June 2020
Published: 24 July 2020

Citation:
Ribeiro JMC and Mans BJ (2020) TickSialoFam (TSFam): A Database That Helps to Classify Tick Salivary Proteins, a Review on Tick Salivary Protein Function and Evolution, With Considerations on the Tick Sialome Switching Phenomenon. Front. Cell. Infect. Microbiol. 10:374. doi: 10.3389/fcimb.2020.00374

Tick saliva contains a complex mixture of peptides and non-peptides that counteract their hosts' hemostasis, immunity, and tissue-repair reactions. Recent transcriptomic studies have revealed over one thousand different transcripts coding for secreted polypeptides in a single tick species. Not only do these gene products belong to many expanded families, such as the lipocalins, metalloproteases, Antigen-5, cystatins, and apyrases, but also families that are found exclusively in ticks, such as the evasins, Isac, DAP36, and many others. Phylogenetic analysis of the deduced protein sequences indicate that the salivary genes exhibit an increased rate of evolution due to a lower evolutionary constraint and/or positive selection, allowing for a large diversity of tick salivary proteins. Thus, for each new tick species that has its salivary transcriptome sequenced and assembled, a formidable task of annotation of these transcripts awaits. Currently, as of November 2019, there are over 287 thousand coding sequences deposited at the National Center for Biotechnology Information (NCBI) that are derived from tick salivary gland mRNA. Here, from these 287 thousand sequences we identified 45,264 potential secretory proteins which possess a signal peptide and no transmembrane domains on the mature peptide. By using the psiblast tools, position-specific matrices were constructed and assembled into the TickSialoFam (TSF) database. The TSF is a rpsblastable database that can help with the annotation of tick sialotranscriptomes. The TSA database identified 136 tick salivary secreted protein families, as well as 80 families of endosomal-related products, mostly having a protein modification function. As the number of sequences increases, and new annotation details become available, new releases of the TSF database may become available.

Keywords: tick, saliva, transcriptome, annotation, sialome switching, feeding, salivary glands

INTRODUCTION

Tick salivary glands serve multiple physiological roles: While off their hosts, special acini (type I) produce a hygroscopic saliva that spreads over the ticks' palps, absorbs atmospheric water vapor, and when re-ingested helps to keep the tick hydrated (Bowman and Sauer, 2004). The salivary glands are also a major excretion/water balance organ in ixodid ticks, as the majority of the water ingested during a blood meal is pumped back into their hosts as saliva (Binnington and Kemp, 1980). In ixodid males, due to their peculiar and successful oral sex reproduction mode, special male acini (type IV) contribute to salivary products that are uniquely male and are molecular homologs of insect seminal gland or vertebrate prostate gland proteins (Tan et al., 2015). Finally, and the focus of this article, tick salivary glands help blood feeding by secreting products that help tick attachment to the host's skin and that inhibit host hemostasis (a physiological response that encompasses platelet aggregation, vasoconstriction, and blood clotting), inhibit the vertebrate tissue repair response, and modulate host immunity (Francischetti et al., 2009).

There are 899 known tick species divided into two major families, the soft tick (*Argasidae*) and the hard tick (*Ixodidae*) families (Guglielmone et al., 2010). A third family, *Nuttalliellidae*, exists, but with a single species. Soft ticks feed relatively rapid (typically <1 h), while hard ticks feed for several days or weeks. Adult soft ticks can feed many times, while adult hard ticks feed only once. Hard ticks are further divided into Prostriate and Metastriate. Metastriate ticks have relatively short mouthparts, producing copious amounts of cement, while Prostriate ticks have longer mouthparts, producing less abundant cement. Adult and nymphal soft ticks do not produce cement. Blood is the only nutritious food for all ticks. It is estimated that there are over 15,000 species of arthropods that feed on blood, and this mode of feeding evolved independently at least 20 times (Mans, 2011)—thus creating a scenario of convergent evolution. Ticks, mosquitoes, sand flies, kissing bugs, and fleas evolved blood feeding independently, but they all share the presence of a salivary apyrase activity, an enzyme (ATP-diphosphohydrolase) that breaks down ATP and ADP released by damaged cells and trigger platelet and neutrophil activation. However, three different gene families were recruited for this task: (1) the 5′-nucleotidase in ticks (Stutzer et al., 2009), some genera of triatomine bugs, and mosquitoes; (2) the Cimex-type apyrase (CD73) in sand flies and the kissing bug genus *Rhodnius*; (3) the CD39 apyrase in fleas (Ribeiro and Arca, 2009). These types of enzymes are ubiquitous in eukaryotes, normally extracellular and bound to the membrane or intracellular and associated to endosomes; their transcripts always display a signal peptide indicative of secretion. Evolution of salivary apyrase, as an adaptation to blood feeding, thus happened by processes of gene duplication of a salivary gland expressed gene with loss of its membrane anchor (Champagne et al., 1995). Another common evolutionary process of adaptation to blood feeding involved further gene duplication events of already established salivary genes, which initially increased the mRNA dosage, but allowed for further functional or antigenic diversification. For example, sand flies and mosquitoes have several related salivary expressed genes of the D7 family, which belong to the odorant binding protein group, and are associated with binding of agonists of hemostasis and inflammation (Valenzuela et al., 2002a; Mans et al., 2007; Calvo et al., 2009; Alvarenga et al., 2010). Ticks and blood sucking Hemiptera had a large expansion of the lipocalin family, which are also associated with binding of agonists of hemostasis and inflammation (Andersen and Ribeiro, 2017). Fleas expanded members of the acid phosphatase family (function unknown) (Andersen et al., 2007; Ribeiro et al., 2012).

While Adult sand fly saliva has <50 polypeptides and mosquito saliva has near 100, hard tick saliva has several hundred, or thousands of polypeptides (Ribeiro and Arca, 2009; Ribeiro et al., 2010). The increased number of components in hard tick saliva was initially thought to derive from the prolonged period of tick feeding, where it would face not only the hemostatic host response, but also its tissue repair and immune responses. However, deep sequencing of salivary transcriptomes at different times of feeding uncovered that ticks change their salivary repertoire frequently, within hours; a process named "sialome switching" (Valenzuela et al., 2002b; Karim and Ribeiro, 2015; Perner et al., 2018). Thus, while in mosquitoes and other non-tick hematophagous organisms, all members of a salivary protein family are simultaneously expressed; in hard ticks, individual genes of the same family, or paralogs, are expressed at different times during the feeding process. Accordingly, when the host mounts an antibody response to a particular antigen, a process that takes a few days, chances are that the antigenic molecule has been substituted by a not antigenically recognizable paralogs. Sialome switching is thus thought to be a mode of immune evasion. It may also serve ticks when they feed on different host species, as they may "find" the best sialome when feeding on a lizard, which may be different then when feeding on a mouse. Sialome switching may thus be a mechanism adapting ticks to feed on different hosts.

The study of the function of saliva in blood feeding by arthropods in the last 30 years was transformed by the revolution of cheap DNA sequencing. In the beginning it was the "grind and find" way: salivary homogenates were used to discover activities determined by a bioassay; followed by chromatographic methods of purification of the biological activity; in the case it was a polypeptide, obtaining Edman sequences allowing the construction of degenerate DNA probes that were used to amplify fragments of the salivary cDNA; that would be used to find, by hybridization, and with luck, a full length clone from which the primary sequence of the studied protein could be determined. The research flow was then from the bioassay to the protein, and from the protein to the DNA or mRNA.

Currently, for <300 $, we can obtain 20 million sequences of 150 nucleotides (nt) in length that can be assembled "*de novo*" (in the absence of a genomic sequence to serve as an assembly scaffold), producing high quality transcript sequences that can be converted to their coding protein sequences. Accordingly, the "sialome" (from the Greek σίελος = saliva) can be obtained inexpensively and in a relatively short amount of time (Ribeiro and Francischetti, 2003). These sialomes have revealed a surprising number of novel protein sequences; they frequently have no similar matches when comparing their

primary sequence to a bank of known proteins. Less frequently, they produce matches to ubiquitous protein families, usually enzymes, but also members of the antigen-5 family or families of protease inhibitors, such as those containing cystatin, serpin, Kazal, or Kunitz domains. These deducted protein sequences can be further used in two ways: First, in the absence of the organism's genomic sequences, they will serve as a data bank for proteomic studies, a technology that requires a reliable "a priori" defined set of sequences; the tandem mass spectrometry (MS/MS) protocol maps the partial sequences.

Theoretically, if the genome sequence of the organism under study is known, then its deducted protein sequences could serve this purpose. However, most blood sucking insects and ticks still do not have a reliable genome sequence. The genome of the tick *Ixodes scapularis* is at best 50% complete (Gulia-Nuss et al., 2016). Even with better genomic data information, such as the anopheline mosquitoes (Holt et al., 2002; Neafsey et al., 2015), a detailed comparison of the protein sequences known to be salivary expressed with the deducted genomic protein sequences indicated that there was an error on ∼50% of the predicted genomic sequences; either because they were missed, or because the intron-exon boundaries were incorrect (Arca et al., 2017). Proteomic studies of the salivary glands of blood sucking arthropods thus rely on carefully curated protein sequences deducted from the salivary transcriptome assembly. Second, the deducted protein sequences can guide production of recombinant proteins to be tested in bioassays to determine their functions, or as immunological markers of vector exposure. Thus, the research flows today from the mRNA to the protein, and from the protein to the bioassay.

Another approach exists, namely the immuno-proteome method, which is based on high throughput cloning and sequencing methods aimed at anti-tick vaccine discovery (Das et al., 2001; de la Fuente et al., 2006; Narasimhan et al., 2007; Radulovic et al., 2014; Becker et al., 2015; Lewis et al., 2015; Garcia et al., 2017). First, an animal is made hyperimmune to tick salivary proteins by previous tick exposure, or injection of salivary homogenates. The hyperimmune serum, and its control, are then used to scan expression cDNA libraries made from tick salivary glands. The positive clones are then sequenced, recombinantly expressed, and tested for their biological activity and as a vaccine to disrupt tick feeding. It has succeeded in discovering and characterizing many tick salivary proteins (Narasimhan et al., 2007; Dai et al., 2009; Schuijt et al., 2010). Somewhat surprisingly, many intracellular tick proteins, not having a signal peptide indicative of secretion, were discovered to be good antigen candidates; as was the case of the conserved tick protein, subolesin (de la Fuente et al., 2006), a member of the Akirin transcription regulator (de la Fuente et al., 2011). Similarly, a tick protein similar to vertebrate histamine releasing factor was found (Mulenga et al., 2003), and named histamine release factor (HRF). This is also a conserved member of the cytoskeletal family named "Translationally controlled tumor protein" (TCTP) and was responsible for the activity of human tissue homogenates to trigger histamine release by mast cells (Xiao et al., 2017). Human TCTP thus has a dual function: as a cytoskeletal protein: and as a cytokine-like protein when cells lyze and their contents are released to the extracellular milieu. ADP and ATP similarly are primarily intracellular molecules; however when released to the extracellular compartment after cellular disruption or secretion, they similarly trigger pro inflammatory reactions. It thus appears that tick saliva contains proteins that are secreted through the classic merocrine pathway, as well as non-conventional secretion pathways, including apocrine or holocrine secretions (Farkas, 2015). Indeed, merocrine and apocrine secretion has been characterized by ultrastructural studies in soft tick salivary glands (Coons and Roshdy, 1981). Hard tick salivary glands suffer a degeneration process after a blood meal (Harris and Kaufman, 1981; Friesen and Kaufman, 2009), and it is possible that this process starts while the tick is still feeding and thus generating a holocrine salivary secretion. Additionally, there is recent evidence that exosomes may be secreted in tick saliva (Hackenberg and Kotsyfakis, 2018; Zhou et al., 2018; Chavez et al., 2019). Exosomes can fuse with host cells and deliver their products intracellularly, including microRNAs that may inhibit translation of some protein types (Keller et al., 2006). The study of salivary exosomal secretion in tick feeding is still in its infancy, and the next decade should uncover its more precise role in feeding by ticks.

Ten years ago, a review on tick sialomes based on 3,500 tick salivary proteins identified more than 30 protein families, most having unknown function (Francischetti et al., 2009). That review was done when the first sialomes were uncovered with the now obsolete Sanger DNA sequencing method. At that point in time, the now defunct 454 and surviving Illumina protocols appeared, and the number of salivary-derived tick protein-coding sequences deposited to the National Center for Biotechnology Information (NCBI) soared, reaching over 287,000 in November/2019 (**Figure 1**). These sequences derive from 44 species within 10 genera; only 19 species from 7 genera are represented with more than one thousand sequences (**Table 1**). Considering that there are 899 tick species from 20 different genera (Guglielmone et al., 2010), we have achieved 1,000 sequences for only 2.7% of the known tick species, which covers 35% of the known genera. Clearly, we are still far from knowing the complete sialome repertoire of ticks (the sialoverse), a task that should take one or more decades for its fulfillment.

To facilitate the task of annotating newly assembled transcriptomes, we present a rpsblastable database of tick salivary families, named TickSialoFam or TSFam. Together with an update on the classification of tick salivary families as proposed in 2009 (Francischetti et al., 2009), we provide further insights into the evolution of the genes coding for these proteins.

METHODS

Sequence Retrieval and Organization

The nucleotide database from NCBI (https://www.ncbi.nlm.nih.gov/nuccore/) was queried with the expression "ixodida[organism] AND salivary," and the resulting records were downloaded in the gb (GenBank) format. Sequences with "mitochondr" in their description were excluded, as well as those results related to unassembled EST's, and those from the REFSEQ database. This resulted in a set of 287,343 sequences

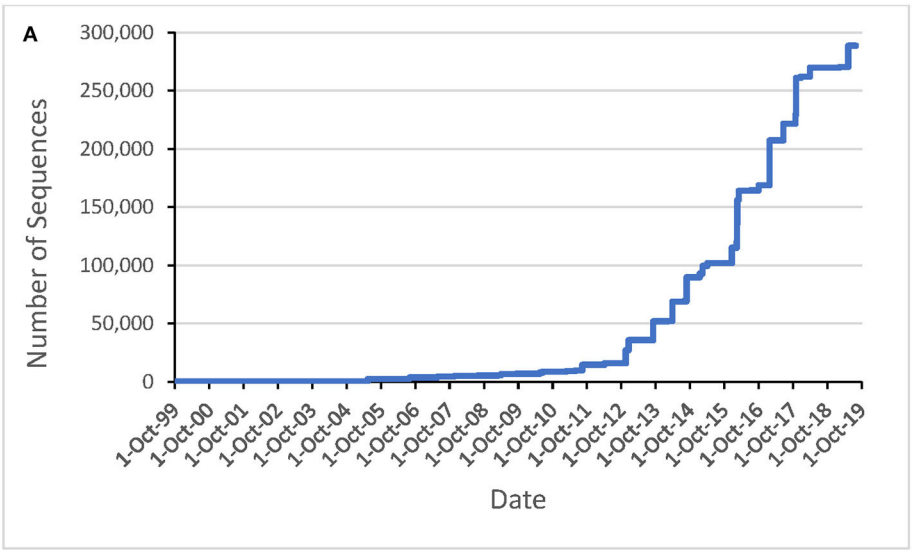

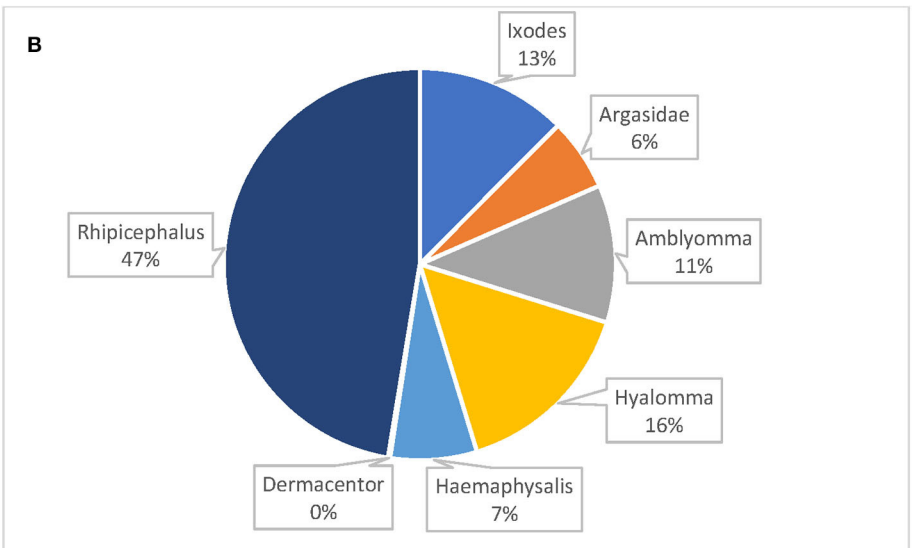

FIGURE 1 | Tick salivary protein coding sequences (excluding EST's) deposited at the National Center for Biotechnology Information (NCBI). **(A)** Number of sequences deposited, 1993–2019. **(B)** Breakdown of sequences available in Nov/2019 by genus or family.

(**Table 1**). It should be noted that up to mid-2018, all protein sequences submitted to the NCBI Transcriptome Shotgun Annotation (TSA) database were deposited in the NCBI protein database, as were the nucleotide sequences deposited to the NCBI nucleotide database. After this time, all TSA submissions appear only in the nuccore database, solely as a link leading to downloading the nucleotide and protein sequences. These TSA databases were then downloaded and added to those of the nuccore database. A script written in visual basic version 6 (VB6) extracted the individual protein sequence in fasta format; this script also built a table that included the sequence accession code, its description, author's, date of publication of the sequence, and bibliographical information (including link to PubMed, when available). When the protein sequence was unavailable, the larger open reading frame was translated. These data were imported into a hyperlinked Excel spreadsheet available as **Supplemental Spreadsheet 1**.

Since this sequence set contained both those related to housekeeping, as well as a salivary secreted function (from now on just called as "housekeeping" or "secreted,") we ran these

TABLE 1 | Tick salivary coding sequences retrieved from NCBI on November 2019.

A		B	
Species	**Number of sequences**	**Species**	**Number of sequences**
Amblyomma americanum	3,967	*Rhipicephalus appendiculatus*	49,146
Amblyomma aureolatum	93	*Rhipicephalus bursa*	39,435
Amblyomma cajennense	7,098	*Hyalomma dromedarii*	38,518
Amblyomma maculatum	4,855	*Ixodes ricinus*	33,250
Amblyomma parvum	2,838	*Rhipicephalus annulatus*	20,753
Amblyomma rotundatum	355	*Haemaphysalis longicornis*	20,592
Amblyomma sculptum	4,249	*Rhipicephalus zambeziensis*	14,393
Amblyomma triste	8,098	*Rhipicephalus pulchellus*	11,227
Amblyomma tuberculatum	67	*Amblyomma triste*	8,098
Amblyomma variegatum	743	*Ornithodoros turicata*	7,560
Antricola delacruzi	317	*Amblyomma cajennense*	7,098
Argas monolakensis	1,059	*Ornithodoros rostratus*	6,587
Carios mimon	4	*Hyalomma excavatum*	5,338
Dermacentor andersoni	505	*Amblyomma maculatum*	4,855
Haemaphysalis longicornis	20,592	*Amblyomma sculptum*	4,249
Haemaphysalis qinghaiensis	2	*Amblyomma americanum*	3,967
Hyalomma anatolicum anatolicum	88	*Amblyomma parvum*	2,838
Hyalomma asiaticum asiaticum	1	*Ixodes scapularis*	2,451
Hyalomma dromedarii	38,518	*Argas monolakensis*	1,059
Hyalomma excavatum	5,338	*Rhipicephalus microplus*	969
Hyalomma rufipes	558	*Rhipicephalus sanguineus*	761
Ixodes affinis	1	*Amblyomma variegatum*	743
Ixodes holocyclus	7	*Hyalomma rufipes*	558
Ixodes pacificus	118	*Ornithodoros parkeri*	544
Ixodes persulcatus	17	*Dermacentor andersoni*	505
Ixodes ricinus	33,250	*Ornithodoros brasiliensis*	440
Ixodes scapularis	2,451	*Amblyomma rotundatum*	355
Ixodes sinensis	5	*Antricola delacruzi*	317
Ornithodoros brasiliensis	440	*Ornithodoros coriaceus*	272
Ornithodoros coriaceus	272	*Ixodes pacificus*	118
Ornithodoros kalahariensis	2	*Amblyomma aureolatum*	93
Ornithodoros moubata	59	*Hyalomma anatolicum anatolicum*	88
Ornithodoros parkeri	544	*Amblyomma tuberculatum*	67
Ornithodoros rostratus	6,587	*Ornithodoros moubata*	59
Ornithodoros turicata	7,560	*Ixodes persulcatus*	17
Rhipicephalus annulatus	20,753	*Ixodes holocyclus*	7
Rhipicephalus appendiculatus	49,146	*Ixodes sinensis*	5
Rhipicephalus bursa	39,435	*Carios mimon*	4
Rhipicephalus haemaphysaloides	1	*Haemaphysalis qinghaiensis*	2
Rhipicephalus microplus	969	*Ornithodoros kalahariensis*	2
Rhipicephalus pulchellus	11,227	*Hyalomma asiaticum asiaticum*	1
Rhipicephalus sanguineus	761	*Ixodes affinis*	1
Rhipicephalus zambeziensis	14,393	*Rhipicephalus haemaphysaloides*	1
Total	287,343	Total	287,343

(A) *Data sorted by species and* ***(B)*** *data sorted by number of sequences.*

sequences through the SignalP program (version 3.0) (Nielsen et al., 1999) to identify whether they had a predicted signal sequence indicative of secretion. We also ran them as well as through the TMHMM program (Sonnhammer et al., 1998) to determine their predicted transmembrane domains. Of the 287,343 sequences, 45,264 had a signal sequence, excluding those having one or more transmembrane domain outside the signal sequence; thus obtaining a set coding for putative classical secreted proteins (**Table 2**). To identify protein families, we clusterized these sequences by blasting each one against the remaining set and joining those that reached variable degrees of identity (varying from 25 to 95% in 5% increments), over at least 75% of the length of the larger sequence. Notice that if a polypeptide A satisfies the rule with polypeptide B, and B with polypeptide C, the cluster ABC would be formed, even though polypeptide A does not satisfy the rule with polypeptide C. For each cluster, we obtained a fasta file with its members. In the cases where the cluster had 5 or more sequences, a clustal (Larkin et al., 2007) alignment was obtained. The resulting fasta files and clustal alignments were hyperlinked to the spreadsheet with the indication of the cluster number (ordered from the most to the least abundant in sequences) and its number of sequences (**Supplemental Spreadsheet 2**).

From the original set of 287,343 sequences, we extracted the 45,264 sequences classified as secreted. The remaining sequences were submitted to the secretomeP program to identify those sequences that could qualify as secreted through non-classical pathways, as indicated by a secretomeP score larger than 0.6 (Bendtsen et al., 2004). The resulting 125,197 sequences are displayed on **Supplemental Spreadsheet 3**.

TickSialoFam Model Construction

A program was written in VB6 that inspected each alignment file from the various clusters of the "Secreted" data set (**Supplemental Spreadsheet 2**). In the cases where it had five or more sequences, and if the alignment indicated at least five sites of identity or conservation, then the fasta file was used to construct a PSIBlast-based model (Altschul et al., 1997; Schaffer et al., 2001). First, all sequences of the cluster were blasted against themselves, and the one that accrued the largest sum of scores (excluding self-blast) was elected as the cluster centroid. The program blastpgp, from the blast package (Psi-blast), was then run using the centroid sequence as input; the formatted cluster fasta sequences (using the blast suit program formatdb) was used as a target databank, with the parameters -W 2 (blastp word size), and -j 5 (maximum number of iterations). The -h switch (inclusion *e* value after the first blast step) was variable, according to the size of the centroid: the chosen values were 1e-15 for length (l) larger than 200; 1e-8 for $100<l<200$; 1e-6 for $60<l<100$; and 1e-4 for $l<60$. These values were arbitrarily adjusted according to size of the sequence: because a smaller sequence accrues a smaller score value than a large sequence and thus has a higher e value. The resulting matrix file was saved using the -C switch. These models were named according to the cluster parameters; for e.g., a model named 35-123 derived from the sequences found in cluster number 123 from the clusterization at 35% identity.

TABLE 2 | Putative secreted class of tick salivary sequences retrieved from NCBI on November 2019.

A		B	
Species	**Number of sequences**	**Species**	**Number of sequences**
Amblyomma americanum	1,369	*Ixodes ricinus*	9,776
Amblyomma aureolatum	27	*Rhipicephalus appendiculatus*	6,690
Amblyomma cajennense	2,072	*Hyalomma dromedarii*	3,833
Amblyomma maculatum	917	*Rhipicephalus bursa*	3,190
Amblyomma parvum	721	*Rhipicephalus zambeziensis*	3,017
Amblyomma rotundatum	164	*Amblyomma triste*	2,542
Amblyomma sculptum	307	*Haemaphysalis longicornis*	2,493
Amblyomma triste	2,542	*Amblyomma cajennense*	2,072
Amblyomma tuberculatum	26	*Rhipicephalus pulchellus*	1,969
Amblyomma variegatum	267	*Rhipicephalus annulatus*	1,467
Antricola delacruzi	83	*Amblyomma americanum*	1,369
Argas monolakensis	301	*Amblyomma maculatum*	917
Dermacentor andersoni	154	*Ixodes scapularis*	890
Haemaphysalis longicornis	2,493	*Ornithodoros turicata*	818
Hyalomma anatolicum anatolicum	27	*Amblyomma parvum*	721
Hyalomma asiaticum asiaticum	1	*Ornithodoros rostratus*	657
Hyalomma dromedarii	3,833	*Hyalomma excavatum*	397
Hyalomma excavatum	397	*Amblyomma sculptum*	307
Hyalomma rufipes	133	*Argas monolakensis*	301
Ixodes affinis	1	*Amblyomma variegatum*	267
Ixodes holocyclus	7	*Rhipicephalus microplus*	257
Ixodes pacificus	74	*Rhipicephalus sanguineus*	224
Ixodes persulcatus	14	*Amblyomma rotundatum*	164
Ixodes ricinus	9,776	*Ornithodoros parkeri*	162
Ixodes scapularis	890	*Dermacentor andersoni*	154
Ixodes sinensis	5	*Hyalomma rufipes*	133
Ornithodoros brasiliensis	61	*Ornithodoros coriaceus*	111
Ornithodoros coriaceus	111	*Antricola delacruzi*	83
Ornithodoros kalahariensis	2	*Ixodes pacificus*	74
Ornithodoros moubata	37	*Ornithodoros brasiliensis*	61
Ornithodoros parkeri	162	*Ornithodoros moubata*	37
Ornithodoros rostratus	657	*Amblyomma aureolatum*	27
Ornithodoros turicata	818	*Hyalomma anatolicum anatolicum*	27
Rhipicephalus annulatus	1,467	*Amblyomma tuberculatum*	26
Rhipicephalus appendiculatus	6,690	*Ixodes persulcatus*	14
Rhipicephalus bursa	3,190	*Ixodes holocyclus*	7
Rhipicephalus haemaphysaloides	1	*Ixodes sinensis*	5
Rhipicephalus microplus	257	*Ornithodoros kalahariensis*	2
Rhipicephalus pulchellus	1,969	*Hyalomma asiaticum asiaticum*	1
Rhipicephalus sanguineus	224	*Ixodes affinis*	1
Rhipicephalus zambeziensis	3,017	*Rhipicephalus haemaphysaloides*	1
Total	45,264	Total	45,264

(A) *Data sorted by species and* ***(B)*** *data sorted by number of sequences.*

These procedures are similar to those used for construction of the COG and KOG databases (Tatusov et al., 2003).

Another method to create matrices was done by psiblasting each sequence against the whole Ixodida database, using the same parameters indicated above. These models are named by the NCBI accession number of the parent protein sequence. These matrix files were then combined with the program makeprofiledb with the parameters -threshold 9.82 -scale 100.0 -dbtype rps -index true, forming the initial TSFam database. Finally, the number of models used in the final database was reduced by selecting those that produced a match with a maximum *e*-value of 1e-20.

Sequence Functional Classification

To further help classification of the protein sequences, possible proline-hydroxylation (Rhoads and Udenfriend, 1969; Bohmer, 1971; Kivirikko et al., 1972) and tyrosine sulfation (Nicholas et al., 1999) sites were determined, including the percentages of glycines, prolines, and tyrosines of each protein sequence, and their number of cysteine residues. These features helped to classify the families within the glycine-rich proteins (GRP) group. Determination of the presence of glycosyl-phosphate-inositol (GPI) anchors were determined with the program DGPI (Pierleoni et al., 2008). This helped to identify secreted proteins that were bound to membranes. The presence of furin cleavage sites were also detected (Duckert et al., 2004), identifying polyproteins with various cleavage sites. The percentages of serines and threonines were determined. The number of possible mucin-type galactosylation sites being measured with the program NetOGlyc (Hansen et al., 1998; Julenius et al., 2005) helps to further identify and classify the mucins. The set of secreted sequences were compared by blastp; to a subset of proteins from the NCBI NR database; to the Swissprot database; to the Enzyme Commission set from the KEGG database; to the salivary Ixodida sequences retrieved as indicated above; to the top 100 proteins associated with exosomes from exocarta (http://exocarta.org/download); and to rpsblast comparisons to the Conserved Domains database (CDD), Kog, Pfam, Smart, and TSF databases. All these comparisons were hyperlinked to the corresponding spreadsheets and allowed manual annotation of the sequences.

The annotations were transferred to the TSF models, which included in their description the following fields of information: (1) model name: as indicated in the previous section (e.g., 35-123 or JAP81818.1). (2) Group: This classification may include non-phylogenetically related sequences, such as the glycine-rich proteins (GRP) and mucins but can include groups such as the Lipocalins or Serpins. For this reason, this field is named group and not family. (3) Family: A subdivision of the group, containing phylogenetically related sequences. This field is empty in many models. (4) H/S/I: Indicates whether the sequence is classified as Secreted, Housekeeping, or in a few cases, Indeterminate. (5) Other: Includes additional information codified as E, enzyme; AM, antimicrobial; and PI, protease inhibitor. These fields are separated by "|" characters, which may be changed to tabs to produce the display shown in the hyperlinked spreadsheets.

The publicly available formatted TSFam database (**Supplemental File 1**) can be used in a rpsblast search using as an input a fasta file of tick salivary proteins, using a command line such as: "[x]blastall -p rpsblast -d [y]TSF -i [z]in.fasta -o [z]tsf.blt -IT -JT -v20 -b10 -e1e-4 -FF." Where [x], [y], and [z] are the paths to the blast program, the TSFam database, and the input fasta and the output files, respectively. We recommend accepting the classifications using the TSFam database when the coverage of the model by the queried protein is at least 2/3 (>66.6%) and having a maximum *e* value of 1e-4. To access the blast programs, use version 2.2.26 available at ftp://ftp.ncbi.nlm.nih.gov/blast/executables/legacy.NOTSUPPORTED/2.2.26/.

Tools That Help With Mining the Database

Three tools, written in visual basic and compiled to run under the Windows environment, are available upon email request to jribeiro@niaid.nih.gov. The tool, fasta2tbl, reads a fasta file and creates a hyperlinked table that can be imported into a spreadsheet. The tool, rpsblast2tbl, reads a rpsblast result file and maps the results and annotation into a hyperlinked table that can be imported into the fasta table done with fasta2tbl. The tool, GetFSA, takes a list of sequence names found in the fasta table or spreadsheet and creates a fasta file that can be used for phylogenetic or other studies.

Phylogenetic Analysis

Phylogenetic analysis were done with Mega7 (Kumar et al., 2016). Alignments were done with Clustal (Larkin et al., 2007) and refined with Muscle (Edgar, 2004) using the MEGA7 program (Kumar et al., 2016). The program FUBAR (Murrell et al., 2013) of the HYPHY (Pond et al., 2005) package was used to find positively selected sites within the in-frame nucleotide sequences. Positively selected codons were identified by their assigned probabilities of the parameter α being smaller than beta. The program RDP4 was used to determine the number of recombination breakpoints within the nucleotide alignments (Martin and Rybicki, 2000).

RESULTS

Table 1 lists the number of retrieved sequences by species, sorted by species name (A), and number of sequences (B); **Table 2** lists the same information for the subset of sequences classified as "secreted."

Because the sequences under this study derive mainly from transcriptome assembly studies, many of the sequences are truncated either at their 5′ or 3′ ends. Only 57% of the 45,264 protein sequences start with a methionine (and even if it starts with one, there is no guarantee that it is the starting methionine); stop codons are found for 57% of the sequences. Both a starting methionine and stop codon occur in 49% of the sequences. Accordingly, identification of signal peptide indicative of secretion can only be found with confidence in a maximum of 57% of the set. Despite these flaws, truncated protein sequences are still important, as they may later serve as sequence templates for MS/MS studies that may include extension of selected coding sequences.

Putative Secreted Proteins

The TSFam database of motifs allowed classification of 18,963 sequences from the 45,264 salivary-derived Ixodida sequences from NCBI, classified as putative secreted proteins (**Supplemental Spreadsheet 2**). These were organized into 136 groups, as indicated in the **Supplemental Table 1**. The criteria for classification of these sequences required an *e*-value <1e-4 and a model coverage of at least 67% (2/3 of the model length). The classifications can be further grouped according to their similarities, or lack of similarities, to other known proteins or protein domains; they can also be grouped according to their known function, leading to the categories "Enzymes," "Protease inhibitors," "Ubiquitous families," "Tick-specific anti-clotting peptides," "Immune-related," "Antimicrobials," and "Tick-specific families" (**Figure 2**). Notice that the category "Tick-specific families" is the larger one, however, most of its members have no known function. Many of the groups are complex in nature and may contain phylogenetically unrelated families; for instance, the "Glycine-rich family," is further subdivided into 19 families in **Supplemental Spreadsheet 2**. Six of the groups contains the majority of sequences (**Figure 3**).

Considering all 136 groups of **Supplemental Table 1**, only 37 have been characterized with at least one member having been recombinantly expressed and its function determined by bioassay, enzymatic assay, or proteomic detection from tick saliva. These studies are referenced in **Supplemental Table 1**. From these 37 characterized families, four have been only enzymatically characterized. Accordingly, the responsible tick protein is only presumed; nine have been found by saliva proteomic studies, but their function has not been characterized. It is also possible that many of the deducted CDS derive from pseudogenes (Kalyana-Sundaram et al., 2012). Thus, we have relative confidence that we know the molecular nature and function of at least one member from 24 of the 136 groups. Confidence should be defined in this case as: (1) Ascertaining that the protein is expressed in the saliva; (2) determining the biological activity of the recombinant protein. Very few protein families have at least one member satisfying these two requirements. Accordingly, this database consists mostly of a hypothetical set to be further characterized by proteomic and functional studies and should be updated as new studies are published.

This new data set provides the mining rounds for further analysis into the evolution of previously known families, including characterization of novel protein families by recombinant expression and functional assay of the predicted proteins.

Evolutionary Insights on Tick Salivary Proteins

What follows is the phylogenetical analysis of selected protein families. Some large families have complex composition (such as, Kunitz, basic tail, Salp15) and will not be analyzed.

Apyrase/5′-Nucleotidase Family

As stated in the introduction, the saliva of unrelated blood feeding arthropods has the ability to hydrolyze ADP and

Tick-specific families	6,805
Ubiquitous families	3,803
Protease inhibitors	2,810
Enzymes	1,737
Immune related	468
Antimicrobial	364
Tick -specific anti-clotting	25
Total	16,012

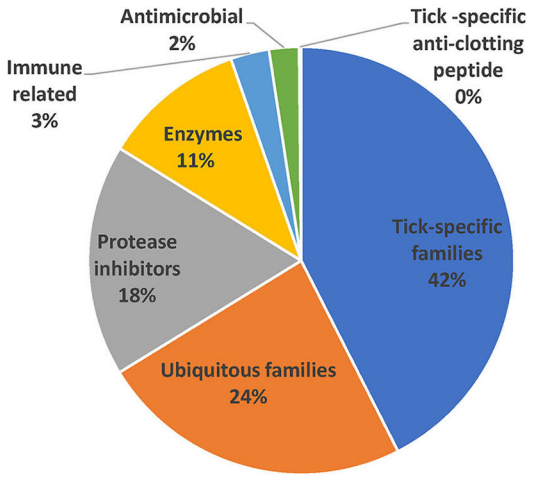

FIGURE 2 | Classification and relative number of sequences for the putative secreted salivary proteins from ticks.

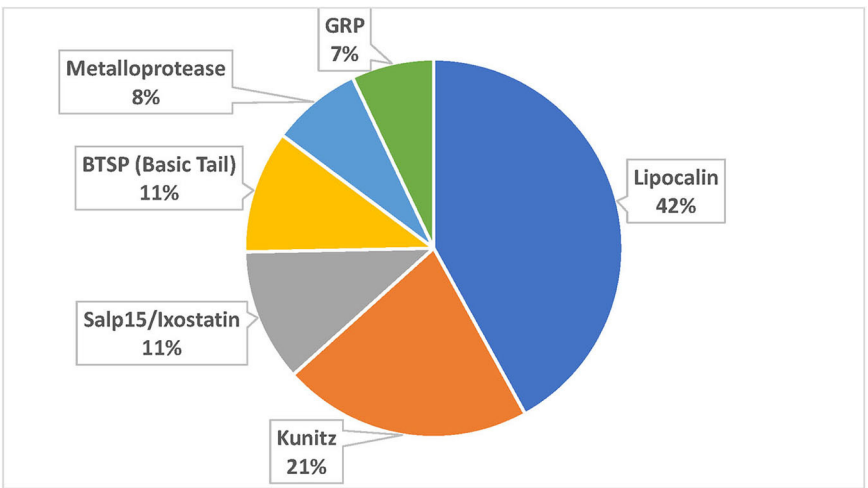

FIGURE 3 | Proportion of sequences accrued by the six larger superfamilies.

ATP, thus inhibiting important pathways of platelet and neutrophil aggregation and other pro-inflammatory reactions (Francischetti et al., 2009). The **Supplemental Spreadsheet 2** and **Table 1** provide for 50 full length sequences belonging to the 5′-nucleotidase family; four of which have a GPI anchor, indicating they are not secreted and could represent the homolog ancestral genes that gave origin to gene versions coding for secreted products. **Supplemental Spreadsheet 1** indicate the presence of 287 annotations for 5′-nucleotidase; fifty of which are full-length. Phylogenetic analysis of these 50 sequences (**Supplemental Figure 1**) confirms this scenario: The GPI-containing sequences group together in a single clade, while the remaining sequences group into three major clades, Clades I and II, with Metastriate and Prostriate sequences, and an Argasidae clade. Clade I has two main branches, one containing Prostriate sequences and another containing only Metastriate sequences. The Prostriate sub clade further divides into two branches, indicative of an ancient gene duplication event. Clade II is similarly organized, with two main branches, and containing a single Prostriate sequence. It is also relevant that the depth of amino acid divergence on the clades I and II are at least 2-fold of the depth of the classic GPI clade, which contains one sequence from *Ixodes, two* from *Rhipicephalus,* and one from *Amblyomma.* Notice that the analysis has many more sequences derived from *I. ricinus* than from other species, reflecting the larger read coverage for the *Ixodes* transcriptomes. As coverage is increased for other species, novel genes coding for products of the 5′-nucleotidase/Apyrase should appear. The phylogram indicates the existence of at least seven genes coding for secreted apyrases from *I. ricinus*, based on the branches having 100% bootstrap support; the amino acid divergence of the secreted proteins is larger than that of the housekeeping, GPI anchored sequences, indicating faster evolution of the genes coding for secreted salivary genes; this was either caused by neutral evolution of these genes when compared to a purifying evolution scenario of the housekeeping genes, or due to positive

selection pressure on the genes coding for secreted enzymes, driven by the immune pressure of their hosts (Mans et al., 2017). Submission of the apyrase coding enzymes to the FUBAR analysis (Murrell et al., 2013) indicated no sites under positive selection. RDP analysis (Martin and Rybicki, 2000) using the same sequence alignment indicated three recombination breakpoints (**Supplemental Spreadsheet 4**).

Lipocalins

There are 3,689 sequences classified as lipocalins in **Supplemental Spreadsheet 2** (considering >66% coverage with a TSFam lipocalin match). A subset of these sequences that had the PFAM His bind domain (with at least 80% coverage) amounted to 1,050 sequences. Attempts to construct a phylogeny (based on the faster Neighbor-Joining algorithm) with this subset were not informative, with most clades having poor bootstrap support. The phylogeny reconstruction of a smaller subset of 32 *I. ricinus* sequences, that were clustered at 40% sequence identity (**Supplemental Figure 2**), shows two main clades that further subdivide in eight smaller clades containing 2 or more sequences. FUBAR analysis indicated 16 codons under positive selection. RDP analysis indicated 11 recombination breakpoints (**Supplemental Spreadsheet 4**).

Metalloproteases

The TSF algorithm indicates 677 sequences as being metalloproteases in **Supplemental Spreadsheet 2**. Eighty-seven of these sequences, from *I. ricinus, A. americanum,* and *R. appendiculatus* were chosen for alignment and phylogenetic analysis based on their completeness and match to the CDD domain cd04272 named ZnMc_salivary_gland_MPs. The cladogram displays five Metastriate-specific clades with strong bootstrap support, plus five Prostriate ones; each clade further subdividing in two or more subclades (**Supplemental Figure 3**). We can conclude that in *I. ricinus,* and possibly in other ticks, there are at least 10 genes coding for this subdivision of the salivary metalloproteases. FUBAR analysis found no sites under positive selection. RDP indicated 3 recombination breakpoints (**Supplemental Spreadsheet 4**).

DAP36 Family

The founding member of this family was identified as an immunosuppressant salivary protein from *Dermacentor andersoni* (Bergman et al., 1995, 1998). In 2009 this family was characterized as a diverse Metastriate-specific family. However, here we find it is also composed of *Ixodes ricinus* members, as depicted in the phylogram of **Supplemental Figure 4**, built with a total of 121 sequences showing eight clades with strong bootstrap support, each containing subclades. These clades are composed of sequences originating from the same genus. FUBAR indicated strong positive selection for seven sites RDP analysis indicated six recombination breakpoints (**Supplemental Spreadsheet 4**).

Cystatins

Cystatins are peptide inhibitors of cysteine proteases that are widespread in vertebrates (Abrahamson et al., 2003). They were first found in tick saliva by screening a salivary transcriptome of *I. scapularis* (Ribeiro et al., 2006). Different from lipocalins, metalloproteases, and Kunitz products, salivary cystatins are poorly transcribed. A recombinant peptide indicated its specificity for cathepsin L, and the protein was named sialostatin L. The expected activity was found in the tick saliva and expression of the protein was confirmed by reactive antibodies raised against the recombinant protein (Kotsyfakis et al., 2006). Naturally infested guinea pigs do not develop antibodies against sialostatin L, but vaccination of guinea pigs with sialostatin L reduced the feeding of ticks, and a boost reaction was observed (Kotsyfakis et al., 2008). A second *I. scapularis* salivary cystatin, named sialostatin L2, has been characterized (Chen et al., 2014; Lieskovska et al., 2015a). The effects of sialostatin L and L2 in mammalian immunity has been well-studied (Sa-Nunes et al., 2009; Kotsyfakis et al., 2010; Horka et al., 2012; Schwarz et al., 2012; Bruhl et al., 2014; Chen et al., 2014; Klein et al., 2015; Lieskovska et al., 2015a,b; Wang et al., 2016; Kotal et al., 2019). **Supplemental Figure 5** depicts the phylogram of 82 tick cystatins, which indicates at least 17 clear clades each being mostly genus specific. FUBAR analysis does not recognize any codon site under positive selection, but RDP indicates the existence of one recombination breakpoint (**Supplemental Spreadsheet 4**).

Proteins Possibly Secreted by Alternative Pathways

Supplemental Spreadsheet 3 contains proteins without a classical secretion signal but containing a secretomeP score indicative of secretion via non-classical pathways. Among these there are the subolesins, described in the introduction. Phylogenetic analysis, based on the alignments of 16 coding sequences, shows three clades of FUBAR indicates no sites under positive selection. RDP analysis indicates one recombination breakpoint.

Housekeeping Proteins

Annotation of the SignalP-containing sequences in **Supplemental Spreadsheet 2** by the TSA algorithm identifies 1,931 coding sequences, organized into 80 groups (**Supplemental Table 2** and **Supplemental Spreadsheet 2**) that probably have a housekeeping function associated with the ER or Golgi compartments. Notably, 1,409 sequences representing 72% of the total group of housekeeping sequences are enzymes.

TABLE 3 | Recombination breakpoints and positive selected sites predicted by RDP4 (Martin et al., 2015) and FUBAR (Murrell et al., 2013).

Family	Number of recombination breakpoints	Number of positive selected sites
Lipocalin	11	16
DAP36	6	7
Apyrase	3	1
Metalloprotease	3	0
Cystatin	1	0
Subolesin	1	0

Among these enzymes, 187 code for glycosyltransferases, most probably associated with glycosylating the salivary secretome. The glycosylation of tick salivary proteins has been under scrutiny recently, due to the epidemics of α-Gal allergy triggered by consumption of beef proteins (Commins and Platts-Mills, 2013). Human cases are associated with previous exposure to tick bites, and spatially correlated with tick abundance (Commins et al., 2011; Mateo-Borrega et al., 2019). A recent search for enzymes coding for α-Gal transferases (GALT) in ticks (Cabezas-Cruz et al., 2018) showed that the classical α1-3 GALTs that produce the Galα1-3Galβ1-(3)4GlcNAc-R (α-Gal) are absent in ticks; their function is taken by other transferases of the α1-4 and β1-4 GALT families. These enzymes are recognizable in **Supplemental Spreadsheet 2** by the TSFam group of Glycosyltransferases and subfamily Lactosylceramide 4-alpha-galactosyltransferase. Other previously identified enzymes that are associated with protein modification (Ribeiro et al., 2006; Francischetti et al., 2009) include those promoting proline hydroxylation and tyrosine sulfation. While tyrosine sulfation has been determined in tick salivary anticlotting peptides (Thompson et al., 2017; Watson et al., 2019), proline hydroxylation, a common modification in collagen (Bohmer, 1971), has not been confirmed in ticks despite the high abundance of salivary collagen-like cement proteins that display the motifs triggering proline hydroxylation (Rhoads and Udenfriend, 1969; de Jong et al., 1991; Shimizu et al., 2005). Proteomic studies should include these possible modifications in the databases used for identification of peptide fragments obtained by MS/MS.

DISCUSSION

The TSFam database, and its associated hyperlinked spreadsheets of tick salivary proteins and associated nucleotide sequences, helps the annotation of tick salivary secreted proteins, as well as the retrieval of these sequences for phylogenetic studies. It has been reported that the genes coding for salivary proteins of blood sucking arthropods show high evolutionary rates; either due to the relaxed constraint of the genes allowing for less negative selection pressure, or for the more rare occurrence of positive selection (Daix et al., 2007; Schroeder et al., 2007; Decrem et al., 2008; Dai et al., 2012; Arca et al., 2014; Mans et al., 2017). The phylogenetic analysis, derived from the alignment of tick salivary coding sequences from the lipocalin, metalloprotease, cystatin, apyrase, DAP36, and subolesin families (**Supplemental Figures 1–6** and **Table 3**), indicate a high number of recombination breakpoints on the genes coding for lipocalins (11 sites) and DAP36 (6 sites); three recombination breakpoint sites for the apyrase and metalloproteases; and one recombination breakpoint on the genes coding for the cystatins and subolesin. No positive selection sites were identified for the metalloprotease, cystatin, and subolesin genes. It is to be noted that the occurrence of recombination breakpoints could lead to false predictions of positive selected sites (Posada and Crandall, 2002; Bay and Bielawski, 2011). While positive selection is associated with fast gene evolution and divergence, intragenic recombination can strongly contribute to genome diversity among individuals, a situation that might be occurring within the lipocalin and DAP36 coding genes (Lauer et al., 2018; Olabode et al., 2019; Salim et al., 2019). As a note of caution, it should be considered that the diversity of transcripts from these multi-gene families could be artifactual due to the "*de novo*" assembly from small reads which could create false recombinant assemblies (Salmon et al., 2010). I A possible way to verify the frequency of these artifacts would be to compare the resulting lipocalin transcripts derived from single tick transcriptomes to those derived from the combined libraries. On the other hand, if recombination exists and leads to new protein variants, is it a classical meiotic recombination derived from a high number of intra-genic breakpoints, or does it occur in a somatic environment, such as occurs with vertebrate immunoglobulins This question could be answered by attempting the genome mapping of each transcript and identifying whether the transcript derives from a mosaic of exons or a "well-behaved" sequence of exons.

DATA AVAILABILITY STATEMENT

The datasets presented in this study can be found in online repositories. The names of the repository/repositories and accession number(s) can be found in the article/**Supplementary Material**.

AUTHOR CONTRIBUTIONS

JR conceived the work and did the bioinformatic analysis. BM contributed in the data analysis and interpretation. All authors contributed to writing the manuscript.

FUNDING

JR was supported by the Intramural Research Program of the National Institute of Allergy and Infectious Diseases (Vector-Borne Diseases: Biology of Vector Host Relationship, Z01 AI000810-19). BM was supported by the National Research Foundation of South Africa (Grant No. 118540).

ACKNOWLEDGMENTS

This work utilized the computational resources of the NIH HPC Biowulf cluster (http://hpc.nih.gov). We are grateful to helpful comments on the manuscript by Drs. Lucas Tirloni and John Andersen. We would like to thank Brian Brown, NIH Library Editing Service, for reviewing the manuscript.

SUPPLEMENTARY MATERIAL

The Supplementary Material for this article can be found online at: https://www.frontiersin.org/articles/10.3389/fcimb.2020.00374/full#supplementary-material

REFERENCES

Abrahamson, M., Alvarez-Fernandez, M., and Nathanson, C. M. (2003). Cystatins. *Biochem. Soc. Symp*. 70, 179–199. doi: 10.1042/bss0700179

Altschul, S. F., Madden, T. L., Schaffer, A. A., Zhang, J., Zhang, Z., Miller, W., et al. (1997). Gapped BLAST and PSI-BLAST: a new generation of protein database search programs. *Nucleic Acids Res*. 25, 3389–3402. doi: 10.1093/nar/25.17.3389

Alvarenga, P. H., Francischetti, I. M., Calvo, E., Sa-Nunes, A., Ribeiro, J. M., and Andersen, J. F. (2010). The function and three-dimensional structure of a thromboxane A_2/cysteinyl leukotriene-binding protein from the saliva of a mosquito vector of the malaria parasite. *PLoS Biol*. 8:e1000547. doi: 10.1371/journal.pbio.1000547

Andersen, J. F., Hinnebusch, B. J., Lucas, D. A., Conrads, T. P., Veenstra, T. D., Pham, V. M., et al. (2007). An insight into the sialome of the oriental rat flea, *Xenopsylla cheopis* (rots). *BMC Genomics* 8:102. doi: 10.1186/1471-2164-8-102

Andersen, J. F., and Ribeiro, J. M. (2017). "Chapter 4 - Salivary kratagonists: scavengers of host physiological effectors during blood feeding," in *Arthropod Vector: Controller of Disease Transmission* (London: Elsevier), 51–63. doi: 10.1016/B978-0-12-805360-7.00004-6

Arca, B., Lombardo, F., Struchiner, C. J., and Ribeiro, J. M. (2017). Anopheline salivary protein genes and gene families: an evolutionary overview after the whole genome sequence of sixteen *Anopheles* species. *BMC Genomics* 18:153. doi: 10.1186/s12864-017-3579-8

Arca, B., Struchiner, C. J., Pham, V. M., Sferra, G., Lombardo, F., Pombi, M., et al. (2014). Positive selection drives accelerated evolution of mosquito salivary genes associated with blood-feeding. *Insect Mol. Biol*. 23, 122–131. doi: 10.1111/imb.12068

Bay, R. A., and Bielawski, J. P. (2011). Recombination detection under evolutionary scenarios relevant to functional divergence. *J. Mol. Evol*. 73, 273–286. doi: 10.1007/s00239-011-9473-0

Becker, M., Felsberger, A., Frenzel, A., Shattuck, W. M. C., Dyer, M., Kugler, J., et al. (2015). Application of M13 phage display for identifying immunogenic proteins from tick (*Ixodes scapularis*) saliva. *BMC Biotechnol*. 15:43. doi: 10.1186/s12896-015-0167-3

Bendtsen, J. D., Jensen, L. J., Blom, N., Von Heijne, G., and Brunak, S. (2004). Feature-based prediction of non-classical and leaderless protein secretion. *Protein Eng. Des. Sel*. 17, 349–356. doi: 10.1093/protein/gzh037

Bergman, D. K., Ramachandra, R. N., and Wikel, S. K. (1995). *Dermacentor andersoni*: salivary gland proteins suppressing T-lymphocyte responses to concanavalin A *in vitro*. *Exp. Parasitol*. 81, 262–271. doi: 10.1006/expr.1995.1117

Bergman, D. K., Ramachandra, R. N., and Wikel, S. K. (1998). Characterization of an immunosuppressant protein from *Dermacentor andersoni* (*Acari: Ixodidae*) salivary glands. *J. Med. Entomol*. 35, 505–509. doi: 10.1093/jmedent/35.4.505

Binnington, K. C., and Kemp, D. H. (1980). Role of tick salivary glands in feeding and disease transmission. *Adv. Parasitol*. 18, 316–340. doi: 10.1016/S0065-308X(08)60403-0

Bohmer, T. (1971). The biosynthesis of collagen. *Acta Rheumatol. Scand*. 17, 209–222. doi: 10.3109/rhe1.1971.17.issue-1-4.28

Bowman, A. S., and Sauer, J. R. (2004). Tick salivary glands: function, physiology and future. *Parasitology* 129 (Suppl), S67–81. doi: 10.1017/S0031182004006468

Bruhl, T. J., Klein, M., Staudt, V., Reuter, S., Grebe, N., Gerlitzki, B., et al. (2014). A new target for the treatment of mast cell dependent asthma? *Respirology* 19:14. doi: 10.1111/resp.12257

Cabezas-Cruz, A., Espinosa, P. J., Alberdi, P., Simo, L., Valdes, J. J., Mateos-Hernandez, L., et al. (2018). Tick galactosyltransferases are involved in alpha-Gal synthesis and play a role during *Anaplasma phagocytophilum* infection and Ixodes scapularis tick vector development. *Sci. Rep*. 8:14224. doi: 10.1038/s41598-018-32664-z

Calvo, E., Mans, B. J., Ribeiro, J. M., and Andersen, J. F. (2009). Multifunctionality and mechanism of ligand binding in a mosquito antiinflammatory protein. *Proc. Natl. Acad. Sci. U.S.A*. 106, 3728–3733. doi: 10.1073/pnas.0813190106

Champagne, D. E., Smartt, C. T., Ribeiro, J. M., and James, A. A. (1995). The salivary gland-specific apyrase of the mosquito *Aedes aegypti* is a member of the 5'-nucleotidase family. *Proc. Natl. Acad. Sci. U.S.A*. 92, 694–698. doi: 10.1073/pnas.92.3.694

Chavez, A. S. O., O'Neal, A. J., Santambrogio, L., Kotsyfakis, M., and Pedra, J. H. F. (2019). Message in a vesicle - trans-kingdom intercommunication at the vector-host interface. *J. Cell Sci*. 132:jcs224212. doi: 10.1242/jcs.224212

Chen, G., Wang, X., Severo, M. S., Sakhon, O. S., Sohail, M., Brown, L. J., et al. (2014). The tick salivary protein sialostatin L2 inhibits caspase-1-mediated inflammation during *Anaplasma phagocytophilum* infection. *Infect. Immun*. 82, 2553–2564. doi: 10.1128/IAI.01679-14

Commins, S. P., James, H. R., Kelly, L. A., Pochan, S. L., Workman, L. J., Perzanowski, M. S., et al. (2011). The relevance of tick bites to the production of IgE antibodies to the mammalian oligosaccharide galactose-alpha-1,3-galactose. *J. Allerg. Clin. Immunol*. 127, 1286–1293 E1286. doi: 10.1016/j.jaci.2011.02.019

Commins, S. P., and Platts-Mills, T. A. E. (2013). Tick bites and red meat allergy. *Curr. Opin. Allergy Clin. Immunol*. 13, 354–359. doi: 10.1097/ACI.0b013e3283624560

Coons, L. B., and Roshdy, M. A. (1981). Ultrastructure of granule secretion in salivary glands of *Argas (Persicargas) arboreus* during feeding. *Parasitol. Res*. 65, 225–234. doi: 10.1007/BF00929188

Dai, J., Wang, P., Adusumilli, S., Booth, C. J., Narasimhan, S., Anguita, J., et al. (2009). Antibodies against a tick protein, Salp15, protect mice from the Lyme disease agent. *Cell Host Microbe* 6, 482–492. doi: 10.1016/j.chom.2009.10.006

Dai, S. X., Zhang, A. D., and Huang, J. F. (2012). Evolution, expansion and expression of the Kunitz/BPTI gene family associated with long-term blood feeding in *Ixodes* Scapularis. *BMC Evol. Biol*. 12:4. doi: 10.1186/1471-2148-12-4

Daix, V., Schroeder, H., Praet, N., Georgin, J. P., Chiappino, I., Gillet, L., et al. (2007). *Ixodes* ticks belonging to the *Ixodes ricinus* complex encode a family of anticomplement proteins. *Insect Mol. Biol*. 16, 155–166. doi: 10.1111/j.1365-2583.2006.00710.x

Das, S., Banerjee, G., DePonte, K., Marcantonio, N., Kantor, F. S., and Fikrig, E. (2001). Salp25D, an *Ixodes scapularis* antioxidant, is 1 of 14 immunodominant antigens in engorged tick salivary glands. *J. Infect. Dis*. 184, 1056–1064. doi: 10.1086/323351

de Jong, L., van der Kraan, I., and de Waal, A. (1991). The kinetics of the hydroxylation of procollagen by prolyl 4-hydroxylase. Proposal for a processive mechanism of binding of the dimeric hydroxylating enzyme in relation to the high kcat/Km ratio and a conformational requirement for hydroxylation of -X-Pro-Gly- sequences. *Biochim. Biophys. Acta* 1079, 103–111. doi: 10.1016/0167-4838(91)90030-4

de la Fuente, J., Almazan, C., Blas-Machado, U., Naranjo, V., Mangold, A. J., Blouin, E. F., et al. (2006). The tick protective antigen, 4D8, is a conserved protein involved in modulation of tick blood ingestion and reproduction. *Vaccine* 24, 4082–4095. doi: 10.1016/j.vaccine.2006.02.046

de la Fuente, J., Moreno-Cid, J. A., Canales, M., Villar, M., de la Lastra, J. M. P., Kocan, K. M., et al. (2011). Targeting arthropod subolesin/akirin for the development of a universal vaccine for control of vector infestations and pathogen transmission. *Vet. Parasitol*. 181, 17–22. doi: 10.1016/j.vetpar.2011.04.018

Decrem, Y., Beaufays, J., Blasioli, V., Lahaye, K., Brossard, M., Vanhamme, L., et al. (2008). A family of putative metalloproteases in the salivary glands of the tick *Ixodes ricinus*. *FEBS J*. 275, 1485–1499. doi: 10.1111/j.1742-4658.2008.06308.x

Duckert, P., Brunak, S., and Blom, N. (2004). Prediction of proprotein convertase cleavage sites. *Protein Eng. Des. Sel*. 17, 107–112. doi: 10.1093/protein/gzh013

Edgar, R. C. (2004). MUSCLE: multiple sequence alignment with high accuracy and high throughput. *Nucleic Acids Res*. 32, 1792–1797. doi: 10.1093/nar/gkh340

Farkas, R. (2015). Apocrine secretion: new insights into an old phenomenon. *BBA Gen. Subj*. 1850, 1740–1750. doi: 10.1016/j.bbagen.2015.05.003

Francischetti, I. M. B., Sa-Nunes, A., Mans, B. J., Santos, I. M., and Ribeiro, J. M. C. (2009). The role of saliva in tick feeding. *Front. Biosci*. 14, 2051–2088. doi: 10.2741/3363

Friesen, K. J., and Kaufman, W. R. (2009). Salivary gland degeneration and vitellogenesis in the ixodid tick *Amblyomma hebraeum*: surpassing a critical weight is the prerequisite and detachment from the host is the trigger. *J. Insect Physiol*. 55, 936–942. doi: 10.1016/j.jinsphys.2009.06.007

Garcia, G. R., Maruyama, S. R., Nelson, K. T., Ribeiro, J. M. C., Gardinassi, L. G., Maia, A. A. M., et al. (2017). Immune recognition of salivary proteins from the cattle tick *Rhipicephalus microplus* differs according to the genotype of the bovine host. *Parasit. Vector* 10:144. doi: 10.1186/s13071-017-2077-9

Guglielmone, A. A., Robbins, R. G., Apanaskevich, D. A., Petney, T. N., Estrada-Pena, A., Horak, I. G., et al. (2010). The *Argasidae*, *Ixodidae* and *Nuttalliellidae* (*Acari: Ixodida*) of the world: a list of valid species names. *Zootaxa* 10, 95–136. doi: 10.11646/zootaxa.2528.1.1

Gulia-Nuss, M., Nuss, A. B., Meyer, J. M., Sonenshine, D. E., Roe, R. M., Waterhouse, R. M., et al. (2016). Genomic insights into the *Ixodes scapularis* tick vector of Lyme disease. *Nat. Commun.* 7:10507. doi: 10.1038/ncomms10507

Hackenberg, M., and Kotsyfakis, M. (2018). Exosome-mediated pathogen transmission by arthropod vectors. *Trends Parasitol.* 34, 549–552. doi: 10.1016/j.pt.2018.04.001

Hansen, J. E., Lund, O., Tolstrup, N., Gooley, A. A., Williams, K. L., and Brunak, S. (1998). NetOglyc: prediction of mucin type O-glycosylation sites based on sequence context and surface accessibility. *Glycoconj. J.* 15, 115–130. doi: 10.1023/A:1006960004440

Harris, R. A., and Kaufman, W. R. (1981)Hormonal control of salivary gland degeneration in the ixodid tick *Amblyomma hebraeum*. *J. Insect Physiol.* 27, 241–248. doi: 10.1016/0022-1910(81)90057-3

Holt, R. A., Subramanian, G. M., Halpern, A., Sutton, G. G., Charlab, R., Nusskern, D. R., et al. (2002). The genome sequence of the malaria mosquito *Anopheles gambiae*. *Science* 298, 129–149. doi: 10.1126/science.1077061

Horka, H., Staudt, V., Klein, M., Taube, C., Reuter, S., Dehzad, N., et al. (2012). Inhibits the Th9-derived production of the asthma-promoting cytokine IL-9 and is effective in the prevention of experimental asthma. *J. Immunol.* 188, 2669–2676. doi: 10.4049/jimmunol.1100529

Julenius, K., Molgaard, A., Gupta, R., and Brunak, S. (2005). Prediction, conservation analysis, and structural characterization of mammalian mucin-type O-glycosylation sites. *Glycobiology* 15, 153–164. doi: 10.1093/glycob/cwh151

Kalyana-Sundaram, S., Kumar-Sinha, C., Shankar, S., Robinson, D. R., Wu, Y.-M., Cao, X., et al. (2012). Expressed pseudogenes in the transcriptional landscape of human cancers. *Cell* 149, 1622–1634. doi: 10.1016/j.cell.2012.04.041

Karim, S., and Ribeiro, J. M. (2015). An Insight into the sialome of the Lone Star tick, *Amblyomma americanum*, with a glimpse on its time dependent gene expression. *PLoS ONE* 10:e0131292. doi: 10.1371/journal.pone.0131292

Keller, S., Sanderson, M. P., Stoeck, A., and Altevogt, P. (2006). Exosomes: from biogenesis and secretion to biological function. *Immunol. Lett.* 107, 102–108. doi: 10.1016/j.imlet.2006.09.005

Kivirikko, K. I., Kishida, Y., Sakakibara, S., and Prockop, D. J. (1972). Hydroxylation of (X-Pro-Gly)n by protocollagen proline hydroxylase. Effect of chain length, helical conformation and amino acid sequence in the substrate. *Biochim. Biophys. Acta* 271, 347–356. doi: 10.1016/0005-2795(72)90209-7

Klein, M., Bruhl, T. J., Staudt, V., Reuter, S., Grebe, N., Gerlitzki, B., et al. (2015). Tick salivary sialostatin L represses the initiation of immune responses by targeting IRF4-dependent transcription in murine mast cells. *J. Immunol.* 195, 621–631. doi: 10.4049/jimmunol.1401823

Kotal, J., Stergiou, N., Busa, M., Chlastakova, A., Berankova, Z., Rezacova, P., et al. (2019). The structure and function of Iristatin, a novel immunosuppressive tick salivary cystatin. *Cell. Mol. Life Sci.* 76, 2003–2013. doi: 10.1007/s00018-019-03034-3

Kotsyfakis, M., Anderson, J. M., Andersen, J. F., Calvo, E., Francischetti, I. M., Mather, T. N., et al. (2008). Cutting edge: Immunity against a "silent" salivary antigen of the Lyme vector *Ixodes scapularis* impairs its ability to feed. *J. Immunol.* 181, 5209–5212. doi: 10.4049/jimmunol.181.8.5209

Kotsyfakis, M., Horka, H., Salat, J., and Andersen, J. F. (2010). The crystal structures of two salivary cystatins from the tick *Ixodes scapularis* and the effect of these inhibitors on the establishment of *Borrelia burgdorferi* infection in a murine model. *Mol. Microbiol.* 77, 456–470. doi: 10.1111/j.1365-2958.2010.07220.x

Kotsyfakis, M., Sa-Nunes, A., Francischetti, I. M., Mather, T. N., Andersen, J. F., and Ribeiro, J. M. (2006). Antiinflammatory and immunosuppressive activity of sialostatin L, a salivary cystatin from the tick *Ixodes scapularis*. *J. Biol. Chem.* 281, 26298–26307. doi: 10.1074/jbc.M513010200

Kumar, S., Stecher, G., and Tamura, K. (2016). MEGA7: molecular evolutionary genetics analysis version 7.0 for bigger datasets. *Mol. Biol. Evol.* 33, 1870–1874. doi: 10.1093/molbev/msw054

Larkin, M. A., Blackshields, G., Brown, N. P., Chenna, R., McGettigan, P. A., McWilliam, H., et al. (2007). Clustal W and clustal X version 2.0. *Bioinformatics* 23, 2947–2948. doi: 10.1093/bioinformatics/btm404

Lauer, S., Avecilla, G., Spealman, P., Sethia, G., Brandt, N., Levy, S. F., et al. (2018). Single-cell copy number variant detection reveals the dynamics and diversity of adaptation. *PLoS Biol.* 16:e3000069. doi: 10.1371/journal.pbio.3000069

Lewis, L. A., Radulovic, Z. M., Kim, T. K., Porter, L. M., and Mulenga, A. (2015). Identification of 24 h *Ixodes scapularis* immunogenic tick saliva proteins. *Ticks Tick Borne Dis.* 6, 424–434. doi: 10.1016/j.ttbdis.2015.03.012

Lieskovska, J., Palenikova, J., Langhansova, H., Campos Chagas, A., Calvo, E., Kotsyfakis, M., et al. (2015a). Tick sialostatins L and L2 differentially influence dendritic cell responses to *Borrelia* spirochetes. *Parasit. Vectors* 8:275. doi: 10.1186/s13071-015-0887-1

Lieskovska, J., Palenikova, J., Sirmarova, J., Elsterova, J., Kotsyfakis, M., Campos Chagas, A., et al. (2015b). Tick salivary cystatin sialostatin L2 suppresses IFN responses in mouse dendritic cells. *Parasit. Immunol.* 37, 70–78. doi: 10.1111/pim.12162

Mans, B. J. (2011). Evolution of vertebrate hemostatic and inflammatory control mechanisms in blood-feeding arthropods. *J. Innate Immun.* 3, 41–51. doi: 10.1159/000321599

Mans, B. J., Calvo, E., Ribeiro, J. M., and Andersen, J. F. (2007). The crystal structure of D7r4, a salivary biogenic amine-binding protein from the malaria mosquito *Anopheles gambiae*. *J. Biol. Chem.* 282, 36626–36633. doi: 10.1074/jbc.M706410200

Mans, B. J., Featherston, J., de Castro, M. H., and Pienaar, R. (2017). Gene duplication and protein evolution in tick-host interactions. *Front. Cell. Infect. Microbiol.* 7:413. doi: 10.3389/fcimb.2017.00413

Martin, D., and Rybicki, E. (2000). RDP: detection of recombination amongst aligned sequences. *Bioinformatics* 16, 562–563. doi: 10.1093/bioinformatics/16.6.562

Martin, D. P., Murrell, B., Golden, M., Khoosal, A., and Muhire, B. (2015). RDP4: Detection and analysis of recombination patterns in virus genomes. *Virus Evol.* 1:vev003. doi: 10.1093/ve/vev003

Mateo-Borrega, M. B., Garcia, B., Larramendi, C. H., Azofra, J., Gonzalez-Mancebo, E., Alvarado, M. I., et al. (2019). IgE-mediated sensitization to galactose-alpha-1,3-Galactose (alpha-Gal) in urticaria and anaphylaxis in Spain: geographical variations and risk factors. *J. Invest. Allerg. Clin.* 29, 436–443. doi: 10.18176/jiaci.0373

Mulenga, A., Macaluso, K. R., Simser, J. A., and Azad, A. F. (2003). The American dog tick, *Dermacentor variabilis*, encodes a functional histamine release factor homolog. *Insect Biochem. Mol. Biol.* 33, 911–919. doi: 10.1016/S0965-1748(03)00097-3

Murrell, B., Moola, S., Mabona, A., Weighill, T., Sheward, D., Pond, S. L. K., et al. (2013). FUBAR: a fast, unconstrained bayesian approximation for inferring selection. *Mol. Biol. Evol.* 30, 1196–1205. doi: 10.1093/molbev/mst030

Narasimhan, S., Deponte, K., Marcantonio, N., Liang, X., Royce, T. E., Nelson, K. F., et al. (2007). Immunity against *Ixodes scapularis* salivary proteins expressed within 24 hours of attachment thwarts tick feeding and impairs *Borrelia* transmission. *PloS oNE* 2:E451. doi: 10.1371/journal.pone.0000451

Neafsey, D. E., Waterhouse, R. M., Abai, M. R., Aganezov, S. S., Alekseyev, M. A., Allen, J. E., et al. (2015). Mosquito genomics. Highly evolvable malaria vectors: the genomes of 16 Anopheles mosquitoes. *Science* 347:1258522. doi: 10.1126/science.1258522

Nicholas, H. B, Jr., Chan, S. S., and Rosenquist, G. L. (1999). Reevaluation of the determinants of tyrosine sulfation. *Endocrine* 11, 285–292. doi: 10.1385/ENDO:11:3:285

Nielsen, H., Brunak, S., and von Heijne, G. (1999). Machine learning approaches for the prediction of signal peptides and other protein sorting signals. *Protein Eng.* 12, 3–9. doi: 10.1093/protein/12.1.3

Olabode, A. S., Avino, M., Ng, G. T., Abu-Sardanah, F., Dick, D. W., and Poon, A. F. Y. (2019). Evidence for a recombinant origin of HIV-1 Group M from genomic variation. *Virus Evol.* 5:vey039. doi: 10.1093/ve/vey039

Perner, J., Kropackova, S., Kopacek, P., and Ribeiro, J. M. C. (2018). Sialome diversity of ticks revealed by RNAseq of single tick salivary glands. *PLoS Negl. Trop. Dis.* 12:e0006410. doi: 10.1371/journal.pntd.0006410

Pierleoni, A., Martelli, P. L., and Casadio, R. (2008). PredGPI: a GPI-anchor predictor. *BMC Bioinformatics* 9:392. doi: 10.1186/1471-2105-9-392

Pond, S. L., Frost, S. D., and Muse, S. V. (2005). HyPhy: hypothesis testing using phylogenies. *Bioinformatics* 21, 676–679. doi: 10.1093/bioinformatics/bti079

Posada, D., and Crandall, K. A. (2002). The effect of recombination on the accuracy of phylogeny estimation. *J. Mol. Evol.* 54, 396–402. doi: 10.1007/s00239-001-0034-9

Radulovic, Z. M., Kim, T. K., Porter, L. M., Sze, S. H., Lewis, L., and Mulenga, A. (2014). A 24-48 h fed *Amblyomma americanum* tick saliva immuno-proteome. *BMC Genomics* 15:518. doi: 10.1186/1471-2164-15-518

Rhoads, R. E., and Udenfriend, S. (1969). Substrate specificity of collagen proline hydroxylase: hydroxylation of a specific proline residue in bradykinin. *Arch. Biochem. Biophys.* 133, 108–111. doi: 10.1016/0003-9861(69)90493-7

Ribeiro, J. M., Alarcon-Chaidez, F., Francischetti, I. M., Mans, B. J., Mather, T. N., Valenzuela, J. G., et al. (2006). An annotated catalog of salivary gland transcripts from *Ixodes scapularis* ticks. *Insect Biochem. Mol. Biol.* 36, 111–129. doi: 10.1016/j.ibmb.2005.11.005

Ribeiro, J. M., Assumpcao, T. C., Ma, D., Alvarenga, P. H., Pham, V. M., Andersen, J. F., et al. (2012). An insight into the sialotranscriptome of the cat flea, *Ctenocephalides felis*. *PLoS ONE* 7:e44612. doi: 10.1371/journal.pone.0044612

Ribeiro, J. M., and Francischetti, I. M. (2003). Role of arthropod saliva in blood feeding: sialome and post-sialome perspectives. *Annu. Rev. Entomol.* 48, 73–88. doi: 10.1146/annurev.ento.48.060402.102812

Ribeiro, J. M., Mans, B. J., and Arca, B. (2010). An insight into the sialome of blood-feeding *Nematocera*. *Insect Biochem. Mol. Biol.* 40, 767–784. doi: 10.1016/j.ibmb.2010.08.002

Ribeiro, J. M. C., and Arca, B. (2009). From sialomes to the sialoverse: An insight into the salivary potion of blood feeding insects. *Adv Insect Physiol* 37, 59–118.. doi: 10.1016/S0065-2806(09)37002-2

Salim, B., Amin, M., Igarashi, M., Ito, K., Jongejan, F., Katakura, K., et al. (2019). Recombination and purifying and balancing selection determine the evolution of major antigenic protein 1 (map 1) family genes in *Ehrlichia* ruminantium. *Gene* 683, 216–224. doi: 10.1016/j.gene.2018.10.028

Salmon, A., Flagel, L., Ying, B., Udall, J. A., and Wendel, J. F. (2010). Homoeologous nonreciprocal recombination in polyploid cotton. *New Phytol.* 186, 123–134. doi: 10.1111/j.1469-8137.2009.03093.x

Sa-Nunes, A., Bafica, A., Antonelli, L. R., Choi, E. Y., Francischetti, I. M., Andersen, J. F., et al. (2009). The immunomodulatory action of sialostatin L on dendritic cells reveals its potential to interfere with autoimmunity. *J. Immunol.* 182, 7422–7429. doi: 10.4049/jimmunol.0900075

Schaffer, A. A., Aravind, L., Madden, T. L., Shavirin, S., Spouge, J. L., Wolf, Y. I., et al. (2001). Improving the accuracy of PSI-BLAST protein database searches with composition-based statistics and other refinements. *Nucleic Acids Res.* 29, 2994–3005. doi: 10.1093/nar/29.14.2994

Schroeder, H., Daix, V., Gillet, L., Renauld, J. C., and Vanderplasschen, A. (2007). The paralogous salivary anti-complement proteins IRAC I and IRAC II encoded by *Ixodes ricinus* ticks have broad and complementary inhibitory activities against the complement of different host species. *Microbes Infect* 9, 247–250. doi: 10.1016/j.micinf.2006.10.020

Schuijt, T., Dai, J. F., van Dam, A., van de Poll, T., and Fikrig, E. (2010). The tick salivary protein Salp9-like inhibits complement-mediated killing of *Borrelia burgdorferi* sensu lato isolates. *Inflamm. Res.* 59, S23–S23. doi: 10.1128/IAI.00232-08

Schwarz, A., Valdes, J. J., and Kotsyfakis, M. (2012). The role of cystatins in tick physiology and blood feeding. *Ticks Tick Borne Dis.* 3, 117–127. doi: 10.1016/j.ttbdis.2012.03.004

Shimizu, M., Igasaki, T., Yamada, M., Yuasa, K., Hasegawa, J., Kato, T., et al. (2005). Experimental determination of proline hydroxylation and hydroxyproline arabinogalactosylation motifs in secretory proteins. *Plant J.* 42, 877–889. doi: 10.1111/j.1365-313X.2005.02419.x

Sonnhammer, E. L., von Heijne, G., and Krogh, A. (1998). A hidden Markov model for predicting transmembrane helices in protein sequences. *Proc. Int. Conf. Intell. Syst. Mol. Biol.* 6, 175–182.

Stutzer, C., Mans, B. J., Gaspar, A. R., Neitz, A. W., and Maritz-Olivier, C. (2009). *Ornithodoros savignyi:* soft tick apyrase belongs to the 5'-nucleotidase family. *Exp. Parasitol.* 122, 318–327. doi: 10.1016/j.exppara.2009.04.007

Tan, A. W., Francischetti, I. M., Slovak, M., Kini, R. M., and Ribeiro, J. M. (2015). Sexual differences in the sialomes of the zebra tick, *Rhipicephalus pulchellus*. *J. Proteomics* 117, 120–144. doi: 10.1016/j.jprot.2014.12.014

Tatusov, R. L., Fedorova, N. D., Jackson, J. D., Jacobs, A. R., Kiryutin, B., Koonin, E. V., et al. (2003). The COG database: an updated version includes eukaryotes. *BMC Bioinformatics* 4:41. doi: 10.1186/1471-2105-4-41

Thompson, R. E., Liu, X. Y., Ripoll-Rozada, J., Alonso-Garcia, N., Parker, B. L., Pereira, P. J. B., et al. (2017). Tyrosine sulfation modulates activity of tick-derived thrombin inhibitors. *Nat. Chem.* 9, 909–917. doi: 10.1038/nchem.2744

Valenzuela, J. G., Charlab, R., Gonzalez, E. C., de Miranda-Santos, I. K., Marinotti, O., Francischetti, I. M., et al. (2002a). The D7 family of salivary proteins in blood sucking diptera. *Insect Mol. Biol.* 11, 149–155. doi: 10.1046/j.1365-2583.2002.00319.x

Valenzuela, J. G., Francischetti, I. M. B., Pham, V. M., Garfield, M. K., Mather, T. N., and Ribeiro, J. M. C. (2002b). Exploring the sialome of the tick, *Ixodes scapularis*. *J. Exp. Biol* 205, 2843–2864.

Wang, X., Shaw, D. K., Sakhon, O. S., Snyder, G. A., Sundberg, E. J., Santambrogio, L., et al. (2016). The tick protein sialostatin L2 binds to annexin A2 and inhibits NLRC4-mediated inflammasome activation. *Infect. Immun.* 84, 1796–1805. doi: 10.1128/IAI.01526-15

Watson, E. E., Ripoll-Rozada, J., Lee, A. C., Wu, M. C. L., Franck, C., Pasch, T., et al. (2019). Rapid assembly and profiling of an anticoagulant sulfoprotein library. *Procee. Natl. Acad. Sci. U.S. A.* 116, 13873–13878. doi: 10.1073/pnas.1905177116

Xiao, B., Yang, Z. M., Xiao, M., Chen, H., and Ma, Q. (2017). The structure and biological functions of translationally controlled tumor protein and its role in tumor progression. *Prog Biochem Biophys.* 44, 148–154.

Zhou, W. S., Woodson, M., Neupane, B., Bai, F. W., Sherman, M. B., Choi, K. H., et al. (2018). Exosomes serve as novel modes of tick-borne flavivirus transmission from arthropod to human cells and facilitates dissemination of viral RNA and proteins to the vertebrate neuronal cells. *PLoS Pathog* 14:e1006764. doi: 10.1371/journal.ppat.1006764

Conflict of Interest: The authors declare that the research was conducted in the absence of any commercial or financial relationships that could be construed as a potential conflict of interest.

frontiers in Cellular and Infection Microbiology

ORIGINAL RESEARCH
published: 29 July 2020
doi: 10.3389/fcimb.2020.00377

IgG Antibody Responses to the *Aedes albopictus* 34k2 Salivary Protein as Novel Candidate Marker of Human Exposure to the Tiger Mosquito

Sara Buezo Montero[1], *Paolo Gabrieli*[2†], *Fabrizio Montarsi*[3], *Alessio Borean*[4], *Stefano Capelli*[4], *Giustina De Silvestro*[5], *Federico Forneris*[2], *Marco Pombi*[1], *Antonio Breda*[6], *Gioia Capelli*[3] *and Bruno Arcà*[1*]

[1] *Division of Parasitology, Department of Public Health and Infectious Diseases, Sapienza University of Rome, Rome, Italy,* [2] *Department of Biology and Biotechnology "L. Spallanzani", University of Pavia, Pavia, Italy,* [3] *Laboratory of Parasitology, Istituto Zooprofilattico Sperimentale delle Venezie, Legnaro, Italy,* [4] *Department of Immunohematology and Transfusion Medicine, San Martino Hospital, Belluno, Italy,* [5] *Department of Transfusion Medicine, Padua University Hospital, Padova, Italy,* [6] *Coordinamento Regionale Attività Trasfusionali (CRAT), Padova, Italy*

Mosquitoes of the *Aedes* genus transmit arboviruses of great importance to human health as dengue, chikungunya, Zika and yellow fever. The tiger mosquito *Aedes albopictus* can play an important role as arboviral vector, especially when *Aedes aegypti* is absent or present at low levels. Remarkably, the rapid worldwide spreading of the tiger mosquito is expanding the risk of arboviral transmission also to temperate areas, and the autochthonous cases of chikungunya, dengue and Zika in Europe emphasize the need for improved monitoring and control. Proteomic and transcriptomic studies on blood feeding arthropod salivary proteins paved the way toward the exploitation of genus-specific mosquito salivary proteins for the development of novel tools to evaluate human exposure to mosquito bites. We previously found that the culicine-specific 34k2 salivary protein from *Ae. albopictus* (al34k2) evokes specific IgG responses in experimentally exposed mice, and provided preliminary evidence of its immunogenicity to humans. In this study we measured IgG responses to al34k2 and to *Ae. albopictus* salivary gland protein extracts (SGE) in individuals naturally exposed to the tiger mosquito. Sera were collected in two areas of Northeast Italy (Padova and Belluno) during two different time periods: at the end of the low- and shortly after the high-density mosquito seasons. Anti-SGE and anti-al34k2 IgG levels increased after the summer period of exposure to mosquito bites and were higher in Padova as compared to Belluno. An age-dependent decrease of anti-saliva IgG responses was found especially in Padova, an area with at least 25 years history of *Ae. albopictus* colonization. Moreover, a weak correlation between anti-saliva IgG levels and individual perception of mosquito bites by study participants was found. Finally, determination of anti-al34k2 IgG1 and IgG4 levels indicated a large predominance of IgG1 antibodies. Overall, this study provides a convincing

OPEN ACCESS

Edited by:
Itabajara Silva Vaz, Federal University of Rio Grande do Sul, Brazil

Reviewed by:
Jessica E. Manning, National Institute of Allergy and Infectious Diseases (NIH), United States
Fabiano Oliveira, National Institute of Allergy and Infectious Diseases (NIH), United States

***Correspondence:**
Bruno Arcà
bruno.arca@uniroma1.it

†Present address:
Paolo Gabrieli, Department of Biosciences, University of Milan, Milan, Italy

Specialty section:
This article was submitted to Parasite and Host, a section of the journal Frontiers in Cellular and Infection Microbiology

Received: *10 March 2020*
Accepted: *18 June 2020*
Published: *29 July 2020*

Citation:
Buezo Montero S, Gabrieli P, Montarsi F, Borean A, Capelli S, De Silvestro G, Forneris F, Pombi M, Breda A, Capelli G and Arcà B (2020) IgG Antibody Responses to the Aedes albopictus 34k2 Salivary Protein as Novel Candidate Marker of Human Exposure to the Tiger Mosquito. Front. Cell. Infect. Microbiol. 10:377. doi: 10.3389/fcimb.2020.00377

indication that antibody responses to al34k2 may be regarded as a reliable candidate marker to detect temporal and/or spatial variation of human exposure to *Ae. albopictus*; a serological tool of this kind may prove useful both for epidemiological studies and to estimate the effectiveness of anti-vectorial measures.

Keywords: *Aedes albopictus*, 34k2 salivary protein, human exposure, marker, vector control, arboviruses, epidemiological tool

INTRODUCTION

Arboviruses as dengue, chikungunya, Zika and yellow fever have been responsible for severe outbreaks in the last decades, causing tens of thousands deaths per year with heavy public health impact and important global economic losses (Wilder-Smith et al., 2017). These four major arboviruses are transmitted by mosquitoes of the *Aedes* genus, with the most important competent vectors being by far the yellow fever mosquito *Aedes aegypti* and the tiger mosquito *Aedes albopictus*. Due to globalization and environmental changes, their distribution is rapidly and progressively expanding into new tropical, subtropical and temperate areas (Kraemer et al., 2015, 2019). Even though *Ae. aegypti* is the main vector of these arboviruses, *Ae. albopictus* can play an important role as an epidemic driver, especially in areas where *Ae. aegypti* is absent or present at low levels. This has been the case for the large chikungunya (2005) and dengue (2018) outbreaks in the Reunion Island (Renault et al., 2007; Vincent et al., 2019), for the several cases of dengue and chikungunya autochthonous transmission (2007–2018) in Italy, France and Croatia (Gossner et al., 2018), or for the more recent cases of Zika virus transmission in southern France (Brady and Hay, 2019; Giron et al., 2019). Importantly, there are currently no specific anti-viral drugs to treat these diseases. A dengue vaccine has been approved by FDA in 2019 but its use appears to have some limitations (CDC, 2019; Espana et al., 2019), and despite the availability of a safe and effective vaccine for yellow fever, the disease is still endemic in Africa and in Central-South America (WHO, 2019). In this scenario, vector monitoring and control, along with the prevention of human-mosquito contact, still represent the main methods to contain the transmission of these arboviral diseases.

Evaluation of human-vector contact is essential to assess the risk of transmission of mosquito-borne diseases and to guide planning and implementation of vector control by public health authorities. For *Aedes* mosquitoes this is currently obtained by entomological methods as ovitraps, larval/pupal indices, adult traps or human landing catches (HLC), which provide estimates of adult and/or immature mosquito densities in a given area (ECDC, 2012). However, entomological measurements have some limitations and drawbacks. First, they only provide an indirect estimation of human exposure to vectors at community level. Second, they can be expensive, labor-intensive and/or difficult to carry out in some epidemiological settings (e.g., logistic constraints or low vector densities) or may raise ethical issues (e.g., for HLC). In addition to classical entomological methodologies, a novel tool for the evaluation of human exposure to disease vectors is emerging. This alternative approach, which allows for a direct estimation of human-vector contact at the individual level, relies on the assessment of host antibody responses against mosquito salivary proteins injected by hematophagous arthropods during blood feeding (Ribeiro and Arcà, 2009). As first shown for ticks (Schwartz et al., 1990), and then for several other blood feeders including anopheline and culicine mosquitoes (Trevejo and Reeves, 2005; Remoue et al., 2006; Doucoure et al., 2012b), these antibody responses can be used to evaluate human exposure to arthropod vectors. Transcriptomic and proteomic studies performed in the last two decades allowed to unravel the complexity of the salivary repertoires of blood feeding insects (Arcà and Ribeiro, 2018) and to identify groups of genus-specific mosquito salivary proteins, i.e., only found in the saliva of either anopheline or culicine mosquitoes (Ribeiro et al., 2010). These findings provided the starting point for shifting from the use of saliva or salivary gland protein extracts (SGE) to the exploitation of individual genus-specific mosquito salivary proteins. In fact, the use of saliva/SGE is inconvenient (difficult to obtain in large amounts) and may even be misleading (content variation according to physiological states, possible cross-reactions). On the other side, genus-specific salivary proteins may represent ideal candidates for the development of immuno-assays suitable for the evaluation of human exposure to either *Anopheles* or *Aedes* vectors.

A solid proof of principle has been already provided for anopheline malaria vectors. IgG responses to the *Anopheles gambiae* gSG6 or the gSG6-P1 peptide have been widely validated as marker of human exposure to Afrotropical malaria vectors in different epidemiological settings in Western and Eastern African countries (Poinsignon et al., 2008; Drame et al., 2010; Rizzo et al., 2011b; Badu et al., 2012; Stone et al., 2012; Proietti et al., 2013; Yman et al., 2016). Moreover, the same antigens have been successfully employed for Asian malaria vectors (Ya-Umphan et al., 2017) and may be of some use with Polynesian (Idris et al., 2017; Pollard et al., 2019) and American Old World anophelines (Montiel et al., 2020). For *Aedes* mosquitoes some promising indications have been obtained with the Nterm-34kDa peptide, which is designed on the culicine-specific *Ae. aegypti* 34k1 salivary protein (Sagna et al., 2018). This peptide allowed to detect variation of human exposure to *Ae. aegypti* bites in studies in Benin, Côte d'Ivoire and Lao PDR (Elanga Ndille et al., 2012; Ndille et al., 2014; Yobo et al., 2018). Moreover, it proved useful to evaluate vector control intervention at La Reunion Island (Indian Ocean), in an urban area where *Ae. aegypti* is not present and individuals are only exposed to *Ae. albopictus* (Elanga Ndille et al., 2016), suggesting it may be of use to assess exposure to both these vectors.

Toward the development of novel additional markers of human exposure to *Aedes* mosquitoes, and more specifically to *Ae. albopictus*, we previously analyzed in a murine model the immunogenic properties of the *Ae. albopictus* 34k2 salivary protein (al34k2). It is worth pointing out that this protein, as the 34k1 mentioned above, is also culicine-specific and a member of the 34kDa salivary protein family. Nevertheless, 34k1 and 34k2 proteins are significantly divergent and only share 32 and 33% amino acid identity in *Ae. albopictus* and *Ae. aegypti*, respectively (Arcà et al., 2007; Ribeiro et al., 2007). We found specific anti-al34k2 IgG responses in mice experimentally exposed to bites of *Ae. albopictus* and in a single human donor hyperimmune to *Ae. albopictus* saliva (Buezo Montero et al., 2019). Moreover, mice immunized by exposure to bites of *Ae. aegypti* had no IgG antibodies cross-reacting to al34k2, suggesting it may be useful for the development of species-specific immunoassays. To follow up these initial observations we analyzed in this study a set of sera collected from healthy human blood donors in two areas with different levels of natural exposure to *Ae. albopictus* (Padova and Belluno, Northeast Italy) during two different periods, at the end of the low-density mosquito season and shortly after the high-density mosquito season.

MATERIALS AND METHODS

Ethical Statement

This study was conceived according to good clinical practices and followed the ethical principles recommended by the Edinburgh revision of the Helsinki declaration. The protocol was approved by the Ethics Committee of Sapienza University (306/17 RIF.CE: 4479, April 10th 2017). All volunteers participating to the study provided written informed consent on the use of their sera to measure antibody responses to mosquito salivary antigens.

Study Areas and Sera Collections

The study was carried out in the Veneto region, Northeast Italy, in the cities of Padova and Belluno (**Supplementary Figure 1A**). Padova (45°24′23"N, 11°52'40"E) is located in a plain area (27 meters a.s.l.), has a relatively high population density (2.287 inhabitants/km²) and counts roughly 213,000 inhabitants. Belluno (46°08′27″N, 12°12′56″E) is situated in a valley at 389 meters a.s.l. and is surrounded by Bellunesi Prealps and Dolomites; total population is of approximately 36,000 inhabitants with a population density lower than Padova (243 inhabitants/km²). *Aedes albopictus* is widely spread almost all over Northeast Italy and Padova is one of the first cities in Europe colonized by this species. After its first finding in 1991 (Dalla Pozza and Majori, 1992), the tiger mosquito got very well established in the area and quickly became an important pest due to its aggressive behavior and daytime biting activity. Afterwards, the tiger mosquito progressively expanded its distribution to the entire Veneto region. Currently, it is by far the most abundant *Aedes* species in the urban areas of Italy, and these two cities were selected as sites with high (Padova) and low to moderate (Belluno) exposure to bites of *Ae. albopictus*. This assumption was mainly based on entomological data from the two areas in the years preceding this study (Montarsi et al., 2015; Montarsi F., unpublished observations) and on history of colonization. In fact, even though *Ae. albopictus* is well established in both municipalities, the two sites markedly differ for the timing of colonization. Padova should be considered of "ancient" colonization: the tiger mosquito was first reported at the beginning of nineties (Dalla Pozza and Majori, 1992) and therefore, at the time of this study, it was established in the city since at least 25 years. On the contrary, Belluno is of "recent" colonization: *Ae. albopictus* reached the area approximately 20 years later, in 2012 (Gobbi et al., 2014), and for this reason at the time of our study was established in Belluno since approximately 5 years. Notably, another exotic mosquito species, *Aedes koreicus*, was found shortly earlier in the Belluno area (Capelli et al., 2011); however, according to entomological surveys performed in the period 2014–2015, the most abundant mosquito species in the Belluno city was *Ae. albopictus* (57%), followed by *Culex pipiens* (32.1%) and *Ae. koreicus* (9.2%), with other *Aedes* species only occasionally found and accounting globally for less than 0.8% of the collected mosquitoes (Baldacchino et al., 2017). It should be also mentioned that another mosquito of Asian origin, *Aedes japonicus japonicus*, was found in 2018 in the far Northeast area of the Belluno province, toward the borders with Austria (Montarsi et al., 2019); however, there is no indication of the presence of *Ae. j. japonicus* in Belluno during the study period.

Planning the sample size for sera collection was not straightforward considering the absence of information on the anti-saliva IgG response in the study sites and the novelty of the al34k2 antigen. A rough estimation was done by conservatively considering an unpaired sample and taking into account previous similar studies (Elanga Ndille et al., 2012, 2016). Hypothesizing for all the comparisons a similar difference of average IgG levels not lower than 0.15 and a variance of 0.16, a minimum number of 112 sera per group could guarantee a power of 80% with a 95% confidence level. In order to increase the power up to approximately 85% we collected around 130 samples/group. Sera were collected among adult healthy volunteers who referred for routine blood donation to the immune transfusion centers of Padova (Padova University Hospital) and Belluno (San Martino Hospital), both located in the Veneto region. A first collection of sera took place in 2017 from May 2nd to May 12th in Padova (PD1, $n = 130$) and from May 4th to June 1st in Belluno (BL1, $n = 130$). According to previous data on mosquito seasonality in the areas (Baldacchino et al., 2017), these sera can be considered as representative of individuals who were not significantly exposed to *Ae. albopictus* bites in the previous 4–5 months. We will refer to these collections in the text as PD1 and BL1 or, more generically, as before (summer) = at the end of the low-density mosquito period. A second collection was done, always in 2017, after the summer period of high mosquito density: from September 11th to November 22nd in Padova (PD2, $n = 132$) and from September 14th to November 21st in Belluno (BL2, $n = 131$). These sera can be considered as representative of individuals who were significantly exposed to *Ae. albopictus* bites. In the text we will refer to this second round of collections as PD2 and BL2 or, more generically, as after (summer) = after the high-density mosquito period. A subset of individuals from Padova ($n = 69$) and Belluno ($n = 97$) could

be enrolled in both surveys. Volunteers participating to the study were also invited to fill a short questionnaire finalized to gather information on (i) cutaneous reaction to mosquito bites (from 0 = absent to 5 = very intense) as well as, with specific reference to the 6-months preceding the donation, on (ii) travels outside Italy and country visited, (iii) perception of intensity of mosquito bites (from 0 = not bitten to 5 = very many bites) and (iv) timing of mosquito bites (during day, at night, day and night).

Entomological Measurements

To evaluate the occurrence and population density of *Ae. albopictus* the two selected sites, Padova and Belluno, were monitored from end of May to July 2017 (low-density) and from end of August to beginning of October 2017 (high-density). The surveys were performed using ovitraps (oviposition standard traps), which is the most used kind of trap for monitoring *Aedes* mosquito species (Velo et al., 2016; Manica et al., 2017). Ovitraps consist of black cylindrical vessels (9.0 × 11.0 cm) with an overflow hole (at 7.0 cm from the bottom) containing ∼300 mL of standing water. A wooden stick (Masonite strip, 10.0 × 2.5 cm) was used as a substrate for oviposition. A larvicide (*Bacillus turingensis* var. *israelensis*, BTI) was added into the ovitraps to avoid larval development. Selection of sites where to set the ovitraps was made by dividing the urban areas into hypothetical squares of 4 km^2 and positioning three traps inside each square. According to these criteria, ovitraps were placed in geo-referenced sites and checked biweekly, with a total of 20 ovitraps in Belluno and 40 in Padova (**Supplementary Figures 1B,C**). The mean number of eggs per positive ovitraps and the proportion of positive ovitraps (number of traps with eggs over total number of ovitraps) were calculated to estimate the seasonal mosquito density.

Mosquito Rearing, Salivary Gland Extracts and 34k2 Salivary Protein

Aedes albopictus mosquitoes (originally collected in Rome, Italy) were reared in the insectary of Sapienza University at 27 ± 1°C, 70 ± 10% relative humidity, 14:10 h light:dark photoperiod. Adult females 3–8 days post-emergence (dpe), and never fed on blood before, were used for all the experiments. Salivary glands were dissected in Phosphate Buffered Saline (PBS), transferred to a microcentrifuge tube kept on ice and containing 20 µl of PBS, then frozen at −80°C (typically in batches of 20–40 salivary gland pairs). *Aedes albopictus* salivary gland protein extracts (SGE) were prepared by three cycles of freezing and thawing, followed by centrifugation at 16,000 × g at 4°C. Supernatants were pooled in order to generate a homogeneous SGE stock to be used for all ELISA assays; protein concentration was measured by the Bradford method (Bio-Rad, 5000002) using the Take3 micro-volume plate in a BioTek microplate reader (BioTek Synergy HT). SGE stocks were stored at −20°C in small aliquots until use. The *Ae. albopictus* al34k2 salivary protein was expressed and purified as previously described (Buezo Montero et al., 2019).

Serological Tests

Enzyme-linked immunosorbent assays (ELISA) were essentially performed as previously described (Rizzo et al., 2011a, 2014a; Buezo Montero et al., 2019). Briefly, flat-bottom 96-well plates (Nunc MaxiSorp, 442404) were coated for 3 h at room temperature (RT) with 50 µl of either *Ae. albopictus* SGE (5.6 µg/ml, equivalent to the amount of proteins per ml obtained from 7 salivary gland pairs) or recombinant al34k2 salivary protein (5 µg/ml) diluted in Coating Buffer (15mM Na_2CO_3, 35mM $NaHCO_3$, 3mM NaN_3, pH 9.6). Afterwards plates were: (i) blocked for 3 h at RT (150 µl 1% w/v skimmed dry milk in PBST, i.e., PBS plus 0.05% Tween 20); (ii) incubated overnight at 4°C with 50 µl of plasma diluted 1:50 (IgG) or 1:20 (IgG1 and IgG4); (iii) incubated for 3 h at RT with 100 µl of polyclonal rabbit anti-human IgG/HRP (Dako P0214, dilution 1:5000) or sheep anti-human IgG1/HRP (Binding Site AP006, dilution 1:1000) or sheep anti-human IgG4/HRP (Binding Site AP009, dilution 1:1000); (iv) incubated in the dark at 25°C for 15 min with 100 µl of o-phenylenediamine dihydrochloride (OPD, Sigma P8287) for colorimetric development. Reactions were terminated by adding 25 µl of 2M H_2SO_4. Three to four washings were performed between each step. OD_{492} were determined using a microplate reader (Biotek Synergy HT).

Data Normalization and Analysis

All samples were analyzed in duplicate with the antigen and once with no antigen. The no-antigen well was used for background subtraction, and IgG levels were expressed as final OD calculated for each sample as the mean OD value with antigen minus the OD value without antigen. Samples whose duplicates showed a coefficient of variation (CV) >20% were re-assayed or not included in the analysis. To control for intra- and inter-assay variation, IgG levels were determined including in each plate negative controls as well as a standard curve made by 2-fold dilution series (1:25–1:1,600) of a human hyperimmune serum. OD values were normalized using titration curves and the Excel software (Microsoft) with a three variable sigmoid model and the Solver add-in application as previously described (Corran et al., 2008). IgG1 and IgG4 OD levels were converted to concentrations (ng/ml) including on each plate standard curves set up as follows. As capturing factors goat anti-human IgG (5 µg/ml, Jackson ImmunoResearch 109005098) or mouse anti-human IgG4 (2 µg/ml, BD Pharmingen 555881) were used for coating (in 50 µl coating buffer, 3 h at RT). After washing, blocking and washing again, wells were incubated overnight at 4°C with two-fold dilution series from 1 µg/ml to 0.0078 µg/ml of purified native human IgG1 (Bio-Rad PHP010) or IgG4 (ABD Serotec 5254–3004) in 50 µl of blocking reagent. Incubation with anti-human IgG1/HRP or IgG4/HRP and colorimetric detection were performed as described above. All datasets were tested for normality and lognormality by different tests (Anderson-Darling, D'Agostino & Pearson, Shapiro-Wilk, Kolmogorov-Smirnov). No dataset passed any normality test and only some datasets passed lognormality tests. For these reasons the statistical analysis was performed using non-parametric tests. Multiple comparisons were performed by the Kruskal-Wallis test. Mann-Whitney *U*-test was used to compare IgG levels between two independent groups. The Wilcoxon matched-pairs test was used for comparison of two paired groups. Graph preparation and

TABLE 1 | Features of the studied population and individual perception of mosquito bites.

		PD1	PD2	BL1	BL2	Total
Date survey (2017)	Start	May 2	Sept 11	May 4	Sept 14	
	End	May 12	Nov 22	June 1	Nov 21	
Sampled individuals		130	132	130	131	
Age range (years)		18–67	19–66	19–65	19–65	
Median age		45.5	47.0	44.0	44.0	
Mean age ± 95% CI		43.8 ± 2.1	45.1 ± 2.1	43.9 ± 1.9	44.8 ± 1.8	
Females (F)		39	34	12	16	
Males (M)		91	98	118	115	
Paired samples		PD, $n = 69$		BL, $n = 97$		
Travel abroad in the preceding 6-months	Country with *Ae. albopictus*	19	30	14	29	96
	Country with no *Ae. albopictus*	7	4	7	6	20
	Not specified	1	4	–	–	5
	No travel	103	94	109	96	402
	Total	130	132	130	131	523
Cutaneous reaction (0–5)	Low (0–1)	73	77	61	92	303
	Mid (2–3)	49	49	18	25	141
	High (4–5)	8	3	4	3	18
	Total	130	129	83	120	462
Number of bites (0-5)	Low (0–1)	117	53	124	64	358
	Mid (2–3)	13	49	6	59	127
	High (4–5)	0	28	0	8	36
	Total	130	130	130	131	521
Timing of bites	Day	11	61	12	38	122
	Night	7	22	7	43	79
	Day and night	6	46	7	36	95
	Total	24	129	26	117	296

statistical analyses were performed using the Prism 8.0 GraphPad Software (San Diego, CA).

RESULTS

The main characteristics of the studied population and the individual perception of mosquito bites are summarized in **Table 1**. Collected sera were used to measure IgG responses to *Ae. albopictus* salivary gland protein extracts (SGE) and to the recombinant *Ae. albopictus* salivary protein al34k2 (Buezo Montero et al., 2019). Considering that male volunteers were largely predominant, and to make sure not to introduce any bias, we preliminarily compared IgG responses to SGE in males versus females and found no statistically significant difference (**Supplementary Figure 2A**); similar results were obtained comparing anti-al34k2 IgG responses in the two sexes. Moreover, in the 6-months preceding the surveys a variable proportion of individuals (16.1–28.8%) had traveled to countries where *Ae. albopictus* was either present or absent. No significant variation of anti-SGE IgG levels was found by pairwise comparisons between individuals who did not travel and those who: (i) traveled, (ii) traveled to countries where *Ae. albopictus* was present or (iii) traveled to countries where *Ae. albopictus* was absent (**Supplementary Figure 2B**). According to these observations, the analyses described below were performed including all the samples collected in the different surveys.

Entomological Monitoring

Oviposition traps were placed in Padova and Belluno (**Supplementary Figures 1B,C**) in the time frame between the two sera collections in order to provide an estimation on the relative population dynamics of *Ae. albopictus*. Both the mean number of eggs per ovitrap and the percentage of positive ovitraps indicated that mosquitoes started appearing around the last week of May in Padova (19.9 eggs/ovitrap, 34.4% positive ovitraps) and shortly later, around the first week of June, in Belluno (36.3 eggs/ovitrap, 30.0% positive ovitraps). The number of eggs per ovitrap progressively increased during the summer period reaching a peak the last week of August

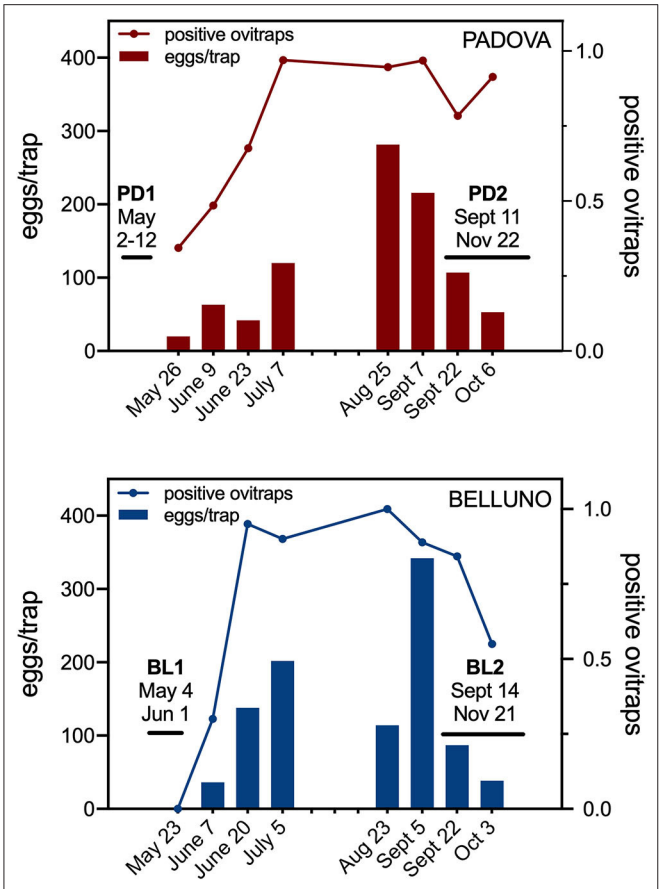

FIGURE 1 | Entomological monitoring by ovitraps in the study areas. Bars show the average number of eggs per positive ovitraps (eggs/trap, left Y axis). Lines represent the proportion of positive ovitraps, i.e., the number of ovitraps with eggs over the total number of ovitraps (positive ovitraps, right Y axis). The time intervals for the two sera collections in each study area are reported.

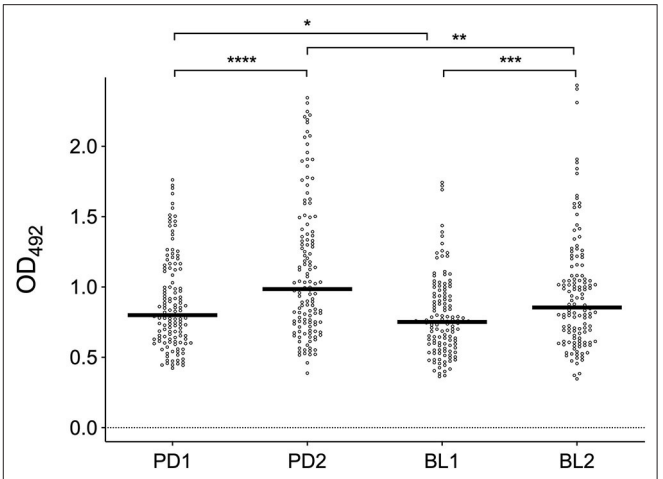

FIGURE 2 | IgG responses to *Ae. albopictus* salivary gland protein extracts. Anti-SGE IgG levels in participants to the four different surveys (PD1, PD2, BL1, and BL2) as indicated at the bottom. IgG levels are expressed as OD values. Number of individuals for each survey according to **Table 1**. Dots mark the individual values and horizontal bars represent the medians. Significant difference in the pairwise comparisons (Mann-Whitney U test) is also reported: $^{*}p < 0.05$; $^{**}p < 0.01$; $^{***}p < 0.001$; $^{****}p < 0.0001$.

in Padova (281.4 eggs/ovitrap, 94.6% positive ovitraps) and first week of September in Belluno (342.1 eggs/ovitrap, 88.9% positive ovitraps) and decreasing afterwards (**Figure 1**). Despite the original assumption of Padova being an area of higher *Ae. albopictus* density than Belluno, ovitraps data did not show a clear difference between the two study sites. On the contrary, the temporal dynamic fully supports the expectations that (i) individuals whose sera were collected before summer were not significantly exposed to *Ae. albopictus* bites for at least 4–5 months and (ii) individuals surveyed after summer were naturally exposed to the tiger mosquito during the warm months, from June to September.

IgG Responses to *Ae. albopictus* Salivary Gland Extracts

IgG antibody responses against mosquito saliva or salivary gland extracts have been previously shown to reliably reflect the intensity of human exposure to bites of either *Anopheles* or *Aedes* species (Remoue et al., 2006; Orlandi-Pradines et al., 2007; Fontaine et al., 2011; Doucoure et al., 2012b, 2014). Therefore, we first analyzed the IgG responses to *Ae. albopictus* SGE in sera collected before and after summer in the two study areas. Anti-SGE IgG responses were significantly higher in sera collected after the summer period of high mosquito density both in Padova (PD2) and Belluno (BL2) as compared to those collected before summer in the same areas (Padova, $p < 0.0001$; Belluno, $p = 0.0009$; **Figure 2**). Moreover, IgG antibody levels against SGE were higher in Padova than Belluno during both before ($p = 0.0341$) and after ($p = 0.0070$) the high-density mosquito seasons. These observations, in contrast to ovitraps data, seems to confirm the original assumption of Padova being an area of higher exposure to *Ae. albopictus* than Belluno.

IgG Responses to *Ae. albopictus* 34k2 Salivary Protein

IgG responses to SGE and al34k2 showed a weak, but clearly positive correlation (Spearman $r = 0.43$, 95% CI 0.36–0.50, $n = 523$, $p < 0.0001$). When the different surveys were compared, a seasonal variation of IgG levels was found in Padova ($p = 0.0043$) and anti-al34k2 IgG responses were higher in Padova than in Belluno both before ($p < 0.0001$) and shortly after the summer season ($p < 0.0001$). Comparison of anti-al34k2 IgG antibody levels between the two sets of sera collected in Belluno failed to show a significant seasonal variation (**Figure 3A**). However, when only paired samples from the two localities were analyzed (i.e., those individuals whose sera were collected both in the first and the second survey), a significant seasonal increase was found not only in Padova ($n = 69$, $p < 0.0001$) but also in Belluno ($n = 97$, $p = 0.0032$) (**Figure 3B**). Overall, despite the relatively weak correlation, anti-al34k2 IgG responses exhibited a pattern of variation fully consistent with the anti-SGE IgG responses. Therefore, these observations convincingly suggest

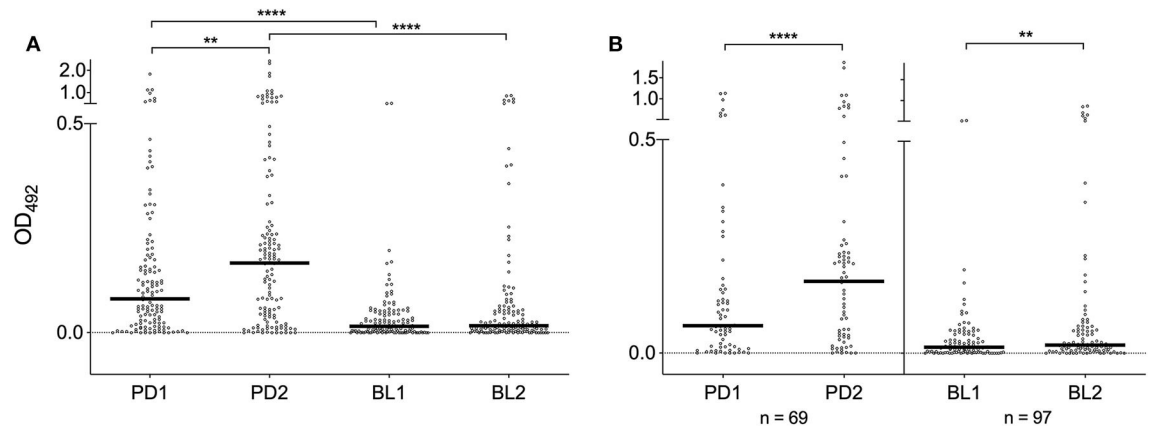

FIGURE 3 | IgG responses to the *Ae. albopictus* salivary gland protein al34k2. **(A)** Anti-al34k2 IgG levels in all participants to the four different surveys. IgG levels, number of individuals, dots, bars and p values as in **Figure 2**. **(B)** IgG responses in paired samples from Padova (left panel) and Belluno (right panel). The number of individuals is indicated at the bottom. Dots and bars as in **(A)**. Significant difference in the pairwise comparisons (Wilcoxon matched-pairs test): $^{**}p < 0.01$; $^{****}p < 0.0001$.

that IgG responses to al34k2 may be suitable to assess spatial and temporal variation of human exposure to bites of the tiger mosquito *Ae. albopictus*.

IgG1 and IgG4 Responses to *Ae. albopictus* 34k2 Salivary Protein

Previous studies showed that the *An. gambiae* gSG6 and cE5 salivary proteins induce in naturally exposed individuals differential antibody responses, with the gSG6 antigen evoking high levels of IgG4 antibodies and cE5, on the contrary, triggering an IgG1-dominated response (Rizzo et al., 2014a,b). To get insights into IgG subclass-specificity of antibody responses to the al34k2 protein we determined IgG1 and IgG4 antibody titers in the sera collected in Padova before (PD1) and after (PD2) the high density mosquito season. As expected a positive correlation was found between anti-al34k2 IgG and IgG1 levels (Spearman $r = 0.64$, 95% CI 0.56–0.70, $n = 262$ $p < 0.0001$), and similar results were obtained for IgG and IgG4 (Spearman $r = 0.68$, 95% CI 0.61–0.74, $n = 262$, $p < 0.0001$) levels. Median IgG1 titers appeared to be over ten-fold higher than corresponding IgG4 titers in both surveys (**Figure 4A**; $p < 0.0001$). A highly significant increase of both anti-al34k2 IgG1 and IgG4 levels was observed in PD2 by pairwise comparisons between paired samples ($n = 68$, $p < 0.0001$; **Figure 4B**); instead, only IgG4 levels showed a weakly significant increase after summer when all samples were considered ($p = 0.0326$, **Figure 4A**). These results clearly indicate that antibody responses against the al34k2 salivary protein show a large predominance of IgG1 antibodies.

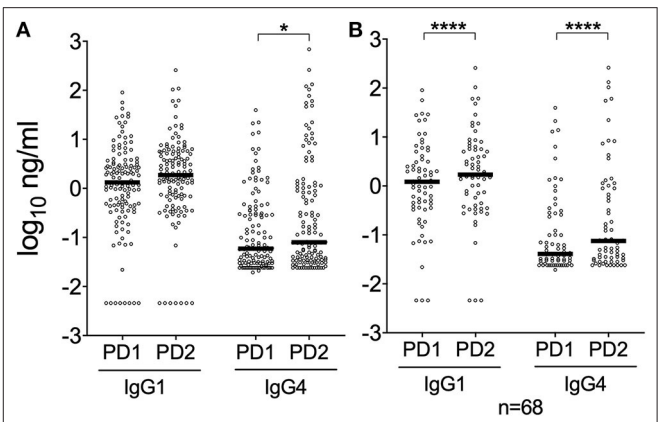

FIGURE 4 | IgG1 and IgG4 responses to the *Ae. albopictus* salivary gland protein al34k2 in Padova. **(A)** Individual anti-al34k2 IgG1 and IgG4 levels in participants to the PD1 ($n = 128$) and PD2 ($n = 128$) surveys. IgG1 and IgG4 levels are expressed in ng/ml. Dots, bars and *p*-values as in **Figure 2**. **(B)** IgG1 and IgG4 responses against al34k2 in paired samples from Padova ($n = 68$). IgG1 and IgG4 levels, dots and bars as above. Pairwise comparisons by the Wilcoxon matched-pairs test ($^{*}p < 0.05$; $^{****}p < 0.0001$).

IgG Responses to *Ae. albopictus* SGE and al34k2 According to Age

Individual IgG responses to *Ae. albopictus* SGE and to al34k2 were also analyzed according to age. Overall, a negative correlation was found between age and IgG responses to *Ae. albopictus* SGE or al34k2. Spearman's rank correlation analysis indicated a clear trend of antibody responses to decrease with age for both Padova surveys, especially when considering the anti-SGE IgG responses; on the contrary, in Belluno a weakly significant negative correlation was only found for the anti-al34k2 IgG responses in the BL2 survey (**Table 2**, **Supplementary Figure 3A**). This general trend was confirmed when participants to the surveys were divided in four different age groups (18–30, 31–40, 41–50 and >50 years old). Pairwise comparisons indicated a clear and significant decrease with age of the anti-SGE and anti-al34k2 IgG responses in Padova; again, this was not the case for Belluno where some decrease was only observed in the over 50 years old category in the BL2 survey (**Supplementary Figure 3B**).

TABLE 2 | Correlation between age and IgG levels.

	Spearman r	95% CI	*n*	*p*-value
PD1-SGE	−0.3861	−0.53 to −0.22	130	<0.0001
PD2-SGE	−0.4570	−0.59 to −0.31	132	<0.0001
BL1-SGE	0.0007	−0.18 to 0.18	130	ns
BL2-SGE	−0.1648	−0.33 to 0.01	131	ns
PD1-al34k2	−0.2548	−0.42 to −0.09	130	0.0030
PD2- al34k2	−0.2435	−0.40 to −0.07	132	0.0049
BL1- al34k2	−0.0961	−0.27 to 0.08	130	ns
BL2- al34k2	−0.2149	−0.38 to −0.04	131	0.0137

To make sure that age distribution did not represent a source of bias we compared the age of the different cohorts of individuals (PD1, PD2, PD paired, BL1, BL2, BL paired) by the Kruskal-Wallis or Mann-Whitney tests and found no significant difference. We also calculated the frequencies of the four age groups in the different cohorts (**Supplementary Figure 4A**) and compared them by the Chi-square test without finding any difference (chi-square 16.37, df 15, $p = 0.358$). Finally, we also compared IgG levels before and after the mosquito season in the two sites by age groups, using both paired and unpaired samples. Median anti-SGE and anti-al34k2 IgG levels were higher after the summer season in almost all the pairwise comparisons (30/32), even though statistical significance was only reached in ∼40% of cases (56% for SGE and 25% for al34k2, **Supplementary Figure 4B**), likely because of the relatively small sample size. Overall, these observations suggest that age should be taken into consideration in similar studies but also indicate that it does not appear to be a relevant source of bias in our investigation.

Anti-saliva IgG Responses and Individual Perception of Exposure to Mosquito Bites

Participants to the surveys, along with the informed consent, were asked to fill a short questionnaire on their individual perception of cutaneous reaction to mosquito bites, intensity/number of bites and timing of occurrence (**Table 1**). Despite the intrinsic limitations of this subjective self-assessment, we verified the possible correlation with anti-SGE and anti-al34k2 IgG antibody levels. Overall, individuals reporting mid to high (2–5) cutaneous reactions showed higher anti-SGE IgG levels as compared to those with absent or low (0–1) reactions. This was supported by the observation that median OD values, as well as 25th and 75th percentiles, were in most cases (PD1, PD2, and BL2) higher for the mid-to-high category, although the difference reached statistical significance only for the PD1 survey ($p = 0.0036$; **Supplementary Figure 5A**). IgG responses to both *Ae. albopictus* SGE and to al34k2 were also compared in individuals reporting a low number of bites (score 0–1) versus those accounting for mid to high number of bites (score 2–5). For both antigens, the 25th and 75th percentiles and median OD values were, in the very large majority of cases, higher in the mid to high category; however, statistical significance was only found when considering the IgG response to SGE in the PD1 ($p = 0.0075$) and BL1 surveys ($p = 0.0320$, **Supplementary Figure 5B**). No general common trend and/or significant difference was recognizable when IgG responses were compared in individuals reporting mainly day- versus night-time bites, only exception being the BL2 survey where anti-al34k2 IgG levels were slightly higher ($p = 0.0280$) in individuals accusing a larger number of bites during daytime.

DISCUSSION

In the last decades the tiger mosquito *Ae. albopictus* impressively expanded its geographic distribution colonizing areas with relative cool climates and gaining the reputation of one of the most invasive species worldwide (Bonizzoni et al., 2013; Lwande et al., 2019). Further spreading in both United States and Europe has been predicted for the next decades (Kraemer et al., 2019), with a consequent expansion of the population at risk from mosquito-borne diseases as dengue, yellow fever, chikungunya and Zika. In this context the cases of autochthonous transmission in Europe (Gossner et al., 2018; Brady and Hay, 2019) and the large outbreaks in the Reunion Island (Renault et al., 2007; Vincent et al., 2019) sound as an alarm bell calling public health authorities for improved monitoring and control of the tiger mosquito.

Historically, the control of vector populations and the reduction of human-vector contact have been the most important weapons in the fight against mosquito-borne diseases. More recently, the identification of genus-specific mosquito salivary proteins (Ribeiro et al., 2010; Arcà and Ribeiro, 2018) paved the way for the development of serological toolboxes that may allow for the simultaneous evaluation of human-vector contact and circulation of pathogens transmitted by the same vector. Such a tool may be useful for epidemiological studies and the evaluation of both transmission risk and efficacy of vector control interventions. The successful outcome of studies with *Anopheles* malaria vectors stimulated efforts to develop similar markers for *Aedes* vectors, leading to the identification of the Nterm-34kDa peptide as candidate biomarker of human exposure to *Ae. aegypti*, with some encouraging indications also for *Ae. albopictus* (reviewed by Sagna et al., 2018).

We previously obtained promising evidence of the immunogenicity of the al34k2 salivary protein to both mice and humans (Buezo Montero et al., 2019). With the aim to validate this antigen as candidate marker of exposure to *Ae. albopictus*, we measured the anti-al34k2 IgG responses in sera collected from adult healthy individuals, before and after the summer high-density mosquito season, in two different areas colonized by the tiger mosquito. It is worth pointing out that, apart from the Nterm-34kda peptide, the availability of additional markers of exposure to the tiger mosquito may prove useful for several reasons. First, the Nterm-34kDa peptide is designed on the *Ae. aegypti* 34k1 salivary protein and the corresponding peptide from the *Ae. albopictus* ortholog is rather divergent (12/19 identical residues with a 3 amino acids gap). This may imply a relatively

low sensitivity, which might be a limiting factor in conditions of low mosquito density, when also traditional entomological approaches become less reliable. Second, human immune responses to mosquito salivary antigens exhibit significant individual variability, as shown for the *An gambiae* gSG6 and cE5 (Rizzo et al., 2014a). As a consequence, multiple antigens may be very helpful providing a more comprehensive view and eventually increasing the sensitivity and/or specificity of the immunoassays.

When we measured the IgG responses to *Ae. albopictus* SGE we found, as expected, a significant increase from low to high mosquito density period. A similar pattern was found for the anti-al34k2 IgG responses: in both study sites they increased shortly after the summer exposure and declined after the winter period of non-exposure to *Ae. albopictus*, even though this was more evident in Padova than in Belluno (**Figure 3**). This is an important finding in view of two considerations. First, an effective marker should evoke an IgG response sufficiently short-term to detect variation in human-vector contact, for example from high to low vector density season or after the implementation of vector control measures. Second, the duration of IgG responses is salivary antigen-dependent, as previously reported for the *An. gambiae* gSG6 and cE5 (Rizzo et al., 2014a). The correlation between individual responses to SGE and al34k2 was positive, as expected, but relatively weak (Spearman $r = 0.43$). However, taking into account (i) that saliva is a complex mixture of more than hundred salivary proteins, (ii) the lower sensitivity of anti-al34k2 IgG responses, and (iii) the individual variability in the response, this observation does not seem really surprising and should not be negatively interpreted. Overall, the observations reported here suggest that in natural conditions the anti-al34k2 IgG responses appear suitable to evaluate seasonal variations of human exposure to the tiger mosquito and eventually to assess the efficacy of vector control interventions at reducing the host-vector contacts.

To our surprise, entomological monitoring by ovitraps did not show the expected difference between the two study sites. Nevertheless, anti-SGE and anti-al34k2 IgG responses were higher in Padova than Belluno both before and after summer, a result that is perfectly in line with the original assumption. Providing a simple and unequivocal explanation to this discrepancy is not easy; however, a few considerations should be kept in mind. First, the correlation between number of eggs and adult females density is not so straightforward and may be affected by several different variables (Manica et al., 2017). Second, the presence of *Ae. koreicus*, whose eggs are practically indistinguishable from those of *Ae. albopictus* (Montarsi et al., 2015), may have contributed to the high numbers found in Belluno. Third, ovitraps were placed within the cities (**Supplementary Figure 1**), but transfusional centers accept blood donors from the whole province. Around 25% of Belluno blood donors were resident in small villages where the tiger mosquito is either absent or present at very low density (Montarsi et al., 2015); on the contrary, all the villages in Padova province are well known to be infested since decades (Romi et al., 1999). In addition, IgG responses to mosquito saliva have been previously shown, in different settings, to be a reliable indicator of host exposure to mosquito bites (Remoue et al., 2006; Orlandi-Pradines et al., 2007; Fontaine et al., 2011; Doucoure et al., 2012a, 2014) and, differently from entomological measures, provide a direct indication of human-vector contact. For these reasons, overall, we feel rather confident suggesting that IgG responses to the al34k2 salivary protein appear a reliable marker also to detect spatial variation of human exposure to *Ae. albopictus*.

Human IgG responses to mosquito saliva are mainly characterized by antibodies of the IgG1 and IgG4 subclasses and very low IgG2 and IgG3 concentrations. High levels of antigen-specific IgG4 antibodies may be related to allergenic properties of insect salivary proteins (Peng and Simons, 2004); they may also be associated with immune tolerance, as is the case for beekeepers who carry elevated levels of venom-specific IgG4 antibodies with anti-inflammatory potential (Garcia-Robaina et al., 1997; Varga et al., 2013). Moreover, higher levels of IgG4 antibodies against *Ae. aegypti* saliva were recently reported in dengue-infected individuals in an endemic area in Colombia (Cardenas et al., 2019). We determined anti-al34k2 IgG1 and IgG4 levels in individuals from the PD1 and PD2 surveys and, in both cases, median IgG1 titers were at least 10-fold higher than corresponding IgG4 levels (**Figure 4**). A similar finding was previously reported for the *An. gambiae* salivary protein cE5 in naturally exposed individuals from a malaria hyperendemic area of Burkina Faso; however, the same individuals carried high levels of anti-gSG6 IgG4 antibodies. This differential responses to the cE5 and gSG6 proteins has been interpreted as a possible indicator of Th1-type and Th2-type polarized immune responses, respectively (Bretscher, 2014; Rizzo et al., 2014a,b). Our findings suggest that the *Ae. albopictus* al34k2 protein may be of limited allergenicity and induces in naturally exposed individuals an IgG1-dominated antibody response that may be indicative of a Th1-type polarization.

IgG antibody responses to SGE and al34k2 showed a trend to decrease with age. This was pronounced in sera collected in Padova but only barely detectable in those from Belluno (**Table 2**, **Supplementary Figure 3**). Human cutaneous reactions and antibody responses to mosquito saliva are known to change over time with the continued natural exposure, most likely because of immune tolerance and progressive desensitization to mosquito salivary proteins (Mellanby, 1946; Feingold et al., 1968; Peng and Simons, 1998, 2004; Doucoure et al., 2012b; Cardenas et al., 2019; Montiel et al., 2020). However, while IgG responses to mosquito saliva (a cocktail of ∼100–150 proteins) decrease with age, the situation with individual salivary proteins is antigen-dependent. For example, a decrease with age was previously reported for the *An. gambiae* gSG6 (Poinsignon et al., 2009; Rizzo et al., 2011b, 2014b; Montiel et al., 2020) and for *Anopheles albimanus* salivary peptides (Londono-Renteria et al., 2020); on the contrary, a positive correlation was found for the *An.* gambiae cE5 (Rizzo et al., 2014a) and the *Ae. aegypti* D7s4 (Ribeiro et al., 2007; Londono-Renteria et al., 2018). Moreover, intensity and persistence of exposure plays a role in natural desensitization to salivary antigens (Mellanby, 1946; Feingold et al., 1968), and this may explain the different trends we observed in Padova, an

area colonized since more than 25 years, and in Belluno, where individuals were exposed to *Ae. albopictus* bites for no more than 5 years.

There are still some possible improvements and a few interesting open questions that wait for answers. First, the absence of unexposed controls prevented the determination of a threshold for seropositivity, which could provide very useful information on seroprevalence. Considering the widespread distribution of the tiger mosquito, getting reliable non-exposed controls may be not so straightforward. Nevertheless, their inclusion in future studies would be very important, especially in view of the encouraging results reported here. Second, it will be of interest to clarify the species-specificity of anti-al34k2 IgG responses. The 34k2 salivary proteins from *Ae. aegypti* and *Ae. albopictus* are 62% identical. However, sera of mice experimentally immunized to *Ae. aegypti* saliva do not carry IgG antibodies recognizing the al34k2 protein. Vice versa, sera from mice exposed to *Ae. albopictus* do not recognize the *Ae. aegypti* orthologous protein ae34k2, which suggests absence of cross-reactivity in the mouse model (Buezo Montero et al., 2019). It will be very interesting to measure the anti-al34k2 IgG responses in naturally exposed individuals living in areas where *Ae. aegypti* is abundant but *Ae. albopictus* is absent. Third, it will be of great value to verify the suitability of the al34k2 antigen for the evaluation of control interventions against the tiger mosquito as for example accomplished by Elanga Ndille and collaborators at La Reunion Island (Elanga Ndille et al., 2016). Finally, it would be very intriguing the validation of the al34k2 antigen in epidemiological settings where arboviral transmission is endemic and maintained by *Ae. albopictus*.

In conclusion, we believe that our study provides promising indications that IgG antibody responses to the *Ae. albopictus* 34k2 salivary protein may be exploited for the evaluation of human exposure to the tiger mosquito. It remains to be established if anti-al34k2 IgG responses represent a species-specific marker or may be useful as more general indicator of exposure to *Aedes* vectors. Serological assays as the one described here have the advantage of providing a direct measure of human-vector contact, not only at the community but also at the individual level, and may be useful to assess the efficacy of vector control interventions in interrupting this interaction. Such a complementary tool can also be employed for epidemiological studies and possibly for estimation of transmission risk. This may be especially helpful when implementation of classical entomological methods is difficult (low vector density, logistic constraints, limited resources, etc.) or when the simultaneous determination of exposure to vector and to specific circulating pathogen(s) by serological measurements may be needed.

DATA AVAILABILITY STATEMENT

The datasets generated for this study are available on request to the corresponding author.

ETHICS STATEMENT

This study involved healthy human volunteers and the protocol was reviewed and approved by the Ethics Committee of Sapienza University (306/17 RIF.CE: 4479, April 10th 2017). The volunteers provided their written informed consent to participate in this study.

AUTHOR CONTRIBUTIONS

BA conceived the study. FM, MP, GC, and BA designed the experiments. SB and FM performed the experiments. PG and FF provided the al34k2 antigen. AlB, SC, GD, and AnB provided the sera. SB, FM, MP, GC, and BA analyzed the data. SB, GC, and BA performed the statistical analysis. BA wrote the first draft of the manuscript. All authors contributed to manuscript revision, read and approved the final submitted version of the manuscript.

FUNDING

This work was partly funded by a grant from Regione Lazio to the Department of Public Health and Infectious Diseases, Sapienza University of Rome (FILAS-RU-2014-1034) and by funds from the Italian Ministry of Defense (PNRM 2017-SENSOR) to MP and BA. SB was supported by a fellowship from the PhD program in Infectious Diseases, Microbiology and Public Health, Sapienza University of Rome. PG was supported from the Fondazione Cariplo (Project 2017-0798). FF was supported by the Giovanni Armenise-Harvard Career Development Award 2013. PG and FF were supported by MIUR (PRIN-2017RPHBCW and Dipartimenti di Eccellenza program 2018-2023) and by the NATO Science for Peace and Security Program (ref. SPS G5701). GC and FM were supported by the Veneto region. The funders had no role in study design, data collection and analysis, decision to publish, or preparation of the manuscript.

ACKNOWLEDGMENTS

We wish to thank all volunteers for their consent in participating to this study. We are grateful and indebted to M. La Raja (Dept. Transfusion Medicine, Padua University Hospital, Padova, Italy) for the precious help and collaboration with sera collection in Padova. We are also very grateful to M. Mazzucato for making the maps, to P. Serini and M. Calzetta for providing the *Ae. albopictus* mosquitoes, M. Dal Pont for the help with the entomological monitoring in Belluno, M.L. Vitale and S. Carlin for the technical assistance.

SUPPLEMENTARY MATERIAL

The Supplementary Material for this article can be found online at: https://www.frontiersin.org/articles/10.3389/fcimb.2020.00377/full#supplementary-material

REFERENCES

Arcà, B., Lombardo, F., Francischetti, I. M., Pham, V. M., Mestres-Simon, M., Andersen, J. F., et al. (2007). An insight into the sialome of the adult female mosquito Aedes albopictus. *Insect. Biochem. Mol. Biol.* 37, 107–127. doi: 10.1016/j.ibmb.2006.10.007

Arcà, B., and Ribeiro, J. M. (2018). Saliva of hematophagous insects: a multifaceted toolkit. *Curr. Opin. Insect. Sci.* 29, 102–109. doi: 10.1016/j.cois.2018.07.012

Badu, K., Siangla, J., Larbi, J., Lawson, B. W., Afrane, Y., Ong'echa, J., et al. (2012). Variation in exposure to *Anopheles gambiae* salivary gland peptide (gSG6-P1) across different malaria transmission settings in the western Kenya highlands. *Malar. J.* 11:318. doi: 10.1186/1475-2875-11-318

Baldacchino, F., Montarsi, F., Arnoldi, D., Barategui, C., Ferro Milone, N., Da Rold, G., et al. (2017). A 2-yr mosquito survey focusing on aedes koreicus (Diptera: Culicidae) in Northern Italy and implications for adult trapping. *J. Med. Entomol.* 54, 622–630. doi: 10.1093/jme/tjw216

Bonizzoni, M., Gasperi, G., Chen, X., and James, A. A. (2013). The invasive mosquito species Aedes albopictus: current knowledge and future perspectives. *Trends Parasitol.* 29, 460–468. doi: 10.1016/j.pt.2013.07.003

Brady, O. J., and Hay, S. I. (2019). The first local cases of Zika virus in Europe. *Lancet* 394, 1991–1992. doi: 10.1016/S0140-6736(19)32790-4

Bretscher, P. A. (2014). On the mechanism determining the TH1/TH2 phenotype of an immune response, and its pertinence to strategies for the prevention, and treatment, of certain infectious diseases. *Scand. J. Immunol.* 79, 361–376. doi: 10.1111/sji.12175

Buezo Montero, S., Gabrieli, P., Severini, F., Picci, L., Di Luca, M., Forneris, F., et al. (2019). Analysis in a murine model points to IgG responses against the 34k2 salivary proteins from Aedes albopictus and Aedes aegypti as novel promising candidate markers of host exposure to Aedes mosquitoes. *PLoS Negl. Trop. Dis.* 13:e0007806. doi: 10.1371/journal.pntd.0007806

Capelli, G., Drago, A., Martini, S., Montarsi, F., Soppelsa, M., Delai, N., et al. (2011). First report in Italy of the exotic mosquito species *Aedes* (Finlaya) *koreicus*, a potential vector of arboviruses and filariae. *Parasit Vectors* 4:188. doi: 10.1186/1756-3305-4-188

Cardenas, J. C., Drame, P. M., Luque-Burgos, K. A., Berrio, J. D., Entrena-Mutis, E., Gonzalez, M. U., et al. (2019). IgG1 and IgG4 antibodies against Aedes aegypti salivary proteins and risk for dengue infections. *PLoS ONE* 14:e0208455. doi: 10.1371/journal.pone.0208455

CDC (2019) *Center for Disease Control and Prevention. Dengue Vaccine*. Available online at: https://www.cdc.gov/dengue/prevention/dengue-vaccine.html (accessed September 23, 2019).

Corran, P. H., Cook, J., Lynch, C., Leendertse, H., Manjurano, A., Griffin, J., et al. (2008). Dried blood spots as a source of anti-malarial antibodies for epidemiological studies. *Malar J.* 7:195. doi: 10.1186/1475-2875-7-195

Dalla Pozza, G., and Majori, G. (1992). First record of Aedes albopictus establishment in Italy. *J Am. Mosq. Control Assoc.* 8, 318–320.

Doucoure, S., Mouchet, F., Cornelie, S., DeHecq, J. S., Rutee, A. H., Roca, Y., et al. (2012a). Evaluation of the human IgG antibody response to Aedes albopictus saliva as a new specific biomarker of exposure to vector bites. *PLoS Negl Trop Dis.* 6:e1487. doi: 10.1371/journal.pntd.0001487

Doucoure, S., Mouchet, F., Cornelie, S., Drame, P. M., D'Ortenzio, E., DeHecq, J. S., et al. (2014). Human antibody response to Aedes albopictus salivary proteins: a potential biomarker to evaluate the efficacy of vector control in an area of Chikungunya and Dengue Virus transmission. *Biomed. Res. Int.* 2014:746509. doi: 10.1155/2014/746509

Doucoure, S., Mouchet, F., Cournil, A., Le Goff, G., Cornelie, S., Roca, Y., et al. (2012b). Human antibody response to Aedes aegypti saliva in an urban population in Bolivia: a new biomarker of exposure to Dengue vector bites. *Am. J. Trop. Med. Hyg.* 87:504–510. doi: 10.4269/ajtmh.2012.11-0477

Drame, P. M., Poinsignon, A., Besnard, P., Cornelie, S., Le Mire, J., Toto, J. C., et al. (2010). Human antibody responses to the Anopheles salivary gSG6-P1 peptide: a novel tool for evaluating the efficacy of ITNs in malaria vector control. *PLoS ONE* 5:e15596. doi: 10.1371/journal.pone.0015596

ECDC (2012). *European Centre for Disease Prevention and Control. Guidelines for the Surveillance of Invasive Mosquitoes in Europe*. Available online at: https://www.ecdc.europa.eu/sites/portal/files/media/en/publications/Publications/TER-Mosquito-surveillance-guidelines.pdf

Elanga Ndille, E., Doucoure, S., Damien, G., Mouchet, F., Drame, P. M., Cornelie, S., et al. (2012). First attempt to validate human IgG antibody response to Nterm-34kDa salivary peptide as biomarker for evaluating exposure to Aedes aegypti bites. *PLoS Negl. Trop. Dis.* 6:e1905. doi: 10.1371/journal.pntd.0001905

Elanga Ndille, E., Doucoure, S., Poinsignon, A., Mouchet, F., Cornelie, S., D'Ortenzio, E., et al. (2016). Human IgG antibody response to aedes Nterm-34kDa salivary peptide, an epidemiological tool to assess vector control in chikungunya and dengue transmission area. *PLoS Negl. Trop. Dis.* 10:e0005109. doi: 10.1371/journal.pntd.0005109

Espana, G., Yao, Y., Anderson, K. B., Fitzpatrick, M. C., Smith, D. L., Morrison, A. C., et al. (2019). Model-based assessment of public health impact and cost-effectiveness of dengue vaccination following screening for prior exposure. *PLoS Negl. Trop. Dis.* 13:e0007482. doi: 10.1371/journal.pntd.0007482

Feingold, B. F., Benjamini, E., and Michaeli, D. (1968). The allergic responses to insect bites. *Ann. Rev. Entomol.* 13, 137–158. doi: 10.1146/annurev.en.13.010168.001033

Fontaine, A., Pascual, A., Orlandi-Pradines, E., Diouf, I., Remoue, F., Pages, F., et al. (2011). Relationship between exposure to vector bites and antibody responses to mosquito salivary gland extracts. *PLoS ONE* 6:e29107. doi: 10.1371/journal.pone.0029107

Garcia-Robaina, J. C., de la Torre-Morin, F., Vazquez-Moncholi, C., Fierro, J., and Bonnet-Moreno, C. (1997). The natural history of Apis-specific IgG and IgG4 in beekeepers. *Clin. Exp. Allergy* 27, 418–423. doi: 10.1111/j.1365-2222.1997.tb00727.x

Giron, S., Franke, F., Decoppet, A., Cadiou, B., Travaglini, T., Thirion, L., et al. (2019). Vector-borne transmission of Zika virus in Europe, southern France, August 2019. *Euro. Surveill* 24:45. doi: 10.2807/1560-7917.ES.2019.24.45.1900655

Gobbi, F., Capelli, G., Angheben, A., Giobbia, M., Conforto, M., Franzetti, M., et al. (2014). Human and entomological surveillance of West Nile fever, dengue and chikungunya in Veneto Region, Italy, 2010-2012. *BMC Infect. Dis.* 14:60. doi: 10.1186/1471-2334-14-60

Gossner, C. M., Ducheyne, E., and Schaffner, F. (2018). Increased risk for autochthonous vector-borne infections transmitted by Aedes albopictus in continental Europe. *Euro. Surveill* 23:1800268. doi: 10.2807/1560-7917.ES.2018.23.24.1800268

Idris, Z. M., Chan, C. W., Mohammed, M., Kalkoa, M., Taleo, G., Junker, K., et al. (2017). Serological measures to assess the efficacy of malaria control programme on Ambae Island, Vanuatu. *Parasit Vectors* 10:204. doi: 10.1186/s13071-017-2139-z

Kraemer, M. U., Sinka, M. E., Duda, K. A., Mylne, A. Q., Shearer, F. M., Barker, C. M., et al. (2015). The global distribution of the arbovirus vectors Aedes aegypti and Ae. albopictus. *Elife* 4:e08347. doi: 10.7554/eLife.08347

Kraemer, M. U. G., Reiner, R. C. Jr., Brady, O. J., Messina, J. P., Gilbert, M., Pigott, D. M., et al. (2019). Past and future spread of the arbovirus vectors Aedes aegypti and Aedes albopictus. *Nat. Microbiol.* 4, 854–863. doi: 10.1038/s41564-019-0376-y

Londono-Renteria, B., Drame, P. M., Montiel, J., Vasquez, A. M., Tobon-Castano, A., Taylor, M., et al. (2020). Identification and pilot evaluation of salivary peptides from anopheles albimanus as biomarkers for bite exposure and malaria infection in Colombia. *Int. J. Mol. Sci.* 21:691. doi: 10.3390/ijms21030691

Londono-Renteria, B. L., Shakeri, H., Rozo-Lopez, P., Conway, M. J., Duggan, N., Jaberi-Douraki, M., et al. (2018). Serosurvey of human antibodies recognizing aedes aegypti D7 salivary proteins in Colombia. *Front. Public Health* 6:111. doi: 10.3389/fpubh.2018.00111

Lwande, O. W., Obanda, V., Lindstrom, A., Ahlm, C., Evander, M., Naslund, J., et al. (2019). Globe-trotting aedes aegypti and aedes albopictus: risk factors for arbovirus pandemics. *Vector Borne. Zoonotic. Dis.* 20, 71–81. doi: 10.1089/vbz.2019.2486

Manica, M., Rosa, R., Della Torre, A., and Caputo, B. (2017). From eggs to bites: do ovitrap data provide reliable estimates of Aedes albopictus biting females? *Peer J.* 5:e2998. doi: 10.7717/peerj.2998

Mellanby, K. (1946). Man's reaction to mosquito bites. *Nature* 158:554. doi: 10.1038/158554c0

Montarsi, F., Drago, A., Martini, S., Calzolari, M., De Filippo, F., Bianchi, A., et al. (2015). Current distribution of the invasive mosquito species, Aedes

koreicus [Hulecoeteomyia koreica] in northern Italy. *Parasit Vectors* 8:614. doi: 10.1186/s13071-015-1208-4

Montarsi, F., Martini, S., Michelutti, A., Da Rold, G., Mazzucato, M., Qualizza, D., et al. (2019). The invasive mosquito Aedes japonicus japonicus is spreading in northeastern Italy. *Parasit Vectors* 12:120. doi: 10.1186/s13071-019-3387-x

Montiel, J., Carbal, L. F., Tobon-Castano, A., Vasquez, G. M., Fisher, M. L., and Londono-Renteria, B. (2020). IgG antibody response against Anopheles salivary gland proteins in asymptomatic Plasmodium infections in Narino, Colombia. *Malar J.* 19:42. doi: 10.1186/s12936-020-3128-9

Ndille, E. E., Dubot-Peres, A., Doucoure, S., Mouchet, F., Cornelie, S., Sidavong, B., et al. (2014). Human IgG antibody response to Aedes aegypti Nterm-34 kDa salivary peptide as an indicator to identify areas at high risk for dengue transmission: a retrospective study in urban settings of Vientiane city, Lao PDR. *Trop. Med. Int. Health* 19, 576–580. doi: 10.1111/tmi.12280

Orlandi-Pradines, E., Almeras, L., Denis de Senneville, L., Barbe, S., Remoue, F., Villard, C., et al. (2007). Antibody response against saliva antigens of Anopheles gambiae and Aedes aegypti in travellers in tropical Africa. *Microbes Infect.* 9, 1454–1462. doi: 10.1016/j.micinf.2007.07.012

Peng, Z., and Simons, F. E. (1998). A prospective study of naturally acquired sensitization and subsequent desensitization to mosquito bites and concurrent antibody responses. *J. Allergy Clin. Immunol.* 101(2 Pt 1), 284–286. doi: 10.1016/S0091-6749(98)70395-1

Peng, Z., and Simons, F. E. (2004). Mosquito allergy: immune mechanisms and recombinant salivary allergens. *Int. Arch. Allergy Immunol.* 133, 198–209. doi: 10.1159/000076787

Poinsignon, A., Cornelie, S., Ba, F., Boulanger, D., Sow, C., Rossignol, M., et al. (2009). Human IgG response to a salivary peptide, gSG6-P1, as a new immuno-epidemiological tool for evaluating low-level exposure to Anopheles bites. *Malar J.* 8:198. doi: 10.1186/1475-2875-8-198

Poinsignon, A., Cornelie, S., Mestres-Simon, M., Lanfrancotti, A., Rossignol, M., Boulanger, D., et al. (2008). Novel peptide marker corresponding to salivary protein gSG6 potentially identifies exposure to Anopheles bites. *PLoS ONE* 3:e2472. doi: 10.1371/journal.pone.0002472

Pollard, E. J. M., Patterson, C., Russell, T. L., Apairamo, A., Oscar, J., Arca, B., et al. (2019). Human exposure to Anopheles farauti bites in the Solomon Islands is not associated with IgG antibody response to the gSG6 salivary protein of Anopheles gambiae. *Malar J.* 18:334. doi: 10.1186/s12936-019-2975-8

Proietti, C., Verra, F., Bretscher, M. T., Stone, W., Kanoi, B. N., Balikagala, B., et al. (2013). Influence of infection on malaria-specific antibody dynamics in a cohort exposed to intense malaria transmission in northern Uganda. *Parasite Immunol.* 35, 164–173. doi: 10.1111/pim.12031

Remoue, F., Cisse, B., Ba, F., Sokhna, C., Herve, J. P., Boulanger, D., et al. (2006). Evaluation of the antibody response to Anopheles salivary antigens as a potential marker of risk of malaria. *Trans. R. Soc. Trop. Med. Hyg.* 100, 363–370. doi: 10.1016/j.trstmh.2005.06.032

Renault, P., Solet, J. L., Sissoko, D., Balleydier, E., Larrieu, S., Filleul, L., et al. (2007). A major epidemic of chikungunya virus infection on Reunion Island, France, 2005-2006. *Am. J. Trop. Med. Hyg.* 77, 727–731. doi: 10.4269/ajtmh.2007.77.727

Ribeiro, J. M., Arcà, B., Lombardo, F., Calvo, E., Phan, V. M., Chandra, P. K., et al. (2007). An annotated catalogue of salivary gland transcripts in the adult female mosquito, *Aedes aegypti*. *BMC Genomics* 8:6. doi: 10.1186/1471-2164-8-6

Ribeiro, J. M., Mans, B. J., and Arcà, B. (2010). An insight into the sialome of blood-feeding Nematocera. *Insect. Biochem. Mol. Biol.* 40, 767–784. doi: 10.1016/j.ibmb.2010.08.002

Ribeiro, J. M. C., and Arcà, B. (2009). From sialomes to the sialoverse: an insight into salivary potion of blood-feeding insects. *Adv. Insect. Physiol.* 37:59. doi: 10.1016/S0065-2806(09)37002-2

Rizzo, C., Lombardo, F., Ronca, R., Mangano, V., Sirima, S. B., Nebie, I., et al. (2014a). Differential antibody response to the *Anopheles gambiae* gSG6 and cE5 salivary proteins in individuals naturally exposed to bites of malaria vectors. *Parasit Vectors* 7:549. doi: 10.1186/s13071-014-0549-8

Rizzo, C., Ronca, R., Fiorentino, G., Mangano, V. D., Sirima, S. B., Nebie, I., et al. (2011a). Wide cross-reactivity between *Anopheles gambiae* and *Anopheles funestus* SG6 salivary proteins supports exploitation of gSG6 as a marker of human exposure to major malaria vectors in tropical Africa. *Malar J.* 10:206. doi: 10.1186/1475-2875-10-206

Rizzo, C., Ronca, R., Fiorentino, G., Verra, F., Mangano, V., Poinsignon, A., et al. (2011b). Humoral response to the *Anopheles gambiae* salivary protein gSG6: a serological indicator of exposure to Afrotropical malaria vectors. *PLoS ONE* 6:e17980. doi: 10.1371/journal.pone.0017980

Rizzo, C., Ronca, R., Lombardo, F., Mangano, V., Sirima, S. B., Nebie, I., et al. (2014b). IgG1 and IgG4 antibody responses to the *Anopheles gambiae* salivary protein gSG6 in the sympatric ethnic groups Mossi and Fulani in a malaria hyperhendemic area of Burkina Faso. *PLoS ONE* 9:e96130. doi: 10.1371/journal.pone.0096130

Romi, R., Di Luca, M., and Majori, G. (1999). Current status of Aedes albopictus and Aedes atropalpus in Italy. *J. Am. Mosq. Control Assoc.* 15, 425–427.

Sagna, A. B., Yobo, M. C., Elanga Ndille, E., and Remoue, F. (2018). New immuno-epidemiological biomarker of human exposure to aedes vector bites: from concept to applications. *Trop. Med. Infect. Dis.* 3:80. doi: 10.3390/tropicalmed3030080

Schwartz, B. S., Ribeiro, J. M., and Goldstein, M. D. (1990). Anti-tick antibodies: an epidemiologic tool in Lyme disease research. *Am. J. Epidemiol.* 132, 58–66. doi: 10.1093/oxfordjournals.aje.a115643

Stone, W., Bousema, T., Jones, S., Gesase, S., Hashim, R., Gosling, R., et al. (2012). IgG responses to *Anopheles gambiae* salivary antigen gSG6 detect variation in exposure to malaria vectors and disease risk. *PLoS ONE* 7:e40170. doi: 10.1371/journal.pone.0040170

Trevejo, R. T., and Reeves, W. C. (2005). Antibody response to *Culex tarsalis* salivary gland antigens among sentinel chickens in California. *Am. J. Trop. Med. Hyg.* 72, 481–487. doi: 10.4269/ajtmh.2005.72.481

Varga, E. M., Kausar, F., Aberer, W., Zach, M., Eber, E., Durham, S. R., et al. (2013). Tolerant beekeepers display venom-specific functional IgG4 antibodies in the absence of specific IgE. *J. Allergy Clin. Immunol.* 131, 1419–1421. doi: 10.1016/j.jaci.2012.08.037

Velo, E., Kadriaj, P., Mersini, K., Shukullari, A., Manxhari, B., Simaku, A., et al. (2016). Enhancement of Aedes albopictus collections by ovitrap and sticky adult trap. *Parasit Vectors* 9:223. doi: 10.1186/s13071-016-1501-x

Vincent, M., Larrieu, S., Vilain, P., Etienne, A., Solet, J. L., Francois, C., et al. (2019). From the threat to the large outbreak: dengue on Reunion Island, 2015 to 2018. *Euro. Surveill.* 24:47. doi: 10.2807/1560-7917.ES.2019.24.47.1900346

WHO (2019). *World Health Organization. Yellow fever Fact Sheets*. Available online at: https://www.who.int/news-room/fact-sheets/detail/yellow-fever

Wilder-Smith, A., Gubler, D. J., Weaver, S. C., Monath, T. P., Heymann, D. L., and Scott, T. W. (2017). Epidemic arboviral diseases: priorities for research and public health. *Lancet Infect. Dis.* 17, e101–e106. doi: 10.1016/S1473-3099(16)30518-7

Ya-Umphan, P., Cerqueira, D., Parker, D. M., Cottrell, G., Poinsignon, A., Remoue, F., et al. (2017). Use of an anopheles salivary biomarker to assess malaria transmission risk along the thailand-myanmar border. *J. Infect. Dis.* 215, 396–404. doi: 10.1093/infdis/jiw543

Yman, V., White, M. T., Rono, J., Arca, B., Osier, F. H., Troye-Blomberg, M., et al. (2016). Antibody acquisition models: A new tool for serological surveillance of malaria transmission intensity. *Sci. Rep.* 6:19472. doi: 10.1038/srep19472

Yobo, C. M., Sadia-Kacou, C. A. M., Adja, M. A., Elanga-Ndille, E., Sagna, A. B., Guindo-Coulibaly, N., et al. (2018). Evaluation of human exposure to aedes bites in rubber and palm cultivations using an immunoepidemiological biomarker. *Biomed. Res. Int.* 2018:3572696. doi: 10.1155/2018/3572696

Conflict of Interest: The authors declare that the research was conducted in the absence of any commercial or financial relationships that could be construed as a potential conflict of interest.

frontiers in Cellular and Infection Microbiology

REVIEW
published: 07 August 2020
doi: 10.3389/fcimb.2020.00407

Aedes Mosquito Salivary Components and Their Effect on the Immune Response to Arboviruses

David Guerrero[1]*, *Tineke Cantaert*[1] and *Dorothée Missé*[2]*

[1] Immunology Unit, Institut Pasteur du Cambodge, Institut Pasteur International Network, Phnom Penh, Cambodia,
[2] MIVEGEC, IRD, University of Montpellier, CNRS, Montpellier, France

Vector-borne diseases are responsible for over a billion infections each year and nearly one million deaths. Mosquito-borne dengue virus, West Nile, Japanese encephalitis, Zika, Chikungunya, and Rift Valley Fever viruses constitute major public health problems in regions with high densities of arthropod vectors. During the initial step of the transmission cycle, vector, host, and virus converge at the bite site, where local immune cells interact with the vector's saliva. Hematophagous mosquito saliva is a mixture of bioactive components known to modulate vertebrate hemostasis, immunity, and inflammation during the insect's feeding process. The capacity of mosquito saliva to modulate the host immune response has been well-studied over the last few decades and has led to the consensus that the presence of saliva is linked to the enhancement of virus transmission, host susceptibility, disease progression, viremia levels, and mortality. We review some of the major aspects of the interactions between mosquito saliva and the host immune response that may be useful for future studies on the control of arboviruses.

Keywords: arbovirus, mosquito saliva, immune response, saliva composition, *Aedes* spp

OPEN ACCESS

Edited by:
Lucas Tirloni,
National Institutes of Health (NIH),
United States

Reviewed by:
Saravanan Thangamani,
Upstate Medical University,
United States
Thiago DeSouza-Vieira,
National Institutes of Health (NIH),
United States
Anderson Sa-Nunes,
University of São Paulo, Brazil

***Correspondence:**
David Guerrero
dguerrero@pasteur-kh.org
Dorothée Missé
dorothee.misse@ird.fr

Specialty section:
This article was submitted to Parasite and Host, a section of the journal Frontiers in Cellular and Infection Microbiology

Received: *05 April 2020*
Accepted: *30 June 2020*
Published: *07 August 2020*

Citation:
Guerrero D, Cantaert T and Missé D (2020) Aedes Mosquito Salivary Components and Their Effect on the Immune Response to Arboviruses. Front. Cell. Infect. Microbiol. 10:407. doi: 10.3389/fcimb.2020.00407

INTRODUCTION

Each year, more than one billion people are infected with vector-borne diseases and nearly one million die as a result. These diseases take a toll on the health and quality of life of the population and have been shown to increase poverty in vulnerable communities due to illness and disability (WHO, 2020). Arboviruses represent an important group of pathogens that cause vector-borne diseases worldwide. There are more than 100 arboviruses known to cause disease in humans and they all share the common characteristic of being transmitted by hematophagous mosquitoes or ticks (LaBeaud et al., 2011). Although many infections are asymptomatic or cause a mild transient fever, progression to more severe pathologies, such as hemorrhagic fever, encephalitis, central nervous system involvement, or arthritis, can occur (Huang et al., 2019). Among the various arboviruses that can infect humans, mosquito-borne dengue (DENV), West Nile (WNV), Japanese encephalitis (JEV), Zika (ZIKV), Chikungunya (CHIKV), and Rift Valley Fever (RVFV) viruses are responsible for major public health problems in regions with high densities of arthropod vectors (Rolin et al., 2013; Wilder-Smith et al., 2017). DENV, WNV, JEV, and ZIKV belong to the *Flavivirus* genus of the *Flaviviridae* family. Their single-stranded positive-sense RNA genomes are typically 11 kb and encode seven non-structural proteins and three structural proteins (C, M, and E) (Laureti et al., 2018). On the other hand, CHIKV and RVFV belong to the *Alphaviridae* and *Phlebovirus* genera, respectively. CHIKV has a single-stranded positive-sense RNA genome that encodes four non-structural and five structural

proteins, whereas RVFV has a tripartite genome, consisting of three single-stranded negative-sense RNA segments that together code for structural and non-structural proteins (Hartman, 2017; Vu et al., 2017). The transmission of most of these viruses is urban/peri-urban in human-mosquito infection cycles (Weaver and Reisen, 2010). As a result, there is a high rate of transmission in densely-populated regions (Struchiner et al., 2015). The successful propagation of these viruses worldwide can be attributed to various factors, amongst the most relevant, the wide distribution of *Aedes* spp. in all continents (Wilder-Smith et al., 2017), human travel and migration (Gould et al., 2017), animal trade (Pfeffer and Dobler, 2010), the creation of ecosystems that favor human-vector interactions (Kilpatrick and Randolph, 2012), and climate change, which favors vector populations (Papa, 2019). Transmission is initiated when a vertebrate host is inoculated with the virus during the blood-feeding of an infected mosquito. During this initial step of the cycle, vector, host, and pathogen converge at the bite site, making this event important for understanding the immune interactions in the skin microenvironment. Once the mosquito locates a vertebrate host, it penetrates the epidermis and dermis with its proboscis, and probes the site until it finds a suitable vessel or hemorrhagic blood pool (Townson, 1993). A salivary mixture containing pharmacologically active compounds, known to modulate host inflammation, hemostasis, and immunity, is injected during probing and facilitates blood intake by the insect by preventing clotting and platelet aggregation and promoting vasodilation (Manning and Cantaert, 2019). It is now known that certain molecules present in the vector's saliva can affect the course of infection, the replication capacity of the virus, and the host immune response (Schneider and Higgs, 2008; Pingen et al., 2017; Vogt et al., 2018). Here, we have provided a comprehensive overview of the anti-arboviral immune response, as well as its modulation by mosquito saliva, within the environment of the skin. We conclude with a prospective appraisal of the development of vaccines.

Aedes MOSQUITO SALIVARY COMPONENTS

Hematophagous mosquito saliva is a mixture of bioactive components known to modulate vertebrate hemostasis, immunity, and inflammation during the insect's feeding process. A recent proteome study identified 1,208 proteins from female *Aedes aegypti* salivary glands using LC-MS/MS analysis (Dhawan et al., 2017). This protein profile was further classified based on molecular functions assigned using bioinformatics databases. Translation, metabolism, oxidation-reduction, and cellular organization were the processes with the highest representation after classification. Furthermore, among the proteins identified in the study, a group of 238 was not attributed with any molecular function. Nevertheless, 64 of these unclassified proteins were predicted to have a signal peptide cleavage site and thought to be secreted. Importantly, salivary factor expression can vary depending on whether the mosquito has fed (blood fed or not) and the infection status (Thangamani and Wikel, 2009; Bonizzoni et al., 2012). These aspects need to be considered in studies examining the effects of mosquito saliva in the infection of target cells with arboviruses. Indeed, several studies have been conducted with saliva from uninfected mosquitoes. The nature of secretory bioactive factors in mosquito saliva is not restricted to proteins alone. In a study conducted by the University of Texas Medical Branch, the authors extracted short non-coding RNAs from the saliva of *A. aegypti* and *Aedes albopictus* mosquitos, infected or not with CHIKV (Maharaj et al., 2015). The researchers found novel microRNAs (miRNAs) expressed only during infection, which they believed could play an important role in regulating the establishment of infection in the vertebrate host during blood feeding. The amount of documented evidence from various disease models, pathogens, and mosquito species has led to the consensus that the presence of saliva and/or mosquito feeding is connected with enhancement of virus transmission, host susceptibility, disease progression, viremia levels, and mortality (Schneider and Higgs, 2008). To date, certain salivary factors have been separately characterized and their immunological role in infection determined (**Table 1**). However, this list is very limited and many studies remain to be conducted in order to better characterize the function of salivary components. The effects of salivary proteins in the host immune response can also vary as a function of the concentration of salivary-gland extracts (SGE). In some studies, high concentrations have been reported to be immune-suppressive, whereas low concentrations have been associated with modulation of the immune response, which normally corresponds to the downregulation of Th1 cytokines and a shift toward a Th2 response (Schneider and Higgs, 2008).

MOSQUITO BITES AND THE EFFECT OF SALIVA ON VIRAL REPLICATION AND DISSEMINATION

The comparison between virus infection dynamics in animals infected through various inoculation routes, has permitted to observe the impact that mosquito-aided viral entry can have on the host. Mice infected with WNV via mosquito bite show higher viral loads and earlier dissemination from local inoculation sites to neighboring tissues than mice infected by needle injection, including earlier breach of the nervous system (Styer et al., 2011). In rhesus macaques, inoculation of DENV through infected mosquito feeding leads to higher and longer viremia than inoculation via subcutaneous, intradermal, or intradermal + SGE needle injection. In addition, macaques infected via mosquito feeding and intradermal + SGE injection show skin inflammation and cellular infiltration at the site of inoculation and higher levels of liver aminotransferase than those infected through other inoculation routes (McCracken et al., 2020). In a similar study, investigators found that macaques infected with ZIKV via mosquito bite developed systemic infection and altered tissue tropism to the virus, which was disseminated mainly in the hemolymphatic tissues, female reproductive tract, liver, and kidneys, whereas the virus was also detected in the cerebrum of one animal and the eyes of the two animals inoculated

TABLE 1 | Summary of salivary factors and their known or suspected role in host immunity.

Factor	Species	Mechanism	Effect	References
A. aegypti venom allergen-1 (*Aa*VA-1)	*A. aegypti*	Binds to autophagy inhibitor LRPPRC. Promotes autophagy activation.	Enhances viral replication in DCs and macrophages.	Sun et al., 2020
Neutrophil stimulating factor 1 (NeSt1)	*A. aegypti*	Induces expression of chemokines (pro-IL-1β, CXCL2 and CCL2)	Enhances viral replication. Promotes the recruitment of macrophages and activation of neutrophils.	Hastings et al., 2019
LTRIN	*A. aegypti*	Inhibits activation of NF-kB	Decreases the expression of pro-inflammatory cytokines	Jin et al., 2018
Anticlotting serpin-like protein (AT)	*A. aegypti*	Unknown	Enhances viral replication	Surasombatpattana et al., 2014
Adenosine deaminase (AD)	*A. aegypti*	Inhibits IFN-α and IFN-β mRNA expression	Enhances viral replication	
Putative 34 kDa family secreted salivary protein	*A. aegypti*	Inhibits type I IFN expression	Enhances viral replication	
Putative secreted protein (VA)	*A. aegypti*	Inhibits IFN-α and IFN-β mRNA expression	Enhances viral replication	
Serine protease CLIPA3	*A. aegypti*	Unknown	Enhances infection	Conway et al., 2014
A. aegypti bacteria-responsive protein 1 (AgBR1)	*A. aegypti*	Upregulates chemo-attractive chemokines, promotes neutrophil recruitment to bite site.	Enhances infection Increased disease severity	Uraki et al., 2019
miRNA-100	*A. aegypti*	Not known	Possible effect on the regulation of immune cell activity and influences viral replication.	Maharaj et al., 2015
miRNA-125	*A. aegypti*	Not known		

via subcutaneous needle injection (Dudley et al., 2017). No significant difference was observed in the peak viral load between the two groups, but the time to reach the viral load was different, with the subcutaneous group reaching the viremia peak faster than the mosquito-infected group. In the case of RVFV, intradermal infection of mice in conjunction with SGE leads to a significant increase in viral titers in blood, brain, and liver, and more severe thrombocyto/leukopenia (Le Coupanec et al., 2013). Additionally, mice intradermally infected with RVFV and exposed to non-infected mosquito bites show shorter survival. Similarly, a mouse model for infection using an avirulent strain of the Semliki Forest virus, a virus closely related to CHIKV, showed that mice exposed to the virus after *A. aegypti* feeding showed higher viral RNA levels at the inoculation site than unbitten mice, as well as earlier dissemination to the brain and evolution to a lethal outcome in some of the mice (Pingen et al., 2016). Although not explored exhaustively, the effect that varying the localization of the saliva inoculum induces in the host has also been investigated. Mice that receive WNV and SGE inoculated together show significantly higher viral titers than those that receive the virus and SGE separately in distal locations, highlighting the local effect of salivary factors on enhancing viremia (Styer et al., 2011).

EFFECT OF SALIVA ON ARBOVIRUS INTERACTIONS WITH THE SKIN ENVIRONMENT

The first cells to interact with the virus are those that constitute the immune system within the skin, as the virus is directly injected into the epidermis and dermis of the host (**Figure 1**). Resident immune skin cells, such as Langerhans cells (LCs), occupy the epidermis together with keratinocytes, whereas various subpopulations of dendritic cells (DCs), macrophages, and T cells reside in the dermis (Matejuk, 2018), all of which can be targets of infection and sites of initial replication for arboviruses (Wu et al., 2000; Limon-Flores et al., 2005; Durbin et al., 2008; Silveira et al., 2018). Since these cells are both permissive to infection and hold the capacity to elicit immune responses, they play a dual role in the infection process: both as replication targets/dissemination vehicles and as the first line of defense. Keratinocytes are able to recognize pathogen-associated molecular patterns (PAMPs) through pattern recognition receptors (PRRs). Upon stimulation, they promote pro-inflammatory responses, along with the production of interferons (IFNs), chemokines, and cytokines (Miller, 2008; Briant et al., 2014). In a recent study, Garcia et al. (2018) observed that keratinocytes produce a type I and III interferon inflammatory response when infected with WNV that is associated with viral load. In addition, the expression of pro-inflammatory cytokines, such as TNF-α and IL-6, and various chemokines by keratinocytes increased significantly after viral infection. In the context of ZIKV, *in vitro* infection of skin fibroblasts leads to active viral replication of the virus (Hamel et al., 2015). Recognition of the virus by skin fibroblast is mostly mediated by RIG-I, MDA5, and TLR3 and induces IFN-α and IFN-β production, as well as that of the CXCR3 ligand CXCL10 and the antiviral chemokine CCL5. Fibroblasts have been reported to be highly susceptible to CHIKV and WNV infection (Ekchariyawat et al., 2015). Activation of these cells following infection appears to elicit similar antiviral responses

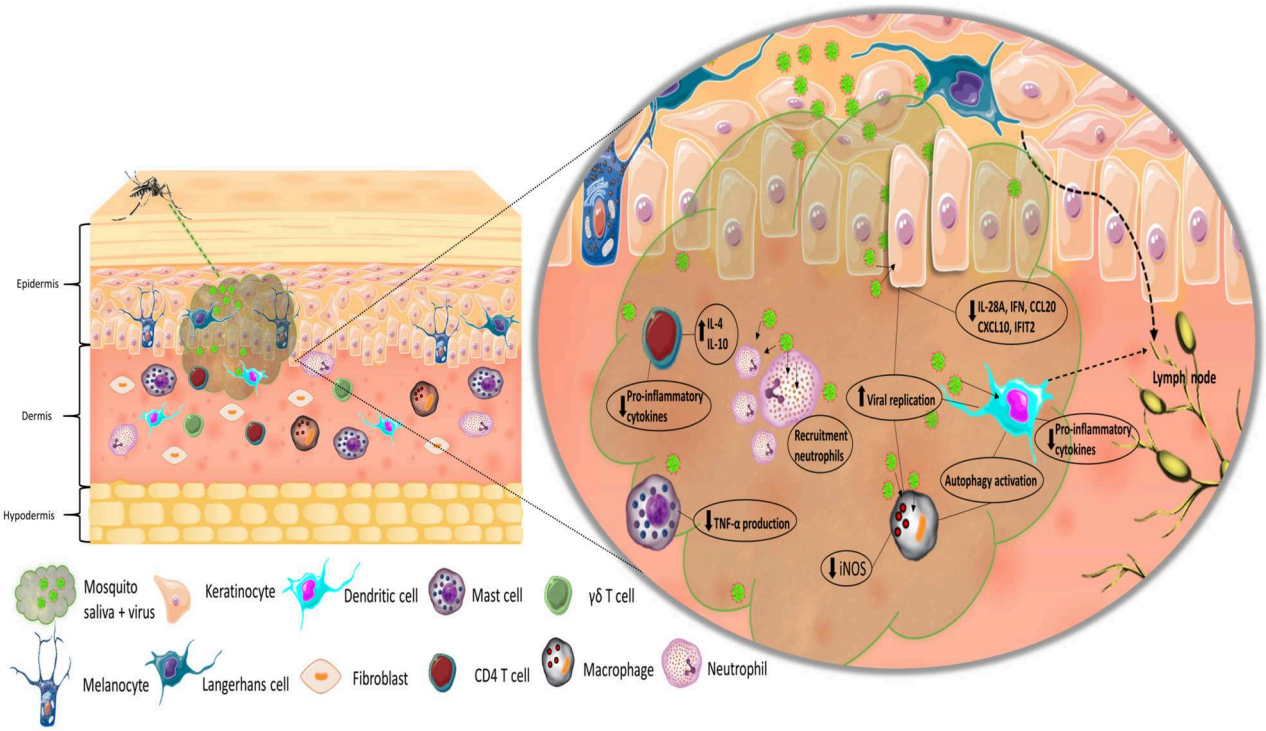

FIGURE 1 | Simplified representation of the inoculation of virus and mosquito saliva into the skin. Recognition of the virus by LCs and DCs, and migration to lymph node. Effect of mosquito saliva on skin immune resident and infiltrating cells.

to both viruses, which consist of increased levels of IL-1β (due to maturation of caspase 1), IFN-β, and other pro-inflammatory cytokines and chemokines. In this case, inflammasome activation via caspase 1 appears to be of particular importance in controlling CHIKV replication in fibroblasts. Keratinocytes infected with WNV in the presence of *A. aegypti* saliva show higher viral replication levels than cells infected without saliva at 48 h post-infection. Saliva-treated cells also present lower levels of mRNA for the inflammatory mediators IL-28A, CXCL10, IFIT2, and CCL20 24 h post-infection. Interestingly, treatment of infected keratinocytes with *Culex quinquefasciatus* saliva also leads to decreased levels of inflammatory mediators, but not to higher viral replication (Garcia et al., 2018). Similarly, keratinocytes show significantly higher viral loads at 6 and 24 h post-infection upon infection with DENV in the presence of *A. aegypti* saliva than those infected with virus alone. Decreased expression levels of β-defensin 3, LL-37, Elafin, and S100A7 at 6 h post-infection and IFNs at 24 h post-infection have also been observed (Surasombatpattana et al., 2012). *A. aegypti* bacteria-responsive protein 1 (AgBR1) is a protein upregulated in the salivary glands of mosquitoes after blood feeding (Ribeiro et al., 2007) that promotes the recruitment of $CD45^{+}CD11b^{+}Ly6G^{+}$ cells, along with the upregulation of neutrophil- and monocytic-attracting chemokine expression at the bite site of mice infected with ZIKV via mosquito bite (Uraki et al., 2019). By stimulating the recruitment of cells susceptible to infection and dampening pro-inflammatory responses, mosquito salivary factors generate an auspicious environment for viral replication. Furthermore, as the earliest interactions of the immune system with arboviruses occur at the inoculation site, modulation of these processes give the virus an advantage in the infection-immune response dynamics.

EFFECT OF SALIVA ON THE INNATE IMMUNE RESPONSE TO ARBOVIRUSES

The modulatory effects of vector saliva factors on the innate immune system are an important contributing factor in the enhancement of viral replication and dissemination. In a recent study, Sun et al. identified a protein, designated *Aa*VA-1, that induces enhancement of viral replication of both ZIKV and DENV in DCs and macrophages (Sun et al., 2020). Silencing of this protein in the mosquitoes led to decreased viremia in ZIKV-infected mice, along with delayed death. Incubation of THP-1 cells, a monocytic cell line, with *Aa*VA-1 did not influence the production of TNF-α, IL-1β, IL-8, monocyte chemotactic protein-1 (MCP-1), IFN-β, IFN-α2, or IFN-α7. The investigators postulated that the protein enhances viral replication by a mechanism other than the modulation of Th1 cytokine production. Interestingly, use of an immuno-pulldown assay to identify proteins that bind to *Aa*VA-1 showed that the protein binds to the autophagy inhibitor, leucine-rich pentatricopeptide repeat-containing protein (LRPPRC). This inhibitor suppresses the initiation of autophagy by binding and sequestering Beclin-1.

The ability of *Aa*VA-1 to bind to LRPPRC and displace Beclin-1, by competing for the same binding motif, enables the initiation of autophagy signaling and thus enhances viral transmission and replication. The effect of this salivary protein could therefore have a major impact on the severity of the disease. It is important to note however that ZIKV, like other flaviviruses, has developed sophisticated mechanisms to overcome autophagy (Chiramel and Best, 2018). Moreover, it has been reported that mosquito SGE significantly suppresses inducible nitric oxide synthase (iNOS) in macrophages. Suppressing the expression of iNOS lowers the levels of the reactive oxygen intermediate NO which is an important factor that regulates the functional activity, growth, and death of macrophages, T cells, NK cells, and neutrophils. Thus, the decrease of NO levels by mosquito saliva deregulates the activity of these immune cells (Schneider et al., 2010; Barros et al., 2019).

Neutrophils are an abundant cell population of the innate immune system. They are effective in controlling pathogens by degranulation, phagocytosis, and the formation of neutrophil extracellular traps (NETs) (Rosales, 2018). Murine neutrophils deploy NETs upon CHIKV infection, in a TLR7- and reactive oxygen species-dependent manner, which can neutralize the virus and lower its infective capacity (Hiroki et al., 2020). Furthermore, mice treated with DNase, which impairs the functionality of NETs, showed increased viral loads and were more susceptible to infection than controls. Indeed, the effect of neutrophils on disease protection can vary depending on the virus and the degree of NETs production (Opasawatchai et al., 2019). Neutrophil stimulating factor 1 (NeSt1) is a newly described salivary protein that enhances ZIKV replication and pathogenesis in mice (Hastings et al., 2019). The protein induces expression of pro-IL-1β, CXCL2, and CCL2, leading to the activation of primary neutrophils and further recruitment of macrophages, which are highly susceptible to infection. Interestingly, passive immunization against the NeSt1 protein prevents early replication and ameliorates pathogenesis in infected mice.

IFNs limit infection by inducing the expression of IFN-stimulated genes (ISGs), disrupting viral replication cycles at various steps (Sen, 2001). PRRs, such as RIG-1 and MDA5, can recognize viral genome particles in the cell cytosol (Hollidge et al., 2011) and their activation leads to type I IFN expression (Sharma, 2003). Other receptors, such as TLR3, TLR7, TLR8, and TLR9, promote type I IFN and NF-kB signaling pathway activation (Yamamoto et al., 2002; Kawai and Akira, 2007). The effectiveness of IFN responses to control arbovirus infections has been documented in several studies. In a hospital-based study in Taiwan, researchers reported that the serum of patients with severe dengue contained less IFN-α than that of patients with non-severe manifestations, supporting the relationship between IFN and protection (Chen et al., 2007). Jiang et al. observed that five ISGs were able to significantly inhibit both WNV and DENV replication and viral entry (Jiang et al., 2010). Additionally, the screening of more than 380 human genes using an overexpression-based approach identified several additional ISGs that suppress WNV replication (Schoggins et al., 2011). In the context of RVFV infection, it has been reported that a critical component of the host immune response to the virus is a robust type I IFN response shortly after infection (do Valle et al., 2010). In addition, early studies performed in rhesus macaques showed that macaques given IFN-α replacement therapy were able to control infection with RVFV (Morrill et al., 1989). In ZIKV *in vitro* studies, treatment of vaginal and cervical epithelial cells, important in the sexual transmission of Zika, with IFN-α/β or IFN-λ inhibited viral infection (Caine et al., 2019). In mouse models, $CD4^+$ T cells, which have the ability to reduce the viral load in the brain, control disease progression, and prevent fatal outcome after ZIKV infection, appeared to be dependent on IFN-γ signaling pathways (Lucas et al., 2018). Additionally, infection of mice lacking IRF-3 and IRF-7 with CHIKV has been shown to lead to fatal outcomes due to hemorrhagic shock (Rudd et al., 2012; Schilte et al., 2012). These studies show the fundamental role of IFN responses in limiting arbovirus infections.

Studies from the early 90's already reported the inhibition of TNF-α production by rat mast cells cultured with SGE from *A. aegypt*i (Bissonnette et al., 1993) and the suppression of IL-2 and IFN-γ production by naïve spleen cells cultured with *A. aegypt*i SGE in mouse models (Cross et al., 1994). The downregulation of cellular pro-inflammatory responses affects viral infection and disease progression, as this mechanism is crucial for controlling viral infections. Polarization toward Th2 responses has been observed in mice after concomitant infection with the virus and salivary proteins. Mice that were exposed to *Culex pipiens* and *A. aegypti* for 4–10 days showed marked downregulation of IFN-γ production after mosquito feeding, along with upregulated production of IL-4 and IL-10 (Zeidner et al., 1999). In a separate study, cytokine expression in the skin of mice was analyzed after intradermal inoculation with *A. aegypti* SGE in combination with Sindbis virus (Schneider et al., 2004). Co-inoculation with the virus and SGE led to reduced production of IFN-β and IFN-γ. In contrast, the expression of IL-4 and IL-10 was significantly upregulated (Schneider et al., 2004). Upregulation of IL-10 production in mice has been associated with impaired Th1 cell responses, thus promoting prolonged and persistent viral infection (Brooks et al., 2006). In addition, humanized mice infected with DENV via mosquito bite show higher viremia than mice infected by injection (Cox et al., 2012). SGE itself appears to enhance thrombocytopenia in these animals.

An *in vitro* study performed on HaCaT and A549 cells showed dampened IL-8 production by cells treated with either CHIKV + SGE or SGE alone, alongside increased viral replication (Puiprom et al., 2013). Additionally, a comparative analysis of cytokine gene expression of mice bitten by uninfected mosquitoes and those bitten by mosquitoes infected with CHIKV showed an altered cytokine expression profile in both cases, characterized by the upregulation of IL-4 and downregulation of IL-2, IFN-γ, and TLR-3 relative to unbitten controls (Thangamani et al., 2010). The investigators also infected mice with CHIKV by needle intradermal injection and observed expression profiles characteristic of a pro-inflammatory response, increased IL-2, IFN-γ, and TLR-3 expression, along with decreased IL-4 and IL-10 expression, contrary to those observed for the mosquito-bitten cases. Interestingly, although the observed cytokine expression profiles of both the mice bitten by uninfected mosquitoes and

those bitten by CHIKV-infected mosquitoes were similar and showed a shift from Th1 to Th2 responses, the effect on IL-4 expression appeared to be greater in the individuals bitten by CHIKV-infected mosquitoes. In a previous study, Thangamani et al. described similar effects of mosquito saliva/bites on the production of IL-4 using a TCR transgenic mouse model (Boppana et al., 2009). Here, exposure to both SGE and mosquito bite induced increased IL-4 expression by $CD4^+$ T cells. Furthermore, the investigators were able to identify a newly described protein, salivary *A. aegypti* IL-4-inducing protein (SAAG-4), which upregulates IL-4 and IL-10 expression and downregulates the expression of IL-12, IFN-γ, and TNF-α in skin. The processes by which salivary proteins modulate cytokine production are not completely understood, but insights about possible mechanisms have become available in recent years.

In a recent study, researchers identified and characterized a 15-kD protein, LTRIN, isolated from *A. aegypti* salivary grands, which was found to be upregulated in blood-fed mosquitos (Jin et al., 2018). The investigators assessed the protein's immunosuppressive activity by infecting human THP-1 cells, human umbilical-vein endothelial cells, mouse BMDMs, and mouse skin fibroblasts with ZIKV in the presence or absence of the protein. In the presence of LTRIN, the level of intracellular transcripts of the virus increased in a dose-dependent manner in all cell types tested. Furthermore, LTRIN binds to the lymphotoxin-β receptor (LTβR), which initiates signaling pathways that regulate various processes, such as cell differentiation, development, and homeostasis of lymph nodes, type I IFN production, and hepatic regeneration (Ware, 2005; Gommerman et al., 2014). Binding of LTRIN to LTβR inhibits the dimerization and activation of the latter, resulting in the inhibition of the NF-κB signaling pathway and the subsequent production of pro-inflammatory cytokines (Jin et al., 2018). This is in accordance with the observations of the gene expression profile of the pro-inflammatory cytokines IL-1, IL-6, and TNF-α, which were expressed at a significantly lower level in cells treated with LTRIN. In a different study, four new proteins that are abundant in mosquito saliva were found to enhance the infection of human keratinocytes by DENV (Surasombatpattana et al., 2014). The proteins were identified after genomic and proteomic analyses of female *A. aegypti* salivary glands and shown to be an anticlotting serpin-like protein (AT), adenosine deaminase (AD), a putative 34-kDa family secreted salivary protein, and a putative secreted protein (VA). Higher DENV mRNA transcripts were found in keratinocytes incubated in the presence of each of these proteins than those incubated with the virus alone. Furthermore, of the four proteins, VA and AD were found to significantly inhibit IFN-α and IFN-β mRNA expression. The 34-kDa protein was reported to completely inhibit type I IFN expression. In accordance with its ability to inhibit type I IFN expression, the 34-kDa protein also inhibited the expression of both IRF3 and IRF7. Despite these advances, additional studies are still needed to determine the individual role that most of the salivary proteins of *A. aegypti* could play in the innate immune response against arboviruses. At present, the lack of these studies could be explained by the difficulty of producing recombinant salivary proteins. Another mechanism that enables *A. aegypti* saliva to modulate interferon responses involves interference of the Janus kinase/signal transducers and activators of transcription (JAK/STAT) signaling pathway. Activation of this pathway leads to the expression of ISG and many antiviral effectors (Nan et al., 2017) and in a recent study, it was observed to be affected by mosquito saliva (Wichit et al., 2017). The study reported downregulation of STAT2 and its phosphorylated form in human skin fibroblast infected with CHIKV in the presence of *A. aegypti* saliva, which led to a marked decrease in type I ISG production.

THE EFFECT OF SALIVA ON THE COMPLEMENT SYSTEM RESPONSE TO ARBOVIRUS

The complement system is a collection of more than 30 soluble and cell-surface proteins that recognize PAMPs. It can be activated by three different pathways: the classical pathway (CP), the lectin pathway (LP), and the alternative pathway (AP) (Stoermer and Morrison, 2011). The involvement of complement as a protective mechanism against arboviruses has been reported in various studies. Mice deficient for C3 or complement receptors 1 and 2 experience a higher WNV burden and higher mortality than wildtype mice (Mehlhop et al., 2005). In addition, in the context of WNV, mice genetically deficient for C1q (CP), C4 (CP, LP), factor B (AP), or factor D (AP) show higher mortality rates than wildtype mice. Additionally, brain infection was observed earlier for mice deficient for any one of these complement factors (Mehlhop and Diamond, 2006). Interestingly, the effects of complement on the dynamics of arbovirus infection may also operate outside of the human host. This is because complement factors can remain active after a blood meal and interact with the virus and cells within the mosquito, which can decrease viral loads in the vector and affect viral transmission (Londono-Renteria et al., 2016). Previous studies have demonstrated the capacity of Anopheline mosquito saliva to inhibit complement activity. SGE from *Anopheles albimanus, Anopheles freeborni*, and *Anopheles aquasalis*, all vectors for malaria, have been reported to inhibit the alternative pathway of the complement system (Mendes-Sousa et al., 2016, 2018). Nevertheless, studies carried out with *A. aegypti* saliva are consistent in demonstrating no direct inhibition of the complement system (Cavalcante et al., 2003; Pereira-Filho et al., 2020).

THE EFFECT OF SALIVA ON THE LYMPHOCYTE RESPONSE TO ARBOVIRUS

T- and B-cell involvement in the response to arbovirus infection has also been shown to be highly important. $CD4^+$ and $CD8^+$ T cells differentiate into more specific subsets defined by different effector functions and cytokine profiles (Golubovskaya and Wu, 2016). The coordinated action of T and B cells leads to the production of specific antibodies against viral proteins. Mice depleted of $CD4^+$ T cells and infected with attenuated RVFV, which is normally not able to generate disease, develop encephalitis, associated with lower virus-specific humoral and T-cell memory responses (Harmon et al., 2018). When mice are

depleted of both $CD4^+$ and $CD8^+$ T cells, the incidence of encephalitis increases. Knockout mice unable to produce γδ T cells infected with CHIKV develop a more severe manifestation of the disease than wildtype controls (Long and Heise, 2015). These mice show increased inflammation-mediated oxidative damage in the feet and ankles and cytokine and chemokine production different from that of wildtype mice. In addition, infection of α/β-T cell deficient mice with JEV results in death over a 10- to 18-day period, in contrast to wildtype mice, which can survive infection, attributable to the granular lytic function of the cells (Jain et al., 2017). For DENV, lower percentages of regulatory B-cell subsets are associated with a more severe disease outcome during acute infection in humans (Upasani et al., 2019). Mosquito salivary factors have an effect on B- and T-cell responses and the proportion of these cell populations. Peripheral blood mononuclear cells treated with 2 μg of *A. aegypti* saliva show a higher proportion of NK T cells than untreated controls (Vogt et al., 2018). In this study, the authors observed no difference in the proportion of activated cells. Thus, the specific influence that this effect could have on the immune response to viral infections is difficult to assess. In the same study, Vogt et al. (2018) used humanized mice exposed to *A. aegypti* saliva through mosquito feeding and observed a lower number of IL-2-producing $CD4^+$ T cells in the blood, and B cells in the skin 12 h after infection. Fewer $CD4^+$ T cells in the blood were also observed at 48 h after infection. In this study, the populations of lymphocytes, NK cells, and other myeloid cells were analyzed at various time points, together with cytokine production, and the overall results are consistent with a mixed Th1/Th2 response, rather than the usual Th1 Th2 shift reported in many other papers. Cell death, together with decreased proliferation rates, is observed when mouse T cells are exposed to *A. aegypti* SGE. This suppressive effect is accompanied by the downregulation of Th1 and Th2 cytokine production (Wanasen et al., 2004; Bizzarro et al., 2013). In addition, B-cell proliferation is inhibited by *A. aegypti* SGE (Wasserman et al., 2004). Lymphocytes cultured in the presence of SGE showed alterations in the cell phenotype and an inversely proportional relationship between the number of viable cells and SGE concentration. The labeling of phosphatidylserine at the cell surface with annexin 5 confirmed the apoptosis of T and B lymphocytes. Lower levels of pro-caspase-3 and pro-caspase-8 expression in total spleen cell lysates than in controls was observed. This suggests that *A. aegypti* SGE mediates apoptosis in T and B lymphocytes via a caspase-3- and caspase-8-dependent pathway (Bizzarro et al., 2013).

VACCINE PROSPECT

In the context of arbovirus, vaccine development has seen several breakthroughs in recent years and vaccines for JEV and yellow fever virus are licensed and used worldwide. Given the extensive diversity of arboviruses and their complex immunological interactions with the host, it is important to consider a variety of approaches to vaccine development. New ideas incorporate vector-based immunological concepts and have become a highly promising area of study. One such new vaccine strategy concerns the delivery of vaccines by microscale needles, which, in additional to being painless, more accurately mimic the natural inoculation of the virus by the arthropod vector and thus might elicit better immune activation in the skin (Manning and Cantaert, 2019). In 2018, researchers described the design of a microneedle based on the biology of mosquito mouth parts and the mechanism behind the painless bite, providing an example of innovative and better-designed vaccine delivery systems (Gurera et al., 2018). In comparison to traditional hypodermic needles, which deliver the vaccine into the subcutaneous strata of the skin, transcutaneous microneedle delivery appears to provide the advantage of promoting robust protective skin-resident responses. Furthermore, the painless and non-invasive nature of microneedle delivery systems, along with the minimal technical training required for their use, are highly desirable traits for a vaccine (Huang et al., 2019). In addition, the viral replication kinetics and evolution to peak viremia in the peripheral blood of macaques infected with DENV via mosquito bite are closer to the data reported for humans than those observed after subcutaneous delivery. Furthermore, the differences in replication kinetics that are observed between infection via mosquito bite and intradermal DENV inoculation do not disappear after the addition of SGE to the intradermal injection (McCracken et al., 2020). These results suggest that delivery systems and localization of the viral inoculum in the skin play an important role in determining viral replication kinetics. The use of salivary components as vaccine targets is also a concept that has gained interest over the years. If the vaccine can elicit an immune response at the very initial step of infection when host, vector, and virus interact, and if that response is triggered by the components present in the mosquito saliva, independent of the virus, then such a vaccine would boost the normal anti-viral response by creating an "anticipated" hostile environment for the virus-saliva mixture. This approach has the added advantage of being vector specific rather than virus specific, possibly opening the door to a catch-all vaccine for different viruses transmitted by a single vector (Manning and Cantaert, 2019). This concept also appears to be promising in the context of other non-viral arthropod-borne diseases. In hamster models, immunization against salivary protein LJM19 from *Lutzomyia longipalpis* provides protection against a fatal outcome from visceral leishmaniasis (Gomes et al., 2008). Also, immunity to salivary components has been documented in various studies with mammalian species after frequent exposure to ticks. This observations, together with studies on the effect of tick salivary proteins on the host immune response, has led to the identification of possible saliva vaccine candidates for tick-transmitted diseases (Manning et al., 2018). In addition, in the context of malaria, mice immunized with antiserum against an *Anopheles gambiae* salivary protein (TRIO) showed partial protection against plasmodium infection (Dragovic et al., 2018). In humans, the results from the first safety and immunogenicity phase 1 clinical trial for an universal mosquito-borne disease vaccine (AGS-v) have recently been published (Manning et al., 2020). The vaccine is composed of four salivary peptides from *A. gambiae* salivary glands that are common in many other mosquito vectors. The aim of the vaccine is to provide

prophylactic protection against various mosquito-transmitted diseases. In the study, adult participants were assigned to one of three treatment groups: AGS-v vaccine, AGS-s vaccine, and adjuvant, or placebo. Treatment was delivered via subcutaneous injection at day 0 and day 21, after which the participants were exposed to uninfected *A. aegypti* feeding at day 42. The vaccine candidate was considered safe for its use in humans. Furthermore, participants who received the vaccine in combination with adjuvant mounted increased vaccine-specific IgG antibodies and cellular responses. All together, the results from this study suggest that AGS-v is an achievable option to implement as a vector-targeted vaccine.

CONCLUSION

Arbovirus infections are a worldwide public health problem. To date, attempts to control the transmission of infection and disease occurrence in vulnerable areas have not been completely successful. Thus, new approaches are needed. Viral entry into the host takes place in the epidermis and dermis of the skin and is mechanically and chemically assisted by the mosquito. The saliva of the vector has the capacity to disturb both innate and adaptive immune responses. Various studies have reported the capacity of saliva components to drive a shift from Th1 (effective, desirable) to Th2 responses. Such a switch is achieved by altering cytokine, chemokine, and interferon production by the cells. Specific salivary compounds have also been reported to induce autophagy, as well as inhibit T and B lymphocyte proliferation and induce apoptosis. Overall, the added effects of these alterations of the immune response lead to enhanced viral replication, disease severity, and ultimately, transmission. Nevertheless, the current state of the art for salivary vaccine development is exciting, as an increasing number of animal studies are showing favorable results and human clinical trials for universal vector vaccines are already in the pipeline.

Required Future Research to Fill Current Knowledge Gaps

Although there has been much research on the composition of mosquito saliva, complete functional proteomic profiles are not yet available. A significant number of studies are still based on transcriptomic or genomic approaches, which, although powerful, lack the capacity to determine 3D protein structure, post-transcriptional modifications, and specific biological functions. In terms of the diversity of the types of compounds being studied, there are also opportunities to expand our current knowledge. Most studies have thus far focused on protein identification and have left the metabolome and miRNA relatively unexplored. Furthermore, although the differential expression of salivary proteins in infected vs. uninfected mosquitoes has been studied (Zhang et al., 2013; Chisenhall et al., 2014), a complete differential proteome/metabolome/miRNA profile is not yet available. In addition, the mechanisms by which the virus affect the composition and abundance of salivary compounds in the vector are not well-understood. Studies on mosquito salivary factors and their effect on immune responses have been carried out using *A. aegypti* saliva. Other important vectors for arboviruses, such as *A. albopictus* and *Culex* ssp., are under-investigated. Thus, there are few comparative analyses of the various effects of saliva on the immune response between different vectors. The same is true for the differential salivary immune-modulatory effects of wildtype mosquitoes relative to those of laboratory-reared mosquitoes. Much has also been accomplished in understanding the host immune response to saliva components, after decades of research, which has set the foundation for the scientific research of recent years. Nevertheless, more extensive characterization of the effector cells involved in the response to mosquito saliva, along with their chemokine and cytokine signatures, is still needed. More complete knowledge of the interactions between saliva and primary host immune cells will make it possible to identify key cell populations/molecules/pathways that control the efficiency of infection. The same is true for the mechanisms by which saliva components reshape the local immune response at the bite site, as a more profound understanding of these mechanisms can be used in the development of treatment.

AUTHOR CONTRIBUTIONS

DG contributed to the writing and editing of the review. DM and TC contributed to the final form of the manuscript and its improvement. DG and DM contributed to designing the table and figure. All authors contributed to the idea and form of the manuscript and approved the submitted version.

FUNDING

This work was supported by the Calmette-Yersin Ph.D. scholarship and funded by the French National Research Agency (ANR-15-CE15-00029) and a Wellcome/HHMI International research scholarship (208710/Z/17/Z).

ACKNOWLEDGMENTS

We would like to thank William Hempel of Alex Edelman & Associates for proofreading of the manuscript.

REFERENCES

Barros, M. S., Lara, P. G., Fonseca, M. T., Moretti, E. H., Filgueiras, L. R., Martins, J. O., et al. (2019). *Aedes aegypti* saliva impairs M1-associated proinflammatory phenotype without promoting or affecting M2 polarization of murine macrophages. *Parasites Vectors* 12:239. doi: 10.1186/s13071-019-3487-7

Bissonnette, E. Y., Rossignol, P. A., and Befus, A. D. (1993). Extracts of mosquito salivary gland inhibit tumour necrosis factor alpha release from mast cells. *Parasite Immunol.* 15, 27–33. doi: 10.1111/j.1365-3024.1993.tb00569.x

Bizzarro, B., Barros, M. S., Maciel, C., Gueroni, D. I., Lino, C. N., Campopiano, J., et al. (2013). Effects of *Aedes aegypti* salivary components on dendritic cell and lymphocyte biology. *Parasites Vectors* 6:329. doi: 10.1186/1756-3305-6-329

Bonizzoni, M., Dunn, W. A., Campbell, C. L., Olson, K. E., Marinotti, O., and James, A. A. (2012). Complex modulation of the *Aedes aegypti* transcriptome in response to dengue virus infection. *PLoS ONE* 7:e50512. doi: 10.1371/journal.pone.0050512

Boppana, V. D., Thangamani, S., Adler, A. J., and Wikel, S. K. (2009). SAAG-4 is a novel mosquito salivary protein that programmes host CD4 T cells to express IL-4. *Parasite Immunol.* 31, 287–295. doi: 10.1111/j.1365-3024.2009.01096.x

Briant, L., Desprès, P., Choumet, V., and Missé, D. (2014). Role of skin immune cells on the host susceptibility to mosquito-borne viruses. *Virology* 464–465, 26–32. doi: 10.1016/j.virol.2014.06.023

Brooks, D. G., Trifilo, M. J., Edelmann, K. H., Teyton, L., McGavern, D. B., and Oldstone, M. B. A. (2006). Interleukin-10 determines viral clearance or persistence *in vivo*. *Nat. Med.* 12, 1301–1309. doi: 10.1038/nm1492

Caine, E. A., Scheaffer, S. M., Arora, N., Zaitsev, K., Artyomov, M. N., Coyne, C. B., et al. (2019). Interferon lambda protects the female reproductive tract against zika virus infection. *Nat. Commun.* 10:280. doi: 10.1038/s41467-018-07993-2

Cavalcante, R. R., Pereira, M. H., and Gontijo, N. F. (2003). Anti-complement activity in the saliva of phlebotomine sand flies and other haematophagous insects. *Parasitology* 127, 87–93. doi: 10.1017/S0031182003003329

Chen, R.-F., Yang, K. D., Wang, L., Liu, J.-W., Chiu, C.-C., and Cheng, J.-T. (2007). Different clinical and laboratory manifestations between dengue haemorrhagic fever and dengue fever with bleeding tendency. *Trans. R. Soc. Trop. Med. Hyg.* 101, 1106–1113. doi: 10.1016/j.trstmh.2007.06.019

Chiramel, A. I., and Best, S. M. (2018). Role of autophagy in zika virus infection and pathogenesis. *Virus Res.* 254, 34–40. doi: 10.1016/j.virusres.2017.09.006

Chisenhall, D. M., Mores, C. N., McCracken, M. K., Christofferson, R. C., and Londono, B. L. (2014). Effect of dengue-2 virus infection on protein expression in the salivary glands of *Aedes aegypti* mosquitoes. *Am. J. Trop. Med. Hyg.* 90, 431–437. doi: 10.4269/ajtmh.13-0412

Conway, M. J., Watson, A. M., Colpitts, T. M., Dragovic, S. M., Li, Z., Wang, P., et al. (2014). Mosquito saliva serine protease enhances dissemination of dengue virus into the mammalian host. *J. Virol.* 88, 164–175. doi: 10.1128/JVI.02235-13

Cox, J., Mota, J., Sukupolvi-Petty, S., Diamond, M. S., and Rico-Hesse, R. (2012). Mosquito bite delivery of dengue virus enhances immunogenicity and pathogenesis in humanized mice. *J. Virol.* 86, 7637–7649. doi: 10.1128/JVI.00534-12

Cross, M. L., Cupp, E. W., and Enriquez, F. J. (1994). Differential modulation of murine cellular immune responses by salivary gland extract of *Aedes aegypti*. *Am. J. Trop. Med. Hyg.* 51, 690–696. doi: 10.4269/ajtmh.1994.51.690

Dhawan, R., Kumar, M., Mohanty, A. K., Dey, G., Advani, J., Prasad, T. S. K., et al. (2017). Mosquito-borne diseases and omics: salivary gland proteome of the female *Aedes aegypti* mosquito. *OMICS J. Integr. Biol.* 21, 45–54. doi: 10.1089/omi.2016.0160

do Valle, T. Z., Billecocq, A., Guillemot, L., Alberts, R., Gommet, C., Geffers, R., et al. (2010). A new mouse model reveals a critical role for host innate immunity in resistance to rift valley fever. *J. Immunol.* 185, 6146–6156. doi: 10.4049/jimmunol.1000949

Dragovic, S. M., Agunbiade, T. A., Freudzon, M., Yang, J., Hastings, A. K., Schleicher, T. R., et al. (2018). Immunization with AgTRIO, a protein in anopheles saliva, contributes to protection against plasmodium infection in mice. *Cell Host Microbe* 23, 523–535.e5. doi: 10.1016/j.chom.2018.03.008

Dudley, D. M., Newman, C. M., Lalli, J., Stewart, L. M., Koenig, M. R., Weiler, A. M., et al. (2017). Infection via mosquito bite alters zika virus tissue tropism and replication kinetics in rhesus macaques. *Nat. Commun.* 8:2096. doi: 10.1038/s41467-017-02222-8

Durbin, A. P., Vargas, M. J., Wanionek, K., Hammond, S. N., Gordon, A., Rocha, C., et al. (2008). Phenotyping of peripheral blood mononuclear cells during acute dengue illness demonstrates infection and increased activation of monocytes in severe cases compared to classic dengue fever. *Virology* 376, 429–435. doi: 10.1016/j.virol.2008.03.028

Ekchariyawat, P., Hamel, R., Bernard, E., Wichit, S., Surasombatpattana, P., Talignani, L., et al. (2015). Inflammasome signaling pathways exert antiviral effect against chikungunya virus in human dermal fibroblasts. *Infect. Genet. Evol.* 32, 401–408. doi: 10.1016/j.meegid.2015.03.025

Garcia, M., Alout, H., Diop, F., Damour, A., Bengue, M., Weill, M., et al. (2018). Innate immune response of primary human keratinocytes to west nile virus infection and its modulation by mosquito saliva. *Front. Cell. Infect. Microbiol.* 8:387. doi: 10.3389/fcimb.2018.00387

Golubovskaya, V., and Wu, L. (2016). Different subsets of T cells, memory, effector functions, and CAR-T immunotherapy. *Cancers* 8:36. doi: 10.3390/cancers8030036

Gomes, R., Teixeira, C., Teixeira, M. J., Oliveira, F., Menezes, M. J., Silva, C., et al. (2008). Immunity to a salivary protein of a sand fly vector protects against the fatal outcome of visceral leishmaniasis in a hamster model. *Proc. Natl. Acad. Sci. U.S.A.* 105, 7845–7850. doi: 10.1073/pnas.0712153105

Gommerman, J. L., Browning, J. L., and Ware, C. F. (2014). The lymphotoxin network: orchestrating a type I interferon response to optimize adaptive immunity. *Cytokine Growth Factor Rev.* 25, 139–145. doi: 10.1016/j.cytogfr.2014.02.002

Gould, E., Pettersson, J., Higgs, S., Charrel, R., and de Lamballerie, X. (2017). Emerging arboviruses: why today? *One Health* 4, 1–13. doi: 10.1016/j.onehlt.2017.06.001

Gurera, D., Bhushan, B., and Kumar, N. (2018). Lessons from mosquitoes' painless piercing. *J. Mech. Behav. Biomed. Mater.* 84, 178–187. doi: 10.1016/j.jmbbm.2018.05.025

Hamel, R., Dejarnac, O., Wichit, S., Ekchariyawat, P., Neyret, A., Luplertlop, N., et al. (2015). Biology of zika virus infection in human skin cells. *J. Virol.* 89, 8880–8896. doi: 10.1128/JVI.00354-15

Harmon, J. R., Spengler, J. R., Coleman-McCray, J. D., Nichol, S. T., Spiropoulou, C. F., and McElroy, A. K. (2018). CD4 T cells, CD8 T cells, and monocytes coordinate to prevent rift valley fever virus encephalitis. *J. Virol.* 92, e01270–18. doi: 10.1128/JVI.01270-18

Hartman, A. (2017). Rift valley fever. *Clin. Lab. Med.* 37, 285–301. doi: 10.1016/j.cll.2017.01.004

Hastings, A. K., Uraki, R., Gaitsch, H., Dhaliwal, K., Stanley, S., Sproch, H., et al. (2019). *Aedes aegypti* NeSt1 protein enhances zika virus pathogenesis by activating neutrophils. *J. Virol.* 93, e00395–19. doi: 10.1128/JVI.00395-19

Hiroki, C. H., Toller-Kawahisa, J. E., Fumagalli, M. J., Colon, D. F., Figueiredo, L. T. M., Fonseca, B. A. L. D., et al. (2020). Neutrophil extracellular traps effectively control acute chikungunya virus infection. *Front. Immunol.* 10:3108. doi: 10.3389/fimmu.2019.03108

Hollidge, B. S., Weiss, S. R., and Soldan, S. S. (2011). The role of interferon antagonist, non-structural proteins in the pathogenesis and emergence of arboviruses. *Viruses* 3, 629–658. doi: 10.3390/v3060629

Huang, Y.-J. S., Higgs, S., and Vanlandingham, D. L. (2019). Arbovirus-mosquito vector-host interactions and the impact on transmission and disease pathogenesis of arboviruses. *Front. Microbiol.* 10:22. doi: 10.3389/fmicb.2019.00022

Jain, N., Oswal, N., Chawla, A. S., Agrawal, T., Biswas, M., Vrati, S., et al. (2017). CD8 T cells protect adult naive mice from JEV-induced morbidity via lytic function. *PLoS Neglected Trop. Dis.* 11:e0005329. doi: 10.1371/journal.pntd.0005329

Jiang, D., Weidner, J. M., Qing, M., Pan, X.-B., Guo, H., Xu, C., et al. (2010). Identification of five interferon-induced cellular proteins that inhibit west nile virus and dengue virus infections. *J. Virol.* 84, 8332–8341. doi: 10.1128/JVI.02199-09

Jin, L., Guo, X., Shen, C., Hao, X., Sun, P., Li, P., et al. (2018). Salivary factor LTRIN from *Aedes aegypti* facilitates the transmission of zika virus by interfering with the lymphotoxin-β receptor. *Nat. Immunol.* 19, 342–353. doi: 10.1038/s41590-018-0063-9

Kawai, T., and Akira, S. (2007). Signaling to NF-κB by toll-like receptors. *Trends Mol. Med.* 13, 460–469. doi: 10.1016/j.molmed.2007.09.002

Kilpatrick, A. M., and Randolph, S. E. (2012). Drivers, dynamics, and control of emerging vector-borne zoonotic diseases. *Lancet* 380, 1946–1955. doi: 10.1016/S0140-6736(12)61151-9

LaBeaud, A.d., Bashir, F., and King, C. H. (2011). Measuring the burden of arboviral diseases: the spectrum of morbidity and mortality from four prevalent infections. *Popul. Health Metrics* 9:1. doi: 10.1186/1478-7954-9-1

Laureti, M., Narayanan, D., Rodriguez-Andres, J., Fazakerley, J. K., and Kedzierski, L. (2018). Flavivirus receptors: diversity, identity, and cell entry. *Front. Immunol.* 9:2180. doi: 10.3389/fimmu.2018.02180

Le Coupanec, A., Babin, D., Fiette, L., Jouvion, G., Ave, P., Misse, D., et al. (2013). *Aedes* mosquito saliva modulates rift valley fever virus pathogenicity. *PLoS Neglected Trop. Dis.* 7:e2237. doi: 10.1371/journal.pntd.0002237

Limon-Flores, A. Y., Perez-Tapia, M., Estrada-Garcia, I., Vaughan, G., Escobar-Gutierrez, A., Calderon-Amador, J., et al. (2005). Dengue virus inoculation to

human skin explants: an effective approach to assess *in situ* the early infection and the effects on cutaneous dendritic cells: cutaneous infection with dengue virus. *Int. J. Exp. Pathol.* 86, 323–334. doi: 10.1111/j.0959-9673.2005.00445.x

Londono-Renteria, B., Grippin, C., Cardenas, J. C., Troupin, A., and Colpitts, T. M. (2016). Human C5a protein participates in the mosquito immune response against dengue virus. *J. Med. Entomol.* 53, 505–512. doi: 10.1093/jme/tjw003

Long, K. M., and Heise, M. T. (2015). Protective and pathogenic responses to chikungunya virus infection. *Curr. Trop. Med. Rep.* 2, 13–21. doi: 10.1007/s40475-015-0037-z

Lucas, C. G. O., Kitoko, J. Z., Ferreira, F. M., Suzart, V. G., Papa, M. P., Coelho, S. V. A., et al. (2018). Critical role of CD4+ T cells and IFNγ signaling in antibody-mediated resistance to zika virus infection. *Nat. Commun.* 9:3136. doi: 10.1038/s41467-018-05519-4

Maharaj, P. D., Widen, S. G., Huang, J., Wood, T. G., and Thangamani, S. (2015). Discovery of mosquito saliva microRNAs during CHIKV Infection. *PLoS Neglected Trop. Dis.* 9:e0003386. doi: 10.1371/journal.pntd.0003386

Manning, J. E., and Cantaert, T. (2019). Time to micromanage the pathogen-host-vector interface: considerations for vaccine development. *Vaccines* 7:10. doi: 10.3390/vaccines7010010

Manning, J. E., Morens, D. M., Kamhawi, S., Valenzuela, J. G., and Memoli, M. (2018). Mosquito saliva: the hope for a universal arbovirus vaccine? *J. Infect. Dis.* 218, 7–15. doi: 10.1093/infdis/jiy179

Manning, J. E., Oliveira, F., Coutinho-Abreu, I. V., Herbert, S., Meneses, C., Kamhawi, S., et al. (2020). Safety and immunogenicity of a mosquito saliva peptide-based vaccine: a randomised, placebo-controlled, double-blind, phase 1 trial. *Lancet* 395, 1998–2007. doi: 10.1016/S0140-6736(20)31048-5

Matejuk, A. (2018). Skin immunity. *Arch. Immunol. Ther. Exp.* 66, 45–54. doi: 10.1007/s00005-017-0477-3

McCracken, M. K., Gromowski, G. D., Garver, L. S., Goupil, B. A., Walker, K. D., Friberg, H., et al. (2020). Route of inoculation and mosquito vector exposure modulate dengue virus replication kinetics and immune responses in rhesus macaques. *PLoS Neglected Trop. Dis.* 14:e0008191. doi: 10.1371/journal.pntd.0008191

Mehlhop, E., and Diamond, M. S. (2006). Protective immune responses against west nile virus are primed by distinct complement activation pathways. *J. Exp. Med.* 203, 1371–1381. doi: 10.1084/jem.20052388

Mehlhop, E., Whitby, K., Oliphant, T., Marri, A., Engle, M., and Diamond, M. S. (2005). Complement activation is required for induction of a protective antibody response against west nile virus infection. *J. Virol.* 79, 7466–7477. doi: 10.1128/JVI.79.12.7466-7477.2005

Mendes-Sousa, A. F., Queiroz, D. C., Vale, V. F., Ribeiro, J. M. C., Valenzuela, J. G., Gontijo, N. F., et al. (2016). An inhibitor of the alternative pathway of complement in saliva of new world anopheline mosquitoes. *J. Immunol.* 197, 599–610. doi: 10.4049/jimmunol.1600020

Mendes-Sousa, A. F., Vale, V. F., Queiroz, D. C., Pereira-Filho, A. A., da Silva, N. C. S., Koerich, L. B., et al. (2018). Inhibition of the complement system by saliva of *Anopheles (Nyssorhynchus) aquasalis*. *Insect Biochem. Mol. Biol.* 92, 12–20. doi: 10.1016/j.ibmb.2017.11.004

Miller, L. S. (2008). Toll-like receptors in skin. *Adv. Dermatol.* 24, 71–87. doi: 10.1016/j.yadr.2008.09.004

Morrill, J. C., Jennings, G. B., Cosgriff, T. M., Gibbs, P. H., and Peters, C. J. (1989). Prevention of rift valley fever in rhesus monkeys with interferon-α. *Clin. Infect. Dis.* 11, S815–S825. doi: 10.1093/clinids/11.Supplement_4.S815

Nan, Y., Wu, C., and Zhang, Y.-J. (2017). Interplay between janus kinase/signal transducer and activator of transcription signaling activated by type I interferons and viral antagonism. *Front. Immunol.* 8:1758. doi: 10.3389/fimmu.2017.01758

Opasawatchai, A., Amornsupawat, P., Jiravejchakul, N., Chan-in, W., Spoerk, N. J., Manopwisedjaroen, K., et al. (2019). Neutrophil Activation and early features of NET formation are associated with dengue virus infection in human. *Front. Immunol.* 9:3007. doi: 10.3389/fimmu.2018.03007

Papa, A. (2019). Emerging arboviruses of medical importance in the mediterranean region. *J. Clin. Virol.* 115, 5–10. doi: 10.1016/j.jcv.2019.03.007

Pereira-Filho, A. A., Mateus Pereira, R. H., da Silva, N. C. S., Ferreira Malta, L. G., Serravite, A. M., Carvalho de Almeida, C. G., et al. (2020). The gut anti-complement activity of *Aedes aegypti*: investigating new ways to control the major human arboviruses vector in the Americas. *Insect Biochem. Mol. Biol.* 120:103338. doi: 10.1016/j.ibmb.2020.103338

Pfeffer, M., and Dobler, G. (2010). Emergence of zoonotic arboviruses by animal trade and migration. *Parasites Vectors* 3:35. doi: 10.1186/1756-3305-3-35

Pingen, M., Bryden, S. R., Pondeville, E., Schnettler, E., Kohl, A., Merits, A., et al. (2016). Host inflammatory response to mosquito bites enhances the severity of arbovirus infection. *Immunity* 44, 1455–1469. doi: 10.1016/j.immuni.2016.06.002

Pingen, M., Schmid, M. A., Harris, E., and McKimmie, C. S. (2017). Mosquito biting modulates skin response to virus infection. *Trends Parasitol.* 33, 645–657. doi: 10.1016/j.pt.2017.04.003

Puiprom, O., Morales Vargas, R. E., Potiwat, R., Chaichana, P., Ikuta, K., Ramasoota, P., et al. (2013). Characterization of chikungunya virus infection of a human keratinocyte cell line: role of mosquito salivary gland protein in suppressing the host immune response. *Infect. Genet. Evol.* 17, 210–215. doi: 10.1016/j.meegid.2013.04.005

Ribeiro, J. M. C., Arca, B., Lombardo, F., Calvo, E., Phan, V. M., Chandra, P. K., et al. (2007). An annotated catalogue of salivary gland transcripts in the adult female mosquito, Ædes ægypti*. *BMC Genomics* 8:6. doi: 10.1186/1471-2164-8-6

Rolin, A. I., Berrang-Ford, L., and Kulkarni, M. A. (2013). The risk of rift valley fever virus introduction and establishment in the United States and European Union. *Emerg. Microbes Infect.* 2, 1–8. doi: 10.1038/emi.2013.81

Rosales, C. (2018). Neutrophil: a cell with many roles in inflammation or several cell types? *Front. Physiol.* 9:113. doi: 10.3389/fphys.2018.00113

Rudd, P. A., Wilson, J., Gardner, J., Larcher, T., Babarit, C., Le, T. T., et al. (2012). Interferon response factors 3 and 7 protect against chikungunya virus hemorrhagic fever and shock. *J. Virol.* 86, 9888–9898. doi: 10.1128/JVI.00956-12

Schilte, C., Buckwalter, M. R., Laird, M. E., Diamond, M. S., Schwartz, O., and Albert, M. L. (2012). Cutting edge: independent roles for IRF-3 and IRF-7 in hematopoietic and nonhematopoietic cells during host response to chikungunya infection. *J. Immunol.* 188, 2967–2971. doi: 10.4049/jimmunol.1103185

Schneider, B. S., and Higgs, S. (2008). The enhancement of arbovirus transmission and disease by mosquito saliva is associated with modulation of the host immune response. *Trans. R. Soc. Trop. Med. Hyg.* 102, 400–408. doi: 10.1016/j.trstmh.2008.01.024

Schneider, B. S., Soong, L., Coffey, L. L., Stevenson, H. L., McGee, C. E., and Higgs, S. (2010). *Aedes aegypti* saliva alters leukocyte recruitment and cytokine signaling by antigen-presenting cells during west nile virus infection. *PLoS ONE* 5:e11704. doi: 10.1371/journal.pone.0011704

Schneider, B. S., Soong, L., Zeidner, N. S., and Higgs, S. (2004). *Aedes aegypti* salivary gland extracts modulate anti-viral and TH1/TH2 cytokine responses to sindbis virus infection. *Viral. Immunol.* 17, 565–573. doi: 10.1089/vim.2004.17.565

Schoggins, J. W., Wilson, S. J., Panis, M., Murphy, M. Y., Jones, C. T., Bieniasz, P., et al. (2011). A diverse range of gene products are effectors of the type I interferon antiviral response. *Nature* 472, 481–485. doi: 10.1038/nature09907

Sen, G. C. (2001). Viruses and interferons. *Annu. Rev. Microbiol.* 55, 255–281. doi: 10.1146/annurev.micro.55.1.255

Sharma, S. (2003). Triggering the interferon antiviral response through an IKK-related pathway. *Science* 300, 1148–1151. doi: 10.1126/science.1081315

Silveira, G. F., Wowk, P. F., Cataneo, A. H. D., dos Santos, P. F., Delgobo, M., Stimamiglio, M. A., et al. (2018). Human T lymphocytes are permissive for dengue virus replication. *J. Virol.* 92, e02181–e02117. doi: 10.1128/JVI.02181-17

Stoermer, K. A., and Morrison, T. E. (2011). Complement and viral pathogenesis. *Virology* 411, 362–373. doi: 10.1016/j.virol.2010.12.045

Struchiner, C. J., Rocklöv, J., Wilder-Smith, A., and Massad, E. (2015). Increasing dengue incidence in Singapore over the past 40 years: population growth, climate and mobility. *PLoS ONE* 10:e0136286. doi: 10.1371/journal.pone.0136286

Styer, L. M., Lim, P.-Y., Louie, K. L., Albright, R. G., Kramer, L. D., and Bernard, K. A. (2011). Mosquito saliva causes enhancement of west nile virus infection in mice. *J. Virol.* 85, 1517–1527. doi: 10.1128/JVI.01112-10

Sun, P., Nie, K., Zhu, Y., Liu, Y., Wu, P., Liu, Z., et al. (2020). A mosquito salivary protein promotes flavivirus transmission by activation of autophagy. *Nat. Commun.* 11:260. doi: 10.1038/s41467-019-14115-z

Surasombatpattana, P., Ekchariyawat, P., Hamel, R., Patramool, S., Thongrungkiat, S., Denizot, M., et al. (2014). *Aedes aegypti* saliva contains a prominent

34-kDa protein that strongly enhances dengue virus replication in human keratinocytes. *J. Invest. Dermatol.* 134, 281–284. doi: 10.1038/jid.2013.251

Surasombatpattana, P., Patramool, S., Luplertlop, N., Yssel, H., and Missé, D. (2012). *Aedes aegypti* saliva enhances dengue virus infection of human keratinocytes by suppressing innate immune responses. *J. Invest. Dermatol.* 132, 2103–2105. doi: 10.1038/jid.2012.76

Thangamani, S., Higgs, S., Ziegler, S., Vanlandingham, D., Tesh, R., and Wikel, S. (2010). Host immune response to mosquito-transmitted chikungunya virus differs from that elicited by needle inoculated virus. *PLoS ONE* 5:e12137. doi: 10.1371/journal.pone.0012137

Thangamani, S., and Wikel, S. K. (2009). Differential expression of *Aedes aegypti* salivary transcriptome upon blood feeding. *Parasites Vectors* 2:34. doi: 10.1186/1756-3305-2-34

Townson, H. (1993). The biology of mosquitoes. Volume 1. Development, nutrition and reproduction. By A.N. Clements. (London: Chapman and Hall, 1992). viii + 509 pp. Hard cover £50. ISBN 0-412-40180-0. *Bull. Entomol. Res.* 83, 307–308. doi: 10.1017/S0007485300034830

Upasani, V., Vo, H. T. M., Ung, S., Heng, S., Laurent, D., Choeung, R., et al. (2019). Impaired antibody-independent immune response of B cells in patients with acute dengue infection. *Front. Immunol.* 10:2500. doi: 10.3389/fimmu.2019.02500

Uraki, R., Hastings, A. K., Marin-Lopez, A., Sumida, T., Takahashi, T., Grover, J. R., et al. (2019). *Aedes aegypti* AgBR1 antibodies modulate early zika virus infection of mice. *Nat. Microbiol.* 4, 948–955. doi: 10.1038/s41564-019-0385-x

Vogt, M. B., Lahon, A., Arya, R. P., Kneubehl, A. R., Spencer Clinton, J. L., Paust, S., et al. (2018). Mosquito saliva alone has profound effects on the human immune system. *PLoS Neglected Trop. Dis.* 12:e0006439. doi: 10.1371/journal.pntd.0006439

Vu, D. M., Jungkind, D., and LaBeaud, A. D. (2017). Chikungunya virus. *Clin. Lab. Med.* 37, 371–382. doi: 10.1016/j.cll.2017.01.008

Wanasen, N., Nussenzveig, R. H., Champagne, D. E., Soong, L., and Higgs, S. (2004). Differential modulation of murine host immune response by salivary gland extracts from the mosquitoes *Aedes aegypti* and *Culex quinquefasciatus*. *Med. Vet. Entomol.* 18, 191–199. doi: 10.1111/j.1365-2915.2004.00498.x

Ware, C. F. (2005). NETWORK COMMUNICATIONS: lymphotoxins, LIGHT, and TNF. *Annu. Rev. Immunol.* 23, 787–819. doi: 10.1146/annurev.immunol.23.021704.115719

Wasserman, H. A., Singh, S., and Champagne, D. E. (2004). Saliva of the yellow fever mosquito, *Aedes aegypti*, modulates murine lymphocyte function. *Parasite Immunol.* 26, 295–306. doi: 10.1111/j.0141-9838.2004.00712.x

Weaver, S. C., and Reisen, W. K. (2010). Present and future arboviral threats. *Antiviral Res.* 85, 328–345. doi: 10.1016/j.antiviral.2009.10.008

WHO (2020). *A Global Brief on Vector-Borne Diseases*. WHO. Available online at: www.who.int (accessed February 22, 2020).

Wichit, S., Diop, F., Hamel, R., Talignani, L., Ferraris, P., Cornelie, S., et al. (2017). *Aedes Aegypti* saliva enhances chikungunya virus replication in human skin fibroblasts via inhibition of the type I interferon signaling pathway. *Infect. Genet. Evol.* 55, 68–70. doi: 10.1016/j.meegid.2017.08.032

Wilder-Smith, A., Gubler, D. J., Weaver, S. C., Monath, T. P., Heymann, D. L., and Scott, T. W. (2017). Epidemic arboviral diseases: priorities for research and public health. *Lancet Infect. Dis.* 17, e101–e106. doi: 10.1016/S1473-3099(16)30518-7

Wu, S.-J. L., Grouard-Vogel, G., Sun, W., Mascola, J. R., Brachtel, E., Putvatana, R., et al. (2000). Human skin langerhans cells are targets of dengue virus infection. *Nat. Med.* 6, 816–820. doi: 10.1038/77553

Yamamoto, M., Sato, S., Mori, K., Hoshino, K., Takeuchi, O., Takeda, K., et al. (2002). Cutting edge: a novel Toll/IL-1 receptor domain-containing adapter that preferentially activates the IFN-? promoter in the toll-like receptor signaling. *J. Immunol.* 169, 6668–6672. doi: 10.4049/jimmunol.169.12.6668

Zeidner, N. S., Higgs, S., Happ, C. M., Beaty, B. J., and Miller, B. R. (1999). Mosquito feeding modulates Th1 and Th2 cytokines in flavivirus susceptible mice: an effect mimicked by injection of sialokinins, but not demonstrated in flavivirus resistant mice. *Parasite Immunol.* 21, 35–44. doi: 10.1046/j.1365-3024.1999.00199.x

Zhang, M., Zheng, X., Wu, Y., Gan, M., He, A., Li, Z., et al. (2013). Differential proteomics of *Aedes albopictus* salivary gland, midgut and C6/36 cell induced by dengue virus infection. *Virology* 444, 109–118. doi: 10.1016/j.virol.2013.06.001

Conflict of Interest: The authors declare that the research was conducted in the absence of any commercial or financial relationships that could be construed as a potential conflict of interest.

frontiers in Cellular and Infection Microbiology

BRIEF RESEARCH REPORT
published: 24 August 2020
doi: 10.3389/fcimb.2020.00427

Phlebotomus perniciosus Recombinant Salivary Proteins Polarize Murine Macrophages Toward the Anti-Inflammatory Phenotype

Petra Sumova[1†], Nikola Polanska[1†], Tereza Lestinova[1], Tatiana Spitzova[1], Barbora Kalouskova[2], Ondrej Vanek[2], Petr Volf[1] and Iva Rohousova[1]*

[1] *Laboratory of Vector Biology, Department of Parasitology, Faculty of Science, Charles University, Prague, Czechia,*
[2] *Laboratory of Structural Biochemistry of Immune Recognition, Department of Biochemistry, Faculty of Science, Charles University, Prague, Czechia*

OPEN ACCESS

Edited by:
Eric Calvo, National Institutes of Health (NIH), United States

Reviewed by:
Maribel Jiménez, Instituto de Salud Carlos III (ISCIII), Spain
Clarissa Romero Teixeira, Fiocruz Ceará, Fundação Oswaldo Cruz, Brazil

***Correspondence:**
Iva Rohousova
iva.kolarova@natur.cuni.cz

[†] *These authors have contributed equally to this work*

Specialty section:
This article was submitted to Parasite and Host, a section of the journal Frontiers in Cellular and Infection Microbiology

Received: *15 June 2020*
Accepted: *14 July 2020*
Published: *24 August 2020*

Citation:
Sumova P, Polanska N, Lestinova T, Spitzova T, Kalouskova B, Vanek O, Volf P and Rohousova I (2020) Phlebotomus perniciosus Recombinant Salivary Proteins Polarize Murine Macrophages Toward the Anti-Inflammatory Phenotype. Front. Cell. Infect. Microbiol. 10:427. doi: 10.3389/fcimb.2020.00427

Phlebotomus perniciosus (Diptera: Phlebotominae) is a medically and veterinary important insect vector. It transmits the unicellular parasite *Leishmania infantum* that multiplies intracellularly in macrophages causing life-threatening visceral diseases. *Leishmania* establishment in the vertebrate host is substantially influenced by immunomodulatory properties of vector saliva that are obligatorily co-injected into the feeding site. The repertoire of *P. perniciosus* salivary molecules has already been revealed and, subsequently, several salivary proteins have been expressed. However, their immunogenic properties have never been studied. In our study, we tested three *P. perniciosus* recombinant salivary proteins—an apyrase rSP01 and yellow-related proteins rSP03 and rSP03B—and showed their anti-inflammatory nature on the murine bone-marrow derived macrophages. Even in the presence of pro-inflammatory stimuli (IFN-γ and bacterial lipopolysaccharide, LPS), all three recombinant proteins inhibited nitric oxide production. Moreover, rSP03 seems to have a very strong anti-inflammatory effect since it enhanced arginase activity, increased the production of IL-10, and inhibited the production of TNF-α even in macrophages stimulated with IFN-γ and LPS. These results suggest that *P. perniciosus* apyrase and yellow-related proteins may serve as enhancing factors in sand fly saliva, facilitating the development of *Leishmania* infection along with their anti-haemostatic properties. Additionally, rSP03 and rSP03B did not elicit the delayed-type hypersensitivity response in mice pre-exposed to *P. perniciosus* bites (measured as visible skin reaction). The results of our study may help to understand the potential function of recombinant's native counterparts and their role in *Leishmania* transmission and establishment within the host.

Keywords: *Phlebotomus*, sand fly saliva, yellow-related proteins, apyrase, macrophage polarization, immunogenicity

INTRODUCTION

Phlebotomus perniciosus (Diptera: Phlebotominae) is a sand fly species distributed in western part of Mediterranean basin. This species is medically and veterinary important as a vector of phleboviruses (e.g., Toscana virus) and, most importantly, as a vector of *Leishmania infantum* (Kinetoplastea: Trypanosomatida), a protozoan intracellular parasite that causes zoonotic human leishmaniasis with canids as the main reservoirs (Maroli et al., 2013).

Sand fly females feed on blood to gain enough nutrients for eggs development. During probing and sucking, the female obligatorily deposits a mixture of salivary molecules into the host skin. Besides being anti-haemostatic, the sand fly salivary molecules are also immunogenic, eliciting both humoral and cellular immune responses in repeatedly bitten host. Such anti-saliva immune response can be employed in leishmaniasis control. The anti-saliva antibody response can be utilized as the tool to screen hosts for the sand fly exposure at the individual level (e.g., in vector control programs), while the anti-saliva cellular immune response has been shown to protect the host against severe leishmaniasis (Lestinova et al., 2017).

The complexity of sand fly salivary proteins has already been revealed for several sand fly species (Coutinho-Abreu and Valenzuela, 2018; Oliveira et al., 2020; Polanska et al., 2020), including *P. perniciosus* (Anderson et al., 2006; Martin-Martin et al., 2013). Several salivary proteins from this sand fly species have been expressed and further tested primarily as markers of exposure (Lestinova et al., 2017; Velez et al., 2018; Willen et al., 2018, 2019; Risueno et al., 2019; Burnham et al., 2020; Maia et al., 2020). However, the functional studies of *P. perniciosus* salivary recombinant proteins are very limited (Sumova et al., 2019), and so far there is no study on their immunomodulatory properties.

In our study, we functionally tested recombinant salivary proteins of *P. perniciosus*, focusing on macrophages as the key cells in leishmaniasis. Macrophages are playing a dual role during *Leishmania* infection. They serve as the main host cell for *Leishmania* parasites as well as the key immune cell controlling the infection (Tomiotto-Pellissier et al., 2018). There are two major macrophage populations with different functions, classically activated M1 macrophages and alternatively activated M2 macrophages. M1 macrophages are activated in the presence of microbial substrates (e.g., bacterial lipopolysaccharide, LPS) and pro-inflammatory cytokines such as IFN-γ and TNF-α. Upon stimulation, they secrete high levels of pro-inflammatory cytokines (e.g., TNF-α, IL-1, IL-6, IL-12) and express the inducible nitric oxide synthetase (iNOS) responsible for the production of microbicide nitric oxide that kills intracellular *Leishmania* and thus controls the infection (Shapouri-Moghaddam et al., 2018; Tomiotto-Pellissier et al., 2018). The latter one, M2 macrophages (also referred as tissue-repairing macrophages), are activated by anti-inflammatory cytokines such as IL-4 and IL-13 toward the expression of the enzyme arginase and high production of IL-10 and TGF-β (Shapouri-Moghaddam et al., 2018). The products of arginase (L-ornithine and its metabolites) then favor *Leishmania* survival and multiplication (Tomiotto-Pellissier et al., 2018). With high functional plasticity, macrophages can switch from one phenotype to another, responding to the changes in the ongoing immune response (Shapouri-Moghaddam et al., 2018).

We focused on the salivary proteins of two abundant protein families; the yellow-related proteins (YRPs) and the apyrases. We compared the effect of these recombinant proteins on the murine macrophages activated either by classical or alternative pathway by measuring nitrite as a marker of iNOS activity and urea as a marker of arginase activity. Additionally, we measured the levels of corresponding secreted cytokines for the recombinant protein with the most pronounced immunomodulatory effect and its ability to elicit delayed-type hypersensitivity immune response in repeatedly bitten mice. The results of our study may help to understand the possible function of their native counterparts.

MATERIALS AND METHODS

Animals and Ethics Statement

Female mice, strain BALB/c and SKH, were purchased from Velaz (the Czech Republic). The mice were used for the experiments at 7–10 weeks of age. Animals were maintained and handled in the animal facility of the Charles University in accordance with the institutional guidelines and Czech legislation (Act No. 246/1992 and 359/2012 coll. on Protection of Animals against Cruelty in present statutes at large), which includes all relevant European Union and international guidelines for experimental animals. The experiments were approved by the Committee on Ethics of Laboratory Experiments of the Charles University and were performed under the permission of the Ministry of the Environment of the Czech Republic (number: MSMT-10270/2015-6) and the Certificate of Competency (number: CZ 02451) approved by the Ministry of Agriculture of the Czech Republic.

Sand Flies and Salivary Gland Dissection

The colony of *P. perniciosus* (originating from Murcia, Spain) was reared under the standard conditions as described in Volf and Volfova (2011). Salivary glands for macrophage stimulation were dissected from 3- to 5-day-old female sand flies, placed into RPMI-1640 medium (Sigma) and stored at −20°C until needed. Salivary glands for delayed-type hypersensitivity test were dissected into the phosphate-buffered saline (PBS; pH 7.2). Before use, the salivary glands were disrupted by three freeze-thaw cycles to prepare the salivary gland homogenate (SGH). All preparations of saliva were sterilized (5 min, 9,300 × g) through 0.22 μm pore centrifugal filters (Millipore) before use in *in vitro* experiments.

Recombinant Proteins

Two yellow-related proteins (rSP03 and rSP03B, Gen Bank ACCN ABA43049 and ABA43050, respectively) and apyrase (rSP01, Gen Bank ACCN ABB00906) derived from *P. perniciosus* salivary proteins were expressed in a human cell line. All proteins were transiently expressed in HEK293S GnTI^{-} cells (ATCC CRL-3022) as previously described (Blaha et al., 2015). Proteins rSP03 and rSP03B were prepared as described in Sumova et al. (2019). Apyrase rSP01 was expressed in a same way as protein

rSP03B. Briefly, transiently transfected HEK293S GnTI$^-$ cells were grown for five to seven days before harvesting the culture medium. The histidine-tagged product was then recovered by IMAC chromatography on HiTrap TALON crude columns (GE Healthcare) and further purified by SEC on Superdex 200 10/300 GL column (GE Healthcare). Finally, the protein identity was verified by mass spectrometry (BIOCEV, the Czech Republic).

Bone Marrow Macrophages Culture

Bone marrow was obtained by flushing of tibias and femurs of euthanized BALB/c mice. The differentiation from the bone marrow precursor cells to the bone marrow-derived macrophages proceeded for 7–9 days in the sterile polystyrene Petri dishes (Thermo Fisher) in the presence of L929 fibroblast cell culture supernatant (20% in RPMI-1640 medium), serving as a source of macrophage colony-stimulating factor (M-CSF), at 37°C with 5% CO_2. Later, after differentiation, the macrophages were cultured in RPMI-1640 medium (Sigma) containing 10% FBS, 1% penicillin-streptomycin (Sigma), 2 mM of L-glutamine (Sigma) and 0.05 mM of β-mercaptoethanol (referred as a complete medium) at 37°C with 5% CO_2.

Bone Marrow Macrophages Stimulation

The sessile bone marrow-derived macrophages (BMMF) were released from the Petri dish with trypsin-EDTA solution (Sigma), washed in 0.9% saline solution and seeded into the 96-wells plates (Costar) at a density of 1×10^6 cells/ml (5×10^4 cells/well). Consequently, the macrophages were co-incubated with *P. perniciosus* SGH (Per-SGH) in the amount equivalent to 0.5 salivary gland per well or with 0.2 μg of one of the recombinant proteins (rSP03, rSP03B, or rSP01) per well. The concentration of Per-SGH and of recombinant proteins has been selected based on our previous studies (Rohousova et al., 2005; Drahota et al., 2009) and on the preliminary experiments (data not shown). Control cells were incubated solely in complete RPMI-1640. Two hours later, cells were stimulated with a combination of IFN-γ (50 U/ml, AbD SEROTEC) and LPS (0.5 μg/ml, Sigma) (referred as classically stimulated macrophages), with IL-4 (25 ng/ml, eBioscience) (referred as alternatively stimulated macrophages), or left unstimulated. After 72 h of incubation, the supernatant and cell lysate were used for the nitrite and urea analysis, respectively. For the cytokine analysis, macrophages were incubated for 24 h and the collected supernatant was stored in −80°C until needed. In all experiments, samples were analyzed in pentaplicates. Six independent experiments were performed with 6 mice in total.

Nitrite Analysis to Measure iNOS Activity

The macrophage iNOS activity was analyzed by measuring the accumulation of nitric oxide in the culture supernatant over a 72 h period. Since the nitric oxide is a short lived free radical, we measured its product, the nitrite ion, using a Griess test in a microplate assay. A total of 100 μl of the culture supernatant was mixed with 50 μl of 60 mM sulfanilamide in 2.5% phosphoric acid and incubated at room temperature in dark for 5 min. Thereafter, 50 μl of 12 mM N-1-naphthylethylenediamine dihydrochloride in 2.5% phosphoric acid was added and incubated in dark for additional 5 min. The absorbance was read at 550 nm using the microplate reader (Tecan Infinite M200). The nitrite concentration was determined using a sodium nitrite as a standard in the range of 12.5–100 μM.

Urea Analysis to Measure Arginase Activity

Arginase activity was analyzed in the lysate of macrophages by measuring the conversion of L-arginine to urea as previously described (Kropf et al., 2007) with slight modifications. Cells were lysed with a solution of Tris–HCl in combination with protease inhibitors (Complete Mini, Roche) and Triton X-100. The enzyme was then activated in the presence of 10 mM $MnCl_2$ by heating and arginine hydrolysis was carried out by incubation of the activated enzyme with 0.5 M arginine (Sigma–Aldrich) at 37°C with 5% CO_2 for 120 min. The reaction was stopped with 400 μl of solution containing H_2SO_4, H_3PO_4 and distilled water (at ratio of 1:3:7). Color reaction was developed in the presence of 20 μl 550 mM α- isonitrosopropiophenone (dissolved in 100% ethanol) after incubation at 100°C for 45 min. Samples were then transferred to microplates and absorbance was read at 540 nm using the microplate reader (Tecan Infinite M200). Urea concentration was determined using urea as a standard in the range of 0.004–0.6 mg/ml.

Detection of Cytokine Production

The production of IL-10 and TNF-α was determined by sandwich enzyme-linked immunosorbent assays (ELISA) using ELISA MAX^{TM} Standard Set kits (BioLegend) according to the manufacturer's instruction with the following modification. Undiluted supernatant was used for determination of IL-10 production, while TNF-α was measured in supernatant diluted twenty-times in RPMI-1640 medium (Sigma). Absorbance was measured using a microplate reader (Tecan Infinite M200).

Skin Test to Measure Delayed-Type Hypersensitivity

The skin test was performed on two females of SKH mice. Mice were exposed to *P. perniciosus* bites, once per week, repeated three times with a 1-week interval between them during three consecutive weeks, with 50–100 bloodfed females per mouse per exposure. Only the dorsal part of the mouse body was available for bloodfeeding. Fourteen days after the last exposure, mice were anesthetized and challenged intradermally on the ventral part of the body with 0.2 μg (in a volume of 12.5 μl) of rSP03 and rSP03B separated from each other as depicted on the **Figure 3B**. The same volume of Per-SGH (equivalent to 0.5 gland) and PBS were used as positive and negative controls, respectively. The delayed-type hypersensitivity (DTH) reaction was measured 48 h post injection as the diameter of erythema.

Endotoxin Test

The level of endotoxin (bacterial LPS) in SGH, recombinant proteins, *Leishmania* and bone marrow macrophages cultures was quantified by ToxinSensor^{TM} Chromogenic LAL Endotoxin Assay Kit (GenScript) according to the manufacturer instructions. Endotoxin levels were measured in the unstimulated macrophage culture and in all stimulants

separately. In all preparations, the concentration of endotoxin was lower than 0.1 EU/ml, a level below the limit to activate the immune cells (Schwarz et al., 2014).

Statistical Analysis

Statistical analyses were carried out using the R software (version 3.6.3, downloaded from http://www.r-project.org). The "nlme" package was used to develop the multilevel regression models to investigate relationship between nitrite concentration, urea concentration and cytokine production as the continuous dependent variables, and exposure of macrophages to saliva or recombinant proteins as the categorical predictor variables. This relationship was examined separately for the macrophages incubated alone in complete RPMI-1640, stimulated with IL-4, and stimulated with a combination of IFN-γ and LPS. Continuous dependent variables with exception of cytokine production were transformed using ln(x+1) formula. $P < 0.05$ indicated statistical significance. Because the samples were analyzed in pentaplicates, we considered the correlation between repeated measurements within the individual mouse.

The fold-change values were calculated as a ratio between the value for cells incubated with salivary proteins (either Per-SGH, rSP01, rSP03, or rSP03B) divided by the mean value of the control cells (marked as neg in figures) treated with the same macrophage stimulus (IFN+LPS, IL-4, or unstimulated).

RESULTS

The Effect of Salivary Proteins on Arginase Activity

Recombinant yellow-related proteins rSP03 and rSP03B, apyrase rSP01, and crude *P. perniciosus* SGH (Per-SGH) were incubated with the bone marrow-derived macrophages to measure the urea production (**Figure 1A**) as a marker of arginase activity that is typical for tissue-repairing macrophages. The most pronounced effect has been observed with rSP03 (**Figure 1A**), which significantly increased urea production regardless of the macrophages' stimulation; the highest production, 3.6-fold the negative control value, was observed in the cells stimulated with IL-4. No significant changes were observed after incubation with rSP03B, rSP01, nor with Per-SGH.

The Effect of Salivary Proteins on iNOS Activity

rSP03, rSP03B, rSP01, and crude Per-SGH were incubated with BMMF to measure nitrite production (**Figure 1B**) as a marker of iNOS activity that is typical for pro-inflammatory macrophages. All tested proteins inhibited the production of NO, regardless of the macrophages' stimulation, and significantly in majority of combinations (**Figure 1B**). The most pronounced effect has been observed in the unstimulated and IL-4-stimulated macrophages incubated with Per-SGH (0.71 and 0.68-fold, respectively), followed by rSP03B (0.68 and 0.64-fold, respectively) and rSP01 (0.66 and 0.66-fold, respectively). All antigens significantly decreased the iNOS activity also in IFN-γ and LPS stimulated macrophages, the most pronounced effect was detected for rSP03 (0.84-fold the negative control value).

The Effect of rSP03 on Cytokine Production

As the protein rSP03 had the most pronounced effect on macrophages' activities, its effect on cytokine production of differentially stimulated macrophages was also evaluated. rSP03 and crude Per-SGH were incubated with bone marrow-derived macrophages to measure the production of anti-inflammatory cytokine IL-10 (**Figure 2A**) and pro-inflammatory cytokine TNF-α (**Figure 2B**). rSP03 markedly increased IL-10 production in unstimulated macrophages (4.18-fold), as well as in macrophages stimulated either with IL-4 (2.52-fold) or a combination of IFN-γ and LPS (1.62-fold). rSP03 also significantly increased TNF-α production in unstimulated cells (1.47-fold), and decreased production of TNF-α in IFN-γ and LPS-stimulated macrophages (0.71-fold). Per-SGH followed similar trends as rSP03 but its effect was less prominent and statistically insignificant.

Intradermal Skin Test With rSP03

Additionally, we tested the ability of rSP03 to elicit delayed-type hypersensitivity (DTH) in the intradermal skin test and compared it with the second yellow-related protein rSP03B and Per-SGH. Neither rSP03, rSP03B, nor the PBS control elicited DTH reaction in the skin of mice pre-exposed to *P. perniciosus* bites measured as the visible redness in the area of inoculation (**Figure 3A**). On the other hand, the site of crude Per-SGH inoculation showed induration and erythema 4.9 and 6.7 mm in diameter per mouse, respectively (**Figure 3**).

DISCUSSION

In this study, we have tested three recombinant salivary proteins from *P. perniciosus* females for their effect on the host immunity. Those recombinant proteins were the apyrase rSP01, and the two proteins of the yellow-related family, rSP03 and rSP03B. We tested their function, focusing on the macrophages as the key host cells for *Leishmania* parasites. Macrophages are known to respond to the different stimuli in their surrounding microenvironment by expressing arginine-processing enzymes, an iNOS or an arginase, whose products are either leishmanicidal (nitric oxide) or essential for *Leishmania* survival (L-ornithine and its metabolites), respectively (Tomiotto-Pellissier et al., 2018). Here we showed that the recombinant *P. perniciosus* apyrase and yellow related proteins possess anti-inflammatory properties on murine macrophages.

Apyrases are present in saliva of all sand fly species studied to date (Oliveira et al., 2020; Polanska et al., 2020). This enzyme hydrolyzes ADP and ATP, thus destroying the important stimulus of platelet aggregation and inflammation at the bite site, which helps the female fly to complete the bloodmeal (Francischetti, 2011). So far, the sand fly apyrases have been tested only in the context of adaptive immunity, employing transfection of the host's cells (Oliveira et al., 2006, 2008; Gomes et al., 2008; Xu et al., 2011; Marzouki et al., 2012; Tlili et al., 2018; Gholami et al., 2019). In previous studies, two recombinant *P. perniciosus* salivary apyrases, rSP01 and rSP01B, have been prepared, however, they have been primarily tested as the markers of exposure with sera of bitten hosts (Martin-Martin et al., 2013,

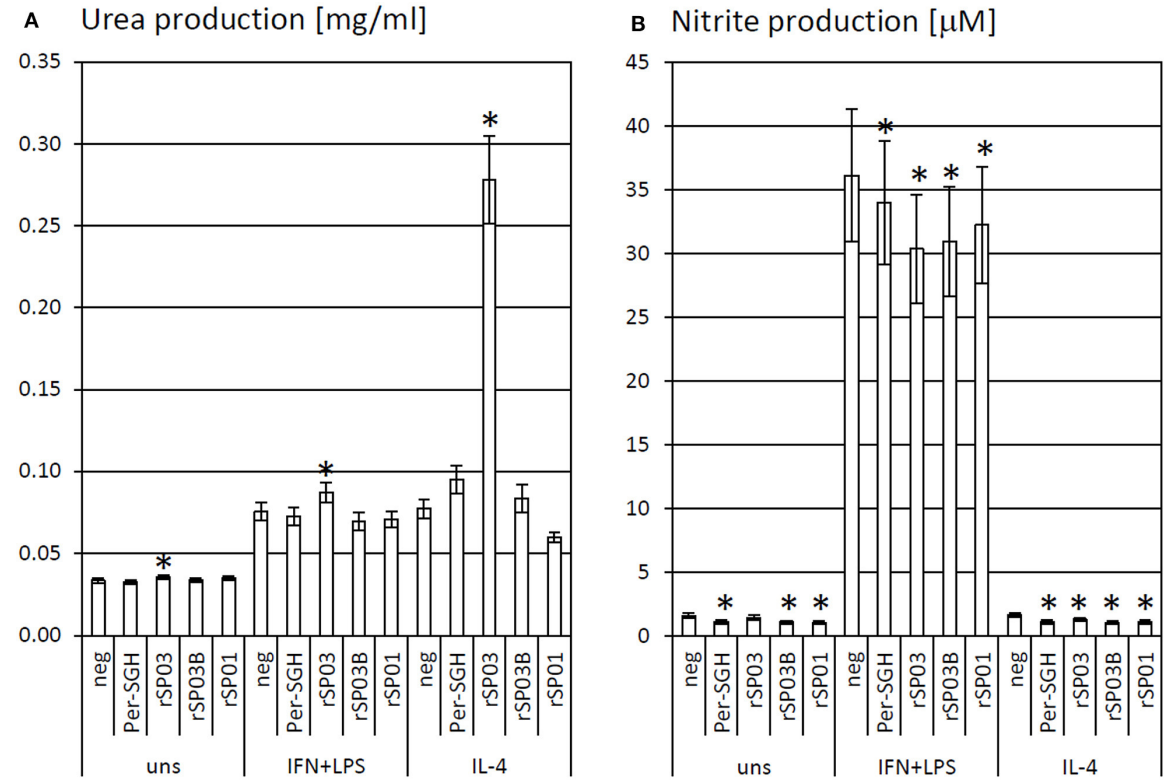

FIGURE 1 | The effect of *Phlebotomus perniciosus* salivary proteins on urea and nitrite production. Bone marrow-derived macrophages of BALB/c mice were incubated with salivary gland homogenate of *Phlebotomus perniciosus* (Per-SGH), or with the following *P. perniciosus* recombinant proteins: Yellow-related proteins rSP03 and rSP03B, or Apyrase rSP01. The cells were stimulated with either IL-4 or a combination of IFN-γ and bacterial lipopolysaccharide (IFN+LPS) and subsequently tested for urea **(A)** or nitrite **(B)** production as markers of arginase and iNOS activity, respectively. Unstimulated (uns) and negative (neg) controls were included. The experiment was performed in six biological replicates (6 mice). The data are presented as mean ± standard error, (*) denotes statistical significance at $p < 0.05$ compared to the neg control of the appropriate stimulant.

2014, 2015; Drahota et al., 2014; Kostalova et al., 2015) and never subjected to test their immunomodulatory properties. Here, we present the first study showing immunomodulatory effect of the recombinant sand fly apyrase on the macrophage activity *in vitro*. In our study, *P. perniciosus* rSP01 significantly inhibited NO production in murine macrophages. The inhibition was pronounced in all three macrophage populations, including the macrophages stimulated toward the pro-inflammatory state, suggesting an anti-inflammatory nature of this recombinant protein.

Yellow-related proteins (YRPs) comprise highly abundant proteins in sand fly saliva. They serve as the binders of biogenic amines (such as serotonin and norepinephrine) thus supporting successful blood feeding by scavenging important stimuli of haemostatic reactions at the bite site (Xu et al., 2011; Sumova et al., 2019). In *P. perniciosus*, two YRPs have been identified and named PpeSP03 and PpeSP03B (Anderson et al., 2006). Although sequentially similar, they differ in several aspects. The PpeSP03B protein has alkaline pI, is more abundant, and serves as a high-affinity binder of serotonin (Anderson et al., 2006; Martin-Martin et al., 2012; Sumova et al., 2019) and a strong binder of anti-saliva antibodies in mice and dogs (Anderson et al., 2006; Vlkova et al., 2011; Martin-Martin et al., 2012; Drahota et al., 2014; Kostalova et al., 2015; Willen et al., 2019). The latter properties of rSP03B made it the best antigen to substitute the sand fly salivary gland homogenate in assays measuring anti-*P. perniciosus* saliva IgG antibodies (Kostalova et al., 2015, 2017), upgraded later into the immunochromatographic test to screen dogs in endemic areas for the vector exposure (Willen et al., 2018, 2019). The other *P. perniciosus* YRP, PpeSP03, has lower pI, is less abundant, and acts as a medium affinity binder of norepinephrine (Anderson et al., 2006; Martin-Martin et al., 2012; Sumova et al., 2019) and a weak binder of anti-saliva antibodies in naturally-exposed dogs (Vlkova et al., 2011; Kostalova et al., 2017).

In our study, both *P. perniciosus* recombinant YRPs showed different immunomodulatory activity but with overall similar anti-inflammatory effect. We demonstrated that the recombinant protein rSP03B acted similar to the *P. perniciosus* rSP01 apyrase; it significantly inhibited NO production in all three murine macrophage populations, while showing no effect on the macrophage arginase activity. The other YRP, rSP03, showed the most pronounced effect on murine macrophages among the three proteins tested. This protein decreased the NO production in stimulated macrophages and increased the arginase activity along with a strong stimulation of IL-10 production in all types of macrophages tested. This anti-inflammatory effect of

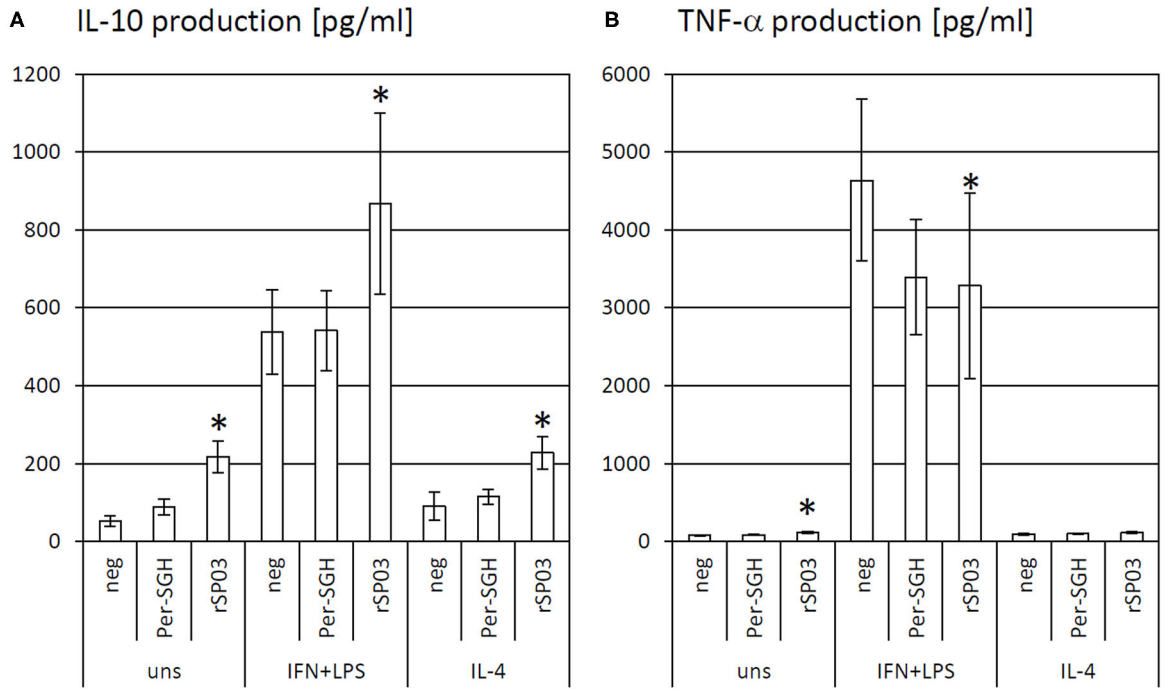

FIGURE 2 | The effect of *Phlebotomus perniciosus* rSP03 on cytokine production. Bone marrow-derived macrophages of BALB/c mice were incubated with salivary gland homogenate of *Phlebotomus perniciosus* (Per-SGH) or with *P. perniciosus* recombinant Yellow-related protein rSP03. The cells were stimulated with either IL-4 or a combination of IFN-γ and bacterial lipopolysaccharide (IFN+LPS) and the supernatant was subsequently tested for the production of IL-10 **(A)** and TNF-α **(B)**. Unstimulated (uns) and negative (neg) controls were included. The experiment was performed in six biological replicates (6 mice). The data are presented as mean ± standard error, (*) denotes statistical significance at $p < 0.05$ compared to the neg control of the appropriate stimulant.

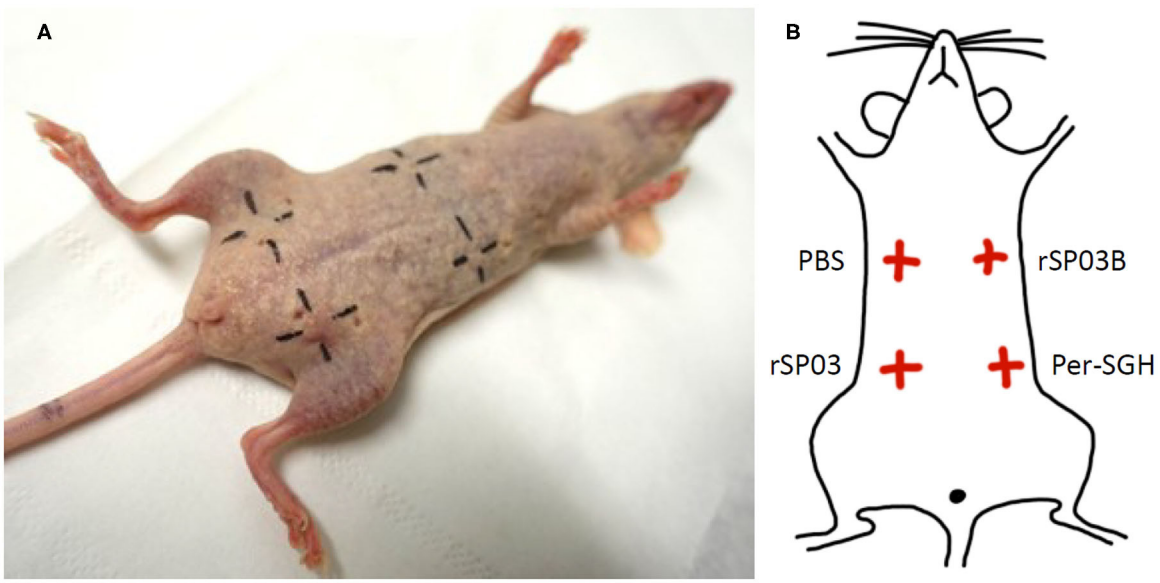

FIGURE 3 | Intradermal skin test with *Phlebotomus perniciosus* recombinant salivary proteins rSP03 and rSP03B. SKH mice were repeatedly exposed to *Phlebotomus perniciosus* bites. Two weeks after the last exposure, mice were challenged intradermally with *P. perniciosus* recombinant Yellow-related proteins rSP03 and rSP03B, and with salivary gland homogenate of *P. perniciosus* (Per-SGH) as depicted on the scheme **(B)**. Phosphate-buffered saline (PBS) was used as a negative control. The representative picture of the two independent experiments is shown **(A)**.

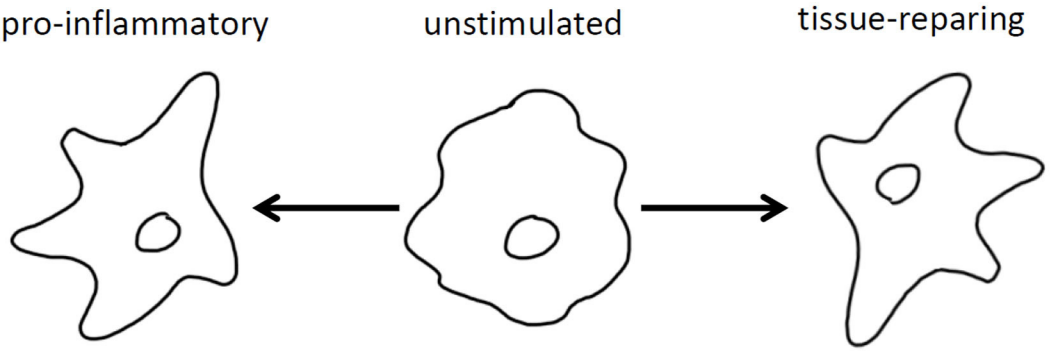

IFN+LPS	ARG	NO	IL-10	TNFa
Per-SGH				
rSP03			**1.62**	
rSP03B			-	-
rSP01			-	-

uns	ARG	NO	IL-10	TNFa
Per-SGH		**0.71**		
rSP03			**4.18**	
rSP03B		**0.68**	-	-
rSP01		**0.66**	-	-

IL-4	ARG	NO	IL-10	TNFa
Per-SGH		**0.68**		
rSP03	**3.60**		**2.52**	
rSP03B		**0.64**	-	-
rSP01		**0.66**	-	-

FIGURE 4 | Graphical summary of the effect of *Phlebotomus perniciosus* salivary proteins on macrophages. Bone marrow-derived macrophages of BALB/c mice were incubated with salivary gland homogenate of *Phlebotomus perniciosus* (Per-SGH), or with one of the three *P. perniciosus* recombinant proteins: Yellow-related proteins rSP03 and rSP03B, or Apyrase rSP01. The macrophages were stimulated with either IL-4 (resulting in tissue-repairing phenotype), a combination of IFN-γ and bacterial lipopolysaccharide (resulting in pro-inflammatory phenotype), or left unstimulated (uns). The experiment was performed in six biological replicates (6 mice). Within the tables, (green) denotes significant increase and (dark gray) significant decrease in the production of urea (ARG), nitrite (NO), IL-10 and TNF-α cytokines. Insignificant changes ($p > 0.05$) are marked (white), (–) means not measured. The numbers represent fold changes above 20% compared to the control.

rSP03 was also seen in macrophages stimulated toward the pro-inflammatory phenotype.

Additionally, we also tested both YRPs for their effect on the adaptive immunity. In mice pre-exposed to *P. perniciosus* bites, injection of the recombinant YRPs did not elicit visible skin reaction compared to *P. perniciosus* crude saliva. This result is in accordance with measured anti-inflammatory effect of both yellow-related proteins. Similar tests have been performed with the YRPs from other sand fly species, employing a different experimental approach; mice were immunized intradermally with a plasmid coding for sand fly YRP and challenged with saliva from the relevant sand fly species (and vice versa; mice first exposed to sand fly saliva and then challenged with plasmid). In these settings, ten YRPs from five different sand fly species were tested with different outcomes (Anderson et al., 2006; Gomes et al., 2008; Oliveira et al., 2008, 2015; Collin et al., 2009; Xu et al., 2011; Abbehusen et al., 2018; Gholami et al., 2019). For instance, in well-studied *Lutzomyia longipalpis*, only one of the three YRPs showed a positive recall response, while the other two proteins did not elicit any DTH response in mice (Gomes et al., 2008; Xu et al., 2011). Such functional divergence of the YRPs is in accordance with the gene duplication events in this protein family (Coutinho-Abreu and Valenzuela, 2018) providing most of the sand fly species with multiple YRPs with various function for scavenging biomolecules essential for host haemostasis and for modulating the host immune system (Sumova et al., 2019).

CONCLUSION

In summary, all three recombinant *P. perniciosus* proteins showed anti-inflammatory properties on murine macrophages (**Figure 4**). Even in the presence of pro-inflammatory stimuli (IFN-γ and LPS), all tested recombinants inhibited NO production. Moreover, rSP03 seems to have a very strong anti-inflammatory effect since it enhanced arginase activity, increased the production of IL-10, and inhibited the production of TNF-α even in macrophages stimulated with IFN-γ and LPS. These results also suggest that *P. perniciosus* apyrase and yellow-related proteins may serve as enhancing factors in sand fly saliva, facilitating the development of *Leishmania* infection along with their anti-haemostatic functions.

In general, sand fly salivary proteins in a recombinant form might be used to understand the possible function of their native counterparts. Importantly, if the recombinant proteins are tested as candidates for leishmaniasis vaccine (Collin et al., 2009; Gomes et al., 2012; Abbehusen et al., 2018; Cunha et al., 2018), their possible immunogenic nature should be also considered since it may negatively influence the vaccinated individuals (Reagan et al., 2012), e.g., by initiating an autoimmune disease in susceptible recipients (Qian et al., 2016). Thus, any vaccine candidate molecules should be thoroughly tested to validate their overall beneficial status for the host immunity.

DATA AVAILABILITY STATEMENT

The raw data supporting the conclusions of this article will be made available by the authors, without undue reservation.

ETHICS STATEMENT

The animal study was reviewed and approved by The Committee on Ethics of Laboratory Experiments, Faculty of Science, Charles University, Czech Republic.

AUTHOR CONTRIBUTIONS

IR and PV conceived the study. IR, PV, PS, and NP designed the experiments. PS and NP performed the experiments. BK expressed and purified the recombinant proteins. TL maintained the *P. perniciosus* colony and designed the methodology of BMMF macrophage cultivation. TS performed statistical analysis. IR analyzed and interpreted the data and drafted the manuscript. PS and NP contributed to the draft writing. OV and PV provided reagents and material and critically read the manuscript. All the authors read and approved the final version of the manuscript.

FUNDING

This work was supported by the Ministry of Education of the Czech Republic through the ERD Fund (project nos. CZ.02.1.01/0.0/0.0/16_019/0000759 and CZ.1.05/1.1.00/02.0109) and by Charles University, the Czech Republic (project nos. UNCE/SCI/012 and SVV260427/2020). The funders had no role in the study design, data collection and analysis, decision to publish, or preparation of the manuscript.

ACKNOWLEDGMENTS

The authors would like to acknowledge Helena Kulikova, Kristyna Srstkova, and Lenka Krejcirikova for their invaluable administrative and technical assistance.

REFERENCES

Abbehusen, M. M. C., Cunha, J., Suarez, M. S., Teixeira, C., Dos Anjos Almeida, V., Da Silva Pereira, L., et al. (2018). Immunization of experimental dogs with salivary proteins from *Lutzomyia longipalpis*, using DNA and recombinant canarypox virus induces immune responses consistent with protection against *Leishmania infantum*. *Front. Immunol.* 9:2558. doi: 10.3389/fimmu.2018.02558

Anderson, J. M., Oliveira, F., Kamhawi, S., Mans, B. J., Reynoso, D., Seitz, A. E., et al. (2006). Comparative salivary gland transcriptomics of sandfly vectors of visceral leishmaniasis. *BMC Genomics* 7:52. doi: 10.1186/1471-2164-7-52

Blaha, J., Pachl, P., Novak, P., and Vanek, O. (2015). Expression and purification of soluble and stable ectodomain of natural killer cell receptor LLT1 through high-density transfection of suspension adapted HEK293S GnTI^{-} cells. *Protein Expr. Purif.* 109, 7–13. doi: 10.1016/j.pep.2015.01.006

Burnham, A. C., Ordeix, L., Alcover, M. M., Martinez-Orellana, P., Montserrat-Sangra, S., Willen, L., et al. (2020). Exploring the relationship between susceptibility to canine leishmaniosis and anti-*Phlebotomus perniciosus* saliva antibodies in Ibizan hounds and dogs of other breeds in Mallorca, Spain. *Parasit. Vectors* 13:129. doi: 10.1186/s13071-020-3992-8

Collin, N., Gomes, R., Teixeira, C., Cheng, L., Laughinghouse, A., Ward, J. M., et al. (2009). Sand fly salivary proteins induce strong cellular immunity in a natural reservoir of visceral leishmaniasis with adverse consequences for *Leishmania*. *PLoS Pathog.* 5:e1000441. doi: 10.1371/journal.ppat.1000441

Coutinho-Abreu, I. V., and Valenzuela, J. G. (2018). Comparative evolution of sand fly salivary protein families and implications for biomarkers of vector exposure and salivary vaccine candidates. *Front. Cell. Infect. Microbiol.* 8:290. doi: 10.3389/fcimb.2018.00290

Cunha, J. M., Abbehusen, M., Suarez, M., Valenzuela, J., Teixeira, C. R., and Brodskyn, C. I. (2018). Immunization with LJM11 salivary protein protects against infection with *Leishmania braziliensis* in the presence of *Lutzomyia longipalpis* saliva. *Acta Trop.* 177, 164–170. doi: 10.1016/j.actatropica.2017.10.009

Drahota, J., Lipoldova, M., Volf, P., and Rohousova, I. (2009). Specificity of anti-saliva immune response in mice repeatedly bitten by *Phlebotomus sergenti*. *Parasite Immunol.* 31, 766–770. doi: 10.1111/j.1365-3024.2009.01155.x

Drahota, J., Martin-Martin, I., Sumova, P., Rohousova, I., Jimenez, M., Molina, R., et al. (2014). Recombinant antigens from *Phlebotomus perniciosus* saliva as markers of canine exposure to visceral leishmaniases vector. *PLoS Negl. Trop. Dis.* 8:45. doi: 10.1371/journal.pntd.0002597

Francischetti, I. M. B. (2011). Platelet aggregation Inhibitors from Hametophagous Animals. *Toxicon* 56, 1130–1144. doi: 10.1016/j.toxicon.2009.12.003. Platelet

Gholami, E., Oliveira, F., Taheri, T., Seyed, N., Gharibzadeh, S., Gholami, N., et al. (2019). DNA plasmid coding for *Phlebotomus sergenti* salivary protein PsSP9, a member of the SP15 family of proteins, protects against *Leishmania tropica*. *PLoS Negl. Trop. Dis.* 13:e0007067. doi: 10.1371/journal.pntd.0007067

Gomes, R., Oliveira, F., Teixeira, C., Meneses, C., Gilmore, D. C., Elnaiem, D. E., et al. (2012). Immunity to sand fly salivary protein LJM11 modulates host response to vector-transmitted leishmania conferring ulcer-free protection. *J. Invest. Dermatol.* 132, 2735–2743. doi: 10.1038/jid.2012.205

Gomes, R., Teixeira, C., Teixeira, M. J., Oliveira, F., Menezes, M. J., Silva, C., et al. (2008). Immunity to a salivary protein of a sand fly vector protects against the fatal outcome of visceral leishmaniasis in a hamster model. *Proc. Natl. Acad. Sci. U.S.A.* 105, 7845–7850. doi: 10.1073/pnas.0712153105

Kostalova, T., Lestinova, T., Maia, C., Sumova, P., Vlkova, M., Willen, L., et al. (2017). The recombinant protein rSP03B is a valid antigen for screening dog exposure to *Phlebotomus perniciosus* across foci of canine leishmaniasis. *Med. Vet. Entomol.* 31, 88–93. doi: 10.1111/mve.12192

Kostalova, T., Lestinova, T., Sumova, P., Vlkova, M., Rohousova, I., Berriatua, E., et al. (2015). Canine antibodies against salivary recombinant proteins of *Phlebotomus perniciosus*: A longitudinal study in an endemic focus of canine leishmaniasis. *PLoS Negl. Trop. Dis.* 9:e0003855. doi: 10.1371/journal.pntd.0003855

Kropf, P., Baud, D., Marshall, S. E., Munder, M., Mosley, A., Fuentes, J. M., et al. (2007). Arginase activity mediates reversible T cell hyporesponsiveness in human pregnancy. *Eur. J. Immunol.* 37, 935–945. doi: 10.1002/eji.200636542

Lestinova, T., Rohousova, I., Sima, M., de Oliveira, C. I., and Volf, P. (2017). Insights into the sand fly saliva: Blood-feeding and immune interactions between sand flies, hosts, and *Leishmania*. *PLoS Negl. Trop. Dis.* 11:e0005600. doi: 10.1371/journal.pntd.0005600

Maia, C., Cristóvão, J., Pereira, A., Kostalova, T., Lestinova, T., Sumova, P., et al. (2020). Monitoring *Leishmania* infection and exposure to *Phlebotomus perniciosus* using minimal and non-invasive canine samples. *Parasit. Vectors* 13:119. doi: 10.1186/s13071-020-3993-7

Maroli, M., Feliciangeli, M. D., Bichaud, L., Charrel, R. N., and Gradoni, L. (2013). Phlebotomine sandflies and the spreading of leishmaniases and other diseases of public health concern. *Med. Vet. Entomol.* 27, 123–147. doi: 10.1111/j.1365-2915.2012.01034.x

Martin-Martin, I., Molina, R., and Jimenez, M. (2012). An insight into the *Phlebotomus perniciosus* saliva by a proteomic approach. *Acta Trop.* 123, 22–30. doi: 10.1016/j.actatropica.2012.03.003

Martin-Martin, I., Molina, R., and Jimenez, M. (2013). Molecular and immunogenic properties of apyrase SP01B and D7-related SP04 recombinant salivary proteins of *Phlebotomus perniciosus* from Madrid, Spain. *Biomed Res. Int.* 2013:526069. doi: 10.1155/2013/526069

Martin-Martin, I., Molina, R., and Jimenez, M. (2015). Kinetics of anti-*Phlebotomus perniciosus* saliva antibodies in experimentally bitten mice and rabbits. *PLoS ONE* 10:e0140722. doi: 10.1371/journal.pone.0140722

Martin-Martin, I., Molina, R., Rohousova, I., Drahota, J., Volf, P., and Jimenez, M. (2014). High levels of anti-*Phlebotomus perniciosus* saliva antibodies in different vertebrate hosts from the re-emerging leishmaniosis focus in Madrid, Spain. *Vet. Parasitol.* 202, 207–216. doi: 10.1016/j.vetpar.2014.02.045

Marzouki, S., Abdeladhim, M., Abdessalem, C., Ben, O.liveira, F., and Ferjani, B., Gilmore, D., et al. (2012). Salivary Antigen SP32 Is the Immunodominant Target of the Antibody Response to *Phlebotomus papatasi* Bites in Humans. *PLoS Negl. Trop. Dis.* 6:e1911. doi: 10.1371/journal.pntd.0001911

Oliveira, F., Giorgobiani, E., Guimaraes-Costa, A. B., Abdeladhim, M., Oristian, J., Tskhvaradze, L., et al. (2020). Immunity to vector saliva is compromised by short sand fly seasons in endemic regions with temperate climates. *Sci. Rep.* 10:7990. doi: 10.1038/s41598-020-64820-9

Oliveira, F., Kamhawi, S., Seitz, A. E., Pham, V. M., Guigal, P. M., Fischer, L., et al. (2006). From transcriptome to immunome: Identification of DTH inducing proteins from a *Phlebotomus ariasi* salivary gland cDNA library. *Vaccine* 24, 374–390. doi: 10.1016/j.vaccine.2005.07.085

Oliveira, F., Lawyer, P. G., Kamhawi, S., and Valenzuela, J. G. (2008). Immunity to distinct sand fly salivary proteins primes the anti-*Leishmania* immune response towards protection or exacerbation of disease. *PLoS Negl. Trop. Dis.* 2:e226. doi: 10.1371/journal.pntd.0000226

Oliveira, F., Rowton, E., Aslan, H., Gomes, R., Castrovinci, P. A., Alvarenga, P. H., et al. (2015). A sand fly salivary protein vaccine shows efficacy against vector-transmitted cutaneous leishmaniasis in nonhuman primates. *Sci. Transl. Med.* 7:290ra90. doi: 10.1126/scitranslmed.aaa3043

Polanska, N., Ishemgulova, A., Volfova, V., Flegontov, P., Votypka, J., Yurchenko, V., et al. (2020). *Sergentomyia schwetzi*: Salivary gland transcriptome, proteome and enzymatic activities in two lineages adapted to different blood sources. *PLoS ONE* 15:e0230537. doi: 10.1371/journal.pone.0230537

Qian, Y., Culton, D. A., Jeong, J. S., Trupiano, N., Valenzuela, J. G., and Diaz, L. A. (2016). Non-infectious Environmental Antigens as a Trigger for the Initiation of an Autoimmune Skin Disease. *Autoimmun. Rev.* 15, 923–930. doi: 10.1016/j.autrev.2016.07.005

Reagan, K. L., Machain-Williams, C., Wang, T., and Blair, C. D. (2012). Immunization of Mice with Recombinant Mosquito Salivary Protein D7 Enhances Mortality from Subsequent West Nile Virus Infection via Mosquito Bite. *PLoS Negl. Trop. Dis.* 6:e1935. doi: 10.1371/journal.pntd.0001935

Risueno, J., Spitzova, T., Bernal, L. J., Munoz, C., Lopez, M. C., Thomas, M. C., et al. (2019). Longitudinal monitoring of anti-saliva antibodies as markers of repellent efficacy against *Phlebotomus perniciosus* and *Phlebotomus papatasi* in dogs. *Med. Vet. Entomol.* 33, 99–109. doi: 10.1111/mve.12343

Rohousova, I., Volf, P., and Lipoldova, M. (2005). Modulation of murine cellular immune response and cytokine production by salivary gland lysate of three sand fly species. *Parasite Immunol.* 27, 469–473. doi: 10.1111/j.1365-3024.2005.00787.x

Schwarz, H., Schmittner, M., Duschl, A., and Horejs-Hoeck, J. (2014). Residual endotoxin contaminations in recombinant proteins are sufficient to activate human CD1c^{+} dendritic cells. *PLoS ONE* 9:e113840. doi: 10.1371/journal.pone.0113840

Shapouri-Moghaddam, A., Mohammadian, S., Vazini, H., Taghadosi, M., Esmaeili, S. A., Mardani, F., et al. (2018). Macrophage plasticity, polarization, and function in health and disease. *J. Cell. Physiol.* 233, 6425–6440. doi: 10.1002/jcp.26429

Sumova, P., Sima, M., Kalouskova, B., Polanska, N., Vanek, O., Oliveira, F., et al. (2019). Amine-binding properties of salivary yellow-related proteins in phlebotomine sand flies. *Insect Biochem. Mol. Biol.* 115:103245. doi: 10.1016/j.ibmb.2019.103245

Tlili, A., Marzouki, S., Chabaane, E., Abdeladhim, M., Kammoun-Rebai, W., Sakkouhi, R., et al. (2018). *Phlebotomus papatasi* Yellow-Related and Apyrase Salivary Proteins Are Candidates for Vaccination against Human Cutaneous Leishmaniasis. *J. Invest. Dermatol.* 138, 598–606. doi: 10.1016/j.jid.2017.09.043

Tomiotto-Pellissier, F., Bortoleti, B. T. D. S., Assolini, J. P., Goncalves, M. D., Carloto, A. C. M., Miranda-Sapla, M. M., et al. (2018). Macrophage Polarization in Leishmaniasis: Broadening Horizons. *Front. Immunol.* 9:2529. doi: 10.3389/fimmu.2018.02529

Velez, R., Spitzova, T., Domenech, E., Willen, L., Cairo, J., Volf, P., et al. (2018). Seasonal dynamics of canine antibody response to *Phlebotomus perniciosus* saliva in an endemic area of *Leishmania infantum*. *Parasit. Vectors* 11:545. doi: 10.1186/s13071-018-3123-y

Vlkova, M., Rohousova, I., Drahota, J., Stanneck, D., Kruedewagen, E. M., Mencke, N., et al. (2011). Canine antibody response to Phlebotomus perniciosus bites negatively correlates with the risk of Leishmania infantum transmission. *PLoS Negl. Trop. Dis.* 5:e1344. doi: 10.1371/journal.pntd.0001344

Volf, P., and Volfova, V. (2011). Establishment and maintenance of sand fly colonies. *J. Vector Ecol.* 36, S1–S9. doi: 10.1111/j.1948-7134.2011.00106.x

Willen, L., Lestinova, T., Kalouskova, B., Sumova, P., Spitzova, T., Velez, R., et al. (2019). Field study of the improved rapid sand fly exposure test in areas endemic for canine leishmaniasis. *PLoS Negl. Trop. Dis.* 13:e0007832. doi: 10.1371/journal.pntd.0007832

Willen, L., Mertens, P., and Volf, P. (2018). Evaluation of the rSP03B sero-strip, a newly proposed rapid test for canine exposure to *Phlebotomus perniciosus*, vector of *Leishmania infantum*. *PLoS Negl. Trop. Dis.* 12:e0006607. doi: 10.1371/journal.pntd.0006607

Xu, X., Oliveira, F., Chang, B. W., Collin, N., Gomes, R., Teixeira, C., et al. (2011). Structure and function of a "yellow" protein from saliva of the sand fly *Lutzomyia longipalpis* that confers protective immunity against *Leishmania major* infection. *J. Biol. Chem.* 286, 32383–32393. doi: 10.1074/jbc.M111.268904

Conflict of Interest: The authors declare that the research was conducted in the absence of any commercial or financial relationships that could be construed as a potential conflict of interest.

frontiers in Cellular and Infection Microbiology

ORIGINAL RESEARCH
published: 31 August 2020
doi: 10.3389/fcimb.2020.00455

Antibody Responses Against *Anopheles darlingi* Immunogenic Peptides in *Plasmodium* Infected Humans

Berlin Londono-Renteria[1], Jehidys Montiel[1], Eric Calvo[2], Alberto Tobón-Castaño[3], Hugo O. Valdivia[4], Karin Escobedo-Vargas[4], Luz Romero[4,5], Maria Bosantes[4,5], Michael L. Fisher[4], Michael J. Conway[6], Gissella M. Vásquez[4] and Audrey E. Lenhart[7]*

[1] Vector Biology Laboratory, Department of Entomology, Kansas State University, Manhattan, KS, United States, [2] Laboratory of Malaria and Vector Research, National Institute of Allergies and Infectious Diseases (NIAID/NIH), Rockville, MD, United States, [3] Malaria Group, Universidad de Antioquia, Medellín, Colombia, [4] U.S. Naval Medical Research Unit No. 6 (NAMRU-6), Callao, Peru, [5] Asociación Benéfica PRISMA, Lima, Peru, [6] Central Michigan University College of Medicine, Mount Pleasant, MI, United States, [7] Division of Parasitic Diseases and Malaria, Entomology Branch, Centers for Disease Control and Prevention, Atlanta, GA, United States

OPEN ACCESS

Edited by:
Ashley Vaughan, Seattle Children's Research Institute, United States

Reviewed by:
Abhai K. Tripathi, Bloomberg School of Public Health, Johns Hopkins University, United States
Anne Poinsignon, Institut de Recherche Pour le Développement (IRD), France

***Correspondence:**
Berlin Londono-Renteria
blondono@ksu.edu

Specialty section:
This article was submitted to Parasite and Host, a section of the journal Frontiers in Cellular and Infection Microbiology

Received: *06 May 2020*
Accepted: *24 July 2020*
Published: *31 August 2020*

Citation:
Londono-Renteria B, Montiel J, Calvo E, Tobón-Castaño A, Valdivia HO, Escobedo-Vargas K, Romero L, Bosantes M, Fisher ML, Conway MJ, Vásquez GM and Lenhart AE (2020) Antibody Responses Against Anopheles darlingi Immunogenic Peptides in Plasmodium Infected Humans. Front. Cell. Infect. Microbiol. 10:455. doi: 10.3389/fcimb.2020.00455

Introduction: Malaria is still an important vector-borne disease in the New World tropics. Despite the recent decline in malaria due to *Plasmodium falciparum* infection in Africa, a rise in *Plasmodium* infections has been detected in several low malaria transmission areas in Latin America. One of the main obstacles in the battle against malaria is the lack of innovative tools to assess malaria transmission risk, and the behavioral plasticity of one of the main malaria vectors in Latin America, *Anopheles darlingi*.

Methods: We used human IgG antibodies against mosquito salivary gland proteins as a measure of disease risk. Whole salivary gland antigen (SGA) from *Anopheles darlingi* mosquitoes was used as antigen in Western blot experiments, in which a ∼65 kDa protein was visualized as the main immunogenic band and sent for sequencing by mass spectrometry. Apyrase and peroxidase peptides were designed and used as antigens in an ELISA-based test to measure human IgG antibody responses in people with different clinical presentations of malaria.

Results: Liquid chromatography–mass spectrometry revealed 17 proteins contained in the ∼65 kDa band, with an apyrase and a peroxidase as the two most abundant proteins. Detection of IgG antibodies against salivary antigens by ELISA revealed a significant higher antibody levels in people with malaria infection when compared to uninfected volunteers using the AnDar_Apy1 and AnDar_Apy2 peptides. We also detected a significant positive correlation between the anti-peptides IgG levels and antibodies against the *Plasmodium vivax* and *P. falciparum* antigens PvMSP1 and PfMSP1. Odd ratios suggest that people with higher IgG antibodies against the apyrase peptides were up to five times more likely to have a malaria infection.

Conclusion: Antibodies against salivary peptides from *An. darlingi* salivary gland proteins may be used as biomarkers for malaria risk.

Keywords: *An. darlingi*, peptides, antibodies, malaria, Colombia

INTRODUCTION

Malaria is one of the most important parasitic diseases of the tropics and subtropics. Despite global decreases in malaria cases, Latin America has experienced an increase in cases since 2015. Colombia is among the top five Latin American countries with the highest numbers of malaria cases reported annually (Chaparro-Narvaez et al., 2016). In 2019 the number of malaria cases officially reported was 78,513 with Chocó, Nariño, Cordoba, and Antioquia, the departments with the highest number of malaria cases (31.4, 20.4, 11.6, and 9.3%, respectively) (Instituto Nacional de Salud, 2019). Several factors contribute to this phenomenon. First, more than 80% of the Colombian territory is suitable for the transmission of malaria due to the presence of a diverse number of mosquito species capable of serving as vectors of *Plasmodium* spp. (Rodriguez et al., 2011). Second, at least three species of *Plasmodium* cause infection in Colombia, with *Plasmodium vivax* as the main species, followed by *Plasmodium falciparum* and *Plasmodium malariae* (Arevalo-Herrera et al., 2012). Forced migration and precarious socioeconomic conditions also favor the spread and prevalence of *Plasmodium* spp. (Martens and Hall, 2000; Jitthai, 2013; Rodrigues et al., 2018).

Globally, most efforts to prevent malaria transmission focus on *P. falciparum*, the deadliest malaria parasite species. However, *P. vivax* is also a significant cause of morbidity and mortality (Chaparro-Narvaez et al., 2016; Geleta and Ketema, 2016; Zain Ul et al., 2016), and improved methods of monitoring its transmission are needed. Malaria transmission in Colombia occurs year-round, with peaks typically occurring between February and June (Ruiz et al., 2006). Malaria incidence is highly associated with changes in climatic conditions (i.e., temperature, elevation, and humidity) (Ruiz et al., 2006; Cassab et al., 2011). More importantly, ∼87% of the reported cases come from people living in rural areas with limited access to health care (Rodriguez et al., 2011). Frequently, research about malaria transmission in these areas is restricted due to the lack of infrastructure to support research, including limited access to electricity.

Currently, the gold standard to determine malaria transmission intensity is the Entomological Inoculation Rate (EIR), which represents the number of infectious mosquito bites a person receives per night. This provides an indirect estimation of the risk of acquiring the disease. One of the challenges of this technique is the need to detect parasites in mosquitoes that are collected in the field. Mosquito trapping systems can be biased and overrepresent the most abundant species in a specific area. In addition, current methods are unable to pinpoint the exact individuals who have been bitten or whether there are differences in the number of bites different people receive. Thus, current surveillance efforts lack individualized, deployable, and cost-effective tools to measure human-vector contact and improve measurement of malaria transmission risk. Such tools would be particularly valuable in assessing the efficacy of vector control interventions in protecting people from malaria vector bites.

Our previous studies demonstrated that IgG antibodies against salivary proteins of major disease vectors correlate with the clinical presentation of dengue fever and malaria (Londono-Renteria et al., 2010; Londoño-Rentería et al., 2015a; Montiel et al., 2020a), and can be used to evaluate vector control interventions (Londono-Renteria et al., 2015c). In fact, IgG antibodies against a salivary peptide (gSG6-P1) from a major African malaria vector has been validated as a reliable marker to measure exposure to several *Anopheles* spp. (Poinsignon et al., 2009; Badu et al., 2012; Sagna et al., 2013). However, recent studies suggest that the gSG6 gene is not present in the subgenus *Nyssorhynchus*, which is the most prevalent American *Anopheles* subgenus (Arca et al., 2017). Although, previous studies have shown that the gSG6-P1 may be useful in areas of the New World where species belonging to subgenus other than *Nyssorhynchus* (Londono-Renteria et al., 2015b; Montiel et al., 2020a), there is a need to detect and validate novel biomarkers for exposure to these *Anopheles* spp. There are at least 40 *Anopheles* species in Colombia (Montoya-Lerma et al., 2011). The main vectors in the country are *Anopheles nuneztovari, Anopheles albimanus* and *Anopheles darlingi*—all three species within the subgenus *Nyssorhynchus* (Montoya-Lerma et al., 2011). Recently, we described several peptides that could be used to determine exposure to *Anopheles albimanus* bites, with antibodies against transferrin and salivary peroxidase proteins associated with the clinical presentation of malaria (Montiel et al., 2020a).

In this study, we evaluated the immunogenicity of salivary proteins in *An. darlingi* salivary gland antigen (SGA) and designed four peptides to measure IgG responses in people living in malaria endemic areas. The objective was to evaluate whether IgG antibodies against these peptides could be reliable markers to detect the risk of disease. *An. darlingi* is one of the most prolific mosquito vectors of malaria in Central and South America (Mirabello and Conn, 2006; Villarreal-Trevino et al., 2015; Prado et al., 2019), known for its behavioral plasticity and highly anthropophilic behavior. This mosquito species bite indoors and outdoors (endophagic/exophagic) and display exophilic/endophilic opportunistic behaviors (Moutinho et al., 2011; Reinbold-Wasson et al., 2012; Moreno et al., 2015). Our study suggests that IgG antibodies against *An. darlingi* salivary proteins are useful to assess malaria risk in areas where this species is endemic. This is the first study describing *An. darlingi* salivary peptides as potential tools to evaluate immune responses against mosquito saliva with the aim to improve accurate estimation of malaria transmission intensity, which is imperative for directing control efforts and predicting the effects of such interventions.

MATERIALS AND METHODS

Ethical Considerations and Human Sample Collection

Serum samples from 179 participants were collected by active and passive case detection from November 2016 to October 2017 in Turbo and El Bagre as part of a malaria study in Colombia. These represent two malaria endemic areas with differing malaria incidence as measured by the Annual Parasite Index (API: confirmed cases during 1 year/population under

TABLE 1 | Description of the serum samples by malaria infection status and location.

Malaria infection status	Turbo	El bagre	Total
P. falciparum	8	18	26
P. vivax	36	29	65
Uninfected	45	43	88
Total	89	90	179

surveillance × 1,000): the API in Turbo was 1.22 in 2016 and 0.77 in 2017, while malaria incidence in El Bagre was higher, with an API of 24.7 in 2016 and 21.3 in 2017 (Londoño-Rentería et al., 2015a; Londono-Renteria et al., 2020; Montiel et al., 2020b). Participant characteristics are described in **Table 1**. No concurrent entomological data was collected for this study. However, these field sites were selected based on a previous study reporting entomological data, where more than 96% of mosquitoes collected in Turbo were *An. albimanus*, while more than 70% of the mosquitos in El Bagre were *An. darlingi* (Gutierrez et al., 2009). Human sample collection and testing protocols were approved by the IRB of Kansas State University (IRB #8956 and IBC #1206) and the Medical School at the Universidad de Antioquia in Medellín, Colombia (Record 011 dated 28 July 2016).

Detection of Malaria Parasites

On-site malaria diagnosis was done by microscopy, then confirmed by nested PCR (nPCR) at the Universidad de Antioquia (Colombia) following methods described previously (Londoño-Rentería et al., 2015a; Londono-Renteria et al., 2020). Based on these results, samples were classified as malaria positive or malaria negative, based on the presence/absence of parasites or a positive PCR result. In case of a disagreement, the PCR results was taken as the final diagnosis.

An. darlingi Mosquito Rearing

All *An. darlingi* were reared in the insectary at the Naval Medical Research Unit No. 6 (NAMRU-6) in Iquitos, Peru as described previously (Villarreal-Trevino et al., 2015). Larvae were reared in a dedicated larvae room (26.8 ± 0.7°C and 76.1 ± 6.3% relative humidity, and 12-h light:12-h dark photoperiod) and adults were maintained in a dedicated adult insectary room (25.9 ± 0.8°C and 69.7 ± 5.7% relative humidity, and 12-h light:12-h dark photoperiod) (Villarreal-Trevino et al., 2015). Eight to ten- day old adult mosquitoes were used for dissections of salivary glands. These mosquitoes were blood fed with chicken blood at an age of 3–5 days post-emergence, and provided with 10% sucrose solution *ad libitum*.

Salivary Gland Antigen (SGA) Preparation

Female *An. darlingi* mosquitoes were cold-anesthetized, washed in 70% ethanol, and placed in PBS (pH 7.2) for salivary gland dissection. Salivary glands were pooled (100 mosquitoes per pool for a total of two pools) and placed in 1X PBS. To prepare the antigen extract, the pool of salivary glands was allowed to freeze at −80°C and thaw at 4°C four times to induce cell rupture and release of proteins; the resulting SGA was kept in PBS at −80°C until use. Protein concentration was determined using a Thermo Scientific NanoDrop™ (Thermo Fisher Scientific, Wilmington, DE, USA) (Londono-Renteria et al., 2013, 2020; Montiel et al., 2020a).

Immunoblotting

To identify immunogenic proteins in *An. darlingi* SGA, pooled sera from ten uninfected subjects were used (five subjects from Turbo and five subjects from El Bagre) were used in the Immunoblotting experiments performed according to Londono-Renteria et al. (2010) (Londono-Renteria et al., 2010). In brief, 2 μg/well of SGA was separated in a 4–15% polyacrylamide gel (BioRad) at 100 V and transferred to a nitrocellulose membrane (Turbo PVDF, 0.45-m pore size, 8.5 by 13.5 cm, Biorad) in a Transblot Turbo following the standard 30 min transference protocol. Membranes were blocked for 1 h with blocking buffer (2% milk in PBST) and incubated with pooled human sera (1/250) at 4°C overnight. Each membrane was washed five times with wash solution (1X PBST) and incubated with HRP-conjugate anti human-IgG, in a 1/1,000 dilution during 1 h at 37°C. Color development was obtained with HRP chromogenic substrate TMB (Novex, Invitrogen). A pre-stained molecular weight marker of 16.5Ð*210 kDa (BioRad) was used for the estimation of the size of the proteins.

Liquid Chromatography/Mass Spectroscopy (LC/MS)

A band of 65 kDa was identified by human serum in the immunoblot. Gel bands corresponding to the immunogenic bands were excised and sent in duplicate to the National Institutes of Health (NIH/NIAID) for identification by mass spectrometry (MS). Briefly, the samples were reduced in solution containing 50 mM HEPES (pH 8.0) 10% acetonitrile and 5 mM DTT for 40 min at 37°C. After cooling to room temperature, the samples were mixed at 15 mM with iodoacetamide. After 15 min of alkylation, 200 ng of trypsin was added and the samples were incubated at 37°C for 15 h in a final volume of 40μl. The solution was evaporated to near dryness under a vacuum at 50°C. Twenty-five microliters of 0.1% trifluoroacetic acid was added and the pH was adjusted to 2.5 with the addition of 10% trifluoroacetic acid. Samples with an estimated protein content of <2 μg were desalted and concentrated with C18 μ Zip Tips. Samples containing up to 10μg were desalted with C18 OMIX 10 solid phase extraction tips. The digests were eluted with 0.1% TFA, 50% acetonitrile and dried under vacuum. The peptides were dissolved in 12 μl 0.1% formic acid, 3% acetonitrile which was used as the injection solvent. Digested peptides were subjected to the LC/MS analysis using an Orbitrap Fusion mass spectrometer (ThermoFisher Scientific, West Palm Beach, FL) connected with EASY nLC 1,000 liquid chromatography (LC) system. Nano-LC was carried out with a 5 μL injection onto a PepMap 100 C18 3-μm trap column (2 cm, ID 75 μm) and a 2 μm PepMap RSLC C18 column (25 cm, ID 75 μm), both from ThermoFisher Scientific. The LC was operated at a 300 μL/min flow rate with a 100-min linear gradient from 100% solvent A (0.1% formic acid, and 99.9% water) to 40% solvent B (0.1% formic acid, 20%

water, and 79.9% acetonitrile) followed by a column wash. A standard data-dependent acquisition performed with a full MS spectrum was obtained by the Orbitrap for m/z 400–2,000 at the resolution of 120,000 with EASY-IC calibration. The precursor ions, with charges from two to eight, were selected, isolated (1.6 m/z window), fragmented by CID, then scanned by the Ion Trap. Survey scans were performed every 2 s and the dynamic exclusion was enabled for 30 s.

Acquisitions were searched against the NCBI-nr (05/2019) proteome and the cRAP.fasta database (theGPM.org) using PEAKS v10 (Bioinformatics Solutions Inc, Ontario, Canada) using a semi-tryptic search strategy with tolerances of 6 ppm for MS and 0.5 Da for MS/MS and carbamidomethylation of cysteine as a fixed modification and oxidation of methionine as a dynamic modification allowing for two missed cleavages. Peptides were filtered with a 0.5% FDR using a decoy database approach and a two spectral matches/peptide requirement.

Anopheles Immunogenic Peptide Selection and *Plasmodium* Antigens

Immunogenic peptides were designed from the most abundant identified proteins: apyrase (Protein Accession # ETN63669.1) and peroxidase (Protein Accession # ETN66035.1) (**Table 2**). Proteins were analyzed for the presence of signal peptide (signal P) sequence using the SignalP 5.0 server and for sequence homologies (at least 50% identity with *E*-value 1 × 10–5) to *Anopheles* and other major culicid disease vector species using online BLAST program. Protein sequence and structure analyses were then performed for the top *Anopheles*-specific proteins using the Protean 3D package of the DNASTAR software (DNASTAR Inc., Madison, WI, USA) (Londono-Renteria et al., 2020). The analysis of linear B-cell epitopes, antigenic regions, flexible regions (turns), hydrophobic regions, stability and/or charge density were conducted by importing the FASTA files from NCBI of sequences of interest into SVMTriP (Center for Plant Innovation, University of Nebraska, Lincoln, NE, USA). Highly antigenic, stable, flexible, charged and <50% hydrophobic regions that were specific to *Anopheles* mosquitoes (>50% homology) were selected using the software for 18–22 amino acid peptides (**Table 3**). The AnDar_PeroX1, AnDar_PeroX2, AnDar_Apy1, and the AnDar_Apy2 peptides of interest were sent for synthesis to GenScript (Piscataway, NJ, USA).

Two recombinant proteins representing the *Plasmodium* Merozoite Surface Protein from *P. falciparum* (Pf-MSP) (Montiel et al., 2020a) and *P. vivax* (Pv-MSP) (Fitzgerald, USA) were used to evaluate antibody responses against the parasite.

ELISA Testing

ELISA conditions were standardized as published elsewhere (Londono-Renteria et al., 2010) and the test was used to measure IgG antibodies against total SGA and individual peptides in human samples. Briefly, 96-well ELISA plates (UltraCruz® ELISA Plate, Santa Cruz Biotechnology, Dallas, TX) were coated with 100 μL/well of 0.5 μg/ml of *An. darlingi* SGA or 2 μg/ml of each peptide in 1X PBS and incubated overnight at 4°C. Plates were blocked for 1 h at room temperature with 2% milk in 1X PBST (blocking buffer) and incubated with 100 μL/well of a 1/100 serum dilution in blocking buffer at 37°C for 2 h. Plates were washed three times with wash solution (1 × PBS and 0.1% Tween) and incubated with 100 μL/well of horseradish peroxidase (HRP)-conjugated goat anti-human IgG (1:1,000), antibodies (Abcam, Cambridge, UK) at 37°C for 1.5 h. Colorimetric development was carried out using tetra-methyl-benzidine (Abcam) as a substrate and incubated for 2 min before the reaction was stopped using 2 N sulfuric acid. Absorbance was measured at 450 nm. Each sample was tested in duplicate. Three controls were included in each plate: (1) control blank: two wells without SGA to control for non-specific induction of color for any of the reagents used in the test; (2) negative control: two wells with SGA but without human serum to control for any non-specific color induction of the coating antigen; and (3) positive control to control for plate to plate variation and normalize OD values. To determine a cut off value of exposure to *Plasmodium* antigens and *An. darlingi*, we tested serum from 12 volunteers living in the US with no history of travel to South America. The OD cut off values to establish exposure were set at 0.167 for Pf-MSP1, 0.153 for Pv-MSP1 and 0.396 for *An. darlingi* SGA.

TABLE 2 | List of proteins identified in an ∼65 kDa protein band from the western-blot using a pool of serum from study participants.

Protein accessions	Description	Avg. mass
ETN63669.1	Apyrase (*An. darlingi*)	63,178
ETN66035.1	Oxidase/peroxidase (*An. darlingi*)	65,566
ACI30180.1	Putative salivary protein SG1B (*An. darlingi*)	51,295
ETN62038.1	ATP synthase beta subunit (*An. darlingi*)	53,768
ETN61268.1	Protein disulfide isomerase (*An. darlingi*)	54,542
ETN64733.1	Venom allergen 5 (*An. darlingi*)	29,387
ETN59462.1	ATP synthase alpha subunit mitochondrial (*An. darlingi*)	59,383
ACI30121.1	SG1-like salivary protein (*An. darlingi*)	44,890
ETN65121.1	Pyruvate kinase (*An. darlingi*)	57,551
ACI30100.1	30 kDa salivary antigen family protein (*An. darlingi*)	25,628
ETN58076.1	Deoxyribonuclease I (*An. darlingi*)	45,530
ETN64604.1	Malic enzyme (*An. darlingi*)	69,409
ETN63240.1	Protein disulfide isomerase (*An. darlingi*)	55,374
ETN62075.1	Apyrase (*An. darlingi*)	62,276
ETN61375.1	Catalase (*An. darlingi*)	62,481
ETN57775.1	Actin (*An. darlingi*)	31,545
ACI30046.1	Long form D7 salivary protein (*An. darlingi*)	37,105

TABLE 3 | *An. darlingi* peptide sequences from the apyrase and the peroxidase/oxidase proteins identified by mass spectrometry.

Peptide name	Peptide sequence	a.a. position
AnDar_PeroX1	RGQCDSTSPYRTYDGRCNNLQN	19–40
AnDar_PeroX2	GQCDSTSPYRTYDGRCNNLQNP	20–41
AnDar_Apy1	GGHSHSFLFSPDSDQPYNKQDT	249–270
AnDar_Apy2	HMNDLHARFDETSNKSSKCRSD	39–60

Data Analysis

After testing for normality, we concluded that the data did not meet the normality requirement. Consequently, we performed non-parametrical statistical tests. Specifically, we used the Mann-Whitney *U*-test to compare two independent groups (i.e., malaria positive vs. negative) and the Kruskal-Wallis test to compare more than two independent groups (i.e., negative, *P. vivax* malaria and *P. falciparum* malaria). Spearman Correlation Coefficients were calculated to measure the strength of association between IgG antibodies against salivary proteins and IgG antibodies against *Plasmodium* antigens as well as age. Odd ratios and Fisher's exact test were used to assess significance of risk calculation. OD values were categorized as low (less than the median OD) or high (equal or above the median OD) for each peptide: AnDar_PeroX1 (median OD = 0.579), AnDar_PeroX2 (median OD = 0.6612), AnDar_Apy1 (median OD = 0.4410) and the AnDar_Apy2 (median OD = 0.4286). All tests were considered significant with a $p\text{-}value < 0.05$.

RESULTS

Immunogenic Proteins in *An. darlingi* SGA

Western blot testing revealed four major immunogenic bands (∼250, ∼62, ∼28, and ∼8 kDa) (**Figure 1**). The most prominent band was a 65 kDa band that was excised and sent for sequencing. Seventeen proteins were identified by LC-MS (**Table 2**). The most abundant proteins found were a ∼63 kDa apyrase (Accession# ETN63669.1) and a 65 kDa oxidase/peroxidase (Accession# ETN66035.1). Two peptides were designed from each of these proteins (AnDar_Apy1, AnDar_Apy2, AnDar_PeroX1, and AnDar_PeroX2) to evaluate immune responses to these specific salivary proteins in people with active malaria infections. The specific sequence of each peptide is described in **Table 3**. Apyrases as well as salivary peroxidases are ubiquitous proteins. The *An. darlingi* apyrase described in the current study has a 63% identity with an apyrase of *Anopheles gambiae* (AGAP011971), and 49% with an apyrase from *Aedes aegypti* (AAEL006347) and an apyrase of *Cx. quinquefasciatus* (CPIJ011010). No significant similarity was found with *An. albimanus* apyrases. The *An. darlingi* salivary oxidase/peroxidase has a 87.8% identity with the *An. albimanus* peroxidase (AAD22196.1). The *An. darlingi* oxidase/peroxidase also presents a 53% similarity with *An. gambiae* (AGAP010735) while similarity with *Ae. aegypti* (AAEL000507) and *Cx. quinquefasciatus* (CPIJ017579) was 48%. However, the selected immunogenic peptides align with identities between 56 and 85% with these proteins (**Supplementary Table 1**).

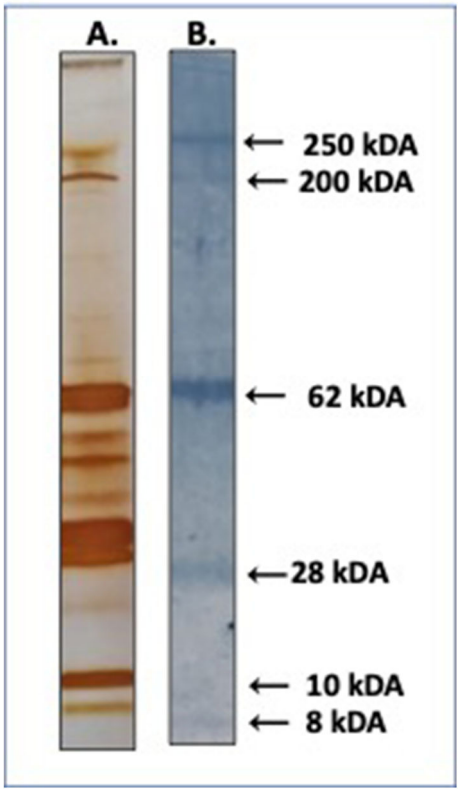

FIGURE 1 | Immunoblot of *An. darlingi* SGA. Pooled serum from uninfected individuals exposed to *An. darlingi* bites was used to identify immunogenic proteins. **(A)** Silver stain of whole SGA. **(B)** Immunoblot.

Antibody Responses Against Salivary Proteins

Serum from a total of 107 females and 72 males with ages between 2 and 83 years old (Age average = 25.1 years old) were included in this study. No significant differences were detected when comparing IgG antibody levels against any of the antigens from either Turbo or El Bagre samples with the exception of AnDarApy2 which was significantly higher in El Bagre (Mann-Whitney test $p = 0.0097$) (**Figure 2**). When comparing IgG antibody levels among groups by their infection status (malaria negative vs. malaria positive), we did not detect significant differences between the groups from either field site using the whole SGA as antigen (Mann-Whitney test $p > 0.05$) (**Figure 3**). However, when using the apyrase peptides, we found that antibodies against AnDar-Apy2 were significantly higher in malaria positive patients in both Turbo (Mann-Whitney test, $p = 0.0001$) and El Bagre (Mann-Whitney test, $p < 0.0001$), while AnDar-Apy1 was higher in malaria positive samples only in El Bagre (Mann-Whitney test, $p < 0.0001$). Interestingly, the peroxidase-derived peptides, only showed significant differences between infected and uninfected samples from El Bagre, where AnDar-PeroX1 was significantly higher in malaria infected people (Mann-Whitney test, $p = 0.0497$). When comparing the antibody levels regardless of the field site, both of the apyrase peptides and AnDarPeroX1 were significantly higher in malaria infected samples.

Antibody Responses Against *Plasmodium* and Mosquito Salivary Proteins

Spearman correlation analysis showed significant associations between three of the salivary proteins (AnDar_Apy1, AnDar_Apy2, and AnDar_PeroX2) and either PvMSP1 or PfMSP1 (Spearman rank correlation test, $p < 0.05$). When

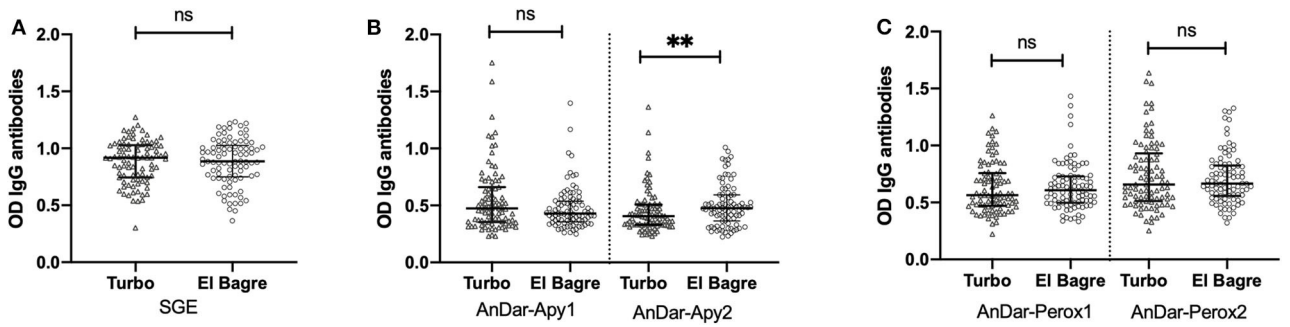

FIGURE 2 | Comparison of IgG antibody levels against *An. darlingi* SGA **(A)** and peptides from Apyrase **(B)** and Peroxidase **(C)** between the study sites (Turbo and El Bagre). ns denotes not significant, $p < 0.05$ (* = 0.01 to 0.05, ** = 0.001 to 0.01, and *** = 0.0001 to 0.001).

divided by malaria infection status, a significant positive association between IgG antibodies against AnDarApy2 and AnDarPeroX2 was maintained with both PvMSP1 and PfMSP1 in both malaria infected and uninfected individuals (**Table 4**). No association with either *Plasmodium* antigen was detected when comparing IgG antibodies against AnDarPeroX1. When comparing whether there were significant differences in the IgG antibody levels against any salivary antigens and the species of *Plasmodium* causing infection, we found that antibodies against both apyrases peptides were significantly higher in people with *P. vivax* infection (Mann-Whitney test, $p < 0.0001$) and *P. falciparum* [Mann-Whitney test, $p = 0.0011$ (AnDar_Apy1), $p = 0.0005$ (AnDar_Apy2)] when compared against IgG antibodies in uninfected participants. In the case of IgG antibodies against the peroxidase peptides, we found only significant higher antibodies against AnDar_Perox1 in *P. vivax* infection (Mann-Whitney test, $p = 0.0114$ (*P. vivax*), $p = 0.1285$ (*P. falciparum*), while antibodies against AnDar_Perox2 were significantly higher only when comparing *P. falciparum* infected against uninfected (Mann-Whitney test, $p = 0.6464$ (*P. vivax*), $p = 0.0131$ (*P. falciparum*). No differences were found with SGE antibodies (Mann-Whitney test, $p > 0.05$) (**Figure 4**).

Malaria Risk and IgG Antibodies Against *An. darlingi* Salivary Proteins

Odd ratios were calculated to determine the risk of malaria infection based on the levels of IgG antibodies against whole SGA and the individual salivary peptides. Our analysis indicated that samples with high levels of antibodies against apyrase peptides had 3.1 (AnDar_Apy1) and 5.1 (AnDar_Apy2) times higher probability of being positive for malaria than samples with lower antibody levels (Fisher's exact test, $p < 0.0001$). Significant odd ratios were not observed when comparing IgG levels of SGA, AnDar_Perox1 or AnDarPerox2 (**Table 5**).

DISCUSSION

An. darlingi is one of the most important malaria vectors in the Americas, and is associated with transmission of both *P. falciparum* and *P. vivax* (de Arruda et al., 1986; Flores-Mendoza et al., 2004). Some data suggest that infected *An. darlingi* tend to bite more outdoors and in the early evening, which reduces the effectiveness of bed nets (Moreno et al., 2015; Newell et al., 2018). The (EIR) is the current gold standard to estimate malaria transmission intensity. However, this technique is labor intensive and requires sensitive methods to accurately detect *Plasmodium* infection in field-captured mosquitoes. In addition, it is impossible to track individual human exposure to infective bites and estimation of risk that can be later used to determine local transmission dynamics. Tools capable of monitoring human-vector contact are needed to more accurately estimate disease risk. Here, we evaluated the IgG responses against *An. darlingi* salivary proteins and showed through ELISA that peptides against a salivary apyrase and peroxidase are suitable antigens to estimate the risk of suffering a malaria infection.

In an effort to identify candidate salivary peptides from *An. darlingi* salivary proteins, an immunogenic ∼65 kDa protein band was identified by antibodies in serum collected from study participants. LC-MS revealed 17 salivary proteins, with apyrase and a peroxidase as the most predominant proteins. Most of the identified proteins have previously been associated with blood feeding. Salivary apyrases hydrolyze ATP and ADP inhibiting platelet aggregation. They are associated with host-seeking behavior and the ability of mosquitoes to find blood vessels (Calvo et al., 2006). Infection status with human pathogens influences mosquito behavior and changes the content of salivary gland and salivary secretions (Chisenhall et al., 2014a,b). A previous study suggested that apyrase activity decreases as sporozoite load increases, rendering the infected mosquitoes more likely to probe and re-feed after an infectious first blood meal (Thievent et al., 2019). Each probing event increases the likelihood of injecting sporozoites into the skin, which increases the chance of infection. Salivary proteins are also injected during each probing event (Ribeiro, 2000; Chisenhall et al., 2014a), which may explain the high antibody responses against salivary proteins in people with active malaria infection. Interestingly, immunization with mosquito saliva leads to the development of anti-apyrase antibodies, which can block its enzymatic activity. However, a decrease in feeding or probing time was not observed in immunized mice even in the presence of higher titers of anti-apyrase antibodies (Mathews et al., 1996). Previous studies

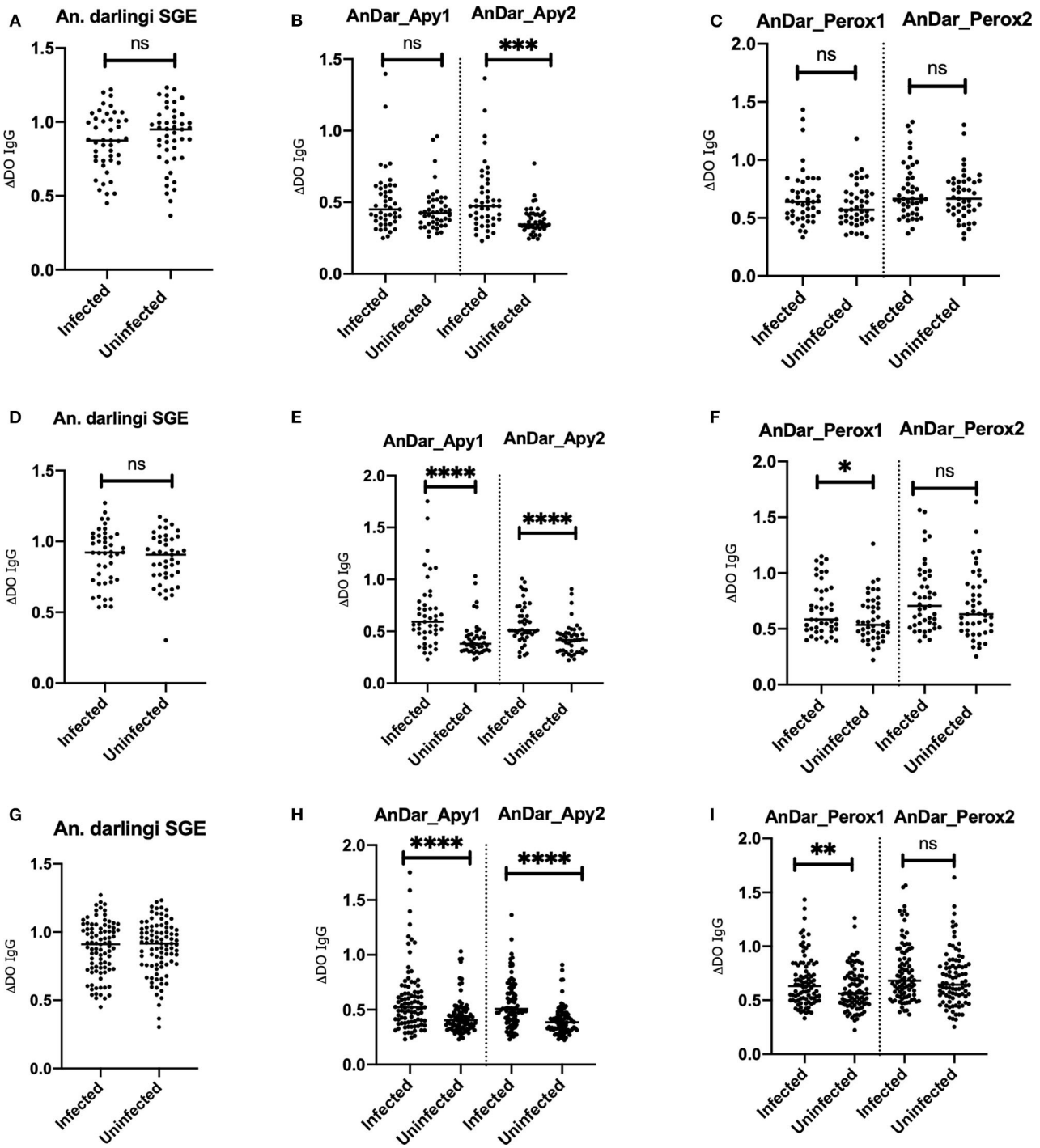

FIGURE 3 | Comparison of IgG antibody levels against *An. darlingi* salivary antigens in samples with malaria infections and uninfected samples from Turbo **(A–C)**, El Bagre **(D–F)** and both sites combined **(G–I)**. ns denotes not significant, $p < 0.05$ (* = 0.01 to 0.05, ** = 0.001 to 0.01, and *** = 0.0001 to 0.001).

have shown changes in salivary gland physiology of infected mosquitoes (Cotama et al., 2013; Pinheiro-Silva et al., 2015). It is unclear if infection with either *P. vivax* or *P. falciparum* changes the expression profile of apyrase or peroxidase proteins in the salivary gland of *An. darlingi* mosquitoes. This information would be helpful to determine a potential function of these proteins in malaria transmission by *An. darlingi* mosquitoes.

Besides the apyrase and the salivary peroxidase described above, other important salivary proteins that had been previously reported were also detected in this study. First, two members of

TABLE 4 | Correlation analysis between IgG antibodies against *An. darlingi* salivary antigens and IgG antibodies against *P. falciparum*, *P. vivax* showing samples grouped by infection status.

All samples ($n = 179$)	**PvMSP1 (*p*-value)**	**PfMSP1 (*p*-value)**
AnDar_Apy1	0.16 (0.0305)*	0.16 (0.0290)*
AnDar_Apy2	0.39 (0.0001)†	0.35 (0.0001)†
AnDar_PeroX1	0.15 (0.0503)*	0.12 (0.1208)
AnDar_PeroX2	0.37 (0.0001)†	0.26 (0.0004)†
SGE	−0.06 (0.4245)	−0.03 (0.6104)
Malaria infected ($n = 89$)	**PvMSP1 (*p*-value)**	**PfMSP1 (*p*-value)**
AnDar_Apy1	0.06 (0.5544)	0.15 (0.1557)
AnDar_Apy2	0.29 (0.0045)*	0.32 (0.0018)*
AnDar_PeroX1	0.13 (0.1971)	0.19 (0.0741)
AnDar_PeroX2	0.35 (0.0008)†	0.26 (0.0106)*
SGE	−0.04 (0.6879)	0.00 (0.9975)
Malaria uninfected ($n = 90$)	**PvMSP1 (*p*-value)**	**PfMSP1 (*p*-value)**
AnDar_Apy1	0.15 (0.1689)	0.11 (0.2770)
AnDar_Apy2	0.41 (0.0001)†	0.33 (0.0013)†
AnDar_PeroX1	0.09 (0.3544)	−0.00 (0.9881)
AnDar_PeroX2	0.39 (0.0001)†	0.24 (0.0184)*
SGE	−0.06 (0.5791)	−0.06 (0.5444)

*$p < 0.05$; †$p < 0.001$.

the SG1 family were detected: the putative salivary protein SG-1B along with a SG1-like salivary protein. The SG-1B appears to be uniquely expressed in the female salivary glands, while the SG1-like can also be expressed in males (Arca et al., 2005). Recently, a member of the SG1 family, TRIO protein, was evaluated as a potential vaccine candidate against *Plasmodium* infection since immunization against these proteins induced partial protection against *Plasmodium berghei* infection. Protection was further improved when animals were co-immunized with saliva and parasite proteins (Dragovic et al., 2018). Second, a long form D7 protein was also detected. Our previous studies demonstrated the immunogenicity of this family of proteins in *Ae. aegypti* saliva (Londono-Renteria et al., 2018). The D7 protein family has been identified as a member of an odorant binding protein (OBP) superfamily known to bind biogenic amines such as histamine, playing an important role as mediators of inflammation and vascular permeability, and facilitating blood feeding (Calvo et al., 2006). Finally, a 30 kDa salivary antigen family protein was identified. These proteins are exclusively found in the salivary glands of adult female mosquitoes and previous work suggested that they may inhibit platelet aggregation (Yoshida and Watanabe, 2006; Calvo et al., 2007b). A venom allergen 5 was also identified, and this family of proteins is found ubiquitously in animals and plants. Their specific function in *Anopheles* mosquitoes is still unknown, but it is thought to function either in the suppression of the host immune system, or as an anticoagulant in a wide range of hematophagous arthropods (Ribeiro and Francischetti, 2003; Calvo et al., 2007a).

It is important to note that whole salivary gland proteins contained in the SGA have been successfully used as antigen to detect IgG antibodies in vertebrate serum (Waitayakul et al., 2006; Badu et al., 2012). However, salivary gland dissection is a tedious process requiring skilled personnel (Coleman et al., 2007) and a continuous source of mosquito salivary glands. Not all mosquitoes are easily colonizable, and although using salivary glands from field mosquitoes can offer a better approximation of the antigens that people are actually exposed to (Andrade et al., 2009), it can be challenging to collect them in sufficient numbers and maintain a proper cold chain and protein stabilization before they are processed for antigen preparation (Fontaine et al., 2011a). Thus, the use of recombinant proteins or peptides is advantageous, particularly when consistency and reproducibility are desired. In that regard, we selected four peptides from the two main immunogenic proteins found after sequencing of the ∼65 kDa band, an apyrase and a salivary peroxidase. The ELISA results revealed that when using the AnDar_Apy1, AnDar_Apy2, and AnDar_PeroX1 peptides as antigens, the IgG antibody levels were significantly higher in samples with active malaria infection as compared to uninfected samples. These results are consistent with our recent study where we observed that malaria-infected samples had significantly higher antibody levels against *An. albimanus* salivary peptides (Londono-Renteria et al., 2020).

Previous studies associated this increase in antibodies with a potentially higher exposure to mosquito bites (Fontaine et al., 2011b). Moreover, this increase in IgG antibodies may also be the result of saliva-dependent activation of immune cells leading to the production of cytokines such as IL4 and IL10 (Vogt et al., 2018). IL4 is involved in the activation of B cells and their differentiation to plasma cells (Granato et al., 2014) and recent studies suggest that IL10 promotes IgG4 antibodies (Jeannin et al., 1998), which is the main antibody subtype that recognizes arthropod salivary antigens (Brummer-Korvenkontio et al., 1994; Cardenas et al., 2019). Further studies are needed to determine the mechanisms involved in the differential antibody profiles between people residing under the same conditions but with different malaria infection status.

In contrast to a previous study in Brazil (Andrade et al., 2009), we did not find significant differences between malaria-infected and uninfected samples when using SGA. One of our previous studies showed the possibility of discrete differences in the responses against *Anopheles* SGA from two different mosquito colony strains, with those differences potentially associated with differences in geographical origins as well as the time of colonization (Londono-Renteria et al., 2020; Montiel et al., 2020a). Another study detected important differences in salivary gland content from wild and colony maintained arthropods from the same species (Maldonado-Ruiz et al., 2019). Consequently, it is possible that the difference between this current study and the one performed in Brazil may reside in the source of the SGA and its components. Specifically, in this study, we used SGA from a recently colonized strain of *An. darlingi* in Iquitos, Peru, while the previous study used SGA from field-caught mosquitoes in Brazil (Andrade et al., 2009).

Regardless, analysis of the immunogenic proteins among mosquito strains may reveal shared immunogenic proteins that represent suitable candidates to measure risk of disease irrespective of the geographical area or the strains. Thus, it was

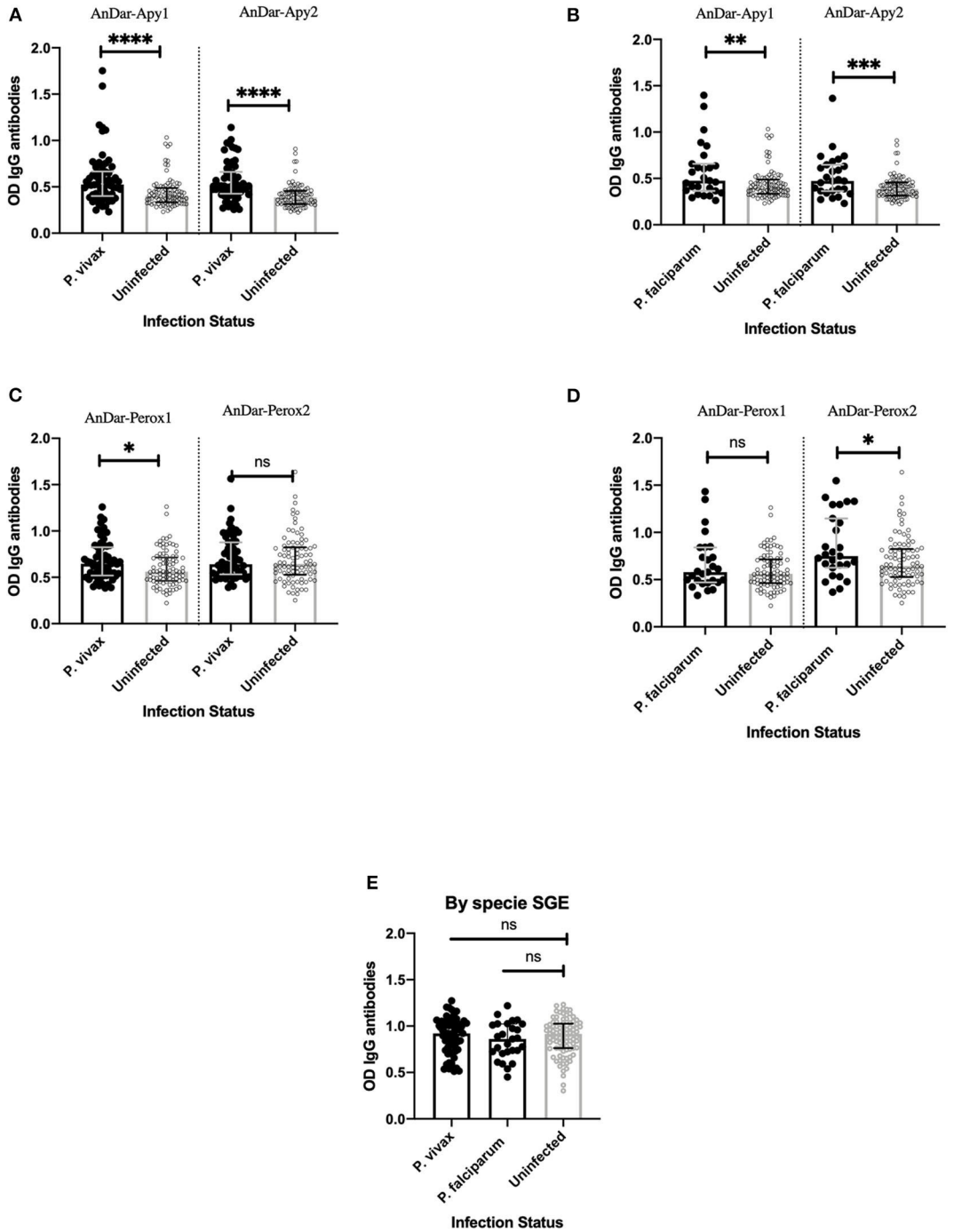

FIGURE 4 | Comparison of IgG antibody levels against *An. darlingi* apyrase peptides **(A,B)**, peroxidase peptides **(C,D)**, and SGA **(E)**, in samples from individuals infected with either *P. falciparum* or *P. vivax*. ns denotes not significant, $p < 0.05$ (* = 0.01 to 0.05, ** = 0.001 to 0.01, and *** = 0.0001 to 0.001).

important to identify the evolutionarily conserved regions within immunogenic proteins as we seek to develop widely applicable biomarkers of malaria risk. Only AnDar_Apy2 was significantly higher in El Bagre, the area with historically higher abundance of *An. darlingi* relative to Turbo (Gutierrez et al., 2009, 2010; Rosero et al., 2013); all other peptides did not show differences between the two sites. The lack of difference in antibody levels against most of the peptides between the two study sites may be explained by the 56 and 80% identity with other major salivary proteins representing a source of cross-reactivity. However, since we did not include concurrent mosquito collection data, we cannot confirm the concurrent *An. darlingi* population density

TABLE 5 | Odds ratio calculations to measure risk of malaria infection based on level of IgG antibodies against *An. darlingi* salivary proteins.

Salivary antigen	Odds ratio	95% Confidence interval	*P*-value
AnDar_Apy1	3.1	1.63197–6.025945	**0.0001**
AnDar_Apy2	5.1	2.617258–10.25419	**0.0001**
AnDar_PeroX1	1.8	0.9509861–3.372674	0.0526
AnDar_PeroX2	1.4	0.7292346–2.560444	0.2967
SGE	0.9	0.5114593–1.788728	0.8815

Bold values indicates p > 0.05.

at the time of this study. Thus, the results presented here are more sensitive at correlating antibodies against salivary proteins with presence of malaria infection rather than *An. darlingi* bite intensity.

Previous studies suggested that there is a significant association between the level of IgG antibodies against the most prominent *Plasmodium* antigens and the development of human immunity against malaria symptoms (Doolan et al., 2009; Rodriguez-Barraquer et al., 2018). Among these antigens, MSP-1 is considered as one of the more important in the development of immunity against malaria and has been investigated as a potential vaccine candidate. Immunity against malaria is thought to be acquired through chronic and sustained exposure to *Plasmodium* antigens (Rodriguez-Barraquer et al., 2018). However, recent evidence suggests that immune responses against salivary proteins may also contribute to the development of immunity against disease (Manning et al., 2018). Our current study revealed that the level of IgG antibodies against AnDar_Apy 2 and the AnDar_PeroX2 were significantly associated with IgG levels against both PvMSP1 and PfMSP1 in all study groups, suggesting a positive association between intensity of exposure to malaria antigens and both peroxidase and apyrase salivary proteins. Furthermore, when measuring the risk of malaria infection through odd ratio calculations, a significant increase in risk was only observed in antibodies against the apyrase peptides. Previous study showed an association between the level of antibodies against PfMSP1 and the only currently validated salivary biomarker from the *An. gambiae* salivary peptide, gSG6-P1 (Badu et al., 2012; Ya-Umphan et al., 2018). Our results suggest that AnDarApy1 and AnDarApy2 may be more suitable biomarkers to estimate malaria risk in areas where *An. darlingi* mosquitoes are endemic. Also interesting is that the correlation between *Plasmodium* antigens and the apyrase peptides salivary was also significant in the uninfected population. It is important to remember that infected individuals present significantly higher IgG antibodies. People in endemic areas may encounter a significant number of bites containing infective sporozoites throughout their lives. Furthermore, in endemic areas for *P. vivax*, as the one where this study was carried out, is very difficult to differentiate a recent infection from a recrudescence, and people may suffer several malaria infections in a year. Since this study did not included follow up of patients, we cannot pinpoint the time of the most recent infection. However, our study showed a significant higher antibody levels against both apyrases peptides and the AnDar_Perox1 in *P. vivax* infected populations suggesting the relevance of these peptides to measure risk of infection with the most prevalent species circulating in this area. Further studies are urgently needed to determine the persistence of antibodies against the salivary proteins and correlate with previous/recent malaria episodes.

Although further studies including a greater number of serum samples from different geographical areas are needed to validate these peptides as biomarkers of both malaria risk and human-vector contact, the current study represents an important advance in evaluating immune responses against mosquito salivary peptides in Latin America.

CONCLUSION

Peptides derived from the *An. darlingi* salivary apyrase and peroxidases are suitable candidate markers for measuring human IgG antibody responses that may be associated with the risk of malaria infections.

DATA AVAILABILITY STATEMENT

All datasets generated for this study in the sequencing data are included in the article and the **Supplementary Material**. Other raw data will be available upon request sent to blondono@ksu.edu.

ETHICS STATEMENT

The studies involving human participants were reviewed and approved by Kansas State University and University of Antioquia. Written informed consent to participate in this study was provided by the participants' legal guardian/next of kin.

AUTHOR CONTRIBUTIONS

BL-R, AL, HV, GV, EC, MF, and MC: study design and data analysis, writing, and reviewing. JM and AT-C: sample collection. KE-V, LR, and MB: mosquito rearing and salivary gland dissection. BL-R and JM: ELISA testing. All authors contributed to the article and approved the submitted version.

FUNDING

This work was supported by the USDA National Institute of Food and Agriculture, hatch multistate project 1021430 and the USAID-CDC - 200-2018-M-00025.

ACKNOWLEDGMENTS

This work was possible thanks to the support provided by the Kansas State University Department of Entomology and the U.S. Naval Medical Research Unit No. 6 (NAMRU-6). Special thanks to the NAMRU-6 Iquitos insectary staff for assisting

in *An. darlingi* rearing. We are grateful to the Ministerio de Agricultura y Riego de Peru, Direccion General Forestal y de Fauna Silvestre for permission to conduct research studies on laboratory reared *An. darlingi* under the auspices of Resolucion Directoral No. 132-2019-MINAGRI-SERFOR-DGGSPFFS. The authors also want to thank the residents of Turbo and El Bagre for participating in our study.

SUPPLEMENTARY MATERIAL

The Supplementary Material for this article can be found online at: https://www.frontiersin.org/articles/10.3389/fcimb.2020.00455/full#supplementary-material

Supplementary Table 1 | Immunogenic peptides alignment between *An. darlingi* and other vectors of human disease.

REFERENCES

Andrade, B. B., Rocha, B. C., Reis-Filho, A., Camargo, L. M., Tadei, W. P., Moreira, L. A., et al. (2009). Anti-*Anopheles darlingi* saliva antibodies as marker of *Plasmodium vivax* infection and clinical immunity in the Brazilian amazon. *Malar. J.* 8:121. doi: 10.1186/1475-2875-8-121

Arca, B., Lombardo, F., Struchiner, C. J., and Ribeiro, J. M. (2017). Anopheline salivary protein genes and gene families: an evolutionary overview after the whole genome sequence of sixteen *Anopheles* species. *BMC Genomics* 18:153. doi: 10.1186/s12864-017-3579-8

Arca, B., Lombardo, F., Valenzuela, J. G., Francischetti, I. M., Marinotti, O., Coluzzi, M., et al. (2005). An updated catalogue of salivary gland transcripts in the adult female mosquito, *Anopheles gambiae*. *J. Exp. Biol.* 208(Pt 20), 3971–3986. doi: 10.1242/jeb.01849

Arevalo-Herrera, M., Quinones, M. L., Guerra, C., Cespedes, N., Giron, S., Ahumada, M., et al. (2012). Malaria in selected non-amazonian countries of Latin America. *Acta Trop.* 121, 303–314. doi: 10.1016/j.actatropica.2011.06.008

Badu, K., Siangla, J., Larbi, J., Lawson, B. W., Afrane, Y., Ong'echa, J., et al. (2012). Variation in exposure to *Anopheles gambiae* salivary gland peptide (gSG6-P1) across different malaria transmission settings in the western Kenya highlands. *Malar. J.* 11:318. doi: 10.1186/1475-2875-11-318

Brummer-Korvenkontio, H., Lappalainen, P., Reunala, T., and Palosuo, T. (1994). Detection of mosquito saliva-specific IgE and IgG4 antibodies by immunoblotting. *J. Allergy Clin. Immunol.* 93, 551–555. doi: 10.1016/S0091-6749(94)70066-4

Calvo, E., Dao, A., Pham, V. M., and Ribeiro, J. M. (2007a). An insight into the sialome of *Anopheles funestus* reveals an emerging pattern in anopheline salivary protein families. *Insect Biochem. Mol. Biol.* 37, 164–175. doi: 10.1016/j.ibmb.2006.11.005

Calvo, E., Mans, B. J., Andersen, J. F., and Ribeiro, J. M. (2006). Function and evolution of a mosquito salivary protein family. *J. Biol. Chem.* 281, 1935–1942. doi: 10.1074/jbc.M510359200

Calvo, E., Tokumasu, F., Marinotti, O., Villeval, J. L., Ribeiro, J. M., and Francischetti, I. M. (2007b). Aegyptin, a novel mosquito salivary gland protein, specifically binds to collagen and prevents its interaction with platelet glycoprotein VI, integrin alpha2beta1, and von willebrand factor. *J. Biol. Chem.* 282, 26928–26938. doi: 10.1074/jbc.M705669200

Cardenas, J. C., Drame, P. M., Luque-Burgos, K. A., Berrio, J. D., Entrena-Mutis, E., Gonzalez, M. U., et al. (2019). IgG1 and IgG4 antibodies against *Aedes aegypti* salivary proteins and risk for dengue infections. *PLoS ONE* 14:e0208455. doi: 10.1371/journal.pone.0208455

Cassab, A., Morales, V., and Mattar, S. (2011). Climatic factors and cases of dengue in Monteria, Colombia: 2003–2008. *Rev. Salud Publica* 13, 115–128. doi: 10.1590/S0124-00642011000100010

Chaparro-Narvaez, P. E., Lopez-Perez, M., Rengifo, L. M., Padilla, J., Herrera, S., and Arevalo-Herrera, M. (2016). Clinical and epidemiological aspects of complicated malaria in Colombia, 2007–2013. *Malar. J.* 15:269. doi: 10.1186/s12936-016-1323-5

Chisenhall, D. M., Christofferson, R. C., McCracken, M. K., Johnson, A. M., Londono-Renteria, B., and Mores, C. N. (2014a). Infection with dengue-2 virus alters proteins in naturally expectorated saliva of *Aedes aegypti* mosquitoes. *Parasit. Vectors* 7:252. doi: 10.1186/1756-3305-7-252

Chisenhall, D. M., Londono, B. L., Christofferson, R. C., McCracken, M. K., and Mores, C. N. (2014b). Effect of dengue-2 virus infection on protein expression in the salivary glands of *Aedes aegypti* mosquitoes. *Am. J. Trop. Med. Hyg.* 90, 431–437. doi: 10.4269/ajtmh.13-0412

Coleman, J., Juhn, J., and James, A. A. (2007). Dissection of midgut and salivary glands from *Ae. aegypti* mosquitoes. *J. Vis. Exp.* 5:228. doi: 10.3791/228

Cotama, S., Dekumyoy, P., Samung, Y., and Lek-Uthai, U. (2013). Salivary glands proteins expression of *Anopheles dirus* a fed on *Plasmodium vivax*- and *Plasmodium falciparum*-infected human blood. *J. Parasitol. Res.* 2013:535267. doi: 10.1155/2013/535267

de Arruda, M., Carvalho, M. B., Nussenzweig, R. S., Maracic, M., Ferreira, A. W., and Cochrane, A. H. (1986). Potential vectors of malaria and their different susceptibility to *Plasmodium falciparum* and *Plasmodium vivax* in northern Brazil identified by immunoassay. *Am. J. Trop. Med. Hyg.* 35, 873–881. doi: 10.4269/ajtmh.1986.35.873

Doolan, D. L., Dobano, C., and Baird, J. K. (2009). Acquired immunity to malaria. *Clin. Microbiol. Rev.* 22, 13–36. doi: 10.1128/CMR.00025-08

Dragovic, S. M., Agunbiade, T. A., Freudzon, M., Yang, J., Hastings, A. K., Schleicher, T. R., et al. (2018). Immunization with AgTRIO, a protein in *Anopheles* saliva, contributes to protection against *Plasmodium* infection in mice. *Cell Host Microbe* 23, 523–535.e525. doi: 10.1016/j.chom.2018.03.008

Flores-Mendoza, C., Fernandez, R., Escobedo-Vargas, K. S., Vela-Perez, Q., and Schoeler, G. B. (2004). Natural *Plasmodium* infections in *Anopheles darlingi* and *Anopheles benarrochi* (Diptera: culicidae) from eastern Peru. *J. Med. Entomol.* 41, 489–494. doi: 10.1603/0022-2585-41.3.489

Fontaine, A., Pascual, A., Diouf, I., Bakkali, N., Bourdon, S., Fusai, T., et al. (2011a). Mosquito salivary gland protein preservation in the field for immunological and biochemical analysis. *Parasit. Vectors* 4:33. doi: 10.1186/1756-3305-4-33

Fontaine, A., Pascual, A., Orlandi-Pradines, E., Diouf, I., Remoue, F., Pages, F., et al. (2011b). Relationship between exposure to vector bites and antibody responses to mosquito salivary gland extracts. *PLoS ONE* 6:e29107. doi: 10.1371/journal.pone.0029107

Geleta, G., and Ketema, T. (2016). Severe malaria associated with *Plasmodium falciparum* and *P. vivax* among children in pawe hospital, Northwest Ethiopia. *Malar. Res. Treat.* 2016:1240962. doi: 10.1155/2016/1240962

Granato, A., Hayashi, E. A., Baptista, B. J., Bellio, M., and Nobrega, A. (2014). IL-4 regulates bim expression and promotes B cell maturation in synergy with BAFF conferring resistance to cell death at negative selection checkpoints. *J. Immunol.* 192, 5761–5775. doi: 10.4049/jimmunol.1300749

Gutierrez, L. A., Gomez, G. F., Gonzalez, J. J., Castro, M. I., Luckhart, S., Conn, J. E., et al. (2010). Microgeographic genetic variation of the malaria vector *Anopheles darlingi* root (Diptera: culicidae) from Cordoba and Antioquia, Colombia. *Am. J. Trop. Med. Hyg.* 83, 38–47. doi: 10.4269/ajtmh.2010.09-0381

Gutierrez, L. A., Gonzalez, J. J., Gomez, G. F., Castro, M. I., Rosero, D. A., Luckhart, S., et al. (2009). Species composition and natural infectivity of anthropophilic *Anopheles* (Diptera: culicidae) in the states of Cordoba and Antioquia, Northwestern Colombia. *Mem. Inst. Oswaldo Cruz* 104, 1117–1124. doi: 10.1590/S.0074-02762009000800008

Instituto Nacional de Salud (2019). *Periodo Epidemiológico XIII*. Bogota: Instituto Nacional de Salud.

Jeannin, P., Lecoanet, S., Delneste, Y., Gauchat, J. F., and Bonnefoy, J. Y. (1998). IgE versus IgG4 production can be differentially regulated by IL-10. *J. Immunol.* 160, 3555–3561.

Jitthai, N. (2013). Migration and malaria. *Southeast Asian J. Trop. Med. Public Health* 44(Suppl 1), 166–200.

Londono-Renteria, B., Cardenas, J. C., Cardenas, L. D., Christofferson, R. C., Chisenhall, D. M., Wesson, D. M., et al. (2013). Use of anti-*Aedes aegypti* salivary extract antibody concentration to correlate risk of vector exposure and dengue transmission risk in Colombia. *PLoS ONE* 8:e81211. doi: 10.1371/journal.pone.0081211

Londoño-Rentería, B., Cárdenas, J. C., Giovanni, J. E., Cárdenas, L., Villamizar, P., Rolón, J., et al. (2015a). *Aedes aegypti* anti-salivary gland antibody concentration and dengue virus exposure history in healthy individuals living in an endemic area in Colombia. *Biomedica* 35, 572–581. doi: 10.7705/biomedica.v35i4.2530

Londono-Renteria, B., Drame, P. M., Montiel, J., Vasquez, A. M., Tobon-Castano, A., Taylor, M., et al. (2020). Identification and pilot evaluation of salivary peptides from *Anopheles albimanus* as biomarkers for bite exposure and malaria infection in Colombia. *Int. J. Mol. Sci.* 21:691. doi: 10.3390/ijms21030691

Londono-Renteria, B., Drame, P. M., Weitzel, T., Rosas, R., Gripping, C., Cardenas, J. C., et al. (2015b). *An. gambiae* gSG6-P1 evaluation as a proxy for human-vector contact in the Americas: a pilot study. *Parasit. Vectors* 8:533. doi: 10.1186/s13071-015-1160-3

Londono-Renteria, B., Patel, J. C., Vaughn, M., Funkhauser, S., Ponnusamy, L., Grippin, C., et al. (2015c). Long-lasting permethrin-impregnated clothing protects against mosquito bites in outdoor workers. *Am. J. Trop. Med. Hyg.* 93, 869–874. doi: 10.4269/ajtmh.15-0130

Londono-Renteria, B. L., Eisele, T. P., Keating, J., James, M. A., and Wesson, D. M. (2010). Antibody response against *Anopheles albimanus* (Diptera: culicidae) salivary protein as a measure of mosquito bite exposure in Haiti. *J. Med. Entomol.* 47, 1156–1163. doi: 10.1603/ME09240

Londono-Renteria, B. L., Shakeri, H., Rozo-Lopez, P., Conway, M. J., Duggan, N., Jaberi-Douraki, M., et al. (2018). Serosurvey of human antibodies recognizing *Aedes aegypti* D7 salivary proteins in Colombia. *Front. Public Health* 6:111. doi: 10.3389/fpubh.2018.00111

Maldonado-Ruiz, L. P., Montenegro-Cadena, L., Blattner, B., Menghwar, S., Zurek, L., and Londono-Renteria, B. (2019). Differential tick salivary protein profiles and human immune responses to lone star ticks (*Amblyomma americanum*) from the wild vs. a laboratory colony. *Front. Immunol.* 10:1996. doi: 10.3389/fimmu.2019.01996

Manning, J. E., Morens, D. M., Kamhawi, S., Valenzuela, J. G., and Memoli, M. (2018). Mosquito saliva: the hope for a universal arbovirus vaccine? *J. Infect. Dis.* 218, 7–15. doi: 10.1093/infdis/jiy179

Martens, P., and Hall, L. (2000). Malaria on the move: human population movement and malaria transmission. *Emerg. Infect. Dis.* 6, 103–109. doi: 10.3201/eid0602.000202

Mathews, G. V., Sidjanski, S., and Vanderberg, J. P. (1996). Inhibition of mosquito salivary gland apyrase activity by antibodies produced in mice immunized by bites of *Anopheles stephensi* mosquitoes. *Am. J. Trop. Med. Hyg.* 55, 417–423. doi: 10.4269/ajtmh.1996.55.417

Mirabello, L., and Conn, J. E. (2006). Molecular population genetics of the malaria vector *Anopheles darlingi* in Central and South America. *Heredity* 96, 311–321. doi: 10.1038/sj.hdy.6800805

Montiel, J., Carbal, L. F., Tobon-Castano, A., Vasquez, G. M., Fisher, M. L., and Londono-Renteria, B. (2020a). IgG antibody response against *Anopheles* salivary gland proteins in asymptomatic *Plasmodium* infections in Narino, Colombia. *Malar. J.* 19:42. doi: 10.1186/s12936-020-3128-9

Montiel, J., Zuluaga, L. M., Aguirre, D. C., Segura, C., Tobon-Castano, A., and Vasquez, A. M. (2020b). Microscopic and submicroscopic *Plasmodium* infections in indigenous and non-indigenous communities in Colombia. *Malar. J.* 19:157. doi: 10.1186/s12936-020-03226-4

Montoya-Lerma, J., Solarte, Y. A., Giraldo-Calderon, G. I., Quinones, M. L., Ruiz-Lopez, F., Wilkerson, R. C., et al. (2011). Malaria vector species in Colombia: a review. *Mem. Inst. Oswaldo Cruz* 106(Suppl. 1), 223–238. doi: 10.1590/S0074-02762011000900028

Moreno, M., Saavedra, M. P., Bickersmith, S. A., Lainhart, W., Tong, C., Alava, F., et al. (2015). Implications for changes in *Anopheles darlingi* biting behaviour in three communities in the peri-iquitos region of Amazonian Peru. *Malar. J.* 14:290. doi: 10.1186/s12936-015-0804-2

Moutinho, P. R., Gil, L. H., Cruz, R. B., and Ribolla, P. E. (2011). Population dynamics, structure and behavior of *Anopheles darlingi* in a rural settlement in the Amazon rainforest of Acre, Brazil. *Malar. J.* 10:174. doi: 10.1186/1475-2875-10-174

Newell, I., Wiskin, C., Anthoney, J., Meza, G., and de Wildt, G. (2018). Preventing malaria in the Peruvian Amazon: a qualitative study in Iquitos, Peru. *Malar. J.* 17:31. doi: 10.1186/s12936-018-2177-9

Pinheiro-Silva, R., Borges, L., Coelho, L. P., Cabezas-Cruz, A., Valdes, J. J., do Rosario, V., et al. (2015). Gene expression changes in the salivary glands of *Anopheles coluzzii* elicited by *Plasmodium berghei* infection. *Parasit. Vectors* 8:485. doi: 10.1186/s13071-015-1079-8

Poinsignon, A., Cornelie, S., Ba, F., Boulanger, D., Sow, C., Rossignol, M., et al. (2009). Human IgG response to a salivary peptide, gSG6-P1, as a new immuno-epidemiological tool for evaluating low-level exposure to *Anopheles* bites. *Malar. J.* 8:198. doi: 10.1186/1475-2875-8-198

Prado, C. C., Alvarado-Cabrera, L. A., Camargo-Ayala, P. A., Garzon-Ospina, D., Camargo, M., Soto-De Leon, S. C., et al. (2019). Behavior and abundance of *Anopheles darlingi* in communities living in the Colombian Amazon riverside. *PLoS ONE* 14:e0213335. doi: 10.1371/journal.pone.0213335

Reinbold-Wasson, D. D., Sardelis, M. R., Jones, J. W., Watts, D. M., Fernandez, R., Carbajal, F., et al. (2012). Determinants of *Anopheles* seasonal distribution patterns across a forest to periurban gradient near iquitos, Peru. *Am. J. Trop. Med. Hyg.* 86, 459–463. doi: 10.4269/ajtmh.2012.11-0547

Ribeiro, J. M. (2000). Blood-feeding in mosquitoes: probing time and salivary gland anti-haemostatic activities in representatives of three genera (*Aedes*, *Anopheles*, *Culex*). *Med. Vet. Entomol.* 14, 142–148. doi: 10.1046/j.1365-2915.2000.00227.x

Ribeiro, J. M., and Francischetti, I. M. (2003). Role of arthropod saliva in blood feeding: sialome and post-sialome perspectives. *Annu. Rev. Entomol.* 48, 73–88. doi: 10.1146/annurev.ento.48.060402.102812

Rodrigues, P. T., Valdivia, H. O., de Oliveira, T. C., Alves, J. M. P., Duarte, A., Cerutti-Junior, C., et al. (2018). Human migration and the spread of malaria parasites to the New World. *Sci. Rep.* 8:1993. doi: 10.1038/s41598-018-19554-0

Rodriguez, J. C., Uribe, G. A., Araujo, R. M., Narvaez, P. C., and Valencia, S. H. (2011). Epidemiology and control of malaria in Colombia. *Mem. Inst. Oswaldo Cruz* 106(Suppl. 1), 114–122. doi: 10.1590/S0074-02762011000900015

Rodriguez-Barraquer, I., Arinaitwe, E., Jagannathan, P., Kamya, M. R., Rosenthal, P. J., Rek, J., et al. (2018). Quantification of anti-parasite and anti-disease immunity to malaria as a function of age and exposure. *eLife* 7:e35832. doi: 10.7554/eLife.35832.045

Rosero, D. A., Naranjo-Diaz, N., Alvarez, N., Cienfuegos, A. V., Torres, C., Luckhart, S., et al. (2013). Colombian *Anopheles triannulatus* (Diptera: culicidae) naturally infected with *Plasmodium* spp. *ISRN Parasitol.* 2013:927453. doi: 10.5402/2013/927453

Ruiz, D., Poveda, G., Velez, I. D., Quinones, M. L., Rua, G. L., Velasquez, L. E., et al. (2006). Modelling entomological-climatic interactions of *Plasmodium falciparum* malaria transmission in two Colombian endemic-regions: contributions to a national malaria early warning system. *Malar. J.* 5:66. doi: 10.1186/1475-2875-5-66

Sagna, A. B., Gaayeb, L., Sarr, J. B., Senghor, S., Poinsignon, A., Boutouaba-Combe, S., et al. (2013). *Plasmodium falciparum* infection during dry season: IgG responses to *Anopheles gambiae* salivary gSG6-P1 peptide as sensitive biomarker for malaria risk in Northern Senegal. *Malar. J.* 12:301. doi: 10.1186/1475-2875-12-301

Thievent, K., Zilio, G., Hauser, G., and Koella, J. C. (2019). Malaria load affects the activity of mosquito salivary apyrase. *J. Insect. Physiol.* 116, 10–16. doi: 10.1016/j.jinsphys.2019.04.003

Villarreal-Trevino, C., Vasquez, G. M., Lopez-Sifuentes, V. M., Escobedo-Vargas, K., Huayanay-Repetto, A., Linton, Y. M., et al. (2015). Establishment of a free-mating, long-standing and highly productive laboratory colony of *Anopheles darlingi* from the Peruvian Amazon. *Malar. J.* 14:227. doi: 10.1186/s12936-015-0733-0

Vogt, M. B., Lahon, A., Arya, R. P., Kneubehl, A. R., Spencer Clinton, J. L., Paust, S., et al. (2018). Mosquito saliva alone has profound effects on the human immune system. *PLoS Negl. Trop. Dis.* 12:e0006439. doi: 10.1371/journal.pntd.0006439

Waitayakul, A., Somsri, S., Sattabongkot, J., Looareesuwan, S., Cui, L., and Udomsangpetch, R. (2006). Natural human humoral response to salivary gland proteins of *Anopheles* mosquitoes in Thailand. *Acta Trop.* 98, 66–73. doi: 10.1016/j.actatropica.2006.02.004

Ya-Umphan, P., Cerqueira, D., Cottrell, G., Parker, D. M., Fowkes, F. J. I., Nosten, F., et al. (2018). *Anopheles* salivary biomarker as a proxy for estimating *Plasmodium falciparum* malaria exposure on the thailand-myanmar border. *Am. J. Trop. Med. Hyg.* 99, 350–356. doi: 10.4269/ajtmh.18-0081

Yoshida, S., and Watanabe, H. (2006). Robust salivary gland-specific transgene expression in *Anopheles stephensi* mosquito. *Insect. Mol. Biol.* 15, 403–410. doi: 10.1111/j.1365-2583.2006.00645.x

Zain Ul, A., Qadeer, A., Akhtar, A., and Rasheed, A. (2016). Severe acute respiratory distress syndrome secondary to *Plasmodium vivax* malaria. *J. Pak. Med. Assoc.* 66, 351–353.

Disclaimer: The views expressed in this article reflect the results of research conducted by the authors and do not necessarily reflect the official policy or position of the Department of the Navy, Department of Defense, the Centers for Disease Control and Prevention, the Department of Health and Human Services, nor the U.S. Government.

Conflict of Interest: The authors declare that the research was conducted in the absence of any commercial or financial relationships that could be construed as a potential conflict of interest.

frontiers in Cellular and Infection Microbiology

ORIGINAL RESEARCH
published: 02 September 2020
doi: 10.3389/fcimb.2020.00459

Proteomic Mapping of Multifunctional Complexes Within Triatomine Saliva

Paula Beatriz Santiago[1], Sébastien Charneau[2], Samuel Coelho Mandacaru[2†], Kaio Luís da Silva Bentes[1], Izabela Marques Dourado Bastos[1], Marcelo Valle de Sousa[2], Carlos André O. Ricart[2], Carla Nunes de Araújo[1] and Jaime Martins Santana[1]**

[1] Pathogen-Host Interface Laboratory, Department of Cell Biology, The University of Brasilia, Brasilia, Brazil, [2] Laboratory of Protein Chemistry and Biochemistry, Department of Cell Biology, The University of Brasilia, Brasilia, Brazil

OPEN ACCESS

Edited by:
Itabajara Silva Vaz Jr,
Federal University of Rio Grande do Sul, Brazil

Reviewed by:
Marcos Sterkel,
Consejo Nacional de Investigaciones Científicas y Técnicas (CONICET), Argentina
Carlo José Freire Oliveira,
Universidade Federal do Triângulo Mineiro, Brazil

***Correspondence:**
Carla Nunes de Araújo
cnunes@unb.br
Jaime Martins Santana
jsantana@unb.br

†Present address:
Samuel Coelho Mandacaru,
UMR 7245 MCAM, Muséum National d'Histoire Naturelle, Centre National de la Recherche Scientifique, Paris, France

Specialty section:
This article was submitted to Parasite and Host, a section of the journal Frontiers in Cellular and Infection Microbiology

Received: 04 May 2020
Accepted: 27 July 2020
Published: 02 September 2020

Citation:
Santiago PB, Charneau S, Mandacaru SC, Bentes KLdS, Bastos IMD, de Sousa MV, Ricart CAO, de Araújo CN and Santana JM (2020) Proteomic Mapping of Multifunctional Complexes Within Triatomine Saliva. Front. Cell. Infect. Microbiol. 10:459. doi: 10.3389/fcimb.2020.00459

Triatomines are hematophagous insects that transmit *Trypanosoma cruzi*, the etiological agent of Chagas disease. This neglected tropical disease represents a global health issue as it is spreading worldwide. The saliva of Triatominae contains miscellaneous proteins crucial for blood feeding acquisition, counteracting host's hemostasis while performing vasodilatory, anti-platelet and anti-coagulant activities, besides modulating inflammation and immune responses. Since a set of biological processes are mediated by protein complexes, here, the sialocomplexomes (salivary protein complexes) of five species of Triatominae were studied to explore the protein-protein interaction networks. Salivary multiprotein complexes from *Triatoma infestans, Triatoma dimidiata*, *Dipetalogaster maxima*, *Rhodnius prolixus,* and *Rhodnius neglectus* were investigated by Blue-Native- polyacrylamide gel electrophoresis coupled with liquid chromatography tandem mass spectrometry. More than 70 protein groups, uncovering the landscape of the Triatominae salivary interactome, were revealed. Triabin, actin, thioredoxin peroxidase and an uncharacterized protein were identified in sialocomplexes of the five species, while hexamerin, heat shock protein and histone were identified in sialocomplexes of four species. Salivary proteins related to triatomine immunity as well as those required during blood feeding process such as apyrases, antigen 5, procalins, and nitrophorins compose different complexes. Furthermore, unique proteins for each triatomine species were revealed. This study represents the first Triatominae sialocomplexome reference to date and shows that the approach used is a reliable tool for the analysis of Triatominae salivary proteins assembled into complexes.

Keywords: Chagas disease, triatominae, salivary proteins, salivary complexes, BN-PAGE, mass spectrometry

INTRODUCTION

Triatominae (Hemiptera: Reduviidae) are the insect vectors of the flagellated protozoan *Trypanosoma cruzi*, which is the pathogen causative of Chagas disease. According to the WHO, Chagas disease is a neglected tropical disease that affects an estimated 6–7 million people worldwide (WHO, 2020). Originally endemic in Latin America countries, in recent decades the disease showed changes in its epidemiological profile due to migratory events, emerging as a global health concern (Pérez-Molina and Molina, 2018). In non-endemic regions, the main routes of *T. cruzi* transmission

are blood transfusion, organ transplantation, and congenital, while the vectorial form occurs in endemic areas where it overlaps with the distribution of triatomine insects (Antinori et al., 2017; Lidani et al., 2019).

The Triatominae subfamily encompasses more than 150 species, grouped in 16 genera and 5 tribes (Monteiro et al., 2018), living in sylvatic, peridomestic, and domestic habitats. After taking a successful blood meal on vertebrates, triatomines are able to transmit *T. cruzi*. In particular, *Triatoma*, *Rhodnius*, and *Panstrongylus* are genera of epidemiological importance, since some of their species complete the biological cycle in human dwellings. During feeding, hematophagous arthropods are challenged by the host's complex hemostatic and immune responses, which prevent blood loss following bite injury. Triatomines use the salivary compounds to overcome these barriers in order to achieve a continuous blood flow at the bite site (Francischetti et al., 2009). In this scenario, the understanding of vector biology, including the complex interaction of its saliva with the host, is an important research priority.

The transcriptomic and proteomic analyses of Triatominae salivary glands (sialomes) highlight the diversity of putative mechanisms of action of the salivary molecules (Santiago et al., 2020). Indeed, triatomine saliva is an important protein mixture that interacts with the host's molecules performing anti-inflammatory, anti-hemostatic, immunomodulatory, and local anesthetic activities (Ribeiro, 1995). The sialomes provide a deep insight into the biology of these vectors, the important aspects of the blood feeding process, as well as the vector-host interactions (Santiago et al., 2020). Among the salivary proteins, one key enzyme in inhibition of platelet aggregation is apyrase (E.C. 3.6.1.5), already reported in the saliva of several hematophagous organisms including arthropods and leeches (Ware and Luck, 2017). Upon injury to a vessel wall, at the insect bite site, damaged cells and dense granules of activated platelets release adenosine diphosphate (ADP), an important physiological agonist of platelet aggregation. This nucleotide binds to platelet membrane purinergic receptors leading to cell shape change and release of granular contents, triggering a positive feedback mechanism that potentiates platelet activation and aggregation (Kahner et al., 2006). Earlier, we have shown that *Triatoma infestans* apyrases are coordinated in a multiprotein complex with the ability to hydrolyze the agonist ADP, as well as adenosine triphosphate (ATP), into adenosine monophosphate (AMP) and inorganic phosphate (iP) (Faudry et al., 2004a, 2006). Thus, apyrases inhibit ADP-mediated activation of host platelets and subsequent aggregation of thrombocytes to facilitate blood feeding. In addition, the enzyme has also been implicated in modulating host inflammation by ATP degradation (Gounaris and Selkirk, 2005).

A fascinating feature concerning proteins is their ability to form supramolecular structures. In this regard, while exerting their functions, a number of proteins do not work as isolated molecules but rather as part of larger complexes formed by two or more associating polypeptide chains, which may be self- or cross-association, forming, respectively, the homo- and the hetero-oligomers (Ali and Imperiali, 2005). The assembly of subunits is based on the chemical and geometrical complementarities and can be either transient or stable (Nooren and Thornton, 2003). Homomers together with heteromers make up more than 50% of protein stoichiometry distribution in Protein Data Bank (PDB, 2020). Functional roles of oligomeric states might be crucial for the regulation of a series of biological processes, mediating gene expression and enzyme activity.

Among a large range of applications, native polyacrylamide gel electrophoresis (BN-PAGE) is a useful approach to analyze native oligomeric states in protein complexes (Schägger et al., 1994; Wittig et al., 2006; Miernyk and Thelen, 2008). Complexes migrate as blue bands through BN-PAGE gels, so they can be sliced off and be subjected to mass spectrometry analyzes, identifying their multiprotein composition. This combined approach provides size and protein-protein interaction data. Moreover, to identify oligomeric states activity, native complexes can be analyzed by in-gel activity assay.

The objective of this work was to unveil the protein-protein interaction network in the saliva (sialocomplexome) of *T. infestans, Triatoma dimidiata*, *Dipetalogaster maxima*, *Rhodnius prolixus,* and *Rhodnius neglectus*. Therefore, we separated and identified salivary multiprotein complexes by blue-native PAGE following mass spectrometry analysis. In addition, the oligomeric apyrase enzyme activity was also investigated by zymographic BN-PAGE. To our knowledge, this is the first insight into the sialocomplexomes of Triatominae.

MATERIALS AND METHODS

Triatomines and Saliva Collection

Triatomine bugs were reared in the insectarium of the University of Brasília (Brasília, Brazil). They were kept at 27 ± 1°C, a relative humidity of 70–75%, under a 12 h/12 h light/dark cycle. The blood source of these insects was *Gallus gallus domesticus*. Twenty-one days post-feeding, as salivary content 20 days after feeding is representative (Faudry et al., 2004a), 15 adults from both sexes of *T. infestans*, *T. dimidiata, D. maxima*, *R. prolixus*, and *R. neglectus*, were immobilized on ice, and under a stereomicroscope the salivary content was obtained by dissection of their salivary glands (SG), which were carefully washed in sterile saline solution before being harvested in microtubes containing EDTA-free protease inhibitor cocktail (Roche, Switzerland), and placed on ice. The pools of saliva from each species were centrifuged at 16,000 × g for 15 min at 4°C. The supernatant collected was kept at −80°C prior to use. The protein concentrations were determined using the Qubit® Protein Assay Kit (Thermo Fisher Scientific).

BN-Page

The salivary gland homogenates of different triatomines were subject to 1D BN-PAGE, as previously described for soluble proteins (Schägger et al., 1994; Wittig et al., 2006). The crude salivary extract from each species (150 μg of total protein) was resuspended in a sample buffer (50 mM Bis-Tris HCl pH 7.0, 15% (w/v) glycerol), and the samples were loaded onto a polyacrylamide gradient gel of 5–18%. Electrophoresis was run at 15 mA constant current for 4 h, at 4°C, in a SE 600 electrophoresis system (Hoefer, Inc., San Francisco, CA, USA). The cathodic

buffer consisted of 15 mM Bis-Tris HCl pH 7.0, 50 mM Tricine and 0.02% (w/v) Coomassie Brilliant Blue G-250 (CBB G-250), while the anodic buffer was composed of 50 mM Bis-Tris HCl pH 7.0. Once electrophoresis was complete, gels were either fixed and stained using CBB G-250 or used for the zymograms. Using a scalpel, the blue bands with high staining intensity containing the potential protein complexes were cut from the gel and stored at −20°C for subsequent LC-MS/MS analysis. The proteins thyroglobulin (669 kDa), ferritin (440 kDa), catalase (232 kDa), aldolase (158 kDa), bovine serum albumin (67 kDa), and ovalbumin (43 kDa) were used as molecular weight markers.

LC-MS/MS Protein Identification

Gel slices excised from the 1D-BN-PAGE were prepared for LC-MS/MS analysis by washing twice 50% acetonitrile por 4 h (in order to remove CBB-250), dehydrating in 100 μL of acetonitrile (ACN) and drying in a speed vacuum (Eppendorf, Hamburg, Germany). The proteins were in-gel reduced with 20 mM dithiothreitol in 25 mM ammonium bicarbonate buffer at 56°C for 45 min and alkylated with 40 mM iodoacetamide in the same buffer at room temperature, in the dark, for 1 h. Subsequently, in-gel proteins were washed in ACN and digested overnight at 37°C with 12.5 ng/μL modified trypsin (Promega, Madison, USA). The supernatants were acidified to a final concentration of 0.1% trifluoroacetic acid (TFA) for the first tryptic peptide extraction and followed by two other steps consisting in 0.1% TFA (v/v) in 50% ACN (v/v) and 0.1% TFA (v/v) in 80% ACN (v/v), respectively. The samples were then lyophilized, solubilized in 50 μL 1% TFA and desalted on a pipette tip packed with C18 membrane (Empore, Supelco). The digests were washed 3 times with 0.5% acetic acid and the peptides eluted with 25, 50, 80, and 100% ACN solutions, all containing 0.5% acetic acid (v/v), prior to LC-MS/MS analysis using an Orbitrap Elite™ hybrid ion trap- orbitrap mass spectrometer (Thermo Fisher Scientific Inc., Waltham, MA, USA). After 4 min washing with solvent A (0.1% (v/v) formic acid), the samples resuspended in 0.1% (v/v) formic acid were loaded into a nano-UPLC-Dionex 3000 system (Thermo Fisher Scientific Inc., Waltham, MA, USA) equipped with a trap type C18 column (100 μm × 3 cm with particles of 5 μm/100 Å) and a C18 analytical column (75 μm × 35 cm with particles of 3 μm/100 Å). The peptides were eluted from the analytical column at a flow rate of 230 nL.min^{-1} directly into the mass spectrometer under ESI ionization with a gradient of 2 to 35% of solvent B (0.1% [v/v] formic acid in ACN) for 30 min, 35–90% B and 90% B for 10 min, and decrease to 2% B to equilibrate the column for 20 min. The Data Dependent Acquisition (DDA) cycle of acquired molecular mass spectra controlled by Xcalibur 2.0 software (Thermo Fisher Scientific Inc., Waltham, MA, USA) comprised the range of m/z 350 to 1,650 and resolution of 120,000 for MS1. The fifteen most abundant precursor ions were fragmented by high energy collision dissociation (HCD), when the MS2 detection was performed at 60,000 resolution in the orbitrap analyzer, with dynamic exclusion for 90 s and collision energy normalized to 35%.

Data Analysis

Raw files were generated by the spectrometer and imported by PEAKS Studio 7.0 (Bioinformatics Solution Inc., Waterloo, Canada) software. Mass spectra data from samples were searched against the Uniprot Triatominae database (57,736 sequences accessed on 04/02/2020) and protein sequences of known contaminant proteins (several human keratins, BSA, and porcine trypsin). The parameters used were 10 ppm peptide mass tolerance, 0.5 Da fragment mass tolerance and two missed cleavages allowed. Methionine oxidations and acetylation of protein N-termini were specified as variable modifications, while carbamidomethylation of cysteine was specified as a fixed modification. Positive protein identities were assigned if at least one unique peptide were matched using a false discovery rate (FDR) of <1%. All contaminant proteins identified were manually removed from the result lists.

As a result of the redundancy of protein databank and protein isoforms derived from the same gene, over-counting of protein inferences might occur. Here, we used a clustering method where an identified protein is classified in a specific protein group (PG) when it has the assignment corresponding to a particular protein family. To be more consistent, these results were subsequently manually curated.

Data Availability

Mass spectrometer output files (Raw data) are available from the MassIVE database (accession number MSV000085118, doi: 10.25345/C5WT30, (http://massive.ucsd.edu/ProteoSAFe/status.jsp?task=364af77ff94b42729ffa5dcaf49fecd0) and ProteomeXchange (accession number PXD018101) (Vizcaíno et al., 2014; Perez-Riverol et al., 2015; Jarnuczak and Vizcaíno, 2017).

Zymogram

In-gel apyrase activity was based on the formation of a white insoluble calcium phosphate precipitate following phosphate production by ADP hydrolysis (Valenzuela et al., 1998). *T. infestans*, *T. dimidiata*, *D. maxima*, *R. prolixus*, and *R. neglectus* salivary contents (150 μg) were subjected to native 1D-BN-PAGE at 4°C. Immediately after running, the gel was washed twice with cold 2.5% (v/v) Triton X-100 and cold Milli-Q water, alternatively for 20 min each wash. The gel was incubated in activity solution (50 mM Tris-HCl, pH 8.3; 100 mM NaCl; 20 mM $CaCl_2$; 20 mM $MgCl_2$; 5 mM ADP) at 37°C for 30 min. The reaction was stopped with the same solution in the absence of the nucleotide.

RESULTS

Triatominae Salivary Protein Complexes Exhibit Unique Profiles

1D-BN-PAGE allowed the separation of the potential salivary multiprotein complexes (**Figure 1**). To minimize technical variation, samples from the five different species were processed in parallel. *R. prolixus* and *R. neglectus* 1D-BN-PAGE maps were almost identical whereas *T. infestans*, *D. maxima,* and *T. dimidiata* displayed unique profiles. Each 1D-BN-PAGE band above 67 kDa was considered as

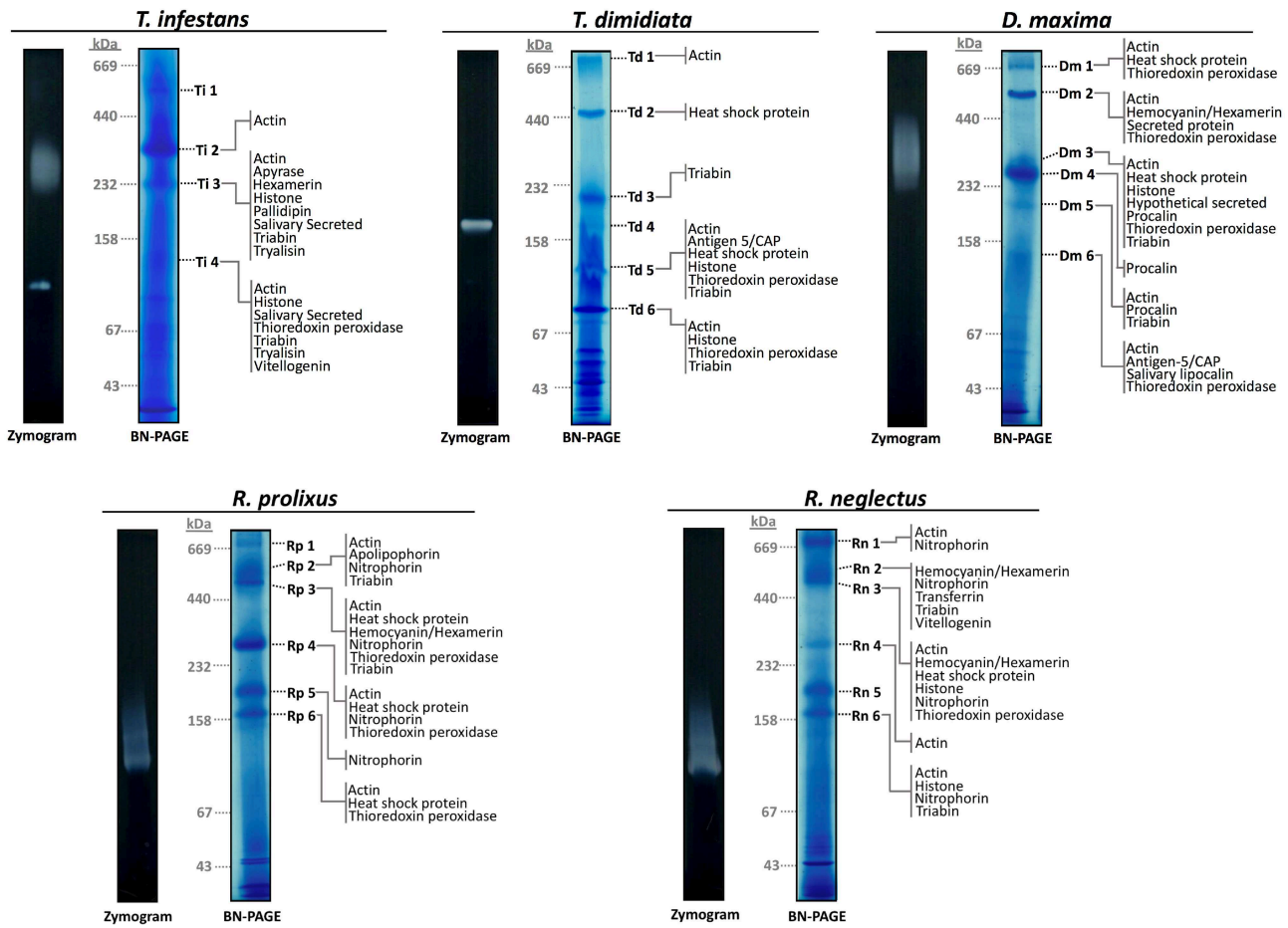

FIGURE 1 | Sialocomplexomes profile and ADPase activity from *Rhodnius prolixus, Rhodnius neglectus, Dipetalogaster maxima, Triatoma dimidiata*, and *Triatoma infestans* in 1D BN-PAGE. Protein complexes present in the saliva from *R. prolixus, R. neglectus, D. maxima,* and *T. dimidiata* are numbered from 1 to 6, and from *T. infestans* are numbered from 1 to 4. Zymography/BN-PAGE assays evaluating the apyrase activity are given to the left of the gels. Gels were run according to the protocols given in Methods. The positions of gel slices are shown by the species initials and number of the band. Hypothetically secreted proteins identified in each band are presented. Gels gradient were 5–18% and they were stained with CBB G-250. Molecular masses (in kDa) are given to the left of the Coomassie-stained gels.

a potential multiprotein complex. In all five species, it is possible to observe that some protein complexes ran above 440 kDa molecular weight. Four potential heteromeric protein complexes were obtained from salivary extracts of *T. infestans* (Ti-1-4), and six from *T. dimidiata* (Td 1-6), *D. maxima* (Dm1-6), *R. prolixus* (Rp1-6), and *R. neglectus* (Rn 1-6) (**Figure 1**).

The Composition of Triatominae Sialocomplexomes

To determine the subunit composition in the protein complexes, the four potential multiprotein bands with high staining intensity from *T. infestans*, and the six from *T. dimidiata*, *D. maxima*, *R. prolixus,* and *R. neglectus* were individually submitted to LC-MS/MS analysis. A comprehensive list of all identified proteins and peptides is provided in **Supplementary Files 1**, **2**, respectively. A total of 72 protein groups (PGs) were identified and several PGs were present in different bands from different triatomine saliva. It was possible to identify 19 different PGs in *T. infestans* sialocomplexomes, while 13 and 32 PGs were identified in *T. dimidiata* and *D. maxima*. *R. prolixus* and *R. neglectus* displayed 21 and 29 PGs, respectively. **Figure 2** shows a diagram representing the relationships among the sets of PGs identified on sialocomplexomes from the five species studied.

The sets of PGs were classified into five categories based on their putative biological functions as follows: Hypothetically secreted, Enzyme, Housekeeping, Unknown, and *Rhodococcus rhodnii*-derived proteins, condensed in **Table 1**. Remarkably, 24 (33.33%) of the PGs were classified as Hypothetically secreted, which are composed by proteins associated with hematophagy. The Enzyme class had 12 (16.67%) of all PGs. The Housekeeping class had 23 PGs, corresponding to 31.94% of the total identified. Approximately 11.11%, corresponding to 8 PGs, were not classified in the Triatominae Uniprot database and were placed in the Unknown class. *Rhodococcus rhodnii*-derived proteins accounted for 6.94% of the PGs.

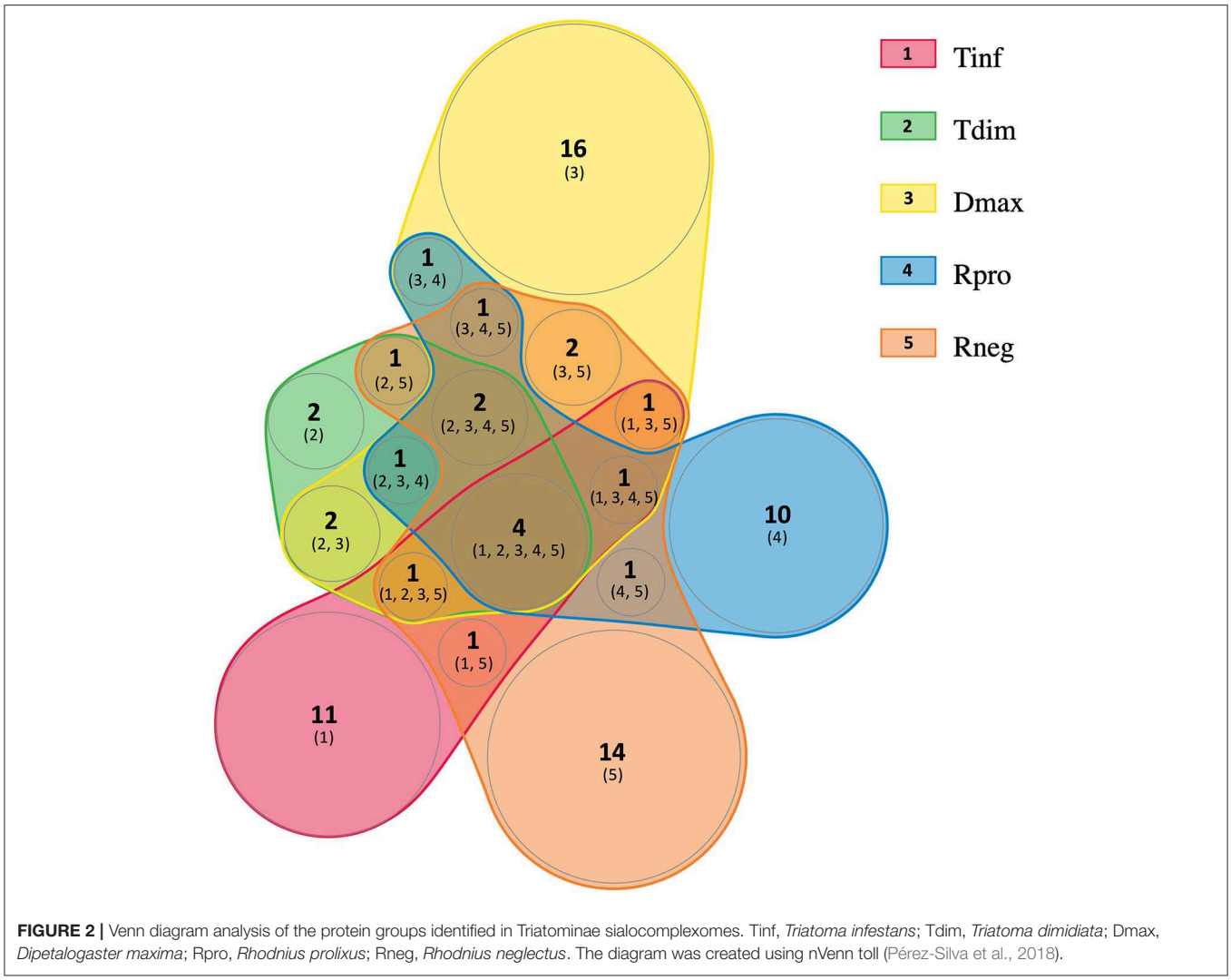

FIGURE 2 | Venn diagram analysis of the protein groups identified in Triatominae sialocomplexomes. Tinf, *Triatoma infestans*; Tdim, *Triatoma dimidiata*; Dmax, *Dipetalogaster maxima*; Rpro, *Rhodnius prolixus*; Rneg, *Rhodnius neglectus*. The diagram was created using nVenn toll (Pérez-Silva et al., 2018).

TABLE 1 | Functional classification of the Protein Groups (PGs) identified on Triatominae sialocomplexomes.

Class	Number of PG	% PGs
Hypothetically secreted	24	33.33
Enzyme	12	16.67
Housekeeping	23	31.94
Unknown	8	11.11
Rhodococcus rhodnii-derived products	5	6.94

The proteins identified in each BN-PAGE complex band can be seen in **Table 2** and in **Figure 1**. Four PGs were common to all five species, three in the Hypothetical secreted class, which are: (i) actin, (ii) thioredoxin peroxidase, (iii) triabin; and (iv) an uncharacterized protein (T1HZ69) from the Unknown class. The hemocyanin/hexamerin, the heat shock protein and the histone PGs were identified in the majority of the species, except for *T. dimidiata*, *T. infestans,* and *R. prolixus,* respectively.

Regarding the Hypothetically secreted class, with the exception of *T. dimidiata*, the species exhibited unique PGs. Apyrase, Ig-like domain-containing protein, pallidipin-like salivary lipocalin, putative salivary secreted protein, and salivary secreted protein PGs were identified only in *T. infestans*; the hypothetically secreted protein, procalin, and putative secreted protein PGs in *D. maxima*; putative apolipophorin, and putative pdz domain-containing protein PGs in *R. prolixus*; and putative drim down-regulated in metastasis-like and transferrin PGs in *R. neglectus*. Furthermore, *Rhodnius* genera showed the unique nitrophorin PG.

Sialocomplexomes From Triatominae Present ADPase Activity in Gel

The apyrase activity was detected above 232 kDa, and in a single band below 158 kDa in *T. infestans*; between 158 and 232 kDa in *T. dimidiata;* and above 232 kDa in *D. maxima*. A smear activity below 158 kDa was observed in both *R. prolixus* and *R. neglectus* (**Figure 1**). The activity smear/bands revealed in *T. infestans*,

T. dimidiata, and *D. maxima* merged with sialocomplexes Ti 3, Td 4, and Dm 3. While enzymatic activity profiles of *R. prolixus* and *R. neglectus* were not associated with stained-CBB bands.

DISCUSSION

Classes of Proteins in the Triatominae Sialocomplexomes

Multiprotein complexes are macromolecular assemblies that regulate essential cellular and physiological processes within biological systems. Despite progresses having been made regarding knowledge of Triatominae saliva and its fundamental role in blood acquisition during feeding (Santiago et al., 2020), insights about the composition and interaction network of salivary protein complexes from triatomines remain unavailable. The proteomic approach used here revealed the salivary proteins identified on BN-PAGE bands ran above their predicted molecular weights, suggesting they form potential protein complexes of higher-order assemblies. Here, when taking a closer look into *Rhodnius* species, a similar electrophoretic profile on BN-PAGE maps from *R. prolixus* and *R. neglectus* was evident. Conversely, Triatomini species showed a diversification of their salivary electrophoretic profiles, in agreement with the observation that this tribe lineage diversified extensively and consistent during evolution. Although, species and genera from Rhodniini and Triatomini tribes exhibit a variety of ecological, morphological, and molecular (salivary proteins) characteristics, recent phylogenetic analyses have suggested the monophyly of the Triatominae subfamily (Monteiro et al., 2018).

As detailed in **Table 1**, around 32% of identified proteins in BN-PAGE maps were attributed to the Housekeeping class. Different proteins associated with DNA or RNA binding/processing, protein synthesis and regulation, cytoskeletal structure were revealed. Previous report suggested a contamination of proteins from salivary gland tissue might have occurred due to salivary glands dissection and saliva collection procedures, not reflecting secreted proteins from saliva (Santiago et al., 2018). However, another hypothesis, supported by the observation that a tick heat-shock cognate protein 70 (HSP70) that interferes with host fibrinogenolysis at the bite site was reported in tick-cell-line-derived exosomes (Vora et al., 2017), is that salivary exosomes may deliver some of these proteins to exert specific biological functions in vertebrate hosts (Hackenberg and Kotsyfakis, 2018). Thus, in our analysis, actin, heat shock protein, histone, and thioredoxin peroxidase, which have already been reported to have a role when secreted, were classified in the Hypothetically secreted class together with typical salivary proteins. New roles for housekeeping secreted proteins may still be unveiled in future works.

Enzymes are abundant in the saliva of plant-feeding hemipterans (Sharma et al., 2014). Here, we showed that enzymes comprised 16% of the proteins identified in the sialocomplexomes. Triatominae subfamily of hemipterans evolved from predatory reduviid bugs, and during the transition to a hematophagous lifestyle, changes in the function of some salivary enzymes may have occurred (Monteiro et al., 2018). Serine and metalloproteases were already reported in different Triatominae sialomes (Assumpcao et al., 2008; Assumpção et al., 2012; Ribeiro et al., 2015; Santiago et al., 2016, 2018), and although their specific roles are unknown, hematophagous salivary enzymes have been associated with host's anti-hemostatic activities during blood acquisition and immunity (reviewed in Santiago et al., 2017). A trypsin-like serine protease, named triapsin, was reported in the salivary glands of *T. infestans* (Amino et al., 2001), and here, was identified in Ti 4 sialocomplex. Triapsin is stored as a zymogen in the luminal content of the SG, and activated during salivation stimulated by biting, suggesting it has a role in blood feeding (Amino et al., 2001). This protease may also be involved in hydrolysis of the superfamily of Proteinase Activated G protein-coupled Receptors (PAR), which regulates growth, development, inflammation, and responses to injury (Amino et al., 2001).

Three metalloproteases were also identified in this study. The aminopeptidase identified in Dm 2 is a member of the M1 family of Zn^{2+} metalloproteases, which are ubiquitous enzymes implicated in many physiological functions (Hooper, 1994). M1 aminopeptidases are found in all insect orders and have been detected in various tissues including salivary glands. They also play important roles in protein digestion (Budatha et al., 2007) and host-pathogen interactions (Denolf et al., 1997; Rajagopal et al., 2003; Aroonkesorn et al., 2015). In Hemipterans, triatomine aminopeptidases have been mainly implicated in the digestion of blood proteins (Garcia et al., 2010). Another zinc-dependent metalloprotease, a member of M16 family (T1HWH5), identified in Dm 2 may also be involved in digestion. In Rn 2, a member of the M13 family of zinc-dependent metallopeptidases was identified. Enzymes from this family have a broad tissue distribution in insects (Macours and Hens, 2004), and have been implicated in metamorphosis (Wilson et al., 2002), immunity to bacteria, fungi and protozoa (Zhu et al., 2003; Aguilar et al., 2005), neuropeptide metabolism (Isaac et al., 2009), and reproduction (Sitnik et al., 2014). Additionally, nuclease, isomerase, carboxylase, transferase, among others (**Table 2**) were also identified in the triatomine sialocomplexomes. These enzymes act on enzymatic cascades regulating various biological processes. The precise function of enzymes in sialocomplexes is unknown, but transient enzymatic complexes association into higher order assemblies have regulatory roles in biological functions.

In the Uncharacterized class, nine proteins with unknown functions were identified. Among them, only the protein T1HZ69 was ubiquitous in the five triatomine species. Another interesting result was the identification of proteins from *Rhodococcus rhodnii* among the sialocomplexomes from all five species. This bacterium was reported composing the low-diversity microbiota associated with the Triatominae salivary glands and was shown to be fundamental to the biological fitness of *R. prolixus* (Lima et al., 2018). *Rh. rhodnii* are members of the Nocardiaceae family, which are symbiont bacteria from triatomines. They are passed from adults to offspring by coprophagy and appear to supplement, the triatomine diet, especially with B vitamins (Brecher and Wigglesworth, 1944). Five proteins from

TABLE 2 | List of Triatominae salivary proteins identified on the oligomeric protein complexes and their putative functions.

Protein group[a]	Putative molecular function[b]	BN-PAGE band[c]
HYPOTHETICALLY SECRETED		
Apyrase		
79 kDa salivary apyrase	Hydrolysis of ADP and ATP	Ti 3
Salivary apyrase	Hydrolysis of ADP and ATP	Ti 3
Actin	Insect immunity/Inhibition of platelet aggregation	Ti 2; Ti 3; Ti 4; Td 1; Td 5; Td 6; Dm 1; Dm 2; Dm 3; Dm 5; Dm 6; Rp 2; Rp 3; Rp 4; Rp 6; Rp 7; Rn 1; Rn3; Rn 4; Rn 6
Antigen-5/CAP family		
Antigen-5-like protein	Inhibition of platelet aggregation; Inhibition of coagulation; Antioxidant activity	Dm 6
SCP domain-containing protein	Inhibition of platelet aggregation; Inhibition of coagulation; Antioxidant activity	Td 5
Cytochrome P450-like protein	Heme binding	Td 6
Histone		
Histone H2A	Insect immunity	Ti 4; Td 5; Td 6; Rn 3
Histone H2B	Insect immunity	Ti 3; Rn 3
Histone H3	Insect immunity	Ti 4; Td 6; Dm 3; Rn3; Rn 6
Hypothetical secreted protein (E2J7B4)	Unknown	Dm 3
Ig-like domain-containing protein	Unknown	Ti 3
Hemocyanin/Hexamerin		
Larval serum protein 2	Insect immunity	Ti 3; Dm 2
Putative basic juvenile hormone	Insect immunity	Dm 2; Rn 2
Putative hexamerin	Insect immunity	Ti 3; Dm 2
Uncharacterized protein (T1HU08)	Insect immunity	Dm 2; Rp 3; Rn2; Rn 3
Nitrophorin		
Nitrophorin 1	Inhibition of platelet aggregation; Vasodilatory; Anti-histaminic	Rp 2; Rp 3; Rp 4; Rp 7; Rn2; Rn3
Nitrophorin 4A	Inhibition of platelet aggregation; Vasodilatory; Anti-histaminic	Rn 2
Nitrophorin-3	Inhibition of platelet aggregation; Vasodilatory; Anti-histaminic	Rn 2; Rp 5
Putative nitrophorin	Inhibition of platelet aggregation; Vasodilatory; Anti-histaminic	Rp 2; Rp 3; Rn1; Rn2; Rn3
Small nitrophorin 2A	Inhibition of platelet aggregation; Vasodilatory; Anti-histaminic	Rp 7; Rn 6
Pallidipin-like salivary lipocalin	Inhibition of platelet aggregation	Ti 3
Procalin	Salivary allergen	Dm3; Dm4; Dm5
Putative apolipophorins	Lipid transporter	Rp 2
Putative drim down-regulated in metastasis-like	Heme binding	Rn 2
Putative heat shock protein	Protein folding, Fibrinogenolysis	Td 2; Td 5; Dm1; Dm3; Rp 3; Rp 4; Rp 6; Rn3
Putative pdz domain-containing protein	Protein-protein interactions mediator	Rp 4
Putative salivary secreted protein	Actin-crosslinking	Ti 4
Putative secreted protein	Unknown	Dm 2
Putative thioredoxin peroxidase	Detoxification of ROS	Ti 4; Td 5; Td 6; Dm 1; Dm 2; Dm 3; Dm 6; Rp 3; Rp 4; Rp 6; Rp 7; Rn3
Salivary lipocalin	Inhibition of hemostasis	Dm 6
Salivary secreted protein	Unknown	Ti 3
Transferrin	Insect immunity	Rn 2
Triabin	Inhibition of thrombin	Ti 3; Ti 4; Td 3; Td 5; Td 6; Dm 3; Dm 5; Rp 2; Rp 3; Rp 7; Rn2; Rn 6
Trialysin	Pore-forming lytic protein	Ti 3; Ti 4
Vitellogenin lipoprotein	Lipid transporter	Ti 4; Rn 2
ENZYME		
Aminopeptidase	Peptidase M1/MetalloAminopeptidase activity	Dm 2
Fanconi-associated nuclease	Phosphodiesterase I activity	Rp 4
Peptidylprolyl isomerase	Peptidyl-prolyl cis-trans isomerase activity	Td 6; Dm 2; Rp 5
PlsC domain-containing protein	Transferase activity, transferring acyl groups	Rp 1

(Continued)

TABLE 2 | Continued

Protein group[a]	Putative molecular function[b]	BN-PAGE band[c]
Putative acetyl-coa carboxylase biotin carboxylase	Biotin carboxylation	Rn 2
Putative heparan sulfate-glucuronic acid c5-epimerase	Heparosan-N-sulfate-glucuronate 5-epimerase activity	Dm 2
Putative trna modification enzyme	tRNA [guanine(37)-N(1)]-methyltransferase activity	Td 6; Rn 2; Rn 6
Putative trypsin-like serine protease	Serine-type endopeptidase activity	Ti 4
Putative vacuolar h+-atpase v1 sector subunit e	Proton-transporting two-sector ATPase	Dm 2; Rp 6
Serine/threonine-protein kinase	Protein serine/threonine kinase activity	Rn 2
Uncharacterized protein (T1HWH5)	Peptidase_M16/metalloendopeptidase activity	Dm 2
Uncharacterized protein (T1I287)	Peptidase_M13/metalloendopeptidase activity	Rn 2
HOUSEKEEPING		
Circadian trip	Ubiquitin-protein transferase activity	Dm 4
CXXC-type domain-containing protein	DNA-binding	Rn 6
Dynein	Microtubule motor activity	Rn 2; Rn 6
Elongation factor 1-alpha	Translation elongation factor activity	Td 5; Td 6
Putative cell cycle control protein crooked neck	RNA processing	Rn 2
Putative endoplasmic reticulum glucose-regulated	ATP binding/protein folding	Dm 1
Putative golgin subfamily protein a member	Golgi organization	Dm 2
Putative guanine nucleotide binding protein mip1	TOR signaling	Ti 3
Putative mediator of rna polymerase ii	Transcription coregulator activity	Dm 2; Dm 3
Putative muscle-specific protein	Cytoskeletal structure	Rn 6
Putative myosin class ii heavy chain	Cytoskeletal structure	Rp 3
Putative retrotransposon-like family	Nucleic acid binding	Dm 3
Putative ribosome-binding protein 1-like isoform x5	Ribosome-binding protein	Ti 4
Putative titin isoform x14	Immunoglobulin-like domain	Rp 4
Putative transcription regulator xnp/atrx dead-box	Nucleic acid binding	Rn 2
Putative ubiquitin	Protein regulation	Ti 3; Dm 2; Rn 2; Rn 3
Putative unconventional myosin-xviiia	Cytoskeletal structure	Td 6; Dm 3
Retinoid-and fatty acid-binding glycoprotein	von Willebrand factor type D domain	Ti 2
Tropomyosin isoform	Cytoskeletal structure	Dm 2; Rp 4; Rn 3
Uncharacterized protein (T1HAV7)	RNA binding/processing	Rn 6
Uncharacterized protein (T1HA71)	DNA binding/regulation of transcription	Rp 7
Uncharacterized protein (T1I899)	DNA binding	Dm 2
Uncharacterized protein (T1IAP4)	Integral component of membrane	Dm 3
UNKNOWN		
Uncharacterized protein (T1HZ69)	-	Ti 4; Td 6; Dm 1; Dm5; Rp1; Rp 3; Rp 4; Rn1
Uncharacterized protein (T1HNL8)	-	Dm 2
Uncharacterized protein (T1HS38)	-	Dm 2; Rn 3
Uncharacterized protein (T1HK09)	-	Rn 6
Uncharacterized protein (T1HX12)	-	Rp 5
Uncharacterized protein (A0A069DS40)	-	Dm 2; Rn 3
Uncharacterized protein (T1HU42)	-	Rp 4
Uncharacterized protein (T1IDW9)	-	Rp 1
RHODOCOCCUS RHODNII		
Elongation factor	Translation elongation factor activity	Rn 6
HNHc domain-containing protein	-	Td 6; Dm 1; Rp 2; Rn 1; Rn 5; Rn 6
P-type ATPase	-	Dm 2
Transferase	Transferase activity	Ti 3
Uncharacterized protein (R7WS93)	-	Rn 6

[a]Protein group name based on protein signature identified by LC/MS-MS.

[b] For the Hypothetical secreted PGs: Putative function of the particular protein group in blood feeding context (vector/host interaction). See references in discussion section. For the Housekeeping and R. rhodnii PGs: Molecular function were based on their classification at Uniprot database.

[c]Triatomine species initials and number of the BN gel band submitted to LC/MS-MS identification.

Rh. rhodnii were identified. Among them, a HNHc domain-containing protein was detected not only in *R. prolixus*, but also in *R. neglectus*, *T. dimidiata* and *D. maxima*. The HNHc domain is associated with DNA-binding proteins involved in cellular processes such as recombination, DNA rearrangement, phage packaging, restriction endonuclease activity and bacterial toxicity (Dalgaard et al., 1997). The possible roles of *Rh. rhodnii* proteins in the saliva of triatomines warrants further investigation.

Our major interest is the Hypothetically secreted proteins since they are involved in the triatomine-host interface. This class accounted for 32% of the identified proteins. When comparing results from the five species, it was seen that actin, thioredoxin peroxidase, triabin, uncharacterized (T1HZ69), hemocyanin/hexamerin, heat shock protein and histone and were identified in various BN-PAGE bands. While the former four are ubiquitous, the last three were not found in *T. dimidiata*, *T. infestans,* or *R. prolixus,* respectively. Apart from triabin, none of the other six proteins were previously highlighted in triatomine saliva before. It is likely that reports have focused on secreted salivary molecules with putative functions already described in literature. Multifunctional molecules, those that await identification of their salivary function or interact with ligands not yet characterized, remain unnoticed.

Proteins commonly described in Triatominae saliva were also revealed. *Rhodnius* sialocomplexes exhibited interacting nitrophorins, which are nitric oxide (NO)-binding heme proteins with vasodilatory function (Champagne et al., 1995). *T. infestans* saliva is distinguished by the presence of apyrases, pallidipin, and trialysin; *T. dimidiata* by antigen-5/CAP; and *D. maxima* by antigen-5/CAP, and procalin (**Table 2**). These molecules account for a diversity of molecular mechanisms of triatomine saliva to overcome host's hemostasis. Pallidipin and antigen-5/CAP members are inhibitors of platelet aggregation mediated by collagen (Noeske-Jungblut et al., 1994; Assumpção et al., 2013). Triabin is a thrombin inhibitor (Noeske-Jungblut et al., 1995), while trialysin is pore-forming lytic protein (Amino et al., 2002), and procalin is a salivary allergen (Paddock et al., 2001). Nitrophorin, pallidipin, procalin, triabin, among other proteins identified here, belong to the lipocalin/calicin superfamily of proteins, which is comprised of low molecular weight proteins with mainly extracellular functions. These proteins share a common structure and are able to bind to small hydrophobic molecules, soluble macromolecules, macromolecular complexes, through non-covalent and covalent bonds; and to specific cell surface receptors (Hernández-Vargas et al., 2016).

Previous triatomine sialome analyses revealed this superfamily is the most abundant and functionally diverse from saliva (reviewed in Santiago et al., 2020).

Salivary Apyrases of Triatominae Are Assembled in Complexes

Apyrase in-gel activity was detected in all samples. In *T. infestans* saliva, an activity band under 158 kDa and a smear above 200 kDa, which is the result of aggregates of active small units, were detected. Moreover, apyrase members were identified by proteomics in Ti 3 sialocomplex, corroborating the in-gel activity is due to true apyrase salivary proteins. This result is in accordance with the 200 kDa apyrase homo-oligomers from the saliva of *T. infestans* reported before (Faudry et al., 2006). A similar pattern of smeared apyrase activity was observed between *T. infestans* and *D. maxima,* and between *R. prolixus* and *R. neglectus.* The various aggregates may reflect several post-translational modifications of the salivary apyrase units, and even other protein units, they contain. Concerning *T. dimidiata,* a single active form (above 158 kDa) was observed. Therefore, different molecular weights were shown to these ADPase activities depending on the triatomine species, indicating heterogeneity of enzyme isoforms and oligomerization.

Although the apyrase in-gel activity was detected in all the samples tested in this study, the specific *T. infestans* apyrase sequences present in the database were not identified by mass spectrometry in *T. dimidiata, D. maxima*, *R. prolixus,* and *R. neglectus* saliva bands. This result appears to reflect the presence of a small amount of apyrase proteins in saliva. In addition, considering the knowledge about the function and composition of the saliva from triatomines, this hydrolase activity acting on ADP typically occurs due to true apyrase (ATP diphosphohydrolase, EC 3.6.1.5) enzymes (Sarkis et al., 1986; Ribeiro, 1995), corroborating this enzyme is well-conserved among triatomines. Because apyrase efficiently affects platelet aggregation, this enzyme has potential as pharmacological candidate for the treatment of thrombotic pathologies, reflecting its importance for research purposes.

Multifunctional Proteins in the Triatominae Sialocomplexomes

Actin is one of the most conserved gene families in Eukarya. Isoforms are expressed in different tissues and are involved in a variety of biological processes, mostly intracellular such as muscle contraction, cell motility, cell division, vesicle and movement (Pollard, 2016). Actin monomers spontaneously polymerize with themselves under physiological conditions (Pollard, 2016), and here may form some homo-oligomeric complexes. Furthermore, in the presence of divalent cations, actin monomers tightly bind adenosine triphosphate (ATP) or diphosphate (ADP) (Pollard, 2016), and thus, polymerized secreted actin may have a role in the counteraction of host's hemostasis by binding to these nucleotides. Despite the description of extracellular actins is not common in insects, it has been proposed that actin is externalized by insect immune competent cells upon immune challenge, mediating antibacterial defense (Sandiford et al., 2015). Actin 5C is a high affinity bacterial binding protein (Sandiford et al., 2015). Here, different actin 5C proteins were identified in salivary complexes by proteomic analyses. These proteins are constitutively expressed and as well as composing the cytoskeletal structure, non-standard functions for triatomine salivary actin can be proposed. In this context, actin 5C proteins may have a role in hematophagy, inhibiting platelet aggregation or in

immunity, inhibiting the growth of bacteria. This is the first-time that secreted actin proteins are mentioned to play a role in triatomine saliva.

Arthropod hemocyanins (Hc) are large and multimeric members of a protein superfamily that also comprises the arthropod phenoloxidase (PO), crustacean pseudohemocyanins, and insect storage hexamerins (Burmester, 2001). Hc participates in microbicidal activity and provides a first line of defense mechanism against microorganisms, emerging as an evolutionary mode of immune surveillance (Coates and Nairn, 2014). Hc and PO show different structures but share almost identical active site architecture, and both contribute to sclerotization of the arthropod cuticle (Decker and Rimke, 1998; Decker et al., 2007). The presence of Hcs in the saliva of triatomines may be related to protection against pathogens acquired during the blood feeding as well as to the initial steps of digestion inside the midgut, once swallowed with the blood meal. Different members from Hc family were found in the sialocomplexomes of *T. infestans*, *D. maxima*, *R. prolixus,* and *R. neglecus*. These large extracellular proteins are found as multiples of 2–8 hexamers (Jaenicke and Decker, 2003). It is likely Hcs form large complexes in the triatomine saliva.

Histones are largely known to control chromatin architecture. It has been suggested that a combination of post-translational modification is able to alter histone functions (Ouvry-Patat and Schey, 2007), including histone antimicrobial activity reported in a wide range of organisms (Patat et al., 2004). Here, histone members were observed in *T. infestans*, *T. dimidiata*, *D. maxima,* and *R. neglectus*. It is feasible that they have a role in innate immunity of triatomines, for instance, by controlling the population growth of bacteria acquired with blood meal in the salivary glands and midgut.

Reactive oxygen species (ROS), including superoxide anions (O^{2-}), hydroxyl radicals (OH^{-}), and hydrogen peroxide (H_2O_2), are reactive molecules generated as by-products of aerobic metabolism. High levels of ROS can be toxic to cells; thus, detoxification is essential to the survival of species. In this context, thioredoxin peroxidase (TPx) is a ubiquitous antioxidant enzyme that scavenges peroxides, mainly H_2O_2, avoiding oxidative damage in inset cells (Arnér and Holmgren, 2000; Radyuk et al., 2001; Imam et al., 2017). Several TPx were reported in hemipterans (Zumaya-Estrada et al., 2018). In hematophagous arthropods, heme metabolism gives rise to iron that catalyzes the conversion of H_2O_2 to hydroxyl free-radical ions, which attack cellular membranes, proteins and DNA (Imam et al., 2017). Thus, TPx could perform a fundamental detoxifying role preventing excessive H_2O_2 generation and iron-driven oxygen toxicity. Nevertheless, it is worth pointing that anopheline salivary peroxidases destroy catecholamine and serotonin, thus inhibiting vasoconstrictors that could interfere with insect feeding (Ribeiro and Nussenzveig, 1993; Ribeiro and Valenzuela, 1999). It is possible that TPx may play a multifunctional physiological role.

A member of apolipophorin (ApoLp) family was revealed in Rp 2 sialocomplex. It is an insect hemolymph protein involved in lipid transport. Three ApoLp have been described, ApoLp-I, ApoLp-II, and ApoLp-III (Blacklock and Ryan, 1994), the latter is homologous to the mammalian Apolipoprotein E (Cole et al., 1987) and facilitates the transport of diacylglycerol from the fat body to muscles (Feingold et al., 1995). ApoLp-III was reported to mediate humoral and cellular immune responses (Kim et al., 2004; Whitten et al., 2004; Song et al., 2008; Zdybicka-Barabas and Cytryńska, 2011). It acts as a pathogen recognition receptor (PRR) as it is able to bind to lipoteichoic acid (LTA), present in cell wall of Gram-positive bacteria (Halwani and Dunphy, 1999; Halwani et al., 2001), lipopolysaccharide (LPS) of Gram-negative bacteria (Kato et al., 1994; Halwani and Dunphy, 1997), and beta 1, 3 glucan of fungal cell wall (Whitten et al., 2004). Moreover, ApoLp-III stimulates encapsulation of foreign substances that are too large to be phagocytized by hemocytes in the hemolymph (Zdybicka-Barabas and Cytryńska, 2013).

Heat-shock proteins (HSPs), also known as chaperones, are responsible to tightly control the *de novo* folding, unfolding, assembly/disassembly, translocation, activation/inactivation, disaggregation, and degradation of proteins and protein complexes. HSPs are highly conserved across species and may act through transient interactions, mediating changes in the composition of a protein complex (Makhnevych and Houry, 2012; Finka et al., 2016). HSP70 proteins bind promiscuously to a wide variety of newly synthesized or unfolded proteins, also preventing their aggregation and allowing correct folding (Finka et al., 2016). A HSP70 from *R. prolixus* was reported to be upregulated during the first hours after blood feeding, and knockdown insects showed impaired blood processing and digestion (Paim et al., 2016). In tick saliva, secreted HSP70 may assist the proper folding of proteins involved in the degradation of fibrinogen at the bite site, thus showing a role in fibrinogenolysis during blood feeding (Vora et al., 2017). Here, HSP70 containing oligomers were observed in sialocomplexomes of *T. dimidiata*, *D. maxima*, *R. prolixus,* and *R. neglectus*. It is apparent that the folding of triatomine salivary proteins is under the control of this protein, which assists the stability and functionality of proteins (Vora et al., 2017). Furthermore, it has been shown HSP70 assembles in dimers stabilized by post-translational modifications and is maintained in the client-loading complex (Morgner et al., 2015). Future studies on triatomine salivary HSP70 may indicate their specific contribution in the blood feeding context.

Vitellogenin is a yolk precursor lipoprotein secreted in the hemolymph that plays a critical role in oocyte development, as it is a source of nutrients during early stages of development (Smolenaars et al., 2007). As it is involved in lipid transport protein, distinct physiological roles are possible for this protein. Regarding blood-feeding it may enable the uptake and transport of dietary lipids. The vitellogenin lipoprotein was previously recognized in assembly stable homodimers (Smolenaars et al., 2007). Vitellogenin protein was identified in Ti 4 and Rn 2 sialocomplexes.

The identification of protein members that may act in the primary effector mechanisms of immunity in the triatomine sialocomplexomes was expected. Studies on how insect immune molecules interact with self-proteins are scarce. It is likely that a dynamic net of protein-protein interactions may improve the immune response, regulating

the molecular events to recognize a variety of foreign targets more efficiently.

In this study, the proteomic analysis revealed a heterogeneous composition in Triatominae sialocomplexomes. From the 72 identifications obtained, 53 were unique, most belonging to the Housekeeping or Enzyme classes. Comparing *R. prolixus* and *R. neglectus* sialocomplexomes, although the identification in the different complexes was not exactly the same, the set of proteins from Secreted class was very similar between them. Concerning the five species, the reduced overlap in proteins composition could be due to changes in gene expression, especially those influenced by adaptive traits. A comparative proteomic analysis of the saliva from *R. prolixus, Triatoma lecticularia,* and *Panstrongylus herreri* showed high interspecific functional biodiversity with only one protein shared among them (Montandon et al., 2016). Moreover, the variation in the salivary protein expression may occur even among individuals within the same species of hematophagous arthropod (Perner et al., 2018). The composition of saliva also changes with time. For instance, in *T. infestans,* recovery of apyrases to maximal activity level takes days after blood feeding, thus suggesting de novo protein synthesis (Faudry et al., 2004b). In addition, even though prior transcriptomic and proteomic analyses of the salivary glands from triatomines have been revealing a conserved set of mRNA that are ubiquitously expressed, they have also found variation in the expression and composition of saliva from triatomines (Santiago et al., 2020). Many of the Secreted proteins have redundant biological roles, and low expression or absence of a protein may not result in impairment of feeding.

The overlap in the protein composition was remarkable among Hypothetically secreted proteins class, indicating that those may be real components of the sialocomplexes. Actin, thioredoxin peroxidase, triabin and uncharacterized (T1HZ69) are shared among the five species, although their positions on complexes showed different range of sizes and low correlated co-migration. It is possible the large salivary complexes occur due to stable homo-oligomeric formations among these proteins, since most are well known to make part of macromolecular complexes in biological systems. It may be worth considering the possibility that smaller secreted proteins such as triabin, antigen-5, nitrophorin, procalin and lipocalin bind with these large macromolecular complexes in a transiently manner, forming multifunctional modules in response to determined stimulus.

All together these results challenge data interpretation but provide significant prediction about native and molecular organization of Triatominae sialocomplexes, suggesting that proteins may undergo several posttranslational modifications to better support stability and functionality not only by one general mechanism, but different routes for oligomerization may occur. Thus, the members of the potential complexes are arranged to form homo- and/or hetero-oligomeric, stable and/or transient assemblies. This dynamic may occur according to the physiological demands of triatomines to give rise to a cooperative functional mechanism, improving the counteraction of host's responses. Finally, the knowledge about the conserved salivary components among triatomine species is fundamental, once may lead to the identification of salivary molecules that might enhance pathogen transmission (Mesquita et al., 2008); and of potential candidates for anti-triatomine vaccines or immunobiologics, concerning their antigenicity and anti-hemostatic and immunomodulatory properties.

CONCLUSION

Protein interaction data is sparse in hematophagous arthropods saliva. This is the first report to give an insight into the potential protein complexes present in the saliva of *T. infestans*, *T. dimidiata*, *D. maxima*, *R. prolixus,* and *R. neglectus* kissing bugs by coupling BN-PAGE to LC-MS/MS. Triatominae salivary proteins may form transient homo- and/or hetero-oligomeric complexes arranged in multifunctional modules to efficiently counteract host's hemostasis, act against pathogens acquired during blood feeding, and in the digestion process once swallowed with the host blood. Oligomeric apyrases were identified only in *T. infestans* through proteomic analysis, despite apyrase in-gel activity was observed across all five species. In addition, unexpected secreted proteins were identified composing the Triatominae sialocomplexomes, ascribing putative novel functions to the poorly characterized protein complexes. For instance, inhibition of platelet aggregation and bacterial growth by actin 5C, and degradation of fibrinogen by HSP70. These proteins, which have primarily functions not related to hematophagy in other tissues, may impact the feeding behavior of triatomines. In the future, more efforts will be needed to elucidate protein-specific interactions and their mechanisms of action. Some questions that remain unanswered are: What triggers these transient interactions? What is the relevance of these complexes in blood feeding behavior, vector-host interaction, and vector immunity?

DATA AVAILABILITY STATEMENT

The datasets presented in this study can be found in online repositories. The names of the repository/repositories and accession number(s) can be found in the article/**Supplementary Material**.

AUTHOR CONTRIBUTIONS

PS, SC, and CA conceived and designed the study. PS and KB were responsible for the triatomines rearing, saliva collection, 1D-BN-PAGE, and zymograms. SM performed LC-MS/MS. PS, CA, SC, and JS performed the data analysis. PS and CA wrote the manuscript. IB, MS, CR, and JS critically revised the manuscript. All authors edited and approved the final manuscript.

FUNDING

This work was supported by grants and fellowships awarded by the Fundacção de Amparo à Pesquisa do Distrito Federal (FAP-DF, grants 0193.001802/2017 and 0193.000.417/2016), Coordenação de Aperfeiçoamento de Pessoal de Nível Superior (CAPES, grant 923/18 CAPES-COFECUB), Conselho Nacional

de Desenvolvimento Científico e Tecnológico (CNPq, INCT-MCTI/CNPq/FAPs 16/2014), Financiadora de Estudos e Projetos (Finep, CT-Infra grants 0439/11 and 0694/13 to MS).

ACKNOWLEDGMENTS

We would like to acknowledge Professor Connie McManus (Institute of Biological Sciences, University of Brasilia) for manuscript editing assistance and Dr. Jaques M. F. Souza for technical assistance.

SUPPLEMENTARY MATERIAL

The Supplementary Material for this article can be found online at: https://www.frontiersin.org/articles/10.3389/fcimb.2020.00459/full#supplementary-material

Table S1 | All saliva protein groups identified from the different bands of the saliva of *Rhodnius prolixus, Rhodnius neglectus, Dipetalogaster maxima, Triatoma dimidiata,* and *Triatoma infestans*, corresponding to the **Figure 1**.

Table S2 | All peptides from the different bands of the saliva of *Rhodnius prolixus, Rhodnius neglectus, Dipetalogaster maxima, Triatoma dimidiata,* and *Triatoma infestans* allowing the protein identification of the sialocomplexes.

REFERENCES

Aguilar, R., Jedlicka, A. E., Mintz, M., Mahairaki, V., Scott, A. L., and Dimopoulos, G. (2005). Global gene expression analysis of Anopheles gambiae responses to microbial challenge. *Insect. Biochem. Mol. Biol.* 35, 709–719. doi: 10.1016/j.ibmb.2005.02.019

Ali, M. H., and Imperiali, B. (2005). Protein oligomerization: how and why. *Bioorg. Med. Chem.* 13, 5013–5020. doi: 10.1016/j.bmc.2005.05.037

Amino, R., Martins, R. M., Procopio, J., Hirata, I. Y., Juliano, M. A., and Schenkman, S. (2002). Trialysin, a novel pore-forming protein from saliva of hematophagous insects activated by limited proteolysis. *J. Biol. Chem.* 277, 6207–6213. doi: 10.1074/jbc.M109874200

Amino, R., Tanaka, A. S., and Schenkman, S. (2001). Triapsin, an unusual activatable serine protease from the saliva of the hematophagous vector of Chagas' disease Triatoma infestans (Hemiptera: Reduviidae). *Insect Biochem. Mol. Biol.* 31, 465–472. doi: 10.1016/S0965-1748(00)00151-X

Antinori, S., Galimberti, L., Bianco, R., Grande, R., Galli, M., and Corbellino, M. (2017). Chagas disease in Europe: a review for the internist in the globalized world. *Eur. J. Intern. Med.* 43, 6–15. doi: 10.1016/j.ejim.2017.05.001

Arnér, E. S., and Holmgren, A. (2000). Physiological functions of thioredoxin and thioredoxin reductase. *Eur. J. Biochem.* 267, 6102–6109. doi: 10.1046/j.1432-1327.2000.01701.x

Aroonkesorn, A., Pootanakit, K., Katzenmeier, G., and Angsuthanasombat, C. (2015). Two specific membrane-bound aminopeptidase N isoforms from Aedes aegypti larvae serve as functional receptors for the Bacillus thuringiensis Cry4Ba toxin implicating counterpart specificity. *Biochem. Biophys. Res. Commun.* 461, 300–306. doi: 10.1016/j.bbrc.2015.04.026

Assumpção, T. C., Eaton, D. P., Pham, V. M., Francischetti, I. M., Aoki, V., Hans-Filho, G., et al. (2012). An insight into the sialotranscriptome of Triatoma matogrossensis, a kissing bug associated with fogo selvagem in South America. *Am. J. Trop. Med. Hyg.* 86, 1005–1014. doi: 10.4269/ajtmh.2012.11-0690

Assumpcao, T. C., Francischetti, I. M., Andersen, J. F., Schwarz, A., Santana, J. M., and Ribeiro, J. M. (2008). An insight into the sialome of the blood-sucking bug Triatoma infestans, a vector of Chagas' disease. *Insect Biochem. Mol. Biol.* 38, 213–232. doi: 10.1016/j.ibmb.2007.11.001

Assumpção, T. C., Ma, D., Schwarz, A., Reiter, K., Santana, J. M., Andersen, J. F., et al. (2013). Salivary antigen-5/CAP family members are Cu2+-dependent antioxidant enzymes that scavenge O_2? and inhibit collagen-induced platelet aggregation and neutrophil oxidative burst. *J. Biol. Chem.* 288, 14341–14361. doi: 10.1074/jbc.M113.466995

Blacklock, B. J., and Ryan, R. O. (1994). Hemolymph lipid transport. *Insect. Biochem. Mol. Biol.* 24, 855–873. doi: 10.1016/0965-1748(94)90015-9

Brecher, G., and Wigglesworth, V. B. (1944). The transmission of Actinomyces rhodnii Erikson in Rhodnius prolixus Stål (Hemiptera) and its influence on the growth of the host. *Parasitology* 35, 220–224. doi: 10.1017/S0031182000021648

Budatha, M., Meur, G., and Dutta-Gupta, A. (2007). A novel aminopeptidase in the fat body of the moth Achaea janata as a receptor for Bacillus thuringiensis Cry toxins and its comparison with midgut aminopeptidase. *Biochem. J.* 405, 287–297. doi: 10.1042/BJ20070054

Burmester, T. (2001). Molecular evolution of the arthropod hemocyanin superfamily. *Mol. Biol. Evol.* 18, 184–195. doi: 10.1093/oxfordjournals.molbev.a003792

Champagne, D. E., Nussenzveig, R. H., and Ribeiro, J. M. (1995). Purification, partial characterization, and cloning of nitric oxide-carrying heme proteins (nitrophorins) from salivary glands of the blood-sucking insect Rhodnius prolixus. *J. Biol. Chem.* 270, 8691–8695. doi: 10.1074/jbc.270.15.8691

Coates, C. J., and Nairn, J. (2014). Diverse immune functions of hemocyanins. *Dev. Comp. Immunol.* 45, 43–55. doi: 10.1016/j.dci.2014.01.021

Cole, K. D., Fernando-Warnakulasuriya, G. P., Boguski, M. S., Freeman, M., Gordon, J. I., Clark, W. A., et al. (1987). Primary structure and comparative sequence analysis of an insect apolipoprotein. Apolipophorin-III from Manduca sexta. *J. Biol. Chem.* 262, 11794–11800.

Dalgaard, J. Z., Klar, A. J., Moser, M. J., Holley, W. R., Chatterjee, A., and Mian, I. S. (1997). Statistical modeling and analysis of the LAGLIDADG family of site-specific endonucleases and identification of an intein that encodes a site-specific endonuclease of the HNH family. *Nucleic Acids Res.* 25, 4626–4638. doi: 10.1093/nar/25.22.4626

Decker, H., and Rimke, T. (1998). Tarantula hemocyanin shows phenoloxidase activity. *J. Biol. Chem.* 273, 25889–25892. doi: 10.1074/jbc.273.40.25889

Decker, H., Schweikardt, T., Nillius, D., Salzbrunn, U., Jaenicke, E., and Tuczek, F. (2007). Similar enzyme activation and catalysis in hemocyanins and tyrosinases. *Gene* 398, 183–191. doi: 10.1016/j.gene.2007.02.051

Denolf, P., Hendrickx, K., Van Damme, J., Jansens, S., Peferoen, M., Degheele, D., et al. (1997). Cloning and characterization of Manduca sexta and Plutella xylostella midgut aminopeptidase N enzymes related to Bacillus thuringiensis toxin-binding proteins. *Eur. J. Biochem.* 248, 748–761. doi: 10.1111/j.1432-1033.1997.t01-1-00748.x

Faudry, E., Lozzi, S. P., Santana, J. M., M., D'Souza-Ault, Kieffer, S., Felix, C. R., et al. (2004a). Triatoma infestans apyrases belong to the 5'-nucleotidase family. *J. Biol. Chem.* 279, 19607–19613. doi: 10.1074/jbc.M401681200

Faudry, E., Rocha, P. S., Vernet, T., Lozzi, S. P., and Teixeira, A. R. (2004b). Kinetics of expression of the salivary apyrases in Triatoma infestans. *Insect Biochem. Mol. Biol.* 34, 1051–1058. doi: 10.1016/j.ibmb.2004.06.016

Faudry, E., Santana, J. M., Ebel, C., Vernet, T., and Teixeira, A. R. (2006). Salivary apyrases of Triatoma infestans are assembled into homo-oligomers. *Biochem. J.* 396, 509–515. doi: 10.1042/BJ20052019

Feingold, K. R., Funk, J. L., Moser, A. H., Shigenaga, J. K., Rapp, J. H., and Grunfeld, C. (1995). Role for circulating lipoproteins in protection from endotoxin toxicity. *Infect. Immun.* 63, 2041–2046. doi: 10.1128/IAI.63.5.2041-2046.1995

Finka, A., Mattoo, R. U., and Goloubinoff, P. (2016). Experimental milestones in the discovery of molecular chaperones as polypeptide unfolding enzymes. *Annu. Rev. Biochem.* 85, 715–742. doi: 10.1146/annurev-biochem-060815-014124

Francischetti, I. M., Sa-Nunes, A., Mans, B. J., Santos, I. M., and Ribeiro, J. M. (2009). The role of saliva in tick feeding. *Front. Biosci.* 14, 2051–2088. doi: 10.2741/3363

Garcia, E. S., Genta, F. A., de Azambuja, P., and Schaub, G. A. (2010). Interactions between intestinal compounds of triatomines and Trypanosoma cruzi. *Trends Parasitol.* 26, 499–505. doi: 10.1016/j.pt.2010.07.003

Gounaris, K., and Selkirk, M. E. (2005). Parasite nucleotide-metabolizing enzymes and host purinergic signalling. *Trends Parasitol.* 21, 17–21. doi: 10.1016/j.pt.2004.10.005

Hackenberg, M., and Kotsyfakis, M. (2018). Exosome-mediated pathogen transmission by arthropod vectors. *Trends Parasitol.* 34, 549–552. doi: 10.1016/j.pt.2018.04.001

Halwani, A., and Dunphy, G. (1997). Haemolymph proteins of larvae of Galleria mellonella detoxify endotoxins of the insect pathogenic bacteria Xenorhabdus nematophilus (Enterobacteriaceae). *J. Insect Physiol.* 43, 1023–1029. doi: 10.1016/s0022-1910(97)00072-3

Halwani, A. E., Dunphy, G. B. (1999). Apolipophorin-III in Galleria mellonella potentiates hemolymph lytic activity. *Dev. Comp. Immunol.* 23, 563–570. doi: 10.1016/s0145-305x(99)00037-3

Halwani, A. E., Niven, D. F., and Dunphy, G. B. (2001). Apolipophorin-III in the greater wax moth, Galleria mellonella (Lepidopteran: Pyralidae). *Arch. Insect Biochem. Physiol.* 48, 135–143. doi: 10.1002/arch.1066

Hernández-Vargas, M. J., Santibáñez-López, C. E., and Corzo, G. (2016). An insight into the triabin protein family of american hematophagous reduviids: functional, structural and phylogenetic analysis. *Toxins (Basel)* 8:44. doi: 10.3390/toxins8020044

Hooper, N. M. (1994). Families of zinc metalloproteases. *FEBS Lett.* 354, 1–6. doi: 10.1016/0014-5793(94)01079-X

Imam, M. U., Zhang, S., Ma, J., Wang, H., and Wang, F. (2017). Antioxidants mediate both iron homeostasis and oxidative stress. *Nutrients* 9:671. doi: 10.3390/nu9070671

Isaac, R. E., Bland, N. D., and Shirras, A. D. (2009). Neuropeptidases and the metabolic inactivation of insect neuropeptides. *Gen. Comp. Endocrinol.* 162, 8–17. doi: 10.1016/j.ygcen.2008.12.011

Jaenicke, E., and Decker, H. (2003). Tyrosinases from crustaceans form hexamers. *Biochem. J. 371 (Pt* 2):515–523. doi: 10.1042/bj20021058

Jarnuczak, A. F., and Vizcaíno, J. A. (2017). Using the PRIDE database and proteomexchange for submitting and accessing public proteomics datasets. *Curr. Protoc. Bioinform.* 59, 13.31.1–13.31.12. doi: 10.1002/cpbi.30

Kahner, B. N., Shankar, H., Murugappan, S., Prasad, G. L., and Kunapuli, S. P. (2006). Nucleotide receptor signaling in platelets. *J. Thromb. Haemost.* 4, 2317–2326. doi: 10.1111/j.1538-7836.2006.02192.x

Kato, Y., Motoi, Y., Taniai, K., Kadono-Okuda, K., Yamamoto, M., Higashino, Y., et al. (1994). Lipopolysaccharide-lipophorin complex formation in insect hemolymph: a common pathway of lipopolysaccharide detoxification both in insects and in mammals. *Insect Biochem. Mol. Biol.* 24, 547–555. doi: 10.1016/0965-1748(94)90090-6

Kim, H. J., Je, H. J., Park, S. Y., Lee, I. H., Jin, B. R., Yun, H. K., et al. (2004). Immune activation of apolipophorin-III and its distribution in hemocyte from Hyphantria cunea. *Insect Biochem. Mol. Biol.* 34, 1011–1023. doi: 10.1016/j.ibmb.2004.05.005

Lidani, K. C. F., Andrade, F. A., Bavia, L., Damasceno, F. S., Beltrame, M. H., Messias-Reason, I. J., et al. (2019). Chagas disease: from discovery to a worldwide health problem. *Front. Public Health* 7:166. doi: 10.3389/fpubh.2019.00166

Lima, M. S., Laport, M. S., Lorosa, E. S., Jurberg, J., Dos Santos, K. R., N. M. A. C., et al. (2018). Bacterial community composition in the salivary glands of triatomines (Hemiptera: Reduviidae). *PLoS Negl. Trop. Dis.* 12:e0006739. doi: 10.1371/journal.pntd.0006739

Macours, N., and Hens, K. (2004). Zinc-metalloproteases in insects: ACE and ECE. *Insect Biochem. Mol. Biol.* 34, 501–510. doi: 10.1016/j.ibmb.2004.03.007

Makhnevych, T., and Houry, W. A. (2012). The role of Hsp90 in protein complex assembly. *Biochim. Biophys. Acta* 1823, 674–682. doi: 10.1016/j.bbamcr.2011.09.001

Mesquita, R. D., Carneiro, A. B., Bafica, A., Gazos-Lopes, F., Takiya, C. M., Souto-Padron, T., et al. (2008). Trypanosoma cruzi infection is enhanced by vector saliva through immunosuppressant mechanisms mediated by lysophosphatidylcholine. *Infect. Immun.* 76, 5543–5552. doi: 10.1128/IAI.00683-08

Miernyk, J. A., and Thelen, J. J. (2008). Biochemical approaches for discovering protein-protein interactions. *Plant J.* 53, 597–609. doi: 10.1111/j.1365-313X.2007.03316.x

Montandon, C. E., Barros, E., Vidigal, P. M., Mendes, M. T., Anh,ê, A. C., H. J., et al. (2016). Comparative proteomic analysis of the saliva of the Rhodnius prolixus, Triatoma lecticularia and Panstrongylus herreri triatomines reveals a high interespecific functional biodiversity. *Insect Biochem. Mol. Biol.* 71, 83–90. doi: 10.1016/j.ibmb.2016.02.009

Monteiro, F. A., Weirauch, C., Felix, M., Lazoski, C., and Abad-Franch, F. (2018). Evolution, systematics, and biogeography of the triatominae, vectors of chagas disease. *Adv. Parasitol.* 99:265–344. doi: 10.1016/bs.apar.2017.12.002

Morgner, N., Schmidt, C., Beilsten-Edmands, V., Ebong, I. O., Patel, N. A., Clerico, E. M., et al. (2015). Hsp70 forms antiparallel dimers stabilized by post-translational modifications to position clients for transfer to Hsp90. *Cell Rep.* 11, 759–769. doi: 10.1016/j.celrep.2015.03.063

Noeske-Jungblut, C., Haendler, B., Donner, P., Alagon, A., Possani, L., and Schleuning, W. D. (1995). Triabin, a highly potent exosite inhibitor of thrombin. *J. Biol. Chem.* 270, 28629–28634. doi: 10.1074/jbc.270.48.28629

Noeske-Jungblut, C., Krätzschmar, J., Haendler, B., Alagon, A., Possani, L., Verhallen, P., et al. (1994). An inhibitor of collagen-induced platelet aggregation from the saliva of Triatoma pallidipennis. *J. Biol. Chem.* 269, 5050–5053.

Nooren, I. M., and Thornton, J. M. (2003). Diversity of protein-protein interactions. *EMBO J.* 22, 3486–3492. doi: 10.1093/emboj/cdg359

Ouvry-Patat, S. A., and Schey, K. L. (2007). Characterization of antimicrobial histone sequences and posttranslational modifications by mass spectrometry. *J. Mass Spectrom* 42, 664–674. doi: 10.1002/jms.1200

Paddock, C. D., McKerrow, J. H., Hansell, E., Foreman, K. W., Hsieh, I., and Marshall, N. (2001). Identification, cloning, and recombinant expression of procalin, a major triatomine allergen. *J. Immunol.* 167, 2694–2699. doi: 10.4049/jimmunol.167.5.2694

Paim, R. M. M., Araujo, R. N., Leis, M. M. R. V., Sant'anna, Gontijo, N. F., Lazzari, C. R., and Pereira, M. H. (2016). Functional evaluation of Heat Shock Proteins 70 (HSP70/HSC70) on Rhodnius prolixus (Hemiptera, Reduviidae) physiological responses associated with feeding and starvation. *Insect Biochem. Mol. Biol.* 77, 10–20. doi: 10.1016/j.ibmb.2016.07.011

Patat, S. A., Carnegie, R. B., Kingsbury, C., Gross, P. S., Chapman, R., and Schey, K. L. (2004). Antimicrobial activity of histones from hemocytes of the Pacific white shrimp. *Eur. J. Biochem.* 271, 4825–4833. doi: 10.1111/j.1432-1033.2004.04448.x

PDB. (2020). Protein Stoichiometry. *Protein Data Bank*. Available online at: https://www.rcsb.org/#Category-search (accessed March 30, 2020).

Pérez-Molina, J. A., and Molina, I. (2018). Chagas disease. *Lancet* 391, 82–94. doi: 10.1016/S0140-6736(17)31612-4

Perez-Riverol, Y., Alpi, E., Wang, R., Hermjakob, H., and Vizcaíno, J. A. (2015). Making proteomics data accessible and reusable: current state of proteomics databases and repositories. *Proteomics* 15, 930–949. doi: 10.1002/pmic.201400302

Pérez-Silva, J. G., Araujo-Voces, M., and Quesada, V. (2018). nVenn: generalized, quasi-proportional Venn and Euler diagrams. *Bioinformatics* 34, 2322–2324. doi: 10.1093/bioinformatics/bty109

Perner, J., Kropáčková, S., Kopáček, P., and Ribeiro, J. M., C. (2018). Sialome diversity of ticks revealed by RNAseq of single tick salivary glands. *PLoS Negl. Trop. Dis.* 12:e0006410. doi: 10.1371/journal.pntd.0006410

Pollard, T. D. (2016). Actin and Actin-Binding Proteins. *Cold Spring Harb. Perspect. Biol.* 8:a018226v1. doi: 10.1101/cshperspect.a018226

Radyuk, S. N., Klichko, V. I., Spinola, B., Sohal, R. S., and Orr, W. C. (2001). The peroxiredoxin gene family in Drosophila melanogaster. *Free Radic. Biol. Med.* 31, 1090–1100. doi: 10.1016/S0891-5849(01)00692-X

Rajagopal, R., Agrawal, N., Selvapandiyan, A., Sivakumar, S., Ahmad, S., and Bhatnagar, R. K. (2003). Recombinantly expressed isoenzymic aminopeptidases from Helicoverpa armigera (American cotton bollworm) midgut display differential interaction with closely related Bacillus thuringiensis insecticidal proteins. *Biochem J.* 370 (Pt 3), 971–978. doi: 10.1042/bj20021741

Ribeiro, J. M. (1995). Blood-feeding arthropods: live syringes or invertebrate pharmacologists? *Infect. Agents Dis.* 4, 143–152.

Ribeiro, J. M., and Nussenzveig, R. H. (1993). The salivary catechol oxidase/peroxidase activities of the mosquito Anopheles albimanus. *J. Exp. Biol.* 179, 273–287.

Ribeiro, J. M., Schwarz, A., and Francischetti, I. M. (2015). A deep insight into the sialotranscriptome of the chagas disease vector, panstrongylus megistus (Hemiptera: Heteroptera). *J. Med. Entomol.* 52, 351–358. doi: 10.1093/jme/tjv023

Ribeiro, J. M., and Valenzuela, J. G. (1999). Purification and cloning of the salivary peroxidase/catechol oxidase of the mosquito Anopheles albimanus. *J. Exp. Biol.* 202 (Pt 7), 809–816.

Sandiford, S. L., Dong, Y., Pike, A., Blumberg, B. J., Bahia, A. C., and Dimopoulos, G. (2015). Cytoplasmic actin is an extracellular insect immune factor which is secreted upon immune challenge and mediates phagocytosis and direct killing of bacteria, and is a Plasmodium Antagonist. *PLoS Pathog.* 11:e1004631. doi: 10.1371/journal.ppat.1004631

Santiago, P. B., Assumpção, T. C., Araújo, C. N., Bastos, I. M., Neves, D., Silva, I. G., et al. (2016). A Deep Insight into the Sialome of Rhodnius neglectus, a Vector of Chagas Disease. *PLoS Negl. Trop. Dis.* 10:e0004581. doi: 10.1371/journal.pntd.0004581

Santiago, P. B., de Araújo, C. N., Charneau, S., Bastos, I. M., D., Assumpção, T. C., et al. (2018). Exploring the molecular complexity of Triatoma dimidiata sialome. *J. Proteomics* 174:47–60. doi: 10.1016/j.jprot.2017.12.016

Santiago, P. B., de Araújo, C. N., Charneau, S., Praça, Y. R., Bastos, I. M., D., et al. (2020). The pharmacopea within triatomine salivary glands. *Trends Parasitol.* 36, 250–265. doi: 10.1016/j.pt.2019.12.014

Santiago, P. B., de Araújo, C. N., Motta, F. N., Praça, Y. R., Charneau, S., Bastos, I. M., et al. (2017). Proteases of haematophagous arthropod vectors are involved in blood-feeding, yolk formation and immunity - a review. *Parasit. Vect.* 10:79. doi: 10.1186/s13071-017-2005-z

Sarkis, J. J., Guimarães, J. A., and Ribeiro, J. M. (1986). Salivary apyrase of Rhodnius prolixus. Kinetics and purification. *Biochem J.* 233, 885–891. doi: 10.1042/bj2330885

Schägger, H., Cramer, W. A., and von Jagow, G. (1994). Analysis of molecular masses and oligomeric states of protein complexes by blue native electrophoresis and isolation of membrane protein complexes by two-dimensional native electrophoresis. *Anal. Biochem.* 217, 220–230. doi: 10.1006/abio.1994.1112

Sharma, A., Khan, A. N., Subrahmanyam, S., Raman, A., Taylor, G. S., and Fletcher, M. J. (2014). Salivary proteins of plant-feeding hemipteroids - implication in phytophagy. *Bull. Entomol. Res.* 104, 117–136. doi: 10.1017/S0007485313000618

Sitnik, J. L., Francis, C., Hens, K., Huybrechts, R., Wolfner, M. F., and Callaerts, P. (2014). Neprilysins: an evolutionarily conserved family of metalloproteases that play important roles in reproduction in Drosophila. *Genetics* 196, 781–797. doi: 10.1534/genetics.113.160945

Smolenaars, M. M., Madsen, O., Rodenburg, K. W., and Van der Horst, D. J. (2007). Molecular diversity and evolution of the large lipid transfer protein superfamily. *J. Lipid Res.* 48, 489–502. doi: 10.1194/jlr.R600028-JLR200

Song, K. H., Jung, M. K., Eum, J. H., Hwang, I. C., and Han, S. S. (2008). Proteomic analysis of parasitized Plutella xylostellalarvae plasma. *J. Insect Physiol.* 54, 1270–1280. doi: 10.1016/j.jinsphys.2008.06.010

Valenzuela, J. G., Charlab, R., Galperin, M. Y., and Ribeiro, J. M. (1998). Purification, cloning, and expression of an apyrase from the bed bug Cimex lectularius. A new type of nucleotide-binding enzyme. *J. Biol. Chem.* 273, 30583–30590. doi: 10.1074/jbc.273.46.30583

Vizcaíno, J. A., Deutsch, E. W., Wang, R., Csordas, A., Reisinger, F., Ríos, D., et al. (2014). ProteomeXchange provides globally coordinated proteomics data submission and dissemination. *Nat. Biotechnol.* 32, 223–226. doi: 10.1038/nbt.2839

Vora, A., Taank, V., Dutta, S. M., Anderson, J. F., Fish, D., Sonenshine, D. E., et al. (2017). Ticks elicit variable fibrinogenolytic activities upon feeding on hosts with different immune backgrounds. *Sci. Rep.* 7:44593. doi: 10.1038/srep44593

Ware, F. L., and Luck, M. R. (2017). Evolution of salivary secretions in haematophagous animals. *Biosci. Horizons* 10:hzw015. doi: 10.1093/biohorizons/hzw015

Whitten, M. M. A., Tew, I. F., Lee, B. L., Ratcliffe, N. A. (2004). A novel role for an insect apolipoprotein (apolipophorin III) in β-1,3-glucan pattern recognition and cellular encapsulation reactions. *J. Immunol.* 172, 2177–2185. doi: 10.4049/jimmunol.172.4.2177

WHO. (2020). *Chagas Disease Key Facts.* Available online at: https://www.who.int/news-room/fact-sheets/detail/chagas-disease-(american-trypanosomiasis) (accessed March 30, 2020).

Wilson, C. L., Shirras, A. D., and Isaac, R. E. (2002). Extracellular peptidases of imaginal discs of Drosophila melanogaster. *Peptides* 23, 2007–2014. doi: 10.1016/S0196-9781(02)00188-2

Wittig, I., Braun, H. P., and Schägger, H. (2006). Blue native PAGE. *Nat. Protoc.* 1, 418–428. doi: 10.1038/nprot.2006.62

Zdybicka-Barabas, A., and Cytryńska, M. (2011). Involvement of apolipophorin III in antibacterial defense of Galleria mellonella larvae. *Comp. Biochem. Physiol. B Biochem. Mol. Biol.* 158, 90–98. doi: 10.1016/j.cbpb.2010.10.001

Zdybicka-Barabas, A., and Cytryńska, M. (2013). Apolipophorins and insects immune response. *Invertebr. Surviv. J.* 10, 58–68.

Zhu, Y., Johnson, T. J., Myers, A. A., and Kanost, M. R. (2003). Identification by subtractive suppression hybridization of bacteria-induced genes expressed in Manduca sexta fat body. *Insect Biochem. Mol. Biol.* 33, 541–559. doi: 10.1016/S0965-1748(03)00028-6

Zumaya-Estrada, F. A., Martínez-Barnetche, J., Lavore, A., Rivera-Pomar, R., and Rodríguez, M. H. (2018). Comparative genomics analysis of triatomines reveals common first line and inducible immunity-related genes and the absence of Imd canonical components among hemimetabolous arthropods. *Parasit. Vect.* 11:48. doi: 10.1186/s13071-017-2561-2

Conflict of Interest: The authors declare that the research was conducted in the absence of any commercial or financial relationships that could be construed as a potential conflict of interest.

frontiers in Cellular and Infection Microbiology

REVIEW
published: 11 September 2020
doi: 10.3389/fcimb.2020.574405

Quantitative Visions of Reality at the Tick-Host Interface: Biochemistry, Genomics, Proteomics, and Transcriptomics as Measures of Complete Inventories of the Tick Sialoverse

Ben J. Mans [1,2,3]*

[1] Epidemiology, Parasites and Vectors, Agricultural Research Council-Onderstepoort Veterinary Research, Pretoria, South Africa, [2] Department of Veterinary Tropical Diseases, University of Pretoria, Pretoria, South Africa, [3] Department of Life and Consumer Sciences, University of South Africa, Pretoria, South Africa

OPEN ACCESS

Edited by:
Lucas Tirloni,
National Institute of Allergy and Infectious Diseases (NIH), United States

Reviewed by:
Shahid Karim,
University of Southern Mississippi, United States
Elisa Azuara-Liceaga,
Universidad Autónoma de la Ciudad de México, Mexico

***Correspondence:**
Ben J. Mans
mansb@arc.agric.za

Specialty section:
This article was submitted to Parasite and Host, a section of the journal Frontiers in Cellular and Infection Microbiology

Received: 19 June 2020
Accepted: 13 August 2020
Published: 11 September 2020

Citation:
Mans BJ (2020) Quantitative Visions of Reality at the Tick-Host Interface: Biochemistry, Genomics, Proteomics, and Transcriptomics as Measures of Complete Inventories of the Tick Sialoverse. Front. Cell. Infect. Microbiol. 10:574405. doi: 10.3389/fcimb.2020.574405

Species have definitive genomes. Even so, the transcriptional and translational products of the genome are dynamic and subject to change over time. This is especially true for the proteins secreted by ticks at the tick-host feeding interface that represent a complex system known as the sialoverse. The sialoverse represent all of the proteins derived from tick salivary glands for all tick species that may be involved in tick-host interaction and the modulation of the host's defense mechanisms. The current study contemplates the advances made over time to understand and describe the complexity present in the sialoverse. Technological advances at given periods in time allowed detection of functions, genes, and proteins enabling a deeper insight into the complexity of the sialoverse and a concomitant expansion in complexity with as yet, no end in sight. The importance of systematic classification of the sialoverse is highlighted with the realization that our coverage of transcriptome and proteome space remains incomplete, but that complete descriptions may be possible in the future. Even so, analysis and integration of the sialoverse into a comprehensive understanding of tick-host interactions may require further technological advances given the high level of expected complexity that remains to be uncovered.

Keywords: tick, sialome, sialoverse, proteome, transcriptome, salivary gland

INTRODUCTION

Organisms are finite creatures in space and time with genomes that are definitive for a given species. As such, within the population of organisms that comprise a specific species, their genomes will be similar in identity and synteny over ~95–99% of the total genome. This last 3–5% of intra-species diversity comprise alleles, epigenetic differences, single nucleotide polymorphisms and lost or rearranged genes that forms the basis for phenotypic or strain differences. The contribution of the microbiome that forms with the tick genome the hologenome, adds considerable diversity at individual and population level (Díaz-Sánchez et al., 2019). Horizontal transfer may occur from the

microbiome to the core genome, but in this case these transferred genes would then become part of the core genome. However, the hologenome is not considered in the current study, since these are exogenous variable factors that may not be part of the core genetic component of a species. The core genetic component comprises not only the genome, but its translational aspects such as the transcriptome and proteome, which are more dynamic in nature, since the final products such as mRNA, proteins and other metabolites show tissue-specific and temporal expression patterns, different half-life's and concentration levels. The impact of concentration levels of proteins and metabolites at the tick feeding site has recently been explored and shown to be critical for effective functioning (Mans, 2019). An extensive summary of functions for tick proteins involved at the tick-host interface was also presented previously (Mans, 2016, 2019; Mans et al., 2016). The acquisition of new functions by gene duplication has also been explored and shown to play an important part in the expansion of gene families in ticks (Mans et al., 2017). The current review considers the progress on quantitative description of molecules at the feeding site and addresses the question on how our understanding of the number of proteins and functions at the feeding site has changed over time due to technological advances and experimental design (**Figure 1**).

COMPLEXITY MEASURED BY MORPHOLOGY AND HISTOCHEMISTRY

The recognition that salivary glands have a complex morphology composed of non-secretory and secretory acini (Robinson and Davidson, 1913), as well as multiple cell types within secretory acini, have been well-recognized once cell staining and tissue sectioning could be applied to tick salivary glands (Till, 1959; Chinery, 1965; Balashov, 1972). While soft ticks have a single granular acini, female hard ticks have two types (II and III), while male hard ticks also have a fourth type (IV) (Till, 1959; Roshdy, 1972). Granular acini from both soft and hard ticks all have multiple cell types, with both histochemical staining and immunolocalization indicating that different cells show differential expression of proteins (Roshdy, 1972; Coons and Roshdy, 1973; Mans et al., 2004). Morphological observation was therefore the first indication that salivary glands have higher complexity than may be expected from a simple secretory organ that may be likened to a bag of proteins.

COMPLEXITY MEASURED BY FUNCTIONAL ACTIVITY

In the absence of fractionation, estimates of complexity may be obtained by measuring unique functions in salivary glands, salivary gland secretions (SGS) or salivary gland extracts (SGE) using empirical methods. As such, it was indicated that tick salivary glands possess numerous functionalities suggesting a complex organ with many functions active at the tick feeding site (Neitz and Vermeulen, 1987). These included enzymatic functions, enzyme inhibitory functions, anticoagulants, cement, toxins and immunogens. Many proteins responsible for these functions were later isolated and identified from numerous tick species, with ∼120 experimentally verified tick protein functions to date (reviewed in Mans, 2019). The difficulty in complexity estimation using functional characterization is the sheer immensity of potential known and unknown functions and the amount of effort necessary to characterize these functions (Ribeiro and Arcà, 2009; Mans, 2016).

COMPLEXITY MEASURED BY COUNTING PEAKS

Kaire (1966) performed the first chromatographic separation of tick proteins from whole tick extracts to purify the neurotoxin from the Australian paralysis tick, *Ixodes holocyclus* (Neumann, 1899). However, the first fractionation of tick salivary proteins arguably occurred in the 1960 and 1970s when Neitz purified the first toxins from SGS from the soft tick *Ornithodoros savignyi* (Audouin, 1826) (sand tampan), now *Ornithodoros kalahariensis* (Neitz et al., 1969; Howell et al., 1975; Bakkes et al., 2018). The fractionation used combinations of size exclusion, ion exchange and iso-electric focusing methods available at the time. Estimation of the number of proteins that was present in the

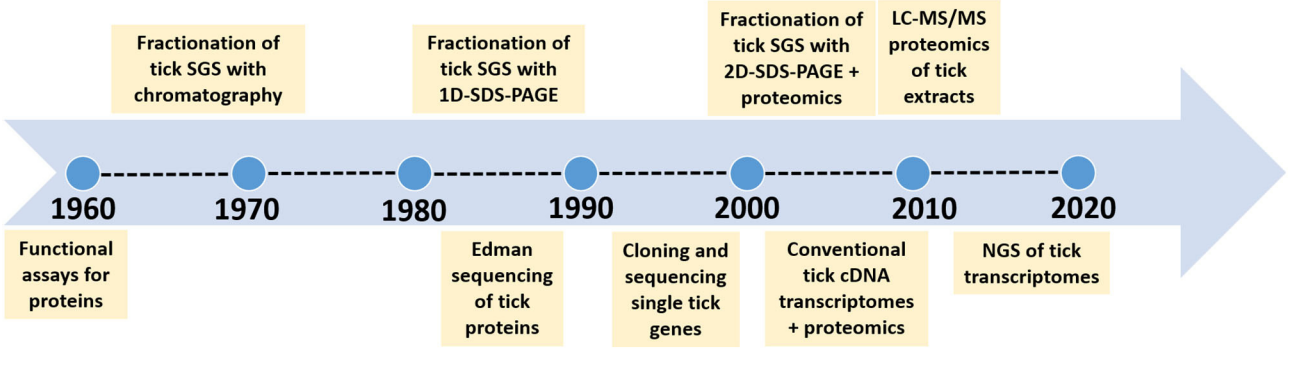

FIGURE 1 | Time line to indicate the major technological advances that improved our estimation of complexity of salivary gland proteins.

SGS is dependent on counting protein peaks with corresponding assumptions regarding the complexity of protein numbers within such peaks. Looking at the work of Neitz et al. (1969) in retrospect and doing back of the envelope estimations suggest a low complexity mixture of <100 proteins. For this specific tick species, even with modern HPLC methods, 1-dimensional sodium dodecyl sulfate poly-acrylamide electrophoresis (1D-SDS-PAGE), or 2-dimensional SDS-PAGE (2D-SDS-PAGE), and using SGE rather than SGS (SGE contain both secretory and non-secretory proteins, while SGS should be more abundant in secretory proteins), the complexity estimates did not change much (Gaspar et al., 1995, 1996; Mans et al., 2001, 2002a; Mans and Neitz, 2004a). For other soft tick species the generalization that <200 proteins may be observed in SGE using HPLC, 1D-SDS-PAGE or 2D-SDS-PAGE also holds (Oleaga et al., 2007; Francischetti et al., 2008a,b; Mans et al., 2008).

For the hard tick *Amblyomma hebraeum* (Koch, 1844) (South African Bont tick), chromatography and microzone electrophoresis suggested a low complexity mixture (Neitz and Vermeulen, 1987). However, it should be noted that the latter study again used SGS from a single feeding stage (partially fed). Whether SGS obtained from chemical induction represents salivary gland complexity has been addressed previously (Mans, 2019), and reservations exist whether such a secretion can be used as accurate measurement of salivary gland protein complexity, since different stimulants results in different proteins secreted (Oliveira et al., 2013).

COMPLEXITY MEASUREMENT BY CHROMATOGRAPHIC FRACTIONATION, EDMAN AND GENE SEQUENCING

Chromatographic fractionation of whole body, SGS or SGE enabled purification of proteins for functional characterization, while development of automated Edman degradation allowed for the first N-terminal amino acid sequences generated for tick salivary gland proteins (Neitz et al., 1983). This approach allowed for the full-length Edman sequencing of a variety of small anticoagulants and platelet aggregation inhibitors (Waxman et al., 1990; Karczewski et al., 1994; Wang et al., 1996). Generation of N-terminal or internal Edman sequences also allowed for the design of degenerate primers or probes that enabled cloning of gene sequences (Keller et al., 1993; Waxman and Connolly, 1993; Gaspar et al., 1996; Joubert et al., 1998; Nienaber et al., 1999; Paesen et al., 1999; Bergman et al., 2000; Valenzuela et al., 2000; Mans et al., 2001, 2002b,c, 2003; Narasimhan et al., 2002; Mulenga et al., 2003). This approach led to generation of ∼30 tick salivary gland sequences by 2003. Our insights into salivary gland complexity were heavily skewed at this point in time by the limited number of functions known (Mans and Neitz, 2004b). Even so, we still remain with very few empirically confirmed functions to date (Mans, 2019), although function assignment by homology allowed thousands of potential functions to be assigned to tick proteins (Mans et al., 2016; Pienaar et al., 2018; Ribeiro and Mans, 2020).

COMPLEXITY MEASURED BY COUNTING BANDS

The development of high resolution 1D-SDS-PAGE by Laemmli (1970) ushered in a new era of estimating complexity, allowing in theory to differentiate proteins with molecular mass differences of <1,000 Da. Linked with high resolution gel photography, this led to the first glimpses of salivary complexity in the Lone Star tick *Amblyomma americanum* (Linnaeus, 1758) (McSwain et al., 1982). This study was significant, since it analyzed changes in protein patterns over the course of feeding and showed that differential expression does indeed occur. Counting of the bands indicated at least 100 proteins with different molecular masses. Other studies soon followed with similar estimates in complexity for *A. hebraeum,* the brown ear tick *Rhipicephalus appendiculatus* (Neumann, 1901) and the red-legged tick *Rhipicephalus evertsi evertsi* (Neumann, 1897; Neitz and Gothe, 1986; Viljoen et al., 1986; Wang and Nuttall, 1994; Wang et al., 1999, 2001). At this point in time 1D-SDS-PAGE promised a glimpse at salivary gland protein complexity. However, our ability to identify these proteins with proteomics was not yet at a technological advanced level that would enable this (Rabilloud, 2020). The limitation of 1D-SDS-PAGE to reveal complexity was also limited by the resolution afforded and the fact that members of the same protein family would have very similar molecular weights, even if they have different iso-electric points resulting in underestimation of complexity. As such, 100 bands may very well indicate a 100 protein families rather than a 100 proteins.

COMPLEXITY MEASURED BY COUNTING SPOTS AND IDENTIFICATION BY PROTEOMIC ANALYSIS

The advent of 2D-SDS-PAGE that included iso-electric focusing in the first dimension followed by 1D-SDS-PAGE in the second dimension (O'Farrell, 1975), again revolutionized the concept of fractionation of complex mixtures. This produced protein expression maps that correlated with protein iso-electric point and molecular weight represented by spots on a gel. In ticks, the first 2D-SDS-PAGE images were published in 2001 for the deer tick *Ixodes scapularis* (Say, 1821) and *O. kalahariensis* (Das et al., 2001; Mans et al., 2001). Analysis of female tick salivary gland extract from *O. kalahariensis* indicated ∼100 proteins on a 2D-electropherogram. The major proteins present in this electropherogram could be confirmed to be soft tick proteins based on protein purification, peptide mass fingerprinting and tick sequences obtained via painstaking single gene sequencing (Mans et al., 2001; Mans and Neitz, 2004a). The 2D-electropherogram for *I. scapularis* revealed almost 500 spots in SGE (Das et al., 2001), and this complexity was again confirmed (Narasimhan et al., 2007). This latter study also indicated that the proteome changes over the time of feeding using Differential 2D Fluorescence Gel Electrophoresis (DIGE).

The first 2D-SDS-PAGE followed by proteomic analysis was performed for the SGS of *A. americanum* and the Gulf Coast tick, *Amblyomma maculatum* (Koch, 1844) (Madden et al., 2002). This

revealed ∼100–200 protein spots on the 2D-electropherogram. Surprisingly, the majority of spots reacted with anti-sheep serum suggesting that they were host derived. Of 16 prominent spots picked for peptide mass fingerprinting, one spot was identified as a tick protein and five spots as host proteins. It should be considered that at this point only 20 protein sequences were available for *A. americanum* and only 287 tick proteins were present in Genbank, which may explain the low number of tick proteins identified. This highlighted the impact that the lack of sequence coverage may have on proteomic detection. Other factors that limited the use of 2D-SDS-PAGE as method for saliva analysis is the high salt concentration found in tick saliva that necessitate extra desalting steps (Madden et al., 2002).

COMPLEXITY MEASURED BY CDNA LIBRARY SEQUENCING AND PROTEOMICS

The advent of complementary DNA (cDNA) library synthesis (Chenchik et al., 1996; Lukyanov et al., 1997) and propagation as unique clones using phage packaging (Kretz et al., 1989), allowed direct sequencing of mRNA derived genes that gave new insight into salivary gland and transcriptome complexity (**Table 1**). The first cDNA libraries constructed were expression libraries used to identify antigenic proteins recognized by host antiserum and subsequent sequencing of immunogenic clones (Das et al., 2000, 2001; Bishop et al., 2002). This yielded 14 immunogenic sequences for *I. scapularis* (Das et al., 2001). Larger scale, studies identified 895 immuno-proteins using similar approached in *A. americanum* (Radulović et al., 2014). Alternative approaches included the use of probes to screen a cDNA library for homologous genes (Sangamnatdej et al., 2002).

The first tick salivary gland cDNA libraries synthesized and systematically sequenced using Sanger sequencing yielded 36 sequences for the castor bean tick *Ixodes ricinus* (Linnaeus, 1758) and 87 sequences for *I. scapularis*, respectively (Leboulle et al., 2002; Valenzuela et al., 2002a). The latter study also identified 19 tick proteins and 2 host proteins using Western blot analysis followed by Edman sequencing and used these sequences to identify corresponding cDNA sequences (Valenzuela et al., 2002a). This already highlighted the importance of having species specific transcriptome sequences available. It also indicated the utility of cDNA library sequencing, when the same cDNA data was used to predict function by homology and subsequent functional characterization of recombinant proteins, leading to the discovery of the anti-coagulant Ixolaris (Francischetti et al., 2002) and a fibrinogenase metalloprotease (Francischetti et al., 2003). The study by Valenzuela et al. (2002a) was further significant in that it represented the first systematic high-throughput randomized sequencing of tick salivary gland cDNA clones (735 clones sequenced that clustered in 410 clusters and yielded 87 unique full-length sequences), that also attempted a systematic classification of salivary transcripts into groups or protein families (7 groups plus various singletons). Secretory proteins accounted for 102 clusters and 310 of the clones sequenced. It also introduced for the first time the term sialome (from the Greek σίελος = saliva) to describe the set of mRNA and proteins expressed in the salivary glands of ticks. A novel algorithm of deconvoluting Edman sequences obtained from crude SGE fractionated on 1D-SDS-PAGE was also presented, that allowed mixed Edman sequences to be matched to the transcriptome (Valenzuela et al., 2002b). This technique was subsequently successfully used in various transcriptome studies to identify abundant proteins (Francischetti et al., 2008a,b, 2011; Mans et al., 2008; Ribeiro et al., 2011).

Shortly after this groundbreaking study, more studies started to report on systematic conventional cDNA library transcriptome Sanger sequencing. For the Tropical Bont tick, *Amblyomma variegatum* (Fabricius, 1794), the salivary gland transcriptome was presented as the AvGI (*A. variegatum* gene index) and sequenced 3,992 clones of which 2,109 was non-redundant and 822 showed similarity to sequences in the database (Nene et al., 2002). No proteomics was performed, and no systematic classification presented, although a high-level gene ontology was assigned. A number of years later the same dataset was re-analyzed with the aim at classifying the genes and resulted in 3,985 EST sequences clustering into 2,077 contigs, of which 605 was submitted to Genbank (Ribeiro et al., 2011). The secretory proteins (379) were classified into 21 groups or families and a 1D-SDS-PAGE fractionation of SGE, from which 24 bands were analyzed by proteomics resulted in the identification of 170 proteins that represented 28% of the EST database submitted to Genbank.

For *R. appendiculatus*, 9,162 clones from an uninfected cDNA library and 9,844 clones from a *Theileria parva* infected cDNA library were sequenced (Nene et al., 2004). This resulted in 7,359 non-redundant sequences. Secretory genes were not classified in any systematic manner although gene ontology was presented. No proteomics was performed. This was followed by the *Rhipicephalus microplus* (Canestrini, 1888) gene index (BmGI) (Asian Blue tick) that was a whole body transcriptome where 11,590 clones were sequenced from a normalized cDNA library resulting in 8,270 unique sequences (Guerrero et al., 2005). A proteomic analysis of larval extract fractionated using 2D-SDS-PAGE, from which 20 spots were selected resulted in 18 proteins being identified (Untalan et al., 2005). This indicated the utility of a representative species specific transcriptome databases.

The salivary gland transcriptome of the Western-Blacklegged tick, *Ixodes pacificus* (Cooley and Kohls, 1943) was constructed via sequencing of only 1,068 clones that clustered into 557 contigs (Francischetti et al., 2005). Even though few clones were sequenced, classification of secretory proteins still resulted in 15 groups and 83 secretory proteins, creating the notion that the most abundant proteins and therefore those most important for feeding would still be represented in small scale transcriptome sequencing projects. However, a project that sequenced 8,150 clones from *I. scapularis* from nymphs and adults from various feeding stages resulted in 3,020 contigs and 863 unique secretory proteins (Ribeiro et al., 2006). This study was the first indication that secretory proteins may be present at levels of more than 500 proteins and possibly extending into thousands, suggesting that tick salivary gland diversity may be much more extensive than previously expected. The transcriptome for *I. ricinus* was also

TABLE 1 | Statistics for conventional cDNA library sequencing.

Species	Clones	Clusters	Genbank	Secretory	Proteomics	Proteomic coverage (%)	References
Ixodes ricinus	96	27	29	–	–	–	Leboulle et al., 2002
Ixodes scapularis	735	410	87	102	19 tick; 2 host	21.8	Valenzuela et al., 2002a
Amblyomma variegatum	3,992	2,109	–	–	–	–	Nene et al., 2002
Rhipicephalus appendiculatus	19,006	7,359	19,046	–	–	–	Nene et al., 2004
Rhipicephalus microplus	11,590	8,270	–	–	–	–	Guerrero et al., 2005
Ixodes pacificus	1,068	557	120	83	–	–	Francischetti et al., 2005
Ixodes scapularis	8,150	3,020	514	863	–	–	Ribeiro et al., 2006
Dermacentor andersoni	1,440	762	1,270	239	–	–	Alarcon-Chaidez et al., 2007
Ornithodoros parkeri	1,529	649	158	130	37	23.4	Francischetti et al., 2008a
Ornithodoros coriaceus	1,089	726	105	127	39	37	Francischetti et al., 2008b
Argas monolakensis	3,087	1,472	193	127	35	18.1	Mans et al., 2008
Ixodes ricinus	1,881	1,274	511	129	–	–	Chmelar et al., 2008
Amblyomma americanum	6,160	4,577	141	193	–	–	Aljamali et al., 2009
Rhipicephalus sanguineus	2,034	1,024	217	219	21 tick; 56 host	9.7	Anatriello et al., 2010; Oliveira et al., 2013
Amblyomma variegatum	3,992	2,077	605	379	170	28.0	Ribeiro et al., 2011
Hyalomma rufipes	2,084	1,167	98	255	72 tick, 22 host	73.4	Francischetti et al., 2011
Antricola delacruzi	1,147	923	38	115	–	–	Ribeiro et al., 2012
Amblyomma americanum	15,390	12,319	14,958	–	–	–	Gibson et al., 2013

Indicated are the tick species, the number of clones sequenced by Sanger sequencing, the non-redundant clusters obtained after clusterization of sequenced clones, final number of genes submitted to Genbank, the number of secretory proteins detected, the number of tick or host proteins detected using proteomics and the proteomic coverage in percentage of proteins detected relative to the genes submitted to Genbank. Transcriptomes are organized based on publication date.

described from four different cDNA libraries (unfed, 24 h after attachment, 4 days—partially fed and 7 days—fully engorged) (Chmelar et al., 2008). A total of 1,881 clones were sequenced that clustered into 1,274 clusters of which 511 was submitted to the nucleotide database. Of these 129 was classified as secretory.

Alarcon-Chaidez et al. (2007) described the salivary gland transcriptome of the Rocky Mountain Wood tick, *Dermacentor andersoni* (Stiles, 1908). The study sequenced 1,440 clones that clustered into 762 unique sequences. Of these ∼75% found homologs in the existing databases. The salivary gland transcriptome for *A. americanum* was described by Aljamali et al. (2009). A total of 6,160 clones were sequenced from both non-normalized and normalized libraries and clustered in 4,577 contigs. Of these 141 were submitted as proteins to Genbank. Reanalysis of the nucleotide sequences identified 193 secretory proteins in the dataset (Mans et al., 2016). A follow up study sequenced 15,390 clones that yielded 12,319 unique sequences (Gibson et al., 2013). The study observed that 71% of all sequences generated could not be annotated by function assignment by homology. Possible reasons presented were divergence in the tick lineage, the presence of lineage specific genes and limited genomic resources for ticks that would allow homology assignment. The study did not attempt to assign these genes to secretory families and the high level of non-homologous orphan sequences that did not find any hits to other tick sequences remain surprising.

Anatriello et al. (2010) described the salivary gland transcriptome of the brown dog tick, *Rhipicephalus sanguineus* (Latreille, 1806) and sequenced 2,034 clones that yielded 1,024 non-redundant sequences. Secretory proteins comprised 219 sequences and were classified into 12 protein family classes. A proteomic study was performed of saliva collected by either dopamine or pilocarpine stimulation (Oliveira et al., 2013). Saliva was fractionated on 1D-SDS-PAGE, bands were excised, followed by tryptic digestion and nanoflow reversed-phase liquid chromatography tandem mass spectrometry (nanoRPLC-MS/MS). The transcriptome database previously generated was used for analysis. The protein profiles obtained with dopamine or pilocarpine stimulation differed significantly with pilocarpine stimulation obtaining more bands. For dopamine stimulation only two lipocalins could be identified. For pilocarpine stimulation, 56 rabbit proteins were identified and only 19 tick proteins. Some of the rabbit proteins may have close homologs in ticks, although 16 rabbit proteins were detected that would be mammal specific. Of interest, is that the lipocalins secreted with dopamine were not found in the pilocarpine secretion, which raised again the question regarding representation of secretory proteins obtained with chemical stimulants.

The final ixodid sialome to be analyzed and described in a systematic manner using conventional cDNA sequencing was for the coarse bont-legged tick, *Hyalomma rufipes* (Koch, 1844) (Francischetti et al., 2011). A total of 2,084 clones were sequenced, clustered into 1,167 contigs of which 255 were classified as secretory and 98 proteins were submitted to Genbank. From 20 1D-SDS-PAGE bands analyzed by MS/MS, 72 tick proteins were identified as well as 22 host proteins. The identified proteins comprised 73.4% of the proteins submitted to Genbank.

By 2006 ∼12 soft tick salivary gland proteins have been functionally characterized and single genes cloned and sequenced. No salivary gland transcriptomes was systematically described up to this point for soft ticks. A proteomic analysis of SGE from *Ornithodoros erraticus* (Lucas, 1849) and *Ornithodoros moubata* (Murray, 1877), the African hut tampan, based on the proteins then present in the databanks underscored the importance of having species specific transcriptome databases necessary for proteomic analysis (Oleaga et al., 2007). For *O. moubata*, 48 non-redundant proteins were present in the databank and for 40 2D-SDS-PAGE spots analyzed only two proteins (TSGP1 and moubatin) could be identified. For *O. erracticus*, no proteins were available in the databanks and from 54 spots analyzed only 7 proteins were identified. In a follow-up study proteomic analysis of saliva from *O. moubata* was performed using *in situ* tryptic digest followed by liquid chromatography-MS/MS (LC-MS/MS) (Díaz-Martín et al., 2013). At this point in time 75 sequences were available in the databanks for *O. moubata* and proteomic analysis identified 193 proteins. Of these, 99.9% of the protein abundance was accounted for by the major lipocalins: TSGP1, TSGP4, and moubatin, while the remaining 0.1% abundance was accounted for by housekeeping proteins similar to sequences from ticks and insects in the database. The presence of housekeeping proteins may be explained by apocrine secretion or perhaps even salivary gland cell degradation given the low abundance found (Mans et al., 2016). As indicated before, the functional provenance of these low abundance proteins at the tick feeding site needs to be confirmed (Mans, 2019).

In 2008, three argasid salivary transcriptomes were reported for the Mono Lake bird tick *Argas monolakensis* (Schwan et al., 1992), the pajaroello tick *Ornithodoros coriaceus* (Koch, 1844) and the relapsing fever tick *Ornithodoros parkeri* (Cooley, 1936) (Francischetti et al., 2008a,b; Mans et al., 2008). For *A. monolakensis*, 3,087 clones were sequenced and clustered to give 1,472 contigs of which 127 was classified as secretory and 193 proteins were submitted to Genbank (Mans et al., 2008). Analyses of 78 2D-SDS-PAGE spots identified 18 spots and 14 proteins, 14 bands analyzed by Edman sequencing identified 13 proteins, and 116 peaks obtained from HPLC fractionation identified 52 peaks and 27 proteins, resulting in a final number of 35 proteins identified. This comprised 18% of the contigs coding for housekeeping and secretory proteins and 40% of the protein samples analyzed. For *O. coriaceus*, 1,089 clones were sequenced, resulting in 726 contigs, 127 classified as secretory and 105 proteins submitted to Genbank. Edman sequencing of 1D-SDS-PAGE fractions identified 3 proteins, analysis of 60 2D-SDS-PAGE spots identified 7 proteins and proteomic MS/MS analysis of 61 bands from 1D-SDS-PAGE analysis identified 37 proteins, resulting in a final number of 39 proteins (Francischetti et al., 2008b). This comprised 37% of the contigs submitted to Genbank. For *O. parkeri*, 1,529 clones were sequenced, resulting in 649 contigs and 158 proteins submitted to Genbank (Francischetti et al., 2008a). Edman sequencing of 1D-SDS-PAGE bands identified 12 proteins, analysis of 60 2D-SDS-PAGE spots identified 11 proteins and proteomic MS/MS analysis of 51 bands from 1D-SDS-PAGE analysis identified 30 proteins, resulting in a final number of 36 proteins (Francischetti et al., 2008a). This comprised 22.7% of the contigs and 42% of the proteomic fractions analyzed. All of the proteins were secretory and the majority belonged to the 5′-nucleotidase (apyrase), basic pancreatic trypsin inhibitor (BPTI), basic tails secretory (BTSP), cystatin, and lipocalin families.

The results obtained for the argasid sialomes indicated that conventional cDNA libraries sequenced at low levels may not represent all proteins present, but that the proteome also do not represent all transcripts found in the sialome. It also indicated that different methodologies may identify different protein sets and are therefore complementary. Even so, it also made the case that specific transcriptomes contribute toward a higher rate of protein identification. It also indicated that for all of these sialomes the major abundant proteins identified were classified as secretory, notably belonging to the BPTI, BTSP and lipocalin families. It also suggested that soft tick sialomes may represent lower complexity than ixodids. Reasons for this may be traced to the short feeding events of soft ticks, where feeding occurs within a few minutes to hours rather than days (Mans and Neitz, 2004b). This result in secretion of a bolus of salivary material and not the differential expression patterns observed for ixodid ticks (McSwain et al., 1982; Wang and Nuttall, 1994).

The salivary transcriptome for female *Antricola delacruzi* (Estrada-Peña et al., 2004) was also described using conventional cDNA library sequencing (Ribeiro et al., 2012). A total of 1,147 clones were sequenced, resulting in 923 contigs, 115 annotated as secretory proteins with 38 proteins submitted to Genbank. The transcriptome differed completely from those of other soft tick species where the major soft tick protein families are BPTI, BTSP and lipocalin families. Instead, ferritin, mucins with chitin-binding domains and TIL-domain-containing proteins were abundant. A reason for this may lie in the fact that *Antricola* adults do not feed on blood. The larvae and possibly nymphs do feed on blood (Estrada-Peña et al., 2008), and it may be expected that these life stages may present the more canonical protein families found in blood-feeding argasids.

Conventional Sanger sequencing of cDNA libraries to generate insights into salivary gland transcriptome composition contributed tremendously to our knowledge of salivary gland complexity, even if in the final analysis it became clear that this approach was not exhaustively descriptive or quantitative. This period saw the classification of secretory salivary gland proteins into well-described families (Francischetti et al., 2009), the detection and description of abundant secretory proteins and the observation that protein families are conserved among tick families. It showed that ticks possess their own lineage specific protein repertoires, that gene duplication plays a significant role in creating lineage specific expansions and that the salivary gland protein repertoire may be much more complex than we expected originally (Mans et al., 2008). The data contributed to our ability to detect and identify salivary proteins by proteomic analysis and showed that species-specific sequence databases are crucial for proteomic identification. Where transcriptome data was available, a significant number of genes in the transcriptome could be confirmed by proteomics. This was

a golden age in salivary gland discovery and we may have happily continued with this low-level description if the next revolution in sequence technology did not occurred, namely next-generation sequencing.

COMPLEXITY MEASURED BY NEXT-GENERATION SEQUENCING OF TRANSCRIPTOMES AND PROTEOMICS

The ability to generate automated high-throughput sequence data that was independent of cDNA library construction was made possible by the development of a wide variety of next-generation sequencing technologies that included Roche 454, Ion Torrent, Illumina HiSeq, and MiSeq technologies (Levy and Myers, 2016). These technologies purified mRNA directly, fragmented and directly sequenced all fragments at the same time resulting in large datasets with millions of reads. The reads are then assembled into contigs using a variety of next-generation algorithms (Martin and Wang, 2011). It enables the complete *de novo* assembly of a whole transcriptomes in the absence of any genome data. It also has the advantage that sequence depth may be converted into sequence coverage, giving an indication of transcript abundance and differential expression.

The first tick salivary gland transcriptome sequenced using these technologies was for *A. maculatum* using the Roche 454 GS FLX titanium pyrosequencing (Karim et al., 2011). The run generated 1,626,969 reads with an average length of 344 bp. An initial 190,646 contigs were assembled, but were reduced to 72,441 using a size cut-off above 149 bp. A final number of 15,814 were analyzed of which 4,849 were submitted to Genbank. An astounding 3,475 secretory proteins were identified with 304 members of the lipocalin family, the latter comprising almost the number of secretory proteins previously found in conventional cDNA libraries. These numbers were orders of magnitude higher than any transcriptome previously produced and hinted a depth of complexity not previously imagined.

The next transcriptome to be described was for *I. ricinus* using a combination of Roche 454 and Illumina technology (Schwarz et al., 2013). For Roche 454, 441,381 reads were generated and for Illumina an astounding 67,703,183 reads for the time. Assembly of the combined reads resulted in a total of 272,220 contigs reduced to 82,907 after a size and coverage cutoff. Of these 34,560 were annotated and 8,586 submitted to Genbank. Of the 82,907 contigs, 13% where classified as secretory and of the Genbank sequences, 3,882 was classified as secretory proteins and an astounding 564 as lipocalins. A follow up study expanded the read coverage by 315 million additional reads that were combined with the previous studies reads to generate a new assembly from which 25,808 contigs were extracted (Schwarz et al., 2014). The study also included midgut transcriptomes and focused on the first 24 h of feeding. These contigs were used for proteomic analysis of SGE and identified 1,510 proteins from nymphs and adults at 12, 24, and 36 h post-attachment. This is an impressive improvement in proteome coverage compared to number of proteins identified using conventional cDNA libraries. However, the direct digestion of SGE without fractionation may have influenced the total number of proteins detected since crude SGE presents a very high complexity mixture. The transcriptome and proteome data did not correlate with regards to abundance or relative changes, even though biological and technical replicates showed good correlation. Interestingly, the proteomes for the salivary gland and midgut did not differ significantly and ∼60% of all proteins did not show any variation in abundance over all time periods sampled. This may reflect that proteomics detect many housekeeping proteins in addition to secreted proteins. Transcriptome levels varied more suggesting transcriptional changes not reflected in the proteome. A sister study classified the same 25,808 contigs according to function and protein family composition as well as for differential expression (Kotsyfakis et al., 2015). This study indicated significant differences in transcript expression profiles between salivary gland and midgut samples. Transcript expression profiles also change over feeding time for different protein families suggesting that "gene switching" occur. It has been suggested that this is a possible way to evade the immune system of the host. In addition, the study indicated higher levels of non-synonymous substitution in secretory proteins suggesting that this indicate higher rates of positive selection.

In a follow up study for *I. ricinus*, transcriptomes from single tick salivary glands were generated (Perner et al., 2018). Salivary glands were sampled from ticks fed on rabbits or artificial membranes at 24, 48, and 72 h. Approximately 435 million Illumina paired reads were generated from 18 libraries and assembled with Illumina reads previously generated in other studies and 40,490 coding contigs were extracted and a final 20,773 contigs with RPKM $>$ 10 were annotated. The study identified 1,907 novel protein sequences of which 406 were identified as secretory. The study indicated that individual ticks show differential expression between ticks and over the course of a blood-meal.

The sialotranscriptomes for three different *Amblyomma* species from Brazil were sequenced using pyrosequencing (Garcia et al., 2014). For *Amblyomma parvum* (Aragão, 1908) 104,817 reads were generated with a final number of contigs of 3,796 of which 493 was annotated as secreted. For *Amblyomma cajennense* (Fabricius, 1787) 67,677 reads were generated with a final number of contigs of 4,604 of which 1,015 was annotated as secreted. For *Amblyomma triste* (Koch, 1844) 442,756 reads were generated with a final number of contigs of 11,240 of which 1,861 was annotated as secreted.

Next-generation sequencing of *A. americanum* sampled unfed, 12, 18, 24, 36, 48, 72, 120, 144, 168, 192, 216, and 264 h after attachment and generated a total of 344,909,378 paired reads (Karim and Ribeiro, 2015). Assembly resulted in a final number of 5,792 contigs that was analyzed. Of these, 2,153 were classified as secretory. Significant differences in transcript levels were observed over the course of feeding, supporting differential expression and the concept of sialome switching was introduced to suggest that the tick switch between different transcriptomes during the course of feeding.

For the zebra tick, *Rhipicephalus pulchellus* (Gerstäcker, 1873) 241,229,128 paired Illumina reads were generated from salivary

glands of males and females that were unfed or fed for 1, 3, and 7 h as well as 1, 2, 3, 4, 5, 6, and 7 days (Tan et al., 2015). Assembly resulted in 50,460 coding sequences of which 7,134 was secretory. Proteomics was performed using SGE and *in situ* trypsin digestion followed by LC-MS/MS. This identified 2,231 proteins of which 221 were secretory. Significant differences in transcriptome and proteome expression were observed between males and females.

For *Haemaphysalis flava* (Neumann, 1897), engorged and semi-engorged female salivary glands were used to generate 162,912,848 paired reads, which after assembly yielded a final number of 54,357 contigs (Xu et al., 2015). Of these, 20,145 had homologs in Genbank and 13,513 could be assigned GO terms. Secretory proteins were not reported.

The salivary gland transcriptomes for brown ear ticks, vectors of *T. parva*, the causative agent of Corridor disease, East Coast fever and Zimbabwe theileriosis were described (de Castro et al., 2016, 2017). For *R. appendiculatus,* 430 million paired reads were generated with a final contig number of 21,410 contigs of which 13,996 coded for proteins, of which 2,135 were secretory proteins and 7,414 were annotated as long non-coding RNA. For *R. zambeziensis* (Walker et al., 1981), ∼190 million paired reads were generated, assembled and resulted in 140,703 transcripts. After a FPKM > 1 cut-off a final contig number of 23,631 transcripts were obtained of which 15,737 were coding for proteins of which 2,569 were classified as secretory.

For *Amblyomma sculptum* (Berlese, 1888), fed and unfed ticks were sampled and ∼567 million single reads were generated (Esteves et al., 2017). Assembly resulted in 9,560 contigs of which 2,314 secretory proteins were found in unfed and 2,592 in the fed transcriptomes. Proteomic analysis identified 124 proteins in saliva of which 58 were secretory. Another study on *A. sculptum*, assembled 195,594,989 Illumina paired reads, 844,529 Ion Torrent reads and 703,210 Roche 454 reads that derived from *Rickettsia amblyommii* infected and uninfected organs that included ovaries, midguts and salivary glands (Moreira et al., 2017). Assembly resulted in 460,445 contigs of which 27,308 were selected for annotation. Of these 2,177 were annotated as secreted salivary gland proteins.

For *Hyalomma excavatum* (Koch, 1844), 138,144,530 Illumina paired reads were generated (Ribeiro et al., 2017). After assembly, 53,228 contigs were obtained and 7,875 coding sequences were annotated with 1,796 classified as secretory. For the camel tick, *Hyalomma dromedarii* (Koch, 1844), male and female ticks at different stages of engorgement were collected from camels in the field (Bensaoud et al., 2018). Illumina sequencing generated 330,285,649 paired-end reads of which 55,819,366 were assembled. After PFAM filtering, 15,342 contigs were annotated of which 1,749 was classified as secretory. The transcriptome study was followed up with proteomic analysis of SGE from ticks collected in the field (Bensaoud et al., 2019a,b). Fractionation of SGE was performed using 1D-SDS-PAGE, after which bands were cut-out, tryptic digested and analyzed using LC-MS/MS. As a target database for the proteomic study, the sialotranscriptome previously generated was used in addition to Acari sequences from Genbank. This identified 1,111 proteins of which 854 were from the Acari database and 257 from the species-specific database. Only 24% of proteins were shared between males and females and 19% of proteins (∼211) were classified as secreted.

For *I. holocyclus*, semi-engorged ticks were collected from animals with confirmed paralysis symptoms, before salivary glands were dissected (Rodriguez-Valle et al., 2018). Illumina sequencing generated 65,035,631 paired reads that produced 134,039 contigs after assembly of which ∼3,149 was classified as secretory.

For the cattle tick *Rhipicephalus annulatus* (Say, 1821), engorged female ticks that were uninfected or infected with *Babesia bigemina* were used to construct salivary gland transcriptomes (Antunes et al., 2019). Illlumina sequencing generated 40,573,988 paired reads that generated 33,379 contigs in the control and 30,435 contigs in the infected sample of which 16,564 and 15,037 gave significant BLAST hits, respectively. This was reduced to 6,823 and 6,475 unigenes, respectively. Proteomics identified 4,594 proteins in female tick extracts.

For *Amblyomma aureolatum* (Pallas, 1772), transcriptomes were generated from *Rickettsia rickettsii* infected and uninfected tissues (Martins et al., 2019). Approximately 242 million reads were generated of which 110 million were from salivary glands. Assembly generated 11,906 contigs of which 11,903 were expressed in salivary glands.

For the Asian longhorned tick, *Haemaphysalis longicornis* (Neumann, 1901), salivary gland transcriptomes were generated that resulted in 18,313 contigs. The transcriptome was not published, but were used for proteomic analysis with iTRAQ labeling to allow for differential quantification of salivary glands from ∼6,000 female ticks that was analyzed as unfed, partially fed, semi-engorged and engorged in three replicates (Ren et al., 2019). Replicate experiments identified 5,059, 5,526, and 5,584 proteins that resulted in 3,667 high-confidence proteins with 2,507 present in all replicates. The majority of proteins identified were housekeeping with significant upregulation of proteins observed during feeding.

A proteomic LC-MS/MS analysis of SGE were performed for the brown ear tick *Rhipicephalus bursa* (Canestrini and Fanzago, 1878) using the Ixodidae database from Genbank (Couto et al., 2020). SGE were prepared from unfed and fed females, which was also either infected, or not with *Babesia ovis*. A total of 1,586 proteins were identified even though only 35 proteins exist in Genbank for this tick species. The majority of proteins were housekeeping, which underscore the utility of sequence databases to identify homologous proteins, but also the impact of the absence of databases to identify species specific proteins.

Giachetto et al. (2020) generated salivary gland transcriptomes for engorged female *R. microplus* that was fed on tick-resistant or tick-susceptible hosts. The transcriptome was assembled from 74,639,552 reads (holstein cattle) and 63,013,658 reads (crossbreed cattle) resulting in 235,451 contigs. Of these 71,757 could be annotated by BLAST analysis but only 1,815 ORFs were extracted of which 20 could be annotated as secretory.

For *R. sanguineus*, female ticks were collected based on weight rather than just days and included unfed, 1.8 mg (day 2), 3.6 mg (day 6), 7.0 mg (day 6), 10.9 mg (day 8), 24 mg (day 8 and 11), 36 mg (days 6, 10, 13), and a sialotranscriptome was constructed (Tirloni et al., 2020). For 20 different libraries that included

replicates, 687 million reads were generated from which 71,643 coding sequences were obtained. These were further reduced to 28,921 transcripts with expression values that would represent a minimum of 0.001% of all transcripts based on TPM value (TPM $\geq$ 10). Of these 8,178 could be annotated with 4,039 identified as secretory proteins. From a similar time series, proteomic analysis of SGE was performed using LC-MS/MS and the transcriptome database generated. This identified 2,125 proteins of that showed a positive correlation between proteome and transcriptome abundance for those transcripts with TPM $>$ 10 (1,745 transcripts). Of 221 with positive correlation, 30% were secretory. A significant number of host proteins (47) were also identified in the SGE. Variability in expression, both in transcript and protein were less marked than previous studies, most probably since the feeding phases of the ticks were better correlated due to weight rather than time. The study again indicated differential expression and the sialome switching phenomenon, both at transcriptome and proteome level.

To date only one salivary gland transcriptome have been described for soft ticks from next-generation sequencing data, namely for *Ornithodoros rostratus* (Aragao, 1911) (Araujo et al., 2019). Salivary glands and midguts were collected from fourth instar nymphs that were unfed or 1 and 4 day fed. Sequencing generated 22,395,831 combined Illumina paired reads that were assembled into 40,058 contigs. Filtering based on ORFs generated a final set of 8,031 contigs that were annotated from which 717 proteins were classified as secretory. In contrast to hard ticks, the secretory proteins in the salivary glands were more abundant than housekeeping proteins and represented 67% of all reads. Another study also sequenced the salivary gland transcriptome of the relapsing fever tick, *Ornithodoros turicata* (Dugès, 1876), but did not describe the transcriptome in a systematic manner (Bourret et al., 2019). The study generated 15,136,406 single-end reads that generated 10,989 contigs after assembly, with 2,138 classified as secretory proteins.

It should be clear from the summary (**Table 2**) that large variations in data generated, numbers of contigs assembled, final contigs selected for annotation and the final number of contigs submitted to Genbank exists for salivary transcriptomes generated with next-generation sequencing. Given this large variation it may be safe to assume that the transcriptomes for salivary glands may not necessarily be representative of the full complement of proteins expressed in the salivary glands. Additionally, it is not yet clear whether the extremely high number of secretory genes found in the transcriptomes (that increase with each new sampling and sequencing effort) is due to artifacts or a tick-specific mechanism to generate genetic diversity (Mans et al., 2016; Ribeiro and Mans, 2020).

NEXT-GENERATION SEQUENCING OF WHOLE BODY TRANSCRIPTOMES

Whole body transcriptomes will by default contain salivary gland derived transcripts. In addition, whole body transcriptomes should at least in theory represent the total protein complexity found in a species at the time of sampling and may as such give a better idea on the upper limits of proteins that may be found in salivary gland transcriptomes.

For the ornate cow tick, *Dermacentor reticulatus* (Fabricius, 1794), 7 day unfed larvae were used to construct a transcriptome to investigate stress responses in larvae (Villar et al., 2014). A total of 18,946 transcripts were obtained that were reduced to 3,808 unigenes. Proteomics on larval extracts identified 74, 239 and 104 proteins using various approaches, respectively. The low number of proteins identified may be due to sample complexity or the reduction of proteins to unigenes that likely represented loss of paralogous genes. For *R. sanguineus*, a larval transcriptome was generated for descriptive purposes (De Marco et al., 2017). A total of 5,566,986 short paired-end reads generated 33,396 contigs after assembly and filtering that represented 16,555 unique genes. Dehydration stress in *D. variabilis* was investigated by sequencing unfed male ticks that was dehydrated (Rosendale et al., 2016). From six libraries, 271,494,907 reads were used for assembly that generated 61,800 contigs that were analyzed, of which ∼40,000 found BLAST hits. For engorged female *H. longicornis*, ∼53 million reads generated 65,916 contigs, of which 23,339 could be annotated (Niu et al., 2019). Whole body transcriptomes for larvae (64,474,326) and nymphs (81,612,022) were also generated (Guo et al., 2019). This resulted in 536,336 transcripts and 440,896 unigenes. Of these 22,347 and 15,112 were annotated by KOG and KEGG databases, respectively. For *I. ricinus*, 15 libraries were constructed for unfed and fed nymphs, unfed males, unfed and fed females (Charrier et al., 2018). From 162,872,698 reads 427,491 contigs were produced that were reduced to a non-redundant dataset of 192,050 contigs. Removal of mammalian and fungal contaminants resulted in 179,316 contigs. Of these 56,809 produced BLAST hits to the Uniref90 or Swissprot databases. Only 12,838 genes were shared with other *I. ricinus* transcriptome studies, while 36,652 were unique to this study and 23,686 was unique to other transcriptomes bringing the potential number of sequences to 73,176 genes. In a follow-up study, the whole body transcriptomes for a number of additional *Ixodes* species were generated for use in phylogenomic analysis using combinations of unfed or fed nymphs, males or females (Charrier et al., 2019). This included *Ixodes acuminatus* (Neumann, 1901) (n = 20,250), *Ixodes arboricola* (Schulze and Schlottke, 1930) (n = 22,179), *Ixodes canisuga* Johnston, 1849 (n = 15,238), *Ixodes frontalis* (Panzer, 1798) (n = 18,187), *Ixodes hexagonus* (Leach, 1815) (n = 3,215), *Ixodes holocyclus* (n = 15,520), *Ixodes uriae* (White, 1852) (49,056), *Ixodes ventalloi* (Gil Collado, 1936) (n = 16,563) and *Ixodes vespertilionis* (Koch, 1844) (n = 21,090) with the final number of contigs assembled indicated.

Whole body transcriptomes indicate that expected upper limits for salivary gland transcriptomes may range from ∼15,000–30,000 genes that can be annotated with our existing annotated databases. One major problem that may exist is overestimation of existing genes due to miss-assembly, such as insertions or deletion not due to exon-intron splicing, or extension of 5′ or 3′ ends that cause such genes to be identified as unique even though the rest of the gene is 100% identical to the canonical gene. While existing algorithms may identify and remove chimeric transcripts (miss-assembly due to linkage of

TABLE 2 | Statistics for salivary gland transcriptomes assembled using next-generation sequencing technologies.

Species	Total reads	Total contigs	Contigs after cut-off	Annotated	HKP	SEC	Genbank	References
Amblyomma maculatum	1,626,969	190,646	72,441	15,814	7,856	3,475	4,849	Karim et al., 2011
Ixodes ricinus	68,144,564	272,220	82,907	34,560	19,491	10,777	8,686	Schwarz et al., 2013
Ixodes ricinus	∼315 million	–	198,504	25,808	12,913	9,048	16,002	Schwarz et al., 2014; Kotsyfakis et al., 2015
Ixodes ricinus	∼435 million	–	40,490	20,773	–	–	7,692	Perner et al., 2018
Amblyomma parvum	104,817	–	–	3,796	2,653	493	2,838	Garcia et al., 2014
Amblyomma cajennense	67,677	–	–	4,604	2,805	1,015	5,770	Garcia et al., 2014
Amblyomma triste	442,756	–	–	11,240	6,854	1,861	8,098	Garcia et al., 2014
Dermacentor andersoni	632,267	21,797	–	21,769	–	–	–	Mudenda et al., 2014
Amblyomma americanum	344,909,378	–	–	5,792	3,465	2,153	3,139	Karim and Ribeiro, 2015
Rhipicephalus pulchellus	241,229,128	–	–	50,460	11,499	7,134	11,227	Tan et al., 2015
Haemaphysalis flava	162,912,848	70,542	55,760	54,357	–	–	–	Xu et al., 2015
Rhipicephalus appendiculatus	∼430 million	87,688	21,410	21,410	8,237	2,135	20,175	de Castro et al., 2016
Rhipicephalus zambeziensis	∼190 million	140,703	23,631	23,631	8,139	2,569	21,529	de Castro et al., 2017
Amblyomma sculptum	∼567 million	–	–	9,560	–	–	4,246	Esteves et al., 2017
Amblyomma sculptum	197,142,728	460,445	27,308	27,308	23,248	2,177	–	Moreira et al., 2017
Hyalomma excavatum	138,144,530	53,228	–	7,875	5,511	1,796	5,337	Ribeiro et al., 2017
Hyalomma dromedarii	55,819,366	142,391	–	15,342	8,063	1,749	142,391	Bensaoud et al., 2018
Ixodes holocyclus	65,035,631	134,039	–	134,039	7,975	3,149	95,717	Rodriguez-Valle et al., 2018
Amblyomma aureolatum	∼242 million	11,903	–	11,903			7,999	Martins et al., 2019
Rhipicephalus annulatus	40,573,988							Antunes et al., 2019
Ornithodoros rostratus	22,395,831	40,058	8,031	8,031	5,125	717	6,588	Araujo et al., 2019
Ornithodoros turicata	15,136,406	–	–	10,989	7,986	2,138	7,560	Bourret et al., 2019
Rhipicephalus microplus	137,653,210	235,451		71,757	–	20	–	Giachetto et al., 2020

Indicated are the total reads generated used in assemblies, the total number of contigs obtained after assembly, number of contigs obtained where a coverage or size cutoff was implemented, the number analyzed for annotation, the number identified as house-keeping (HKP) or secretory (SEC). The number of sequences coding for proteins or contigs deposited in Genbank is also indicated.

two canonical genes or fragments), identifying miss-assembled transcripts due to small inserts, deletions or extensions is more difficult with existing algorithms and require extensive manual curation.

PROTEOMICS OF TICK SALIVA

Apart from the studies mentioned above that specifically focused on salivary gland transcriptome descriptions with added proteomic analysis, some studies focused more specifically on the analysis of tick saliva using proteomics (**Table 3**). The salivary transcriptome of *D. andersoni* were sequenced using Roche 454 technology for the purpose of proteomic analysis (Mudenda et al., 2014). A total of 632,267 reads were generated at three time points (Day 0, Day 2, and Day 5). Assembly yielded 21,769 unique sequences coding for proteins. Each time point presented unique transcripts as well as up- or down-regulation of genes during the course of feeding. The study also collected saliva for day 2 and day 5 of feeding and fractionated this with 2D chromatography (in-line cation exchange linked with reversed phase) yielding 30 fractions analyzed by MS/MS. An impressive number of 677 proteins were detected.

Tirloni et al. (2014) performed proteomic analysis on saliva collected from partially and fully fed *R. microplus*. For this, saliva was fractionated on 1D-SDS-PAGE and 42 bands for partially engorged and 15 bands for fully engorged was excised, in-gel trypsin digested and analyzed on LC-MS/MS. Saliva was also directly digested *in situ* before LC-MS/MS analysis. Spectra were analyzed against an in-house database of 22,009 protein sequences. The study identified 187 tick and 68 host proteins. Another study that also compared saliva collected from partially and fully fed *R. microplus* by iTRAQ labeling followed by LC-MS/MS analysis, identified 322 unique proteins of which 41 was considered high-confidence and was found in both partially and fully fed samples (Feng et al., 2019).

Using a similar approach to Tirloni et al. (2014), performing *in situ* trypsin digestion of saliva from nymphs and adults from *H. longicornis,* followed by LC-MS/MS analysis, 135 tick and 100 rabbit proteins were identified (Tirloni et al., 2015). The authors used the in-house salivary gland transcriptome database of 22,009 sequences from *R. microplus* and the Ixodidae sequences from Genbank. In a study using a similar methodology that collected saliva from *I. scapularis* females at 24, 48, 72, 96, and 120 h as well as engorged and detached, a total of 769 tick and 130 rabbit proteins were identified (Kim et al., 2016). The NCBI non-redundant database (62,246 Ixodidae entries) were used for identification, rather than a species-specific database, since this database presumably presents the

TABLE 3 | Summary of proteomic analysis for tick salivary gland proteins using various technologies.

Species	Extract type	Technology	Tick Proteins	Percentage of Genbank	Species specific sequences in Genbank/Study	HKP	SEC	References
Ixodes scapularis	SGS	Edman	12	13.7	87	0	12	Valenzuela et al., 2002a
	SGE	Edman	11	12.6		4	7	
Ornithodoros erraticus	SGE	MALDI-MS	6	–	0	5	2	Oleaga et al., 2007
Ornithodoros moubata	SGE	MALDI-MS	2	4.1	48	0	2	Oleaga et al., 2007
Ornithodoros parkeri	SGE	Edman	12	7.6	158	0	12	Francischetti et al., 2008a
		1D-LC-MS	29	18.3		0	29	
		2D-LC-MS	11	6.9		2	9	
		Total	37	23.4		2	35	
Ornithodoros coriaceus	SGE	Edman	3	2.8	105	0	3	Francischetti et al., 2008b
		2D-LC-MS	7	6.6		0	7	
		1D-LC-MS	36	34.3		0	36	
		Total	39	37.0		0	39	
Argas monolakensis	SGE	Edman	14	7.2	193	0	14	Mans et al., 2008
		2D-LC-MS	14	7.2		0	14	
		LC-MS	28	14.5		0	28	
		Total	35	18.1		0	35	
Rhipicephalus sanguineus	SGS	1D-LC-MS	21	9.7	217	12	9	Oliveira et al., 2013
Amblyomma variegatum	SGE	1D-LC-MS	170	28.0	605	151	19	Ribeiro et al., 2011
Hyalomma rufipes	SGE	1D-LC-MS	72	73.4	98	75	23	Francischetti et al., 2011
Ornithodoros moubata	SGS	LC-MS	193	257.3	75	72	3	Díaz-Martín et al., 2013
Dermacentor andersoni	SGS	LC-MS	677	3.1	21,797	–	–	Mudenda et al., 2014
Rhipicephalus microplus	SGS	1D-LC-MS	187	–	22,009	41	145	Tirloni et al., 2014
Haemaphysalis longicornis	SGS	1D-LC-MS	135	–	–	106	29	Tirloni et al., 2015
Ixodes scapularis	SGS	1D-LC-MS	582	–	62,246	–	–	Kim et al., 2016
Amblyomma americanum	SGS	1D-LC-MS	1,182	–	110,587	–	–	Kim et al., 2020

Protein mixtures analyzed were obtained via induction of salivary gland secretion (SGS) or salivary gland extracts (SGE). Mixtures were analyzed by one-dimensional SDS-PAGE followed by blotting and Edman sequencing (Edman), matrix-assisted laser desorption ionization (MALDI-MS), one-dimensional SDS-PAGE from which bands were cut out for tryptic digest followed by MS/MS analysis (1D-LC-MS), or two-dimensional SDS-PAGE from which bands were cut out for tryptic digest followed by MS/MS analysis (2D-LC-MS), or salivary gland proteins fractionated using liquid chromatography followed by MS/MS (LC-MS).

most up to date collection of *I. scapularis* sequences derived from both the genome and transcriptomes. The authors indicate that protein profiles change over the course of feeding and suggest that this switching mechanism is used as immune evasion strategy. More recently, the saliva profile of *A. americanum* was determined using the *in situ* digestion, LC-MS/MS approach (Kim et al., 2020). Saliva was collected from ticks attached for 24, 48, 72, 96, 120, 144, 168, and 192 h, as well as engorged and detached. The database used was from sequences generated previously (Radulović et al., 2014). This transcriptome was reassembled from the datasets and generated 110,587 contigs used for analysis. This study identified 1,182 tick and 335 rabbit proteins.

From these studies, saliva complexity at any given point seems low and corresponds with roughly 200 proteins. Complexity increase with number of sampling points, since protein expression patterns change over time, but it would seem, also with the size of the species-specific database. With regard to sampling points, the current practice is to sample at 24 h intervals and protein expression patterns may change between sampling events, suggesting that change can occur within hours. At yet, it is not clear how fast this change can occur. Even so, not all proteins identified are secretory, but many are housekeeping and some host-derived (**Tables 1**, **3**). The numbers identified still do not correlate with the almost 10-fold larger number of transcripts identified in the transcriptomes (Mans et al., 2017). This would suggest that transcriptomes generate an over-estimation of complexity or that proteomic analysis are not yet technologically advanced to identify all proteins present in complex salivary mixtures.

The above sections detailed both transcriptome and proteomic studies since these are generally closely linked. It has been indicated that species-specific transcriptomes are essential for detection of lineage specific proteins and to increase proteome coverage. Even so, the use of proteomes to validate transcriptomes is just as valid. In a perfect world, each contig produced by a transcriptome sequencing project should be confirmed and validated by proteomic analysis, since proteins represents functional entities (Mans, 2019). However, the coverage of transcriptomes by proteomes has been dismal to date (**Figure 2**). In the case of transcriptomes derived from conventional cDNA libraries the transcriptome coverage detected by proteomics was decent, ranging from 10 to 73% (**Table 1**; **Figure 2**). This could be explained by the representation of highly abundant transcripts in relatively small transcriptomes, correlating with highly expressed proteins in

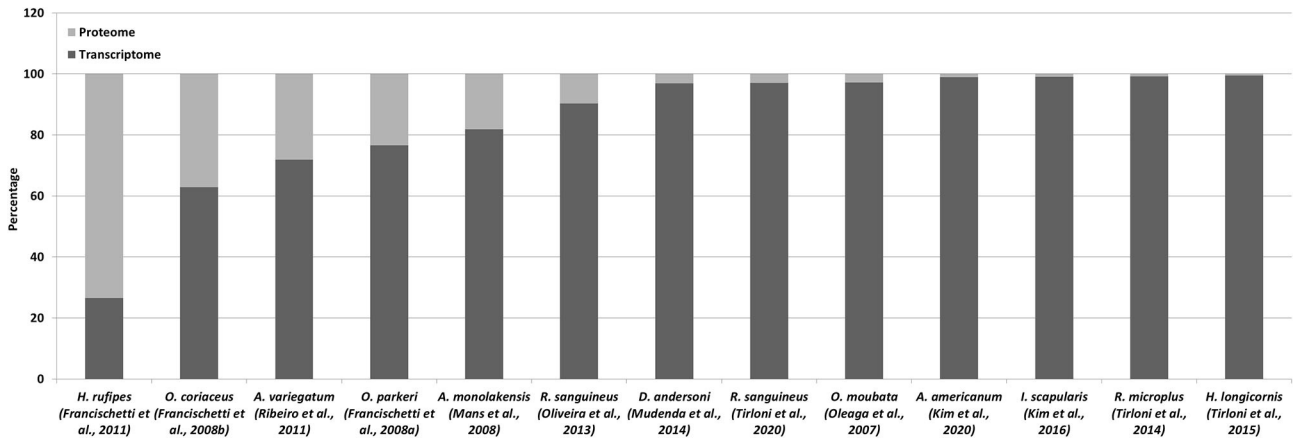

FIGURE 2 | Proteomics of tick transcriptomes. Indicated is the percentage of proteins identified using proteomics relative to the transcriptome database used for identification.

the proteome. As transcriptome sizes increased, the number of proteins detected in the proteome also increased, but not at the same ratio. As such, while proteins detected by proteomics may range in the thousands, the percentage of transcriptome coverage is lower compared to conventional cDNA derived transcriptomes (**Table 3**). The potential reasons for this are numerous. Proteomic technology may not yet be sensitive enough to obtain the depths attained by next-generation sequencing of transcriptomes. This may be linked to both hardware limitations of mass spectrometry equipment, but also to sample fractionation strategies. In regard to the latter, the more complex the sample, the lower the expected coverage that may be obtained. Fractionation of samples that decrease sample complexity but retain yields for low abundance proteins should yield higher detection numbers for proteins. The number of time points sampled for proteomics may impact on the number of proteins identified, with more sampling points yielding more proteins. Transcriptomes may present artifacts, i.e., transcripts that do not represent proteins present in a given sample. This may be due to misassemblies or transcription of pseudogenes that are not translated into protein (Mans et al., 2017).

PROTEOMICS OF TICK CEMENT

An integral part of salivary complexity is the cement cone produced by some *Ixodes* and metastriate ticks (Chinery, 1973; Suppan et al., 2018). These are proteins secreted in soluble form in the saliva that then harden to a matrix that can anchor the tick to the host during feeding. Analysis of the cement cone was historically difficult due to its insolubility. However, the use of chaotropic agents such as urea and SDS to solubilize the cement cone, followed by proteomic analysis have allowed a deeper insight into cement composition. For *A. americanum,* cement were dissolved in 8M urea followed by SDS-PAGE, before bands were cutout for proteomic analysis. This identified 7 proteins that included a glycine-rich and metalloprotease as well as proteins considered housekeeping using the *A. americanum* salivary transcriptome and tick database (Karim and Ribeiro, 2015; Bullard et al., 2016). A follow up study solubilized the cement cone in 8M urea, after which alkylation and tryptic digestion were followed with LC-MS/MS identification. This identified 160 proteins using an in-house *A. americanum* database (Porter et al., 2015; Hollmann et al., 2018). The proteins identified included as major proteins glycine-rich proteins and protease inhibitors as well as a large proportion of house-keeping proteins. A more recent study identified 654 proteins in urea+SDS extracted vs. 388 proteins in SDS vs. 266 proteins in urea alone from cement cones of *R. microplus* (Villar et al., 2020). The protein profile from cement was also termed the "cementome." The study also identified 2,264 proteins from salivary gland extract. Of the proteins identified in the cement only 81 seem to be tick-derived while the rest were host-derived. The tick proteins were composed of glycine-rich proteins, protease inhibitors and various enzymes proposed to play a role in cement formation, solidification and maintenance. Complexity of the cement cone therefore seem to increase as extraction methodologies improve. A question that obviously remain is how many proteins may be entrapped during cement formation that do not play a primary role in the cement plug.

THE COMPLETENESS OF SIALOTRANSCRIPTOMES

Next-generation sequencing technologies raised the problem of what would be considered to be true in transcriptomics. In all publications published to date several recurring issues may be observed. Assemblies lead to large numbers of contigs and cut-off values needs to be implemented to reduce the number of contigs analyzed. This is generally based on coverage, either RPKM or TPM values or a subjective selection of the cutoff value. While this result in more trustworthy final assemblies, it raises the question of the origin of those contigs that do not make the selection criteria. Are these assembly artifacts, background transcription artifacts, environmental contamination or contamination from other tick tissues?

To determine how representative a transcriptome is, the presence of expected household genes can be determined. The

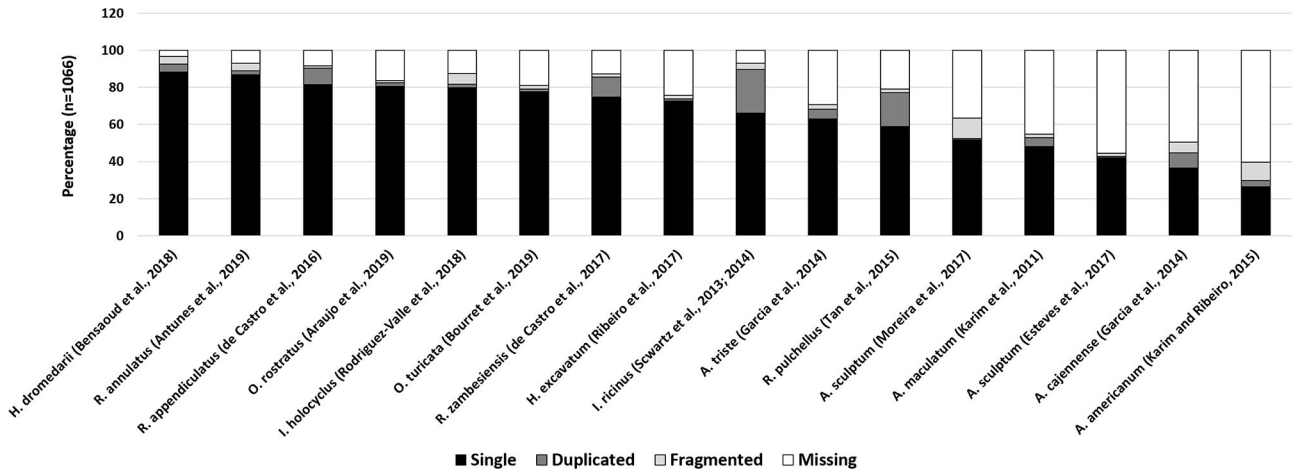

FIGURE 3 | BUSCO analysis of tick salivary gland transcriptomes. Indicated are various published tick transcriptomes and their BUSCO analysis. Complete genes were detected as single copies (single) or multiple copies (duplicated). Genes that are fragmented or missing are also reported.

"completeness" of this set may then be used as a proxy for the quality of a transcriptome. The program "Benchmarking Universal Single-Copy Orthologs or BUSCO" uses the concept of universal genes that are present as singletons in both genomes and transcriptomes (Waterhouse et al., 2018). BUSCO analysis of all published salivary gland transcriptomes generated with next-generation sequence technologies, indicate that the "completeness" of these transcriptomes ranges from 40 to 97% (**Figure 3**). This would imply that salivary transcriptomes have not been sequenced to depths necessary to recover all genes. However, as indicated above, the BUSCO scores may also have been influenced by the cut-off values used in post-assembly analysis. While universal genes may certainly be indicative of how well housekeeping genes may be represented in transcriptomes, their function as proxy for the completeness of secreted protein families should be considered with caution. Small, abundant, multi-copy, polymorphic families such as the BPTI, BTSP, and lipocalins, may present their own problems during assembly since these genes are likely to be lost during assembly due to non-uniform sequence coverage and assembly artifacts. As such, while salivary gland transcriptomes have been expanded by NGS technologies the results suggest that we may still be missing a third or more of the transcriptome.

COMPLEXITY MEASURED BY GENOME SEQUENCING

While transcriptome sequencing can certainly give insight into gene diversity, the above discussion indicate that it may not be possible to derive at a final number of genes using transcriptomics. The gold standard for definitively estimating gene numbers remains whole genome sequencing. For ticks, draft genomes of *I. scapularis*, *I. ricinus*, *H. longicornis,* and *R. microplus* has been published (Cramaro et al., 2015, 2017; Gulia-Nuss et al., 2016; Barrero et al., 2017; Miller et al., 2018; Guerrero et al., 2019).

The first genome for *I. scapularis* was sequenced using Sanger sequencing (Gulia-Nuss et al., 2016). The estimated genome size was 2.1 Gb with 20,486 predicted genes. BUSCO analysis indicated 69% completeness based on 2,675 reference genes (Mans et al., 2017). The ISE6 cell line from *I. scapularis* was also sequenced (Miller et al., 2018). This estimated the genome size at 2.8 Gb but if duplications are taken into account the size reduces to 2.2 Gb. BUSCO analysis indicated 95% completeness for 1,066 reference genes. The total number of genes associated with this genome is 37,259 with 24,501 protein coding. However, it has been estimated that as much as 50% of salivary gland proteins may be missing or incomplete in the genome (Ribeiro and Mans, 2020).

The genome for *I. ricinus* has been sequenced with both Illumina and Pacific Biosciences (PacBio) long read technologies (Cramaro et al., 2015, 2017). The estimated size of the genome is 2.65 Gb from which 516 Mb were sequenced which represent 19.4% of the genome but 67% of the non-repetitive genome. A total of 25,263 proteins were identified based on BLAST similarity searches. However, BUSCO only indicated 55.5% completeness.

The genome for *H. longicornis* was sequenced using PacBio long read technology (Guerrero et al., 2019). Genome sequencing was facilitated by the parthenogenicity of this species (ability to asexually reproduce with mating) that reduce genome heterogeneity. The total length of the genome was 7.3 Gbp in 34,208 contigs and was 96% complete as assessed with BUSCO. To date a gene count is not available.

The genome of *R. microplus* was sequenced using an Illumina/PacBio hybrid assembly approach (Barrero et al., 2017). Given the highly repetitive nature of the genome (70%) and the large estimated size (7.1 Gbp), Cot filtration was used to enrich for single, low copy, and moderately repetitive genomic DNA. This yielded an assembly of 2 Gbp with 38,827 genes of which 24,758 is protein coding. BUSCO analysis indicated a completeness of 53.1%. Conversely, a 63,416 non-redundant transcriptome dataset showed 85% completeness, suggesting

that the genome assembly still miss 47% proteins encoded in the genome.

While all available tick genomes yield protein coding genes ranging from ∼20,000 to 30,000 it is clear that their incomplete nature also do not allow accurate estimations of complexity of the whole genome, nor what may be expected at the tick-host interface.

COMPLEXITY MEASUREMENTS ONLY AS GOOD AS THE EXISTING DATABASES

It has been indicated that database repositories for sequences has an immense impact on the coverage and complexity detected during proteomic analysis, but also impact on the ability to annotate transcriptomes. In this regard, tick sequences are scattered across many different databases, none which present a complete non-redundant set of sequences. For VectorBase (Giraldo-Calderón et al., 2015), the only datasets available is for *I. scapularis*, *I. ricinus,* and *R. microplus* which is effectively those for which genome datasets exist. For Genbank, the nucleotide core database contain the majority of historical sequences deposited in Genbank, but only links to transcriptome shotgun assembly (TSA) sequences (that include EST and next-generation sequencing assemblies contained in the small read archive database -SRA). For many tick transcriptomes, data is only available in the small read archive database (SRA) as contigs (that may or may not contain full length ORFs) and no protein or nucleotide coding sequences exist. In some instances, no contigs were deposited and only raw sequence read data is available. This generally necessitates either extraction of ORFs or reassembly and annotation to make this data useful for comparative or proteomic analysis, although given the diversity of methods available for transcriptome assembly and analysis, the reproducibility of constructing a published transcriptome is debatable. In many cases as indicated, researchers use in-house sequence databases not deposited anywhere and therefore not available. There is therefore a need for a centralized database that would address all of these shortcomings and would include comprehensive inclusion of all tick transcriptomes sequenced to data as well as accurate annotation. To compound this, the unique lineage specific expansions observed in ticks make extraction of functionally relevant information difficult since proteins may only be annotated as "potential secretory protein" or "unknown function" (Ribeiro and Mans, 2020). In many cases, such proteins cannot even be assigned to existing protein families. In an attempt to partially address this, a database of secretory proteins has recently been constructed that can be searched by reverse position specific BLAST to assign potential secretory proteins to known secretory families (Ribeiro and Mans, 2020). However, this database only attempted classification of those proteins present in the NCBI non-redundant sequence database and excluded TSA and SRA databases. The searchable database will however, allow for better annotation of transcriptomes using a consistent nomenclature.

With regard to proteomic analysis, the data described in publications in tables or supplementary materials is generally useful to document the snapshot provided by a specific study. However, the main usefulness of proteomic data lies in the re-analysis potential of the raw data once sequence databases has been expanded since this may result in higher numbers of proteins identified from the proteomic data. To this end, raw proteomic data can be submitted to the PRoteomics IDEntification database (PRIDE) (Perez-Riverol et al., 2019). To this end, proteomic data for at least 6 tick species is available in PRIDE and include *A. americanum* (Crispell et al., 2019; Kim et al., 2020), *A. sculptum* (Esteves et al., 2017), *I. scapularis* (Villar et al., 2015; Kim et al., 2016), *I. ricinus* (Cramaro et al., 2015), *H. longicornis* (Ren et al., 2019), and *R. sanguineus* (Tirloni et al., 2020).

OTHER MEASURES OF COMPLEXITY: ALTERNATIVE SPLICING, RECOMBINATION, NON-CODING RNA AND POSTTRANSLATIONAL MODIFICATION

The current study has thus far largely focused on detection and quantification of genes and the proteins encoded by them, as measures of salivary gland complexity. The impact of exon shuffling and gene duplication has not been considered yet, since these are mechanisms to generate diversity during long-term evolution which is detected retrospectively (Mans et al., 2017). However, alternative splicing may contribute significantly to increase complexity since this may be tissue specific and give rise to protein isoforms (Nilsen and Graveley, 2010). The impact of alternative splicing on complexity has not yet been analyzed in depth in ticks or salivary gland products. For example, the search terms "alternative splicing" and "ticks" retrieve 11 hits in PubMed. Of these, 9 deals with potential alternative splicing in single genes, the majority which is housekeeping (Baxter and Barker, 1998; Guo et al., 1998; Saravanan et al., 2003; Xu et al., 2003; Tabish et al., 2006; Buresova et al., 2009; Olafson et al., 2011; Temeyer et al., 2012; Urbanová et al., 2018). None of the genome, proteome or transcriptome studies described in the current study considered alternative splicing or isoforms extensively, except for the study of Oleaga et al. (2007) that detected numerous isoforms on a two-dimensional gel for the histamine and serotonin-binding protein, TSGP1. It is unclear whether these isoforms were due to alternative splicing or post-translational modification. The absence of extensive detection of alternative splicing in salivary gland proteins may be partially due to the consideration that most secretory tick families are single domain proteins such as the BPTI, BTSP, cystatin or lipocalin families, or composed of multiple domains of these core folds such as for example the various BPTI proteins with double, triple, quadruple and quintuple domains, or composed of multi-domain proteins with well-defined domain structures such as 5'-nucleotidase and the metalloproteases (Francischetti et al., 2009). On this, large scale proteomic studies support the observation that a single main isoform exist for most proteins and that other isoforms may not be functional, or under selective pressure or even expressed (Tress et al., 2017), while splicing of whole domains is also unlikely (Light and Elofsson, 2013). The

potential for alternative splicing, exon shuffling and intragenic recombination to generate "new genes on the fly" has been considered to explain the sheer diversity of secretory proteins observed in the salivary glands (Ribeiro and Mans, 2020). Real data is, however, needed to confirm this.

A further level of complexity that may be emerging is that of non-coding RNA. Abundant long non-coding RNA was found in tick transcriptomes (de Castro et al., 2016), while microRNA may perform important housekeeping functions (Barrero et al., 2011; Zhou et al., 2013; Luo et al., 2015, 2019; Shao et al., 2015; Malik et al., 2019; Liu et al., 2020). However, of more interest for the current study is the potential that some of these non-coding RNA may play a role in the regulation of host defense mechanisms. As such, exosomes that carry microRNAs has been described in the saliva of ticks (Hackenberg et al., 2017). It has been proposed that these exomes may deliver microRNAs to immune cells to down-regulate immune modulatory pathways (Hackenberg and Kotsyfakis, 2018; Bensaoud et al., 2019b; Chávez et al., 2019). This will add another layer of complexity to salivary glands of which the magnitude is difficult to estimate. As yet, down-regulation of such immune pathways needs to be proven and it needs to be shown that concentrations of these microRNAs can break the chemical equilibrium barrier to be effective (Mans, 2019).

Post-translational modifications play a large role in regulation of functional networks and in protein function. With regard to protein function involved in tick-host interaction a number of post-translational modifications have been shown to be important for functionality, especially tyrosine sulfation (Shabareesh et al., 2017; Thompson et al., 2017; Vechtova et al., 2018; Franck et al., 2020). Many of the transcriptome studies listed also report many potential modification sites or motifs. However, large scale confirmation of post-translational modifications by proteomic analysis has not yet been performed for ticks (Vechtova et al., 2018). As such, the impact of post-translational modifications on complexity of salivary gland proteins is as yet unknown, but could be quite significant.

FUTURE PERSPECTIVES ON SALIVARY GLAND COMPLEXITY

We are undoubtedly much further along the road to describing and understanding tick salivary gland protein complexity than ever before. It is likely that the next 10–20 years will see the completion of many tick genomes, the validation of many tick transcriptomes by proteomics and final estimates on the complexity of salivary gland protein repertoires for many tick species. This will be facilitated by new technologies such as third generation nanopore sequencing that will hopefully make transcriptome and genome sequencing affordable for the high number of species required to map all orthologs and paralogs. Other challenges are defined by our ignorance of the mechanisms regulating sialome switching, and the mode and possible physiological role of host protein secretion by tick salivary glands. The next challenge will be to analyze all this information to generate a comprehensive, holistic and ultimately understandable synthesis of tick evolution and tick-host interaction. Even so, we may find out that many genes identified in the genomes or transcriptomes may never be validated by proteomics. This may be due to the presence of pseudogenes or expression so transient to remain undetectable by proteomics, or even be functionally irrelevant (Mans et al., 2017; Mans, 2019). In the end, validation by empirical testing will remain crucial.

As indicated, the salivary gland is a complex organ composed of multiple acini with each comprising multiple cell types. While temporal differential expression over the course of feeding has been well-characterized, differential expression also occur within different cell types and acini. To define this expression well is important, since some cells are prone to infection by pathogens, such as *T. parva* that infect the e-cells of type III acini (Fawcett et al., 1982). In this case the impact of parasite infection on vector expression (Nene et al., 2004), is confounded by non-infected/non-affected members of the same cell type and other cell types since the parasite do not infect all cells of a particular type at the same time (McKeever, 2009). Other cell types are involved in specific biological functions such as water secretion by the e-cells of type III acini (Fawcett et al., 1981). An accurate picture of global differential expression is therefore confounded by the differential expression that occur on smaller scales. The potential to address this issue exist via single cell sequencing approaches (Chattopadhyay et al., 2018). These approaches are hampered by the pyramidal structure of acini and the fragility of salivary gland cell types, but future innovations on non-disruptive separation of acinar cell types may enable single cell sequencing. Alternatives may also be found in laser capture microdissection of cell regions followed by single cell sequencing (Chattopadhyay et al., 2018). It is foreseen that these approaches will certainly enable a deeper dissection of salivary function, localization and parasite-vector interaction.

The majority of studies described for salivary gland transcriptomics are for adult ticks, while whole body transcriptomes are generally generated for larvae or nymphs. Single cell and related technologies that allow sequencing of minute quantities of genetic material may open up the possibility of sequencing larval or nymphal glands made accessible via laser microdissection. This will certainly advance tick salivary gland transcriptomics, since differential expression between life stages is well-recognized (Schwarz et al., 2013; Andreotti et al., 2018).

AUTHOR CONTRIBUTIONS

The author confirms being the sole contributor of this work and has approved it for publication.

FUNDING

This work is based on the research supported in part by the National Research Foundation of South Africa (Grant Number: 118540).

ACKNOWLEDGMENTS

I thank Jose Ribeiro for critical reading of the manuscript.

REFERENCES

Alarcon-Chaidez, F. J., Sun, J., and Wikel, S. K. (2007). Transcriptome analysis of the salivary glands of *Dermacentor andersoni* Stiles (*Acari*: *Ixodidae*). *Insect Biochem. Mol. Biol.* 37, 48–71. doi: 10.1016/j.ibmb.2006.10.002

Aljamali, M. N., Hern, L., Kupfer, D., Downard, S., So, S., Roe, B. A., et al. (2009). Transcriptome analysis of the salivary glands of the female tick *Amblyomma americanum* (*Acari*: *Ixodidae*). *Insect Mol. Biol.* 18, 129–154. doi: 10.1111/j.1365-2583.2009.00863.x

Anatriello, E., Ribeiro, J. M., de Miranda-Santos, I. K., Brandão, L. G., Anderson, J. M., Valenzuela, J. G., et al. (2010). An insight into the sialotranscriptome of the brown dog tick, *Rhipicephalus sanguineus*. *BMC Genomics* 11:450. doi: 10.1186/1471-2164-11-450

Andreotti, R., Giachetto, P. F., and Cunha, R. C. (2018). Advances in tick vaccinology in Brazil: from gene expression to immunoprotection. *Front. Biosci.* 10, 127–142. doi: 10.2741/s504

Antunes, S., Couto, J., Ferrolho, J., Sanches, G. S., Merino Charrez, J. O., De la Cruz Hernández, N., et al. (2019). Transcriptome and proteome response of *Rhipicephalus annulatus* tick vector to Babesia bigemina infection. *Front. Physiol.* 10:318. doi: 10.3389/fphys.2019.00318

Araujo, R. N., Silva, N. C. S., Mendes-Sousa, A., Paim, R., Costa, G. C. A., Dias, L. R., et al. (2019). RNA-seq analysis of the salivary glands and midgut of the argasid tick *Ornithodoros rostratus*. *Sci. Rep.* 9:6764. doi: 10.1038/s41598-019-42899-z

Bakkes, D. K., De Klerk, D., Latif, A. A., and Mans, B. J. (2018). Integrative taxonomy of Afrotropical Ornithodoros (*Ornithodoros*) (*Acari*: *Ixodida*: *Argasidae*). *Ticks Tick Borne Dis.* 9, 1006–1037. doi: 10.1016/j.ttbdis.2018.03.024

Balashov, Y. S. (1972). Bloodsucking ticks (*Ixodideae*)—vectors of disease of man and animals. *Misc. Pub. Entomol. Soc. Amer.* 8, 161–376.

Barrero, R. A., Guerrero, F. D., Black, M., McCooke, J., Chapman, B., Schilkey, F., et al. (2017). Gene-enriched draft genome of the cattle tick *Rhipicephalus* microplus: assembly by the hybrid Pacific biosciences/illumina approach enabled analysis of the highly repetitive genome. *Int. J. Parasitol.* 47, 569–583. doi: 10.1016/j.ijpara.2017.03.007

Barrero, R. A., Keeble-Gagnère, G., Zhang, B., Moolhuijzen, P., Ikeo, K., Tateno, Y., et al. (2011). Evolutionary conserved microRNAs are ubiquitously expressed compared to tick-specific miRNAs in the cattle tick *Rhipicephalus* (Boophilus) microplus. *BMC Genomics* 12:328. doi: 10.1186/1471-2164-12-328

Baxter, G. D., and Barker, S. C. (1998). Acetylcholinesterase cDNA of the cattle tick, Boophilus microplus: characterisation and role in organophosphate resistance. *Insect Biochem. Mol. Biol.* 28, 581–589. doi: 10.1016/S0965-1748(98)00034-4

Bensaoud, C., Aounallah, H., Sciani, J. M., Faria, F., Chudzinski-Tavassi, A. M., Bouattour, A., et al. (2019a). Proteomic informed by transcriptomic for salivary glands components of the camel tick *Hyalomma dromedarii*. *BMC Genomics* 20:675. doi: 10.1186/s12864-019-6042-1

Bensaoud, C., Hackenberg, M., and Kotsyfakis, M. (2019b). Noncoding RNAs in parasite-vector-host interactions. *Trends Parasitol.* 35, 715–724. doi: 10.1016/j.pt.2019.06.012

Bensaoud, C., Nishiyama, M. Y. Jr., Ben Hamda, C., Lichtenstein, F., Castro de Oliveira, U., Faria, F., et al. (2018). *De novo* assembly and annotation of *Hyalomma dromedarii* tick (*Acari*: *Ixodidae*) sialotranscriptome with regard to gender differences in gene expression. *Parasit. Vectors* 11:314. doi: 10.1186/s13071-018-2874-9

Bergman, D. K., Palmer, M. J., Caimano, M. J., Radolf, J. D., and Wikel, S. K. (2000). Isolation and molecular cloning of a secreted immunosuppresant protein from *Dermacentor andersoni* salivary gland. *J. Parasitol.* 86, 516–525. doi: 10.1645/0022-3395(2000)086[0516:IAMCOA]2.0.CO;2

Bishop, R., Lambson, B., Wells, C., Pandit, P., Osaso, J., Nkonge, C., et al. (2002). A cement protein of the tick *Rhipicephalus appendiculatus*, located in the secretory e cell granules of the type III salivary gland acini, induces strong antibody responses in cattle. *Int. J. Parasitol.* 32, 833–842. doi: 10.1016/S0020-7519(02)00027-9

Bourret, T. J., Boyle, W. K., Zalud, A. K., Valenzuela, J. G., Oliveira, F., and Lopez, J. E. (2019). The relapsing fever spirochete *Borrelia turicatae* persists in the highly oxidative environment of its soft-bodied tick vector. *Cell. Microbiol.* 21:e12987. doi: 10.1111/cmi.12987

Bullard, R., Allen, P., Chao, C. C., Douglas, J., Das, P., Morgan, S. E., et al. (2016). Structural characterization of tick cement cones collected from *in vivo* and artificial membrane blood-fed lone star ticks (*Amblyomma americanum*). *Ticks Tick Borne Dis.* 7, 880–892. doi: 10.1016/j.ttbdis.2016.04.006

Buresova, V., Hajdusek, O., Franta, Z., Sojka, D., and Kopacek, P. (2009). IrAM-An alpha2-macroglobulin from the hard tick *Ixodes ricinus*: characterization and function in phagocytosis of a potential pathogen *Chryseobacterium* indologenes. *Dev. Comp. Immunol.* 33, 489–498. doi: 10.1016/j.dci.2008.09.011

Charrier, N. P., Couton, M., Voordouw, M. J., Rais, O., Durand-Hermouet, A., Hervet, C., et al. (2018). Whole body transcriptomes and new insights into the biology of the tick *Ixodes ricinus*. *Parasit. Vectors* 11:364. doi: 10.1186/s13071-018-2932-3

Charrier, N. P., Hermouet, A., Hervet, C., Agoulon, A., Barker, S. C., Heylen, D., et al. (2019). A transcriptome-based phylogenetic study of hard ticks (*Ixodidae*). *Sci. Rep.* 9:12923. doi: 10.1038/s41598-019-49641-9

Chattopadhyay, P. K., Roederer, M., and Bolton, D. L. (2018). A deadly dance: the choreography of host-pathogen interactions, as revealed by single-cell technologies. *Nat. Commun.* 9:4638. doi: 10.1038/s41467-018-06214-0

Chávez, A. S. O., O'Neal, A. J., Santambrogio, L., Kotsyfakis, M., and Pedra, J. H. F. (2019). Message in a vesicle-trans-kingdom intercommunication at the vector-host interface. *J. Cell Sci.* 132:jcs224212. doi: 10.1242/jcs.224212

Chenchik, A., Diachenko, L., Moqadam, F., Tarabykin, V., Lukyanov, S., and Siebert, P. D. (1996). Full-length cDNA cloning and determination of mRNA 5' and 3' ends by amplification of adaptor-ligated cDNA. *Biotechniques* 21, 526–534. doi: 10.2144/96213pf02

Chinery, W. A. (1965). Studies on the various glands of the tick *Haemaphysalis spinigera* Neumann 1897. 3. the salivary glands. *Acta Trop.* 22, 321–349.

Chinery, W. A. (1973). The nature and origin of the "cement" substance at the site of attachment and feeding of adult *Haemaphysalis spinigera* (*Ixodidae*). *J. Med. Entomol.* 10, 355–362. doi: 10.1093/jmedent/10.4.355

Chmelar, J., Anderson, J. M., Mu, J., Jochim, R. C., Valenzuela, J. G., and Kopecký, J. (2008). Insight into the sialome of the castor bean tick, *Ixodes ricinus*. *BMC Genomics* 9:233. doi: 10.1186/1471-2164-9-233

Coons, L. B., and Roshdy, M. A. (1973). Fine structure of the salivary glands of unfed male *Dermacentor variabilis* (say) (*Ixodoidea*: *Ixodidae*). *J. Parasitol.* 59, 900–912. doi: 10.2307/3278433

Couto, J., Villar, M., Mateos-Hernández, L., Ferrolho, J., Sanches, G. S., Sofia Santos, A., et al. (2020). Quantitative proteomics identifies metabolic pathways affected by Babesia infection and blood feeding in the sialoproteome of the vector *Rhipicephalus bursa*. *Vaccines* 8:91. doi: 10.3390/vaccines8010091

Cramaro, W. J., Hunewald, O. E., Bell-Sakyi, L., and Muller, C. P. (2017). Genome scaffolding and annotation for the pathogen vector *Ixodes ricinus* by ultra-long single molecule sequencing. *Parasit. Vectors* 10:71. doi: 10.1186/s13071-017-2008-9

Cramaro, W. J., Revets, D., Hunewald, O. E., Sinner, R., Reye, A. L., and Muller, C. P. (2015). Integration of *Ixodes ricinus* genome sequencing with transcriptome and proteome annotation of the naïve midgut. *BMC Genomics* 16:871. doi: 10.1186/s12864-015-1981-7

Crispell, G., Commins, S. P., Archer-Hartman, S. A., Choudhary, S., Dharmarajan, G., Azadi, P., et al. (2019). Discovery of alpha-gal-containing antigens in North American tick species believed to induce red meat allergy. *Front. Immunol.* 10:1056. doi: 10.3389/fimmu.2019.01056

Das, S., Banerjee, G., DePonte, K., Marcantonio, N., Kantor, F. S., and Fikrig, E. (2001). Salp25D, an *Ixodes scapularis* antioxidant, is 1 of 14 immunodominant antigens in engorged tick salivary glands. *J. Infect. Dis.* 184, 1056–1064. doi: 10.1086/323351

Das, S., Marcantonio, N., Deponte, K., Telford, S. R., Anderson, J. F., Kantor, F. S., et al. (2000). Salp16, a gene induced in *Ixodes scapularis* salivary glands during tick feeding. *Am. J. Trop. Med. Hyg.* 62, 99–105. doi: 10.4269/ajtmh.2000.62.99

de Castro, M. H., de Klerk, D., Pienaar, R., Latif, A. A., Rees, D. J., and Mans, B. J. (2016). *De novo* assembly and annotation of the salivary gland transcriptome of *Rhipicephalus* appendiculatus male and female ticks during blood feeding. *Ticks Tick Borne Dis.* 7, 536–548. doi: 10.1016/j.ttbdis.2016.01.014

de Castro, M. H., de Klerk, D., Pienaar, R., Rees, D. J. G., and Mans, B. J. (2017). Sialotranscriptomics of *Rhipicephalus* zambeziensis reveals intricate expression profiles of secretory proteins and suggests tight temporal transcriptional regulation during blood-feeding. *Parasit. Vectors* 10:384. doi: 10.1186/s13071-017-2312-4

De Marco, L., Epis, S., Comandatore, F., Porretta, D., Cafarchia, C., Mastrantonio, V., et al. (2017). Transcriptome of larvae representing

the *Rhipicephalus sanguineus* complex. *Mol. Cell. Probes* 31, 85–90. doi: 10.1016/j.mcp.2016.02.006

Díaz-Martín, V., Manzano-Román, R., Valero, L., Oleaga, A., Encinas-Grandes, A., and Pérez-Sánchez, R. (2013). An insight into the proteome of the saliva of the argasid tick *Ornithodoros moubata* reveals important differences in saliva protein composition between the sexes. *J. Proteomics* 80, 216–235. doi: 10.1016/j.jprot.2013.01.015

Díaz-Sánchez, S., Estrada-Peña, A., Cabezas-Cruz, A., and de la Fuente, J. (2019). Evolutionary insights into the tick hologenome. *Trends Parasitol.* 35, 725–737. doi: 10.1016/j.pt.2019.06.014

Esteves, E., Maruyama, S. R., Kawahara, R., Fujita, A., Martins, L. A., Righi, A. A., et al. (2017). Analysis of the salivary gland transcriptome of unfed and partially fed *Amblyomma* sculptum ticks and descriptive proteome of the saliva. *Front. Cell Infect. Microbiol.* 7:476. doi: 10.3389/fcimb.2017.00476

Estrada-Peña, A., Venzal, J. M., Kocan, K. M., Tramuta, C., Tomassone, L., de la Fuente, J., et al. (2008). Observations on Antricola ticks: small nymphs feed on mammalian hosts and have a salivary gland structure similar to ixodid ticks. *J. Parasitol.* 94, 953–955. doi: 10.1645/GE-1371.1

Fawcett, D. W., Büscher, G., and Doxsey, S. (1982). Salivary gland of the tick vector of East Coast fever. *IV. cell type selectivity and host cell responses to Theileria parva. Tissue Cell* 14, 397–414. doi: 10.1016/0040-8166(82)90035-0

Fawcett, D. W., Doxsey, S., and Büscher, G. (1981). Salivary gland of the tick vector (R. *appendiculatus) of East Coast fever. II. cellular basis for fluid secretion in the type III acinus. Tissue Cell* 13, 231–253. doi: 10.1016/0040-8166(81)90003-3

Feng, L. L., Liu, L., and Cheng, T. Y. (2019). Proteomic analysis of saliva from partially and fully engorged adult female *Rhipicephalus microplus* (*Acari*: *Ixodidae*). *Exp. Appl. Acarol.* 78, 443–460. doi: 10.1007/s10493-019-00390-4

Francischetti, I. M., Anderson, J. M., Manoukis, N., Pham, V. M., and Ribeiro, J. M. (2011). An insight into the sialotranscriptome and proteome of the coarse bontlegged tick, *Hyalomma marginatum* rufipes. *J. Proteomics* 74, 2892–2908. doi: 10.1016/j.jprot.2011.07.015

Francischetti, I. M., Mans, B. J., Meng, Z., Gudderra, N., Veenstra, T. D., Pham, V. M., et al. (2008a). An insight into the sialome of the soft tick, *Ornithodorus parkeri*. *Insect Biochem. Mol. Biol.* 38, 1–21. doi: 10.1016/j.ibmb.2007.09.009

Francischetti, I. M., Mather, T. N., and Ribeiro, J. M. (2003). Cloning of a salivary gland metalloprotease and characterization of gelatinase and fibrin(ogen)lytic activities in the saliva of the Lyme disease tick vector *Ixodes scapularis*. *Biochem. Biophys. Res. Commun.* 305, 869–875. doi: 10.1016/S0006-291X(03)00857-X

Francischetti, I. M., Meng, Z., Mans, B. J., Gudderra, N., Hall, M., Veenstra, T. D., et al. (2008b). An insight into the salivary transcriptome and proteome of the soft tick and vector of epizootic bovine abortion, *Ornithodoros coriaceus*. *J. Proteomics* 71, 493–512. doi: 10.1016/j.jprot.2008.07.006

Francischetti, I. M., My Pham, V., Mans, B. J., Andersen, J. F., Mather, T. N., Lane, R. S., et al. (2005). The transcriptome of the salivary glands of the female western black-legged tick *Ixodes pacificus* (*Acari*: *Ixodidae*). *Insect Biochem. Mol. Biol.* 35, 1142–1161. doi: 10.1016/j.ibmb.2005.05.007

Francischetti, I. M., Sa-Nunes, A., Mans, B. J., Santos, I. M., and Ribeiro, J. M. (2009). The role of saliva in tick feeding. *Front. Biosci.* 14, 2051–2088. doi: 10.2741/3363

Francischetti, I. M., Valenzuela, J. G., Andersen, J. F., Mather, T. N., and Ribeiro, J. M. (2002). Ixolaris, a novel recombinant tissue factor pathway inhibitor (TFPI) from the salivary gland of the tick, *Ixodes scapularis*: identification of factor X and factor Xa as scaffolds for the inhibition of factor VIIa/tissue factor complex. *Blood* 99, 3602–3612. doi: 10.1182/blood-2001-12-0237

Franck, C., Foster, S. R., Johansen-Leete, J., Chowdhury, S., Cielesh, M., Bhusal, R. P., et al. (2020). Semisynthesis of an evasin from tick saliva reveals a critical role of tyrosine sulfation for chemokine binding and inhibition. *Proc. Natl. Acad. Sci. U.S.A.* 117, 12657–12664. doi: 10.1073/pnas.2000605117

Garcia, G. R., Gardinassi, L. G., Ribeiro, J. M., Anatriello, E., Ferreira, B. R., Moreira, H. N., et al. (2014). The sialotranscriptome of *Amblyomma triste*, *Amblyomma parvum* and *Amblyomma cajennense* ticks, uncovered by 454-based RNA-seq. *Parasit. Vectors* 7:430. doi: 10.1186/1756-3305-7-430

Gaspar, A. R., Crause, J. C., and Neitz, A. W. (1995). Identification of anticoagulant activities in the salivary glands of the soft tick, *Ornithodoros savignyi*. *Exp. Appl. Acarol.* 19, 117–127. doi: 10.1007/BF00052551

Gaspar, A. R., Joubert, A. M., Crause, J. C., and Neitz, A. W. (1996). Isolation and characterization of an anticoagulant from the salivary glands of the tick, *Ornithodoros savignyi* (*Acari*: *Argasidae*). *Exp. Appl. Acarol.* 20, 583–598. doi: 10.1007/BF00052809

Giachetto, P. F., Cunha, R. C., Nhani, A. Jr., Garcia, M. V., Ferro, J. A., and Andreotti, R. (2020). Gene expression in the salivary gland of *Rhipicephalus* (*Boophilus*) microplus fed on tick-susceptible and tick-resistant hosts. *Front. Cell Infect. Microbiol.* 9:477. doi: 10.3389/fcimb.2019.00477

Gibson, A. K., Smith, Z., Fuqua, C., Clay, K., and Colbourne, J. K. (2013). Why so many unknown genes? *partitioning orphans from a representative transcriptome of the lone star tick Amblyomma americanum. BMC Genomics* 14:135. doi: 10.1186/1471-2164-14-135

Giraldo-Calderón, G. I., Emrich, S. J., MacCallum, R. M., Maslen, G., Dialynas, E., Topalis, P., et al. (2015). VectorBase: an updated bioinformatics resource for invertebrate vectors and other organisms related with human diseases. *Nucleic Acids Res.* 43, D707–D713. doi: 10.1093/nar/gku1117

Guerrero, F. D., Bendele, K. G., Ghaffari, N., Guhlin, J., Gedye, K. R., Lawrence, K. E., et al. (2019). The Pacific biosciences *de novo* assembled genome dataset from a parthenogenetic New Zealand wild population of the longhorned tick, *Haemaphysalis longicornis* Neumann, 1901. *Data Brief* 27:104602. doi: 10.1016/j.dib.2019.104602

Guerrero, F. D., Miller, R. J., Rousseau, M. E., Sunkara, S., Quackenbush, J., Lee, Y., et al. (2005). BmiGI: a database of cDNAs expressed in *Boophilus microplus*, the tropical/southern cattle tick. *Insect Biochem. Mol. Biol.* 35, 585–595. doi: 10.1016/j.ibmb.2005.01.020

Gulia-Nuss, M., Nuss, A. B., Meyer, J. M., Sonenshine, D. E., Roe, R. M., Waterhouse, R. M., et al. (2016). Genomic insights into the *Ixodes scapularis* tick vector of Lyme disease. *Nat. Commun.* 7:10507. doi: 10.1038/ncomms10507

Guo, J., Sun, Y., Luo, X., Li, M., He, P., He, L., et al. (2019). *De novo* transcriptome sequencing and comparative analysis of *Haemaphysalis flava* Neumann, 1897 at larvae and nymph stages. *Infect. Genet. Evol.* 75:104008. doi: 10.1016/j.meegid.2019.104008

Guo, X., Xu, Q., Harmon, M. A., Jin, X., Laudet, V., Mangelsdorf, D. J., et al. (1998). Isolation of two functional retinoid X receptor subtypes from the ixodid tick, *Amblyomma americanum* (L.). *Mol. Cell. Endocrinol.* 139, 45–60. doi: 10.1016/S0303-7207(98)00073-2

Hackenberg, M., and Kotsyfakis, M. (2018). Exosome-mediated pathogen transmission by arthropod vectors. *Trends Parasitol.* 34, 549–552. doi: 10.1016/j.pt.2018.04.001

Hackenberg, M., Langenberger, D., Schwarz, A., Erhart, J., and Kotsyfakis, M. (2017). *In silico* target network analysis of *de novo*-discovered, tick saliva-specific microRNAs reveals important combinatorial effects in their interference with vertebrate host physiology. *RNA* 23, 1259–1269. doi: 10.1261/rna.061168.117

Hollmann, T., Kim, T. K., Tirloni, L., Radulović, Ž. M., Pinto, A. F. M., Diedrich, J. K., et al. (2018). Identification and characterization of proteins in the *Amblyomma americanum* tick cement cone. *Int. J. Parasitol.* 48, 211–224. doi: 10.1016/j.ijpara.2017.08.018

Howell, C. J., Neitz, A. W., and Potgieter, D. J. (1975). Some toxic and chemical properties of the oral secretion of the sand tampan, *Ornithodoros savignyi* (Audouin) (1827). *Onderstepoort J. Vet. Res.* 43, 99–102.

Joubert, A. M., Louw, A. I., Joubert, F., and Neitz, A. W. (1998). Cloning, nucleotide sequence and expression of the gene encoding factor Xa inhibitor from the salivary glands of the tick, *Ornithodoros savignyi*. *Exp. Appl. Acarol.* 22, 603–619. doi: 10.1023/A:1006198713791

Kaire, G. H. (1966). Isolation of tick paralysis toxin from *Ixodes holocyclus*. *Toxicon* 4, 91–97. doi: 10.1016/0041-0101(66)90003-1

Karczewski, J., Endris, R., and Connolly, T. M. (1994). Disagregin is a fibrinogen receptor antagonist lacking the Arg-Gly-Asp sequence from the tick, *Ornithodoros moubata*. *J. Biol. Chem.* 269, 6702–6708.

Karim, S., and Ribeiro, J. M. (2015). An insight into the sialome of the Lone Star tick, *Amblyomma americanum*, with a glimpse on its time dependent gene expression. *PLoS ONE* 10:e0131292. doi: 10.1371/journal.pone.0131292

Karim, S., Singh, P., and Ribeiro, J. M. C. (2011). A deep insight into the sialotranscriptome of the Gulf Coast tick, *Amblyomma maculatum*. *PLoS ONE* 6:e28525. doi: 10.1371/journal.pone.0028525

Keller, P. M., Waxman, L., Arnold, B. A., Schultz, L. D., Condra, C., and Connolly, T. M. (1993). Cloning of the cDNA and expression of moubatin, an inhibitor of platelet aggregation. *J. Biol. Chem.* 268, 5450–5456.

Kim, T. K., Tirloni, L., Pinto, A. F., Moresco, J., Yates, J. R. 3rd, da Silva Vaz, I. Jr., and Mulenga, A. (2016). *Ixodes scapularis* tick saliva proteins sequentially secreted every 24 h during blood feeding. *PLoS Negl. Trop. Dis*. 10:e0004323. doi: 10.1371/journal.pntd.0004323

Kim, T. K., Tirloni, L., Pinto, A. F. M., Diedrich, J. K., Moresco, J. J., Yates, J. R. III., et al. (2020). Time-resolved proteomic profile of *Amblyomma americanum* tick saliva during feeding. *PLoS Negl. Trop. Dis*. 14:e0007758. doi: 10.1371/journal.pntd.0007758

Kotsyfakis, M., Schwarz, A., Erhart, J., and Ribeiro, J. M. (2015). Tissue- and time-dependent transcription in *Ixodes ricinus* salivary glands and midguts when blood feeding on the vertebrate host. *Sci. Rep*. 5:9103. doi: 10.1038/srep09103

Kretz, P. L., Reid, C. H., Greener, A., and Short, J. M. (1989). Effect of lambda packaging extract mcr restriction activity on DNA cloning. *Nucleic Acids Res.* 17:5409. doi: 10.1093/nar/17.13.5409

Laemmli, U. K. (1970). Cleavage of structural proteins during the assembly of the head of bacteriophage T4. *Nature* 227, 680–685. doi: 10.1038/227680a0

Leboulle, G., Rochez, C., Louahed, J., Ruti, B., Brossard, M., Bollen, A., et al. (2002). Isolation of *Ixodes ricinus* salivary gland mRNA encoding factors induced during blood feeding. *Am. J. Trop. Med. Hyg*. 66, 225–233. doi: 10.4269/ajtmh.2002.66.225

Levy, S. E., and Myers, R. M. (2016). Advancements in next-generation sequencing. *Annu. Rev. Genomics Hum. Genet*. 17, 95–115. doi: 10.1146/annurev-genom-083115-022413

Light, S., and Elofsson, A. (2013). The impact of splicing on protein domain architecture. *Curr. Opin. Struct. Biol*. 23, 451–458. doi: 10.1016/j.sbi.2013.02.013

Liu, W., Guo, J., Luo, J., Ren, Q., Chen, Z., Qu, Z., et al. (2020). Analysis of microRNA expression profiles dynamic in different life stages of *Haemaphysalis longicornis* ticks by deep sequencing of small RNA libraries. *Ticks Tick Borne Dis*. 11:101427. doi: 10.1016/j.ttbdis.2020.101427

Lukyanov, K., Diatchenko, L., Chenchik, A., Nanisetti, A., Siebert, P., Usman, N., et al. (1997). Construction of cDNA libraries from small amounts of total RNA using the suppression PCR effect. *Biochem. Biophys. Res. Commun*. 230, 285–288. doi: 10.1006/bbrc.1996.5948

Luo, J., Liu, G. Y., Chen, Z., Ren, Q. Y., Yin, H., Luo, J. X., et al. (2015). Identification and characterization of microRNAs by deep-sequencing in Hyalomma anatolicum anatolicum (*Acari*: *Ixodidae*) ticks. *Gene* 564, 125–133. doi: 10.1016/j.gene.2015.01.019

Luo, J., Ren, Q., Chen, Z., Liu, W., Qu, Z., Xiao, R., et al. (2019). Comparative analysis of microRNA profiles between wild and cultured *Haemaphysalis longicornis* (*Acari*, *Ixodidae*) ticks. *Parasite* 26:18. doi: 10.1051/parasite/2019018

Madden, R. D., Sauer, J. R., and Dillwith, J. W. (2002). A proteomics approach to characterizing tick salivary secretions. *Exp. Appl. Acarol*. 28, 77–87. doi: 10.1023/A:1025342015065

Malik, M. I., Nawaz, M., Hassan, I. A., Zhang, H., Gong, H., Cao, J., et al. (2019). A microRNA profile of saliva and role of miR-375 in *Haemaphysalis longicornis* (*Ixodida*: *Ixodidae*). *Parasit. Vectors* 12:68. doi: 10.1186/s13071-019-3318-x

Mans, B. J. (2016). "Glandular matrices and secretions: blood- feeding arthropods," in *Extracellular Composite Matrices in Arthropods,* eds E. Cohen and B. *Moussian (Springer International Publishing Switzerland),* 625–688.

Mans, B. J. (2019). Chemical equilibrium at the tick-host feeding interface: a critical examination of biological relevance in hematophagous behavior. *Front. Physiol*. 10:530. doi: 10.3389/fphys.2019.00530

Mans, B. J., Andersen, J. F., Francischetti, I. M., Valenzuela, J. G., Schwan, T. G., Pham, V. M., et al. (2008). Comparative sialomics between hard and soft ticks: implications for the evolution of blood-feeding behavior. *Insect Biochem. Mol. Biol*. 38, 42–58. doi: 10.1016/j.ibmb.2007.09.003

Mans, B. J., de Castro, M. H., Pienaar, R., de Klerk, D., Gaven, P., Genu, S., et al. (2016). Ancestral reconstruction of tick lineages. *Ticks Tick Borne Dis*. 7, 509–535. doi: 10.1016/j.ttbdis.2016.02.002

Mans, B. J., Featherston, J., de Castro, M. H., and Pienaar, R. (2017). Gene duplication and protein evolution in tick-host interactions. *Front. Cell Infect. Microbiol*. 7:413. doi: 10.3389/fcimb.2017.00413

Mans, B. J., Louw, A. I., and Neitz, A. W. (2002b). Amino acid sequence and structure modeling of savignin, a thrombin inhibitor from the tick, *Ornithodoros savignyi*. *Insect Biochem. Mol. Biol*. 32, 821–828. doi: 10.1016/S0965-1748(01)00169-2

Mans, B. J., Louw, A. I., and Neitz, A. W. (2002c). Savignygrin, a platelet aggregation inhibitor from the soft tick, *Ornithodoros savignyi*, presents the RGD integrin recognition motif on the Kunitz-BPTI fold. *J. Biol. Chem*. 277, 21371–21378. doi: 10.1074/jbc.M112060200

Mans, B. J., Louw, A. I., and Neitz, A. W. (2003). The major tick salivary gland proteins and toxins from the soft tick, *Ornithodoros savignyi*, are part of the tick Lipocalin family: implications for the origins of tick toxicoses. *Mol. Biol. Evol*. 20, 1158–1167. doi: 10.1093/molbev/msg126

Mans, B. J., and Neitz, A. W. (2004a). The sand tampan, *Ornithodoros savignyi*, as a model for tick–host interactions. *S. Afr. J. Sci.* 100, 283–288.

Mans, B. J., and Neitz, A. W. (2004b). Adaptation of ticks to a blood-feeding environment: evolution from a functional perspective. *Insect Biochem. Mol. Biol*. 34, 1–17. doi: 10.1016/j.ibmb.2003.09.002

Mans, B. J., Steinmann, C. M., Venter, J. D., Louw, A. I., and Neitz, A. W. (2002a). Pathogenic mechanisms of sand tampan toxicoses induced by the tick, *Ornithodoros savignyi*. *Toxicon* 40, 1007–1016. doi: 10.1016/S0041-0101(02)00098-3

Mans, B. J., Venter, J. D., Coons, L. B., Louw, A. I., and Neitz, A. W. (2004). A reassessment of argasid tick salivary gland ultrastructure from an immuno-cytochemical perspective. *Exp. Appl. Acarol*. 33, 119–129. doi: 10.1023/B:APPA.0000030012.47964.b3

Mans, B. J., Venter, J. D., Vrey, P. J., Louw, A. I., and Neitz, A. W. (2001). Identification of putative proteins involved in granule biogenesis of tick salivary glands. *Electrophoresis* 22, 1739–1746. doi: 10.1002/1522-2683(200105)22:9<1739::AID-ELPS1739>3.0.CO;2-7

Martin, J. A., and Wang, Z. (2011). Next-generation transcriptome assembly. *Nat. Rev. Genet*. 12, 671–682. doi: 10.1038/nrg3068

Martins, L. A., Malossi, C. D., Galletti, M. F. B. M., Ribeiro, J. M., Fujita, A., Esteves, E., et al. (2019). The transcriptome of the salivary glands of *Amblyomma aureolatum* reveals the antimicrobial peptide microplusin as an important factor for the tick protection against *Rickettsia rickettsii* infection. *Front. Physiol*. 10:529. doi: 10.3389/fphys.2019.00529

McKeever, D. J. (2009). Bovine immunity - a driver for diversity in *Theileria* parasites? *Trends Parasitol*. 25, 269–276. doi: 10.1016/j.pt.2009.03.005

McSwain, J. L., Essenberg, R. C., and Sauer, J. R. (1982). Protein changes in the salivary glands of the female lone star tick, *Amblyomma americanum*, during feeding. *J. Parasitol*. 68, 100–106. doi: 10.2307/3281330

Miller, J. R., Koren, S., Dilley, K. A., Harkins, D. M., Stockwell, T. B., Shabman, R. S., et al. (2018). A draft genome sequence for the *Ixodes scapularis* cell line, ISE6. *F1000Res* 7:297. doi: 10.12688/f1000research.13635.1

Moreira, H. N. S., Barcelos, R. M., Vidigal, P. M. P., Klein, R. C., Montandon, C. E., Maciel, T. E. F., et al. (2017). A deep insight into the whole transcriptome of midguts, ovaries and salivary glands of the Amblyomma sculptum tick. *Parasitol. Int*. 66, 64–73. doi: 10.1016/j.parint.2016.10.011

Mudenda, L., Pierlé, S. A., Turse, J. E., Scoles, G. A., Purvine, S. O., Nicora, C. D., et al. (2014). Proteomics informed by transcriptomics identifies novel secreted proteins in *Dermacentor andersoni* saliva. *Int. J. Parasitol*. 44, 1029–1037. doi: 10.1016/j.ijpara.2014.07.003

Mulenga, A., Tsuda, A., Onuma, M., and Sugimoto, C. (2003). Four serine proteinase inhibitors (serpin) from the brown ear tick, *Rhiphicephalus* appendiculatus; cDNA cloning and preliminary characterization. *Insect Biochem. Mol. Biol*. 33, 267–276. doi: 10.1016/S0965-1748(02)00240-0

Narasimhan, S., Deponte, K., Marcantonio, N., Liang, X., Royce, T. E., Nelson, K. F., et al. (2007). Immunity against *Ixodes scapularis* salivary proteins expressed within 24 hours of attachment thwarts tick feeding and impairs Borrelia transmission. *PLoS ONE* 2:e451. doi: 10.1371/journal.pone.0000451

Narasimhan, S., Koski, R. A., Beaulieu, B., Anderson, J. F., Ramamoorthi, N., Kantor, F., et al. (2002). A novel family of anticoagulants from the saliva of *Ixodes scapularis*. *Insect Mol. Biol*. 11, 641–650. doi: 10.1046/j.1365-2583.2002.00375.x

Neitz, A. W., Bezuidenhout, J. D., Vermeulen, N. M., Potgieter, D. J., and Howell, C. J. (1983). In search of the causal agents of tick toxicoses. *Toxicon S* 3, 317–320. doi: 10.1016/0041-0101(83)90219-2

Neitz, A. W., and Gothe, R. (1986). Changes in the protein pattern in the salivary glands of paralysis inducing female *Rhipicephalus* evertsi evertsi during infestation. *Zentralbl. Veterinarmed. B* 33, 213–320. doi: 10.1111/j.1439-0450.1986.tb00025.x

Neitz, A. W., Howell, C. J., and Potgieter, D. J. (1969). Purification of the toxic component in the oral secretion of the sand tampan *Ornithodoros savignyi* (Audouin) (1827). *J. S. Afr. Chem. Ind.* 22, 142–149.

Neitz, A. W., and Vermeulen, N. M. (1987). Biochemical studies on the salivary glands and haemolymph of Amblyomma hebraeum. *Onderstepoort J. Vet. Res.* 54, 443–450.

Nene, V., Lee, D., Kanga, S., Skilton, R., Shah, T., de Villiers, E., et al. (2004). Genes transcribed in the salivary glands of female *Rhipicephalus* appendiculatus ticks infected with *Theileria parva*. *Insect Biochem. Mol. Biol.* 34, 1117–1128. doi: 10.1016/j.ibmb.2004.07.002

Nene, V., Lee, D., Quackenbush, J., Skilton, R., Mwaura, S., Gardner, M. J., et al. (2002). AvGI, an index of genes transcribed in the salivary glands of the ixodid tick *Amblyomma variegatum*. *Int. J. Parasitol.* 32, 1447–1456. doi: 10.1016/S0020-7519(02)00159-5

Nienaber, J., Gaspar, A. R., and Neitz, A. W. (1999). Savignin, a potent thrombin inhibitor isolated from the salivary glands of the tick, *Ornithodoros savignyi* (*Acari*: *Argasidae*). *Exp. Parasitol.* 93, 82–91. doi: 10.1006/expr.1999.4448

Nilsen, T. W., and Graveley, B. R. (2010). Expansion of the eukaryotic proteome by alternative splicing. *Nature* 463, 457–463. doi: 10.1038/nature08909

Niu, D., Zhao, Y., Yang, Y., Yang, R., Gong, X., and Hu, L. (2019). *De novo* RNA-seq and functional annotation of *Haemaphysalis longicornis*. *Acta Parasitol.* 64, 807–820. doi: 10.2478/s11686-019-00103-2

O'Farrell, P. H. (1975). High resolution two-dimensional electrophoresis of proteins. *J. Biol. Chem.* 250, 4007–4021.

Olafson, P. U., Temeyer, K. B., and Pruett, J. H. (2011). Multiple transcripts encode glucose 6-phosphate dehydrogenase in the southern cattle tick, *Rhipicephalus* (Boophilus) microplus. *Exp. Appl. Acarol.* 53, 147–165. doi: 10.1007/s10493-010-9392-6

Oleaga, A., Escudero-Población, A., Camafeita, E., and Pérez-Sánchez, R. (2007). A proteomic approach to the identification of salivary proteins from the argasid ticks *Ornithodoros moubata* and *Ornithodoros erraticus*. *Insect Biochem. Mol. Biol.* 37, 1149–1159. doi: 10.1016/j.ibmb.2007.07.003

Oliveira, C. J., Anatriello, E., de Miranda-Santos, I. K., Francischetti, I. M., Sá-Nunes, A., Ferreira, B. R., et al. (2013). Proteome of *Rhipicephalus* sanguineus tick saliva induced by the secretagogues pilocarpine and dopamine. *Ticks Tick Borne Dis.* 4, 469–477. doi: 10.1016/j.ttbdis.2013.05.001

Paesen, G. C., Adams, P. L., Harlos, K., Nuttall, P. A., and Stuart, D. I. (1999). Tick histamine-binding proteins: isolation, cloning, and three dimensional structure. *Mol. Cell* 3, 661–671. doi: 10.1016/S1097-2765(00)80359-7

Perez-Riverol, Y., Csordas, A., Bai, J., Bernal-Llinares, M., Hewapathirana, S., Kundu, D. J., et al. (2019). The PRIDE database and related tools and resources in 2019: improving support for quantification data. *Nucleic Acids Res.* 47, D442–D450. doi: 10.1093/nar/gky1106

Perner, J., Kropáčková, S., Kopáček, P., and Ribeiro, J. M. C. (2018). Sialome diversity of ticks revealed by RNAseq of single tick salivary glands. *PLoS Negl. Trop. Dis.* 12:e0006410. doi: 10.1371/journal.pntd.0006410

Pienaar, R., Neitz, A. W. H., and Mans, B. J. (2018). Tick paralysis: solving an enigma. *Vet. Sci.* 5:53. doi: 10.3390/vetsci5020053

Porter, L., Radulović, Ž., Kim, T., Braz, G. R., Da Silva Vaz, I. Jr., and Mulenga, A. (2015). Bioinformatic analyses of male and female *Amblyomma americanum* tick expressed serine protease inhibitors (serpins). *Ticks Tick Borne Dis.* 6, 16–30. doi: 10.1016/j.ttbdis.2014.08.002

Rabilloud, T. (2020). Paleoproteomics explained to youngsters: how did the wedding of two-dimensional electrophoresis and protein sequencing spark proteomics on: let there be light. *J. Proteomics* 107, 5–12. doi: 10.1016/j.jprot.2014.03.011

Radulović, Ž. M., Kim, T. K., Porter, L. M., Sze, S. H., Lewis, L., and Mulenga, A. (2014). A 24-48 h fed *Amblyomma americanum* tick saliva immuno-proteome. *BMC Genomics* 15:518. doi: 10.1186/1471-2164-15-518

Ren, S., Zhang, B., Xue, X., Wang, X., Zhao, H., Zhang, X., et al. (2019). Salivary gland proteome analysis of developing adult female *Haemaphysalis longicornis* ticks: molecular motor and TCA cycle-related proteins play an important role throughout development. *Parasit. Vectors* 12:613. doi: 10.1186/s13071-019-3864-2

Ribeiro, J. M., Alarcon-Chaidez, F., Francischetti, I. M., Mans, B. J., Mather, T. N., Valenzuela, J. G., et al. (2006). An annotated catalog of salivary gland transcripts from *Ixodes scapularis* ticks. *Insect Biochem. Mol. Biol.* 36, 111–129. doi: 10.1016/j.ibmb.2005.11.005

Ribeiro, J. M., Anderson, J. M., Manoukis, N. C., Meng, Z., and Francischetti, I. M. (2011). A further insight into the sialome of the tropical bont tick, Amblyomma variegatum. *BMC Genomics* 12:136. doi: 10.1186/1471-2164-12-136

Ribeiro, J. M., Labruna, M. B., Mans, B. J., Maruyama, S. R., Francischetti, I. M., Barizon, G. C., et al. (2012). The sialotranscriptome of *Antricola delacruzi* female ticks is compatible with non-hematophagous behavior and an alternative source of food. *Insect Biochem. Mol. Biol.* 42, 332–342. doi: 10.1016/j.ibmb.2012.01.003

Ribeiro, J. M., Slovák, M., and Francischetti, I. M. (2017). An insight into the sialome of Hyalomma excavatum. *Ticks Tick Borne Dis.* 8, 201–207. doi: 10.1016/j.ttbdis.2016.08.011

Ribeiro, J. M. C., and Arcà, B. (2009). From sialomes to the sialoverse: an insight into salivary potion of blood-feeding insects. *Adv. Insect Physiol.* 37, 59–118. doi: 10.1016/S0065-2806(09)37002-2

Ribeiro, J. M. C., and Mans, B. J. (2020). TickSialoFam (TSFam): a database that helps to classify tick salivary proteins, a review on tick salivary protein function and evolution, with considerations on the tick sialome switching phenomenon. *Front. Cell. Infect. Microbiol.* 10:374. doi: 10.3389/fcimb.2020.00374

Robinson, L. E., and Davidson, J. (1913). The anatomy of *Argas persicus* (Oken 1818). part II. *Parasitology* 6, 217–256. doi: 10.1017/S0031182000003073

Rodriguez-Valle, M., Moolhuijzen, P., Barrero, R. A., Ong, C. T., Busch, G., Karbanowicz, T., et al. (2018). Transcriptome and toxin family analysis of the paralysis tick, *Ixodes holocyclus*. *Int. J. Parasitol.* 48, 71–82. doi: 10.1016/j.ijpara.2017.07.007

Rosendale, A. J., Romick-Rosendale, L. E., Watanabe, M., Dunlevy, M. E., and Benoit, J. B. (2016). Mechanistic underpinnings of dehydration stress in the American dog tick revealed through RNA-Seq and metabolomics. *J. Exp. Biol.* 219, 1808–1819. doi: 10.1242/jeb.137315

Roshdy, M. A. (1972). The subgenus Persicargas (*Ixodoidea*, *Argasidae*, *Argas*). 15. histology and histochemistry of the salivary glands of A. (P.) persicus (Oken). *J. Med. Entomol.* 9, 143–148. doi: 10.1093/jmedent/9.2.143

Sangamnatdej, S., Paesen, G. C., Slovak, M., and Nuttall, P. A. (2002). A high affinity serotonin- and histamine-binding lipocalin from tick saliva. *Insect Mol. Biol.* 11, 79–86. doi: 10.1046/j.0962-1075.2001.00311.x

Saravanan, T., Weise, C., Sojka, D., and Kopácek, P. (2003). Molecular cloning, structure and bait region splice variants of alpha2-macroglobulin from the soft tick *Ornithodoros moubata*. *Insect Biochem. Mol. Biol.* 33, 841–851. doi: 10.1016/S0965-1748(03)00083-3

Schwarz, A., Tenzer, S., Hackenberg, M., Erhart, J., Gerhold-Ay, A., Mazur, J., et al. (2014). A systems level analysis reveals transcriptomic and proteomic complexity in *Ixodes ricinus* midgut and salivary glands during early attachment and feeding. *Mol. Cell. Proteomics* 13, 2725–2735. doi: 10.1074/mcp.M114.039289

Schwarz, A., von Reumont, B. M., Erhart, J., Chagas, A. C., Ribeiro, J. M., and Kotsyfakis, M. (2013). *De novo Ixodes ricinus* salivary gland transcriptome analysis using two next-generation sequencing methodologies. *FASEB J.* 27, 4745–4756. doi: 10.1096/fj.13-232140

Shabareesh, P. R. V., Kumar, A., Salunke, D. M., and Kaur, K. J. (2017). Structural and functional studies of differentially O-glycosylated analogs of a thrombin inhibitory peptide - variegin. *J. Pept. Sci.* 23, 880–888. doi: 10.1002/psc.3052

Shao, C. C., Xu, M. J., Chen, Y. Z., Tao, J. P., and Zhu, X. Q. (2015). Comparative profiling of microRNAs in male and female *Rhipicephalus sanguineus*. *Appl. Biochem. Biotechnol.* 176, 1928–1936. doi: 10.1007/s12010-015-1688-x

Suppan, J., Engel, B., Marchetti-Deschmann, M., and Nürnberger, S. (2018). Tick attachment cement - reviewing the mysteries of a biological skin plug system. *Biol. Rev. Camb. Philos. Soc.* 93, 1056–1076. doi: 10.1111/brv.12384

Tabish, M., Clegg, R. A., Turner, P. C., Jonczy, J., Rees, H. H., and Fisher, M. J. (2006). Molecular characterisation of cAMP-dependent protein kinase (PK-A) catalytic subunit isoforms in the male tick, Amblyomma hebraeum. *Mol. Biochem. Parasitol.* 150, 330–339. doi: 10.1016/j.molbiopara.2006.09.006

Tan, A. W., Francischetti, I. M., Slovak, M., Kini, R. M., and Ribeiro, J. M. (2015). Sexual differences in the sialomes of the zebra tick, *Rhipicephalus pulchellus*. *J. Proteomics* 117, 120–144. doi: 10.1016/j.jprot.2014.12.014

Temeyer, K. B., Olafson, P. U., and Pruett, J. H. (2012). Sequence polymorphism in acetylcholinesterase transcripts and genotyping survey of BmAchE1 in laboratory and Mexican strains of *Rhipicephalus* (*Boophilus*) microplus. *J. Med. Entomol.* 49, 555–562. doi: 10.1603/ME11215

Thompson, R. E., Liu, X., Ripoll-Rozada, J., Alonso-García, N., Parker, B. L., Pereira, P. J. B., et al. (2017). Tyrosine sulfation modulates activity of tick-derived thrombin inhibitors. *Nat. Chem.* 9, 909–917. doi: 10.1038/nchem.2744

Till, W. M. (1959). New cell types in the salivary glands of the brown ear tick, *Rhipicephalus appendiculatus* Neumann. *Nature* 184, 1078–1079. doi: 10.1038/1841078a0

Tirloni, L., Islam, M. S., Kim, T. K., Diedrich, J. K., Yates, J. R. III, Pinto, A. F., Mulenga, A., et al. (2015). Saliva from nymph and adult females of Haemaphysalis longicornis: a proteomic study. *Parasit. Vectors* 8:338. doi: 10.1186/s13071-015-0918-y

Tirloni, L., Lu, S., Calvo, E., Sabadin, G., Di Maggio, L. S., Suzuki, M., et al. (2020). Integrated analysis of sialotranscriptome and sialoproteome of the brown dog tick *Rhipicephalus sanguineus* (s.l.): insights into gene expression during blood feeding. *J. Proteomics*. 103899. doi: 10.1016/j.jprot.2020.103899

Tirloni, L., Reck, J., Terra, R. M., Martins, J. R., Mulenga, A., Sherman, N. E., et al. (2014). Proteomic analysis of cattle tick *Rhipicephalus* (*Boophilus*) microplus saliva: a comparison between partially and fully engorged females. *PLoS ONE* 9:e94831. doi: 10.1371/journal.pone.0094831

Tress, M. L., Abasca, F., and Valencia, A. (2017). Alternative splicing may not be the key to proteome complexity. *Trends Biochem. Sci.* 42, 98–110. doi: 10.1016/j.tibs.2016.08.008

Untalan, P. M., Guerrero, F. D., Haines, L. R., and Pearson, T. W. (2005). Proteome analysis of abundantly expressed proteins from unfed larvae of the cattle tick, *Boophilus microplus*. *Insect Biochem. Mol. Biol.* 35, 141–151. doi: 10.1016/j.ibmb.2004.10.009

Urbanová, V., Hajdušek, O., Šíma, R., Franta, Z., Hönig-Mondeková, H., Grunclová, L., et al. (2018). IrC2/Bf - A yeast and Borrelia responsive component of the complement system from the hard tick *Ixodes ricinus*. *Dev. Comp. Immunol.* 79, 86–94. doi: 10.1016/j.dci.2017.10.012

Valenzuela, J. G., Charlab, R.,Mather, T. N., and Ribeiro, J. M. (2000). Purification, cloning, and expression of a novel salivary anticomplement protein from the tick, *Ixodes scapularis*. *J. Biol. Chem.* 275, 18717–18723. doi: 10.1074/jbc.M001486200

Valenzuela, J. G., Francischetti, I. M., Pham, V. M., Garfield, M. K., Mather, T. N., and Ribeiro, J. M. (2002a). Exploring the sialome of the tick *Ixodes scapularis*. *J. Exp. Biol.* 205, 2843–2864.

Valenzuela, J. G., Pham, V. M., Garfield, M. K., Francischetti, I. M., and Ribeiro, J. M. (2002b). Toward a description of the sialome of the adult female mosquito *Aedes aegypti*. *Insect Biochem. Mol. Biol.* 32, 1101–1122. doi: 10.1016/S0965-1748(02)00047-4

Vechtova, P., Sterbova, J., Sterba, J., Vancova, M., Rego, R. O. M., Selinger, M., et al. (2018). A bite so sweet: the glycobiology interface of tick-host-pathogen interactions. *Parasit. Vectors* 11:594. doi: 10.1186/s13071-018-3062-7

Viljoen, G. J., Bezuidenhout, J. D., Oberem, P. T., Vermeulen, N. M., Visser, L., Gothe, R., et al. (1986). Isolation of a neurotoxin from the salivary glands of female *Rhipicephalus evertsi* evertsi. *J. Parasitol.* 72, 865–874. doi: 10.2307/3281836

Villar, M., Ayllon, N., Alberdi, P., Moreno, A., Moreno, M., Tobes, R., et al. (2015). Integrated metabolomics, transcriptomics and proteomics identifies metabolic pathways affected by *Anaplasma phagocytophilum* infection in tick cells. *Mol. Cell. Proteomics* 14, 3154–3372. doi: 10.1074/mcp.M115.051938

Villar, M., Pacheco, I., Merino, O., Contreras, M., Mateos-Hernández, L., Prado, E., et al. (2020). Tick and host-derived compounds detected in the cement complex substance. *Biomolecules* 10:555. doi: 10.3390/biom10040555

Villar, M., Popara, M., Ayllón, N., Fernández de Mera, I. G., Mateos-Hernández, L., Galindo, R. C., et al. (2014). A systems biology approach to the characterization of stress response in *Dermacentor reticulatus* tick unfed larvae. *PLoS ONE* 9:e89564. doi: 10.1371/journal.pone.0089564

Wang, H., Kaufman, W. R., Cui, W. W., and Nuttall, P. A. (2001). Molecular individuality and adaptation of the tick *Rhipicephalus* appendiculatus in changed feeding environments. *Med. Vet. Entomol.* 15, 403–412. doi: 10.1046/j.0269-283x.2001.00328.x

Wang, H., Kaufman, W. R., and Nuttall, P. A. (1999). Molecular individuality: polymorphism of salivary gland proteins in three species of ixodid tick. *Exp. Appl. Acarol.* 23, 969–975. doi: 10.1023/A:1006362929841

Wang, H., and Nuttall, P. A. (1994). Comparison of the proteins in salivary glands, saliva and haemolymph of *Rhipicephalus* appendiculatus female ticks during feeding. *Parasitology* 109, 517–523. doi: 10.1017/S003118200008077X

Wang, X., Coons, L. B., Taylor, D. B., Stevens, S. E. Jr., and Gartner, T. K. (1996). Variabilin, a novel RGD-containing antagonist of glycoprotein IIb-IIIa and platelet aggregation inhibitor from the hard tick *Dermacentor variabilis*. *J. Biol. Chem.* 271, 17785–17790. doi: 10.1074/jbc.271.30.17785

Waterhouse, R. M., Seppey, M., Simão, F. A., Manni, M., Ioannidis, P., Klioutchnikov, G., et al. (2018). BUSCO applications from quality assessments to gene prediction and phylogenomics. *Mol. Biol. Evol.* 35, 543–548. doi: 10.1093/molbev/msx319

Waxman, L., and Connolly, T. M. (1993). Isolation of an inhibitor selective for collagen-stimulated platelet aggregation from the soft tick *Ornithodoros moubata*. *J. Biol. Chem.* 268, 5445–5449.

Waxman, L., Smith, D. E., Arcuri, K. E., and Vlasuk, G. P. (1990). Tick anticoagulant peptide (TAP) is a novel inhibitor of blood coagulation factor Xa. *Science* 248, 593–596. doi: 10.1126/science.2333510

Xu, G., Fang, Q. Q., Keirans, J. E., and Durden, L. A. (2003). Cloning and sequencing of putative acetylcholinesterase cDNAs from the American dog tick, *Dermacentor variabilis*, and the brown dog tick, *Rhipicephalus sanguineus* (*Acari*: *Ixodidae*). *J. Med. Entomol.* 40, 890–896. doi: 10.1603/0022-2585-40.6.890

Xu, X. L., Cheng, T. Y., Yang, H., Yan, F., and Yang, Y. (2015). *De novo* sequencing, assembly and analysis of salivary gland transcriptome of *Haemaphysalis* flava and identification of sialoprotein genes. *Infect. Genet. Evol.* 32, 135–142. doi: 10.1016/j.meegid.2015.03.010

Zhou, J., Zhou, Y., Cao, J., Zhang, H., and Yu, Y. (2013). Distinctive microRNA profiles in the salivary glands of *Haemaphysalis longicornis* related to tick blood-feeding. *Exp. Appl. Acarol.* 59, 339–349. doi: 10.1007/s10493-012-9604-3

Conflict of Interest: The author declares that the research was conducted in the absence of any commercial or financial relationships that could be construed as a potential conflict of interest.

frontiers in Cellular and Infection Microbiology

ORIGINAL RESEARCH
published: 18 November 2020
doi: 10.3389/fcimb.2020.563349

The Central Role of Salivary Metalloproteases in Host Acquired Resistance to Tick Feeding

Jan Perner[1], Dominic Helm[2], Per Haberkant[2], Tereza Hatalova[1], Sara Kropackova[1], Jose M. Ribeiro[3] and Petr Kopacek[1]*

[1] Institute of Parasitology, Biology Centre, Czech Academy of Sciences, Ceske Budejovice, Czechia, [2] Proteomics Core Facility, The European Molecular Biology Laboratory (EMBL), Heidelberg, Germany, [3] Laboratory of Malaria and Vector Research, National Institute of Allergy and Infectious Diseases, Bethesda, MD, United States

OPEN ACCESS

Edited by:
Herbert Leonel de Matos Guedes, Federal University of Rio de Janeiro, Brazil

Reviewed by:
Jiří Černý, Czech University of Life Sciences Prague, Czechia
Dania Richter, Technische Universitat Braunschweig, Germany

***Correspondence:**
Jan Perner
perner@paru.cas.cz

Specialty section:
This article was submitted to Parasite and Host, a section of the journal Frontiers in Cellular and Infection Microbiology

Received: *18 May 2020*
Accepted: *20 October 2020*
Published: *18 November 2020*

Citation:
Perner J, Helm D, Haberkant P, Hatalova T, Kropackova S, Ribeiro JM and Kopacek P (2020) The Central Role of Salivary Metalloproteases in Host Acquired Resistance to Tick Feeding. Front. Cell. Infect. Microbiol. 10:563349. doi: 10.3389/fcimb.2020.563349

During feeding on vertebrate hosts, ticks secrete saliva composed of a rich cocktail of bioactive molecules modulating host immune responses. Although most of the proteinaceous fraction of tick saliva is of little immunogenicity, repeated feeding of ticks on mammalian hosts may lead to impairment of tick feeding, preventing full engorgement. Here, we challenged rabbits with repeated feeding of both *Ixodes ricinus* nymphs and adults and observed the formation of specific antibodies against several tick salivary proteins. Repeated feeding of both *I. ricinus* stages led to a gradual decrease in engorged weights. To identify the salivary antigens, isolated immunoglobulins from repeatedly infested rabbits were utilized for a protein pull-down from the saliva of pilocarpine-treated ticks. Eluted antigens were first identified by peptide mass fingerprinting with the aid of available *I. ricinus* salivary gland transcriptomes originating from early phases of tick feeding. To increase the authenticity of immunogens identified, we also performed, for the first time, *de novo* assembly of the sialome from *I. ricinus* females fed for six days, a timepoint used for pilocarpine-salivation. The most dominant *I. ricinus* salivary immunogens identified in our study were zinc-dependent metalloproteases of three different families. To corroborate the role of metalloproteases at the tick/host interface, we fed ticks micro-injected with a zinc metalloprotease inhibitor, phosphoramidon, on a rabbit. These ticks clearly failed to initiate feeding and to engorge. However, neither feeding to ticks immune blood of repeatedly infested rabbits, nor phosphoramidon injection into ticks, prevented their engorgement when fed *in vitro* on an artificial membrane system. These data show that Zn metalloproteases play a decisive role in the success of tick feeding, mediated by complex molecular interactions between the host immune, inflammatory, and hemostatic processes, which are absent in *in vitro* feeding. This basic concept warrants further investigation and reconsideration of the current strategies towards the development of an effective "anti-tick" vaccine.

Keywords: ticks, acquired resistance, antigen, immunoprecipitation, vaccine, *Ixodes ricinus*, metalloprotease

INTRODUCTION

Ticks and tick-borne diseases (TBD) represent a growing global burden for both human and animal health (de la Fuente et al., 2008) and are a major constraint for the improvement of livestock industries, particularly in developing countries (Peter et al., 2005). Host immunity-mediated rejection of ticks has potential in the search for a vaccine that offers an effective and environmentally sound approach for controlling ticks and TBDs (de la Fuente et al., 2016).

Ticks salivate proteinaceous saliva into the host during the course of feeding (Francischetti et al., 2009). The individual protein components are secreted into a feeding site at functional concentrations and with adequate affinities for host targets to establish biomolecular associations at the feeding site, thereby modulating host intrinsic hemostatic processes and defence responses (Mans, 2019). To escape immune recognition by the host, tick salivary proteins have evolved low immunogenicity (Chmelar et al., 2016), leading to low or no tick rejection reactions when *Ixodes ricinus* ticks feed on their natural hosts such as mice, voles, or passerine birds (Dizij and Kurtenbach, 1995; Dusbábek et al., 1995; Heylen et al., 2010). In contrast, tick saliva induces an antibody-mediated response in distinct less adapted hosts (Brossard and Wikel, 2005).

The production of anti-salivary gland-specific antibodies against *Amblyomma variegatum* and *I. ricinus* ticks was reported in rabbits (Jongejan et al., 1989; Schorderet and Brossard, 1993). Furthermore, sera from sheep that were exposed to a repeated infestation of *Amblyomma americanum* ticks were shown to recognize multiple tick antigens (Barriga et al., 1991). The presence of specific anti-tick antibodies has been correlated with the inability of ticks to feed and/or reproduce, leading to the concept of acquired resistance to ticks in sensitive host species (Bowessidjaou et al., 1977). The presence of host antibodies in the tick's blood meal might thus be a decisive defence factor preventing tick infestations.

The cellular fraction of host immunity is also clearly involved in the phenomenon of acquired resistance to ticks. In fact, cellular infiltration into the tick feeding site was described in the original seminal paper (Trager, 1939) showing that ticks fed on resistant animals were pale in colour due to a higher leukocyte content in their gut. It was established that repeated tick infestation on guinea pigs is characterized by a large accumulation of eosinophils and basophils in the dermis and epidermis (Allen, 1973). Similarly in mice, basophils are recruited to the tick feeding site during the second, but rarely the first, infestation (Wada et al., 2010). The indispensable role of basophils in acquired resistance to ticks was demonstrated convincingly by diminishing the manifestation of acquired resistance in basophil-ablated mice (Wada et al., 2010).

In the more-than-20-year-old review (Willadsen and Jongejan, 1999), it was stated: "Disappointingly, little progress has been made in the identification of the protective antigens of naturally acquired immunity." A few studies have addressed this challenge in various tick species since then by using yeast surface display (Schuijt et al., 2011) or gel-based proteomics (Garcia et al., 2017). To fill the knowledge gap as to what are the *bona fide* immunogens introduced into the host by tick feeding, we exploited a laboratory model of repetitive infestations of *I. ricinus* adult females and nymphs on rabbits to induce the production of antibodies. Using pull-down enrichment of proteins present in *I. ricinus* saliva *via* their specific binding to immunoglobulins from resistant rabbits, and following differential proteomic analysis, we identified natural tick antigens against which, antibodies are formed in the acquired immunity of rabbits. Our data suggest that zinc-dependent metalloproteases in tick saliva play the most prominent role in mounting an antibody response in resistant rabbits.

MATERIAL AND METHODS

Tick Colony Maintenance and Natural Feeding on a Rabbit

I. ricinus ticks (nymphs and adults) were collected by flagging in the forest near České Budějovice, Czech Republic. Ticks were kept at 24°C and 95% humidity under a 15:9 h day/night regime. Repeated feeding of adult *I. ricinus* ticks was performed by placing 50 freshly collected females into two chambers (25 each with an equal number of males) on the opposing sides of the shaven back of a laboratory rabbit (Hy-Plus strain) and ticks were allowed to feed naturally until replete. The feeding was repeated three times at 2–3 week intervals, and engorged females were weighed after each feeding. Feeding of *I. ricinus* nymphs on a laboratory rabbit was performed in total, eight times: 4 x 2 subsequent feedings (10 days overall) followed by a resting interval of 2–3 weeks (1st, 2nd, 3rd, or 4th nymphal infestation). For each feeding, a total number of 500 nymphs were equally distributed into two chambers on the opposing sides of the rabbit and allowed to feed till replete. Fifty representative fully fed nymphs were weighed per feeding.

All laboratory animals were treated in accordance with the Animal Protection Law of the Czech Republic No. 246/1992 Sb., ethics approval No. 25/2018. The study was approved by the Institute of Parasitology, Biology Centre of the Czech Academy of Sciences (CAS) and Central Committee for Animal Welfare, Czech Republic (protocol no. 1/2015).

Membrane Tick Feeding

Membrane feeding of ticks was performed according to the original protocol (Krober and Guerin, 2007) in a 6-well plate format kept at 37°C. Bloods from repeatedly infested and naive rabbits were collected in 50 ml conical centrifuge tubes and manually defibrinated using glass beads (diameter 4 mm). Fifteen females were placed into each feeding unit lined with a thin (80–120 μm) silicone membrane, previously pre-treated with a bovine hair extract in dichloromethane (0.5 mg of low volatile lipids). After 24 h, unattached or dead females were removed and an equal number of males were added to the feeding unit containing attached females. Diets were exchanged in a 12 h regime, with concomitant addition of 1 mM adenosine triphosphate (ATP) and gentamicin (5 μg/ml).

Micro-Injection of Unfed *I. ricinus* Females

Phosphoramidon [*N*-(α-rhamnopyranosyl-oxyhydroxyphosphinyl)-Leu-Trp] (Merck; Sigma-Aldrich 525276), a competitive inhibitor of several soluble zinc metalloproteases (Kitagishi and Hiromi, 1984),

was solubilized in PBS and 300 nl were micro-injected in a concentration series ranging from 5–50 µg/µl, through the coxa of the third pair of legs into the hemocoel of each unfed adult *I. ricinus* female using a Nanoinject II (Drummond). Next day, ticks were allowed to feed naturally on a rabbit or were fed *in vitro* on a membrane (see above). The feeding ability of ticks was monitored, and their post-engorgement weights were determined.

Salivary Gland Transcriptome Assembly

Five pairs of salivary glands were dissected from adult *I. ricinus* females fed for 6 days on a naïve rabbit. These were homogenized using a 29G needle syringe and RNA was extracted using Nucleospin RNA (Macherey-Nagel). The RNA extract was sent to Novogene for library preparation and NovaSeq 600 M (Illumina) sequencing. Paired end unstranded sequencing (PE 150) generated 39,825,389 clean reads with a Q30 of 95%. Transcriptome assembly and coding sequence extraction were carried out as described previously (Ribeiro et al., 2014). Briefly, reads were stripped of their contaminating primers, and bases with equal values <20 were trimmed. Clean reads were assembled using the Abyss (Birol et al., 2009) and Trinity (Grabherr et al., 2011) assemblers. These assemblies were merged using a parallelized pipeline of blastn and cap3 assembler (Huang and Madan, 1999) as described previously (Karim et al., 2011). All open reading frames larger than 200 nucleotides were extracted and those matching known proteins or having a signal peptide were retained. The resulting peptide and coding sequences were mapped to a hyperlinked spreadsheet, including blastp and rpsblast matches to several databases, as well as an indication of the signal peptide (Nielsen et al., 1999), transmembrane domains (Sonnhammer et al., 1998) and O-galactosylation sites (Hansen et al., 1998). The sequence data are available in GenBank as BioProject: 589581 and a hyperlinked excel sheet is available to download at https://proj-bip-prod-publicread.s3.amazonaws.com/transcriptome/Perner/Ixric/Perner-Ir2019.zip (further referred to as Source data 1), which also provides semi-quantitative data on transcript expression. Column AR in the Source data 1 spreadsheet indicates a Y if the new sequence is at least 2% different from the public one, or if it extends the length of a known sequence. The Y actually represents 3 classes: (a) novel sequences, if less than 95% identical to a known sequence, (b) similar sequences, possibly due to alleles (95–98% identity and full or at least 90% coverage, (c) extensions, with 98–100% id and longer new sequences as indicated in column AQ of the Source data 1 spreadsheet.

Immunoprecipitation

Saliva was collected from one hundred *I. ricinus* adult females fed on naïve rabbits for 6 days and they were then manually detached and removed. Salivation was induced by application of 1.2 µl of pilocarpine (5 mg dissolved in 100 µl of 100% ethanol) onto the tick scutum (Tatchell, 1967). Saliva was collected into 10-µl capillaries for 2 h in a wet chamber kept at 30°C. IgG fractions were obtained from the rabbit sera by caprylic acid precipitation of non-IgG proteins (Russo et al., 1983) and dialysed against 50 mM Tris, pH 8.0, 150 mM NaCl. A volume of 125 µl of Protein A Mag Sepharose bead slurry (GE Healthcare) was equilibrated with 1 ml of binding buffer: 50 mM Tris, pH 8.0, 150 mM NaCl. Immunoglobulins (82.5 µg) were then added to equilibrated beads and incubated for 1 h at 7°C. Beads were washed three times with binding buffer and then saliva was added to the Ig-loaded beads. These were incubated over-night at 7°C in a head-over-head rotator. Beads were washed five times with binding buffer and antigens were eluted with 0.2% SDS, 0.1% Tween-20, 50 mM Tris-HCl, pH = 8.0, 150 mM NaCl incubated for 7 min at 25°C, shaking at 1,000 rpm (Antrobus and Borner, 2011). The eluates were separated by non-reducing SDS-PAGE in 4–12% Bis Tris Plus gel (Life Technologies) and stained with Coomassie Brilliant Blue.

Sample Preparation for Mass Spectrometry

Coomassie-stained bands were excised, chopped into small pieces and transferred to 0.5-ml Eppendorf tubes. For all following steps, buffers were exchanged in two consecutive 15-min incubation steps of gel pieces with 200 µl of acetonitrile (ACN), with the ACN being removed after each step. Proteins were reduced by the addition of 200 µl of a 10 mM DTT solution in 100 mM ammonium bicarbonate (AmBiC, Sigma Aldrich, A6141) and incubated at 56°C for 30 min. Proteins were alkylated by the addition of 200 µl of 55 mM iodoacetamide (IAA) in 100 mM AmBiC and incubated for 20 min in the dark. A 0.1 µg/µl stock solution of trypsin (Promega, V511A) in trypsin resuspension buffer (Promega, V542A) was diluted with ice-cold 50 mM AmBiC buffer to achieve a final concentration of 1 ng/µl. 50 µl were then added to the gel pieces, which were incubated first for 30 min on ice and then overnight at 37°C. Gel pieces were sonicated for 15 min, spun down and the supernatant was transferred into a glass vial (VDS Optilab, 93908556). Remaining gel pieces were washed with 50 µl of an aqueous solution of 50% ACN and 1% formic acid and sonicated for 15 min. The combined supernatants were dried in a speedvac and reconstituted in 10 µl of an aqueous solution of 0.1% (v/v) formic acid.

LC-MS/MS

Briefly, peptides were separated using an UltiMate 3000 RSLC (Thermo Scientific) equipped with a trapping cartridge (Precolumn; C18 PepMap 100, 5 lm, 300 lm i.d. × 5 mm, 100 A°) and an analytical column (Waters nanoEase HSS C18 T3, 75 um × 25 cm, 1.8 µm, 100 A°). Solvent A: aqueous 0.1% formic acid; Solvent B: 0.1% formic acid in acetonitrile (all solvents were of LC-MS grade). Peptides were loaded onto the trapping cartridge using solvent A for 3 min at a flowrate of 30 µl/min. Peptides were separated on the analytical column at a constant flowrate of 0.3 µl/min applying a 30 min gradient of 2–25% of solvent B in A, followed by an increase to 85% B. Peptides were directly analyzed in positive ion mode applied with a spray voltage of 2.2 kV and a capillary temperature of 275°C using a Nanospray-Flex ion source and a Pico-Tip Emitter 360 lm OD × 20 lm ID; 10 lm tip (New Objective). The MS spectra with a mass

range of 350–1.500 m/z were acquired using a resolution of 120.000 (maximum injection time of 100 ms). Fragmentation was triggered by HCD in fixed collision energy mode with fixed collision energy of 30% for peaks with a charge state of 2–6 on the MS scan and a 5-second exclusion window. MS2 spectra were acquired by the Ion Trap with a rapid ion trap scan rate and a max injection time of 35 ms. The mass spectrometry proteomics data have been deposited to the ProteomeXchange Consortium *via* the PRIDE (Perez-Riverol et al., 2019) partner repository with the dataset identifier PXD021370.

Data Analysis

Acquired data were processed using MaxQuant 1.6.7.0 with cDNA databases based on transcriptomics data. Apart from the default settings, the following modifications were considered: Carbamidomethyl (C) (fixed modification), Acetyl (N-term), and Oxidation (M) (variable modifications). Gel slices were considered as fractions of the naïve or immunized samples. Proteins were identified by a minimum of four assigned unique peptides and, with zero assignment in the naïve sample, are shown in **Table 1**. Only sequence coverages of more than 2% and Q values (representing the probability that the protein is a false hit) that equal zero were considered. Full proteomics assignment data are shown in the excel spreadsheet available as **Supplementary Data File**.

Statistical Analysis

Data on tick weights failed to meet the criteria for normal data distribution according to the Shapiro-Wilk normality test. Individual datasets were, therefore, analyzed by the unpaired non-parametric Mann-Whitney test. Individual statistical significances are stated in the Figure legends.

RESULTS

Repeated *Ixodes ricinus* Feeding Induces Acquired Resistance in Rabbits

We subjected laboratory rabbits to repeated feeding of *Ixodes ricinus* adults and nymphs. After initial feeding, any following feeding of adult females led to significantly decreased engorged weights (**Figure 1A**). Similarly, the immediate weight reduction of nymphs following feeding of the first cohort was observed with a gradual and continuous decrease in nymphal weights until the 4th infestation (**Figure 1B**). To verify if the acquired resistance to adult ticks would also lead to resistance against nymphal stages, we added *I. ricinus* nymphs to a rabbit with previously developed resistance to *I. ricinus* adults. Nymphs were placed onto the same spot where adults had previously fed, and also onto a new unexposed spot on the rabbit's back (**Figure 1C**). Nymphs gained significantly lower engorged weights compared to control nymphs fed on a naïve rabbit, demonstrating cross-reactivity between adult and nymphal antigens and cross-protection between adult and nymphal *I. ricinus* ticks (**Figure 1C**). There was no significant difference between ticks placed on the old and new spot of the rabbit, indicating a systemic response to the tick feeding rather than local rejection (**Figure 1C**).

Immunoprecipitation of Antigens From Tick Saliva Using Antibodies Developed Under Naturally Acquired Immunity

Tick secretory material is derived predominantly from salivary glands but can also contain components from midgut regurgitate (Brown, 1988). To select the source material for pull-down, we inspected the background avidity of naïve rabbit immunoglobulins against midgut homogenates, salivary gland homogenates, and saliva

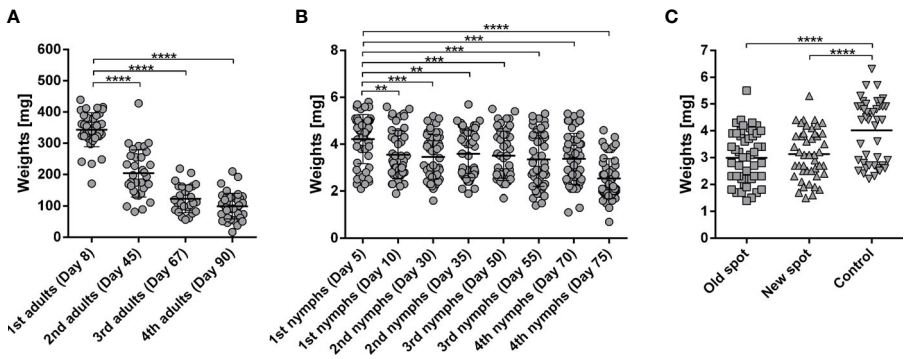

FIGURE 1 | **(A)** Weights of *Ixodes ricinus* adults repeatedly fed on one rabbit. *I. ricinus* adult females were fed on a laboratory rabbit in subsequent feedings with 2–3-week intervals between feedings. Adult females were placed in two chambers on opposing sides of the rabbit (25 ticks into each chamber); n ≥ 30; Days indicate the date of detachment of respective groups after attachment of the first ticks. **(B)** Weights of *I. ricinus* nymphs repeatedly fed on one rabbit. *I. ricinus* nymphs were fed on a laboratory rabbit in two subsequent feedings (10 days overall) and with 2–3-week intervals between feedings. Nymphs were placed in two chambers on opposing sides of the rabbit (125 nymphs into each chamber). Two subsequent feedings (1st, 2nd, 3rd, or 4th nymphs) totaled each 500 nymphs. Days indicate the date of detachment of the respective groups after attachment of first ticks. Fifty representative fully fed nymphs were weighed per feeding. Note, the clusters above and below the average weight represent weights of female and male nymphs, respectively (Dusbabek, 1996). **(C)** Weights of *I. ricinus* nymphs fed on a repeatedly adult-infested rabbit. *I. ricinus* nymphs were fed on a laboratory rabbit previously fed on by *I. ricinus* adults. Nymphs were placed on a rabbit two weeks after the last *I. ricinus* adult feeding (Day 90). Nymphs were placed either on a spot of previous feeding (old) or the feeding chamber was moved to a previously un-infested spot on the same rabbit (new). Nymphs fed on a naive rabbit were used as a control. Mean + SEM are shown, n ≥40. Asterisks indicate statistical significance, ****p < 0.0001, ***p < 0.001, **p < 0.01, when compared to tick weights after first feeding.

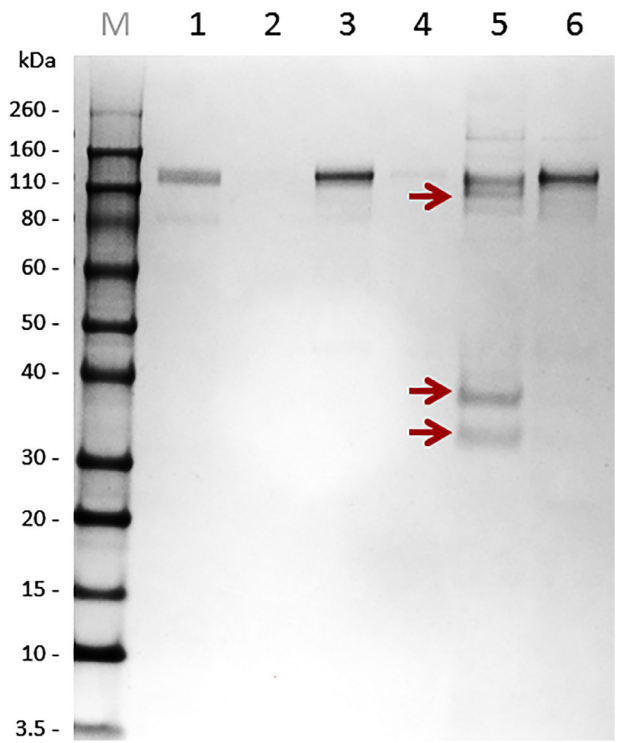

FIGURE 2 | Non-reducing SDS-PAGE separation of immunoprecipitated salivary antigens using protein A paramagnetic beads. Immunoglobulins (Ig's) from both immunized (repeated feeding) and naïve rabbit sera were immobilized on Protein A magnetic beads. These immunoglobulin-loaded beads were used for antigen fishing in pilocarpine-induced saliva of *I. ricinus* females fed on a rabbit for six days. Bound antigens to immunoglobulins from immunized and naïve rabbits were eluted and subjected to SDS-PAGE. M – Novex Sharp Marker, 1 – immunoglobulin fraction from "immunised" rabbits, 2 – SN after bead pelleting (indicates immobilization of "immunised" Ig's on Protein A beads), 3 – immunoglobulin fraction from naïve rabbits, 4 – SN after bead pelleting (indicates immobilization of naive Ig's on Protein A beads), 5 – elution fraction from "immune" beads, 6 – elution fraction from "naïve" beads. Bands from experimental group (red arrows) and corresponding areas from the control gel control were sliced out the gel and subjected to proteomic analysis.

(**Supplementary Figures S1–3**). While immunoglobulins from naïve rabbits markedly cross-reacted with proteins of the tick midgut and salivary gland homogenates (**Supplementary Figures S1, 2**, respectively), reduced immuno-detection was found in tick pilocarpine-induced saliva using immunoglobulins from naïve rabbits (**Supplementary Figure S3**). Therefore, for identification of immunogens, we used saliva of *I. ricinus* ticks, rather than a tissue homogenate. Isolated immunoglobulins from sera of immunized or naïve rabbits were immobilized on paramagnetic ProteinA beads, and target antigens were pulled-down from the saliva of adult *I. ricinus* females. To prevent co-elution (leaking) of immunoglobulins with the antigens, we used mild elution conditions for retrieval of a pure, yet possibly not exhaustive, set of antigens. The elution fraction from immunoglobulins of the repeatedly infested rabbit clearly contained specific antigens that were not present in the elution fraction from immunoglobulins of a naive rabbit (**Figure 2**). The elution fractions were separated by SDS-PAGE and the area around the visible bands were excised for proteomic identification, together with the corresponding gel areas in the lane from the naïve rabbit control.

Tick Antigens Recognized by Naturally Acquired Immunity Are Mostly Secreted Metalloproteases

Proteins were, by default, identified by assignment of obtained peptides in available *I. ricinus* transcriptomes from the early phase of feeding. Existing transcriptomes of *I. ricinus* salivary glands, however, so far have covered a transcript repertoire of salivary glands only during the initial three days of tick feeding (Schwarz et al., 2013; Kotsyfakis et al., 2015; Perner et al., 2018). In order to fine-tune the protein identification of salivary gland antigens at the timepoint of saliva collection, we assembled a new transcriptome from salivary glands of adult *I. ricinus* females fed for six days. Additionally, we have identified 19,559 novel or extended transcripts (see *Material and Methods* section for the filtering criteria). The full list of assembled contigs, their sequences and expression values are accessible through the Source data 1, a hyper-linked excel sheet (see *Material and Methods* for a download link). Using this new transcriptome as a search database for peptide assignments (BioProject: 589581), we have identified only one unique antigen-encoding transcript on top of those identified from already existing transcriptomes (**Table 1**). Out of ten identified antigens, six are enzymes, one is a binding protein, and three are proteins of unknown function (containing a distant domain similarity with the catalytic domain of phosphoinositide-specific phospholipase C-like phosphodiesterases) (**Table 1**). Among the identified salivary antigens, the MA clan metalloproteases of the GluZincin superfamily (based on MEROPS nomenclature), and the zinc-dependent metallopeptidases, which contain the HEXXH motif as part of their active site, clearly dominate. These mainly include the M13 family neprilysin-like metalloprotease, the M2 family angiotensin converting enzyme-like dipeptidyl carboxypeptidase (kininase), and the M1 family aminopeptidase N, venom metalloprotease 3, and Metis5 (venom antarease-like) metalloprotease. Additionally, a non-proteolytic enzyme identified among the enriched antigens was the ATP diphosphohydrolase (apyrase), a frequently reported constituent of tick saliva (Mans, 2016). The full list of identified antigens and numbers of assigned peptides is available as **Supplementary Data File**. To gain an insight into expression dynamics throughout tick feeding, we inspected the transcription expression profiles of those transcripts that were present in our new 6 days fed SG library and compared their expression patterns in SG RNAseq databases from earlier timepoints of feeding (Source data 1 spreadsheet, columns ER-EZ). Most of the antigen transcripts were apparently present in the salivary glands during the early phases of feeding. In fact, most were highly abundant transcripts and their levels decreased only slightly as feeding progressed (**Table 1**). A unique transcript, present only in the new 6 days fed SG library, was the venom metalloprotease 3. Based on software predictions, most of the identified antigens are secretory proteins except aminopeptidase N that lacks the signal peptide (**Table 1**). The antigens identified were predicted to be frequently post-translationally modified,

bearing O-glycosylation at Ser and Thr residues, and/or N-glycosylation at Asn residues (**Table 1**). This is in line with the recent corroboration that the presence of a glycan moiety on salivary proteins is critical for eliciting tick rejection by a host, a guinea pig in that case (Narasimhan et al., 2020). Of note, a clear motif ANGD**Y**DDWQ, found in the sequence of aminopeptidase N and apolipophorin, indicates sulfation of the tyrosine residue of the enzyme (**Table 1**), a key post-translational modification that determines the capacity of tick salivary proteins to inhibit host clotting enzymes (Thompson et al., 2017).

Tick Membrane Feeding of Immunized Rabbit Blood Did Not Lead to Decreased Engorged Weights

To examine whether the decreased weights of ticks fed on repeatedly infested rabbits is caused by the presence of "toxic" immunoglobulins in the blood, we performed the following *in vitro* feeding experiment. Ticks were fed artificially on blood collected from repeatedly infested rabbits and naïve rabbits. The results clearly show that both groups achieved comparable engorged weights irrespective of the presence of anti-tick immunoglobulins (**Figure 3**). This observation indicates that integration of antibodies in acquired resistance to ticks is not an independent cause but is likely linked to other fractions of host immunity absent in the artificial membrane feeding. This is in line with a previous observation that the humoral response of the immunized animals alone did not affect tick feeding (Knorr et al., 2018). Also, this result rather negates the expectations of using this *in vitro* feeding platform as a valuable tool for screening anti-tick sera from vaccinated animals, as previously proposed (de la Fuente et al., 2016).

Injection of Metalloprotease Inhibitor Impairs Tick Feeding *In Vivo* on a Rabbit but Not Feeding *In Vitro* on a Membrane

To investigate the role of metalloproteases at the tick-host interface, we performed a comparative feeding on a rabbit (*in vivo*) and using an artificial membrane system (*in vitro*) with ticks that were microinjected with phosphoramidon, a potent naturally occurring inhibitor of neprilysin-like and ACE-like metalloproteases (Campbell, 2018). Ticks were micro-injected with different concentrations of phoshoramidon solution in PBS, ranging from 50 to 5 μg/μl, in a volume of 300 nl (25 to 2.5 nanomoles/tick injection). Ticks rested over-night before being placed for feeding. Ticks were then either put on a rabbit or on the membrane of an artificial feeding system. The highest concentration injected (50 μg/μl) was toxic and ticks died before feeding initiation or shortly thereafter, irrespective of the feeding mode (**Figure 4**). However, the lower concentrations (5–25 μg/μl), impaired the feeding of ticks on a rabbit, while ticks fed on a membrane managed to initiate and accomplish feeding until full engorgement (**Figure 4**). These data clearly show that tick salivary metalloproteases play a critical role in the feeding process on a living host.

DISCUSSION

Tick salivary gland transcriptomic (Perner et al., 2018) and proteomic (Narasimhan et al., 2007) repertoires wax and wane as functions of time during the initial period of tick feeding on a host. The salivary proteome repertoire also appeared to adjust according to the host species (Tirloni et al., 2017; Narasimhan et al., 2019). For increased authenticity in identifying peptide mass fingerprints, it is critical to have transcriptomic databases relevant to particular tick feeding stages and host type. We, therefore, assembled a salivary gland transcriptome from ticks fed on a rabbit for six days, i.e. the common time-point for pilocarpine-induced saliva collection, to match in time with proteomic pull-down and mass spectrometry. In this study, we identified and experimentally demonstrated that salivary enzymes and scavenging proteins play a critical role in interactions between the tick and host at the expense of immunological recognition during prolonged exposure to the

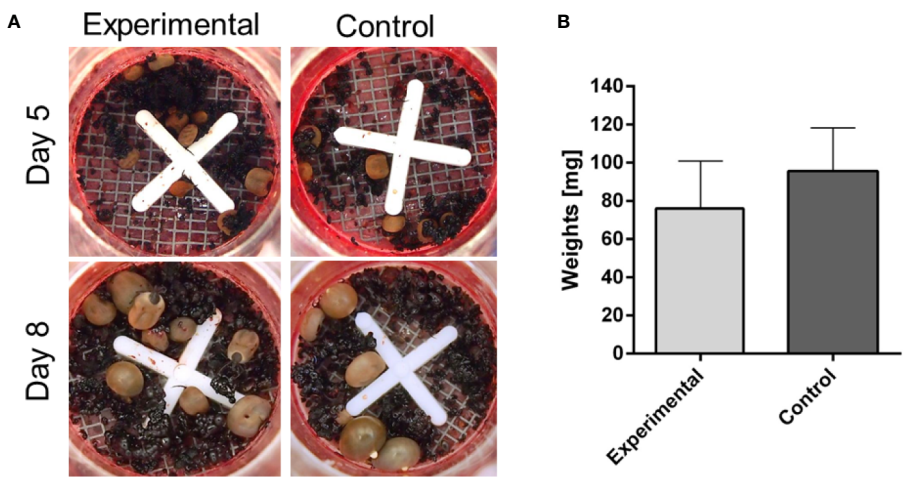

FIGURE 3 | Membrane feeding of *Ixodes ricinus* adults on blood from infested rabbit. *I. ricinus* adults were fed on reconstituted rabbit blood (haematocrit 60%) either from a previously infested rabbit, by repeated adult *I. ricinus* feeding (experimental), or from a naïve rabbit (control). **(A)** Pictures of feeding units during the course of artificial feeding. **(B)** Weights of dropped-off females and females removed on Day 10. Bars represent a mean and SEM, n ≥6.

TABLE 1 | Identification and characterization of tick *I. ricinus* salivary antigens.

Protein name[a]	Transcript IDs[b]GenBank SG 6D transcriptome	Unique peptides[c] Immunised	Sequence coverage[d] (unique)[%]	SignalP[e]	PTM[f] predictions	Expression in SG[g][FPKM values]			
						1D	2D	3D	6D
Neprilysin-like peptidase	GADI01003586 **IrSigP-237310_FR2_13-780**	**13**	14.5 (14.5)	**Y**	**O5_N2**_Y0	**156**	**92**	**60**	**42**
Apolipophorin	GANP01007796 GANP01012862	**7**	30.7 (2.7)	**Y**	**O4_N1_Y1**	nd	nd	nd	nd
ACE-like (Kininase)	**IrSigP-1798_FR1_163-82**	**7**	45.9 (10)	**Y**	O0_**N2**_Y0	**957**	**971**	**1,406**	**448**
Aminopeptidase N	GADI01006478 **234210_FR3_1-970**;	**5**	11.4 (9.7)	N	O0_N0_**Y1**	**489**	**376**	**279**	**148**
Putative secreted protein	GADI01006537 GANP01014738	**5**	20.1 (20.1)	**Y**	O0_**N1**_Y0	nd	nd	nd	nd
Venome MP3-like	GADI01008036 **IrSigP-37829_FR4_7-380**	**5**	10.8 (8.4)	**Y**	O0_N0_Y0	**0**	**0**	**0**	**443**
Secreted protein	**16939_FR1_1-184 IrSigP-16941_FR1_1-451**	**4**	12.1 (12.1)	**Y**	**O4**_N0_Y0	**13**	**10**	**12**	**48**
Metis5	**1791_FR1_58-521 IrSigP-245384_FR2_35-602**	**4**	4.8 (4.8)	**Y**	**O6**_N0_Y0	**791**	**731**	**422**	**476**
Uncharacterised protein	GADI01001927 GANP01013656	**4**	13.5 (8.8)	**Y**	**O2**_N0_Y0	nd	nd	nd	nd
Apyrase (5'-nucleotidase)	GADI01003062 **IrSigP-91535_FR1_1-605**	**4**	10 (7.9)	**Y**	O0_**N1**_Y0	**18**	**11**	**14**	**7**

*Legend to the **Table 1**: Counts of assigned peptides to an individual protein were identified and quantified by the MaxQuant software engine. Proteins with a minimum of four assigned unique peptides and with zero assignment in the naïve sample are shown in the table. Only sequence coverages of more than 2% and Q values (representing the probability that the protein is a false hit) that equal zero are shown. Full proteomics assignment data are shown in the excel spreadsheet available as **Supplementary Data File**. Antigens present in the novel transcriptome of salivary glands from the I. ricinus ticks fed for six days are shown in bold, and their sequences are accessible through column "A" in the hyperlinked Source data 1 spreadsheet (see Material and Methods for download link).*

[a]individual protein identified and quantified by the MaxQuant software engine.

[b]Normal font - accession number of the assigned protein in the GenBank; In bold - antigens present in the novel transcriptome of salivary glands from the I. ricinus ticks fed for six days. Sequences are accessible through column "A" in the hyperlinked Source data 1 spreadsheet (see Material and Methods for download link).

[c]Number of unique peptides used for the antigen identification.

[d]Sequence coverage.

[e]Signal peptide prediction using SignalP with >0.90 probability threshold (Almagro Armenteros et al., 2019). For Metis 5 metalloprotease, which lacks an N-terminus in our database, antarease I. scapularis homologue (XP_029834648.1; E value = 0; aa identity = 83%) was used for the SignalP prediction.

[f]Prediction of posttranslational modification. Numbers of O-glycosylation (O) and N-glycosylation (N) sites were predicted (> 0.75 prediction threshold) by NetOGlyc 4.0 and NetNGlyc 1.0, respectively (Steentoft et al., 2013). Y prediction of tyrosine sulfation (Chang et al., 2009) (threshold > 0.90).

[g]Average FPKM values in I. ricinus salivary glands transcriptomes (1D, 2D, 3D, 6D - days of feeding).

host immune system. During this period, the host antibody response had sufficient time to develop. Antigens identified by repeated feeding of ticks thus have the potential to be harnessed for research into vaccination against tick feeding. Importantly, the recent study on guinea pigs and their acquired resistance to *I. scapularis* infestation revealed that tick salivary glycoproteins are the critical elicitors of tick resistance (Narasimhan et al., 2020). This finding agrees with our results showing that the majority

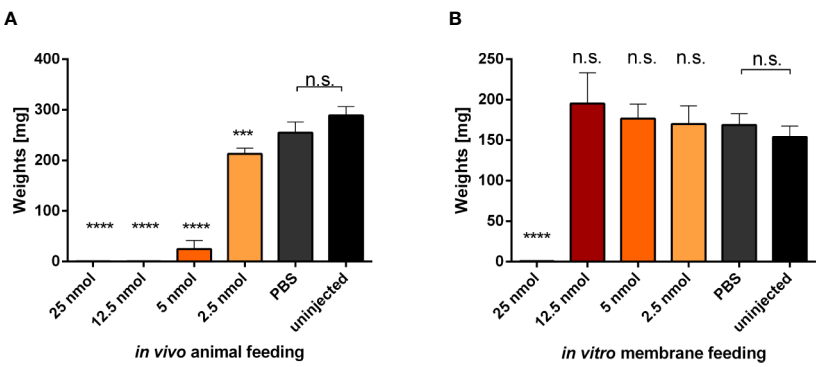

FIGURE 4 | Evaluation of micro-injected phosphoramidon effect on tick feeding. Adult *I. ricinus* females were micro-injected indicated amounts of phosphoramidon solubilized in PBS. **(A)** Weights of engorged females fed on a rabbit. Bars represent the mean and SEM, n ≥25. **(B)** Weights of engorged females fed on an artificial membrane system. Data were obtained from two independent experiments. Bars represent a mean and SEM, n ≥12. Asterisks indicate statistical significance, *** indicate p = 0.0003, **** indicate p < 0.0001, n.s, not significant, when compared to the uninjected control.

of antigenic metalloproteases from *I. ricinus* saliva are predicted to be post-translationally modified by O-type and/or N-type glycosylation. If glycans need to be retained on the enzymes to induce protectivity, this needs to be taken into consideration in recombinant protein expression strategies for vaccination against ticks and tick-borne pathogens (Šimo et al., 2017).

Metalloproteases comprise the majority of coding sequences in the tick salivary gland transcriptomes, accounting for more than 5% of the total read of the entire transcriptome (Schwarz et al., 2013), as well as of salivary proteomes of various tick species, e.g. *Dermacentor andersoni* (Mudenda et al., 2014), *Haemaphysalis longicornis* (Tirloni et al., 2015), *Ixodes scapularis* (Kim et al., 2016), *A. americanum* (Kim et al., 2020). Despite their abundance, the physiological function of most metalloproteases in tick saliva remains unknown, although some were characterized as fibrinogenases (Francischetti et al., 2003). We can speculate about their additional possible interference with the host peptide signalling cascade of inflammatory responses or host matrix modulation. Our results show that some of the MA clan zinc-dependent metalloproteases of different families are the major immunogens present in the saliva of *I. ricinus* ticks and thus corroborate previous studies showing the recognition of metalloproteases by sera of repeatedly infested dogs and rabbits (Decrem et al., 2008) as well as by sera from people with an immune reaction to tick feeding (Becker et al., 2015). Vaccination trials with the metalloprotease Metis1 in rabbits led to decreased fecundity in *I. ricinus* ticks (Decrem et al., 2008), as well as with the metalloprotease BrRm-MP4 from *R. microplus* (Ali et al., 2015).

Three of five identified antigenic metalloproteases in *I. ricinus* saliva presumably act as endopeptidases, cleaving host (vertebrate) large protein or peptide substrates. M13-neprilysin-like metalloprotease is an endopeptidase and shares a 32% amino-acid identity with mammalian neprilysin, and contains a HEITH Zn-binding motif (Bland et al., 2008). Invertebrate M13 peptidases have been found in various organisms playing diverse roles from metamorphosis to immune responses (Bland et al., 2008). Neprilysin-like peptidases have undergone genome expansion and the *I. scapularis* genome encodes more than a hundred different isoforms (Gulia-Nuss et al., 2016). M2 Metallo-dipeptidyl carboxypeptidase (kininase) is a broad substrate specificity exopeptidase, containing an HEMGH Zn-binding motif, and sharing a 42% amino acid identity with insect and mammalian angiotensin-converting enzyme (ACE). However, it has been shown that the ACE-related protein from *R. microplus* does not cleave mammalian angiotensin as a substrate (Jarmey et al., 1995; Bastiani et al., 2002). Instead, the *I. scapularis* dipeptidyl carboxypeptidase was shown to exert a kininase activity, with the capacity to cleave host bradykinin, a key pro-inflammatory molecule (Ribeiro and Mather, 1998). The identified *I. ricinus* antigenic kininase is a likely homologue of the *I. scapularis* enzyme (XP_029826915.1; 90% amino acids identity over 99% coverage) and *R. microplus* ACE-like protein (54% amino acid identity over 95% sequence coverage), designated as Bm91 antigen (Riding et al., 1994). Vaccination with recombinant Bm91 produced in the eukaryotic *Pichia pastoris* system, however, did not confirm any effect against tick feeding or reproduction (Lambertz et al., 2012). When silenced, no significant deviations from feeding and reproduction in Bm91-RNAi ticks were observed either (Nijhof et al., 2007). M1 Puromycin-sensitive aminopeptidase is another exopeptidase, containing the HELAH Zn-binding motif, and shares a 44% amino acid identity with mammalian aminopeptidase N. The tick aminopeptidase N homologue has a strong predication for tyrosine sulfation. Such post-translational modification plays a critical role in its capacity to inhibit host haemostatic targets (Thompson et al., 2017). In insects, aminopeptidase N is mainly localized to the midgut membrane (Adang, 2004) and is a candidate molecule from the mosquito *Anopheles gambiae* for a *Plasmodium falciparum* transmission-blocking vaccine (Dinglasan et al., 2007). Interestingly, using specific rabbit polyclonal antibodies, nearly a 100% neutralisation of protease activity was achieved, which supports the concept of immunoglobulin-mediated neutralisation of proteases at the parasite-host interface (Dinglasan et al., 2007).

Besides the dominant metalloproteases, we also identified the enzyme apyrase as an immunogenic constituent of tick saliva. Apyrases hydrolyse host ADP and ATP, inhibiting key pathways of platelet and neutrophil aggregation and other pro-inflammatory reactions (Francischetti et al., 2009). Anti-apyrase immunoglobulins have been reported as markers of the sand fly *Lutzomyia longipalpis* bite, indicating an immunogenic nature of these enzymes, even in non-tick blood feeders (Milon et al., 2010). Vaccination of rabbits with *E.coli*-produced recombinant *Ornithodoros moubata* apyrase (GenBank: AGJ90350.1; 52% amino acid identity and 97% coverage with the *I. ricinus* immunogenic apyrase) led to a strong reduction in feeding in all developmental stages (Díaz-Martín et al., 2015), indicating a protective effect when used as a single-antigen vaccine.

Another natural *I. ricinus* antigen was identified as an apolipophorin-related molecule. Apolipophorins were originally described as important lipid transporters in insect hemolymph (Chino et al., 1981; Chino and Downer, 1982). Insect apolipophorins show a resemblance to tick vitellogenins and carrier proteins (Donohue et al., 2009), all of which are derived from a common ancestor and belong to the large lipid transfer protein superfamily (Smolenaars et al., 2007). This finding is not new, as homologous lipoproteins have previously been identified proteomically in pilocarpine-induced saliva of partially- and fully-fed *R. microplus* ticks (Tirloni et al., 2014), dopamine-induced saliva of partially-fed *D. andersoni* (Mudenda et al., 2014), dopamine- and pilocarpine-induced saliva of *H. longicornis* nymphs and adults (Tirloni et al., 2015), pilocarpine-induced saliva of *I. scapularis* (Kim et al., 2016), *A. americanum* (Kim et al., 2020), as well as by antibody-mediated identification in phage display cDNA expression SG libraries from early timepoints of *A. americanum* feeding (Radulovic et al., 2014). Genetically tick-resistant bovines recognize more tick salivary proteins than sera of susceptible ones. Among *R. microplus* antigens identified by sera of resistant bovines, and not of susceptible ones, are apolipophorin and lipocalins (Garcia et al., 2017). The role of lipoproteins in tick saliva is currently unknown. The transcript encoding apolipophorin/vitellogenin (SigP-149886; GenBank: JAB71606.1) is predominantly expressed in the midgut rather than salivary glands in nymphs and adults of *I. ricinus* (Kotsyfakis et al., 2015), suggesting that it might not be a specific salivary secretory protein.

Using artificial membrane feeding of ticks, we demonstrated that the mere presence of anti-tick immunoglobulins in the blood meal

had no significant effect on the progress of tick feeding. This can be explained by the fact that the processes by which antigens interact with the *in vivo* system are absent in the membrane feeding system. Such processes might include blood coagulation (ticks fed on defibrinated blood in the membrane feeding system), or leukocyte infiltration and degranulation. Host production of specific immunoglobulins may bring about neutralisation of the antigenic metalloprotease enzymatic activity. When fed repeatedly, potential antibody-mediated neutralisation of the proteases might lead to increased levels of peptidic inflammatory mediators and leukocyte infiltration, eventually causing rejection of ticks. Alternatively, as tick salivary Zn-metalloproteases were implicated in the prevention of fibrin clot formation and dissolution of the fibrin clots (Francischetti et al., 2003), we speculate that the ability of ticks exposed to protective immunoglobulins or a specific inhibitor to fully engorge in an *in vitro* membrane feeding system is due to the fact that ticks are served defibrinated blood. Any neutralisation of tick anti-clotting activity is, therefore, not physiologically penalized in this apparently "luxurious" feeding system.

CONCLUSION

In this work, we have: 1) identified tick salivary proteins that are recognized by antibodies produced in a tick-immunized host (rabbit), using peptide mass fingerprinting; 2) assembled and made publicly available the tick salivary gland transcriptome of adult *I. ricinus* females from the 6th day of tick feeding; 3) demonstrated that neutralization of tick Zn-dependent metalloproteases by rabbit immunoglobulins or inhibition by a specific inhibitor prevent ticks from initiating and progressing through natural feeding but not artificial feeding.

We conclude that metalloproteases present in tick saliva target the components of the host hemostatic and defence systems that are absent during artificial membrane feeding. This explains why ticks feed successfully *in vitro* even in the presence of protective immunoglobulins or metalloprotease inhibitors.

DATA AVAILABILITY STATEMENT

The datasets presented in this study can be found in online repositories. The names of the repository/repositories and accession number(s) can be found in the article/**Supplementary Material**.

ETHICS STATEMENT

The animal study was reviewed and approved by Central Committee for Animal Welfare, Czech Republic.

AUTHOR CONTRIBUTIONS

JP: conceptual design, membrane feeding of ticks and immunoprecipitation of antigens, wrote the manuscript draft. DH and PH: mass spectrometry. TH: phosphoramidon experiments and membrane feeding. SK: western blotting. JR: transcriptome assembly and edited the manuscript. PK: co-wrote and edited the manuscript. All authors contributed to the article and approved the submitted version.

FUNDING

This study was funded mainly by the Czech Science Foundation (GACR) Grant No: 18-01832S to PK. JP and PK were additionally supported by the "Centre for research of pathogenicity and virulence of parasites" (no. CZ.02.1.01/0.0/0.0/16_019/0000759) funded by the European Regional Development Fund (ERDF) and Ministry of Education, Youth and Sport (MEYS).

ACKNOWLEDGMENTS

We are grateful to Jan Erhart for excellent technical support.

SUPPLEMENTARY MATERIAL

The Supplementary Material for this article can be found online at: https://www.frontiersin.org/articles/10.3389/fcimb.2020.563349/full#supplementary-material

REFERENCES

Adang, M. J. (2004). "Insect Aminopeptidase N," in *Handbook of Proteolytic Enzymes, 2nd Edition*. Eds. A. J. Barrett, D. A. Rawlings and J. F. Woessner (Academic Press: Elsevier), 296–299. doi: 10.1016/B978-0-12-079611-3.50079-3

Ali, A., Fernando Parizi, L., Garcia Guizzo, M., Tirloni, L., Seixas, A., Vaz Ida, S. Jr, et al. (2015). Immunoprotective potential of a Rhipicephalus (Boophilus) microplus metalloprotease. *Veterinary Parasitol.* 207, 107–114. doi: 10.1016/j.vetpar.2014.11.007

Allen, J. R. (1973). Tick resistance: basophils in skin reactions of resistant guinea pigs. *Int. J. Parasitol.* 3, 195–200. doi: 10.1016/0020-7519(73)90024-6

Almagro Armenteros, J. J., Tsirigos, K. D., Sonderby, C. K., Petersen, T. N., Winther, O., Brunak, S., et al. (2019). SignalP 5.0 improves signal peptide predictions using deep neural networks. *Nat. Biotechnol.* 37, 420–423. doi: 10.1038/s41587-019-0036-z

Antrobus, R., and Borner, G. H. (2011). Improved elution conditions for native co-immunoprecipitation. *PloS One* 6, e18218. doi: 10.1371/journal.pone.0018218

Barriga, O. O., Andujar, F., Sahibi, H., and Andrzejewski, W. J. (1991). Antigens of Amblyomma americanum ticks recognized by repeatedly infested sheep. *J. Parasitol.* 77, 710–716. doi: 10.2307/3282703

Bastiani, M., Hillebrand, S., Horn, F., Kist, T. B. L., Guimarães, J. A., and Termignoni, C. (2002). Cattle tick Boophilus microplus salivary gland contains a thiol-activated metalloendopeptidase displaying kininase activity. *Insect Biochem. Mol. Biol.* 32, 1439–1446. doi: 10.1016/S0965-1748(02)00064-4

Becker, M., Felsberger, A., Frenzel, A., Shattuck, W. M., Dyer, M., Kugler, J., et al. (2015). Application of M13 phage display for identifying immunogenic proteins from tick (Ixodes scapularis) saliva. *BMC Biotechnol.* 15, 43. doi: 10.1186/s12896-015-0167-3

Birol, I., Jackman, S. D., Nielsen, C. B., Qian, J. Q., Varhol, R., Stazyk, G., et al. (2009). De novo transcriptome assembly with ABySS. *Bioinf. (Oxford England)* 25, 2872–2877. doi: 10.1093/bioinformatics/btp367

Bland, N. D., Pinney, J. W., Thomas, J. E., Turner, A. J., and Isaac, R. E. (2008). Bioinformatic analysis of the neprilysin (M13) family of peptidases reveals complex evolutionary and functional relationships. *BMC Evolution. Biol.* 8, 16. doi: 10.1186/1471-2148-8-16

Bowessidjaou, J., Brossard, M., and Aeschlimann, A. (1977). Effects and duration of resistance acquired by rabbits on feeding and egg laying in Ixodes ricinus L. *Experientia* 33, 528–530. doi: 10.1007/BF01922254

Brossard, M., and Wikel, S. K. (2005). Tick immunobiology. *Parasitology* 129, S161–S176. doi: 10.1017/s0031182004004834

Brown, S. J. (1988). Evidence for regurgitation by Amblyomma americanum. *Veterinary Parasitol.* 28, 335–342. doi: 10.1016/0304-4017(88)90081-7

Campbell, D. J. (2018). Neprilysin Inhibitors and Bradykinin. *Front. Med. (Lausanne).* 5, 257. doi: 10.3389/fmed.2018.00257

Chang, W. C., Lee, T. Y., Shien, D. M., Hsu, J. B., Horng, J. T., Hsu, P. C., et al. (2009). Incorporating support vector machine for identifying protein tyrosine sulfation sites. *J. Comput. Chem.* 30, 2526–2537. doi: 10.1002/jcc.21258

Chino, H., Downer, R. G. H., Wyatt, G. R., and Gilbert, L. I. (1981). Lipophorins, a major class of lipoproteins of insect haemolymph. *Insect Biochem.* 11, 491. doi: 10.1016/0020-1790(81)90085-8

Chino, H., and Downer, R. G. (1982). Insect hemolymph lipophorin: a mechanism of lipid transport in insects. *Adv. Biophysics* 15, 67–92. doi: 10.1016/0065-227X(82)90005-3

Chmelar, J., Kotal, J., Kopecky, J., Pedra, J. H. F., and Kotsyfakis, M. (2016). All For One and One For All on the Tick-Host Battlefield. *Trends Parasitol.* 32, 368–377. doi: 10.1016/j.pt.2016.01.004

de la Fuente, J., Estrada-Pena, A., Venzal, J. M., Kocan, K. M., and Sonenshine, D. E. (2008). Overview: Ticks as vectors of pathogens that cause disease in humans and animals. *Front. Biosci. J. Virtual Lib.* 13, 6938–6946. doi: 10.2741/3200

de la Fuente, J., Kopacek, P., Lew-Tabor, A., and Maritz-Olivier, C. (2016). Strategies for new and improved vaccines against ticks and tick-borne diseases. *Parasite Immunol.* 38, 754–769. doi: 10.1111/pim.12339

Decrem, Y., Mariller, M., Lahaye, K., Blasioli, V., Beaufays, J., Zouaoui Boudjeltia, K., et al. (2008). The impact of gene knock-down and vaccination against salivary metalloproteases on blood feeding and egg laying by Ixodes ricinus. *Int. J. Parasitol.* 38, 549–560. doi: 10.1016/j.ijpara.2007.09.003

Díaz-Martín, V., Manzano-Román, R., Oleaga, A., and Pérez-Sánchez, R. (2015). New salivary anti-haemostatics containing protective epitopes from Ornithodoros moubata ticks: Assessment of their individual and combined vaccine efficacy. *Veterinary Parasitol.* 212, 336–349. doi: 10.1016/j.vetpar.2015.08.005

Dinglasan, R. R., Kalume, D. E., Kanzok, S. M., Ghosh, A. K., Muratova, O., Pandey, A., et al. (2007). Disruption of Plasmodium falciparum development by antibodies against a conserved mosquito midgut antigen. *Proc. Natl. Acad. Sci.* 104, 13461–13466. doi: 10.1073/pnas.0702239104

Dizij, A., and Kurtenbach, K. (1995). Clethrionomys glareolus, but not Apodemus flavicollis, acquires resistance to Ixodes ricinus L, the main European vector of Borrelia burgdorferi. *Parasite Immunol.* 17, 177–183. doi: 10.1111/j.1365-3024.1995.tb00887.x

Donohue, K. V., Khalil, S. M., Sonenshine, D. E., and Roe, R. M. (2009). Heme-binding storage proteins in the Chelicerata. *J. Insect Physiol.* 55, 287–296. doi: 10.1016/j.jinsphys.2009.01.002

Dusbábek, F., Borský, I., Jelínek, F., and Uhlíř, J. (1995). Immunosuppression and feeding success of Ixodes ricinus nymphs on BALB/c mice. *Med. Veterinary Entomol.* 9, 133–140. doi: 10.1111/j.1365-2915.1995.tb00169.x

Dusbabek, F. (1996). Nymphal sexual dimorphism in the sheep tick Ixodes ricinus (Acari: Ixodidae). *Folia Parasitol.* 43, 75–79.

Francischetti, I. M. B., Mather, T. N., and Ribeiro, J. M. C. (2003). Cloning of a salivary gland metalloprotease and characterization of gelatinase and fibrin (ogen)lytic activities in the saliva of the Lyme disease tick vector Ixodes scapularis. *Biochem. Biophys. Res. Commun.* 305, 869–875. doi: 10.1016/S0006-291X(03)00857-X

Francischetti, I. M., Sa-Nunes, A., Mans, B. J., Santos, I. M., and Ribeiro, J. M. (2009). The role of saliva in tick feeding. *Front. Biosci. (Landmark Ed)* 14, 2051–2088. doi: 10.2741/3363

Garcia, G. R., Maruyama, S. R., Nelson, K. T., Ribeiro, J. M., Gardinassi, L. G., Maia, A. A., et al. (2017). Immune recognition of salivary proteins from the cattle tick Rhipicephalus microplus differs according to the genotype of the bovine host. *Parasites Vectors* 10, 144. doi: 10.1186/s13071-017-2077-9

Grabherr, M. G., Haas, B. J., Yassour, M., Levin, J. Z., Thompson, D. A., Amit, I., et al. (2011). Full-length transcriptome assembly from RNA-Seq data without a reference genome. *Nat. Biotechnol.* 29, 644–652. doi: 10.1038/nbt.1883

Gulia-Nuss, M., Nuss, A. B., Meyer, J. M., Sonenshine, D. E., Roe, R. M., Waterhouse, R. M., et al. (2016). Genomic insights into the Ixodes scapularis tick vector of Lyme disease. *Nat. Commun.* 7, 10507. doi: 10.1038/ncomms10507

Hansen, J. E., Lund, O., Tolstrup, N., Gooley, A. A., Williams, K. L., and Brunak, S. (1998). NetOglyc: prediction of mucin type O-glycosylation sites based on sequence context and surface accessibility. *Glycoconj J.* 15, 115–130. doi: 10.1023/A:1006960004440

Heylen, D. J. A., Madder, M., and Matthysen, E. (2010). Lack of resistance against the tick Ixodes ricinus in two related passerine bird species. *Int. J. Parasitol.* 40, 183–191. doi: 10.1016/j.ijpara.2009.07.011

Huang, X., and Madan, A. (1999). CAP3: A DNA sequence assembly program. *Genome Res.* 9, 868–877. doi: 10.1101/gr.9.9.868

Jarmey, J. M., Riding, G. A., Pearson, R. D., McKenna, R. V., and Willadsen, P. (1995). Carboxydipeptidase from Boophilus microplus: a "concealed". *Antigen Similarity Angiotensin-Convert. Enzyme Insect Biochem. Mol. Biol.* 25, 969–974. doi: 10.1016/0965-1748(95)00038-W

Jongejan, F., Pegram, R. G., Zivkovic, D., Hensen, E. J., Mwase, E. T., Thielemans, M. J., et al. (1989). Monitoring of naturally acquired and artificially induced immunity to Amblyomma variegatum and Rhipicephalus appendiculatus ticks under field and laboratory conditions. *Exp. Appl. Acarol.* 7, 181–199. doi: 10.1007/BF01194059

Karim, S., Singh, P., and Ribeiro, J. M. (2011). A deep insight into the sialotranscriptome of the gulf coast tick, *Amblyomma maculatum*. *PloS One*, 6, e28525. doi: 10.1371/journal.pone.0028525

Kim, T. K., Tirloni, L., Pinto, A. F. M., Moresco, J., Yates, J. R., da Silva Vaz, I., et al. (2016). Ixodes scapularis Tick Saliva Proteins Sequentially Secreted Every 24 h during Blood Feeding. *PloS Neglected Trop. Dis.* 10, e0004323. doi: 10.1371/journal.pntd.0004323

Kim, T. K., Tirloni, L., Pinto, A. F. M., Diedrich, J. K., Moresco, J. J., Yates, J. R., et al. (2020). Time-resolved proteomic profile of Amblyomma americanum tick saliva during feeding. *PloS Neglected Trop. Dis.* 14, e0007758. doi: 10.1371/journal.pntd.0007758

Kitagishi, K., and Hiromi, K. (1984). Binding between Thermolysin and Its Specific Inhibitor, Phosphoramidon. *J. Biochem.* 95, 529–534. doi: 10.1093/oxfordjournals.jbchem.a134635

Knorr, S., Anguita, J., Cortazar, J. T., Hajdusek, O., Kopáček, P., Trentelman, J. J., et al. (2018). Preliminary Evaluation of Tick Protein Extracts and Recombinant Ferritin 2 as Anti-tick Vaccines Targeting Ixodes ricinus in Cattle. *Front. Physiol.* 9. doi: 10.3389/fphys.2018.01696

Kotsyfakis, M., Schwarz, A., Erhart, J., and Ribeiro, J. M. (2015). Tissue- and time-dependent transcription in Ixodes ricinus salivary glands and midguts when blood feeding on the vertebrate host. *Sci. Rep.* 5, 9103. doi: 10.1038/srep09103

Krober, T., and Guerin, P. M. (2007). In vitro feeding assays for hard ticks. *Trends Parasitol.* 23, 445–449. doi: 10.1016/j.pt.2007.07.010

Lambertz, C., Chongkasikit, N., Jittapalapong, S., and Gauly, M. (2012). Immune Response of Bos indicus Cattle against the Anti-Tick Antigen Bm91 Derived from Local Rhipicephalus (Boophilus) microplus Ticks and Its Effect on Tick Reproduction under Natural Infestation. *J. Parasitol. Res.* 2012, 907607. doi: 10.1155/2012/907607

Mans, B. (2016). "Glandular Matrices and Secretions: Blood-Feeding Arthropods", in *Extracellular Composite Matrices in Arthropods*. Eds. E. Cohen and B. Moussian. (Cham: Springer), 625–688. doi: 10.1007/978-3-319-40740-1_17

Mans, B. J. (2019). Chemical Equilibrium at the Tick–Host Feeding Interface: A Critical Examination of Biological Relevance in Hematophagous Behavior. *Front. Physiol.* 10. doi: 10.3389/fphys.2019.00530

Milon, G., Teixeira, C., Gomes, R., Collin, N., Reynoso, D., Jochim, R., et al. (2010). Discovery of Markers of Exposure Specific to Bites of Lutzomyia longipalpis, the Vector of Leishmania infantum chagasi in Latin America. *PloS Neglected Trop. Dis.* 4, e638. doi: 10.1371/journal.pntd.0000638

Mudenda, L., Pierle, S. A., Turse, J. E., Scoles, G. A., Purvine, S. O., Nicora, C. D., et al. (2014). Proteomics informed by transcriptomics identifies novel secreted proteins in Dermacentor andersoni saliva. *Int. J. Parasitol.* 44, 1029–1037. doi: 10.1016/j.ijpara.2014.07.003

Narasimhan, S., Deponte, K., Marcantonio, N., Liang, X., Royce, T. E., Nelson, K. F., et al. (2007). Immunity against Ixodes scapularis salivary proteins expressed within 24 hours of attachment thwarts tick feeding and impairs Borrelia transmission. *PloS One* 2, e451. doi: 10.1371/journal.pone.0000451

Narasimhan, S., Booth, C. J., DePonte, K., Wu, M.-J., Liang, X., Mohanty, S., et al. (2019). Host-specific expression of Ixodes scapularis salivary genes. *Ticks Tick-Borne Dis.* 10, 386–397. doi: 10.1016/j.ttbdis.2018.12.001

Narasimhan, S., Kurokawa, C., Diktas, H., Strank, N. O., Cerny, J., Murfin, K., et al. (2020). Ixodes scapularis saliva components that elicit responses associated with acquired tick-resistance. *Ticks Tick-Borne Dis.* 11, 101369. doi: 10.1016/j.ttbdis.2019.101369

Nielsen, H., Brunak, S., and von Heijne, G. (1999). Machine learning approaches for the prediction of signal peptides and other protein sorting signals. *Protein Eng.* 12, 3–9. doi: 10.1093/protein/12.1.3

Nijhof, A. M., Taoufik, A., de la Fuente, J., Kocan, K. M., de Vries, E., and Jongejan, F. (2007). Gene silencing of the tick protective antigens, Bm86, Bm91 and subolesin, in the one-host tick Boophilus microplus by RNA interference. *Int. J. Parasitol.* 37, 653–662. doi: 10.1016/j.ijpara.2006.11.005

Perez-Riverol, Y., Csordas, A., Bai, J., Bernal-Llinares, M., Hewapathirana, S., Kundu, D. J., et al. (2019). The PRIDE database and related tools and resources in 2019: improving support for quantification data. *Nucleic Acids Res.* 47, D442–D450. doi: 10.1093/nar/gky1106

Perner, J., Kropackova, S., Kopacek, P., and Ribeiro, J. M. C. (2018). Sialome diversity of ticks revealed by RNAseq of single tick salivary glands. *PloS Negl. Trop. Dis.* 12, e0006410. doi: 10.1371/journal.pntd.0006410

Peter, R. J., Van den Bossche, P., Penzhorn, B. L., and Sharp, B. (2005). Tick, fly, and mosquito control–lessons from the past, solutions for the future. *Veterinary Parasitol.* 132, 205–215. doi: 10.1016/j.vetpar.2005.07.004

Radulovic, Z. M., Kim, T. K., Porter, L. M., Sze, S. H., Lewis, L., and Mulenga, A. (2014). A 24-48 h fed Amblyomma americanum tick saliva immuno-proteome. *BMC Genomics* 15, 518. doi: 10.1186/1471-2164-15-518

Ribeiro, J. M., and Mather, T. N. (1998). Ixodes scapularis: salivary kininase activity is a metallo dipeptidyl carboxypeptidase. *Exp. Parasitol.* 89, 213–221. doi: 10.1006/expr.1998.4296

Ribeiro, J. M., Chagas, A. C., Pham, V. M., Lounibos, L. P., and Calvo, E. (2014). An insight into the sialome of the frog biting fly, Corethrella appendiculata *Insect Biochem. Mol. Biol.* 44, 23–32. doi: 10.1016/j.ibmb.2013.10.006

Riding, G. A., Jarmey, J., McKenna, R. V., Pearson, R., Cobon, G. S., and Willadsen, P. (1994). A protective "concealed". *Antigen Boophilus. Microplus Purification Localization Possible Funct. J. Immunol.* 153, 5158–5166.

Russo, C., Callegaro, L., Lanza, E., and Ferrone, S. (1983). Re.: Purification of IgG monoclonal antibody by caprylic acid precipitation. *J. Immunol. Methods* 65, 269–271. doi: 10.1016/0022-1759(83)90324-1

Schorderet, S., and Brossard, M. (1993). Changes in immunity to Ixodes ricinus by rabbits infested at different levels. *Med. Veterinary Entomol.* 7, 186–192. doi: 10.1111/j.1365-2915.1993.tb00673.x

Schuijt, T. J., Narasimhan, S., Daffre, S., DePonte, K., Hovius, J. W., Van't Veer, C., et al. (2011). Identification and characterization of Ixodes scapularis antigens that elicit tick immunity using yeast surface display. *PloS One* 6, e15926. doi: 10.1371/journal.pone.0015926

Schwarz, A., von Reumont, B. M., Erhart, J., Chagas, A. C., Ribeiro, J. M., and Kotsyfakis, M. (2013). De novo Ixodes ricinus salivary gland transcriptome analysis using two next-generation sequencing methodologies. *FASEB J. Off. Publ. Fed. Am. Soc. Exp. Biol.* 27, 4745–4756. doi: 10.1096/fj.13-232140

Šimo, L., Kazimirova, M., Richardson, J., and Bonnet, S. I. (2017). The Essential Role of Tick Salivary Glands and Saliva in Tick Feeding and Pathogen Transmission. *Front. Cell. Infect. Microbiol.* 7. doi: 10.3389/fcimb.2017.00281

Smolenaars, M. M., Madsen, O., Rodenburg, K. W., and Van der Horst, D. J. (2007). Molecular diversity and evolution of the large lipid transfer protein superfamily. *J. Lipid Res.* 48, 489–502. doi: 10.1194/jlr.R600028-JLR200

Sonnhammer, E. L., von Heijne, G., and Krogh, A. (1998). A hidden Markov model for predicting transmembrane helices in protein sequences. *Proc. Int. Conf. Intell. Syst. Mol. Biol.* 6, 175–182.

Steentoft, C., Vakhrushev, S. Y., Joshi, H. J., Kong, Y., Vester-Christensen, M. B., Schjoldager, K. T. B. G., et al. (2013). Precision mapping of the human O-GalNAc glycoproteome through SimpleCell technology. *EMBO J.* 32, 1478–1488. doi: 10.1038/emboj.2013.79

Tatchell, R. J. (1967). A modified method for obtaining tick oral secretion. *J. Parasitol.* 53, 1106–1107. doi: 10.2307/3276849

Thompson, R. E., Liu, X., Ripoll-Rozada, J., Alonso-Garcia, N., Parker, B. L., Pereira, P. J. B., et al. (2017). Tyrosine sulfation modulates activity of tick-derived thrombin inhibitors. *Nat. Chem.* 9, 909–917. doi: 10.1038/nchem.2744

Tirloni, L., Reck, J., Terra, R. M., Martins, J. R., Mulenga, A., Sherman, N. E., et al. (2014). Proteomic analysis of cattle tick Rhipicephalus (Boophilus) microplus saliva: a comparison between partially and fully engorged females. *PloS One* 9, e94831. doi: 10.1371/journal.pone.0094831

Tirloni, L., Islam, M. S., Kim, T. K., Diedrich, J. K., Yates, J. R. ,. 3., Pinto, A. F., et al. (2015). Saliva from nymph and adult females of Haemaphysalis longicornis: a proteomic study. *Parasites Vectors* 8, 338. doi: 10.1186/s13071-015-0918-y

Tirloni, L., Kim, T. K., Pinto, A. F. M., Yates, J. R., da Silva Vaz, I., and Mulenga, A. (2017). Tick-Host Range Adaptation: Changes in Protein Profiles in Unfed Adult Ixodes scapularis and Amblyomma americanum Saliva Stimulated to Feed on Different Hosts. *Front. Cell. Infect. Microbiol.* 7. doi: 10.3389/fcimb.2017.00517

Trager, W. (1939). Acquired Immunity to Ticks. *J. Parasitol.* 25, 57. doi: 10.2307/3272160

Wada, T., Ishiwata, K., Koseki, H., Ishikura, T., Ugajin, T., Ohnuma, N., et al. (2010). Selective ablation of basophils in mice reveals their nonredundant role in acquired immunity against ticks. *J. Clin. Invest.* 120, 2867–2875. doi: 10.1172/JCI42680

Willadsen, P., and Jongejan, F. (1999). Immunology of the tick-host interaction and the control of ticks and tick-borne diseases. *Parasitol. Today* 15, 258–262. doi: 10.1016/S0169-4758(99)01472-6

Conflict of Interest: The authors declare that the research was conducted in the absence of any commercial or financial relationships that could be construed as a potential conflict of interest.

Advantages of publishing in Frontiers

OPEN ACCESS
Articles are free to read for greatest visibility and readership

FAST PUBLICATION
Around 90 days from submission to decision

HIGH QUALITY PEER-REVIEW
Rigorous, collaborative, and constructive peer-review

TRANSPARENT PEER-REVIEW
Editors and reviewers acknowledged by name on published articles

Frontiers
Avenue du Tribunal-Fédéral 34
1005 Lausanne | Switzerland

Visit us: www.frontiersin.org
Contact us: frontiersin.org/about/contact

REPRODUCIBILITY OF RESEARCH
Support open data and methods to enhance research reproducibility

DIGITAL PUBLISHING
Articles designed for optimal readership across devices

FOLLOW US
@frontiersin

IMPACT METRICS
Advanced article metrics track visibility across digital media

EXTENSIVE PROMOTION
Marketing and promotion of impactful research

LOOP RESEARCH NETWORK
Our network increases your article's readership